e-ISSN : 2320-0847
p-ISSN : 2320-0936

American Journal of Engineering Research (AJER)

Volume 4 Issue 8– August 2015

www.ajer.org ajer.research@gmail.com

Editorial Board

American Journal of Engineering Research (AJER)

CONTENTS

Volume-4 Issue-8

American Journal of Engineering Research (AJER)
e-ISSN: 2320-0847 p-ISSN : 2320-0936
Volume-4, Issue-8, pp-01-08
www.ajer.org
Research Paper Open Access

Performance Analysis of DWDM System Considering the Effects of Cascaded Optical Amplifiers with Optimum Receiver Gain

Abu Jahid[1], Zahangir Alam[1]
[1]*Department of EEE, Bangladesh University of Business and Technology (BUBT), Dhaka, Bangladesh*

ABSTRACT: *Tremendous growth of rate of traffic due to demands for different multimedia services urges the development of a suitable transmission system capable of handling a large bandwidth. The inherent potential of DWDM like large bandwidth, flexibilities, scopes to upgrade and so many other feature have made it most frequently implied multiplexing technique. In this paper a system has been proposed where an optimum number of amplifiers have been used and an improved APD receiver has been proposed. Theoretical analysis has been carried out to evaluate the performance limitations of DWDM system with intensity modulation direct detection (IM/DD) due to the effects of amplified spontaneous emission (ASE) noise of optical amplifiers and other noises due to an optical receiver. The analysis is presented to find the expression of signal to noise ratio (SNR) and bit error rate (BER) up to the optical receiver taking into account the effect of number of amplifiers and receiver type. Also the system performance has been analyzed by varying amplifier gain, hop length, receiver bandwidth and receiver gain. Result shows that the system performance deteriorates significantly due to power penalty and path penalty.*

Keywords- *Optical Amplifier, BER, Avalanche Photodiode (APD), ASE, IM/DD.*

I. INTRODUCTION

Recently increased bandwidth demand for a large number of growing utilities such as High Definition Television (HDTV), World Wide Web etc. has taken the attention of the recent researchers. Different models have been available for the increased demand without the further extension of the existing facility.

One of the promising techniques to access the huge bandwidth is Wavelength Division multiplexing (WDM). By assigning the incoming signal a specific frequency of light in a limited bandwidth, it increases the bandwidth, flexibility and upgrades the system capacity [1]. Each of the input signals is carried independently, where a dedicated bandwidth for each input signal is allocated. By using WDM, a link capacity on the order of 50 THz can be achieved [2]. An increased number of amplifier affect the Signal to Noise Ratio (SNR) and hence the Bit Error Rate (BER) because of increased amount of spontaneous emission noise. The use of many optical amplifiers in a WDM system after a certain interval makes the signal amplified spontaneous emission beat noise dominate over other noises such as thermal receiver noise and other receiver noises [3]. However, the transmission length increases with the increase in the bit rate and the parameters have the capability of absenting in the network [4]. In Dense Wavelength Division Multiplexing (DWDM), the wavelengths are spaced more closely than that in WDM, which makes it capable of accessing a huge bandwidth. The earlier DWDM systems operated with 4 to 16 wavelengths, while todays DWDM systems support 160 wavelengths transmitting at a speed of 10 Gb/s [5]. A DWDM system has two important features, first the ability to amplify all wavelengths without converting them to electrical system. Second it can carry different type of signals with different speeds simultaneously. The first means that DWDM combines multiple optical signals to amplify them as a group. The second is mainly about the fact that it can carry signals of different types and speeds [6].

Optical amplifier plays an important role by communicating with the other optical amplifiers towards the destination. An optical amplifier regenerate, amplify and control the flow of optical energy from source to destination by reducing the amount of noise. Additionally, in the 1550nm range, it offers a relatively lower insertion loss. Electronic feedback arrangements are also used to control the output power from the amplifier [7]. The most attractive feature of a DWDM system is that the gain region of Erbium Doped Fiber Amplifiers (EDFA) has a gain region located in C band. So the losses due to long span and also the high passive noise are overcome [8].

EDFA is superior in the amplification of the optical signal without any crosstalk penalty even while operating in deep in gain compression. EDFA finds its use in the applications where high output power and high data rate has the major concern. It can reduce a huge amount of data loss and can simultaneously amplify the signal having multi wavelengths. So this type of optical amplifier is used frequently in DWDM systems [9] [10]. In order to achieve a faithful and efficient reception, a handsome amount of optical power should be available at the receiving end. A successful transmission ends with the proper separation of the 0's and 1's from the raw input optical signal [11] [12]. The transmitted signal should have a minimum amount of power that can be sensed by the receiver which is called the sensitivity of the receiver. The receiver sensitivity or the target Bit Error Rate (BER) should be stated otherwise BER is taken as 10^{-12}. The transmitted power should be large enough so that it can maintain a minimum signal power equal to the receiver sensitivity despite the attenuation along the optical fiber. Yet it is not guaranteed that a higher level of transmitted power is surely to maintain the minimum signal power over a long distance at the receiving end. The reason behind this is an increased amount of input signal power gives rise of channel impairment and nonlinearities [13] [14]. The received signal power should lie between the dynamic ranges of the receiver. Otherwise the receiver will be permanently damaged or it will lose the capability to distinguish between 0's and 1's.

In this paper a system model has been proposed where the performance has been analyzed with respect to different parameters and the result has been discussed for better system performance. The paper has been organized as following, section I describes the introduction, section II describes the proposed model, mathematical model is discussed in section III, section IV discusses the result and in section V the conclusion has been drawn.

II. SYSTEM MODEL

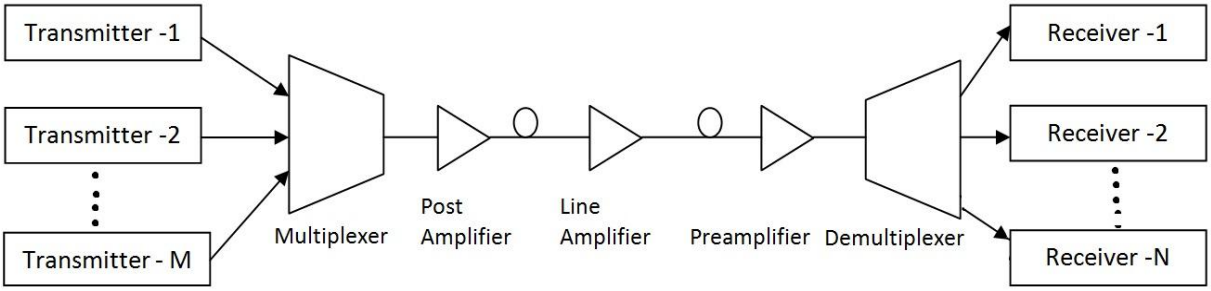

Fig. 1: DWDM system with optical amplifier in cascaded

The proposed model in Fig. 1 shows a simple block diagram of a unidirectional Wavelength Division Multiplexing link having M number of transmitter and N number of receivers. A transmitter consists of laser source, coupling optics and electrons convert electrical signal to optical signal. The multiplexer multiplex the optical signal from different WDM channels. The resultant signal is then sent to optical fiber link. After a certain distance a number of optical amplifiers are used to compensate the loss in fiber. The distance between two successive optical amplifiers is called span length. The typical span length is 60-120 km. There are three different types of optical amplifiers, optical preamplifier, optical power amplifier and linear amplifier. They have different use in different place of the optical link. An optical preamplifier is used in front of a receiver to provide high sensitivity and high gain. After the transmitter the power of the transmitted signal is increased by a power amplifier. An essential feature of a WDM system is add-drop multiplexer (WADM). A WADM separates only one or two channels from a large number of channels while a full demultiplexer separates all the optical channels in a fiber.

III. MATHEMATICAL MODEL

Amplified spontaneous emission is the dominant noise in an optical amplifier. The spontaneous recombination of electrons and holes in the amplifier medium is mainly responsible for this noise. This recombination generates a broad spectral background of photons that gets amplified along with the optical signal. The Power Spectral Density (PSD) of the ASE noise is- [16]

$$N_{sp}(f) = n_{sp}(G-1)hf = Khf \quad (1)$$

Where,

n_{sp} =Spontaneous emission factor, G=Amplifier gain, h=Plank's constant, f=Frequency of radiation

But despite the ASE noise the optical amplifiers are used in order to compensate the fiber losses. The gain of optical amplifier should be such that it can eliminate the loss along the optical fibers. The total number of optical amplifier will be used solely depends on the span length and the ASE noise. A large span length is preferable to reduce the number of optical amplifier but a large span length reduces the signal strength sufficiently. Receiving a weak signal and amplifying it requires the sensitivity of the optical receiver to be high. So a tradeoff should be made between these limitations.

Let,

P_i= Power output from the Transmitter=Power input to the fiber,

If the amplifier gain is adjusted to compensate for the total losses, then

$$G\ (dB) = P_L\ (dB) = (\alpha fc + \alpha j)\ L\ (dB) \quad (2)$$

Where,

α_{fc}=Fiber cable loss(dB/km), α_j=Joint loss(dB/km),

L=Length of each hop (Distance between two line amplifier in km)

$$G = 10^{-[(\alpha fc + \alpha j)L]/10,} \quad (3)$$

The total number of amplifiers= N = L_t/L, [L_t=Total transmission distance in km]

Then total spontaneous emission noise at the input of the receiver is,

$P_{ase} = NKhfB$,

Where, B =Bandwidth of the receiver,

The optical power received by the receiver, $P_r = P_i G$,

Therefore, the signal to noise ratio at the receiver input

$$\frac{S}{N} = \frac{P_i G}{P_{ase}} = \frac{P_i^{10-(\alpha_{fc}+\alpha_f)L/10}}{NKhf} \quad (4)$$

Another important fact should be considered while using optical amplifier is Path Penalty Factor (F_{path}). It is the factor by which path average signal energy must be increased (as G increases) in a chain of N cascaded optical amplifiers to maintain a fixed SNR.[15]

Path penalty factor F_{path} (G) = $\frac{1}{G}\left(\frac{G-1}{\ln G}\right)^2$ (5)

The signal to noise ratio is defined as the ratio of signal power to the noise power. For a P-i-N photodiode in an optical fiber communication is given by the following equation-

$$\text{SNR} = \frac{I_p^2}{I_n^2} \quad (6)$$

Where I_p is the photocurrent and I_n is the total noise current. The total noise current is defined as-

$$I_n = \sqrt{i_s^2 + i_t^2}$$

Where i_s is the shot noise current and i_t is thermal noise current. The thermal noise contribution may be reduced by increasing the value of R_L (Load resistance), although this reduction may be limited by bandwidth considerations

$$i_s = \sqrt{2e(Ip)B}\ , \quad i_t = \sqrt{4kTB\ /\ R_L}$$

Another negligible amount of noise, dark current noise associated with the receiver, $i_d = \sqrt{2e(I_D)B}$

k is the Boltzmann constant ($1.38*10^{-23}$ J/K), B is the photodiode bandwidth, and T(K) is the absolute temperature.

So the overall signal to noise ratio is -

$$\frac{S}{N} = \frac{I_P{}^2}{2eB\,(I_P + I_D) + \frac{4kTBF_n}{R_L}} \tag{7}$$

Where F_n represents the noise figure, defined by- [15]

$$F_n = \frac{(S/N)_{in}}{(S/N)_{out}}$$

In the Avalanche Photodiode the signal current in the amplifier is increased and the overall SNR is increased as thermal noise remains the same. But the multiplication factor (M) increases the dark current noise and quantum noise which may be a limiting factor. The signal-to-noise ratio for APD receiver can be expressed as- [11]

$$\frac{S}{N} = \frac{I_P{}^2 M^2}{2eB\,(I_P + I_D) M^{2+x} + \frac{4kTBF_n}{R_L}} \tag{8}$$

Where the factor *x* ranges between 0 and 1.0 and depending on photodiode material.

It is apparent from Eq. (8) that the first term in the denominator increases with increasing *M* whereas the second term decreases. For low *M* the combined thermal and amplifier noise term dominates and the total noise power is virtually unaffected when the signal level is increased, giving an improved SNR. However, when *M* is large, the thermal and amplifier noise term becomes insignificant and the SNR decreases with increasing *M* at the rate of M^x. Therefore, an optimum value of the multiplication factor *M* should be used. [11]

IV. RESULT AND DISCUSSION

From the mathematical model described above the system performance has been analyzed with various parameters. The SNR is determined for different input power, bandwidth, amplifier gain and hop length. Also the system performance has been demonstrated for different types of receivers and their gains. And finally the system performance has been plotted for different receiver gain and bandwidth for the selection of these parameters.

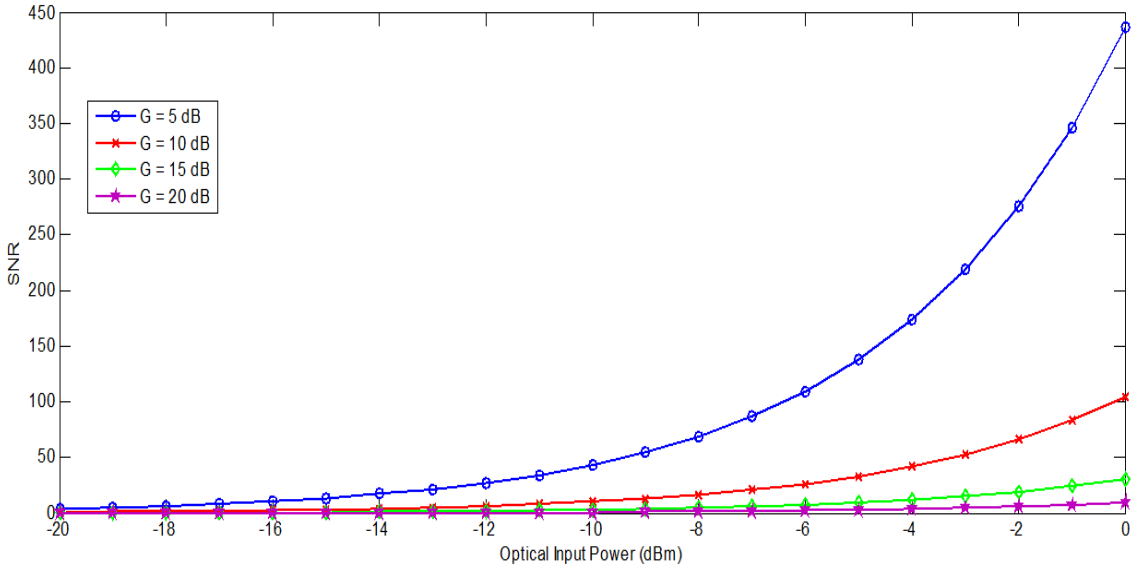

Fig. 2 Amplifier SNR vs input Power for Hop length L=100km, N=10 varying Gain (G=5dB, 10dB, 15dB, 20 dB)

Fig. 2 demonstrate the variation of SNR with the input power to the optical amplifier with a hop length of 100km, no of amplifier 10 and various amplifier gain of 5dB, 10dB, 15 dB and 20 dB. The SNR increases with the increase of optical input power. The SNR is highest for the amplifier gain of 5dB. So the SNR increases with the decrease of amplifier gain.

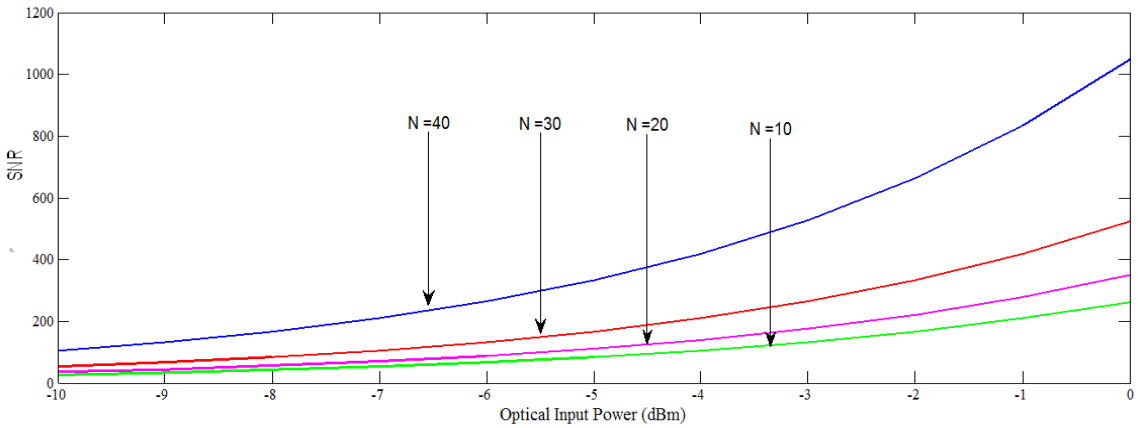

Fig. 3 SNR vs input Power for Hop length L=100km G=10dB varying N=10, 20, 30, 40

In Fig. 3, the SNR has been demonstrated for different amplifier numbers. The SNR has been plotted for the number of amplifiers 10, 20, 30, 40. The output is maximum when the number of amplifiers 40. So it can be concluded that the SNR increases with the increase of number of amplifier.

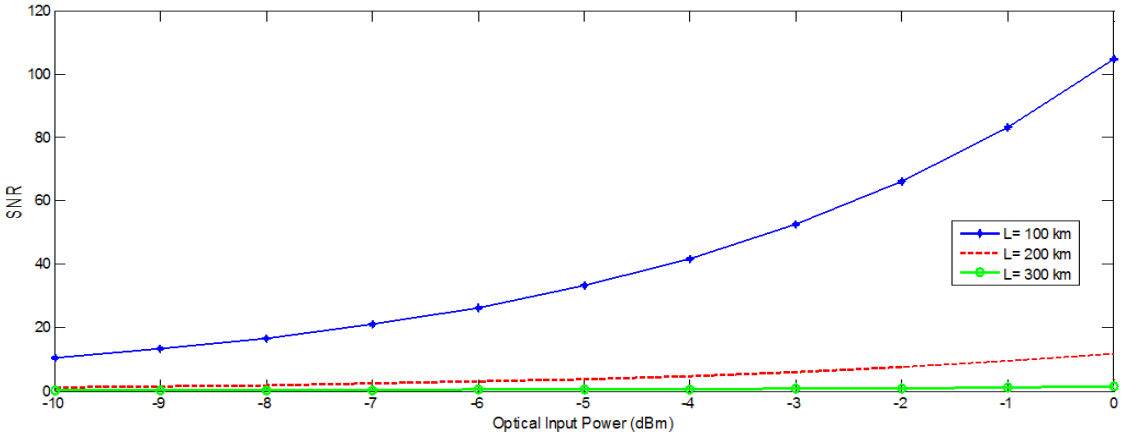

Fig. 4 Amplifier SNR vs Optical Input Power Varying Hop Length L

In Fig. 4, the SNR has been plotted against optical input power with a hop length of 100 km, 200km and 300 km. The SNR is highest for the hop length of 100km. So the SNR increases with the decrease of hop length.

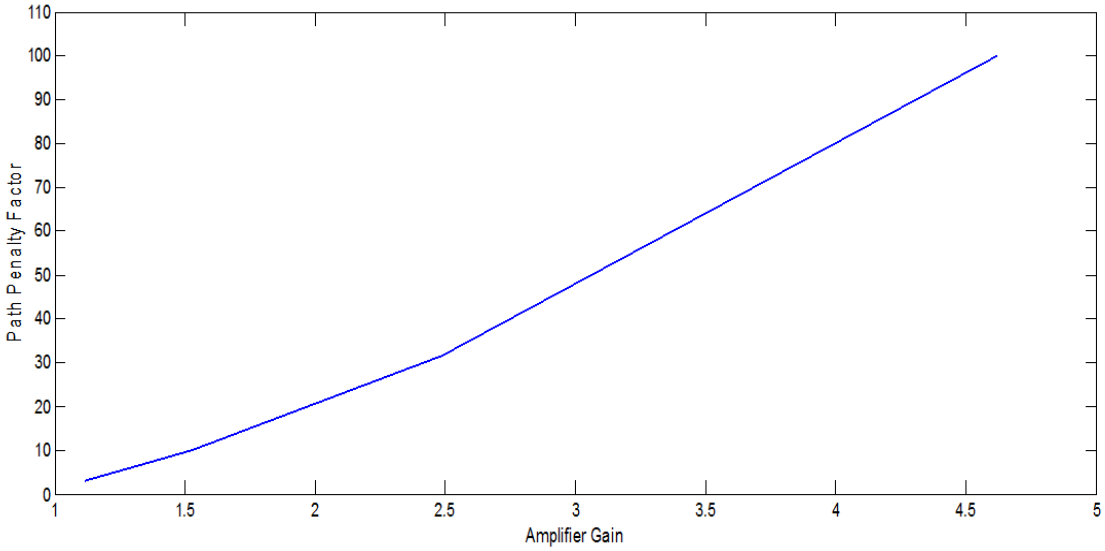

Fig. 5 Path Penalty Factor (F_{path}) vs amplifier gain

Fig. 5 shows the path penalty factor for different amplifier gain. For a higher amplifier gain the path penalty factor increases.

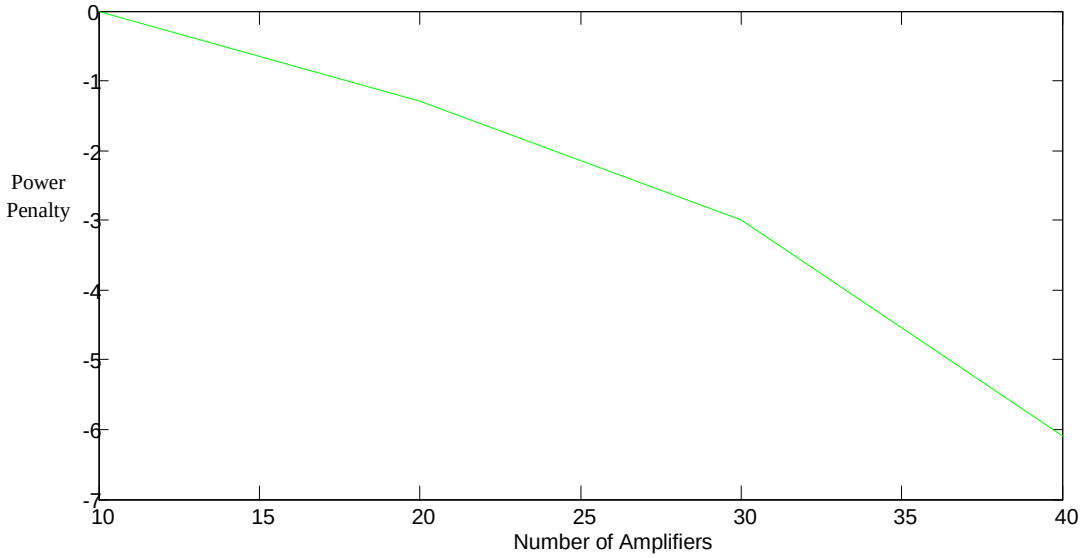

Fig. 6 Power Penalty vs No. of Amplifiers for a fixed SNR=200

In Fig. 6, the power penalty vs no of amplifiers have been demonstrated with a fixed SNR. The power penalty decreases with the increase of number of amplifier.

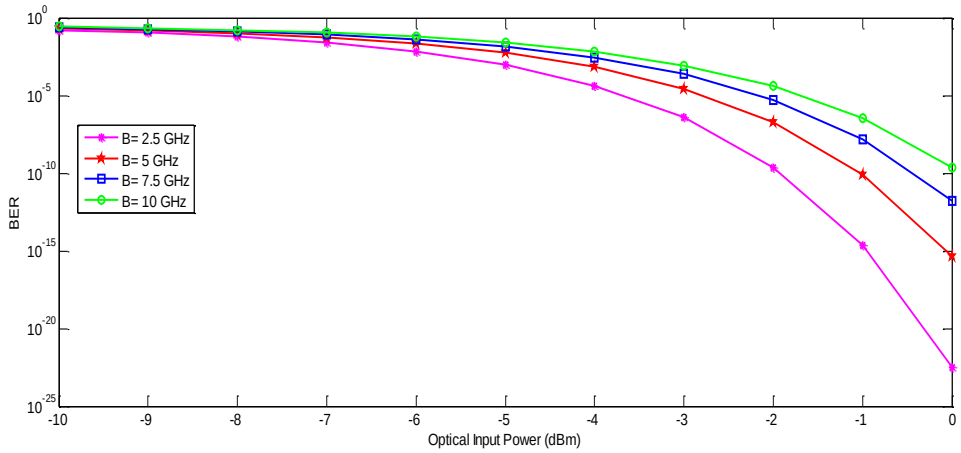

Fig. 7 BER vs Optical Input Power Varying Bandwidth for P-i-N Receiver

In Fig. 7, Bit Error Rate (BER) vs Optical input power has been plotted for different bandwidth. From Eq. (7) and (8) it can be seen that both in a p-i-n photodiode and APD receiver, the noises increase with the increase of bandwidth. Hence the SNR decreases with the increase of bandwidth. When SNR decreases, BER increases. In Fig. 7, the BER is highest when the bandwidth is 10GHz.

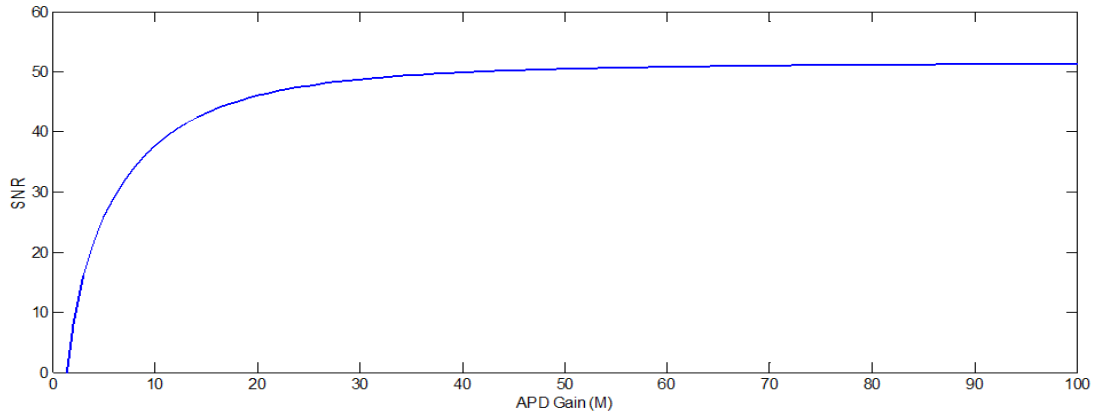

Fig.8 SNR vs APD Gain

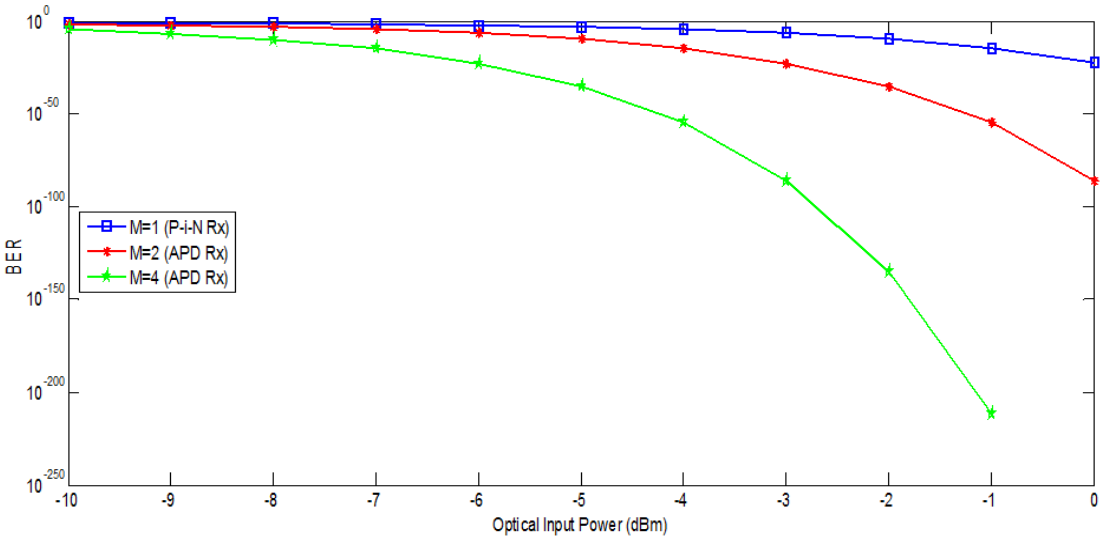

Fig. 9 BER vs Input Power varying APD Gain for a fixed Bandwidth B=5GHz

In Fig 8, the SNR has been plotted against APD gain (M). From M=0 to M=30, the SNR increases rapidly, but after M=30, the increase of the SNR is not significant. In Fig. 9, the BER is plotted vs optical input power for different APD gain. From equation (7) & (8), when the value of M=1, the SNR expression is similar to P-i-N receiver. From Fig. 9, it can be concluded that the BER decreases when the value of M increases. So APD receiver is shows better performance in respect of SNR.

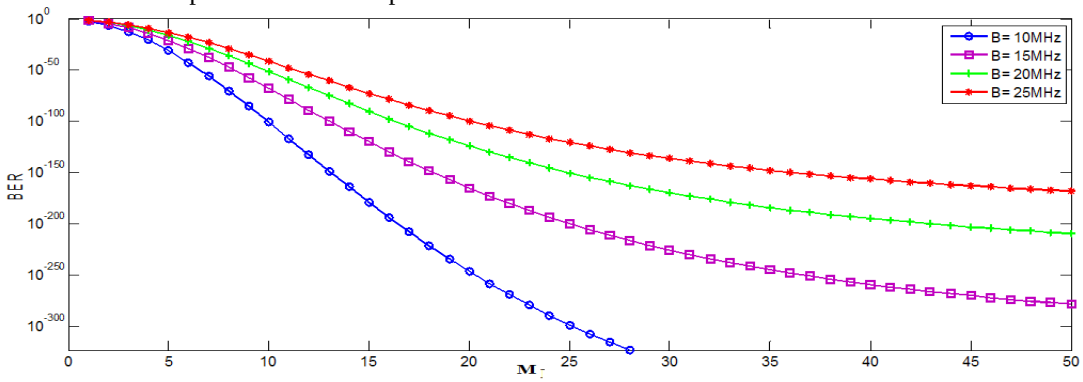

Fig. 10 BER versus APD gain (M) varying bandwidth

In Fig. 10, BER has been plotted against APD gain varying bandwidth. The BER increases when the bandwidth is increased. So combining Fig. 8 and Fig. 10, it can be concluded that for better performance only the value of M should not be limited but also the bandwidth should be limited. Again a small bandwidth corresponds to a smaller receiver size thus minimizes the cost.

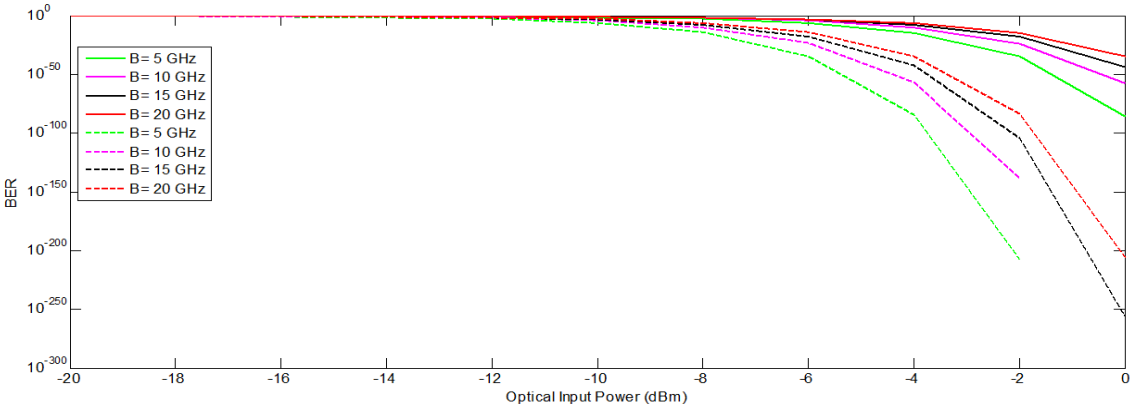

Fig. 11 BER vs Input Power varying Bandwidth for APD Receiver with APD gain M=2 (solid line) and M=5 (dotted line)

In Fig. 11, BER vs input power has been plotted with varying bandwidth and APD gain. The solid line shows the result for M=2 and the dotted line is for M=5. The Figure combines the overall result of analysis of the system. It shows the value of BER is higher for M=2 lower for M=5. Again relatively smaller bandwidth has a lower BER than that of a larger bandwidth.

V. CONCLUSION

A very basic approach to analyze the performance of DWDM systems considering the effect of cascaded optical amplifiers and receiver type has been described. The SNR of optical amplifiers and BER performance has been investigated by varying different parameters. We have also quantified BER performance of DWDM link in terms of receiver bandwidth. It is found that the system has been suffered by power penalty and path penalty and the system performance has also degraded due to higher receiver bandwidth. Both the penalty factor is higher for higher amplifier gain and longer hop length. Therefore, it has been concluded that the system performance can be substantially improved by using marginal amplifier gain and optimum number of amplifiers.

REFERENCES

[1] Gyselings T., Morthier G., and Baets R., "Crosstalk analysis of multiwavelength optical cross connects," *J. Lightwave Technol.*, vol. 17, pp. 1273–1283, Aug. 1999.

[2] Bracket, C., "Dense wavelength division multiplexing networks: principles and applications", *IEEE Journal Select. Areas Commun.*, August 1990, Vol. 8, No. 6, pp. 948-964.

[3] Dods S. D., Anderson T. B., "Calculation of bit-error rates and power penalties due to incoherent crosstalk in optical networks using Taylor series expansions," *J. Lightwave Technol.*, vol. 23, pp. 1828– 1837, April 2005.

[4] Kelvin B. A., Afa J. T., "Bit Error Rate Performance of Cascaded Optical Amplifiers Using Matlab Computation Software," *European Scientific Journal*, vol. 9, No. 3, January 2013.

[5] Bracket, C., "Dense wavelength division multiplexing networks: principles and applications", *IEEE Journal Select. Areas Commun.*, August 1990, Vol. 8, No. 6, pp. 948-964.

[6] Tian, C. and Kinoshita, S., "Analysis and control of transient dynamics of EDFA pumped by 1480- and 980-nm lasers", *IEEE/OSA Journal of Lightwave Technology*, August 2003, vol. 21, No. 8, pp. 1728- 1734.

[7] Reza S. E., Ahsan N., Ferdous S., Dhar R. K., Rahimi M. J., " Analyses on the Effects of Crosstalk in a Dense Wavelength Division Multiplexing (DWDM) System Considering a WDM Based Optical Cross Connect (OXC)" *International Journal of Scientific & Engineering Research*, vol. 4, issue 1, January 2013.

[8] Elrefaie, A., Goldstein, E., Zaidi, S. and Jackman, N., "Fiber-amplifier cascades with gain equalization in multiwavelength unidirectional inter-office ring network," *IEEE Photon. Technol. Lett.*, vol. 5, pp. 1026- 1031, Sept. 1993.

[9] Feuer, M., Kilper, D. and Woodward, S., "ROADMs and their system applications" in "Optical fiber telecommunications V, B: Systems and Networks", ed. Kaminow, I., T. and Willner, A., Academic press editors, EUA, 2008, ch.8.

[10] Senior, J.M. ''*Optical fibre communication principles and practice*'' 3rd edition Prentice Hall 2009.

[11] Connely, M. J., "*Semiconductor optical amplifiers*", Kluwer Academic, 2002.

[12] Ramamurthiu, B., "*Design of Optical WDM Networks*, LAN, MAN, and WAN Architectures:, Kluvier, 2001.

[13] Ramaswami, R. and K. Sivarajan, "*Optical Network: A Practical Perspective"*, 3rd edition, Morgan Kaufmann, 2002.

[14] Keiser, G., "Optical Fiber Comunications", 3rd edition,McGraw-Hill, 2000.

[15] Iqbal, A., Elahee, M., Jahid, A. and Majumder, S.P., "*Performance analysis of WDM system with optical amplifiers in cascade in presence of crosstalk*", Military Institute of Science and Technology (MIST), Dhaka, Bangladesh, 2009,

American Journal of Engineering Research (AJER)
e-ISSN: 2320-0847 p-ISSN : 2320-0936
Volume-4, Issue-8, pp-09-13
www.ajer.org
Research Paper Open Access

Modeling Slope-Descending Sight Distance for Overtaking Maneuvre in Double Lane Highway

Onuamah Patrick
Civil Engineering Department, Enugu State University of Science and Technology, Enugu, Nigeria.

Abstract: *Many vehicles on the highway move at speeds below the design speed obviating overtaking maneuvers by vehicles that move at the design speeds. The paper is an attempt to formulate a model to determine the minimum overtaking sight distance to be maintained by a descending overtaking vehicle driver on an inclined double lane divided highway. The vehicle and road user characteristics as well as the vertical road geometry are combined to assess the overtaking distance by formulating a mathematical model that satisfies the laws of the mechanics of motion.*
Keywords*: Overtaking maneuver, graphic model, one-way traffic, perception-reaction time, visibility.*

I. Introduction

For proper movement of vehicles, roads must be visible to the driver for quite some long distance, to enable the moving vehicle slow down as may be required before any obstructions for safe motion. Visibility therefore, is a vital factor for vehicle operation and for acquiring high speeds on the highway.

II. Sight Distance

Sight distance is the actual distance per length of road over which a driver sitting at a specific height in a vehicle can see objects either moving or stationary, on the road surface. Sight distance is affected by myriads of factors including the sharpness of curves (horizontal and vertical), objects obstructing visibility, buildings or corners at road intersections, etc.

2.1 Stopping Sight Distance

Also the stopping sight distance for a vehicle in motion is the required distance for which the vehicle moving at a design speed can be stopped without colliding with a stationary object on the road. The stopping site distance depends on the features of the road ahead, height of the driver's eye above the road surface, height of the object above the road surface, the road horizontal and vertical curves, traffic conditions, positions of obstructions, etc. At the summit of curves, the stopping sight distance is that distance measured along the road surface which a vehicle driver whose eye is 1.22 m above the road surface can see an object of 10 cm height also situated on the road surface [1], [7].

The distinction between stopping sight distance and decision sight distance must be understood. Stopping sight distance is used when the vehicle is traveling at design speed on a poor wet pavement when one clearly discernable object or obstacle is present in the roadway. Decision sight distance applies when conditions are complex, driver expectancies are different from the situation, or visibility to traffic control or design features is impaired [2]. Most situations presented on arterials for access management require stopping sight distance at a minimum; however, decision sight distance should be provided for safety and smoother operations. More factors affecting sight distance include speed of vehicle, efficiency of brakes, total reaction time, longitudinal slope of the road, frictional resistance between the road surface and the vehicle tyres, etc.

2.2 Perception-Reaction Time

The reaction time is the time it takes the driver to apply the brakes effectively from the time the object is seen and the perception time is the time the average driver realizes a danger ahead for which the brake should be applied. Recent studies have checked the validity of 2.5 seconds as the design perception-reaction time. Four recent studies [3], [4], [5], [6] (Table 1) have shown a maximum of 1.9 seconds as the perception-reaction time for an 85th percentile time and about 2.5 seconds as the 95th percentile time.

TABLE 1: Brake Reaction Times Studies

Researcher	85th Percentile Time (Seconds)	95th Percentile Time (Seconds)
Gazis et al	1.48	1.75
Wortman et al	1.80	2.35
M.S. Chang	1.90	2.50
M. Sivak	1.78	2.40

By road type, some researchers [6] have suggested that the perception-reaction \should reflect the complexity of traffic conditions, expectancy of drivers and the driver's state. They suggest that the perception-reaction times may be altered accordingly (Table 2).

TABLE 2: Perception-Reaction Times Considering Complexity and Driver's State

Road Type	Driver's State	Complexity	Perception-Reaction time
Low Volume Road	Alert	Low	1.5 s
Two-Lane	Fatigued	Moderate	3.0 s
Primary Rural Road Urban Arterial	Alert	High	2.5 s
Rural Freeway	Fatigued	Low	2.5 s
Urban Freeway	Fatigued	High	3.0 s

2.3 Overtaking Graphic Cum Mathematical Model

For overtaking manoeuvre in the one-way traffic, the overtaking vehicle traveling at the design speed, V_d, has to leave its own track, overtake and return to the track, without expecting any traffic from the opposite direction. The distance visible to the driver of the vehicle intending to overtake another slow moving vehicle without causing any inconvenience or possible accident is called the overtaking site distance. This can be depicted graphically as in (Fig. 1). The model goes to show vehicle A initially at position A_1 and travelling at the design speed of V_d which takes a reaction time of t_r through the distance d_1 to start overtaking vehicle B which is moving at a slower speed and at position B_1 at that instant**.**

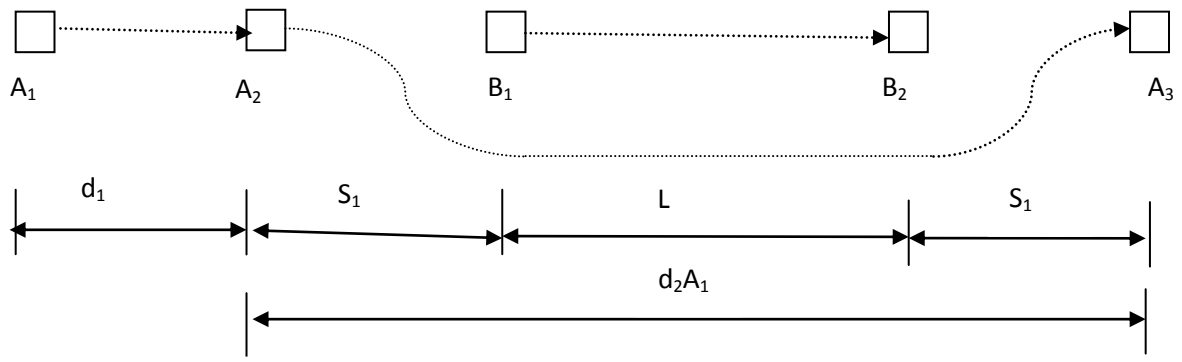

Fig1: Overtaking Manoeuvre Graphic Model

Now, vehicle A overtakes vehicle B through the distance d_2 in time t_2. This distance must not be less than the sum of the stopping site distances, S_1, between vehicles A and B before and after the overtaking movement of vehicle A moving from position A_2 to position A_3 plus the distance, L, covered by vehicle B moving from position B_1 to position B_2 within the same time of t_2 by which Vehicle A moved from position A_2 to A_3. For a one-way traffic in a double lane divided carriageway, no vehicle is expected from the opposite direction. That is,

$$d_1 = V_B t_r \qquad (1)$$

where d_1= reaction distance
V_B = velocity of vehicle B,
and t_r = reaction time of vehicle A driver.

From laws and mechanics of motion,

$$d_2 = V_B t_2 + \frac{1}{2} a_A t^2 \qquad (2)$$

Also, from fig.1,

$$d_2 = 2S_1 + L \qquad (3)$$

where d_2= overtaking distance,
t_2 = overtaking time,
a_A = acceleration of vehicle
S_1 = stopping site distance
and L = distance moved by vehicle B from position B_1 to position B_2.

But

$$L = V_B t_2 \qquad (4)$$

Combining Eqns (2), (3) and (4),

$$\frac{1}{2} a_A {t_2}^2 = 2S_1 \qquad (5)$$

$$\Rightarrow$$

$$t_2 = \pm \sqrt{\frac{4S_1}{a_A}} \qquad (6)$$

The work done against friction, W_f, in stopping a moving vehicle equals the kinetic energy, E_k, of the moving vehicle.

That is,

$$W_f = \mu F S_1 \qquad (7)$$

where F= braking force
S_1 = braking/stopping sight distance of moving vehicle in the single lane two-way traffic, and μ= coefficient of friction between tyre and the brake pad.

Also

$$E_k = \frac{1}{2} m {V_d}^2 \qquad (8)$$

where m = mass of vehicle and V_d = design speed of vehicle.

That is $E_k = \frac{1}{2}\frac{W}{g}{V_d}^2$ (9)

where W= weight of vehicle and S = stopping distance of vehicle.

When the vehicles is descending on a slope of α°, the total work done to overcome friction is

$$W_f = (\mu W + W\, Sin\, \alpha) S_1 \qquad 10)$$

For small angle of slope,

$$Sin\, \alpha \approx \tan \alpha \approx \frac{h}{100} \qquad (11)$$

where h=elevation.

Using Eqn (11) in Eqn (10),

$$W_f = \left(\mu W + \frac{Wh}{100}\right) S_1 \qquad (12)$$

Since $W_f = E_k$, Eqns (9) and (12) combine to give that

$$S_1 = \frac{{V_d}^2}{2g\left(\mu + \frac{h}{100}\right)} \qquad (13)$$

Using Eqn (13) in Eqn (6),

$$t_2 = \pm \sqrt{\frac{{V_d}^2}{g\left(\mu + \frac{h}{100}\right) a_A}} \qquad (14)$$

and hence, using Eqn (14) in Eqn (2),

$$d_2 = V_B t_2 + \frac{{V_d}^2}{2g\left(\mu + \frac{h}{100}\right)} \qquad (15)$$

where V_d = design velocity

Hence, minimum overtaking distance, OSD_m, is

$$OSD_m = d_1 + d_2 \qquad (16)$$

and the safe overtaking zone OSD_z [1], [7] is given by

$$OSD_z = 3(d_1 + d_2) \qquad (17)$$

III. Conclusion

A comprehensive understanding of stopping distance and overtaking manoeuvring distance are essential requirements in planning, design and operation of transportation systems. Many researchers [2], [3] have investigated the stopping site distance and overtaking site distance (OSD) under homogeneous traffic conditions. The OSD is theoretically derived and the results indicate that the proposed model is able to represent the OSD of the heterogeneous and less lane-disciplined traffic stream under study with reasonable accuracy.

References

[1] G. Singh, J. Singh, *Highway Engineering*, 5th Edition, reprint, India, 2013, ch. 6, pp. 138-152.

[2] R. Layton, "Stopping Sight Distance and Decision Sight Distance", *Transport Research Institute,, Oregon State University, 1997, Discussion Paper 8A, pp. 1-25.*

[3] D.C. Gazis, D. C. Azis, F.S Hiller, "The Problem of the Amber Signal in Traffic Flow," *Operations Research 8, March-April 1960.*

[4] R.H.Wortman, J.S. Matthaas, "Evaluation of Driver Behavior at Signalized Intersections," *Transportation Research Record 904, T.R.B, Washington, D.C., 1983.*

[5] M.S. Chang, "Timing Traffic Signal Change Intervals Based on Driver Behavior," *T.R. Record 1027, T.R.B, Washington, D.C., 1985.*

[6] Sivak, M., "Radar Measured Reaction Times of Unalerted Drivers to Brake Signals," *Perceptual Motor Skills 55, 1982*

[7] S. K. Khanna, C.E.J. Justo, *Highweay Engineering*, 8th Edition, reprint, India, 2001, ch. 4, pp. 86-114.

American Journal of Engineering Research (AJER)
e-ISSN: 2320-0847 p-ISSN : 2320-0936
Volume-4, Issue-8, pp-14-18
www.ajer.org
Research Paper Open Access

Stable, bounded and periodic solutions in a non-linear second order ordinary differential equation.

Eze, Everestus Obinwanne, Ukeje, Emelike and Hilary Mbadiwe Ogbu
Department of Mathematics, Michael Okpara University of Agriculture Umudike, Umuahia, Abia State.

ABSTRACT: *Results are available for boundedness and periodicity of solution for a second order non-linear ordinary differential equation. However the issue of stability of solutions in combination with boundedness and periodicity is rare in literature. In this paper, stability boundedness and periodicity of solutions have been shown to exist in a non-linear second order ordinary differential equation. This task has been achieved through the following:*

a. *The use of Lyapunov functions $v:\mathbb{R}^2 \to \mathbb{R}$ with some peculiar properties to achieve stability and boundedness in the non-linear second order ordinary differential equation.*
b. *The use of Leray-Shauder fixed point technique and an integrated equation as the mode for estimating the apriori bounds in achieving stability and boundedness of solutions.*

KEYWORDS: *Lyapunov functions, integrated equations, apriori bounds, fixed point technique, completely continous.*

I. INTRODUCTION

Consider the non-linear second order ordinary differential equation

$$\ddot{x} + a\dot{x} + h(x) = p(x) \qquad (1.1)$$

Subject to the boundary conditions

$$D^{(r)}x(0) = D^{(r)}x(2\pi), r = 0,1 \qquad (1.2)$$

where $a > 0$ *and* $h(x), p(x)$ are continous functions depending on their argument. For the constant coefficient equation.

$$\ddot{x} + a\dot{x} + bx = p(x) \qquad (1.3$$

Ezeilo (1986)has shown that if the Ruth-Hurwitz's conditions

$$a > 0, b > 0 \qquad (1.4)$$

hold, the roots of the ordinary equation

$$\lambda^2 + a\lambda + b = 0 \qquad (1.5)$$

Have negative real parts, then asymptotic stability and ultimate boundedness of solutions can be verified for (11.3) when $p(t) = 0$. The existence of periodic solutions can be verified (1.3) when (1,4) holds: Ezeilo (1960), Tejumola (2006), Coddington and Levinson (1965), Ogbu (2006) , Ezeilo and Ogbu (2009).
A close look at equations (1.1) and (1.3) give some clue to the theorem stated below.
Theorem 1.1
Suppose there exists $a > 0, b > o$ *and* $\beta > o$ *such that*

I. $h(x) < b, \beta^2 = b,\ 1 = \frac{d}{dt}$.
II. $|h(x) - x| > 0$ for all x
III. $|h(x)| \to \infty\ \ |x| \to \infty$
IV. $x^2 + y^2 \to \infty$ as $|x| \to \infty, |y| \to \infty$

Then equations (1.1)- (1.2) has stable, bounded and periodic solutions when $p(t) = 0$.

Theorem 1.2
Suppose further in theorem 1.1, the condition (i) is replaced by

(i') $h'^{(x)} < b, \beta^2 \neq b,\ |a\dot{x} - p(t)| > 0$.

Then equation (1.1)- (1.2) has stable, bounded and periodic solutions when $p(t) \neq 0$.

II. PRELIMINARIES

Consider the scalar equation

$$\dot{x} = f(x), x\epsilon\mathbb{R}^n, f(0) = 0 \qquad (2.1)$$

Where f is sufficiently smooth.

Theorem 2.1

Assume that

i. $f\epsilon c'$

ii. There exists a c' function $v: \mathbb{R}^n \to \mathbb{R}$ such that $v(x) > 0\ \forall x$ and $v(x) = 0\ if\ x = 0$

iii. Along the solution paths of equation (2.1) $\dot{v} \leq 0$

Then the solution $x = 0$ of equation (2.1) is stable in the sense of Lyapunov.

Theorem 2.2

Assume that

i. $f\epsilon c'$

ii. There exists a c' function $v: \mathbb{R}^n \to \mathbb{R}$ such that $v(x) > 0\ \forall x$ and $v(x) = 0\ if\ x = 0$

iii. Along the solution paths of equation (2.1) $\dot{V} < 0,\ x \neq 0$ and $\dot{V} = 0,\ x = 0,\ i.e\ \dot{V}$ is negative definite.

Then the solution $x = 0$ of equation (2.1) is asymptotically stable in the sense of Lyapunov.

Theorem 2.3 (Yoshizawa)

Consider the system

$$\dot{x} = f(t, x, y), \dot{y} = g(t, x, y) \qquad (2.2)$$

Where f and g satisfy conditions for existence of solutions for any given initial values. Suppose there exists a function $v: \mathbb{R}^n \to \mathbb{R}$ with the first partial derivatives in its argument such that

$$v(x, y) \to \infty\ as\ x^2 + y^2 \to \infty \qquad (2.3)$$

and such that for any solution $(x(t), y(t))$ of equation (2.2)

$$\dot{V} = \frac{d}{dt}V\big(x(t), y(t)\big) \leq -\delta < 0\ if\ x^2(t) + y^2(t) \geq R > 0 \qquad (2.4)$$

Where δ and R are finite constants. Then every solution $\big(x(t), y(t)\big)$ of equation (2.2) is (uniformly) ultimately bounded with bounding constants depending on R and how $v \to +\infty\ as\ x^2 + y^2 \to \infty$. The conclusion here is that there exists a a constant $D, 0 < D < \infty$ such that

$$|x(t)| \leq D, |y(t)| \leq D \qquad (2.5)$$

The proof of theorem (1) entails establishing stability, boundedness and periodicity for equation (1.1)-(1.2) when $p(t) = 0$. That is

$$\ddot{x} + a\dot{x} + h(x) = 0 \qquad (2.6)$$

Or the equivalent system

$$\dot{x} = y$$
$$\dot{y} = -ay - h(x) \qquad (2.7)$$

Consider the function $v: \mathbb{R}^2 \to \mathbb{R}$ defined by

$$v = \frac{1}{2}y^2 + H(x) \qquad (2.8)$$

Where $H(x) = \int_0^x h(s)ds$

Clearly the V defined above is positive semi definite. The time derivative $\dot{v}$ along the solution path of (2.7) is

$$\begin{aligned}\dot{v} &= y\dot{y} + h(x)\dot{x}\\ &= y\big(-ay - h(x)\big) + h(x)y\\ &= -ay^2 - h(x)y\\ &= -ay^2\end{aligned}$$

Which is negative definite. Therefore by Lyapunov theorem the system (2.6)-(2.7) is asymptotically stable. Hence it is stable. Therefore the system (2.6)-(2.7) is stable in the sense of Lyapunov when $p(t) = 0$

Now for the proof of boundedness in equation (2.6)-(2.7), consider the c' function $v: \mathbb{R}^2 \to \mathbb{R}$ defined by

$$V = \tfrac{1}{2}x^2 + \tfrac{1}{2}y^2 \qquad (2.9)$$

The V is defined in equation (3.4) is positive semi definite. The time derivative V along the solution path of (3.2) is

$$\begin{aligned}\dot{v} &= x\dot{x} + y\dot{y}\\ &= xy - ay^2 - yh(x)\\ &= -ay^2 - y(h(x) - x)\end{aligned}$$

Since $|h(x) - x| > 0$ for all x (condition (ii) in theorem1) then

$$\dot{v}=-ay^2 - y|h(x) - x| < 0 \qquad (2.10)$$

Without loss of generality, v is such that $\dot{v} \leq -1$ since $x^2 + y^2 \to \infty$ as $|x| \to \infty$ as $|y| \to \infty$
By Yoshizawa's theorem, equation (3.1) has a bounded solution. Therefore equation (1.1) has bounded solution when $p(t) = 0$
Now the condition (i) in theorem (1) which is $\beta^2 = b$ implies that $i\beta$ is a root of the auxiliary equation. Therefore the solution to (2.6) is the form $A\cos\beta(t) + B\sin\beta(t)$. this clearly shows that the solution is periodic. Therefore equation (2.6) is stable, bounded and periodic. Hence, the proof of theorem 1.
The proof of theorem 2 is as follows
Consider equation (1.1) or its equivalent system,

$$\left.\begin{aligned} \dot{x} &= y \\ \dot{y} &= -ay^2 - h(x) + p(t) \end{aligned}\right\} \qquad (2.11)$$

And the function $v: \mathbb{R}^2 \to \mathbb{R}$ defined by

$$v = \tfrac{1}{2}y^2 + h(x) \qquad (2.12)$$

Where $H(x) = \int_0^x h(s)ds$
clearly the V defined above in equation (2.12) is positive semi-definite. The time derivative $\dot{v}$ along the solution paths of (2.11) is

$$\begin{aligned} \dot{v} &= y\dot{y} + h(x)y \\ &= y\big(-ay - h(x) + p(t)\big) + h(x)y \\ &= -ay^2 - yh(x) + yp(t) + h(x)y \\ &= -ay^2 - yp(x) \\ &= -y(ay - p(t)) \\ &= -y(a\dot{x} - p(t)) < 0 \text{ for } |a\dot{x} - p(t)| \end{aligned}$$

This is a negative definite.
Therefore by Lyapunov theorem, the system (2.11) is asymptotically stable in the sense of Lyapunov.
Next we proceed to establish boundedness and periodicity in equation (1.1) a parameter λ, dependent equation.

$$\ddot{x} + a\dot{x} + h_\lambda(x) = \lambda p(t) \qquad (2.13)$$

where $h_\lambda(x) = (1 - \lambda)bx + \lambda h(x) \qquad (2.14)$
where λ is in the range of $0 \leq \lambda \leq 1$ and b is a constant satisfying (1.4). The equation (2.13) is equivalent to the system

$$\left.\begin{aligned} \dot{x} &= y \\ \dot{y} &= -ay^2 - h(x) + p(t) \end{aligned}\right\} \qquad (2.15)$$

the system of equation (2.10) can be represented in the vector form

$$\dot{x} = Ax + \lambda F(t, x). \qquad (2.16)$$

where

$$x = \begin{Bmatrix} x \\ y \end{Bmatrix}, A = \begin{pmatrix} 0 & 1 \\ -b & -a \end{pmatrix}, F = \begin{bmatrix} 0 \\ p(t) - h(t) + bx \end{bmatrix} \qquad (2.17)$$

We remark that the equation (3.8) reduces to a linear equation

$$\ddot{x} + a\dot{x} + bx = 0 \qquad (2.18)$$

when $\lambda = 0$ and to equation (1.1) when $\lambda = 1$.
If the roots of the auxiliary equation (2.18) has no root of the form

$$\beta^2 \neq b, \beta^2 \neq 0 \qquad (2.19)$$

(β is an integer), then equation (1.1) –(1.2) has at least one 2π periodic solution that is the matrix. As defined in equation (2.17) has no imaginary roots so that the matrix $(e^{-2\pi A} - 1)$ where (1) is the identity (2×2) matrix is invertible. Therefore x is a 2π periodic solution of equation (3.11) if and only if $x = \lambda TX, 0 \leq \lambda \leq 1 \qquad (2.20)$
Where the transformation T is defined by

$$(TX)(t) = \int_0^{2\pi} \big(e^{(-2\pi A)} - 1\big)^{-1} e^{((t-s)A)} F\big(S, X(s)\big)ds \qquad (2.21)$$

Hale (1963)
Let s be the space of all real valued continuous 2-vector function $x(t) = (\bar{x}(t), \bar{y}(t))$ which are of period 2π. If the mapping T is completely continuous mapping of S into itself. Then existence of a 2π periodic solution to equation (1.1)-(1.2) correspond to $X \epsilon S$ satisfying equation (2.20) for $\lambda = 1$. Finally using Scheafer's lemma (Scheafer 1955) We establish that

$$|x|_\infty \leq c_6, |\dot{x}|_\infty \leq c_3 \qquad (2.22)$$

where the c's are the apriori bounds.

III.RESULTS

Let $x(t)$ be a possible 2π periodic solution of equation (2.13). The main tool to be used here in this verification is the function $W(x,y)$ defined by

$W(x,y) = \frac{1}{2}y^2 + H_\lambda(x)$ (3.1)

where $H_\lambda(x) = \int_0^x h_\lambda(s)ds$

The time derivative $\dot{W}$ of equation (3.1) along the solution paths of (2.15) is

$$\begin{aligned} \dot{w} &= y\dot{y} + h_\lambda(x)\dot{x} \\ &= -ay^2 - h_\lambda(x)y + \lambda p(t)y + h_\lambda(x)y \\ &= -ay^2 + \lambda p(t)y \end{aligned} \quad (3.2)$$

Integrating the equation (3.2) with respect to t from $t = 0$ to $t = 2\pi$

$$\int_0^{2\pi} \dot{w}dt = \int_0^{2\pi} -a\dot{x}^2 dt + \int_0^{2\pi} \lambda p(t)\dot{x}\ dt$$

$$[W(t)]_0^{2\pi} = \int_0^{2\pi} -a\dot{x}^2 dt + \lambda \int_0^{2\pi} p(t)\dot{x}\ dt$$

Since $W(0) = W(2\pi)$ implies that $[W(t)]_0^{2\pi} = 0$ because of 2π periodicity. Thus

$$0 \le -\int_0^{2\pi} a\dot{x}^2 dt + \lambda \int_0^{2\pi} p(t)\dot{x}\ dt$$

$$a\int_0^{2\pi} \dot{x}^2 dt \le |\lambda|\,|p(t)| \int_0^{2\pi} \dot{x}\ dt \quad (3.3)$$

Since $|\lambda| \le 1$ and $p(t)$ is continous then

$$\int_0^{2\pi} a\dot{x}^2 dt \le c_1(2\pi)^{1/2}\left(\int_0^{2\pi} \dot{x}dt\right)^{1/2}$$

by Schwartz's inequality. Therefore

$$\left(\int_0^{2\pi} \dot{x}^2 dt\right)^{1/2} \le c_1 2\pi^{1/2} \equiv c_2$$

That is $\left(\int_0^{2\pi} \dot{x}^2 dt\right)^{1/2} \le c_2$

Now since $x(0) = x(2\pi)$, it is clear that there exists $\dot{x}(\tau) = 0$ for $\tau \in [0, 2\pi]$. Thus the identity

$$\begin{aligned} \dot{x}(t) &= \dot{x}(\tau) + \int_0^{2\pi} \ddot{x}^2\, ds \\ &= \int_0^{2\pi} \ddot{x}^2(s)\, ds \end{aligned}$$

$max_{0\le t\le 2\pi}|\dot{x}(t)|dt \le \int_0^{2\pi}|\ddot{x}(t)|dt \le 2\pi^{1/2}\left(\int_0^{2\pi} \ddot{x}^2(s)ds\right)^{1/2}$ (3.4)

By Schwartz's inequality.

Using Fourier expansion of

$$x^{\sim} \sum_{r=0}^{\infty} (ar\cos 2\pi l + br \sin 2\pi l)$$

and its derivative in Ezeilo and Onyia (1984) we obtain

$$\int_0^{2\pi} \ddot{x}^2 dt \le |\lambda||p(t)| \int_0^{2\pi} \dot{x}dt$$

$\int_0^{2\pi} \ddot{x}^2 dt \le c_1(2\pi)^{1/2}\left(\int_0^{2\pi} \ddot{x}^2 dt\right)^{1/2}$ by Schwartz's inequality. Therefore

$\left(\int_0^{2\pi} \ddot{x}^2 dt\right)^{1/2} \le c_1(2\pi)^{1/2} \equiv c_2$ (4.5)

From equation (4.5)

$$max_{0\le t\le 2\pi}|\dot{x}(t)| \le (2\pi)^{1/2}.c_1(2\pi)^{1/2} \equiv c_3$$

$|\dot{x}|_\infty \le c_3$ (4.6)

Now integrating equation (3.8) with respect to t from $t = 0$ to $t = 2\pi$, we obtain

$\int_0^{2\pi} \ddot{x}dt + \int_0^{2\pi} a\dot{x}dt + \int_0^{2\pi} h_\lambda(x)dt = \int_0^{2\pi} \lambda p(t)dt.$ (4.7)

Using equation (3.9) on (4.8) we obtain

$$\int_0^{2\pi} \ddot{x}dt + \int_0^{2\pi} a\dot{x}dt + \int_0^{2\pi} (1-\lambda)bx\ dt + \int_0^{2\pi} h(x)dt = \int_0^{2\pi} \lambda p(t)dt.$$

using the 2π periodicity of solution in equation (1.2) then equation (4.8) yields

$\int_0^{2\pi}(1-\lambda)bx\,dt + \int_0^{2\pi} h(x)dt = \int_0^{2\pi}\lambda p(t)dt.$ (4.8)

The continuity of $p(t)$ assures boundedness and the fact that $0 \le \lambda \le 1$, the right hand side of equation (4.8) is bounded. That is

$\left|\int_0^{2\pi}\lambda p(t)dt.\right| \le c_4$ (4.9)

So

$\left|\int_0^{2\pi}(1-\lambda)bxdt + \int_0^{2\pi}\lambda h(x)dt\right| \le c_4$ (4.10)

Therefore given $\alpha > 0$, there exists $\eta > 0$ such that $\tau \in [0, 2\pi]$

$|x(\tau)| \le c_5$ (4.11)

$\tau = 0$ We are done.

Suppose NOT, i.e $x(\tau) \neq 0$ for any τ then equation (4.9) yields

$\int_0^{2\pi}(1-\lambda)b|x|dt + \int_0^{2\pi}|\lambda||h(x)|dt > \int_0^{2\pi}(1-\lambda)b\eta dt + \int_0^{2\pi}\lambda\alpha dt > 2\pi(1-\lambda)b\eta + 2\pi\lambda a$ (4.12)

but equation (4.13) implies that $\int_0^{2\pi}(1-\lambda)bxdt + \int_0^{2\pi}\lambda h(x)dt$ is no more bounded.

This is a negation of equation (4.10). Thus $|h(x)| \to \infty$ as $|x| \to \infty$ and equation (4.12) holds. The identity.

$x(t) = x(\tau) + \int_\tau^t \dot{x}\,dt$ Holds.

Thus

$$max_{0\le t\le 2\pi}|x(t)| \le |x(t)| + \int_0^{2\pi}|\dot{x}(t)|dt \le c_5 + (2\pi)^{1/2}\left(\int_0^{2\pi}\dot{x}^2 dt\right)^{1/2}$$

By Schwartz's inequality

$\le c_5 + (2\pi)^{1/2}.c_2$ by equation (4.4)

Thus $|x|_\infty \le c_5 + (2\pi)^{1/2}.c_2 \equiv c_6$

so

$|x|_\infty \le c_6$ (4.13)

IV. CONCLUSION:-

By equations (4.7) and (4.13) equation (2.22) is established and hence complete proof of theorem 2. Note also that equation (4.7) and (4.12) indicate that the solution $x(t)$ and $\dot{x}(t)$ are bounded.

REFERENCES

[1] E.A. Coddington and N. Levinson, Theory of Ordinary Differential Equations, MC Graw Hill, New York, Toronto, London, (1965).

[2] J.O.C. Ezeilo, Existence of Periodic Solutions of a certain Third Order Differential Equations, Pro. Camb. Society (1960) 56, 381-387.

[3] J.O. C. Ezeilo and J. O. Onyia, Non resonance oscillations for some third order differential equation, J. Nigerian Math. Soc. Volume1 (1984), 83-96.

[4] J. O. C. Ezeilo, Periodic solutions of third order differential equation in the post twenty-five years or so, a paper presented at 2nd Pan-African Congress of African Mathematical Union at the University of Jos, Jos, Nigeria, 1986.

[5] J. O. C. Ezeilo and H. M. Ogbu, Construction of Lyapunov type of functions for some third order non-linear differential equation by method of integration, J. Sci. Teach. Assoc. Nigeria Volume/issue 45/1&2 (2009)

[6] J. K. Hale, Oscillations in Non-linear System, McGraw-Hill, New York, Toronto, London, 1963.

[7] H. M. Ogbu, A necessary and sufficient condition for stability and harmonic oscillations in a certain second order non-linear differential equation, Pacific J. Sci. Tech. Akamai University, Hilo, Hawaii (USA) 7(2) (2006), 126-129.

[8] R. Reissig, G. Sansone and R. Couti, Non Linear Differential Equation of Higher Order, Noordhoff, International Publishing Leyden (1974).

[9] H. Schaefer, Uber dei, Methods der aproiri Schranken Mathematics, Ann 129 415-416. (1995)

[10] H.O. Tejumola, Periodic Boundary Value Problems for Some Fifth and Third Order Ordinary Differential Equations, Journal of Nigeria mathematical Society, Volume 25, 37-46 (2006)

NOTE

We are publishing this article in honour of late Professor Hillary Mbadiwe Ogbu who died on the 2nd of June 2014 and May His gentle soul rest in Peace. Amen.

This was his last Article --- THE FINAL EQUATION

American Journal of Engineering Research (AJER)
e-ISSN: 2320-0847 p-ISSN : 2320-0936
Volume-4, Issue-8, pp-19-30
www.ajer.org
Research Paper Open Access

Evaluation of optimum modes and conditions of contact ultrasonic treatment of wound surface and creation of tools for its implementation

V.N. Khmelev[1], R.N. Golykh[1], A.V. Shalunov[1], V.V. Pedder[2], V.A. Nesterov[1], R.S. Dorovskikh[1]

[1] *Biysk Technological Institute (branch) of Altai State Technical University named after I.I. Polzunov, Russia*
[2] *Scientific production enterprise "Metromed" Ltd, Russia*

ABSTRACT: *The paper presents results of researches on evaluation of optimum modes and conditions of contact ultrasound influence on wound surface to remove (extract) pathological contents (infectant) (separation between liquid and solid phases). In order to optimize modes and conditions of process model of converse ultrasonic capillary effect was proposed. It considers capillary-porous system "solid-liquid" as a whole, but takes into account effects and phenomena inside separate capillary. Among effects and influencing factors it should be underlined following factors: change of dielectric constant leading to changes of disjoining pressure and consequently to the origin of converse ultrasonic capillary effect; bending and radial deformation of the capillary; formation of cavitation fog preventing extraction of wound content. The model allows to determine determine extraction rate depending on amplitude of ultrasonic vibrations, area of radiating surface of the waveguide radiator, amount of drainage canals in it and physical properties of wound content. It was obtained, that for the most widely spread in surgical practice types of wound content (viscosity of no more than 110 mPa·s) vibration amplitude of the radiator of the waveguide-tool should not exceed 39…90 μm at the insonification of the nidus of infection and radiating surface of the radiator of the waveguide-tool should contain no less than 12 draining canals per unit area in 20 cm^2. Evaluated optimum modes and conditions let develop and make ultrasonic waveguide-tools for implementation of extraction process. Designed waveguide-tools are recommended to use in specialized medical surgery and conservative therapy devices.*

Keywords - *Ultrasonic, extraction, biological tissue, wound infection, converse ultrasonic capillary effect*

I. INTRODUCTION

Wound infection developing at 35-45% of patients of the surgical hospitals and even more number of oncological patients is not only clinical problem, but also general biological problem [1, 2]. Most of the patients have post-operative wound complications accompanied by syndrome of endogenous toxicosis [3]. At the syndrome of endogenous toxicosis endotoxins are accumulated that leads to the death of cells. The analysis of syndrome of endogenous toxicosis appearance shows, that it is possible to suppress it by the application of the methods of therapeutic action on different stages of pathological development of the disease locally influencing on endotoxins substrates in the nidus of wound infection.

One of the most promising approaches to local remove of wound content including endotoxins is the possibility of use of ultrasonic energy.

It is known that at the application of mechanical vibrations of ultrasonic frequency on the biological tissue – natural capillary-porous system "liquid-solid" - remove of pathological content can be realized due to the appearance of converse ultrasonic capillary effect [3]. The action of converse ultrasonic capillary effect causes mass transfer of pores and capillaries content of the biological tissue to surface of the wound.

However at present converse ultrasonic capillary effect is not widely used in medicine, as there is no scientific data on the modes (ultrasonic vibration amplitude) and the conditions of ultrasonic action (the area of insonified wound surface, number of drainage channels of the waveguide-tool), at which the most productivity (rate) of the extraction can be provided. To determine optimum modes and conditions required for practical realization of the converse capillary effect it is necessary to carry out complex theoretical studies of mass transfer process in the capillary-porous system "liquid-solid" allowing analyze characteristic properties of converse capillary effect action and its power characteristics.

II. Problem Statement

Until present most researches of liquid medium flow in the capillaries under the action of ultrasonic action considered direct ultrasonic capillary effect discovered and studied by Konovalov E.G., Kitaygorodskiy U.A., Prokhorenko P.P., Dezhkunov N.V., Rozin U.P. and others [4–7]. The main point of the effect is the acceleration of the process, which is opposite to the extraction – penetration of liquid to the capillary cavity under the action of ultrasonic vibrations.

At that very few studies are devoted to the investigation of converse ultrasonic capillary effect observed at the size of the capillaries of less than 10^{-5} m [3, 8], which are specific for the biological tissues. However existing theoretical descriptions do not allow explaining the mechanism of the converse capillary effect [3, 8, 9] and determining interaction of extraction rate of pathological content with the modes and conditions of ultrasonic action in order to develop means of the practical realization of the process.

Thus, final aim of the paper is to design means (waveguide-tools) for ultrasonic extraction of pathological content from the biological tissues due to theoretical determination of optimum modes and conditions of the action.

Implementation of developed waveguide-tools in the surgery and conservative therapy by their use as a part of medical apparatuses lets realize contact ultrasonic action on the nidus of wound infection at stationary and ambulance patients. Proposed method of influence makes possible to stop the development of the syndrome of endogenous toxicosis due to ultrasonic capillary extraction of the endotoxins from the smallest pores of the biological tissue (up to 20 nanometers and less) and improves clinical symptoms independently of the illness stage.

To achieve stated objective it is necessary to solve following particular tasks:

– development of physical-mathematical model and determination of optimum modes and conditions of the realization of mass transfer process in the capillary-porous system "liquid-solid" at the interaction of insonified biological tissues with the transducer – the waveguide-tool having one or several drain holes on the radiating surface;

– definition of optimum vibration amplitude, the area of radiating surface of the wave-guide-tool and the number of the drainage channels in it to provide maximum productivity of extraction on the base of the developed model analysis;

– development of the procedure of engineering calculations of the waveguide-tools on the base of carried out theoretical studies;

– construction of the waveguide-tool samples calculated with the use of proposed procedure and study of their functional possibilities.

Following sections are devoted to the solution of stated tasks.

III. The Model of Mass Transfer Process in the Biological Tissue

To solve the first of stated tasks it is necessary to formulate the model of the mass transfer process in the capillary-porous system "liquid-solid" allowing determine optimum modes and conditions of extraction according to ultrasonic vibration amplitude, area of simultaneously insonified wound surface and number of the drainage channels of the waveguide-tool.

The model should take into account effects and phenomena leading to the extraction of pathological content from a single pore or a capillary, and also it allows analyzing extraction efficiency from the capillary-porous system in a whole.

Theoretically considered mass transfer process in the biological tissue (capillary-porous system "liquid-solid") can be presented in a following way (Fig. 1).

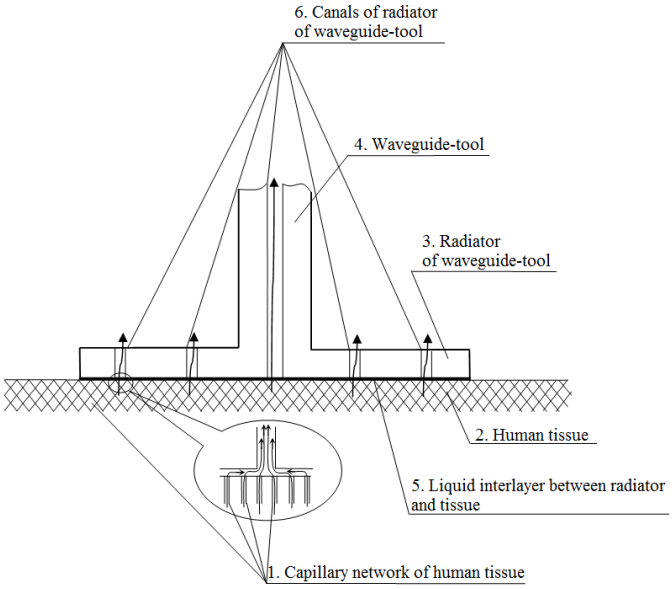

Fig.1. Diagram of mass transfer process in the biological tissue at the contact ultrasonic action

According to the diagram mass transfer of wound content initially occurs from the capillary network 1 to the gap between the radiator 3 of the waveguide-tool 4 and biological tissue 2 generating a layer of liquid medium (infectant) 5. Further wound content is transferred to the drainage channels 6 of the radiator 3 of the waveguide-tool 4, and then it comes to the technological chamber of the ultrasonic extractor, which realizes draining of nidus of infection. The presence of intermediate layer of liquid medium 5 between the wound surface and the radiator 3 of the waveguide-tool 4 is caused by wetting effect and also by untight fit of the radiator 3 of the waveguide-tool 4 to the wound surface, where there is wound effluent in the interface.

To determine optimum modes and conditions of the action providing the realization of the process with maximum efficiency the flow of wound content is described by Navier-Stokes equations (1-4) with the boundary conditions (5-6) on the surface of the biological tissue:

$$\frac{\partial u}{\partial r}+\frac{u}{r}+\frac{\partial v}{\partial z}=0 \tag{1}$$

$$\rho\left(u\frac{\partial u}{\partial r}+v\frac{\partial u}{\partial z}\right)=-\frac{\partial p}{\partial r}+\eta\left(\frac{1}{r}\frac{\partial u}{\partial r}-\frac{u}{r^2}+\frac{\partial^2 u}{\partial r^2}+\frac{\partial^2 u}{\partial z^2}\right) \tag{2}$$

$$\rho\left(u\frac{\partial v}{\partial r}+v\frac{\partial v}{\partial z}\right)=-\frac{\partial p}{\partial z}+\eta\left(\frac{1}{r}\frac{\partial v}{\partial r}+\frac{\partial^2 v}{\partial r^2}+\frac{\partial^2 v}{\partial z^2}\right) \tag{3}$$

$$\rho\left(\left\langle u_1\frac{\partial v_1}{\partial r}+v\frac{\partial v_1}{\partial z}\right\rangle+\frac{1}{4}\left\langle U_{us}^{*}\frac{\partial V_{us}}{\partial r}+U_{us}\frac{\partial V_{us}^{*}}{\partial r}+\frac{\partial}{\partial z}\left(V_{us}V_{us}^{*}\right)\right\rangle\right)=\frac{F-F_B}{lS_c}+2\eta\frac{\partial^2}{\partial z^2}\langle v_1\rangle-\frac{\partial^2}{\partial z^2}\langle p_1\rangle \tag{4}$$

$$u=\langle u_1\rangle=\frac{G_{sp}}{\rho} \tag{5}$$

$$p=\langle p_1\rangle \tag{6}$$

where u and v are the radial and axial components of rate of movement of pathological content in the channels of the radiator of the waveguide-tool, respectively, m/s; p is the static pressure in liquid, m/s; ρ is the density of liquid, kg/m^3; η is the viscosity of liquid, Pa·s, u_1 and v_1 are the radial and axial rate of stationary liquid movement in a single capillary of the biological tissue, respectively, m/s; U_{us} and V_{us} is the complex amplitude of the radial and axial vibrational speed of the capillary wall, respectively, m/s; F is the force magnitude acting on liquid in a single capillary, N; F_B is the Bjerknes force acting on the cavitation fog in the intermediate layer and defined according to the papers [10–12], N; S_c is the capillary cross-section area, m^2; l is the length of the capillary, m; <> is the averaging sign of the capillary cross-section area.

Numerical solution of the system of equations (1-6) by finite element method allows find velocity distribution in the capillary network of insonified biological tissue and in the channels of the waveguide-tool. Obtained distribution lets calculate total extraction velocity depending on the modes and the conditions of action on the base of the expression (7):

$$G=N\frac{\pi d^2}{4}\langle V\rangle\rho \tag{7}$$

where N is the number of drainage channels in the radiator of the waveguide-tool; d is the diameter of the single channel, m; $\langle V \rangle$ is the average extraction velocity of pathological content along the cross-section of the single drainage canal, m/s; ρ is the density of wound content, kg/m^3.

However to determine distribution of liquid phase flow velocities total force F (see equation (4)) acting on the volume of liquid in the single capillary (Fig. 2) and leading to its ultrasonic extraction remains unknown.

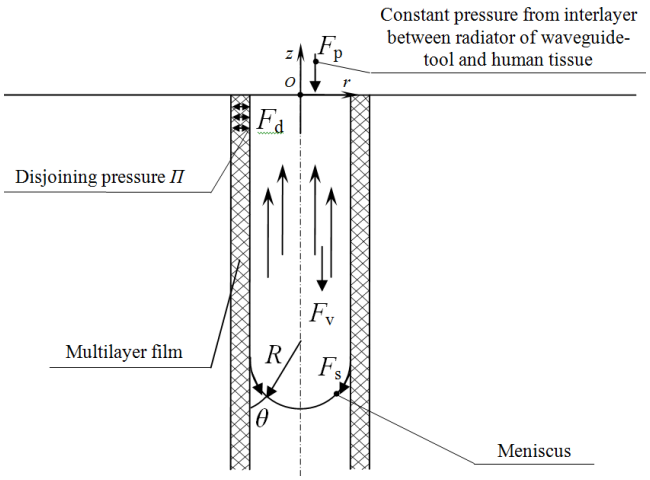

Fig. 2. Diagram mass transfer process in a single capillary

This force balances additional pressure F_p occurring on the surface of the biological tissue (Fig. 3) due to hydraulic resistance of the drainage channels and viscous friction force F_v in liquid phase. Liquid moves uniformly. According to the hypothesis [6, 10], force F is the increment sum of disjoining pressure in the multilayer film ΔF_d on the walls of the capillary [3, 8] and surface tension forces ΔF_s [3] caused by meniscus curvature ($F = \Delta F_d + \Delta F_s$).

Obtained equation for force acting on liquid in the single capillary can be expressed in a following way:

$$F = \frac{\pi d^2 c_2^2 V_0^2}{2} \times \left[\left(\frac{\partial h}{\partial \Pi} \left[\frac{1}{\varepsilon_{l0}^2} - \frac{\ln \varepsilon_{l0}}{\varepsilon_{l0}^2} \right] \frac{A_0}{A_1 + p_0} \right)^2 \times \left(6\pi\, k\, q_e n_0^2 N_A\, h^2 z \rho_2 F\right)^2 \times \left(\frac{\rho_2 (\omega z_0)^2}{4R^2} + \frac{\sigma \cos\theta}{R^3} \right) + \frac{\sigma \cos\theta}{R} \left(\frac{4\nu}{\omega^2} \right)^2 \right] \quad (8)$$

where z is the ion valence in the multilayer film; F is the Faraday constant equals to 96485.33(85) C/mol; k is the electrostatic constant equals to $9 \cdot 10^9$ J·m/C^2; q_e is the ion charge $1.6 \cdot 10^{19}$ C; ε_{l0} is the liquid dielectric constant in the capillary; N_A is the Avogadro's number equals to $6.02 \cdot 10^{23}$ mole^{-1}; n_0 is the ion concentration at the boundary between multilayer liquid film and internal cavity of the capillary, mol/m^3; h is the thickness of the multilayer film, m; Π is the disjoining pressure in the film, Pa; d is the diameter of the capillary, m; c_2 is the velocity of sound in wound content, m/s; V_0 is the amplitude of vibrational velocity of wound content, m/s; ρ_2 is the density of wound content, kg/m^3; A_0 (dimensionless) and A_1 (Pa) are the constant coefficients defining dependence of dielectric constant of liquid phase on pressure [9]; σ is the surface tension of wound content, N/m; θ is the wetting angle between the meniscus boundary and capillary wall; ω is the circular frequency of ultrasonic vibrations, s^{-1}; z_0 is the length of the capillary, m; ν is the Poisson constant of the biological tissue.

The substitution of the expression (8) in Navier-Stokes system of equations (1-6) allows defining total extraction rate (flow rate) of pathological content, which is necessary for the solution of the second task - determination of optimum modes and conditions of ultrasonic action.

IV. Results of Calculations of Extraction Rate of Wound Content from the Biological Tissue

To determine optimum modes and conditions of ultrasonic action we carried out calculations of the total extraction rate depending on amplitude of ultrasonic vibrations, area of insonified wound surface and number of drainage channels of the radiator.

Fig. 3 shows obtained pictures of wound content flow with physical properties close to water (the viscosity is 1 mPa·s; the surface tension is 72 N/m) at different number of the channels in the waveguide-tool.

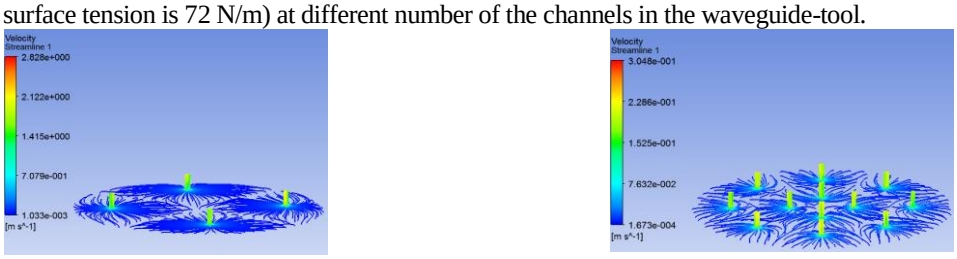

a) 4 channels b) 12 channels

Fig. 3. Pictures of wound content flow at different number of the drainage channels in the radiator of the waveguide-tool of 20 cm^2

Further the dependences of extraction rate on the conditions, modes of influence and physical properties of extracted pathological content (Fig. 4–8) are presented (the diameter of the pores of biological tissue model is 10^{-7} m). As it was mentioned above, the conditions are the area of insonified surface of the biological tissue and the number of the drainage channels in the radiator (Fig. 4–5), and the mode is the vibration amplitude of the radiator (Fig. 7–9).

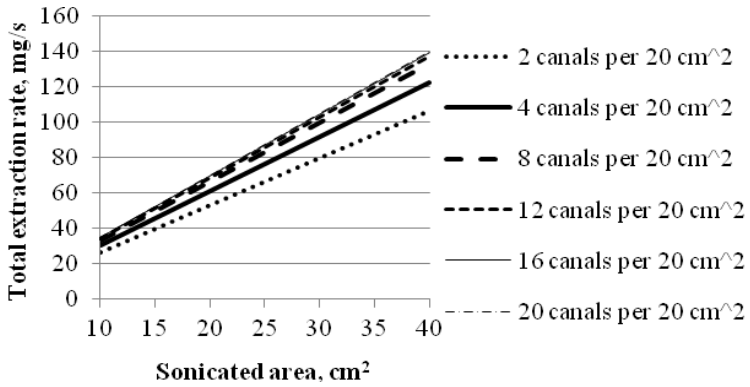

Fig. 4. Dependences of extraction rate of wound content, which physical properties are close to water (the viscosity is 1 mPa·s, the surface tension is 72 N/m) on the area of the radiating surface of the waveguide-tool at different number of the channels in it (the vibration amplitude is 10 μm, the frequency *f* is 23.85 kHz)

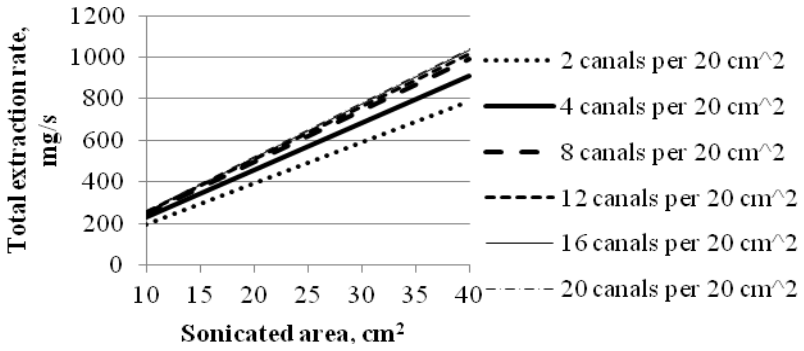

Fig. 5. Dependences of extraction rate of wound content, which physical properties are close to water on the area of the radiating surface of the waveguide-tool at different number of the channels in it (the vibration amplitude is 35 μm, the frequency *f* is 23.85 kHz)

As it follows from presented dependences (Fig. 4–5), extraction rate depends linearly on the area of the radiating surface of the waveguide-tool and at the increase of the number of drainage channels it approaches asymptotically to maximum possible value observed at hydraulic resistance of the canals, which tends to zero.

Presented dependences of specific extraction rate (Fig. 4–5) allow concluding, that the action by the waveguide-tool containing no less than 12 channels on the radiating surface of 20 cm^2 area is the most appropriate. It can be caused by the fact, that in this case extraction rate exceeds 95% of maximum possible value. The use of less channels number leads to the decrease of extraction rate up to 20%. Maximum number of the channels is selected from the condition that they do not influence on distribution of vibration amplitudes and

cyclical strength of the waveguide-tool.

Further the dependences of total extraction rate on vibration amplitude of the radiator of the waveguide-tool at the frequency of f = 23.85 kHz made in the disk form with the area of 20 см^2 (the diameter is 50 mm) containing 12 drainage channels at different viscosities and surface tension of extracted liquid (Fig. 6–8) are shown.

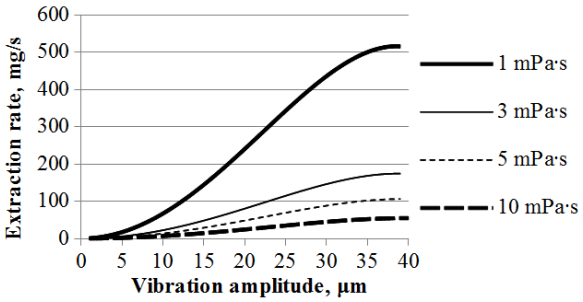

a) for the range of viscosities of 1...10 mPa·s

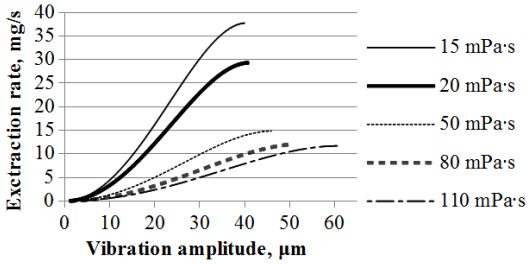

b) for the range of viscosities of 15...110 mPa·s

Fig. 6. Dependences of extraction rate on vibration amplitude of the radiator of the waveguide-tool at different viscosities of wound content (the surface tension is 72 N/m)

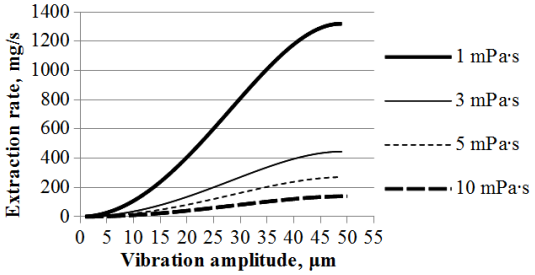

a) for the range of viscosities of 1...10 mPa·s

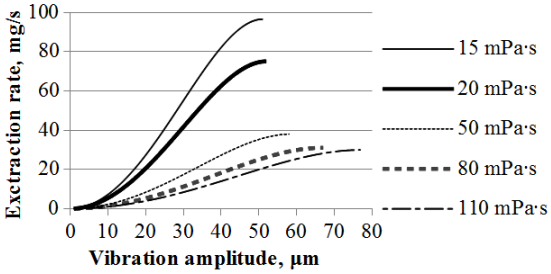

b) for the range of viscosities of 15...110 mPa·s

Fig. 7. Dependences of extraction rate on vibration amplitude of the radiator of the waveguide-tool at different viscosities of wound content (the surface tension is 45 N/m)

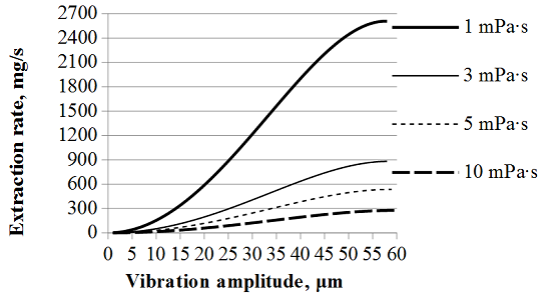

a) for the range of viscosities of 1...10 mPa·s

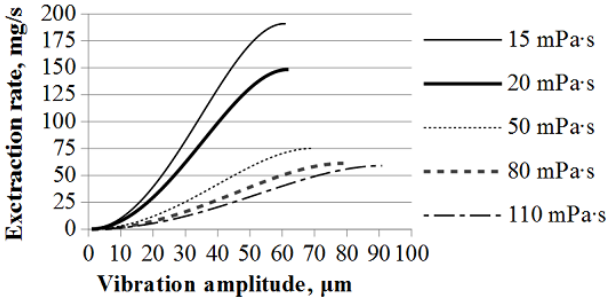

b) for the range of viscosities of 15...110 mPa·s

Fig. 8. Dependences of extraction rate on vibration amplitude of the radiator of the waveguide-tool at different viscosities of wound content (the surface tension is 32 N/m)

Presented diagrams (Fig. 5–9) allows along with the conditions of action (the area of the radiator and the number of drainage channels) choose necessary vibration amplitude, at which required productivity of wound content extraction can be achieved at the application of the waveguide-tool with the 50-mm-diameter radiator.

In particular, extraction rate of wound content, which is close to water in physical properties having low viscosity of 1 mPa·s and surface tension of 72 N/m, achieves 500 mg/s at the amplitude of no more than 35 μm. At the amplitude of 12 μm the extraction rate is 100 mg/s. Whereas for wound content in the viscosity close to detritus (110 mPa·s) with the surface tension of 32 N/m the extraction rate achieves 60 mg/s.

Moreover presented dependences prove quadratic growth of extraction rate with the increase of vibration amplitude of the radiator of the waveguide-tool. However starting with some threshold value of the amplitude, which is 39 μm for liquid with the viscosity of 1 mPa·s and the surface tension of 72 N/m, the growth of the extraction rate stops due to the realization of cavitation mode [13–14]. It is caused by the action of

Bjerknes force on cavitation fog near the surface of insonified biological tissue, which prevents extraction.

These forces are known to lead to the occurrence of direct ultrasonic capillary effect [12].

This fact is the evidence of necessity to limit vibration amplitude of the radiator of the waveguide-tool by the value, at which cavitation mode is realized and extraction rate is maximum. Exceeding of this value does not lead to the increase of extraction efficiency, but it can cause thermo-ultrasonic destruction of the biological tissue in the insonification area. Based on the obtained dependences vibration amplitude should not exceed 39…90 μm for insonification of the biological tissues with wound content having viscosity in the range of 1…110 mPa·s.

The dependences of extraction rate of pathological content on vibration amplitude of the radiator of the waveguide-tool with other constructions and dimensions are similar to ones shown in Fig. 7–9 and they differ from them in some adjustment coefficient *K*. The value of coefficient *K* according to carried out calculations depends on the area of the radiating surface *S* and the drainage channels on it *N* on the base of the expression (9):

$$G(A,\sigma,\eta,N)=K(N,S)\,G_{sp.MAX}(A,\sigma,\eta),$$
$$K(N,S)=k(N)\,S. \qquad (9)$$

where $G_{sp.\,MAX}$ is the maximum possible specific extraction rate (per unit area of wound surface), kg/(s·m^2); *A* is the vibration amplitude of the radiator of the waveguide-tool, m; σ and η are the surface tension (N/m) and viscosity (Pa·s) of wound content, respectively; *k*(*N*) is the constant depending on the number channels per surface unit area of the waveguide-tool radiator; *S* is the radiator surface area, m^2; *N* is the number of drainage channels per unit area of the radiator, m^{-2}.

Obtained results are the base for the selection of optimum modes and conditions of ultrasonic action, which are necessary for providing required extraction productivity.

Discovered optimum modes and conditions can be used for the solution of the third stated task – development of procedure of engineering calculations of special-purpose ultrasonic waveguide-tools of various types.

V. Procedure of Engineering Calculations of the Waveguide Tools

The ultrasonic waveguide-tools intended for practical realization of ultrasonic extraction of wound content from the biological tissues should have specified character of vibrations (longitudinal or bending) of the waveguide tract and its working ending [13, 14] and also provide required range of vibration amplitudes, which is 5–90 μm according to the results of carried out theoretical studies.

That is why working tools can be made in the form of flexural-vibrating disk (a), longitudinal-vibrating rod with the central channel (b) and rod with the disk ending (c) (Fig. 9).

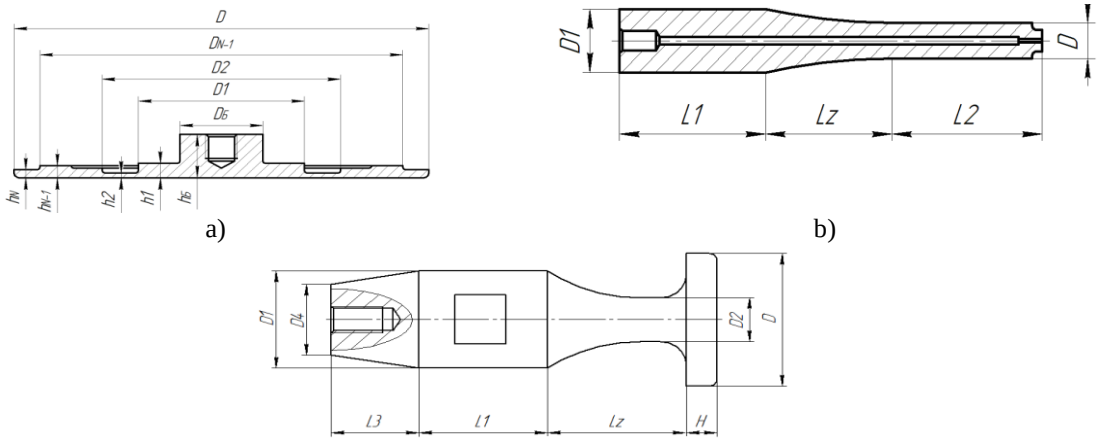

Fig. 9. Drafts of working tools of three types: a) in the form of flexural-vibrating disk; b) in the form longitudinal-vibrating rod with the central channel; c) in the form of longitudinal-vibrating rod with the disk ending

In order to make it possible to remove pathological content from the nidus of infection the tool should have through drainage holes of small diameter (0.5…1 mm).

If the working ending of the waveguide-tool is in the form of disk (Fig. 9a) [13], the holes are made on the zones of the disk vibrating with maximum amplitude to provide the highest extraction productivity (see Fig. 6-8). If the working tool is made in the form of the rod with the ending of small diameter (Fig. 9b), it should

contain one central channel with the diameter of no more than 1 mm.

According to carried out theoretical studies extraction productivity depends on the number of holes and vibration amplitude in zones of holes location. At that vibration amplitudes in the different zones of the working tool, where the holes are located, are determined by the diameter (D), width and height of the thickenings ($D_1...D_{N-1}$, $h_1…h_N$) of the working tool, and also lengths of the parts of the waveguide tract (l_1, l_2, l_z, l_3). For the selection of optimum geometric parameters of the working tool, number and location of the holes in order to provide maximum efficiency of influence on wound surface we develop the procedure of engineering calculations.

According to the procedure following characteristics of the waveguide-tool, which influence on extraction productivity, are defined:

1. **Resonance frequency.** It is selected lower than operating frequency of the piezoelectric transducer in 100–1000 Hz in order to provide the best matching.

2. **Radiator diameter *D*.** It is defined on the base of the requirements to ultrasonic extraction process of infectant (the size of simultaneously insonified wound surface).

3. **Thicknesses $h_1…h_N$ and diameters $D_1...D_{N-1}$** of different ring zones of the radiator**,** if it is made in the form of flexural-vibrating disk (Fig. 10a). The parameters $h_1…h_N$ and $D_1...D_{N-1}$ are selected with the use of finite element modeling in a following way, that relative amplitude difference A_n and A_{n+1} in the neighboring maximum points does not exceed $|(A_n – A_{n+1})/A_n| < 0{,}1$.

4. **Lengths of cylindrical (l_1, l_2) and exponential (l_z)** zones of the waveguide tract (Fig. 10b, c) on the base of the ratio (10) [14]:

$$l_z = \frac{c}{12\pi f}\ln\frac{D_1}{D_2}, \qquad l_1 = l_2 = \frac{c}{12\pi f}. \tag{10}$$

where c is the propagation rate of longitudinal vibrations in the material of the waveguide-tool, m/s; f is the resonance frequency of the tool, Hz; D_1 is the largest diameter of the exponential zone, m; D_2 is the smallest diameter of the exponential zone, m.

At that the ratio D_1/D_2 is selected based on the conditions, which provide necessary amplification coefficient and stiffness of the construction. For the most part of ultrasonic working tools applied in practice it is 2…4 [13, 14].

5. **Number of the drainage holes** based on the ratio (11):

$$N = \left\lfloor N_0 \frac{\pi D^2}{4S_0} \right\rfloor \tag{11}$$

where D is the diameter of the radiator, m; N_0 is specific number of holes per surface unit area of the capillary-porous sample S_0=20 cm^2 determined on the base of obtained theoretical dependences.

Using proposed procedure geometric parameters of three types of waveguide-tools for insonification of wound surface with the diameters of 9 mm, 20 mm, 30 mm, 50 mm and 75 mm were calculated. All developed radiators are intended for the application combined with the piezoelectric transducer at the frequency of 23.85 kHz.

The distributions of vibration amplitudes of designed waveguide-tools are shown in Fig. 10–12.

a) radiator of 50 mm in diameter b) radiator of 75 mm in diameter

Fig. 10. Distributions of vibration amplitude of flexural-vibrating disk radiators

According to presented distributions flexural-vibrating disk radiators of 50 and 75 mm in diameter operate on the second ring vibration mode. At that relative difference of vibration amplitude in the local maximum points is 5...10 %. It proves the fact, that proposed procedure allows design working tools providing uniformity of extraction on all insonified wound surface.

Fig. 11 shows the form of vibrations of the rod working tool with the central channel and diameter of working ending of 9 mm obtained during the calculations with the use of developed procedure.

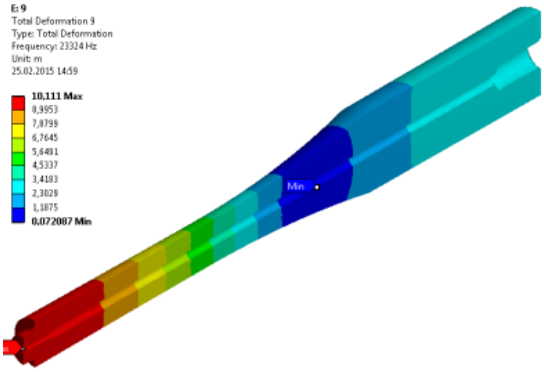

Fig. 11. Distributions of vibration amplitudes of longitudinal-vibrating tool with the central tract

According to Fig. 11 the tip of the tool vibrates uniformly. There is no any essential bend of the butt surface at the operation of the tool.

Fig. 12 shows distributions of vibration amplitudes of the working tool in the form of rod with disk ending of 20 and 30 mm in diameter.

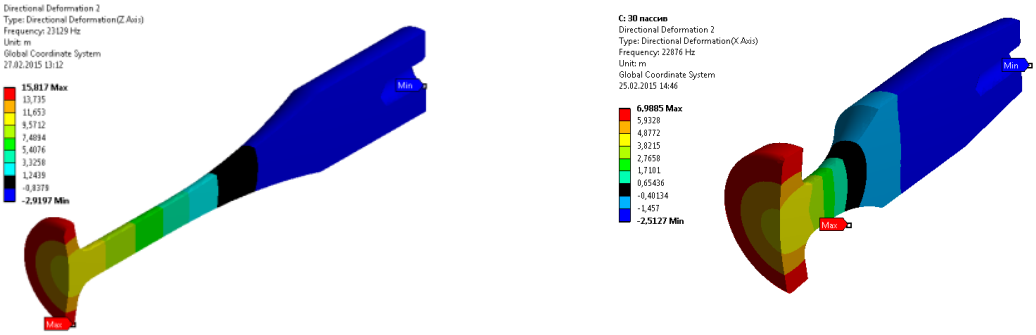

a) 20 mm in diameter b) 30 mm in diameter

Fig. 12. Distributions of vibration amplitude of longitudinal-vibrating disk radiators

At the analysis of the longitudinal-vibrating tools with the disk endings of 20 and 30 mm in diameter (Fig. 12) it was found out, that vibration amplitude at the edge of the disk is in 1.2…1.3 higher than in the central part. It is caused by the fact, that the construction of the disk tip is not rigid. That is why we decided to perform the holes at the periphery, which vibrates with maximum amplitude.

Further we produced one sample of developed working tools (Fig. 10–12) within the frames of solution of the fourth stated task.

The photos of produced working tools are shown in Fig. 13.

a) 20 mm in diameter b) 30 mm in diameter

c) 50 mm in diameter d) 75 mm in diameter

e) rod working tool with the central channel

Fig. 13. Produced working tools

On the disk flexural-vibrating working tools the holes are made within the limits of ring zone vibrating with maximum amplitude. Produced longitudinal-vibrating tool with the central channel (Fig. 13e) has a possibility to change the tip with metered orifice. It was made for carrying out studies with different diameters of the central channels due to the tip change.

Further we present the results of experiments on the determination of the parameters of produced working tools and studies of their functional possibilities in order to prove adequacy of proposed calculation procedure.

VI. Results of the Experiments

Carried out experiments include both determination of the zones, in which limits vibration amplitude is close to zero, and measurement of maximum vibration amplitude. The measurements were performed with the application of the test bench shown in Fig. 14.

The results of measurements of geometric sizes of "zero" vibration and amplitude and also proportional level of acoustic pressure in the air at the distance of 100 mm from the radiating surface for the waveguide-tools of various constructions are shown in Table 1. The measurements of amplitudes were carried out at consumed power of the electronic generator of 35…300 W, which is in proportion to the area of the radiating surface of the disk.

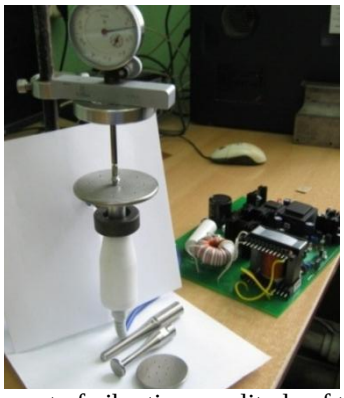

Fig. 14. Test bench for measurement of vibration amplitude of the radiating surface of the tools

Table 1. Characteristics of the working tool found theoretically and experimentally

Type of tool	f_T, kHz	f_M, kHz	ξ, μm	L_{SP}, dB	Diameter of the rings of vibration "zero" (theoretically), mm	Diameter of the rings of vibration "zero" (experiment), mm
Longitudinal-vibrating with the central channel	23.3	22.6	30	152	–	–
Disk D=20 mm	23.1	22.08	60	157	–	–
Disk D=30 mm	22.87	23.35	40	155	–	–
Disk D=50 mm	23.5	23.7	46	154	17; 42.8	16.4; 42.5
Disk D=75 mm	23.4	22.85	40	156	28; 62	29; 64

Symbols used in Table 1: D is the diameter of the disk ending of the working tool; f_T is the theoretically calculated value of resonance frequency; f_M is the measured value of resonance frequency; ξ is the vibration amplitude of the radiator in the maximum points; L_{SP} is the level of acoustic pressure generated by the radiator in at the distance of 100 mm from its surface.

The difference between experimental and theoretical values of the resonance frequencies of the waveguide-tools can be explained by error at their production and difference of tool material properties.

Theoretically determined parts of the surfaces of the radiating disk, on which there are vibration "zeros", and maximum amplitudes vary from the parameters obtained as a result of measurements in no more than 5% that proves adequacy of proposed procedures of calculations of the tools.

To determine functional possibilities of produced tools we carried out research on the example of the extraction process of the model of wound content (physiological solution) with simultaneous atomization. As a model of capillary-porous system we used porous foam-rubber impregnated by water.

Fig. 15 shows the photo of extraction process with simultaneous atomization at the contact of the tool of 75 mm in diameter with the porous material.

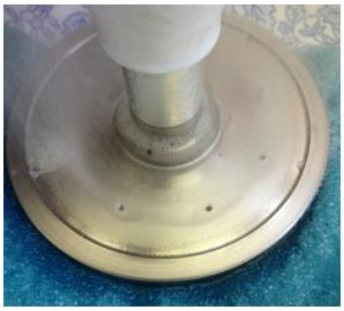

Fig. 15. Photo of moisture extraction process from the porous material

As a result of carried out experimental studies it was determined, that extracted liquid spreads on the surface of the disk radiator. Thus, it was proved principal possibility of realization of extraction of pathological content from the biological tissue, which is natural capillary-porous system.

VII. Conclusion

As a result of carried out studies we discovered optimum modes and conditions of ultrasonic extraction of wound content from the biological tissue and means of practical realization of the process were designed.

To achieve main goal of the paper all the tasks were solved, namely:

1. Physical-mathematical model of converse ultrasonic capillary effect allowing determine extraction rate (in mg/s) depending on vibration amplitude, radiator area, number of the channels in it and physical properties of wound content was developed.
2. Optimum modes (vibration amplitude) and conditions (area and number drainage channels of the waveguide-tool) of ultrasonic action providing maximum productivity of wound content extraction depending on its viscosity and surface tension were determined. It was stated, that extraction rate could achieve 500 mg/s at vibration amplitude of the waveguide-tool, which did not exceed 35 μm.
3. Based on the results of carried out theoretical studies the procedure of engineering calculation of three types of the waveguide-tools intended for ultrasonic action on wound surface was developed.
4. Having applied proposed procedure working tools of three types were designed and produced, experimental studies, which proved adequacy of proposed procedure and possibility of extraction of pathological content by contact ultrasonic action, were carried out.

Developed tools are recommended for the application as a part of specialized medical devices for surgery and conservative therapy.

VIII. Acknowledgements

The reported study was partially supported by RFBR. Research project No. 14-08-31716 mol_a.

REFERENCES

[1] U.K. Abaev, *Reference book for surgeon. Wound and wound infection. Manual* (Rostov: Fenix, 2006). In Russian.

[2] V.K. Kosyonok, V.V. Pedder, V.N. Mironenko, M.V. Naboka, N.V. Rumyantsev, G.Z. Rot, S.P. Popova, and I.V. Surgutskova, New approaches in palliative therapy of the patients with malignant neoplasm, *Palliative medicine and rehabilitation*, 2008, 5-11. In Russian.

[3] V.V. Pedder, L.V. Loshchilova, V.V. Byaller, G.V. Savrasov, and N.V. Shepelev, Converse ultrasonic capillary effect and its usage in surgery, *Technical problems in medicine*, *Abstracts of IV Scientific conference*, Tbilisi, GE, 1986, 90-91. In Russian.

[4] E.G. Konovalov, and I.N. Germanovich, Ultrasonic capillary effect, *Thesis of AS BSSR*, Vol. 6, 8, 1962, 492-493. In Russian.

[5] Y. Tsunekawa, S. Tamura, M. Okumiya, and N. Ishihara, Hot-dip coating of lead-free aluminium on steel substrates with ultrasonic vibration, *J. Mater. Sci. Technol., 24 (01)*, 2008, 41-44.

[6] U.I. Kitaygorodskyi, and V.I. Drozhalova, Calculation of height and liquid rise rate in the capillaries under the action of ultrasonic vibrations, *Application of ultrasound in metallurgy*, *90*, 1977, 12–16. In Russian.

[7] N.V. Dezhkunov, A. Francescutto, P. Ciuti, and P. Ignatenko, Ultrasonic capillary effect and sonoluminescence, *WCU'2003*, Paris, FR, 2003, 597-600.

[8] D.E. Moulton, and J. Lega, Effect of disjoining pressure in a thin film equation with non-uniform forcing, *European Journal of Applied Mathematics*, *Vol. 24, 6*, 2013, 887-920.

[9] W.B. Floriano, and M.A.C. Nascimento, Dielectric Constant and Density of Water as a Function of Pressure at Constant Temperature, *Brasilian journal of physics*, *Vol. 34, 1*, 2004, 38-41.

[10] V.N. Khmelev, R.N. Golykh, S.S. Khmelev, and K.A. Karzakova, Determination of optimum modes and conditions of ultrasonic cavitation treatment of high-viscous liquids, *Scientific-technical bulletin of Povolzhiye, 2*, 2013, 249-251. In Russian.

[11] V.N. Khmelev, A.V. Shalunov, R.N. Golykh, and S.S. Khmelev, Determination of modes of ultrasonic action providing formation of cavitation area in high-viscous and non-Newtonian liquids, *E-magazine «South-Siberian scientific bulletin»*, 1, 2014, 22-27. In Russian.

[12] E.U. Rozina, On nature of force acting on cavitation medium near the capillary cut, *Acoustic bulletin, Vol. 6, 3*, 2003, 60-68. In Russian.

[13] V.N. Khmelev, A.V. Shalunov, S.N. Tsyganok, R.V. Barsukov, and K.V. Shalunova, The application of high-intensity ultrasonic vibrations for the intensification of processes in gas media, *Chemical engineering*, *1*, 2010, 23–28. In Russian.

[14] S.N. Tsyganok, *Study and improvement of piezoelectric ultrasonic vibrating systems for intensification of processes of chemical technologies*, Ph.D. diss., Biysk, RU, 2005. In Russian.

American Journal of Engineering Research (AJER)
e-ISSN: 2320-0847 p-ISSN : 2320-0936
Volume-4, Issue-8, pp-31-37
www.ajer.org
Research Paper Open Access

Factors Affecting Adoption of Cloud Computing Technology in Technical Educations (A Case Study of Technical Institution in Meerut City)

Dr. Sudhir Pathak(Academic Director) NGI
Dr. M.K.Madan(Director General) NGI

Abstract: *Cloud Computing Technology is perceived by many as a new asset of Information technology for the IT companies, educational institutions, government sectors, etc. In the ever fast growing economy apart from the challenges faced due to recession, the educational institutes find this a big hurdle as to how to provide necessary Information technology support for educational activities and research areas. Cloud Computing, the latest buzzword in IT sector, may come to the rescue, as it can provide an easy and inexpensive access to the state of the art IT technology, software and its applications. Cloud computing is a recent concept that is still evolving across the information technology industry and academia. Cloud computing is Internet (cloud) based development and use of computer technology whereby dynamically scalable and often virtualized resources are provided as a service over the Internet. The main aims & Objectives of this research paper is to study the factors which affect the adoption of Cloud Computing Technology in a technical educational institutions, a case study of Engineering colleges in Meerut city(UP.). Questionnaire was used a data collection tool and the results were analyzed by SPSS & R program for statistical analysis.*

I. INTRODUCTION

Cloud computing is internet based computing where shared servers supply software, infrastructure, and platform devices on a pay-as-you –use basis. All information that a digitized system has to offer is provided as a service in the cloud computing technology. Users can focus more on their core business processes rather than spending time and gaining knowledge on resources wanted to customize their processes. According to NIST Cloud Computing consists of five essential characteristics, three service models and four deployment Models. Five essential characteristics are: on demand self-service, broad network access, resource pooling, and rapid elasticity and optimize resource use. There are four different deployment models of cloud computing. Private cloud, the cloud may be managed by the organization or a third party and may present on premise or off premise. Community cloud, the cloud infrastructure is shared by several organizations and supports a specific community that has shared concerns (e.g., mission, security requirements, policy, and compliance considerations). Public cloud, the cloud infrastructure is made existing to the general public or a large industry group and is owned by an organization advertising cloud services. Hybrid cloud, the cloud infrastructure is a composition of two or more clouds (private, community, or public). Cloud Models can be segmented into Software as a Service (Saas), Platform as a service (PaaS) and Infrastructure as a Service (IaaS). Software as a Service, this is typically where end user applications are delivered on demand over a network on a pay per use basis. The software requires no client installation, just a browser and network connectivity. Platform as a Service is used by software development companies to run their software products. Infrastructure as a Service is a model in which an organization outsources the equipment used to support operations, including storage, hardware, servers and networking components. [1], [2]

Cloud computing in education sector:

The benefits of cloud computing are being appreciated by many sectors of business and industry and now are being adopted by education sector also. Cloud computing presents many advantages to e-learning by providing the infrastructure, platform and educational services directly through cloud providers. There are many examples of using cloud computing for education. Virginia virtual computing lab (VCL) uses cloud computing technology and provides students with access to the architectural, geographical, mathematical, research, statistical applications at any time and any location with an Internet broadband connection.

Software in a virtual lab is used more than a software in a physical lab, reducing the peruse cost of each software license and unlike physical computer labs, a virtual lab is available to students 24 hours a day, during every day of the year. [3]

The VCL which began in 2002 by North Carolina State University, with support from IBM, and in 2009 it became available as a free, hardware-agnostic Apache open source project. There are now similar education clouds based on the VCL in California, Georgia, and South Carolina. Cloud computing is an innovative concept, it allows for more than the use of text books and it is a tool to bridge the digital divide and to solve educational problems. For students, cloud computing makes real-time collaboration easy. Online meeting spaces and video chat also make it possible for students to meet and attend classes online. And with assignments which are online and can be accessed anywhere, students can take their learning with them anywhere. All of these things are made possible through cloud computing and have the potential to transform education as we know it. Cloud computing allows institutions, business sectors and education sectors to access real time information from anywhere in the world in at any time. In the field of education, this is pretty important as it gives the teachers and the learners to continuously update their domain knowledge. Cloud computing allows teachers and learners to access applications and other useful tools free of charge. Cloud computing technology is a new technology for our education sector so it is efficient and also environment friendly. Because cloud computing allows for interconnectivity, students are uncovered to openness. Students are able to experience and feel what is processing in the real world. Educators point to cloud computing as a solution for instructors' obstacles in preparation and development of courses and strengthening curriculum. Which material can be taught and learned using textbooks and chalk boards, it is now gathered and absorbed much more quickly and easily through Internet access, using cloud computing technology in the classroom. This research paper aims at studying the factors which affect the adopting of Cloud computing technology in a Technical education institution, with a particular case study at a renowned public school in Delhi.

II. PROBLEM STATEMENT

The process of purchasing, maintaining, and monitoring Computing assets requires a large investment of financial and manpower resources for any technical institution. An option which centralizes computing assets and can lower the costs and manpower requirements for the organizations is the use of centralized computing assets provided as cloud computing. Currently, many technical institutions are interested in using cloud computing capabilities, but they do not know where to expect changes when choosing for the cloud computing concept.[4] This research attempts to identify the factors taken into consideration by education institutions, when deciding about adoption of cloud computing technology.

III. RESEARCH DESIGN

3.1. RESEARCH QUESTION

The study deals with the factors which affect the adoption of Cloud Computing Technology in education institution, a case study on a Neelkanth Group of Institutions, Meerut City (UP). Hence, the research question will be: ***"What are the Factors observed by NGI considering the adoption of cloud computing into their operations?"***

3.2. RESEARCH HYPOTHESIS

There is a significant effect between independent variables and Cloud Computing Adoption in NGI (at level of significance α=0.05)

3.3. RESEARCH VARIABLES

The dependent variable: Cloud Computing Adoption
The independent variables:
1. Top Management Support
2. Support and integration with School Services
3. Skills of IT human resources
4. Security effectiveness
5. Cost reduction

3.4. SCOPE AND LIMIT OF RESEARCH

The scope of research is limited to education institution practically in NGI. The population of study consists of academic and administrative staff.

3.5. RESEARCH METHODOLOGY

The research population includes a study of each of the Director General, Director, Principal, Professor, Associate professor, Asst. Professor; Lab Technicians of different departments, Supervisors, Non-Technical

Staffs, Accounts Department and the other administrative staff at NGI, The population is selected according to the research variables. Where (175) questionnaires are distributed, (155) are retrieved; as the result, the percentage of responses is (89.07%). After reviewing the literature and interviewing the specialists, the questionnaire is the most appropriate tool for this research. The questionnaire is provided with a cover letter which explains the purpose of this research. The questionnaire is composed of three parts as follows:

- **First Part:** General Personal Information, which consists of (6) items.
- **Second Part:** The adoption of Cloud Computing technology, which consists of (9) items.
- **Third section:** Skills of IT staff at the institution. It consists of (12) items.
- **Fourth section:** Security effectiveness in adoption of Cloud Computing. It consists of (12) items.
- **Fifth section:** Cost Reduction through the

Adoption of Cloud Computing. It consists of (11) items.

3.6. STATISTICAL ANALYSIS

In order to test the fields of research tool (questionnaire), and paragraphs analysis, parametric tests were used (One sample T test, Independent Samples T-test, Analysis of Variance- ANOVA). Testing paragraphs of each research variable about the average score equal to answer neutrality (degrees approval medium).

- *Null hypothesis:* tests that the average answer degree is equal to 3, which in conversely equal with "Agree" by the Likert scale.
- *The alternative hypothesis*: The average score answer is not equal to 3 If the Sig.>0.05 (Sig. greater than 0.05), according to SPSS program results , it cannot reject the null hypothesis, so in this case the average views of respondents on the phenomenon under study does not differ materially from "Agree" which is 3 in Likert scale. On other hand, if the Sig. <0.05 (Sig. less than 0.05), then it can reject the null hypothesis, and accept the alternative hypothesis that the average views of respondents varies materially from the medium approval degree "Agree".

Table: 1

Likert Means and Test values for the "The adoption of cloud computing technology"

Sl. no.	Paragraph s	Likert Mean	Proportional Likert Mean	p-values Sig.	Rank
1	Cloud Computing technology is an attractive technological option to the Technical Institutions	3.89	77.78	p<0.05	4
2	2 Cloud Computing technology is an attractive economic option to the Technical Institution	3.76	75.25	p<0.05	9
3	The Technical Institution Focuses on new IT system projects, which aim to increase the efficiency and quality of services provided for the beneficiaries.	3.95	78.99	p<0.05	3
4	The Technical Institution Focuses on new IT system projects, which aim to maintain competitive advantage	3.88	77.56	p<0.05	5
5	The Technical Institution has high speed internet lines, and uninterrupted services.	4.09	81.71	p<0.05	1
6	The Technical Institution Focuses on new IT system projects, which aim to increase students satisfaction.	3.81	76.30	p<0.05	6
7	The Technical Institution Focuses on new IT system projects, which aim to increase employees satisfaction.	3.77	75.31	p<0.05	8
8	The Technical Institution Focuses on new IT system projects, which aim to increase data and information security.	4.06	81.23	p<0.05	2
9	The adoption of Cloud Computing technology in IT operations will support the learning process.	3.79	75.75	p<0.05	7
	All paragraphs	3.89	77.77	p<0.05	

*The Likert Mean is significantly different from 3

Table 2:

Likert Means and Test values for "Top management Support of the Adoption of Cloud Computing Technology"

Sl. no.	Paragraphs	Likert Mean	Proportional Likert Mean	p-values Sig.	Rank
1	Top management informed of ongoing developments of Cloud Computing technology and the importance of its use	3.10	61.95	0.199	7
2	Top management concerns to provide the staff with the needed trainings and skills for any new technology so as to keep up with development.	3.28	65.61	p<0.05	4
3	Top management develops plans which are flexible enough to accommodate any changes required by the adoption of Cloud Computing technology	3.06	61.22	0.278	8
4	Top management supports the new technologies which serve the learning process, and the Institution students	3.51	70.24	p<0.05	3
5	Top management seeks to maintain competitive advantage through the adoption of new technologies, and its uses in its Operations	3.52	70.37	p<0.05	2
6	There is a support from top management in IT field to adopt everything new such as Cloud Computing technology	3.14	62.	0.094	6
7	Top Management has a future plan to adopt Cloud Computing, and its uses in IT operations	2.78	55.56	0.039*	11
8	Top management has plans to get rid of obstacles that hinder the use of any new technology at the Institution such as Cloud Computing technology.	2.85	57.04	0.061	9
9	Top management provides the support and the needed requirements to adopt Cloud Computing technology.	2.73	54.50	p<0.05	12
10	The adoption of Cloud Computing technology is included in Strategic Plan for IT Center	2.84	56.88	0.085	10
11	The administration's decision is wise in the use one of Cloud Computing applications at the Institution	3.84	76.79	p<0.05	1
12	Top management supports a shift policy in all or some of the IT operations towards Cloud Computing technology.	3.20	64.05	p<0.05	5
	All Paragraphs	3.16	63.19	p<0.05	

*The Likert Mean is significantly different from 3

Table 3:
Likert Means and Test values for "Skills of IT human resource"

Sl. no.	Paragraphs	Likert Mean	Proportional Likert Mean	p-values Sig.	Rank
1	Cloud Computing technology helps on the development of IT staff abilities and skills	3.83	76.59	p<0.05	2
2	Training provided to staff in the field of IT enough, and makes them sophisticated and looks forward to some extent to the latest technology.	3.23	64.69	p<0.05	9
3	Cloud Computing technology helps on the development of the spirit of creativity and innovation.	3.60	71.95 5	p<0.05	6
4	The Institution provides training programs for employees relating to the new technologies (such as Cloud Computing Technology)	2.76	55.19	p<0.05	12
5	IT staff realize the importance of the adopting of Cloud Computing at the Institution	3.58	71.65	p<0.05	7
6	IT Management staff continuously on the lookout for new technological developments (such as Cloud Computing Technology)	3.64	72.75	p<0.05	4
7	The staff is sent to scientific missions to take advantage of technological developments surrounding	2.80	56.05	0.064	11
8	The staff dissatisfaction and disability to change is one of the challenges that hinder the adoption of any new technology (such as Cloud Computing Technology)	3.45	69.00	p<0.05	8
9	I do not need high effort to inquire or to identify any new technology such as Cloud Computing Technology	3.61	3.61	p<0.05	5
10	Technological developments encourage positive competition among staff to motivate them to serve the general interest of the institution	3.70	74.07	p<0.05	3
11	The Institution holds meetings, lectures and materials for the definition of human resources the importance and the use of Cloud	2.96	59.25	0.380	10
12	IT staff needs training in the Cloud Computing, especially in The (construction, development, deployment) cloud services	3.95	79.01	p<0.05	1
	All paragraphs	3.43	68.53	p<0.05	

*The Likert Mean is significantly different from 3

Table 4:

Likert Means and Test values for "Support and Integration of institution services with cloud computing"

Sl. no.	Paragraph s	Likert Mean	Proportional Likert Mean	p-values Sig.	Rank
1	The possibility of moving existing applications and services provided by IT Department at the Institution to the cloud	3.28	65.61	p<0.05	12
2	Systems, technological services and applications at the Institution are continuously updated to keep pace with technological development	3.65	72.93	p<0.05	7
3	Technological services and applications at the Institution characterized by sufficient flexibility.	3.46	69.27	p<0.05	10
4	The adoption of Cloud Computing technology at the Institution helps to activate new services.	3.85	77.04	p<0.05	4
5	The adoption of Cloud Computing technology at the Institution helps to improve quality of its services.	3.93	78.52	p<0.05	2
6	The adoption of Cloud Computing technology at the Institution helps in distinguishing the Institution in its provided services, which is different from that provided by other universities.	3.91	78.29	p<0.05	3
7	The adoption of Cloud Computing technology at the Institution helps to improve the performance of currently Institution services.	3.83	76.54	p<0.05	5
8	The transfer of e-mail service from the old system to one of Cloud Computing applications (Gmail) easily without suffering.	3.60	72.05	p<0.05	9
9	The facilities of integration services and IT applications with the services provided by Cloud Computing (e.g. Gmail)	3.76	75.12	p<0.05	6
10	Cloud Computing providers offer free services to students, to help them in the learning process by providing disk service to store and share data, e-mail and others.	3.64	72.84	p<0.05	8
11	Cloud Computing provides working environment for students to conduct their scientific experiments that need special devices they cannot provide	3.38	67.56	p<0.05	11
12	It's possible to access to the services provided in the cloud from anywhere and any device.	4.09	81.71	p<0.05	1
	All paragraphs	3.69	73.90	p<0.05	

The Likert Mean is significantly different from 3

Table 5:

Likert Means and Test values for "Security effectiveness in adoption of cloud computing"

Sl. no.	Paragraph s	Likert Mean	Proportional Likert Mean	p-values Sig.	Rank
1	The data security is the biggest challenges facing the Institution to adopt any new technology	4.43	88.64	p<0.05	1
2	We must know where the data is stored in the Cloud Computing	3.78	75.61	p<0.05	6
3	The strength of data security depends on the strength of service provider in terms of security	4.15	82.96	p<0.05	2
4	It can be considered a contract agreement between the Institution and the service provider as a safety and reliability of the data.	3.74	74.75	p<0.05	8
5	There is confidence in new technologies and the providers of these services (e.g. Google, Microsoft, Amazon,)	3.36	67.25	p<0.05	12
6	The adoption and use of Cloud Computing Technology Lead to develop a plan to protect the security and confidentiality of the information	3.85	77.04	p<0.05	4
7	The confidence increases with companies Cloud Computing service providers in the event of clear agreements related to hacking and electronic security breaches	3.75	75.00	p<0.05	7
8	The Cloud Computing service provided by Google Inc., which is the e-mail service (Gmail) used in the Institution safer than the old system.	3.49	69.88	p<0.05	10
9	The services and applications of Cloud Computing provided by service providers companies (e.g. Google, Amazon, Microsoft,) are difficult to hack and piracy	3.41	68.10	p<0.05	11
10	The cloud for students is safer than traditional methods (flash, the device profile,) in putting their researches, reports and home work.	3.63	72.66	p<0.05	9
11	The things that will help the Institution to overcome fears of safety is not put sensitive data or applications in the cloud	3.79	75.75	p<0.05	5
12	Could be the Institution a hybrid cloud, which consists of a Public Cloud to put non-sensitive and public applications and also from the Private Cloud to maintain the confidentiality and security of data?	3.95	79.01	p<0.05	3
	All paragraphs	3.77	75.37	p<0.05	

The Likert Mean is significantly different from 3

Table 6:
Likert Means and Test values for "Cost reduction through the adoption of cloud computing"

Sl. no.	Paragraph s	Likert Mean	Proportional Likert Mean	p-values Sig.	Rank
1	The Institution focuses on modern IT system projects, which aim to reduce costs.	1 4.02	80.49	p<0.05	1
2	Transfer the operations and services of Institution to the cloud will reduce costs.	3.87	77.32	p<0.05	4
3	The service of Cloud Computing provided by Google Inc., (e.g. an email Service - Gmail) at the Institution is less expensive than the old system.	3.85	76.96	p<0.05	6
4	Many Cloud Computing service providers offer free services to higher education institutions.	3.58	71.65	p<0.05	11
5	There are free services in the cloud help students to communicate with each other, save and share data and others.	3.85	77.04	p<0.05	5
6	The Cloud computing helps to reduce the expenses that go to buy hardware, servers, software or maintenance.	3.98	79.51	p<0.05	3
7	The most important feature of Cloud Computing is the ability to control costs by use.	3.73	74.57	p<0.05	7
8	The most important feature of Cloud Computing is getting rid of unnecessary costs (place - electricity - air ... etc.).	4.01	80.24	p<0.05	2
9	The Cloud Computing Technology provides innovative Institution services without increasing the cost or the price of the service.	3.68	73.58	p<0.05	8
10	The cloud provides the needs of lab such as (special specifications of high expensive computers, or scientific applications), which it needs to work for a few hours or days continuously to bring out the desired results.	3.67	73.33	p<0.05	9
11	When to adopt Cloud Computing Technology, the cost is greatly reduced and capital expenditure is converted in the IT operations to ongoing expenses.	3.60	72.10	p<0.05	10
	All paragraphs	3.81	76.12	p<0.05	

*The Likert Mean is significantly different from 3

Stepwise Regression:
Table 7 shows the regression coefficients and their P values (sig.). Based on the Standardized coefficients, the significant independent variable is "Support and integration of Institution services" with cloud computing and "top management support of the adoption of cloud computing technology".

Table 7:
The Regression Coefficients

No	Paragraph	Unstandardized Coefficients		Standardized Coefficients	T	Sig.
		B	Std. Error	Beta		
1	Constant	1.183	0.270		4.378	0.000
2	Support and Integration of institution services with cloud computing	0.491	0.086	0.512	5.699	0.000
3	Top management support for the adoption of Cloud computing	0.282	0.076	0.335	3.730	0.000

The regression equation is:
The adoption of cloud computing in NGI = **1.183** +**0.491***(Support and Integration of institution services with cloud computing) + **0.282***(Top management support for the adoption of Cloud computing) By using stepwise regression the following results were obtained: R square = **0.572**, this implies **57.2%** of the variation in the adoption of Cloud computing in NGI is governed by "Support and Integration of institution services with cloud computing and Top management support for the adoption of Cloud computing".

Table 8: ANOVA for Regression

No.	Paragraph Sum	Sum of Squares	D F	Likert Mean Square	F	Sig.
1	Regression	15.053	2	7.527	52.705	0.000
2	Residual	11.282	79	0.143		
	Total	26.335	81			

Table 8 Shows the Analysis of Variance for the regression model. Sig. = **0.000**, so there is a significant relation between the dependent variable "Adoption of Cloud computing in NGI " and independent variables "Support and Integration of Institution services with Cloud Computing" and "Top management support for the adoption of Cloud Computing".

IV. CONCLUSIONS:

Engineering College is governed by many factors, from which the main factors are: "Support and Integration of Institution services with Cloud Computing" and "Top management support for the adoption of Cloud Computing".

REFERENCES:

[1] (2010, August) Virginia's virtual computing lab. [Online].HYPERLINKwww.education.virginia.gov/.../VAVCLthoughtdoc_081510.docwww.education.virginia.gov/./VAVCLthoughtdoc_081510.doc [2] Albrecht Fortenbacher Wen-Yu Liu, "Digital Divide and Clo Computing-A Case Study in a Rural Area of Taiwan," 2011.[3] Yefim Natis, "Key Issues for Cloud-Enabled Application Infrastructure," April 2008. [4] Jeffrey,K & Neidecker-Lutz, B.(2009): The future of cloud computing: Opportunities for European cloud computing beyond 2010.

American Journal of Engineering Research (AJER) 2015
American Journal of Engineering Research (AJER)
e-ISSN: 2320-0847 p-ISSN : 2320-0936
Volume-4, Issue-8, pp-38-40
www.ajer.org
Research Paper Open Access

A Random Evolution of Stochastic difference Equations related to M/M/1 Queueing System

M.Reni Sagayaraj[1], P.Manoharan[2], S. Anand Gnana Selvam[3]
R.Reynald Susainathan[4]
[1,2,3]*Department of Mathematics, Sacred Heart College (Autonomous), Tirupattur - 635601, Vellore District.Tamil Nadu, S.India.*
[4]*Reckitt Benckiser, India Limited (Gurgaon), New Delhi. India.*

ABSTRACT : *We propose a stochastic model for evolution with single server queue. Birth and death of species occur with constant probabilities. It is shown that the Poisson like arrival process (births) with slowly diffusing like time dependent average inter-event time may be represented as a super statistical one and exhibits* $1/\mu$ *arrival (birth). We obtain customers induces less to the system and they alter the dynamics of the net profit. We associate various costs and analysis the Markov evolution of the net profit functions.*

Keywords - *Random evolution, stochastic Difference Equation, Birth and death process. net profit functions, point process*

I. INTRODUCTION

A random evolution is a natural but apparently new generalization of this notion. In this note we hope to show that this concept leads to simple and powerful applications of probabilistic tools to initial-value problems of both parabolic and hyperbolic type. The term `random evolution' first appeared in the year 1968 paper of Griego and Harris [9] where the further acknowledgments paper The two-state Markov chain, often called the telegraph process, is the continuous-time counterpart of the classical Bernoulli process of Discrete-parameter probability theory. A Simpler proof of the telegraph equation was obtained by Kaplan [4].Recent approaches to large deviation of random evolution are contained in the works of Bezuidehout [2] and Eizenberg-Freidin [3].

A random evolution $M(t,\omega)$ is the product. It is shown that the Poisson process with diffusing average time may be represented by the equation.

$$M(t) = T_{\tau 0}(t_1)Tv_{(t_1)}(t_2 - t_1) \dots\dots Tv_{(t_{N(t)})}\left(t - T_{N(t)}\right) \qquad (1)$$

The study of Markov diffusion process has played an important role in the development of stochastic processes both from theoretical as well as the applied points of view, one of the earliest applications was to the study of the fluctuations of arrival variables due to various aspects were studied.

Assume that stochastic differential equations is

$$\frac{dx}{dt} = a(x;t)$$

Describe a one dimensional dynamical system. Assume that (1) fulfils conditions such that a unique solution exists, thus $x(t) = x(t;x_0;t_0)$ is a solution satisfying the initial condition $(t_0) = x_0$. Given the initial condition, we know how the system behaves at all times t, even if we cannot find a solution analytically. We can always solve it numerically up to any desired precision.

A way of modelling these elements is by including stochastic influences of birth. A natural extension of a deterministic differential equations model is a system of stochastic differential equations, where relevant parameters are modelled as suitable stochastic processes, or stochastic processes are added to the driving system

equations. This approach assumes that the dynamics are partly driven by arrival of the variable.
A natural extension of a deterministic ordinary differential equations model is given by a stochastic differential equations model, where relevant parameters are randomized or modelled as random processes of some suitable form, or simply by adding a arrival term to the driving equations of the system. This approach assumes that some degree of arrival is present in the dynamics of the process. Here we will use the Wiener process. It leads to a mixed system with both a deterministic and a stochastic part in the following way:

$$dX_t = \mu(X_t;t)dt + \sigma(X_t;t)dW_t \qquad (3)$$

When $X_t = X(t)$ is stochastic processes, not a determined function like in[1].This isindicated by the capital letter. Here $W_t = W(t)$is a wiener process and since it is now here differentiable, we need to define what the differential means. It turns out that it is very useful to write $dw_t = \xi_t dt$ where a white arrival process is, define as being normally distributed for any fixed `t' and uncorrelated.
We have proposed stochastic model of $\frac{1}{\mu^{\beta}}$ arrival with 0.5, β < 2, based on the simple point process models [10] and on nonlinear stochastic differential equations [5], [6]. Here we show that the Poisson like point process with slowly diffusing time-dependent average interevent. The distribution of the Poisson like interevent time may be expressed as an exponential distribution of the Non extensive statistical Mechanics. We describe the problem as Random evolution with single server Queue. The Markov evolution of a net profit function determined.

II. MODEL DESCRIPTION OF THE PROBLEM

We consider a counter where the customers arrive according to a Poisson Process wit rate λ .There is a single server at the counter and he serves the customers according to the order of their arrival. The service time for a customer has exponential distribution with mean $\frac{1}{\mu}$ .An arriving customer joins the queue with probability 1 if the system size is 0.If the system size is 1 when the customers arrives, he join the queue with probability p and he balks with probability q[11].
The basic concept of queueing theory

$$p + q = 1$$

And $P_0(t) = p$, for all n ≥ 2. We assume that $P_0(t) = b$ using probability arguments, we have

$$P_0(t+\Delta) = P_0(1-\lambda\Delta) + P_1(t)\mu\Delta + o(\Delta) \qquad (4)$$
$$P_1(t+\Delta) = P_1(1-\mu\Delta) + P_0(t)\lambda\Delta + o(\Delta) \qquad (5)$$

From the above equation we have

$$P_0'(t) = -\lambda P_0(t) + \mu P_1(t) \qquad (6)$$
$$P_1'(t) = -\mu P_0(t) + \lambda P_1(t) \qquad (7)$$

We observe the if the initial probabilities are assumed to be the steady state values, then queueing process is stationary at any time.
If we are assume that the process starts with 1 customer at time t=0, then a=0 and b=1.In this situation, we obtain the steady state probabilities are,

$$P_0(t) = \frac{\mu}{\lambda+\mu}\left\{1 - e^{-(\lambda+\mu)t}\right\} \qquad (8)$$
$$P_1(t) = \frac{\mu}{\lambda+\mu} + \frac{\mu}{\lambda+\mu}\left\{1 - e^{-(\lambda+\mu)t}\right\} \qquad (9)$$

III. A RANDOM EVOLUTION WITH SINGLE SERVER QUEUE

We consider the queueing model M/M/1 starting with one customer at time t=0.As busy periods always fetch utility of the system by the customers and in turn provide profit to the system. We attach a positive cost $C_1, C_2 > 0$ per unit time, to busy periods .In the same way a negative cost $-C_1, C_2 > 0$ per unit time is attached to idle periods. Considering the epochs of beginning and ending of the busy periods ,we note that these epochs constitute an alternating point process on the time axes characteristic by the two densities like $\mu e^{-\mu t}$ and $\lambda e^{-\lambda t}$. Let C(t) be the cost per unit time at time t. Then it can be easily given that

$$C(t) = \frac{1}{2}(C_1 - C_2) + \frac{1}{2}(C_1 + C_2)(-1)^N(t) \qquad (10)$$

Let P(t) be the net gain of the system up to time t. Then it can be easily seen that

$$P(t) = \int_0^t C(u)du$$

Solve the above we get two random quantities p(t)and C(t) constitute a random motion.

IV. THE MARKOV EVOLUTION OF A NET PROFIT FUNCTION

Let r(t) be the value of the service per unit time per customer in the system at time t. We define

$$r(t) = \begin{cases} -r_1 \ if \ n(t) = 0 \\ r_2 \ if \ n(t) = 1 \\ r_3 \ if \ n(t) > 1 \end{cases}$$

Where n(t) represents the number of customers in the system at time t. Here we assumed that $r_i > 0 \, , i - 0, 2, 3 \ldots$

It is to be noted that r1 is the negative cost due to the idle time of the server and r_2 and r_3 corresponds to the state dependent positive gain due to the customer who join the system. Clearly r_2 and r_3 contribute positive revenue to the net profit function. Then the net profit function L(t) is given the stochastic integral.

$$L(t) \int_0^t r(u)du \qquad (11)$$

In [8] by using r(u) as the instantaneous velocity of the server , L(t) gives the distance traveled by the server in time t. Then the time evolution of the net gain can be studied by identifying the server as a particle under a random motion [7] on the real line with three velocities in a cyclic manner. We now study the time evolution of L(t) .for this ,we assume that the server enter in to the idle state at time t=0.Then we note that n(0)=0 and $r(0) = r_1$.

It is easy to note that the discrete component of L(t) given by

$$P_r\{L(t) = -r_{(t)}\} e^{-\lambda t} \qquad (12)$$

From the assumption made on the input and output processes, it may be verified that the stochastic process.

V. CONCLUSION

The special non-linear stochastic difference equation, generating the distribution density with $\frac{1}{\mu}$ mean arrival. We derive two random quantities P(t) and C(t) constitute of a random variable with random motion. We analyze cost of the Markov evolution of the net profit. We describe the explicit expression of the transient probabilities Pn(t) are found in a direct way along with steady state solution. It can be applied for telecommunication network.

REFERENCES

[1] Bailey, N. T. J. (1963). Stochastic birth, death and migration processes for spatially distributed populations. *Biometrika* 55 189-198.

[2] Bezuidehout, "Degeneration of the solutions of certain well-posed systems of partial differential equations depending on a small parameter," *J. Math. Anal. Appl.*, 16, 419-454 (1966).

[3] Einstein, A. (1905). ber die von molekularkinetischen Theorie der Wrme geforderte Bewegung von in ruhenden Flssigkeiten suspendierten Teilchen. Annelen der Physik, 17:549560.

[4] Kaplan, S., "Differential equations in which the Poisson process plays a role," *Bull. Am. Math.* Soc., 70, 264-268 (1964).

[5] B.Kaulakyas,and M.Alaburda,*J.Stat.Mech*.P02051 (2009).

[6] B.Kaulakys, J.Ruseckas,VGontis and M.Alaburda,Physica A 365,217(2006)

[7] Klesnik,a.(1998):The equations of Markovian random evolution on the line ,*J.Appl.Prob*. Vol.35,pp27-35.

[8] Krishnakumar.B, Parthasarathy.P.R and Sharafali,M(1993)Transient solution of an M/M/1 queue with balking ,queueing system(Theory and application) vol13 pp441-447.

[9] HARRIS, T. E. (1968). Counting measures, monotone random set functions. 2. Wuhr. 10 102-119.

[10] D. J. Higham, An algorithmic introduction to numerical simulation of stochastic differential Equations, *SIAM Review* 43 (2001), 525546.

[11]. M.Reni Sagayaraj, S.Anand Gnana Selvam, R.Reynald Susainathan, "A Study on Random Evolution Associated with a M/M/1/∞ Queueing System with Balking" The *International Journal Of Science & Technoledge (*ISSN 2321 – 919X), Vol. 2(5), May 2014.PP130-132.

American Journal of Engineering Research (AJER) 2015
American Journal of Engineering Research (AJER)
e-ISSN: 2320-0847 p-ISSN : 2320-0936
Volume-4, Issue-8, pp-41-54
www.ajer.org
Research Paper Open Access

Study and Evaluation of Liquid Air Energy Storage Technology For a Clean and Secure Energy Future

Challenges and opportunities for Alberta wind energy industry

Hadi H. Alyami[*1], Ryan Williams[*2]
[1] *School of Electrical and Computer Engineering*
[2] *School of Business*
[*] *Faculty of Graduate Studies and Research*
University of Alberta, Edmonton, Canada

Abstract: *Global energy demand is steadily increasing each year. Many jurisdictions are seeking to incorporate sustainable and renewable energy sources to help meeting the demand and doing so in a responsible method to the environment and the next generation. In a wide-context, renewable energy sources are promising, yet cannot be controlled in such a way that is responsive to energy demand fluctuation. Liquid Air Energy Storage (LAES) technology seeks to bridge the gap that exists between energy supply and demand in an effort to mitigate the current demand deficiency. The volume ratio of air to liquid air is nearly 700:1. Liquid air is a dense energy carrier that is by converting renewable energy at off-peak periods into liquid air the energy can be stored until a peak-demand period when energy producers are maximising output to meet the demand. The energy is then retrieved from the liquid air through rapid expansion as it re-gasifies through a gas turbine and converted into electricity. A commercial scale pilot plant in Slough, UK illustrates the application of this technology empirically. The application of this technology in Canada might have challenges as public policy respective jurisdictions play a role. A case of point of applications where LAES can be integrated is the renewable energy market; particularly the wind power in Alberta. This paper's analysis embraces wind power industry in Alberta from the perspective of both the electric system operator and the power generation plant. As such, it serves as an alleviating proposal of the current wind energy issues in Alberta – including the uncertainty of forecasting system. The analysis assumed energy storage technologies as a viable stand-alone mitigation with no consideration of the current technological and operational advancements in power systems such HVDC grids, distributed generation concepts and among others.*

Key Words: LAES technology, Wind power in Alberta, Power shifting, LAES arbitrage opportunities, Energy demand.

I. Introduction

Power energy is a key element of the modern life that is usually taken for granted in many developed nations. This paper's motivation is to accelerate the flexibility of the current base-load facilities toward a future of power energy where production can more easily meet demand peaks without the use of peak-load facilities. Therefore, the major motivation for LAES technology deployment is enabling more efficient utilisation of existing base-load facilities via load-levelling demand response technique and renewable-based energies integration. LAES system is among the best energy storage technologies and can be readily deployed anywhere in which air is available [1], [2].

At present, power grids operate in a momentary-time strategy that matches instantaneous supply with instantaneous demand. This strategy serves the power grid well; however, the aspiration to eliminate GHG emissions through the integration of renewable energies introduces critical challenges that affect the momentary-time strategy [3], [4]. Renewable energies, also referred to as variable generation, are variable and intermittent in nature for which their power outputs fluctuate and are difficult to predict. As a result, in the last two decades, the need to deploy energy storage systems as a vital component of the future power grid that incorporates more renewable energies has been rapidly growing [5].

1. Background

I. Demand for Energy Storage Systems

Energy storage systems have been adapted to numerous small-scale, low-powered apparatuses and to large-scale, high-powered systems. Although they are mature in low-powered (less than a few kW) applications, technical and economic obstacles still exist for high-powered applications (more than $1MW$) [6]. The evolution from variable generations to stochastic generation, the resurgence of micro-grids as essential component in distributed grid construction, the gradually strained infrastructure of transmission systems as new lines lag behind power demand, and the necessity for growth in the security and reliability of power supply are all emerging grid technological advancements whose operations will stimulate the need for energy storage systems [7], [8]. Fig. (1) illustrates the benefits of energy storage systems to the emerging technologies in the electric power grid industry.

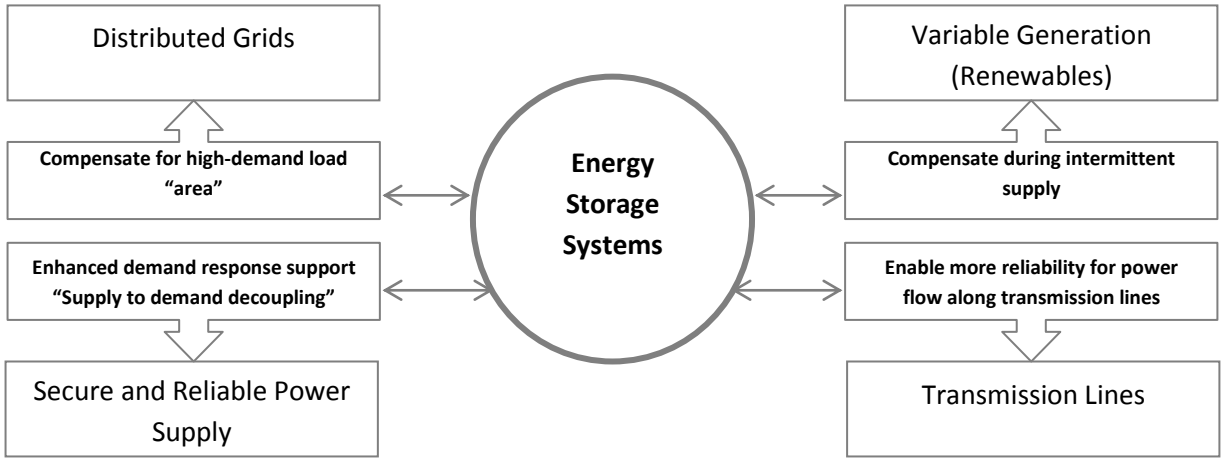

Figure 1: Factors for grid energy storage systems

In stationary applications, energy storage systems play a major role in the overall reliability of the power grid system [9]. The power supply-to-demand needs must be precisely balanced so that as the natural fluctuation of power demand increases or decreases, the power supply compensates accordingly. However, it is reported in [10] that power demand is fairly stable to some extent and only varies considerably during a short period relative to the annually-operated power grids. This means power grids must be designed to satisfy peak demands that only last for short durations [5], [11]. Thus the power grid's capacity is utilised optimally. Instead, the excess power can be stored during off-peak demands and released back when demand returns. Therefore, energy storage systems can serve as a penance for which the power supply can be decoupled from power demand, thereby ensuring higher security and reliability. Power supply-to-demand decoupling can also significantly reduce power costs, as dissipated power is lower, allowing more renewable energy deployment, which is in fact the main driving force behind the development of power storage systems.

II. Energy Storage Technologies in Electricity Network

Energy storage technologies are not recent advances but comprised the plethora of 18^{th} century discoveries, for instance, the gasoline-filled tank in vehicles and airplanes [14]. In pumped-hydro storage (PHS), an example of a stationary application that put into use since the 1990s, water is pumped overnight into a high reservoir and released during the day when demand peaks [9]. However, energy storage technologies have only gained serious

attention over the last decade when the electricity industry became more complex; as a result of the integration of renewable energies, the spanning of long distances by transmission and distribution systems and the steady increase in power demand. Therefore, due to the prevalent introduction of electric power, energy storage systems became a major factor in economic development. A case in point is that electricity must be consumed as it is being produced, otherwise, it will be dissipated as heat if not promptly stored [15]. In general, electric power can be effectively converted into potential, kinetic or chemical energy forms. Each form has different requirements and is suitable for certain applications and systems. The potential of electric energy storage is complicated by the fact that the wide range of storage technologies are either already commercialised, in development or under examination, from which the selection among the various technologies will be critical. Energy storage systems can be classified based on their stored energy form and their tangible functions [4], [7]. In terms of tangible functions, these technologies can be classified based on their power ratings and storage durations as shown in Fig. (2).

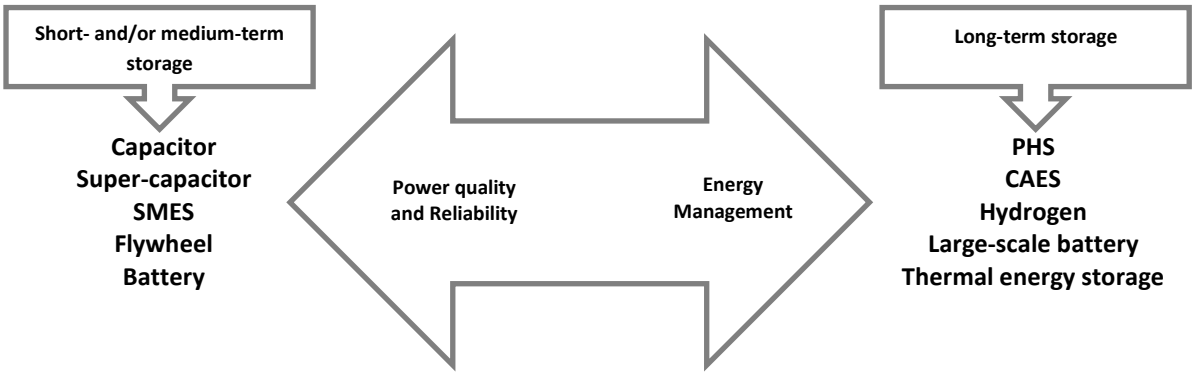

Figure 2: Evaluation of energy storage technologies

In terms of power quality and reliability, energy storage systems should be cap able of responding to power demands on a momentary basis without the need of continuous discharge at any given time, whereas in terms of energy management, energy storage systems should be capable of shifting bulk amount of power over long periods of time (hours and days) [16]. Technologies within the energy management category can be deployed as either Demand Side Management (DSM) for electric and thermal loads, or Supply Side Management (SSM) for reliable and economic power supplies [16].

Pumped-hydro system (PHS), compressed air system, and sodium sulphur and lead acid batteries are currently the most widely considered storage technologies [3]. They are mature and reliable technologies; nevertheless, they still offer some challenges, including geographical requirements and risks for PHS and the underground compressed air system as well as the usual high cost and low power density of batteries. Liquid air energy storage (LAES) is an emerging power storing technology that could play a major role in storage systems development.

III. Liquid Air Energy Storage Technology

The philosophy that air could be turned into an energy vector, or "energy carrier", dates back to the 1900s, when the US company, Tripler, attempted to establish a simple liquid air-driven vehicle that competed with the electric and steam vehicles [2]. However, the emergence of the internal-combustion engine, along with the required inefficient and bulky external heat exchanger for the liquid air-driven vehicle has decelerated liquid air technology development [18]. This was not until the beckoning of the 20th century when serious interest in liquid air technology or cryogenic energy in general was rekindled. This technology thus expanded to include stationary systems, besides automobile applications, where it has found great acceptance [19].

In 2001, P. Dearman established and patented the Dearman-engine, whose operation is based upon vaporised liquid air inside an engine cylinder utilising heat obtained through a thermal fluid mixture of antifreeze and water [20]. This led to eliminating the necessity for the external inefficient, bulky heat

exchangers of traditional liquid air engines. In 2006, the Highview Power Storage Plant, the first plant incorporating liquid air "nitrogen" as an energy storage carrier in the world, developed Dearman's insight into a grid-scale ($25MW$) energy storage system [10]. The remarkable success of the Highview Power Storage Plant has brought great interest in the technology particularly for large-scale storage applications.

Air can be liquefied when its temperature is reduced to $-195℃$ using standard industrial mechanisms – compressors, heat exchangers and turbines [10]. The air liquefaction process is illustrated in Fig. (3).

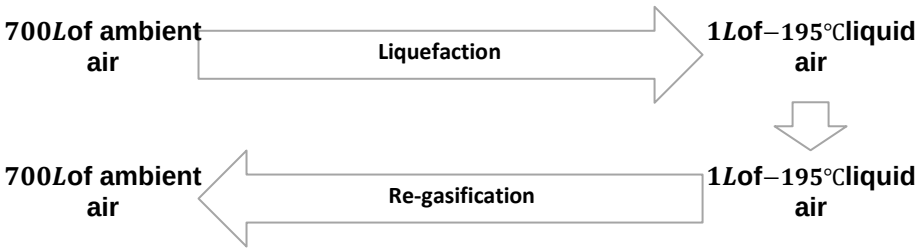

Figure 3: Air liquefaction process

It is clear that through liquefaction,$700L$ of ambient air can yield $1L$ of low-temperature liquid air, which can therefore be stored in an unpressurised insulated tank. When heat is re-established during re-gasificationto the stored liquid air it expands 700 times in volume. This expansion is capable of spinning a turbine to generate electric power via an electric generator. Air mainly consists of nitrogen (78%), and oxygen (21%), among other gases, which can be separated, as they liquefy at different temperatures (nitrogen at $-195℃$ and oxygen at $-182℃$). An air separation unit is used for this purpose [21]. Air is firstly cleaned from contaminants, such as CO_2, using dust filters, and compressed to 6 bars. The compressed air is then refrigerated to 16℃. Water and CO_2, which are produced at this stage, need to be removed in a process called adsorption, otherwise they would freeze and block the pipes [21]. The partially cooled air is then extremely cooled down to liquefaction temperatures and then passed through a heat exchanger. The super cold air (below $-150℃$) is now separated in a manner in which the liquid settles to the bottom and gas rises to the top. When the temperature decreases to $-182℃$ oxygen liquefies, as does nitrogen when the temperature decreases to $-195℃$. Accordingly, they can be stored in an unpressurised insulated tank. The amount of liquefied nitrogen is almost four-fold greater than liquefied oxygen; this attribute provides more credibility to the liquefied nitrogen. Therefore, a new method, called "Frond-end", is developed in which air can be turned directly into liquefied nitrogen. Liquefaction methods, which have developed rapidly, can be categorised as Cascade Cycle, Mixed Refrigerant Cycle (MRC) and Expander Cycle. Cascade cycle and MRC incorporate throttle valves with mixed refrigerants for the production of cold whereas expander cycle employs compression and expansion equipment with gas-phase refrigerant to produce cold [7]. The liquid air energy storage cycle consists of three main components charging, storage and discharging, which are in fact three physically varied components that can be independently sized. From the charge to the discharge cycles, cryogenic energy is captured, stored and recovered [10].The schematic diagram can be simplified for analysis as shown in Fig. (4).

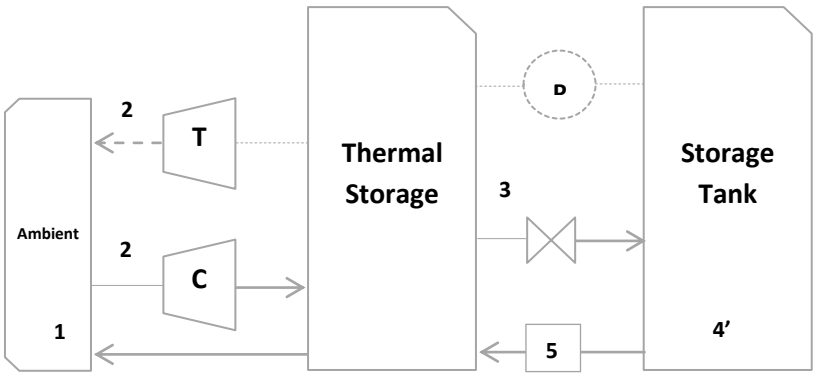

Figure 4: Simplified schematic workflow diagram of LAES

The net-work recycled during compression work "discharging" during charging is known as the round-trip efficiency, which is expressed as [13]

$$\eta = y\frac{(w_t - w_p)}{wc} \quad (2)$$

where: y is the mass of liquid produced/total mass (3-4).
w_t is the turbine work (2-1).
w_p is the pump work (4'-3).
w_c is the compressor work (1-2).

At the commercial scale $(8 - 300MW)$, liquid air technology is capable of having a 60%round-trip efficiency [10]. However, harvesting the waste cold during re-gasification can well enhance the efficiency to 80% [13].If gas compression (1-2) and gas expansion (2-1) are assumed as isothermal process and fluid work behaves as an "ideal gas", the main loss in the cycle is due to adiabatic work (4'-3), followed by isenthalpic expansion (3-4) loss [10] ,[16]. This results in incomplete work fluid condensation. The inclusion of the cooling work of the cold recovery (2-3) yields;

$$y = \frac{h_1 - h_2 + Q_r}{h_1 - h_l} \quad (3)$$

where: h_1 is the enthalpy at (1).
h_2 is the enthalpy at (2).
h_l is the enthalpy at (4').
Q_r is the enthalpy recycled during discharge for cold recovery.

$$Q_r = h_2 - (h_1 + W_p) \quad (4)$$

The isothermal work (1-2) and (2-1) can now be determined from the pressure ration, P_r, of the process, gas constant, R, and temperature, T_1:

$$W = R\,T_1\,InP_r \quad (5)$$

Therefore, from Eq. (2) through Eq. (5), η can be determined as a function of a charge/discharge pressure ratio [8], [20].

The concept behind the LAES system has been successfully validated at a demonstration plant called the Highview Power Storage Plant in Slough, the UK. In 2008, the Scottish and Southern Energy (SSE) Station hosted the idea of the Highview Power Storage Plant during which time the pilot plant was built on a scale 70 times larger than the $5kW$ lab-scale [10]. The plant was fully commissioned in 2011 with a storage capacity about $300kW/2.5MWh$. In 2014, the Highview Power Storage Plant was awarded £$8M$of funding from the British government to further increase the storage capacity to $5MW/15MWh$. Much of the gas and electricity industry technologies can be transferred to the liquid air system; therefore, the Highview Power Storage Plant is built from mature and widely employed equipment. However, equipment combined in a novel design called a Cryo-Energy System, or Liquid Air Energy Storage system [10]. The system can be divided into three main components – a charging cycle, power storage and discharging cycle. First, excess power from the nearby SSE station is harvested to power the air liquefier (Air Separation Unit) to convert air into liquid. The resulting liquid, which is the energy carrier, is hence stored in the storage tank at $-195℃$. When the demand at SSE station peaks, the liquid air is obtained from the storage tank and pumped to ambient temperature into a heat exchanger, where the liquid turns back into highly pressurised air. Accordingly, this air is utilised to spin a turbine and electric generator, which supplies the electric power back to the SSE station. The duration for the system to deliver the power back takes only $150sec$, which is promising for applications requiring a fast recovery response [10].

II. LAES Concept Evaluation

I. Energy Storage System for Electric Grid and Renewable Energy

At present, power grids operate in a momentary-time strategy that matches instantaneous supply with instantaneous demand [1]. The global demand for electric power is steadily increasing2% annually, posing a challenge for the power grid to satisfy this ongoing demand. The emanation of the increasing demand is mainly from commercial, industrial and domestic end-users, where demand is constantly changing as a product of time [17]. The penetration of variable generation (renewable energies)exacerbates the momentary-time strategy further because not only do power demands currently fluctuate, but also the power supply. If power demand exceeds power supply, or vice versa, the frequency of this imbalance increases or decreases, causing great instability in the power grid system [18]. Thus, power storage technologies can provide vital opportunities in bridging the future gap between the increased power demand and the power supply. *Power-shifting* and *Time-shifting* are two main opportunities that can decarbonise and secure the future of power energy.

The practice of managing electric power supply and demand so that power during off-peak periods is shifted to power during on-peak periods is the principle behind the power-shifting strategy [22]. On average, power grids operate at a capacity of 40% below their maximum due to on-peak periods lasting only a few hours a day during which time the power grid operates at higher capacities to satisfy the demand [8]. However, if the excess power during off-peak periods is stored and delivered back during on-peak periods, the power grid can exploit its capacity more efficiently. Even if the power demand or on-peak power increase, the power grid does not necessarily increase its capacity to meet only a few hours of demand. Instead, it can use the stored power. Similarly, renewable-based energies can greatly benefit from energy storage technologies where intermittency and unpredictability are met through absorbing excess power when resources are available, (when the sun is shining and wind is blowing), and delivering it back when it is needed,regardless of weather conditions.

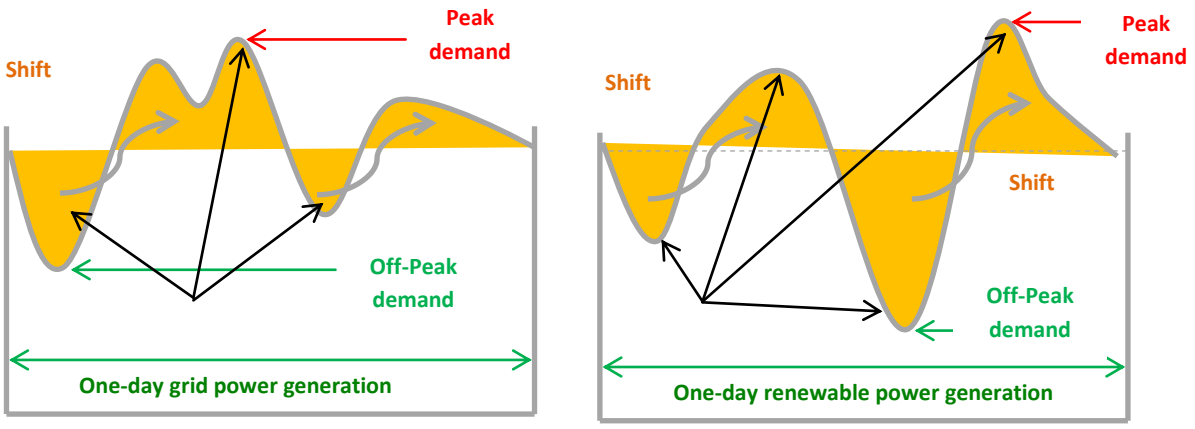

(a) (b)

Figure 6: Power generation fluctuations for (a) grid and (b) renewable sources

Fig. (6) exhibits the principle of shifting excess power based on the demand. In Figure (6-a) the pattern illustrates the normal operation for a power grid during a one-day period, while Figure (6-b) illustrates the fluctuation of a renewable power energy operation. It is evident in both cases how a power-shifting strategy can play a major role in the power generation industry, particularly if a great fraction of the power generated derives from renewable energies [22].

The time-shifting strategy is related to the electricity market, rather than to the electric power operation. It allows taking advantage of the benefits of the differences in wholesale electric power prices over the course of a daily period. It is also known as “energy arbitrage”. Power storage systems can be implemented to achieve this strategy via storing electric power when prices are low and releasing it for sale when prices are higher [20]. This reflects the prices during on-peak and off-peak periods. Time-shifting is even more effective in deregulated markets, such as Alberta’s electricity market where prices vary based on the power demand. Likewise, it is mostly beneficial for renewable-based plants where the prices vary as the power demands from the power grid vary [22].

II. Wind Energy in Alberta

Alberta Wind Energy has grown from 563 MW at the end of 2009 to 1088 MW at the end of 2013 and plans to add an additional 1800 MW by 2020. Currently 4% of the power generation within Alberta comes from wind energy, even though 8% of installed capacity is at wind projects. Lifting of the cap placed on wind power has increased the proportion of wind power in the electricity pool. Coal power still dominates power production in Alberta. Wind power can be integrated with viable energy storage systems to increase reliability of wind power and increase flexibility with fluctuating demand. Barriers exist for energy storage systems' widespread adoption. Key barriers to that adoption are competitive cost, validated performance specifications, regulatory uncertainty, industry acceptance [23]. Costs are typically too high for energy storage systems to make them feasible for grid scale application. Especially when we compare the cost of established production methods that compete for the same dollars. Many of the storage technologies have not been around long enough to validate the claims made by the manufacturers. For instance, a battery manufacturer may claim 30 years of high efficiency charging and discharging but if the technology has only been around for 2 years how is that information validated. Another key barrier is regulatory and uncertainty as governments have yet to adapt to these new technologies industry is uncertain of how they will be regulated. This uncertainty prevents adoption. Lastly, industry acceptance prevents widespread adoption of energy storage technology. Industry must have confidence in the products before investing the time and money into these storage technologies. In order for a storage technology to gain widespread adoption it must overcome these main obstacles.

III. Deployment Potential

This suggests the potential benefits for employing power-shifting and time-shifting strategies for the electricity industry in Alberta, Canada through the use of a storage system namely LAES. Alberta Innovates Technology Future (AITF) has already suggested a number of mature storage technologies from which the Alberta electricity industry can incorporate in the future. However, LAES technology was not on the list; therefore, a critical comparison between the listed technologies and LAES technology was conducted in order to exhibit how LAES technology is able to compete.

I. The Liquid Air Energy Storage System for Alberta Wind Energy (Power-shifting)

Coal and gas are currently the main fuels used in Alberta electricity generation, accounting for 82% of its capacity in 2013 [4]. Hydropower has until recently comprised the next source of Alberta's electricity generation capacity, but it is almost surpassed by wind power. Alberta has excellent wind resources, with an over 1,468 MW of installed capacity as of Sep. 2014. It is even expected to grow rapidly by1,800 MW by 2020 [22]. However, the intermittent nature of wind power exists as an obstacle for its wide penetration into the electricity market in Alberta.

At present, Alberta wind power projects only predict the available wind power to Alberta Electric System Operator (AESO) through a complex forecasting system managed by Alberta Wind Power Forecasting Projects. However, this does not ensure a superior correlation between the forecasted wind power and the actual generated wind power. The use of this forecasting system is somewhat unreliable because a critical difference may occur between the forecasted and actual wind powers upon which the AESO may suffer from system instability and/or the skyrocketing of power prices. A power-shifting strategy can provide a superior penance to mitigate this uncertain challenge through which LAES technology can be deployed. The correlation data between the wind power forecasts received from the Alberta Wind Power Forecasting Projects and the measured "actual" wind power production for the month of January, 2014 are plotted in Fig. (7). Data source is attached in Appendix (A).

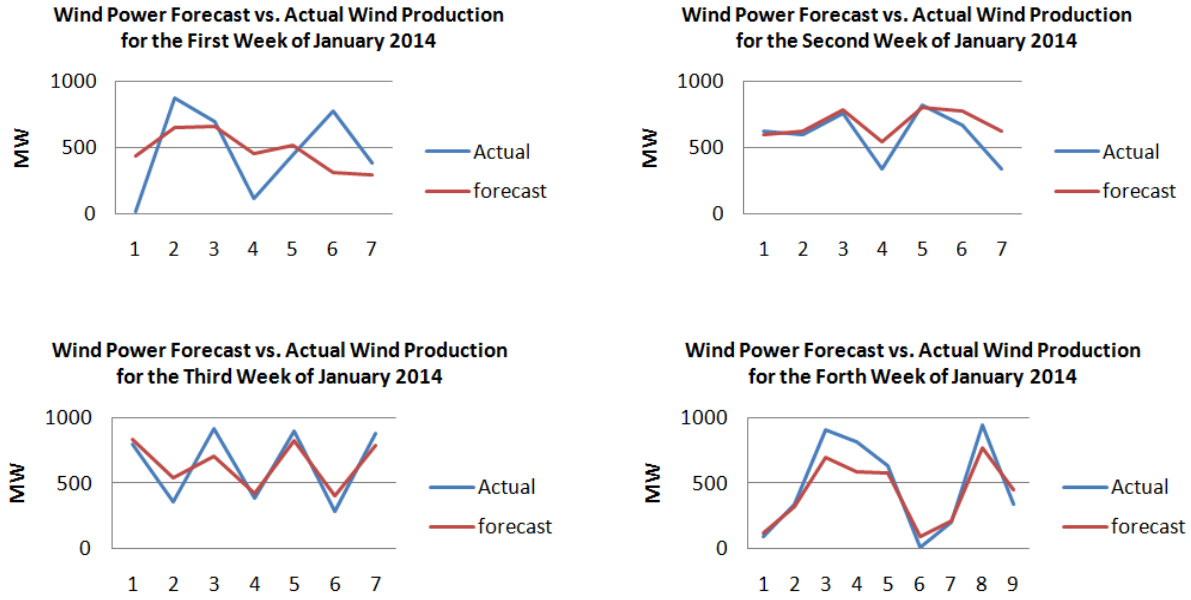

Figure 7: Wind power forecast comparison to actual production for the weeks of January 2014

II. Energy Storage Technologies Compared to LAES Technology

Energy storage technologies in Alberta have been examined in conjunction with wind power production by the AESO and AITF. In collaboration with the AESO, the AITF conducted a study in 2011 on adopting energy storage technologies to support the dispatch of Alberta wind projects. A number of mature storage technologies were suggested for the future of wind power energy in Alberta, discounting LAES. Nonetheless, the maturity of LAES is promising based on the Highview Power Plant know-how. The inherent feature of LAES is summarised in Table (1).

Table 1: Comparison of the most mature energy storage systems to LAES

Technology	Size Range (MW)	Efficiency (Round-trip%)	Geographical Requirement	Maturity
Pumped Hydro (PHS)	> 280	75-85	Mountains/ reservoirs	Commercialised and widely deployed at scales up to a few GW.
Compressed Air (CAES)	Up to 290	45-48	caverns	Demonstrated via two plants in operation up to 290MW.
Sodium Sulphur Batteries (NaS)	< 40	60 experienced for whole system; 80 at cell level	None	Commercialised and most widely deployed battery in stationary applications at scales up to 32MW.
Lead Acid Batteries	Up to 20	65-80 (conventional); 85-90 (advanced)	None	Commercialised in conventional form, deployed up to 20 MW scale; piloted to commercial in advanced form.
LEAS	10 -200	55-85 (depending on thermal waste recycle)	Air	Demonstrated via a pilot plant in operation up to 25MW.

IV. Discussion

I. Liquid Air Energy Storage Systems for Alberta Wind Energy (Power-shifting)

Alberta has energy-only wholesale markets, governed by the AESO whose main responsibility is ensuring the reliability of the electric power supply and establishing an hourly real-time price for electric power. Prices vary with higher prices occurring during on-peak demands. Thus, if the power demand is greater than the available power, the prices for "power generated at that time" increase. In other words, the larger the gap between the power demand and the power supply, the higher the prices and the greater the uncertainty of the AESO. Presently, wind power has attracted serious attention in Alberta, with plans to reach 1,800 MW by 2020; however, this will further exacerbate the uncertainty in the AESO spanning the gap between power demand and power supply. In 2006, the AESO imposed a 900 MW cap on wind power. The cap was lifted in late 2007 after the AESO lunched a wind integration initiative which suggested an energy storage solution to mitigate the intermittency of wind power generation. The wind integration initiative also suggested that the Alberta wind power projects submit firm offers two hours prior to delivering their electric supply. A firm offer that "Must Offer Must Comply" (MOMC rule) adopted by the AESO would challenge the Alberta wind power projects in which they currently only predict the available wind power via a complicated forecasting system. The system uses near real-time meteorological data at wind power sites to indicate the amount of wind power that will be available to the Alberta grid system in the near-term. Although the MOMC rulehas not yet been applied to Alberta wind power projects, they are required to submit a 12-h ahead wind power forecast so that a rough estimate of the available wind power is obtained. Wind power is highly variable, possessing the ability to rapidly ramp up or down and which may be in the opposite direction of load patterns, all of which make predicting wind power and maintaining the reliability of the power system even more challenging.

Alberta wind power projects submit offers based mainly on previously forecasted wind power for which delivery of that amount of power could be a challenge due to wind power variations. However, if an LAES system was installed, offers can be more easily satisfied due to applying a power-shifting strategy. For example, if the actual wind power is greater than the forecasted wind power, the excess can be stored, whereas when the actual wind power is less than the forecasted, the previously stored power can be released, making electric power delivery more reliable. In Fig. (7), the correlation between forecasted wind power and actual wind power was variable. On days 2, 3, 6 and 7, the actual wind power ranged from $900MW$ to $790MW$, whereas the forecasted wind power ranged from $630MW$to$360MW$. Therefore, the power delivery matched the power that the AESO anticipated to receive. However, on days 1, 4 and 5, the actual power was less than the previously forecasted power in which less power was delivered to the AESO. The AESO now suffers from this uncertainty and needs to promptly bridge the gap between the forecasted and actual wind power. However, this would not be the case if a LAES system was installed because the excess power generated during days 2, 3, 6 and 7 could be stored and then shifted to days 1, 4 and 5 when needed. The schematic operation of LAES technology in supplementing Alberta wind power energy can be depicted in Fig. (8).

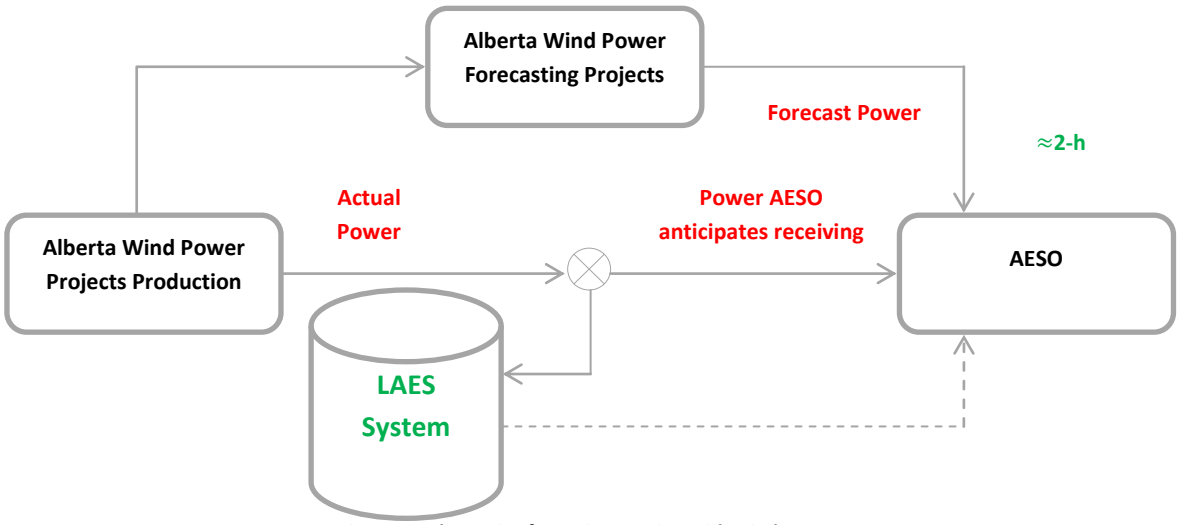

Figure 8: Schematic of LAES integration with wind power

When the actual wind power is less than the forecasted wind power, the difference can be drawn from the power previously stored, whereas when the actual wind power is greater than the forecasted wind power and the AESO cannot absorb the difference (during off-peak periods), the excess power can be then stored (otherwise it is lost). In this regard, wind power projects in Alberta benefit from storing the power generated at the "wrong time" and the AESO benefits from being more certain about the available wind power.

It is clear in Figure (7) that a power-shift strategy will be instrumental for Alberta wind power projects mitigating forecasting system uncertainty. Similarly, for other plots, the forecasted and actual wind powers correlated for some days but not others.

II. The Technical Maturity of Liquid Air Energy Storage Technology

- *The Required Equipment*

Much of the power generation industry, turbo-machinery and gas sectors equipment can be transferred to LAES technology in which all the used equipment is advanced – including compressors, a cold box, and storage medium. This should makeLAES more attractive to Alberta wind power projects compared toNaS and lead acid batteries, which deploy new cells and chemistry techniques requiring long validation periods. Although PHS utilises mature equipment, the hydroelectric nature of the system suffers from the drawback of having long construction times (normally 8-12 years) and requiring large physical land features (mountains). A gas turbine is also a crucial mechanical component in PHS whose operation costsare high because of the use of expensive gas/oil ($\sim 300 g/kWh$). CAES eliminates the gas turbine deficiency in PHS through the employment of a modified gas turbine (turbo-machinery); nevertheless, its usage of a CAES cavern poses a technical challenge. The pressure in a CAES cavern varies during charging and discharging cycles which increases throttle losses between compression and expansion equipment. LAES has the benefit of gas turbine removal and the pressure in the system is independent and can be kept consistent during any operation cycles (charging, storage, discharging). The round-trip efficiency is promising and can be depicted as shown in Fig. (9). It is clear how the round-trip efficiency can be increased with cold-waste recycle.

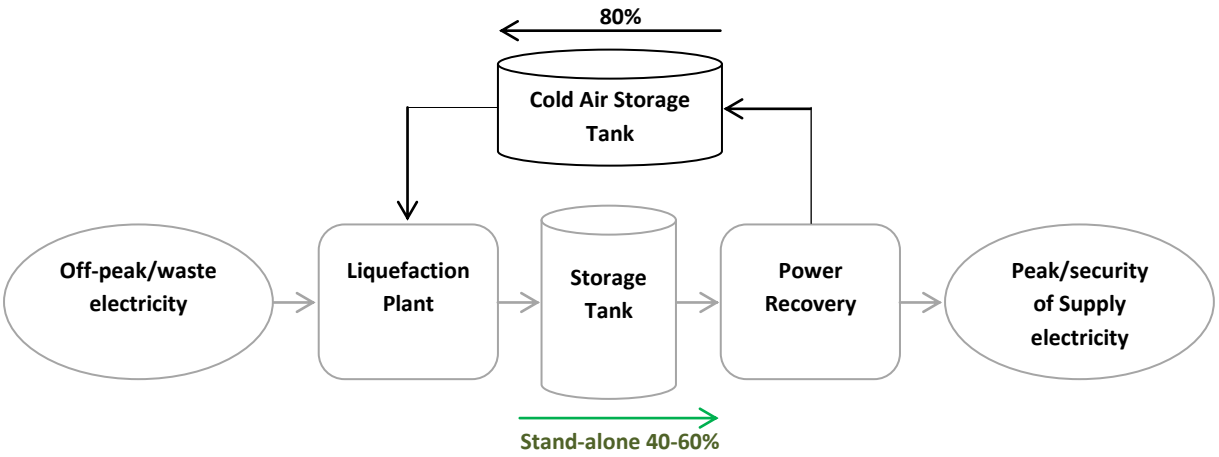

Figure 9: Round-trip efficiency of LAES with and without cold-waste recycle

- *Power Rating and Response Time*

In Alberta wind power projects, PHS, CAES and LAES are more applicable than batteries due to their low power ratings, as shown in Table (1). Thus, batteries are not suitable for large-scale stationary applications. Although PHS and CAES have higher power capabilities than LAES, their response times are inappropriate for Alberta Wind power projects. It is essential that if the forecasted wind power is less than the actual wind power, compensation made promptly to avoid power demands to supply gap issues. LAES technology can be in full operation to supply the stored power in $150 sec$ only.

- *Storage Duration and Self-discharge*

Alberta wind power projects would greatly benefit from a storage system that is capable of storing excess power on an hourly basis. This is because Alberta has energy-only wholesale markets, governed by the AESO whose main responsibility is ensuring the reliability of electric power supply and establishing an hourly real-time price for electric power. Therefore, the AESO requires electric power on an hourly basis. In this case, all the listed technologies in Table (1) are well suitable, except the NaS battery, which has a storage time on a second basis. Self-discharge percentages in all the listed technologies are minimal; nevertheless, LAES technology seems to have the highest self-discharge rate of$0.5 - 1\%$. However, this is not a serious drawback for Alberta wind power projects though, since charging and discharging occur repeatedly based on the gap between forecasted and actual generated wind power.

- *Geographical Requirement*

Most of the wind power projects in Alberta are clustered in the southern region of Alberta, as shown in Fig (10), which lacks mountains for which PHS technology is not applicable. CAES also requires complex underground construction as well as caverns, which are considered geographical limitations. However, LAES technology only requires air and excess power for which it is deployable globally with a minimal footprint and very little restrictions.

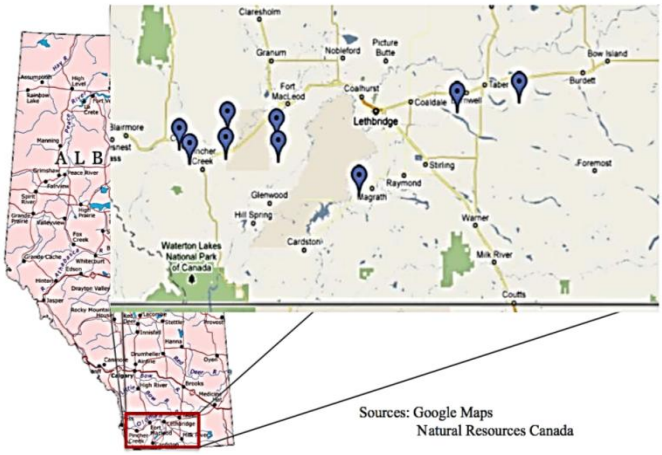

Figure 10: Map of wind power projects in southern Alb Natural Resources Canada]

Two different cases were considered for adoption of LAES technology in the electricity production sector. One case from the perspective of AESO and the other case from the perspective of a wind power electricity producer. Each scenario illustrates different needs that LAES can provide.

III. LAES for Firming Electricity Production

From the perspective of AESO, it is predictable electricity production that is most pivotal for market economics to maintain reasonable production bids. Dealing with fluctuations from renewable energy technologies can present a great challenge for the Alberta System Electricity Operator that must meet the instantaneous electricity demands of consumers. Unexpected outages can create limit the supply of electricity to which pushes bid prices toward the ceiling of $1000/MWh. In 2013, the system marginal price (SMP) exceeded $990/MWh for 53 hours [. These unexpected outages do not come only from wind power facilities but there is a strong negative correlation between high bid prices (over $500/MWh) and wind power production shown implicitly These periods can be very costly for AESO and in turn the province of Alberta.

Use of LAES systems would assist technologies with intermittent production concerns such as wind power to firm up offers to the grid and create better reliability of their electrical production. Table (2) illustrates the annual contribution of wind power in Alberta as compared to the other sources of electricity generation.

Table (2). Pool price range of electricity by fuel type

Pool Price Range MWh	Contribution to Annual Average Pool Price	Coal	Cogen	Gas	Peaker	Hydro	Wind	Other
$0 to $99.99	$27.59	36%	34%	26%	13%	28%	47%	29%
$100 to $149.99	$3.43	4%	4%	4%	4%	4%	4%	4%
$150 to $249.99	$4.76	6%	6%	6%	6%	5%	6%	6%
$250 to $499.99	$10.26	13%	13%	15%	16%	12%	11%	14%
$500 to $899.99	$18.66	23%	24%	25%	32%	24%	21%	26%
$900 to $1000	$15.49	19%	19%	23%	29%	27%	11%	22%
Average Revenue ($/MWh)	$80.19	$77.25	$83.13	$112.18	$213.59	$98.02	$54.97	$95.85

The average load factor of the overall grid producers is 79.4% of the installed 14,568 MW of capacity. However, for the wind power segment of the installed 1,088 MW only generates 31.6% of its load capacity. Wind power consists of 8% of the electricity capacity by nameplate capacity it only generates 4% of the power. Interestingly, during peak hours in 2013 wind power exhibited a capacity factor of 53%. This means that the capacity in off-peak times is dramatically reduced. Capturing this off-peak capacity using LAES would help make the power assets more efficient and ease grid pressures during peak times if the energy was discharged later.

IV. LAES for Arbitrage Opportunities

The advantages of LAES for firming might not be fully appreciated by an electricity producers as their aim is to generate revenue not ensure adequate power supply for the entire province. LAES does present opportunities to increase revenue from the same assets thus increasing their efficiency and the return on the assets. Wind power in Alberta from the perspective of the electricity producer must consider the best methods to yield the most efficient results as it competes in a deregulated market. Perhaps, in a regulated market, electricity producers would not be as concerned with the timing of electricity production but in Alberta the rate that a producer offers can vary greatly as demand fluctuates throughout the day. The ability to meet instantaneous demand can increase the acceptable bid price. In Table 3, the breakdown of the pool price range for wind and other common forms of energy are compared. Wind only generates half of average revenue per MWh because the power it sells is almost half sold at a price ranging between zero and $100/MWh. Wind power has limited control over when the wind blows and so cannot dispatch power that is not generated. And when it does blow it might not be the busier portion of the day so it is sold at a lower value than a peaker plant has the ability to command a higher price because it can meet the peak load demands that the collective baseload facilities do not have capacity to meet. While the peaker plant may be more costly to operate they are able to generate a price/MWh four times that of wind power. LAES would provide an opportunity to store a portion of the energy currently being dispatched at the $0 – 100/MWh range and store the energy until a much greater bid can be offered and accepted.

By shifting a portion of the power generated at off peak times to the higher demand periods similar to yield an average pool price similar to the gas plants or the peaker plants. This strategy will increase revenue by an upper limit of $330 million for the overall wind production within Alberta. If a single wind project (Halkirk) was considered with a capacity of 150MW. Deploying twenty percent of the lower pool price range at peak times may increase revenues at the site by approximately $10,000,000 per annum. This is does not rely on generating any more electricity from the assets only shifting the existing supply to on-peak windows using LAES. Further revenues could be generated depending on the reason for such a low off-peak capacity factor. As stated previously the on-peak capacity factor is 53% percent while the overall capacity factor for wind is 31.6%. If the off-peak is not being exploited because of the minimal returns, LAES could be employed to store the extra wind energy for release. An additional 20% would be a fair assumption yielding another $10 million dollars in revenue for the Halkirk Project. However, if the off-peak reduction in capacity factor is naturally occurring, for instance, wind patterns reduced at night then this additional revenue would not be recognized.

V. Conclusion

Liquid Air Energy Storage Technology demonstrates great potential for delivering reliable and efficient power when partnered with a wind power project. The key barriers of cost competitiveness, validation of performance specifications, uncertainty of regulations and industry acceptance are best overcome by the potential of LAES. LAES uses existing equipment from the cryogenic and power generation industries. This easily bridges the gap between small scale studies, pilot projects and grid-scale operations as equipment for grid-scale capacity have already been in use and the efficiencies and operating costs are known empirically not just theoretically. This is a great advantage over other competing technologies that would require extensive development for grid-scale operations. Utilising existing equipment keeps costs competitive and provides valid performance and safety specifications. All of these factors will encourage industry acceptance. Industry confidence will lead to the greatest adoption of the technology. The only piece still missing is the uncertainty of regulations. If Alberta specifies regulations standards or includes storage technologies in the same category of power generation then industry would be able to plan accordingly. Also, government partnership would entice private industry to develop this technology further.

Acknowledgment: *Hadi Alyami gratefully acknowledges the financial support of the Ministry of Education in Saudi Arabia.*

References

[1] Paul W. Parfomak "Energy Storage for Power Grids and Electric Transportation: A Technology Assessment" Congressional Research Service; March 2012.
[2] B. Rehfeldt, C. Stiller "Process Engineering and Thermodynamic Evaluation of Concepts for Liquid Air Energy Storage: Liquid Air Energy Storage: A flexible and widely applicable medium-term large-scale energy storage" Hitachi Power Europe GmbH, Germany; 2012.
[3] Yongliang Li "Cryogen Based Energy Storage: Process Modelling and Optimisation" PhD Thesis, University of Leeds, England; 2012.
[4] D. Strahan et al. "Liquid Air Technologies – a guide to the potential" Conference Report; Centre for Low Carbon Futures and Liquid Air Energy Network, ISBN: 978-0-9927328-0-6; October 2013.
[5] R. Morgan, S. Nelmes, E. Gibson, G. Brett "Liquid air energy storage – Analysis and first results from a pilot scale demonstration plant" ScienceDirect, Applied Thermal Engineering: 2014.
[6] Y. Li, H. Chen, X. Zhang, C. Tan, Y. Ding "Renewable energy carriers: Hydrogen or liquid air/nitrogen?" ScienceDirect, Applied Thermal Engineering 30 (2010) 1985-1990.
[7] H. Chen, T. Ngoc Cong, W. Yang, C. Tan, Y. Li, Y. Ding "Progress in electrical energy storage system: A critical review" Progress in Natural Science 19 (2009) 291–312: ScienceDirect; April 2008.
Sean Davies "Grid Gets The Smarts" Power Smart Grid, Engineering and Technology Magazine; May 2012, P. 42-45.
[8] Bob Yirka "Energy companies testing "liquid air" as a means of storing backup electricity" PHYS. Org; 22 May 2013.
[9] E. Heureux Zara "Cryogenic Energy Storage and Residential Demand Response" PhD Candidate, Department of Earth and Environmental Engineering, Columbia university; 2014.
[10] Highview Power Storage: Technology and Performance Review, England; March 2012.
[11] C. Ordonez, M. Plummer, "Cold Thermal Storage and Cryogenic Heat Engines for Energy Storage Applications," Energy Sources, 19:389-396, 1997.
[12] M. Akhurst, L. Aworks et al. "Liquid Air in the energy and transport systems" The Centre for Low Carbon Futures; ISBN: 978-0-9575872-2-9; May 2013.
[13] C. Knowlen, A. Mattick, A. Bruckner and A. Hertzberg "High Efficiency Energy Conversion Systems for Liquid Nitrogen Automobiles" Aerospace and Energetics Research Program, University of Washington, Seattle, WA; 2007: 981898.
[14] M. Conte, P. Prosini, S. Passerini "Overview of energy/hydrogen storage: state-of-the-art of the technologies and prospects for nanomaterials" Materials Science and Engineering B108 (2004) 2–8.
[15] GOV.UK "Increasing the use of low-carbon technologies: Policy" Available from: https://www.gov.uk/government/policies/increasing-the-use-of-low-carbon-technologies#background; accessed on Nov.1, 2006.
[16] B. Byers "Risks Associated with Liquid Nitrogen Cryogenic Storage Systems" Dana–Farber Cancer Institute, Boston, Massachusetts, USA: 1999.
[17] H. Khani, R. Seethapathy "Optimal Weekly Usage of Cryogenic Energy Storage in an Open Retail Electricity Market" University of Western Ontario, London, ON, Canada; 2013.
[18] Y. Ding, J. Yang "UK-China Collaboration on Energy Storage Research: Electrical energy storage using mechanical and thermal methods and integration with industrial processes" MPCS; May 2012.
[19] G. Brett, M. Barnett "Utility-scale energy storage: Liquid air a pioneering solution to the problem of energy storage" Presentation; IET; 2012.
[20] H. Knight "The Power of Cool" Daily Technologies; NewScientists; February 2011.
[21] T. Peters "Liquid Air Energy Storage secures £8M of Government funding for multi-MW demonstration" Liquid Air Energy Network, England; February 2014.
[22] Alberta Innovates Technology Future "Energy Storage making Intermittent Power Dispatchable" Final Report, Vesion1.1; October 2011.
[23] Department of Energy "Grid Energy Storage" U.S Department of Energy; December 2013.

Appendix (A)

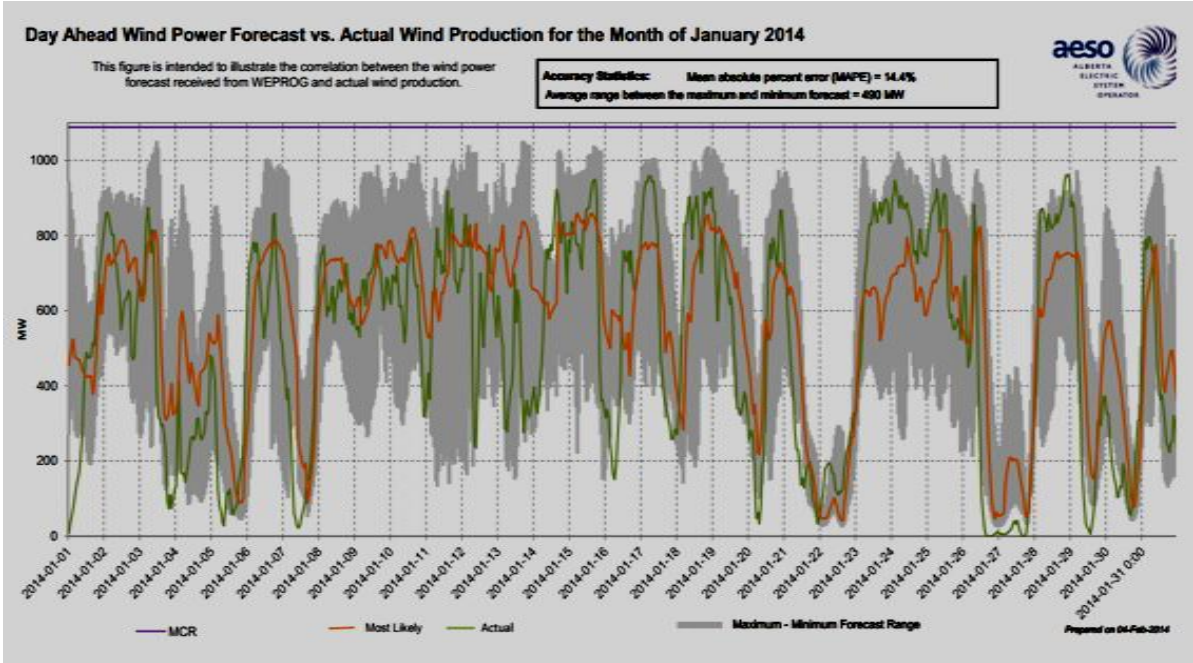

Figure (A) Day ahead wind power forecast obtained from AESO Web-site [2015]

List of Symbols and Acronyms

LAES:	*Liquid Air Energy Storage*
GHG:	*Greenhouse Gas*
ΔE_{total}:	*The total change in energy form*
PHS:	*Pumped-Hydro Storage*
DSM:	*Demand Side Management*
SSM:	*Supply Side Management*
CO_2:	*Carbon-oxide*
MRC:	*Mixed Refrigerant Cycle*
AITF:	*Alberta Innovates Technology Future*
AESO:	*The Alberta Electric System Operator*
MOMC:	*Must Offer Must Comply*
CAES:	*Compressed Air Energy Storage*
SMP:	*The system marginal price*
PEST:	*Political, Economic, Socio and Technical analysis*

American Journal of Engineering Research (AJER)
e-ISSN: 2320-0847 p-ISSN : 2320-0936
Volume-4, Issue-8, pp-55-63
www.ajer.org
Research Paper Open Access

Exploitation of Groundwater in Fractured Basement of Ado-Ekiti, Nigeria

Oluwadare Joshua OYEBODE, KayodeOluwafemiOLOWE,
Sunday Olakunle OYEGOKE, Ekom EDEM
Civil Engineering Department, College of Engineering,Afe Babalola University, Ado-Ekiti, Ekiti State, Nigeria

ABSTRACT:*Groundwater is the most efficient resource for meeting water demand in the basement complex areas. Basement complexes worldwide shared common hydrogeological indicators and the situation in the entire Ado Ekiti is not like to be far from that of Afe Babalola University Ado-Ekiti, Ekiti State (ABUAD).This study examined groundwater exploitation in fractured basement of Ado Ekiti and environs. The scope was narrowed to groundwater supply and potential in ABUAD. Seventeen boreholes have been drilled in ABUAD and yet there is a seeming perennial water scarcity in the University. The data generated in this study could provide benchmarks to unravel the prevailing conditions on groundwater potential and exploitation in fractured basement in the whole of Ado Ekiti and environs. The study revealed that most appealing geologic sequence for good groundwater potential is overburden thickness of ≥ 25m and weathered/fractured basement having resistivity range between 20 - 100Ω-m with thickness ranging between 12 – 30m. Present daily water demand for ABUAD stands at 420,000litres/day and in a decade's time the daily projection is expected to be 934200liters/day. If the University is experiencing water scarcity, it means that all the boreholes put altogether is currently producing below 37% efficiency. The problem probably could be attributed to poor borehole completion operation, 'hanging borehole' and incomplete development. Pumping test is very vital for successful borehole completion and benchmark for future operation and maintenance. Efforts should be geared towards the redevelopment of all the boreholes in ABUAD to increase their efficiencies. Pumping test should be carried out to ascertain the true status of the remaining boreholes. Efforts should only be concentrated in areas designated to have good groundwater potential for new borehole schemes. As a long term measures and also to meet up with the decade's forecast on water demand, dam should be constructed for water supply and power generation.*

I. INTRODUCTION

1.1 Background of Study

Exploitation of groundwaterresources involves apart from the location ofsuitable source, the construction of properlydesigned wells. The design and the execution of water supplysystems and their maintenance is also an integralpart of the scheme of exploitation andmanagement. The common groundwater abstracting structures are dug wells and boreholes and are to be designed to get theoptimum quantity of water eco economically from a given geological formation.

Fractured basement complex are good sources for potable water in many part of the world. However, sitting of highly productive wells in these rock units remains a challenging and expensive task because fracture development at regional scale is both **heterogeneous** and **anisotropic (**Manda et al., 2006). Aquifers can be developed either in weathered overburden basement or fractured basement of crystalline rocks of intrusive and/or metamorphic origin which are mainly Precambrian age (Wright, 1992). Sustainable well yields for bedrock, therefore, may strongly depend on the quantity of water stored in materials that can break downwards into bedrock and on periodic replenishment by recharge (Lyford, 2004). The discontinuous nature of the basement aquifer systems makes detailed knowledge and application of geological, hydro-geological and geophysical investigations inevitable (Amudu et al, 2008). In Ado Ekiti or Ekiti State generally, groundwater is found in fractured basement complex as the State is underlain by Precambrian basement rocks. It is also stated that aquifer found in fractured basement in Ado Ekiti and its environs has relatively very low yield, (Gabriel et al, 2014).

1.2 Statement of the Problem

Perennial water scarcity in ABUAD calls for great concern in spite of untiring efforts of the management in providing not less 17 boreholes water sources. The study intends to unravel the root cause of the problem with a view of proffering the solution. EK-RUWASSA, 2014, reported failure rate in previously drilled boreholes in Ekiti State to be around 54%. Reasons advanced for this were probably due to lack of detailed hydrogeological and pre-drilling geophysical investigation or poor understanding of hydro-geological characteristics of the basement complex environment which could probably give rise to improper exploitation framework of groundwater in fractured basement.

1.3 Aim of Study

The aim of this research is to determine sustainable groundwater exploitation in fractured basement complex of Ado-Ekiti.

1.4 Objectives of Study

The specific objectives are:

(i) To re-appraise geophysical investigations carried out in all the boreholes in ABUAD.
(ii) To determine if the boreholes were drilled and constructed in accordance with the result of the investigation.
(iii) To determine aquifer characteristics, draw down, yield, specific capacity, recovery, efficiency of the borehole, pump sizing, etc.
(iv) To determine if all the boreholes in ABUAD put together can guarantee the expected water demands under a given pumping duration per day.
(v) To determine if the boreholes are sited in a way to avoid interference during pumping.
(vi) To determine the estimation of borehole efficiency or variation of in performance with a discharge rate;
(vii) Determine the measurement of transmissivity, storativity and hydraulic conductivity;

1.5 Justification of Study

It is hoped that this study would reveal the level of groundwater exploitation in fractured basement complex in Ado-Ekiti and highlight areas of concern. The research is also intended in a way to improve the analysis and decision support on groundwater exploitation in fractured basement complex in Ado-Ekiti. This research would undoubtedly be the most in-depth studies on the exploitation of groundwater in fractured basement complex in ABUAD in particular and Ado-Ekiti in general.

1.6Scope of Study.

In this study only boreholes data in Afe Babalola University, Ado Ekiti (ABUAD) will be considered in coming up with a generalized sustainable groundwater exploitation in fractured basement of Ado Ekiti. This phenomenon more or less calls for in-depth hydrogeological and geophysical studies to evaluate these conditions.

1.7 Study Area

Ado-Ekiti is located between latitude $7^0$31 and $7^0$491 north of the equator and longitude $5^0$71 and $5^0$71 east of the Greenwich Meridian. Afe Babalola University is located in Ado-Ekiti along Ijan road, opposite The Federal Polytechnics. The study college is located at the north-western part of the University campus opposite Alfa Belgore Hall and adjacent female hall of residence. It lies at longitudes 5°18'25.87"E and latitudes 7°36' 23.82"N. The terrain in the study area is gently undulating, with topographic elevation ranging from 350m to 370m above sea level. ABUADis located on 130 hectares at an altitude of 1,500ft above sea level which *ipso facto* provides a cool and ideal climate for learning, sporting activities and commercial agriculture (Oyegoke and Oyebode, 2014).

1.7.1Population and Demography of study area

Ado-Ekiti is inhabited by the Yoruba of South Western Nigeria.According to 2006 census the population is about 308,621 inhabitants (Ekiti State Government Portfolio);the increase has made people in the town to depend on sub-surfacewater to compliment the pipe borne water which is always neversufficient.

1.7.2Hydrogeology of Ado-Ekiti

The major surface waters in the study area are rivers Ogbese, Osun, Oni, Osse and Ero. Others are the small tributaries joining the major rivers. It has been observed that wells dug close to the river normally contained water at shallow depths Shemang, (1990). Within the weathered zone, discontinuous water table occurs and

water level shows marked seasonal fluctuations Dan-Hassan (1993). As shown in plate 1, The highest groundwater yield in basement terrains is found in areas where thick overburden overlies fractured zones OlorunniwoandOlorunfemi (1987); Olorunfemi sand Fasuyi (1993).

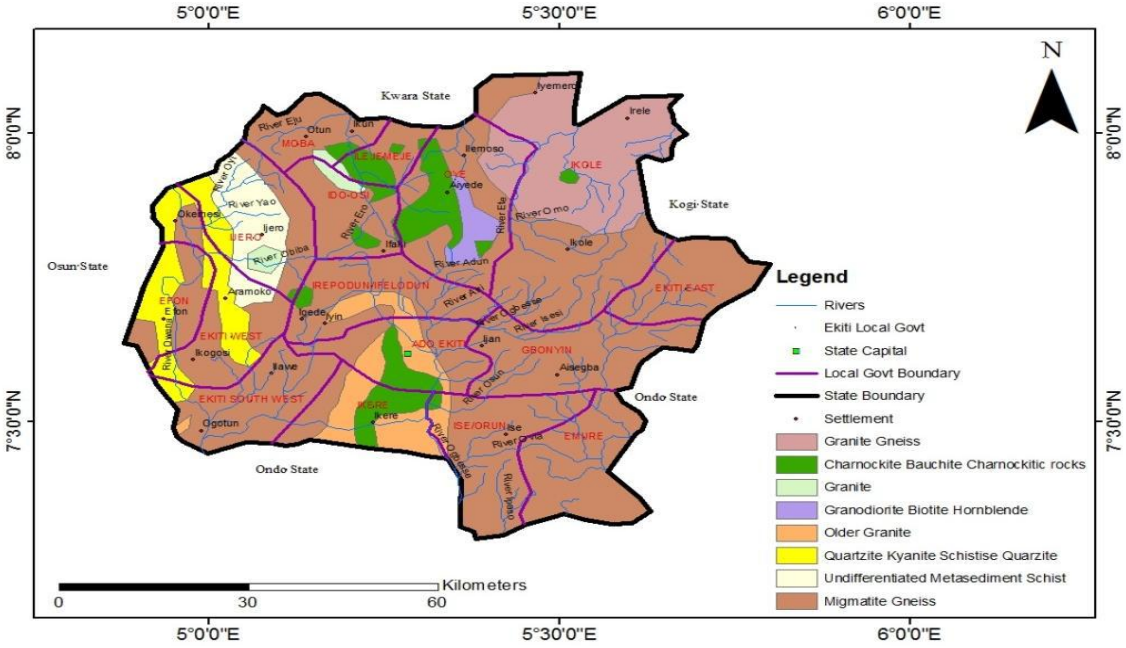

Plate 1: Hydrogeology of Ado-Ekiti

II. METHODOLOGY

The research methods adopted for the study against the backdrop of the research aim and objectives are Water demand determination, Reappraisal of Geophysical Survey, Pumping Test, Recovery Test, Constant Rate Test and Analysis.

2.1 Water Demand (WD) Determination

From the reviews it is observed that per capita and population method is favoured in developing countries like Nigeria in the computation of WD. NWSSP (2000) gives credence to this method hence this work will adopt the method in computing water demand for ABUAD.

In computing the water demand for ABUAD, it will be assumed that University falls within semi settlement and according to NWSSP (2000), water per capita for urban areas of Nigeria is put at 60litres. Under this method of per capita and population, it therefore means that water per capita (Wpc) value will be multiplied with the projected population (Pp) of ABUAD to forecast its water demand using the empirical equation below: WD = Wpc x Pp

The result will thereafter be evaluated against the total water supply output of the University. The essence is to see if the total water supply output is more or less than the water demand of the University.

2.2 Reappraisal of Geophysical Survey

Under this method, the research adopted groundwater potential map compiled by Oladimeji et al (2013) to reappraise geophysical survey of boreholes in ABUAD. Seventy one survey stations were conducted across nooks and crannies of ABUAD. From the survey major electrolyteunits were delineated and it included overburden rocks (clayey lateritic rocks), weathered basement/fractured basement and fresh basement. Using Wright (1992) groundwater potential classification scheme, groundwater potential zones were classified. The scheme was used in reappraising the 17 boreholes in the University.

2.3Pumping Tests

Pumping test was conducted in four out of seventeen boreholes strategically located in the University and based groundwater potential zones. The whole idea was to have a benchmark of groundwater hydraulics in each zone for easy generalization and computation. Borehole in ABUAD Inn and that of Talent Discovery Centre were selected to represent boreholes in moderate groundwater potential zone while borehole at the back of College of Engineering and that of Old Staff Quarters were selected to represent that of poor groundwater potential zone. The borehole at the back of Female Hall of Residence 2 located within the good groundwater potential zone could not be selected because it was not productive at the time of the test.

2.3.1 Recovery Test

The primary aim of recovery test was used in evaluating borehole performance rather than the aquifer performance by measuring the borehole performance. From field experience and as a **"Rule of Thumb",** an inefficient well isthe onethatif the pump is shut off after one hour of pumping and 90% or more of the drawdown is recovered after five minutes, the well is concluded to be unacceptably inefficient.

2.3.2 Constant Rate Test and Analysis

The constant rate test provides data which can be interpreted by comparison with the behaviour of type aquifers. The intent of the test is:

- To assess the borehole performance;
- To obtain values of the aquifer transmissivity and storativity;
- To obtain that values that could be used to predict long-term aquifer and borehole performance; and
- To obtain the specific capacity of the borehole which give the basis for selecting pump size and pump size and pump setting for the borehole in long term production.

The analyses of the pumping test data will be based on information obtained from the pumped borehole itself since there will be no observation borehole.

The constant rate-pumping test will be conducted with a discharged rate. Some hydrological data parameters could be calculated from the field data so generated and analysed. Basic assumptions in computing well hydraulics derived from constant rate test include the following:

- The aquifer is semi to unconfined
- Thickness of the aquifer is about 12m minimum, that is 12 m will be used for the computation and analysis
- Length of screen is 12m
- Radius of screen is 0.0625m

2.4.2.1 Transmissivity:

Transmissivity (T) could be calculated from the general equation: $T = 0.183Q/\Delta Sw$

Where T= Transmissivity (m^2/d), Q= Discharge Rate (m^3/d), ΔSw = difference in drawdown during one log cycle; between 10m and 10m since pumping started which is the slope of time drawdown graph.

Table 1: Classification of Transmissivity

S/N	Magnitude	Class	Designation	Specific Capacity (m^2/day)	Groundwater Supply Potential	Expected Q if S=5m
1.	> 1000	I	Very high	> 864	Regional importance	> 4320
2	100-1000	II	High	86.4 – 864	Lesser regional Importance	432 – 4320
3	10-100	III	Intermediate	8.64 – 86.4	Local water Supply	43.2 – 432
4.	1-10	IV	Low	0.864 – 8.64	Private Consumption	4.32 – 43.2
5.	0.1-1	V	Very low	0.0864 – 0.864	Limited Consumption	0.423 – 4.32
6.	<0.1	VI	Imperceptible	< 0.0864	Very difficult to utilize for local water supply	< 0.432

Source: Driscoll, F.G (1986)

2.3.2.2 Storativity:

With no observation borehole, the storativity would be estimated through the coefficient of permeability (K) derived from BABUSKIN'S Equation: K = (0.306Q/ls) x (log 1.321/r); Where; K – coefficient of permeability (m/d), Q – Discharge rate employed in test, l – Length of screen assumed to be equivalent to thickness of aquifer. S – Maximum drawdown at end of test, r – Radius of screen.

The BABUSKIN'S equation assumes stabilization of the dynamic water level (DWL) under unconfined condition and BEICINKI's equation relates specific yield and coefficient of permeability (K) through; u = 0.117 x 7√K where u = specific Yield ratio and K = coefficient of permeability (m/d). Under unconfined condition, specific yield is equivalent to storativity.

2.3.2.3 Specific Capacity:
Specific Capacity q = Q/s; q = specific capacity in m³/h/m, Q = Discharge Rate in m³/h, s = Drawdown at end of test in m

2.3.2.4 Entrance Velocity through Screens:
Entrance Velocity at envisaged pumping rate could be calculated from the general equation:
V = Q/πRLP; V= entrance velocity in m/s, Q = envisage discharge rate in m³/s, R= radius of screen, L = length of screen, P = percentage of opening in screen

2.3.2.5 Range of Cone of Depression:
The range of cone of depression for the pumping rate is calculated from SICHARDI'S formula: R = 10s x √K; R = Range of cone of depression, S = Maximum drawdown at stabilization, K = Permeability coefficient.The value of R will indicate whether the borehole within the field will have mutual interference during pumping activity.

III. DATA ANALYSIS AND DISCUSSION

This chapter focuses on the analysis of the data collected using the methods as described in chapter 3. Determination of water demand, borehole development, sitting of borehole and reappraisal of geophysical reports and pumping test in ABUAD will be analyzed and discussed.

3.1 Determination of Water Demand

3.1.1 Water Quantity Estimation

The daily water demand of as calculated based on per capita demand of NWSSP (2000) for ABUAD is420000 liters/day

3.1.2 Population Forecast of Water Demand

Using the arithmetical progression method of estimation is 934200 litres/day

3.2 Reappraisal of Geophysical Report andBorehole Construction

Table 2 showed geophysical report reappraisal of 17 boreholes in ABUAD in line with groundwater potential map parameters recommended byOladimeji et al (2013) adopted to have a firsthand knowledge of the probable production potential level of the boreholes. These parameters are thickness of overburden and weathered/fractured basement lithounits including resistivity of weathered/fractured basement.

Table 2: Analysis of Geophysical Report Based on Groundwater Potential Map of ABUAD

S/N	Name	UTM		OBT (m)	RWF (Ω-m)	WFT (m)	GP
		ETX	**NTY**				
1.	Back of College of Social &MgtSc	754896	841587	10 (Ltd groundwater potential	30 (Optimum aquifer potential)	11 (poor ground-water potential)	Poor groundwater potential
2	Left back of Coll. Soc. & Mgt. Sc.	754743	841525	16 (Ltd groundwater potential	55 (Optimum aquifer potential)	14 (Fair ground-water potential)	Moderate groundwater potential
3.	Back of MHS	754925	841525	14 (Ltd groundwater potential	45 (Optimum aquifer potential)	13 (Fair ground-water potential)	moderate groundwater potential
4.	Back of male Hall of	755142	841280	18 (Ltd groundwater potential	40 (Optimum aquifer	10 (poor ground-water	Poor groundwater potential

	Residence .				potential)	potential	
5.	Female Hall of Resc.1	755107	842264	10 (poor groundwater potential	16 (Ltd aquifer potential)	9 (poor ground-water potential	Poor groundwater potential
6.	Back of female hall of Resc. 2	754198	841652	22 (Ltd groundwater potential	75 (Optimum aquifer potential)	17 (Fair ground-water potential)	Good groundwater potential
7.	Female hall of Resc.	754958	84217	10 (Ltd groundwater potential	10 (Ltd aquifer potential)	6 (poor ground-water potential	Poor groundwater potential
8.	Local Kitchen	755355	841617	14 (Ltd groundwater potential)	15 (Ltd aquifer potential)	11 (poor ground-water potential)	Poor groundwater potential
9.	Front of Local Kitchen	754472	841617	10 (Ltd groundwater potential)	60 (Optimum aquifer potential)	13 (poor ground Water potential)	Slightly moderate groundwater potential)
10.	Laundry	755447	841744	14 (Ltd groundwater potential)	15 (Ltd aquifer potential)	10 (poor ground-water potential)	Poor groundwater potential
11.	Back of Water Plant	755538	841836	14 (Ltd groundwater potential)	20 (Ltd aquifer potential)	10 (poor ground-water potential)	Poor groundwater potential
12.	Old Staff Qtrs. (Front of BLK C)	755628	842206	12 (Ltd groundwater potential)	20 (Ltd aquifer potential)	10 (poor ground-water potential)	Poor groundwater potential
13.	Old Staff Qtrs. (Front of BLK E)	755189	842299	14(Ltd groundwater potential)	15 (Ltd aquifer potential)	10 (poor ground-water potential)	Poor groundwater potential
14.	Old Staff Qtrs. (Front of BLK F)	755658	843590	10 (Ltd groundwater potential)	10 (Ltd aquifer potential)	6 (poor ground-water potential)	Poor groundwater potential
15.	ABUAD INN	754008	841183	22 (Ltd groundwater potential)	Optimum aquifer potential	14 (Fair ground-water potential)	Moderate groundwater potential
16.	TDC	754008	841801	22 (Ltd groundwater potential)	60 (Optimum aquifer potential)	14 (Fair ground-water potential)	Moderate groundwater potential
17.	Back of Engr. BLK	754649	841801	14 (Ltd groundwater potential)	30 (Optimum ground-water potential	9 (poor ground-water potential)	Poor groundwater potential

Source: Oladimeji et al (2013)

Where NTY - Northing (Y-Axis), OBT - Overburden thickness, RWF - Resistivity of weathered/fractured layer, WFT - Weathered/fractured layer thickness, GP- Groundwater potential

3.3 Pumping Test

3.3.1 Recovery Test

The research project relied on the recovery test method, which is both time and cost effective, in arriving at a qualitative way of having first-hand information on the borehole efficiency and performance. Any well that is shut off after one hour of pumping and 90% or more recovery is achieved after five minutes is considered to be inefficiently unacceptable. Basically, well efficiency more or less serves as a monitoring tool in which future maintenance of the well could be predicated upon. All the boreholes in question recovered between 45 – 86% on or before the expiration of 5 minutes.

3.3.2 Constant Rate Pumping Test

Refer to appendices 1 – 4 showing graphical analysis of constant rate pumping test.

Table 3: Boreholes Hydraulic Parameters Summary

S/N	NAME	Q (m^3/d)	T(m^2/d)	K	S_O	q (m^2/d)	V (m/sec)	R (m)	Expected Q if S is 5m (m^3/d)
1.	Talent Discovery Centre	108	274.5	0.238	0.057	7.03	$2.7x10^{-3}$	74.93	35.15
2.	ABUAD INN	130	1321.67	1.1206	0.124	33.08	$3.2x10^{-3}$	41.60	165.4
3.	Back Of College of Engr.	64.08	488.61	0.286	0.063	8.454	$1.6x10^{-3}$	40.54	42.27
4.	Front Of Old Staff Quarters	48	109.8	0.153	0.046	4.50	$1.12x10^{-3}$	41.70	22.5

Source: Field Survey (Compiled from Appendices 1, 2, 3, 4, 5, 6a, 7a, 8a and 9a)

Where Q - Discharge Rate, T - Transmissivity, K – Permeability, S– Storativity, Q - Specific Capacity, V- Entrance Velocity, R - Radius of Depression

3.4 Discussion of Findings

The study aims at determining sustainable groundwater exploitation in weathered/fractured basement complex of Ado-Ekiti vis-a-vis ABUAD.

3.4.1 Water Demand

Water demand for the University as computed during the study stands at 42, 0000 litres/day ($420m^3$/day or $17.5m^3$/hr) and 93, 4200 litres/day ($934.2m^3$/day or $38.93m^3$/hr), water quantity estimation and population forecast of water demand methods respectively. The expected daily water production at 100% assumed installed capacity should be $1142.12m^3$/day, which is 24hrs pumping. But at 60% operational efficiency, the expected daily output should be $685.3m^3$day, which could be adequate to meet the present day water demand of the University. If the present daily consumption is not met, it probably implies that the functionality/operational efficiency of the water schemes is below 37% installed capacity.

3.4.2 Geophysical Survey and Borehole Construction

Findings revealed that lithological sequence of overburden, weathered basement and fractured basement identification is first step in groundwater exploitation in Ado Ekiti and environs. The second step is to establish whether resistivity and thickness of weathered/fractured basement in addition to the thickness of overburden unit. Resistivity range of 20 - 100Ω-m and thickness of 12m to 30m with overburden thickness of ≥ 25m are considered to have good groundwater potential but regrettably none of the boreholes located in ABUAD within this zone. What prevailed in most cases are the resistivity and thickness values of weathered/fractured basement meeting these conditions without overburden unit thickness of ≥ 25m.

Three boreholes are located in zone with moderate groundwater potential and the rest (14 in number) are located in poor groundwater potential zone. (Table 3) and pumping test result actually confirmed the groundwater potential classification scheme adopted as there was clear demarcation between the pumping rate of the three boreholes situated in moderate groundwater potential zone against those fourteen boreholes situated in the poor groundwater potential zone. Two boreholes situated in the moderate groundwater has a mean discharge rate of 119m^3/day whereas those boreholes (2) situated in poor groundwater potential zone had a mean discharge value of56.08m^3/day.

Very importantly, findings also revealed that construction design of a borehole can impact negatively on the yield of a borehole no matter how appealing the geophysical survey result of the groundwater potential can be as was seen in the significant difference in the performance level between the borehole at the back of College of Engineering and the one located in front of Old Staff Quarters, even though both of them shared to the same zone, poor groundwater potential zone. The borehole at the back of College of Engineering has relatively more promising hydraulic parameter than the one in front of Old Staff Quarters (Block F).

3.4.3 Pumping Test

Although all the boreholes could be accepted with certain measures of efficiency based on application of recovery tool but in terms of specific capacity tool, it is below acceptable standard. As mentioned earlier the specific capacity values in all the boreholes were not in tandem with transmissivity values proposed by Driscol, F.G. (1986). This simply an indication that development was incomplete and boreholes were likely not constructed according to standard best practices. In fact out of four boreholes pumping test was conducted only the borehole at the back of College of Engineering could be said to meet the minimum standard of borehole construction. The remaining three could be tagged in local parlance as **"Hanging Borehole"**

Transmissivity values of all the boreholes pump tested should guarantee adequate yield for industrial, municipal or irrigational purposes under Driscol, F.G (1986) classification scheme as all of the boreholes pump tested except the one in the front of Old Staff Quarters (Block F) had transmissivity values well above 124m^2/day, but the specific capacity of the boreholes would not guarantee this. Even the storativity values of the pump tested boreholes were within the acceptable range of 0.01 and 0.3. The entrance velocity values of the boreholes were within the laminar flow range and all the boreholes were located away from radius of depression of each borehole. The question is where the problem lies. The answer could still be traced to construction/development procedures adopted.

IV. CONCLUSIONS AND RECOMMENDATIONS

4.1 Conclusions

Sustainable groundwater exploitation is achievable in Ado Ekiti and ABUAD in particular if boreholes are located and constructed based on standard best practices. Lithological unit sequence needed for good groundwater yield and sitting of boreholes is overburden unit of thickness ≥ 25m and weathered/fractured basement with resistivity ranging from 20 - 100Ω-m and thickness between 12 -30m. More over hydraulic parameters gotten from the pump tested boreholes have revalidated the groundwater potential map of ABUAD proposed by Oladimeji et al (2013).

Judging from the number of boreholes and their assumed production level, the present daily water demand in ABUAD put at 420,000litres/day could be met even if the production level is put at 37% of installed capacity. The focus now should be on how the demand will be met in ten years time considering the fact that projected demand is put at 934,200litres/day. The lingering water scarcity in ABUAD could probably be largely due to the fact that most of the boreholes are functioning far below installed capacity. As noted that most of the boreholes have constructional problems

4.2 Recommendations

In view of the research questions answered coupled with the aim and objectives realized, there are needs for the following recommendations:

1) To improve the efficiency in boreholes in ABUAD, the boreholes need to be re-developed by surging and airlifting method until sand free nature is achieved. This should be done annually considering the manner the boreholes were constructed.
2) Pumping test should be carried out in the remaining boreholes to really confirm their functionality status. This should be planned during long vacation when student population is low because the process will require long time of borehole shut down.
3) Subsequence boreholes should be sited in zone earmarked for good groundwater potential and water piped to central reservoir for re-distribution to areas of needs.
4) National borehole completion format should be used in documenting completed borehole history to enable monitoring, operation and maintenance.

5) Finally, as a long term measures, there should be an urgent plan to dam the nearby river for both water supply and power generation.

References

[1] Ariyo, S.O and Adeyemi, G.O. 2009. Role of Electrical Resistivity Method for Groundwater Exploration in Hard Rock Areas: A Case Study from Fidiwo/Ajebo Areas of Southwestern Nigeria. The Pacific Journal of Science and Technology. 10 (1): 483 – 486.

[2] Bayowa G.O. Olorunfemi M.O. and Ademilua O.L. (2014a*);* A Geoelectric Assessment and Classification of the aquifer systems in a Typical Basement Complex Terrain: Case study of Ekiti State, Southwestsern Nigeria. *Research Journal in Engineering and Applied Sciences 3 (1) 55- 60*

[3] Bayowa O.G., Olorunfemi, M.O., and Ademilua, O.L. (2014b). Preliminary Geomorphological, Geological Hydrogeological Assessment of the Groundwater potential of Ekiti State, Southwestern

[4] Clerk L (1985). Groundwater Abstraction from Basement Complex Areas of Africa. J. Eng. Geol., London 18: 25-34.

[5] Department of Geography and Planning Science, Ekiti State University, P.M.B. 5363, Ado Ekiti, Ekiti State, Nigeria. segunaros2002@yahoo.com

[6] Department of Geography and Planning Science, Ekiti State University, P.M.B. 5363, Ado Ekiti, Ekiti State, Nigeria. *omotsonnat@yahoo.com*

[7] Eduvie M.O. (2006). Borehole Failures and Groundwater Development in Nigeria. National Seminar on the Occasion of Water Africa Exhibition (Nigeria 2006), Lagos, Nigeria.Available at http://www.nwri.gov.ng/userfiles/file/Borehole_Failure_in_ Nigeria.pdf Accessed 20 Dec. 2012

[8] FMWR (2000). National Water Supply and Sanitation Policy. 1st edition, Fed Republic of Nigeria.http://www.nwri.gov.ng/userfiles/file/National_Water_Supply_and_Sanitation_Policy.pdf. Accessed 20 December 2012

[9] OECD. (2012). Development Co-operation Report 2012: Lessons in Linking Sustainability and Development, OECD Publishing. Available at: http://dx.doi.org/10.1787/dcr- 2012-en. Accessed 14 December 2012

[10] M.I. Oladapo, O.J. Akintorinwa, Hydrogeophysical Study of OgbeseSouth-western, Nigeria. *Global J. Pure and Applied Sci., 13(1)*, 2007, 55-61.

[11] M.O. Olorunfemi, J.S. Ojo, O.M Akintunde, Hydrogeophysical evaluation of the groundwater potential of Akure metropolis, southwestern Nigeria. *J. Min. Geol., 35(2)*, 1999, 207-228.

[12] Obasi, R.A., Ademilua O.L., and Eluwole A.B. (2013). Geoelectric Sounding for Groundwater Potential Appraisal Around the Northeastern - Southwestern Parts of the Federal Polytechnic Ado – Ekiti Campus, Southwestern Nigeria. Research Journal in Engineering and Applied Sciences. vol. 2, No. 3, pp. 211-219

[13] Omole, D.O. and Isiorho, S.A. (2011). Waste Management and Water Quality Issues in Coastal States of Nigeria: The Ogun State Experience. Journal of Sustainable Development in Africa, 13(6):207-217

[14] Osuagwu, B.C., 2009, Geophysical investigation for groundwater in a difficult terrain around Modomo Area, Ife, Osun State: Unpublished Bachelor of Science Thesis, Obafemi Awolowo University, Ile-Ife, Osun State, p. 88.

[15] Oyawoye, M.O., 1972, The Basement Complex of Nigeria, *in*, T.F.J. Dessauvagie, and A.J. Whiteman, (eds.), African Geology: University of Ibadan, Nigeria, p. 67-99.

[16] Oyebode O.J and Oyegoke, O.J (2014). Water Supply Challenges of a University Community: The Case Study of ABUAD" Proceedings of International Conference on Science, Technology, Education, Arts, Management and Social Sciences iSTEAMS Research Nexus Conference, Afe Babalola University, Ado-Ekiti, Nigeria, between 29 and 31st May, 2014. pp. 969-976.

[17] Rahaman, M.A. (1976).Review of the Basement Geology of Southwestern Nigeria. In Geology of Nigeria. Elizabeth publishing Company, Nigeria. pp. 23 -33.

[18] Transnational Journal of Science and Technology July 2012 edition vol. 2, No.6

[19] UNICEF/WHO (2012). Progress on drinking water and sanitation: 2012 update. UNICEF and World Health Organization. ISBN: 978-92-806-4632-0

[20] Vander Velpen, B.P.A. 1988. "Resist Version 1.0". M.Sc. Research Project. ITC: Delft, Netherlands.

[21] Wright, C. P, 1992. The hydrogeology of crystalline basement aquifers in Africa. In: C. P. Wright and W. C. Burgess (eds). Hydrogeology of Crystalline Basement aquifer in Africa. Geological Society of London Special Publication No. 66 Pp. 1 – 27.

American Journal of Engineering Research (AJER) 2015
American Journal of Engineering Research (AJER)
e-ISSN: 2320-0847 p-ISSN : 2320-0936
Volume-4, Issue-8, pp-75-88
www.ajer.org
Research Paper Open Access

Comparison the Efficiency of Cajanus Cajan and Ficus Benghalensis for Lead and Zinc Removal From Waste Water.

Tanushka Parashar
Jiwaji University , Gwalior, India

ABSTRACT: *Water is one of the most important natural resources, essential for all forms of life. These natural resources are being contaminated everyday by anthropogenic activities. Water is a vital natural resource, which is essential for multiplicity purposes. Therefore, it is essential to remove heavy metals from water throughbio adsorption process.*

"Cajanus Cajan seed coat and Ficus Benghalensis aerial root has been used for the removal of Pb (II) and Zn (II) from synthetic wastewater. The synthetic wastewater concentration was 1000 mg/l.Temperature kept constant as 35°C.Sorption kinetics models viz., pseudo first order and pseudo second order were applied for the experiment. It was revealed that Pb (II) and Zn (II) removal follows pseudo second order rate expression. Adsorption isotherm was justified by Langmuir and Freudlich adsorption isotherm. IR spectra,NMR spectra andXRD spectra shows the presence of following groups such as –COOH,-OH, aliphatic,-NH_2 which increases the efficiency of bioadsorbents at moderate pH.Proximate analysis also explains the percentage of carbon that means the presence of aliphatic hydrocarbon.The suitable pH for maximum removal of Pb (II) and Zn(II) ions from synthetic water by Cajanus cajan and Ficus benghalensis were 6.

Keywords: *Bioadsorption, Proximate analysis, Sorption Kinetics, Sorption Isotherm and Anthropogenic.*

I. INTRODUCTION

Water pollution is a serious global problem. It causes disease and death.[2]Heavy metal contamination of water is mainly caused by industrialization, modernization, urbanization, mining, electroplating, metal processing, textile, battery manufacturing industries, paper pulp industries, storage battery, automotive discharge and bisleries [1].Heavy metals threat to environment and public health by bioaccumulation, toxicity and reaches in food chain of the ecosystem.Heavy metals ions such as Pb, Cd, Hg, Cr, Ni, Zn and Cu are non-biodegradable. They are natural component of the earth crust. To, small extent, it enters in our bodies via food, drinking water and air. As trace elements, some heavy metals are essential to maintain the metabolism of human body[2]. However at high concentration they lead to poisoning. Main sources of lead release in water are leaded gasoline, tire wear, lubricating oil and grease bearing wear.Zinc emission take place from tire wear, motor oil, grease and brake emission.Lead accumulation causes acute or chronic damage to nervous systems, renal systems, decreases hemoglobin formation, infertility and abnormality in women.[3-4]Excess of zinc suppress Cupper and iron absorption and cause anosmia, acidity in stomach, lethargic, ataxia (lack of coordination of muscle movement). There are several technologies for removing heavy metal from water such as chemical oxidation, ion exchange, reverse osmosis, electrochemical application, membrane process, evaporation, filtration, solvent extraction, chemical precipitation[5-8]. The main disadvantages of these methods are high prize non viable,scale and sludge formation take place. Therefore,the best alternatives to remove heavy metal from the water source arebioadsorption. Due to practical limitation with living microbes, dead biomass agricultural waste or byproducts are preferably used for adsorption. Recent research has been focused on the development of unique materials which increased affinity, capacity and selectivity for the target metals[9].The objective of this research is to develop low cost, easily viable, highly efficient and ecofriendly bioadsorbent like Cajanus Cajan and Ficus Benghalensis for removal of heavy metals Pb and Zn removal.Therefore by the use of Cajanus Cajan seed coat cover and Ficus Benghalensis aerial root as bioadsorbent for the removal of lead and zinc from the water.Because they are easily available, low cost, highly efficient, ecofriendly. Lead and Zinc is chosen due to its presence in water of the Gwalior region.

II. MATERIALS AND METHODS

1.1. Physico-Chemical Analysis Of The Bioadsorbents:*Cajanus Cajan coverings collected from pulse industries.Soluble and colored components of coverings were removed by repeated washing with distilled water then coverings dried at 30^{o}C, powdered and sieved. Ficus benghalensis aerial root are collected by local areas. It is washed with distilled water many times dried in sunlight then dried in oven. Grounded into powder with electrically grinded mixture. Powder is sieved to get proper size particles (350 to 850 micrometer).*

Fig. 1a Aerial Roots of Ficus Benghalensis

Fig.1b Seed coat of Cajanus cajan

In order to analyze physico chemical properties ofbioadsorbents IR spectra, NMR spectra, XRD and proximate analysis are conducted.

1.2. Infra Red Spectra-Infra –Red spectra of the bioadsorbent were recorded using Infra – Red spectrophotometer.

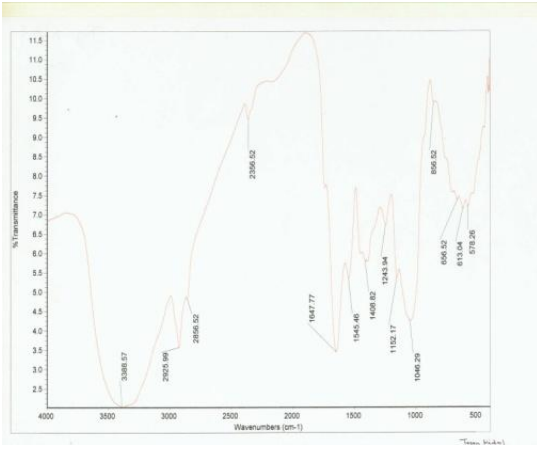

Fig. 2a IR Spectra of Cajanus Cajan

Table I: IR ranges Cajanus Cajan

3388.57	-OH stretching of alcohol, phenols, and carboxylic acids.
2925.99	-C=C-stretching of aliphatic hydrocarbons.
2856.52	-C-H-stretching of aldehyde.
1647.77	-C=O stretching of amide.
1545-1647	-N=O stretching of nitro group.
1152.17	Presence of tertiary alcohol.
1243.94	-C=O stretching of ether group present.
1152.17	-S=O stretching of sulphur dioxide
656 and 613	-Si-O stretching of silicate.
656&613	-Si-O- stretching.

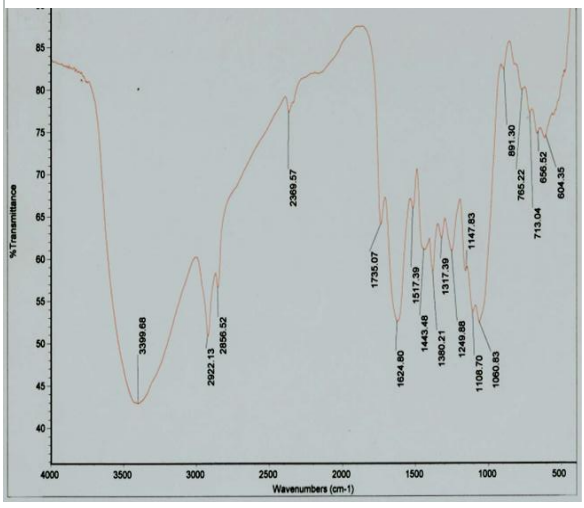

Fig. 2b IR spectra of Ficus Benghalensis

Table II: IR ranges of Ficus benghalensis

Ranges (cm^{-1})	**Functional group posses by Ficus benghalensis**
3399.68	-OH stretching of alcohol (Polymeric association of intermolecular hydrogen bonding).
2922.13	-CH stretching of aliphatic hydrocarbon.
2856.52	-$COCH_3$ shows presence of ether group.
1735.07	-C=O stretching of aldehyde, Carbonyl group.
1624.80	-NH deformation of amine group.
1443.48-1380.21	-CH deformation of –CH2, -CH3.
1317.39	-C=O stretching of t-alcohol.
49.88	-OH group present.
1108.70	Secondary alcohol present.
1060.83	-C=C-O-C stretching of ether.
765.22-713.04	-CH_2 rocking.

Table III:The results of proximateanalysis of Cajanus Cajan and Ficus Benghalensis are-

Bioadsorbent	*Cajanus cajan*	*Ficus benghalensis*
% of moisture	18.838	18.96
% of volatile matter	17.86	18.22
% of ash	18.83	17.71
% of fixed Carbon	44.88	45

More the percentage of fixed carbon in bioadsorbent is far better.

1.4. Nuclear Magnetic Resonance *–It is general methodology in which encoding and detection occurs in different physical and molecular environment. NMR spectra of adsorbent by using NMR spectrophotometer(model aV-500).*

Table IV a: NMR ranges of Cajanus cajan.

Tau value	*Functional group*
1.5	Methyne
1.3	sec R_2CH_2
1.5	t-R_3CH

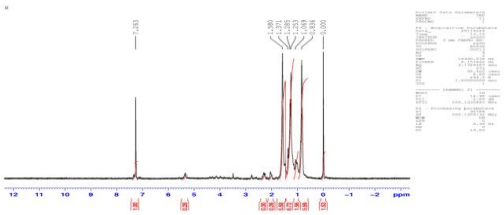

Fig.3a: NMR spectra of Cajanus Cajan

Table IV b: NMR ranges of Ficus benghalensis

Tau value	*Functional group*
7.263	Alcohol group, CH_3NHCOR
3.492	RNH_2, RNHR
1.5, 1.371, 1.333, 1.286, 1.253	$RCONH_2$ RCONHR
0.843, 0.069	=N-OH

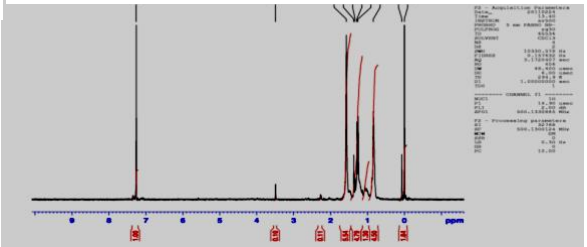

Fig.3b: NMR spectra of Ficus Benghalensis

2.4 .X- Ray Diffraction *-It represents the amorphous nature of bioadsorbents.*

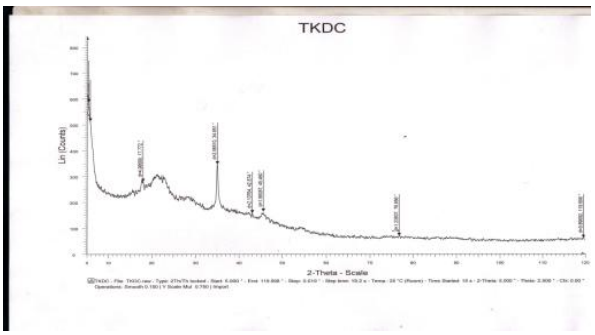

Fig. 4a XRD of Cajanus Cajan

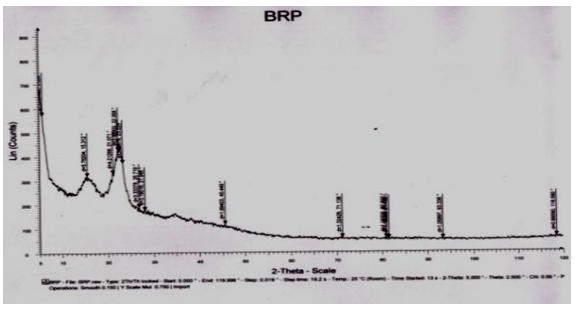

Fig. 4b XRD of Ficus benghalensis

2.5. Biosorption Experiment:*Batch adsorption experiments were carried out at different pH, contact time, different concentration and adsorbent loading weight.Different pH of the solution was monitored by adding 0.1NHCl and 0.1N NaOH solution. Different concentration of the solution was prepared by diluting stock solution. Required amount of bioadsorbent was then added content was shaken up to required contact time on an electrically rotator shaker at 1200 rpm. The filtration was done using Whatman Filter paper of 125ppm. The filtrates were treated with dithiozone.Lead ions forms lead dithiozonate and Zinc ions forms zinc dithiozonate.Filtrate were separated and analyzed by using U.V.Visible spectrophotometer (Schimadzu) for the percentage of metal removal. Spectra for the percentage of metal removal obtained at wavelength 515 nm .The percentage of metal removal were calculated as:*

% of removal of metal = Ci – Ce / Ci x 100

III. RESULT AND DISCUSSION

3.1. Effect Of pH: *Experiment were performed at 35°c, concentration of adsorbate 100mg/l and varying the pH from 1to 12. It was observed that uptake of Pb (II) and Zn (II) increased with the increase in pH.These optimum uptakes for maximum adsorption of Pb(II)and Zn(II) was found to be 6. Slightly acidic pH supports maximum of adsorption, as the surface of bioadsorbent contains carboxyl group, hydroxyl group, enol group, ester,-SO_2, amide linkage. So the positive end of metal binded to this group of adsorbent at low pH. At the highest pH the surface of bioadsorbent becomes negatively charged and in addition there will be abundance of negatively charge in aqueous solution both of these factors hinders the bioadsorption at high pH.It was observed that at lowest pH when the solution was treated by potassium chromate (K_2CrO_4) dark yellowish color obtained. It also indicates higher percentage of adsorption at low pH as compared to higher pH .So, it represents that the efficiency of adsorption higher at lowest pH .It is highest at 6 .More binding sites are available at this pH.*

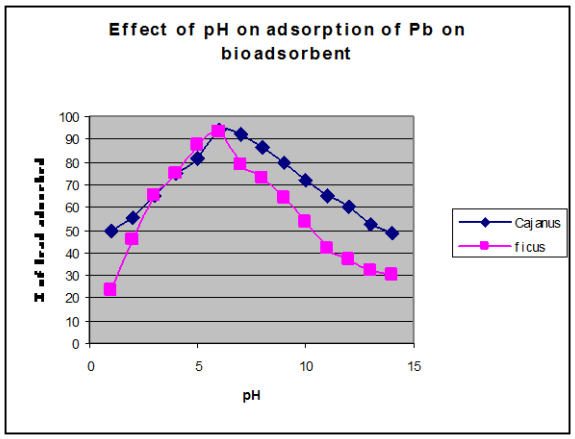

Fig. 5a Effect of pH on adsorption of lead by Cajanus cajan and Ficus benghalensis

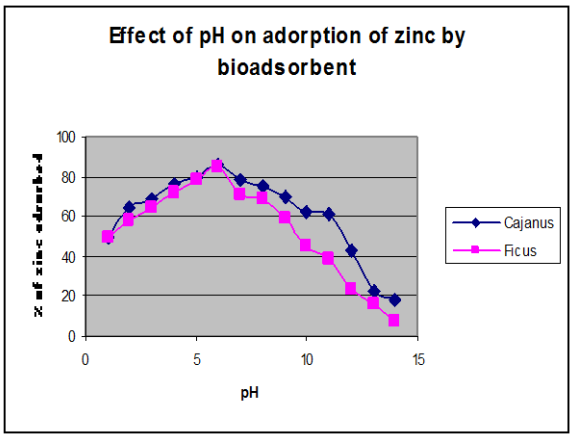

Fig.5b Effect of pH on adsorption of zinc by Cajanus cajan and Ficus benghalensis

3.2. Adsorption Isotherm: *The isotherm constant was calculated from the slope and intercept from Langmuir adsorption isotherm and Freudlich adsorption isotherms.R^2 represents the adsorption process very well.Bioadsorption Isotherms describes how adsorbate interacts with bioadsorbents and equilibrium is established between adsorbed metal ions and residual metal ions during surface bioadsorption. Sorption Isotherm represents the capacity and efficiency of bioadsorbent to metal ions. The Langmuir adsorption explains monolayer coverage of adsorbate over a homogenous adsorbent surface, biosorption of each molecule on to the surface has equal biosorption activation energy. While Freudlich adsorption Isotherm explains heterogeneous surface with a non-uniform distribution of heat of biosorption over a surface and a multilayer biosorption.*

Table V: Sorption Isotherm constants and RL values for sorption of Pb (II) on Cajanus Cajan at different concentration with respect to time.

Different concentration (ppm) Pb^{2+}	*Langmuir Model*			*Freudlich Model*			
	q°	*B*	*r^2*	*N*	*K_F*	*r^2*	*R_L*
50	33.079	-2.5380	0.957	-0.963	0.28	0.88	1.04
100	45.024	-5.470	0.969	0.77	0.36	0.7881	1.018
150	56.338	-12.376	0.983	0.80	0.34	0.99	0.141
200	69.108	-40.65	0.99	0.87	0.31	0.99	0.68

In the table values of $r^2$is higher of Langmuir than Freudlich adsorption Isotherm, which means Langmuir equation represented the adsorption process very well. Value of Q° which is defined as the maximum capacity of adsorbent was calculated from Langmuir plots. The equilibrium parameter R_L, which is defined as $R_L = 1 / 1+bC_{A0}$:$O<R_L<1$ reflects the favorable adsorption process.In the present research the equilibrium parameter was found to be in the range $O<R_L<1$ which is shown in table. This indicated to the fact that the adsorption process was favorable and the adsorbent utilizedhave a great potential.

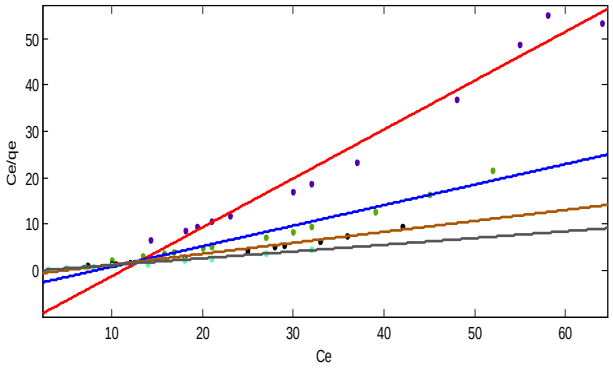

Fig. 6a Langmuir plot: Different Concentration of lead removal by Cajanus cajan verses time

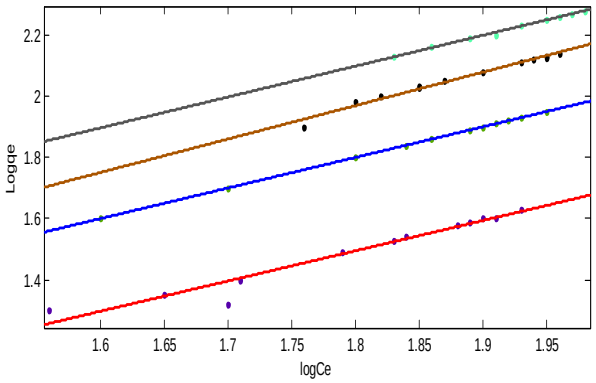

Fig. 6b Freudlich plot: Different concentration of lead removal by Cajanus cajan verses time

Table VI:Sorption Isotherm constants for sorption of different concentration of Zn(II) by Cajanus cajan.

Differentconcentration (ppm)Zn^{2+}	***Langmuir model***			***Freudlich model***			
	q°	***b***	***r^2***	***R_L***	***N***	***K_F***	***r^2***
50	26.413	1.518	0.93	1.03	0.575	0.466	0.98
75	29.985	1.090	0.847	1.052	48.614	-9.57	0.89
100	39.154	1.057	0.95	1.022	61.31	-0.066	0.57
150	45.24	1.3068	0.96	1.013	65.74	-0.068	0.24

From the table it is clear that in the case of adsorption of Zn^{2+} on Cajanus cajan follows Freundlich adsorption isotherm as the value of correlation coefficient exists in the range 0.57 to 0.98 which support it.

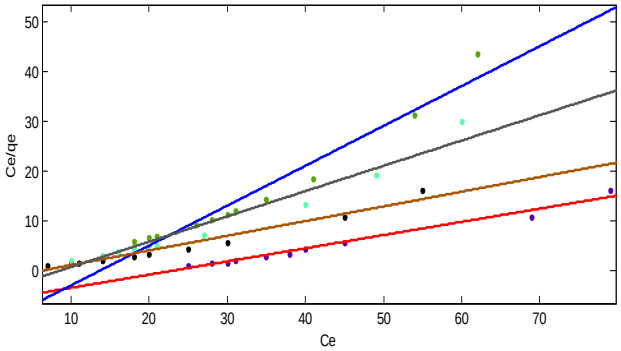

Fig.7a Langmuir plot: Different concentration of zinc removal by *Cajanus cajan* verses time

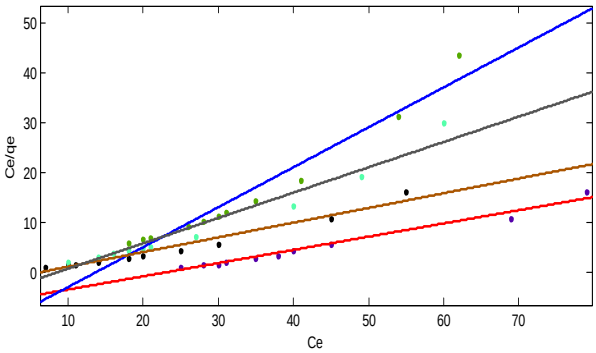

Fig. 7b Freudlich plot: Different concentration of zinc removal by *Cajanus cajan* verses time

TableVII: Sorption isotherm constant and R_L values for sorption of Pb (II)by different doses of Cajanus cajan.

Metal Pb^{2+}	***Langmuir model***			***Freudlich model***			
Different Doses(gm)	***q°***	***b***	***r^2***	***R_L***	***N***	***K_F***	***r^2***
0.25	24.02	-0.063	0.94	1.09	0.53	-0.49	0.98
0.50	1	-0.183	1	1.18	0.64	-0.41	0.99
1	45.45	-0.811	0.99	1.020	0.62	-0.33	0.98
2	60.75	-1.1447	0.98	0.4	0.89	-0.30	0.99

The Isotherm constant were calculated from the slope and intercept. The value of r^2 is higher of Langmuir isotherm than Freudlich Isotherm that indicates that Langmuir Isotherm explains adsorption process better.

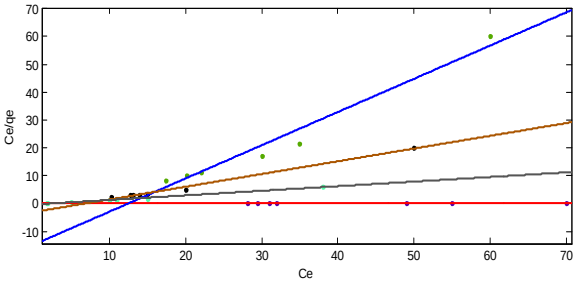

Fig. 8a Langmuir Plot–Different doses of Cajanus *cajan* for lead removal verses time

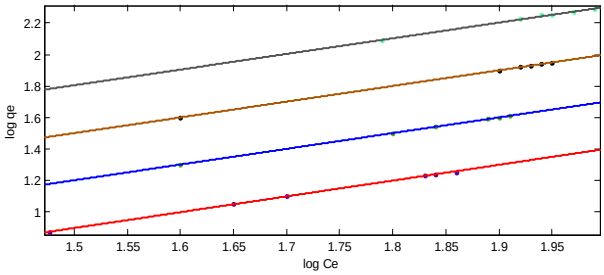

Fig. 8b Freudlich Plot: Different doses of *Cajanus cajan* for lead removal verses time

TableVIII:Sorption Isotherm constant and $R_L$values for sorption of Zinc (II) by different doses of Cajanus cajan.

Metal Zn^{2+}	*Langmuir model*			*Freudlich model*			
Different Doses (gm)	*q°*	*b*	*r^2*	*R_L*	*N*	*K_F*	*r^2*
0.25	384.6	6.06	0.079	1.647	6.92	-1.211	0.01
0.50	425.5	2.46	0.05	4.048	0.512	0.509	0.91
1.00	62.42	1.06	0.92	9.345	0.50	0.018	0.99
2.00	41.6	0.87	0.98	0.011	85.4	-0.027	0.37

The correlation coefficient supported Freudlich isotherms.

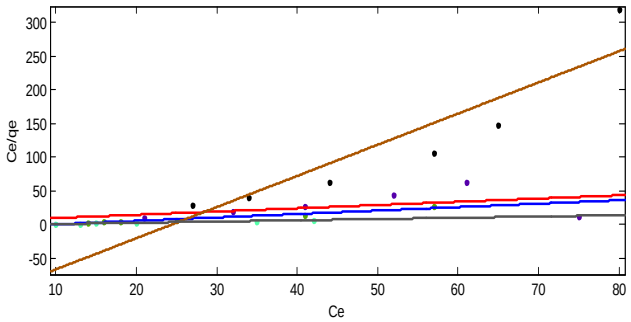

Fig. 9a Langmuir plot: Effect of different doses of *Cajanus cajan* for zinc removal verses time

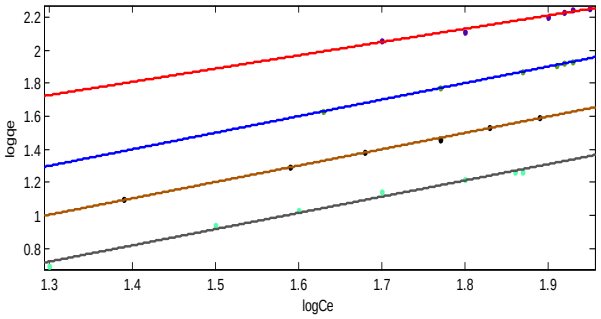

Fig. 9b Freundlich plot: Effect of different doses of *Cajanus cajan* for zinc removal verses time

Table IX: Sorption isotherm constant for different concentration of Pb (II) removal by Ficus benghalensis.

Parameter Pb^{2+} ion	*Langmuir Parameter*		*r^2*	*Freudlich Parameter*		*r^2*
Concentration (ppm)	*Q_o*	*b*		*N4*	*K_f*	
75	0.8064	0.033	0.84	0.983	1.32	0.99
150	2.12	0.073	0.90	0.99	1.48	0.99
200	10.20	0.158	0.39	1.149	3.5	0.27
250	5.414	0.190	0.97	0.71	1.86	0.97

Correlation coefficient of Freudlich adsorption isotherm supports the adsorption of different concentration of lead by Ficus benghalensis.

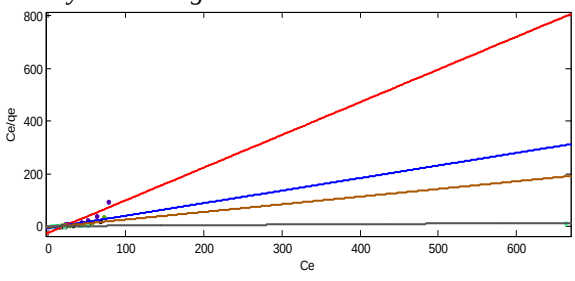

Fig. 10a Langmuir plot - Different concentration of lead removal by Ficus benghalensis verses time

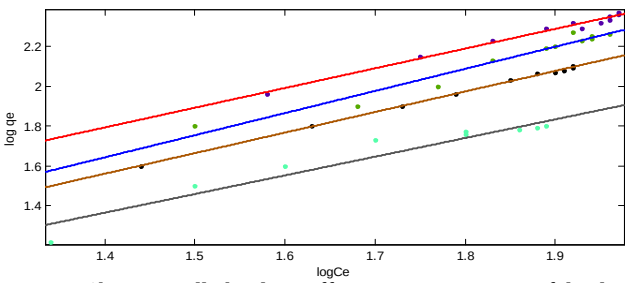

Fig. 10b Freundlich plot-Different concentration of lead removal by Ficus benghalensis verses time.

Table X:Sorption isotherm constant for different doses of Ficus benghalensis for Pb (II) removal verses time.

Parameter Pb^{2+} `ion	Langmuir Parameter		r^2	Freudlich Parameter		r^2
Doses(gm)	Q_{max}	b		N	K_f	
0.75	0.36	0.067	0.95	1.010	1.94	1
1	0.79	0.080	0.95	1	1.99	1
2	4.34	0.12	0.96	0.98	1.86	0.99
3	9.090	0.28	0.97	0.83	1.28	0.96

Freudlich adsorption isotherm is best fitted for different doses of Ficus benghalensis for lead removal verses time. Correlation coefficient supports it.

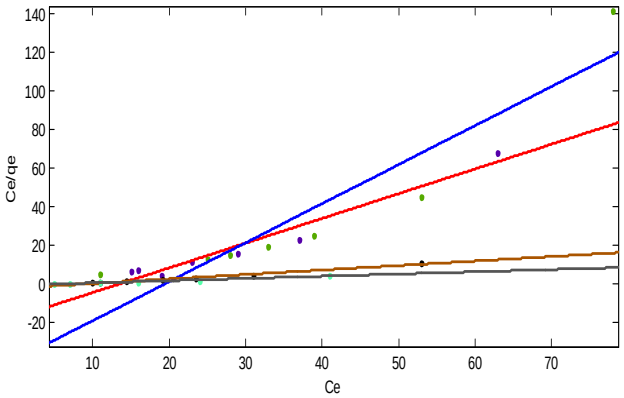

Fig. 11a Langmuir plot-Different doses of *Ficus benghalensis* for lead removal verses time

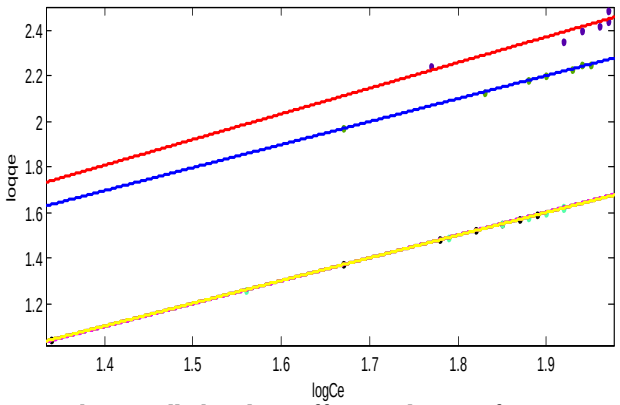

Fig. 11b Freudlich plot-Different doses of *Ficus benghalensis* for lead removal verses time

TableXI: Sorption isotherm constant for different concentration of Zn (II) removal by Ficus benghalensis.

Parameter Zn^{2+} ion	Langmuir Parameter		r^2	Freudlich Parameter		r^2
Concentration (ppm)	Q_{max}	B		N	K_f	
75	0.66	-0.039	0.90	1.010	1.32	0.99
150	1.92	-0.060	0.92	0.98	1.40	0.99
200	3.703	-0.1032	0.89	1.020	2.13	0.99
250	5.800	0.23	0.95	0.99	2.48	0.99

Freudlich adsorption isotherm supports the adsorption of different concentration of zinc by Ficus benghalensis verses time. Value of r^2 favors it.

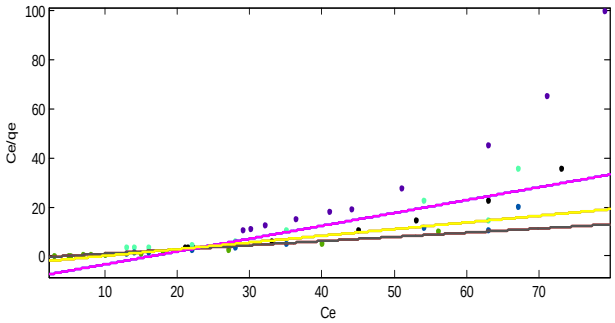

Fig.12a Langmuir plot- Different concentration of zinc removal by *Ficus benghalensis* verses time

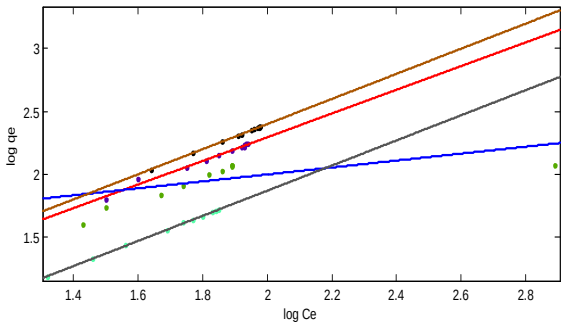

Fig. 12b Freundlich plot-Different concentrations of zinc removal by *Ficus benghalensis* verses time

Table XII:Sorption isotherm constant for different doses of Ficus benghalensis for Zn (II) removal.

Parameter Zn^{2+} ion	Langmuir Parameter		r^2	Freudlich Parameter		r^2
Doses (gm)	Q_{max}	b		N	K_f	
0.75	0.59	-0.049	0.91	1.018	1.8	0.99
1	2.406	-0.125	0.98	1.000	-	1.00
2	4.694	-0.148	0.96	1.000	1.99	1.00
3	8.410	-0.33	0.97	1.030	3.3	0.99

Freudlich adsorption isotherms explain adsorption of zinc by different doses of Ficus benghalensis verses time. Correlation coefficient supports it.

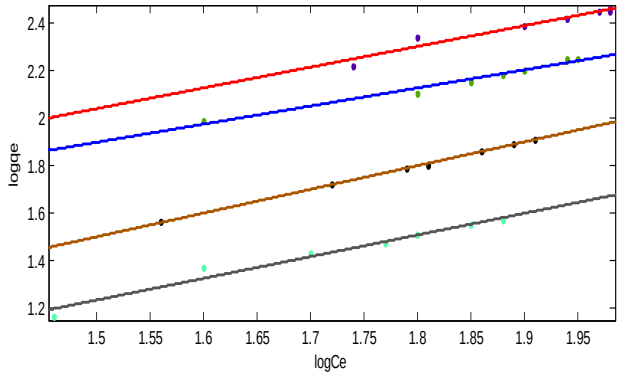

Fig. 13a Langmuir plots-Different doses of *Ficus benghalensis* for zinc removal verses time

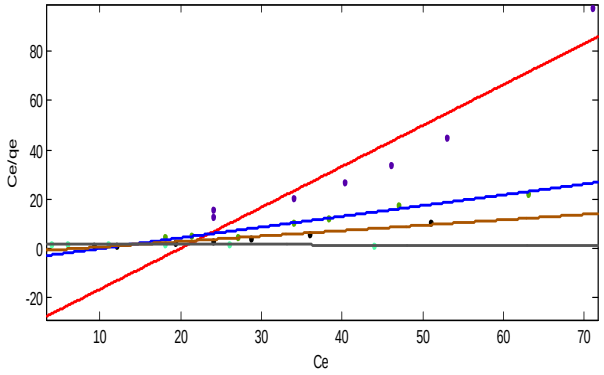

Fig. 13b Freudlich plot-Different doses of *Ficus benghalensis* for zinc removal verses time

3.3. ***Sorption Kinetics****:In order to predict the adsorption kinetics model Pb(II) and Zn(II) pseudofirstorder and pseudo second order were applied to the data .The effect of the different concentration verses time were investigated to find best kinetic models. Linear fit models were generally observed for all the concentration and time.*

TableXIV:Sorption kinetics constant for different concentration of Pb(II) removal by Cajanus cajan.

Pb(II) Parameters)	***Pseudo first order***			***Pseudo second order***		
Concentration(ppm)	K_1	q_e	r^2	K_1	***h***	r^2
50	-161.08	0.28	0.98	106.3	3.2	0.973
100	-164.41	0.248	0.98	88.8	6.57	0.793
150	-145.34	0.236	0.97	101.0	7.19	0.989
200	-96.8	0.212	0.98	117.6	7.75	0.970

The value of correlation coefficient supports Pseudo second order model.

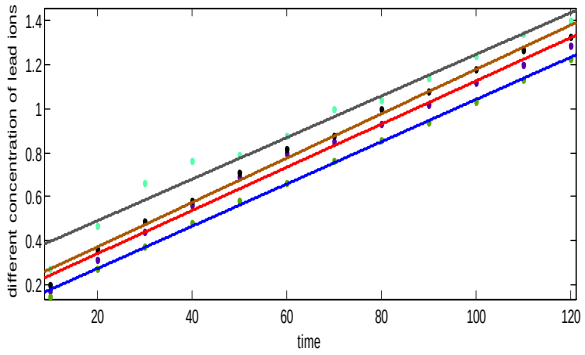

Fig.14a Pseudo first order model- Different concentration of lead removal by *Cajanus* verses time

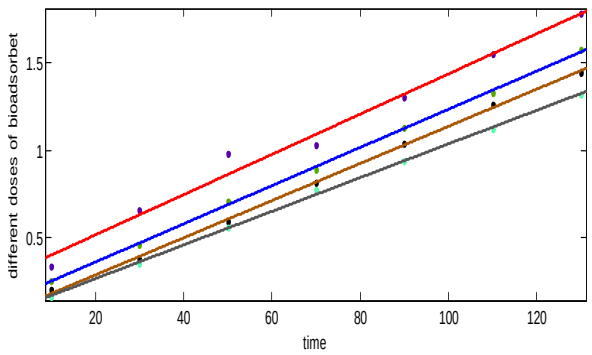

Fig.14b Pseudo second order model – Different concentration of lead removal by *Cajanus cajan* with respect to time

Table XV:Sorption Kinetics constant obtained for different doses of Cajanus cajan.

Parameters Doses (gm) Pb^{2+}	***Pseudo first order***			***Pseudo second order***		
	K_1	q_e	r^2	K_1	***h***	r^2
0.25	-0.0035	1.87	0.90	0.012	5.58	0.71
0.5	-0.0024	1.75	0.080	0.0103	9.407	0.55
1	-0.0039	1.52	0.78	0.0083	7.40	0.48
2	0.0076	0.73	0.88	0.0092	8.13	0.99

In order to predicts sorption kinetic models of Pb (II) pseudo first order and pseudo second order were applied. The effect on the Pb (II) by different doses of adsorbent verses time were investigated to find best kinetic model. Good correlation coefficient was observed for Pseudo second order equation.

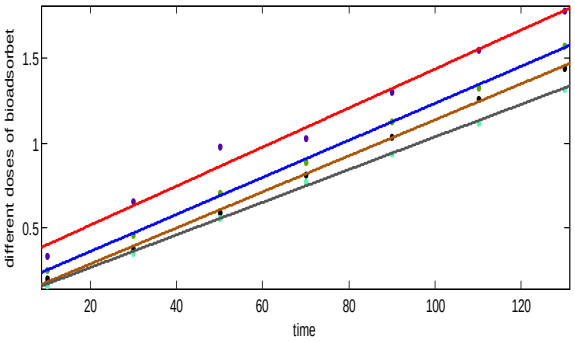

Fig. 15a Pseudo first order model – Different doses of *Cajanus cajan* for lead removal respect to time

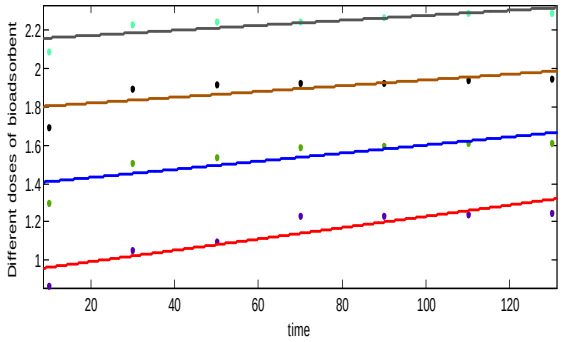

Fig. 15b Pseudo second order model- Different doses of *Cajanus cajan* for lead with respect to time

TableXVI:Sorption kinetics constant for different concentration of zinc (II) removal by Cajanus cajan.

Parameters ConcentrationZn (II)	***Pseudo first order***			***Pseudo second order***		
	K_1	***q_e***	***r^2***	***K_1***	***h***	***r^2***
50	-0.0046	0.28	0.99	133.3	1.618	0.96
100	-0.004741	0.280	0.92	98.4	6.30	0.99
150	-0.006257	0.245	0.92	98.4	6.30	0.99
200	-0.007881	0.254	0.93	158.4	2.299	0.72

The good correlation coefficient is obtained for Pseudo second order equation so it is best fitted model.

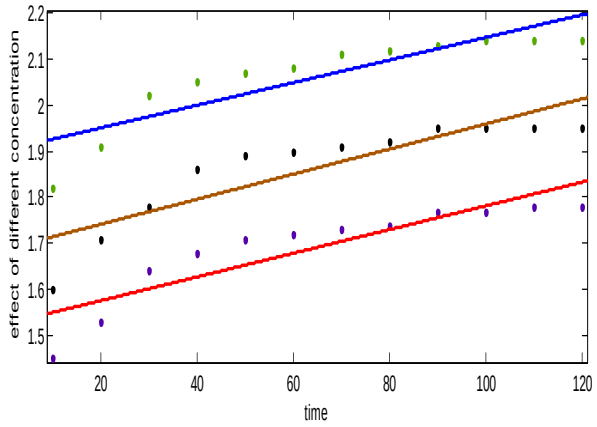

Fig.16a Pseudo first order model: Different concentration of zinc removal by *Cajanus cajan* verses time

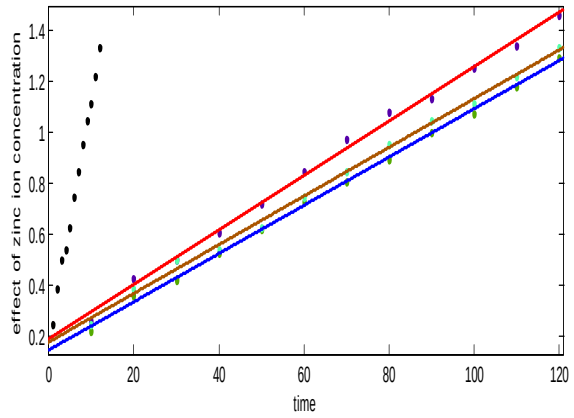

Fig.16b Pseudo second order model: Different concentration of zinc removal by *Cajanus cajan* verses time

Table XVII:Sorption kinetics rate constant obtained for zinc removal by different dosesof Cajanus cajan.

Parameters Doses (gm) Zn^{2+}	***Pseudo first order***			***Pseudo second order***		
	K_1	***Qe***	***r^2***	***K_1***	***h***	***r^2***
0.25	0.0045	1.94	0.99	0.036	0.617	0.96
0.50	0.0075	1.90	0.92	0.045	0.158	0.99
1.00	0.0081	1.75	0.92	0.098	0.158	0.99
2.00	0.0098	1.79	0.93	0.109	0.434	0.72

The value of r^2supports Pseudo second order kinetics equation for the adsorption of Zn(II) ions by Cajanus Cajan .

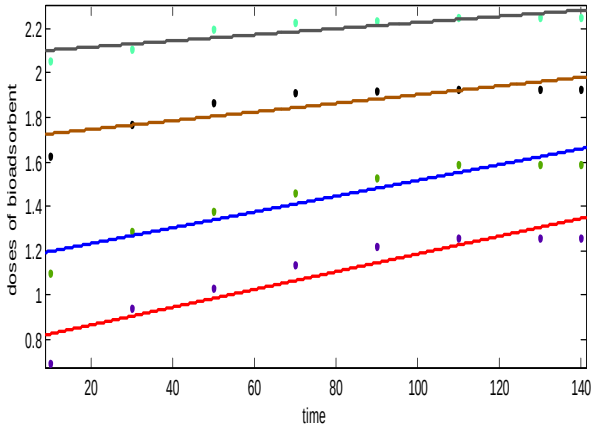

Fig.17a Pseudo first order model Effect of different doses of *Cajanus cajan*for zinc removal with respect to time

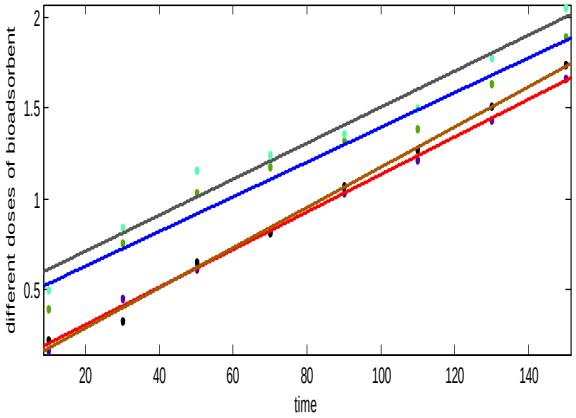

Fig.17b Pseudo second order model- Effect of different doses of *Cajanus cajan* for zinc removal with respect to time

Table XVIII: Sorption kinetics rate constant for different concentration of lead and zinc removal by Ficus benghalensis verses time.

Parameter Concentration (ppm)	***Pseudo first order lead ion***		r^2	***Pseudo second order lead ion***		r^2	***Pseudo first order zinc ion***		r^2	***Pseudo second order zinc ion***		r^2
	K_s	Q_e		K_1	h		K_s	Q_e		K_1	h	
75	0.0090	26.8	0.6	102.8	0.0003	0.9	3.4	8.12	0.9	1.003	-	0.99
150	0.0082	57.6	6	107.3	0.0003	8	6	$4.0X10^7$	0	7	8.03	0.99
200	0.0075	86.8	0.7	111.9	0.036	0.9	1.1	4.12X1	0.9	0.98	7.04	0.99
250	0.0064	127.	2	112.3	0.0000	9	9	0^2	2	1.003	0	0.99
		3	0.7		5	0.9	0.6	5.37	0.8	7	3.16	
			4			9	2		9	1.003	2.45	
			0.6			0.9	0.3		0.9	7		
			9			9	9		5			

Pseudo Second order kinetics is followed by different concentration of lead and zinc removal by Ficus benghalensis verses time. It is well supported by correlation coefficient.

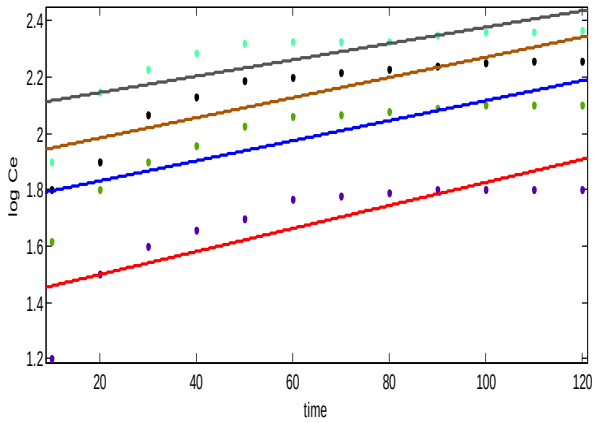

Fig.18a Pseudo first order model- Effect of different concentration of lead removal by *Ficus benghalensis* verses time

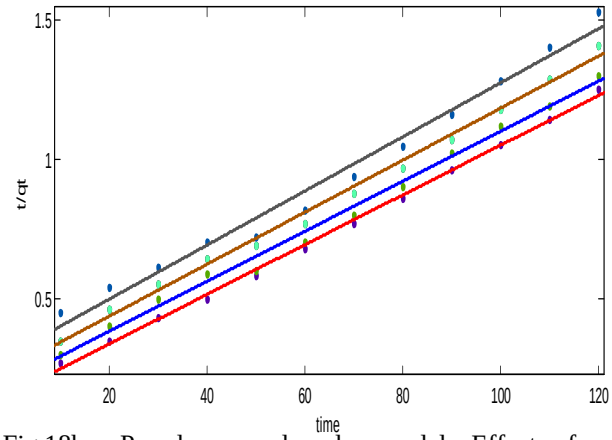

Fig.18b Pseudo second order model: Effect of different concentration of lead removal by *Ficus benghalensis* verses time

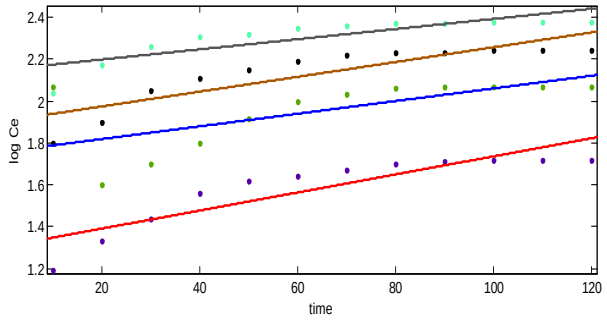

Fig.19a Pseudo first order model- Effect of different concentration of zinc removal by *Ficus benghalensis* verses time.

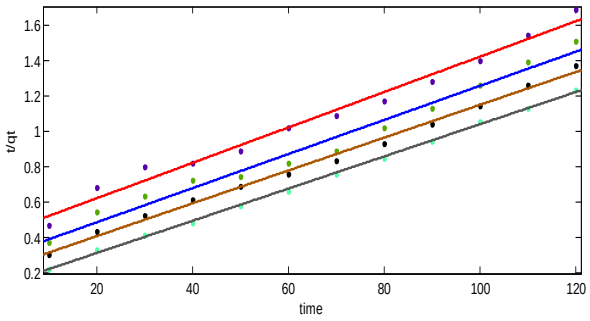

Fig.19b Pseudo second order model: Effect of different concentration of zinc removal by *Ficus benghalensis* verses time

TableXIX:Sorption Kinetics constant for lead and zinc adsorption by different doses of Ficus benghalensis verses time.

Doses gm	***Pseudo first order lead ion***		***r^2***	***Pseudo second order lead ion***		***r^2***	***Pseudo first order zinc ion***		***r^2***	***Pseudo second order zinc ion***		***r^2***
	K_s	***Q_e***		***K_1***	***h***		***K_s***	***Q_e***		***K_1***	***h***	
0.75	0.008	15.17	0.99	98.81	0.0003	0.99	0.002	17.7	0.81	84	0.0004`	0.98
1	0.005	22.3	0.70	96.24	0.0005	0.98	0.005	42.2	0.83	94.07	0.0004	0.90
2	0.004	107.6	0.77	98.42	0.0008	0.99	0.003	108.1	0.86	99.8	0.0006	0.99
3	0.004	186.2	0.88	101.9	0.0011	0.99	0.003	190.5	0.75	104.1	0.00009	0.99

Pseudo second order kinetics explains the adsorption of lead and zinc by different doses of Ficus benghalensis verses time. Good correlation coefficient supports it.

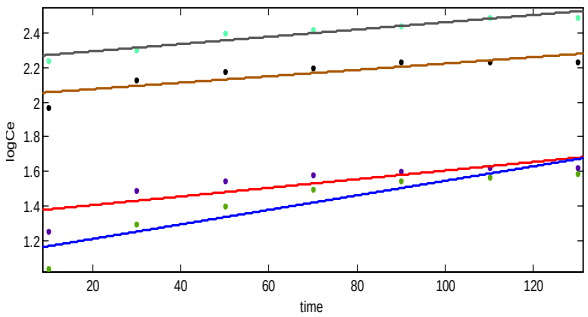

Figure:20a Pseudo first order model- Effect of different doses of *Ficus benghalensis* for removal of lead verses time

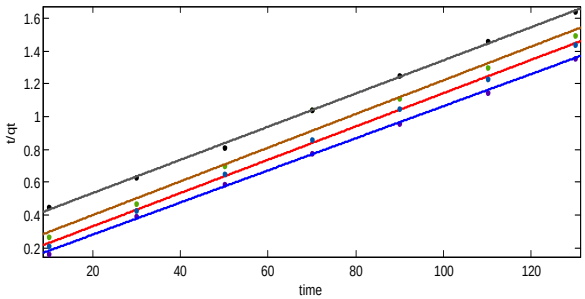

Figure:20b Pseudo second order model- Effect of different doses of *Ficus benghalensis* for lead removal verses time

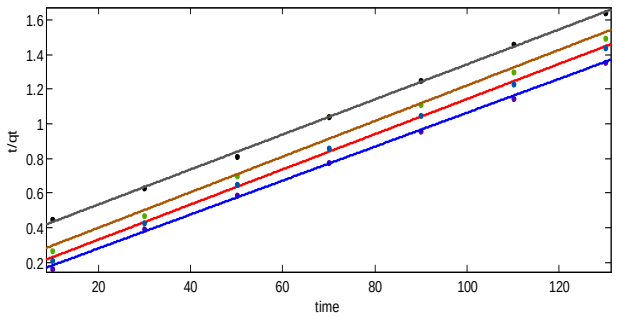

Fig. 21a Pseudo First order: Effect of different doses of *Ficus benghalensis* for zinc removal verses time

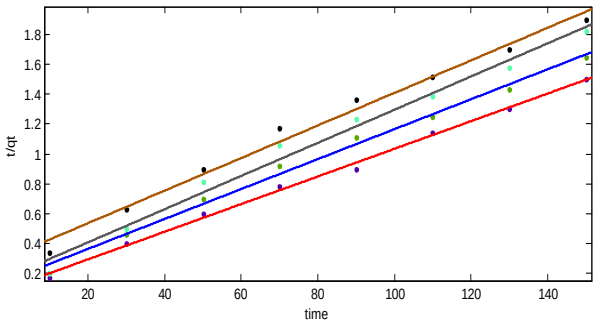

Fig. 22b Pseudo second order model- Effect of different doses of *Ficus benghalensis* for zinc removal verses time

IV. CONCLUSION

Cajanus Cajan and Ficus benghalensis is considered as an effective and efficient bioadsorbent for the removal of lead and Zinc ions from wastewater. It was observed that the suitable pH for the removal is 6 .The value of correlation coefficient for lead ions were higher for Langmuir adsorption isotherm which indicates monolayer adsorption takes place.On the other hand for the Zinc ions follows Freundlich sorption isotherms. The best correlation coefficient for lead ions was obtained by Pseudo second order reaction for concentration and doses with respect to time and zinc ions by pseudo second order for concentration and for doses. The removal of lead and zinc ions take place at low pH more effectively which was observed when treated with dithiozone. Dark colored at pH 6. For Ficus Benghalensis follows Freundlich adsorption isotherm for different concentration as well as for different doses. But for sorption kinetics it follows Pseudo second order for different concentration as well as well as different doses.

IR spectra, NMR spectra, XRD spectra explained that there are many functional group such as –COOH, -OH ,-CHO, aliphatic hydrocarbon which increase the process of bioadsorption at low pH and follows Langmuir and Freundlich adsorption isotherms and pseudo second order kinetics . The data thus useful in designing an efficient treatment plant for lead and zinc ions from wastewater by Cajanus cajan and Ficus benghalensis. These bioadsorbents are chosen for the metal removal because they are easily available, biodegradable,cheap, ecofriendly, efficient and effective.

Bioadsorbent	**Cajanus cajan**		**Ficus benghalensis**	
Metal ions	**Pb(II) ions**	**Zn(II) ions**	**Pb(II) ions**	**Zn(II) ions**
ph	6	6	6	6
Sorption Isotherm				
Concentration	Langmuir Isotherm	Freundlich Isotherm	Freundlich Isotherm	Freundlich isotherm
Doses	Freundlich Isotherm	Freundlich Isotherm	Freundlich Isotherm	Freundlich Isotherm
Sorption Kinetics				
Concentration	Pseudo First Order reaction	Pseudo Second Order reaction	Pseudo Second Order reaction	Pseudo Second Order reaction
Doses	Pseudo Second Order reaction	Pseudo Second Order reaction	Pseudo Second Order reaction	Pseudo Second Order reaction

V. ACKNOWLEDGEMENT

I am thankful to my husband Mr. Pradeep Parashar who always helps me at each & every step of my research work.

6. Schematic presentation for the process of bioadsorption

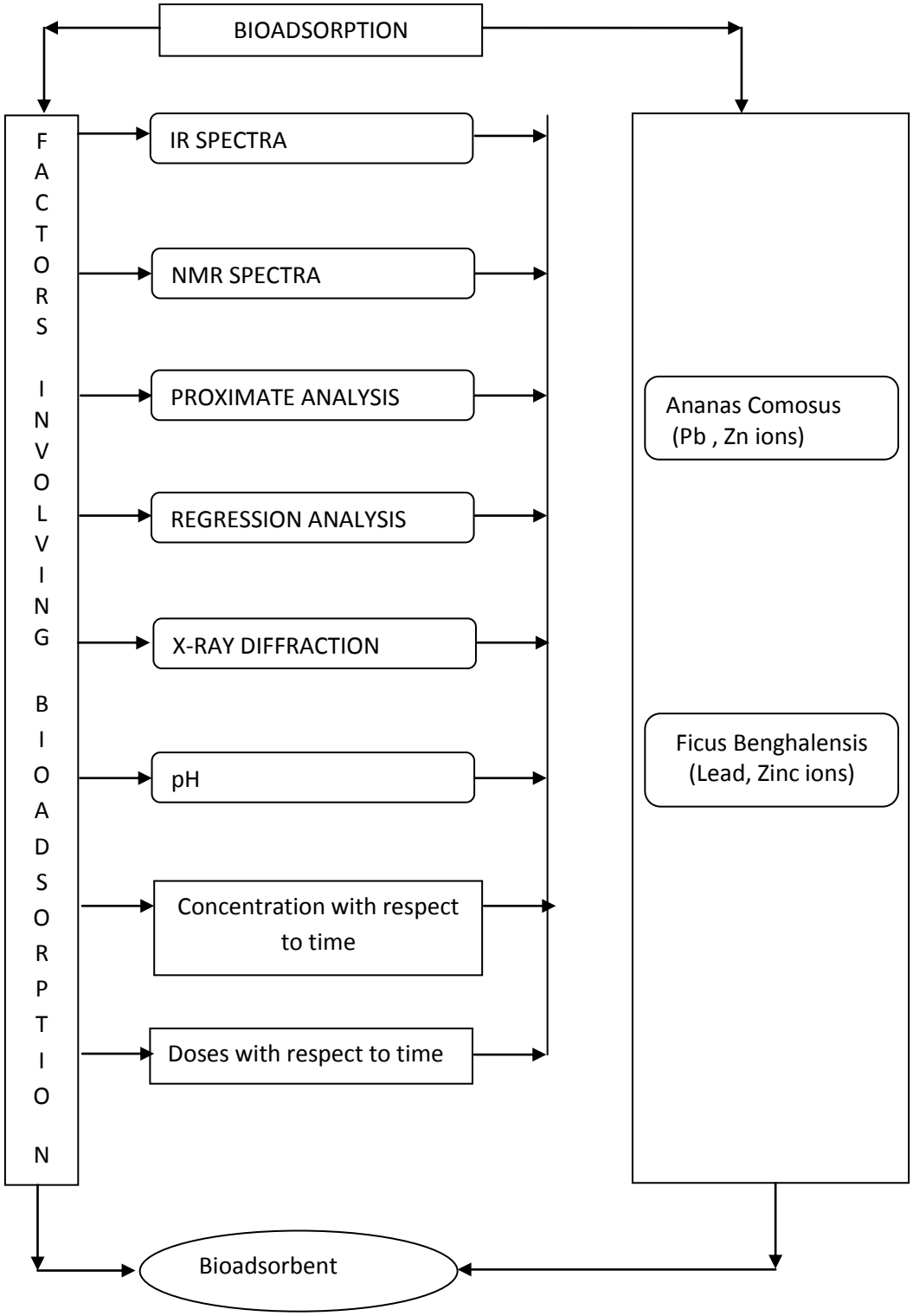

REFERENCE

[1] R. W. Gaikwad, Removal of Cd [II] from aqueous solution by activated charcoal derived from coconut shell, *EJEAF, Agric. Food Chem.*,2004, ISSN 1579-4377.

[2] Ning chuan, Fengb,Xueyi Guoa, Bioadsorption of heavy metals from aqueous solution by chemically modified orange peel,*Journal of hazardous material, Volume 185,*2011, 49-54.

[3] Meral Yurtsever, Bioadsorption of Pb (II)ions by quebracho tannin resin,*Journal of Hazardous materials, 163,*2009, 58-64.

[4] Hala .Y.EI –Kassas and Eman M.El –Taher, Optimization of batch Process Parameters by response surface Methodology for Mycorhiza remediation of chrome –VI by a chromium resistant strain of Marine Trichoderma Viride, *American – EurasianJ.Agric.&Environ.Sci., 5(5):*2009, ISSN 1818 -6769.

[5] A. K. Bhattacharya, Adsorption ofZn (II) from aqueous solution by using different adsorbent,*Thermal Eng .,123,* 2006, 43-5.

[6] B. Volesky, Z. H. Holan, Bioadsorption of heavy metals, *Biotechnology Prog*., 1995, 235-250.

[7] B. Volesky,Detoxification of metal bearing effluents bioadsorption for the next century.*Hydrometallurgy*,2001,59.

[8] N. Ahalya, Bioadsorption of heavy metals also review paper. *Res.J.Chem. Environment*, 2003, 71-79.

[9] K. K. Singh, Removal of lead from aqueous solution by agricultural waste maize bran,*Bioresource Technol., 97* , 2006, 2124-2130.

[10] Nuria Miralles, Cesar Valderrama, Ignasi casas, Maria Martinez, and Antonio Florida, Cadmium and lead removal from aqueous solution by Grape stalk waste: Modeling of a Fixed Bed column,*J.Chem.Eng*., *55*, 2010, 3548-3554.

[11] Zhen Wu, Hong Li, Jian Ming and Ghoul Zhao, Optimization of Adsorption of Tea Polyphenol into oat beta – Glucan using Response surface Methodology, *J.Agric.FoodChem.59*, 2011, 378-385.

[12] Juddith Kammerer, Reinhold Carle and Dietmar R., Kammre, Adsorption and Ion Exchange Basic Principles and their Application in Food Processing. *J.Agric. Food Chem., 59,* 2011, 22-42.

[13] M. M. Aslam, Removal of copper from industrial effluent by adsorption with economically viable materials,*EJEAF chemistry*, 3(2), 2011, ISSN 1579-4377.

[14] N. T. Abdel - Ghani, M. Hefny, G. A. F. El - Chaghaby, Removal of lead from aqueous solution using low cost abundantly available adsorbents, Int. *J. Environ. Sci. Tech.*,2007, 67 - 73.

[15] B. M. W. P. K. Amarasingh, R. A. William, Tea waste as a low cost adsorbent for removal of Cu and Pb from wastewater. *Chemical Engineering Journal*, Vol. – 132, 2007, 299 - 509.

American Journal of Engineering Research (AJER) 2015
American Journal of Engineering Research (AJER)
e-ISSN: 2320-0847 p-ISSN : 2320-0936
Volume-4, Issue-8, pp-89-92
www.ajer.org
Research Paper Open Access

ANXIETY LEVEL OF KHO-KHO PLAYERS AT NATIONAL LEVEL: A SCIENTIFIC VIEW

Rajinder Singh Koura, Jatinder pal Singh
Pggc, Chandigarh

ABSTRACT: *Anxiety is an unpleasant feeling of worry, nervousness, discomfort, and unease. Though it may be normal to experience anxiety once in a while, too much of it can definitely affect one's behaviour and productivity. People who are always having anxiety attacks worry too much that it affects the outcome of their whole day activity. Athletes are not spared of anxiety and just like any anxiety attack; it greatly affects physical and sports performance. Sports and anxiety is always related. The competition in sport gives an athlete the adrenalin to push himself to the win. However, it is also very likely that negative thoughts find its way to the brain which affects the athlete's activity and performance.*

KEY WORDS: *Anxiety, motivation, aggression,*

I. INTRODUCTION

Sports performance is the outcome of many capacities of a sports person. A variety of factors are involved in actually attaining performance goals. Among all performance factors, psychological development is the most important factor. Psychological variables such as anxiety, motivation, aggression and cohesion among team members play a vital role in performance of a sports person. Psychology as behavioral science has made its contribution for improving sports performance. The competitive nature of sports is the major reason for the aggressive behavior of the sportsperson. The struggle for supremacy, dominance and excellence involve all sorts of aggression. The term aggression means violent behavior with intent to hurt a person. Aggressive behavior is also used to depict a strong and adventurous effort. Anxiety is a feeling of nervousness, fear or worry. Anxiety may occur without a cause, or it may occur based on a real situation. Many athletes who perform well during training can suffer from performance anxiety on the day of competition. If feeling of nervousness, anxiety or fear interferes with your sports performance, learning to use a few tips from sports psychologists may help you get your anxiety under control and reduce game day nervousness. Motivation is an internal energy force that determines all aspects of our behaviour, it also impact on how we think, feel and interact with others. In sports, high motivation is widely accepted as an essential prerequisite is getting athletes to fulfill their potential. It is a force that is often difficult to exploit fully. Kho-Kho is an Indian traditional game. Kho-Kho game is played particularly is rural & urban areas. This game has become popular in many states of India. All states have their own association which are affiliated to Kho-KhoFederation of India. In todays competitive era, for getting success in any sports, we should keep in mind the number of factors. In these factors psychological factors plays a important role for improving sports performance.

II. HYPOTHESIS OF THE STUDY

1. There is significant relationship between Anxiety level of motivation of male kho-kho players at National Level.
2. There is significant relationship between. Anxiety or Aggression of male kho-kho players at National level.
3. There is significant relationship between motivation and aggression of male kho-kho players at National level.
4. There is significant relationship between Anxiety level and motivation of female kho-kho players at National level.
5. There is significant relationship between anxiety and aggression of female kho-kho players at National level.
6. There is significant relationship between motivation and aggression of female kho-kho players at National level.

7. There is significant relationship among anxiety, motivation and aggression of male kho-kho players at National level.
8. There is significant relationship among anxiety, motivation and aggression of female kho-kho players at National level.
9. There is significant relationship among anxiety, motivation and aggression of female kho-kho players at National level.

III. SIGNIFICANCE OF THE STUDY

1. The present study may be helpful to find out relationship among Anxiety level motivation and aggression level of kho-kho players at National Level.
2. The present study may be helpful to physical Education teachers, coaches and sports psychologists to understand the relationship of kho-kho players at National level.
3. The present study may be helpful in designing the psychological tests of the various games.

IV. METHODOLOGY

1. Design of the study – In order to solve the purpose of the sample will be collected from kho-kho players of North Zone states of India i.e. Punjab, Haryana, Himachal Pradesh, J&K. Chandigarh, Rajasthan, Delhi, Uttar Pradesh, Uttrakhand, through purposive sampling. The players will be assessed in three Psychological variables i.e.sports competition anxiety, Aggression and sports achievement Motivation level.

SELECTION OF THE TEST ITEMS

To measure anxiety sports competition anxiety test by R.MARTIN (1990) was used.

To measure motivation level sports ACHIEVEMENT motivation test by M. L. Kamlesh was used.

To measure aggression level ,aggression scale by Dr. Roma PAL AND Dr. Tasneem Naqvi was used.

V. STATISTICAL TECHNIQUES USED

In order to test the hypothesis mean, standard deviation (S.D.), correlation and Analysis of Variance (ANOVA) will be used.

COMPARISON OF ANXIETY TEST OF ATHELETES

MEAN PB	2.833333	2.666667	2.583333	2.666667	2.666667	2.083333	2.25	2.75
MEAN JK	2.5	2.5	2.333333	2.583333	2.666667	1.916667	2.25	2.416667
MEAN RAJ	2.333333	2.416667	2.25	2.5	2.5	2.166667	2.5	2.416667
MEAN UK	2.583333	2.5	2.583333	2.416667	2.25	2.083333	2.083333	2.333333
MEAN UP	2.416667	2.583333	2.5	2.25	2.25	1.916667	2.25	2.583333
MEAN HP	2.416667	2.25	2.25	2.416667	2.333333	1.916667	2.25	1.583333
MEAN DELHI	2.5	2.75	2	2.5	2.25	2.083333	2.166667	1.833333

TABLE 1

COMPARATIVE ANXIETY TEST FOR ATHELETE OF VARIOUS STATES

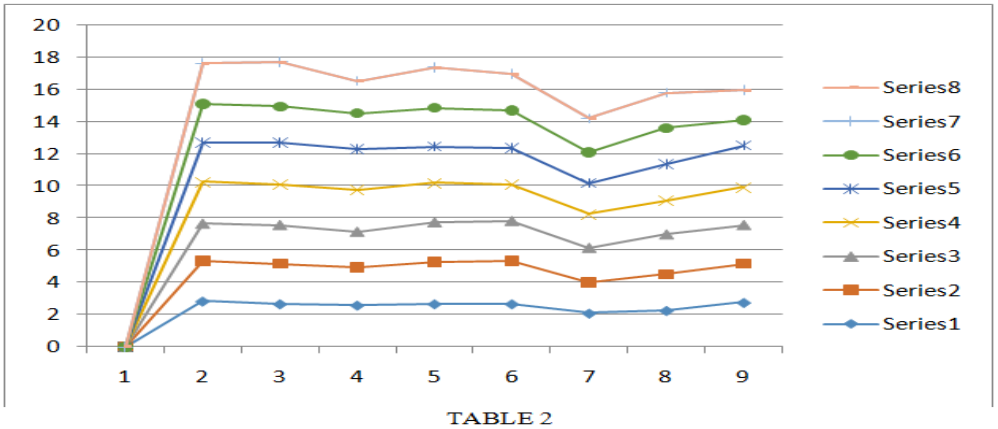

TABLE 2

COMPARISON OF SPORTS ANXIETY TEST WITH KEY(BOYS)

KEY	25-30	12-17	25-30	25-30	15-24	25-30	25-30
SCORE	26	13	30	27	24	30	28
INTERPRETATION	HIGHLY AVERAGE	AVERAGE	HIGHLY AVERAGE	HIGHLY AVERAGE	ABOVE AVERAGE	HIGHLY AVERAGE	HIGHLY AVERAGE

TABLE 3

COMPARISON OF SPORTS ANXIETY TEST WITH KEY(GIRLS)

KEY	15-24	12-17	25-30	15-24	15-24	25-30	15-24
SCORE	24	12	26	22	19	26	20
INTERPRETATION	ABOVE AVERAGE	AVERAGE	HIGHLY AVERAGE	ABOVE AVERAGE	ABOVE AVERAGE	HIGHLY AVERAGE	ABOVE AVERAGE

TABLE 4

RESULTS OF SPORTS ACHIEVMENT MOTIVATION TEST(GIRLS)

key	>17	>17	>17	>17	7 or less	>17	>17	14 or more	>17	8-16
SCORE	17	19	18	16	7	18	19	14	20	9
INTERPRETATION	EXTROVERSION	EXTROVERSION	EXTROVERSION	EXTROVERSION	INTROVERSION	EXTROVERSION	EXTROVERSION	NEUROTICISM	EXTROVERSION	AMBIVERT

TABLE 5

RESULTS OF SPORTS ACHIEVMENT MOTIVATION TEST(BOYS)

key	>17	>17	>17	>17	7 or less	>17	>17	14 or more	>17	>17
SCORE	20	21	19	18	9	22	20	15	21	18
INTERPRETATION	EXTROVERSION	EXTROVERSION	EXTROVERSION	EXTROVERSION	INTROVERSION	EXTROVERSION	EXTROVERSION	NEUROTICISM	EXTROVERSION	EXTROVERSION

TABLE 6

The scoring key was constructed by Dr Roma pal and Dr Tasneem Naqvi was employed and scoring key is given below:

S. NO	RANGE OF SCORE	INTERPRETATION
1	107 AND ABOVE	THE SATURATED
2	90-106	THE HIGH
3	61-89	THE AVERAGE
4	46-60	THE LOW
5	45 AND BELOW	THE C LEAN

TABLE 7

SCORE AS PER KEY	SCORE OF GIRLS AGGRESSION	INTERPRETATION
107 AND ABOVE	170	THE SATURATED

TABLE 8

VI. SIGNIFICANCE OF THE STUDY

4. The present study may be helpful to find out relationship among Anxiety level motivation and aggression level of kho-kho players at National Level.
5. The present study may be helpful to physical Education teachers, coaches and sports psychologists to understand the relationship of kho-kho players at National level.
6. The present study may be helpful in designing the psychological tests of the various games.

REFERENCES

[1] Feldenkrais, M., (1972). *Awareness through movement*. New York: Harper & Row.

[2] Hendricks, G, & Fadiman, J. (Eds). (1976). *transpersonal education: A curriculum for feeling and being*. New York: Prentice-Hall.

[3] International Society of Sport Psychology (1992). Physical activity and psychological benefits: International Society of Sport Psychology Position Statement. *The Physician and Sports medicine*, *20*(10), 179-184.

[4] Miller, H. B. (1969). *Emotions and malignancy (hypnosis-psychiatry and organic tissue changes)*. Paper presented at American Society of Clinical Hypnosis Convention, San Francisco

[5] Bhusan-(2002), - Anxiety, Aggression and Team cohesion as Related to performance in Selected Team Sports. Unpublished Ph.D thesis, Panjab University Chandigarh.

[6] Bjorkqvist, K., &Nicmcli, P. (1992). New trends in the study of female aggression, *In K. Bjorkqvist& P. Nienrelli (Eds.), O/women: Aspects of female aggression. SanDiego, CA: Academic Press.*

[7] Ellis, S.R., & Janelle, C.M. (2000).Legitimacy Judgments of Perceived Aggression and Assertion by Contact and Non-Contact Sports Participants. Research Quarterly for Exercise and Sports, 71(1), 88-89.

[8] Gould, D., Horn, T.S., Spreemann, J. (1983). Competitive anxiety in junior elite wrestlers.***Journal of sports and exercise psychology,*** 5*(1)*, 58-71.

[9] Maria Kavussanu, Glyn C. Roberts (1996) Motivation in Physical Activity Contexts: The Relationship of Perceived Motivational Climate to Intrinsic Motivation and Self-Efficacy **Journal of Sports and Exercise Psychology,** Volume 18, Issue 3, September, 264-280.

[10] Mintah, J.K., Huddleston, S, &Doody, S.G. (1999).Justification of Aggressive Behavior in Contact and Semi contact sports. Journal of Applied Social Psychology, 29, 597-605.

[11] Ommundsen Y., B.H. Pedersen (1999)*The role of achievement goal orientations and perceived ability upon somatic and cognitive indices of sport competition trait anxiety A study of young athletes,* Scandinavian Journal of Medicine & Science in Sports, SJMSS Volume 9, Issue 6, 333-343, December 1999.

[12] Ommundsen, Y., vaglum, P. (1991). Soccer competition anxiety and enjoyment in young boy players.The influence of perceived competence and significant others emotional involvement.***International journal of sports psychology,*** 2(2), 35-45.

American Journal of Engineering Research (AJER)
e-ISSN: 2320-0847 p-ISSN : 2320-0936
Volume-4, Issue-8, pp-93-97
www.ajer.org
Research Paper Open Access

An Evaluation of the Plane Wave properties of Light using Maxwell's Model

Nwogu O. Uchenna [1], Emerole Kelechi [2], Osondu Ugochukwu [3], Imhomoh E. Linus [4]

[1](*Department of Electrical and Electronics Engineering, Federal Polytechnic Nekede ,Owerri, Imo State, Nigeria)*

ABSTRACT: *The only two forces of nature that human beings can directly experience through their 5 senses are gravity and light. The other sensations such as a smell, heat, sound etc detect macroscopic properties of mater and not its constituents. Electrostatic and electromagnetic charges are deeply likened with light. It is the accelerated movement of these charges that gives light. The movement is at the speed of light. This part of electromagnetic radiation (light) is the only one that is visible to human being. Here, the language of engineering electromagnetism; the second grand unification of science that unifies the 3 most powerful forces of light, magnetisms and electricity (Maxwell's four equations) and underlying vector calculus equations were invoked to decouple the component parts of a typical electromagnetic radiation to bring out this phenomenon called light, as a basic component part of an electromagnetic radiation.*

Keywords *- current, displacement, field, magnitude, phasor, vector*

I. INTRODUCTION

Light is a transverse wave having an oscillating electric and magnetic field. Both fields are perpendicular to each other and to the direction of their propagation. The ratio of the electric field intensity ($\bar{E}$) and magnetic field intensity ($\hat{H}$) is equal to a constant thus;

$$\rightarrow \frac{E}{B} = \text{constant (c)}$$

Therefore an electromagnetic waves is defined as plane if at any given instant of time, the electric intensity ($\bar{E}$) and the magnetic intensity ($\bar{H}$), remain the same (in magnitude and phase), over a plane normal to the direction of wave propagation and are completely propagating in the Z direction and the X-Y plane is called the plane of the wave or the wave front.

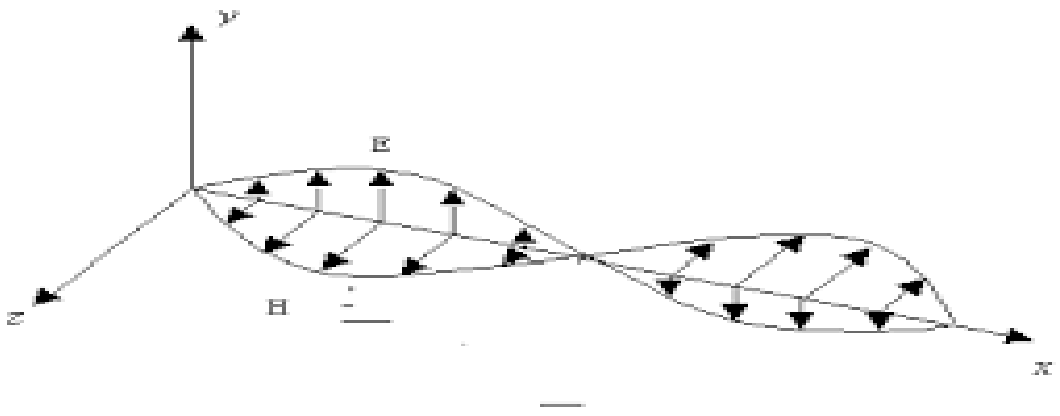

Figure 1: Plane Wavefront.

From the above definition;

$\frac{\partial B}{\partial X} = \frac{dB}{dy} = 0$

$\frac{\partial E}{\partial X} = \frac{dE}{dy} = 0$

$\therefore \frac{dEX}{dBX} = \frac{dEY}{dBy}$ = Constant = field strength ≅ 377 (intrinsic impedance)

According to Maxwell equationfor plane wave:

$E=E_{\circ}Cos\Phi X^{:H} = H_{\circ}Cos\Phi\bar{y}$ where X and Y are unit vector in a given direction.

II. METHODOLOGY

Maxwell's original equation where broken down into four equations. These four equations are a refined form of the 22 previous equations. It unifies the 3 most powerful forces of nature: Light, Electricity and Magnetisms. It consists of the electromagnetic language that binds these 3 universal forces [4]. Also Maxwell's equations play a central role in the analysis in the transmission media [2].

The four sets of equations satisfied everywhere by the electric field vectors ($\bar{E}$ and $\bar{D}$), and magnetic field vectors ($\bar{H}$ and $\bar{B}$) are;

$div\ \bar{D}=p$

$div ß=0$

$curl\ \bar{E} = -\frac{d\bar{B}}{dt} = \mu_r\mu_{\circ}\frac{-dH}{dt}$

$curl\ \bar{H} = \bar{J} + \frac{d\bar{D}}{dt} = \delta\varepsilon + \epsilon_r\epsilon_{\circ}\frac{d\bar{E}}{dt}$

Where $\bar{D}$ and $\frac{\delta\bar{D}}{dt}$ are electric displacement and displacement current density respectively and $\bar{J}$ is the conduction current density.

$\bar{D} = \epsilon_r\epsilon_{\circ}\bar{E}$ and $H = \frac{\bar{B}}{UrUo}$ with ρ = free charge density

$\epsilon_{\circ}$= permittivity of free space = 8.854 X 10^{-2}fm $^{-1}$

ϵ_r=dielectric constant or relative permittivity of the material

ϵ_r = 1 in a vacuum, $\epsilon_r > 1$ in homogenous, isotopic medium

$\mu_{\circ}$ = permeability of free space

$\mu\epsilon_{\circ} = \frac{1}{C2}$ where c speed of light.

However, in the words of Maxwellians [4]; in the beginning God said;

$\bar{V}\ X\ \bar{H} = \bar{J} + \frac{\delta\bar{D}}{dt}$

$\bar{V}\ X\ \bar{E} = -\frac{\delta\bar{B}}{dt}$

$\bar{V}.\bar{B} = 0$

$\bar{V}.\bar{D} = p$ and there was light.

This Maxwell's equation is made up of electromagnetism and light. The equations can be decoupled and by applying constitutive relations and other vector calculus conditions, thus as a component of electromagnetic wave can be unveiled.

III. PHYSICAL INTERPRETATIONS

$$\bar{V} \text{ X } \bar{H} = \bar{J} + \frac{\delta \bar{D}}{dt}$$

$$\bar{V} \text{ X } \bar{E} = - \frac{\delta \bar{B}}{dt}$$

$\bar{V}.\bar{B} = 0$

$\bar{V}.\bar{D} = p$

Where,

$\bar{J}$ = Conduction current density

$\frac{\delta \bar{D}}{dt}$ = time varying electric flux density

$\bar{B}$ = magnetic flux density

$\frac{\delta \bar{B}}{dt}$ = time varying magnetic flux density

ρ = electric charge density

The four equations describe the experimental al facts that [4].

Equation 1: Magnetic field is not only produced by a conductor current but also by a displacement current or time varying electric flux density (Ampere's law)

Equation 2: Electric field can be produced by a time varying magnetic field (Faraday and Lenz's law)

Equation 3: There is no isolated magnetic change in nature i.e. the existence of a monopole.

Equation 4: Establishes the occurrence of isolated electric charges in nature (Gauss law).

IV. MAXWELL'S EQUATION IN FREE SPACE(CHARGE FREE ZONE)

A free space or charge free zone is space with nothing in it at all. It doesn't exist in the known universe, but interstellar space is a good approximation [6]

Features of free include: Uniformity everywhere, no electric charge in and around it. It carries no electric current and nothing that electromagnetic radiations are propagated in free space by electromagnetic theorem, we use Maxwell's equation as well as a constitutive tool to understand and decipher plane waves into their constituent parts.

Using Maxwell's equations (M.E) (1) and decoupling it by multiplying it by a vector $\bar{V}$ we have that [4]:

$$\bar{V} \text{ X } [\bar{V} \text{ X } \bar{H}] = \bar{V} \text{ X } \bar{J} + \bar{V} \text{ x } \frac{\delta \bar{D}}{dt} \ldots\ldots\ldots (1)$$

Invoking constitute relations to decouple the L.H.S. of the equation (1), we have, assuming

$\bar{D} = \epsilon \bar{E}$

:. R.H.S = $\bar{\nabla}$ X $\bar{J}$ + $\bar{\nabla}$ X[$\frac{d\epsilon\bar{E}}{dt}$]= $\bar{\nabla}$ X $\bar{J}$ +Є$\frac{d}{dt}$ [$\bar{\nabla}$ X $\bar{E}$]……..(1a)

To decouple L.H.S of the equation, we use the vector identity theorem, which state the curl of the curl of a vector is equal to the gradient of divergence minus the laplacian. Thus:

L.H.S = $\hat{V}$ [$\hat{V}$.$\hat{H}$] – $\hat{V}^2\hat{H}$

Where $\hat{V}$ [$\hat{V}$.$\hat{H}$] = gradient of the divergence of the vector = 0

$\bar{\nabla}^2\bar{H}$ = Lapalcian

Bringing the L.H.S and R.H.S of the equations together, we have that

0-$\bar{\nabla}^2\bar{H}$=$\bar{\nabla}$X$\bar{J}$+Є$\frac{d}{dt}$[$\bar{\nabla}$X$\bar{E}$]… ……..(2)

Form the L .H.S, $\bar{\nabla}$X$\bar{E}$ = Maxwell's equation (M.E) (2), applying the constitutive relations to further decouple, we have;

[$\bar{\nabla}$ X $\bar{E}$] = $\frac{dB}{dt}$

B=μ$\bar{H}$:.[$\bar{\nabla}$X$\bar{E}$]=– $\frac{\delta\mu\bar{H}}{\delta t}$……..……(3)

Substituting equation (3) back in equation (2) we have,

$$0 - \bar{\nabla}^2\bar{H} = -\frac{\mu\epsilon d2\bar{H}}{dt2} = -\bar{\nabla}\,X\,\bar{J}$$

The above equation (4) is called the general wave equation for the H field [4]. We can further deduce the wave equation on the $\bar{E}$ field by decoupling Maxwell's equation 2 by taking the curl of the equation:

$\bar{\nabla}$X [M.E (2)]

$\bar{\nabla}$ X $\bar{\nabla}$ X $\bar{E}$ = $\bar{\nabla}$ X -$\frac{\delta\bar{B}}{dt}$

$\bar{\nabla}$ X $\bar{\nabla}$ X $\bar{E}$ = - $\frac{d}{dt}$ [$\bar{\nabla}$ X $\bar{B}$]…….. …….(5)

By applying vector identity to the L.H.S and the constitutive relations on the R.H.S, we have that;

$\bar{\nabla}$ ($\bar{\nabla}$ X $\bar{E}$) - $\bar{\nabla}^2$ X $\bar{E}$ =μ $\frac{d}{dt}$ ($\bar{\nabla}$ X $\bar{H}$) = μ $\frac{d}{dt}$ (J $\bar{J}$+ Є $\frac{d\bar{E}}{dt}$)

The L.H.S. can also be decoupled further with M.E (4)

$\bar{\nabla}$.($\bar{\nabla}$ X $\bar{E}$) where $\bar{\nabla}$.$\bar{D}$ = ρ, substituting we have that $\bar{\nabla}$ ($\frac{\rho}{Є}$)

Bringing the two sides of the equations, together we have; ……..…(6)

$$\bar{\nabla}^2\,\bar{E} - \mu Є\frac{d2\bar{E}}{dt2} = \mu\frac{d\tau}{dt} + \bar{\nabla}\left(\frac{\rho}{E}\right)$$

equation for the $\bar{E}$ field. But for a source free region

$\bar{J} = 0$ and $p = 0$

Substituting equation (4) and (6) we can deduce the general vector wave equation for a source free region in the $\bar{H}$ and $\bar{E}$ field respectively:

$$\bar{V}^2 H - \mu\epsilon \frac{d2H}{dt2} = 0$$

$$\bar{V}^2 E - \mu\epsilon \frac{d2E}{dt2} = 0$$

time sinusoidally , the time derivative can be replaced by factors of jw to

$\frac{\delta 2}{dt2} = (jw)^2 = -w^2$ substituting in the wave equations, we have [4]:

$$\bar{V}^2 \bar{H} + w^2 \mu\epsilon\bar{H} = 0$$

$$\bar{V}^2 \bar{E} + w^2 \mu\epsilon\bar{E} = 0$$

Comparing the general equations with the source velocity equation

$\bar{V}^2 w - \frac{1}{\sqrt{2}} \frac{\delta co2}{\delta t2} = S^o$ (free space)

where $\sqrt{}$ =source velocity

We have that

$$\therefore \sqrt{sp} = \frac{1}{\sqrt{2}} = \mu\epsilon = \frac{1}{\sqrt{\mu\epsilon}}$$

Assume free space, $\epsilon = \epsilon_\circ = \frac{1}{36\pi} \text{ X } 10^{-9} = 8.854\text{X}10^{-6}\text{C}^2/\text{nm}^2$,

$\mu = \mu_\circ = 4\pi \text{ X}10^{-7}\text{Tm/A}$

$$= \sqrt{sp} = \frac{1}{\sqrt{4\pi}\text{X}10-7\text{X}\frac{1}{36\pi}\text{ X }10-9} = 3\text{X}10^8\text{m/s} = \text{speed of light.}$$

This shows that light is an integral part of both the electric field $\bar{E}$ and the magnetic field $\bar{H}$.

V. CONCLUSION

The above derived equation shows that light can behave like a projecting magnetic or electric field. That is, we have light embedded in both the electric and magnetic fields. Electromagnetic waves are produced that propagates through a vacuum at the speed of light.

REFERENCES

[1] George Kennedy and Bernard Davis, *Electronic Communication systems* (McGraw-Hill Education, 1992).
[2] Johnson Ejimanya, Communication Electronics(Print Konsult, 2005).
[3] Jeff Hecht, *Understanding Fiber optics* (Prentice Hall, 2006).
[4] S. Adekola, A. Ayorinde, I. Moete On the Radiation fields of the Helical Hyperbolic Antenna, *PIERS Proceedings Kuala Lumpur,MALAYSIA, March 27-30, 201, 1644-1647*
[5] J. Parryhill, *Basic Electromagnetic wave properties of ligh t(*2009).
[6] www.icbse.org/education: Introduction to light waves (2012).

American Journal of Engineering Research (AJER)
e-ISSN: 2320-0847 p-ISSN : 2320-0936
Volume-4, Issue-8, pp-98-103
www.ajer.org
Research Paper Open Access

Reassessment of Islamic Astronomical Sciences

Md. Sharif Ikbal[1],
[1](Department of Islamic Studies, The People's University of Bangladesh, Bangladesh)

ABSTRACT: *This paper attempts to reevaluate Muslim input to astronomy. Underling the efforts and the contributions of Al–Biruni and Al–Battani to astronomy is the core concern of this paper. Astronomy is one of the sciences that have existed since the dawn of recorded civilization. It has been called the queen of sciences and it incorporates many disciplines such as physics, optics in particular, and mathematics, as well as celestial mechanics. Reassessing the contributions of Muslim scholars and Qur'anic views on astronomy is an urgent call in a time when knowledge is claimed by one civilization, the Western civilization.*
Keywords -*Islamic astronomy, Quranic views on astronomy, Muslim contributions to astronomy, Al–Biruni*

I. INTRODUCTION

Astronomy is that branch of engineering sciences that deals with the origin, evolution, composition, distance and the motion of all bodies and scattered matter in the universe. In the Arabic peninsular before the advent of Islam, there was an intimate knowledge of the sun and the moon as well as the night sky whereby meteorological phenomena were associated with the changing patterns of these celestial objects throughout the year with reasons.

The expansion of the Islamic intellectualism began in 622 AD with the journey of Prophet Mohammed from Mecca. Within a century, Muslims dominated the whole Middle East and extended eastwards across northern India to the borders of China, and westwards across Asia Minor and North Africa, from there to Spain and part of Europe. Muslim scholars became enthusiastic intellectuals and benefited from the achievements of the great civilizations of the past developing interest for astronomy and other fields. This was in line with one of the characteristics of Islam, that is, to have love for wisdom and knowledge. The Qura'nic dictum on astronomy reads:

"We have not created the heaven and the earth and all that is between them in mere idle play. None of this have we created without an inner truth." (Al–Quran, Surah al–Dukhan, verse 38)

II. THE NATURE OF ASTRONOMY

ShaharirMohd Zain argues that the word *Astro*is a Greek word which brings into mind the meaning of stars – astronomy can thus be regarded as the science that investigates all matter–energy in the universe, which includes its distribution, composition, physical states, movements and evolution. (ShaharirMohd Zain, 1985) [1].

According to Sharma astronomy in the etymological level denotes the *law of the stars* - from the Greek word αστρονομία- is a science involving the observation and the explanation of events occurring outside earth and its atmosphere. Astronomy studies the origins, evolution, physical and chemical properties of objects that can be observed in the sky as well as the processes involving them. (Arvind Sharma, 1983) Astrophysics, which discusses the physical properties and structure of all cosmic matter, is thus, a branch of this field.

Dick Teresi contends that a tolerant, multiracial, highly literate society, with a predominant language, Arabic, also fostered the growth of astronomy in Islam. (Dick Teresi, 2003) The stars were used for navigation in the desert whereas the moon regulated the Islamic calendar. The Quran states in that line that:

"They ask you about new crescent moons, say they are but signs to mark fixed period of times for mankind and Hajj." (Al–Quran, Surah Al–Baqara, verse 189)

The sun was used in calculating the five daily prayer times as well as the fasting period based on the position of the sun in the horizon [2]. It was also by the means of astronomy that Muslims determined the precise direction of the *Qibla*, the holy figure they face five times a day in fulfilling their daily prayers.

Teresi confirms that Astronomy entered the Islamic tradition from three directions: Persia, India and Greece. He wrote: "With conquest, they brought an Arab folk astronomy that mixed with local knowledge, especially the mathematical traditions of Indian, Persian, and Greek astronomy, which they mastered and adapted to their needs." (Dick Teresi, 2003)

The first major astrological text translated into Arabic came from India. This was the *Siddhanda*, translated in Baghdad around 770 and known to the Muslims, as the *Sindhind*. (Dick Teresi, 2003). Nonetheless, the Greek contribution to the Islamic astrology was by far the greatest. The conquests of Alexander the Great had spread Greek civilization right across the ancient world; consequently, Greek ideas had greatly influenced the indigenous astrology of Persia and India. The great cultural center of Alexandria in Egypt which was renowned as 'The Hub of the World' in Hellenistic times fell to Muslims in 642 [3]. This enabled the intellectual legacy of Greece which was contained in thousands of manuscripts in its famous library to be opened up to Islamic scholars. In the early ninth century, Al–Ma'mun, the caliph of Baghdad, founded an academy called the House of Wisdom which became the center of an ambitious project to translate all the surviving texts of antiquity into Arabic. (J. J. O' Conner & E. F. Robertson, 1999) Aristotle's work in physics, the astronomy of Hipparchus and Ptolemy's astrology, which revolutionized Islamic science were some of the many works that were translated here.

The mathematical astronomy possessed a pronounced Islamic flavor until the nineteenth century. The discovery of the theories of Ptolemy and Hipparchus brought new scientific rigors to the field. This was further stimulated by contact with India and the application of the advanced techniques. The numerical symbols 1, 2, 3, and the decimal system of notation based on the symbol zero, which were unknown to the Greeks and Romans, came originally from India. Toby Huff contends that: "It is useful to consider the history of astronomical thinking in medieval Islam. For astronomical work in Islam during this period was both intense and far in advance of equivalent thought in Europe". (Toby E. Huff, 1993). Theories and designs were gradually improved until the precision of Islamic Astronomy surpassed to that of the Greeks. The philosophical foundation to Islamic astrology was laid down by Al–Kindi, Ma'mun's physician, and one of the most learned man of all times. Drawing upon classical ideas, Al–Kindi evolved a philosophy of 'cosmic sympathy' that linked macrocosm and microcosm. The correspondence between celestial configurations and events on earth demonstrated the wholeness of creation – the theories of Aristotle and Ptolemy provided a respectable scientific framework for the former.

The fatalism implicit in astrology was broadly compatible with the teachings of Islam, which means, 'submission' to the Will of Allah. Astrological symbolism became an important element in the esoteric doctrines of the Sufi mystics, though more orthodox theologians argued that astrology was irrelevant at best; at worst, it was a dangerous, delusion bordering on the magical and demonic – since Allah is all–powerful. Similar objections were raised by the Christian theologians when astrology began to filter into medieval Europe through Islamic universities of Moorish Spain.

The Mathesis of FirmicusMaternus was the first classical text to be translated from Arabic to Latin around 1000 AD. (David Plant, 2005) It was followed by a flood of astrological, scientific and philosophical works over the next two centuries that revitalized all aspects of European learning. The original Arabic texts mixed with that of the classical authors gave a distinctly Islamic flavor to medieval astrology that can be traced down to the 17th century.

Some of the rules and aphorisms of Islamic scholars like Albumazar (Abu–Ma'shar), Alfraganas (Al–Farghani) and AlKindus (Al–Kindi) were even quoted in Lilly's Christian Astrology. However, with the historical enmity between Islam and Christianity, it was fashionable amongst European astrologers to regard any dubious methods such as the Arabic distortions of classical doctrines [4].

As an example, the high–minded and progressive Kepler dismissed horary and most other traditional practices as 'Islamic Sorcery', though horary and even the much–maligned 'Arabian parts' were well–known in classical astrology [5]. Virtually all the Arabic texts that influenced medieval astrology remain in Latin translation, making them inaccessible to most astrologerstoday.David King agrees the history of astronomy in Islamic civilization has been documented by a series of scholars of diverse backgrounds. (David A. King, 1986) Yaqubibn Tariq, Al–Khawarizmi, Al–Battani, Al–Farghani, Al–Sufi, Al–Biruni, Al–Tusi, and Omar Khayyam are just a few scholars who have left a lasting mark in the annals of astronomy. Among these scientists however al-Biruni and al-Batani's contributions to Astronomy stand high on the rostrum.

III. AL-BIRUNI'S CONTRIBUTIONS TO ASTRONOMY

Astronomy, a prime interest to the human mind since the Stone Age itself, has been approached in every way possible by the Muslim astronomers – Al–Biruni was of no exception. In fact, SeyyedHossein Nasr argues that no other Muslim astronomer had dealt with astronomy as thorough and as rigor as Al–Biruni.(Seyyed Hussein Nasr, 1979) In one of his masterpiece, the al–Qanun al–Masudi, fi al–Hai'awa al–Nujum, he had discussed

about many astronomical theories that require a great deal of time and deep thought to be understood. Al–Biruni had always pondered upon the controversy of egocentrism and heliocentric. The Encyclopedia of Britannica defines a geocentric system as any theory of the structure of the solar system (or the universe) in which earth is assumed to be at the center of all. (Encyclopedia Britannica) The same reference defines a heliocentric system as a cosmological model in which the Sun is assumed to lie at or near a central point (of the solar system or of the universe), while the Earth and other bodies revolve around it. (Encyclopedia

Britannica) According to Nick: "Al Biruni proposed the notion that the earth rotates around its axis [6]. Although adhering to the then broadly accepted geocentric view of the world, with the earth in the middle of the universe, he was curious of the heliocentric view of the world – with the sun being in the middle. Because of this, Al Biruni was the first to undertake experiments related to such astronomical facts. Eventually however, he left the heliocentric argument because of his inability to present actual confirmation." (Martin Nick)Some modern scholars criticized Al–Biruni for accepting the geocentric theory, a theory he shared with his teacher, Abu Mansur Nasr. Scholars like A–Razi, IbnSina and the others their own opinion regarding this matter. (Abd. LatifSamian 1992) the absence of the telescope and other modern scientific apparatus during that era made it difficult for them to come to a common ground. They did not accept any new theory without clear scientific evidences [7]. The geocentric model was well accepted, though false in actuality, until the late 16th century. Al–Biruni had also discussed the question on whether the earth rotates around its axis centuries before the rest of the world.In his well-known book, the al–Athar al–Baqia, he had discussed the rotation of the earth and has given the correct values of latitudes and longitudes of various places. (Abu Raihan) He had also discussed this issue in his al–Qanun al–Masudi, fi al–Hai'awa al–Nujum. SeyyedHossein Nasr asserted that it was one of the most important Muslim astronomical encyclopedias that discussed for the first time, the idea that the earth rotates around its own axis. (Seyyed Hussein Nasr, 1979)In relation to his interest in the planetary motions of the universe (geocentrism&heliocentrism), Al–Biruni had also delved greatly into the study of Cosmogony. Unlike cosmology, which studies the universe at large throughout its existence, cosmogony is the study of the evolutionary behavior of the universe and the origin of its characteristic features. (Encyclopedia Britannica) That is, it is the study of the origination or the coming into existence and the creation of the universe [8].

Although his al–Qanun al–Masudi, fi al–Hai'awa al–Nujumdid not discuss the origin of the universe,Al–Biruni had reported the findings of his work on cosmogony in detail in his book Al–Tahdid. (Abd. LatifSamian, 1992) He denied the opinions that say that this world is everlasting. He also objected to Aristotle's concept of movement, which states that there is neither a beginning nor an end to life and that everything is constantly moving.After having delved into several fundamental tribulations related to planetary motion, Al–Biruni's next interest was on imaginary spheres and signs that have always been discussed in astronomy, such as the pole, equator line, horizontal line, vertical line and zodiacal signs. Al–Biruni believed that there was no way to know the parallax of stars – the stellar parallax phenomenon in particular. The stellar parallax phenomenon can be exemplified by the event of the movement of the earth along the orbital path which gives an illusion of the stars moving. This phenomenon (stellar parallax) was of great interest during that era because of its significance in measuring the distance between the earth and the sun. Al–Biruni had doubts in Ptolemy's opinion that the distance between the earth and sun is about 286 times the earth's circumference.He claimed that Ptolemy's theory was based on the occurrence of an eclipse – however, Ptolemy did not bring into consideration of the occurrence if a full eclipse. Al–Biruni, however, proposed that the distance between moon and earth can be measured unlike the distance between earth and sun which could not be measured using apparatus available at that time. In his treatises, the al–Qanun al–Masudi, fi al–Hai'awaal–Nujumand the Tahdid–i–Amaken, he had given an accurate approximation of the earth's radius and circumference. This is suggested by Mohaini Mohamed when she wrote: "Even in modern calculations, his measurements of earth's radius fell short by less than 12 miles and its circumference only by 70 miles. If the greatest scientist of the seventeenth century, Newton, had known the work of al–Biruni and knew that the earth's circumference is approximately 25,000 miles, he might not have to wait for more than a decade to publish his famous theory" (Mohaini Mohamed, 2000)Al–Biruni's interest in planetary motion had also driven him into studying the moon and the amazing phenomena associated with it. Al–Biruni stated that the moon returns to the initial position relative to the sun but with a difference in a minute increase. He also claimed that the movement of the moon and all the matter that move in the sky could not be determined by a single observation – the observation must be carried on continuously. Al–Biruni had successfully explained the rule of tide. He stated that the increase and decrease of the level of tide happens based on the moon phase. He gave a clear definition about tides in Somnath and its etymological relationship with the moon.

An astronomer as well as a historian at the same time, the science of chronology was of great importance to Al–Biruni. Chronology is the science of locating events in time. As an astronomer, he was drawn into the natural events that occur in daily life such as the transition between dawn and dusk, the actual time period of daytime, the difference between day and night between different places and many more. He had made the incentive to study the taqwims(calendars) of the other races.The quest to find the exact times for

solat(prayers) drove him to perform more researches. His books from the al–Athar al–Baqiato al–Qanun al–Masudi, fi al–Hai'awa al–Nujumwere the result of these research works. He invented an apparatus to measure the daytime and wrote about it in Ta'bir Al–Mayzan

Al–Taqdir Al Azman. He had also written an article in which, he described about day and night as well as proving the total daytime in a year at the pole area. In addition to that, Al–Biruni had arranged a simple article that describes how the Indian measure their time. His book, Tanqih Al–Tawarikhdiscuss about date. N another of his, the Tasawwaramr Al–Fajrwa Al Shafaq fi Jahat Al–Gharbwa Al Sharq, he had discussed about sunrise. He studied the motive behind the time period between dawn and dusk.Ibn Al Haytham stated that the time for dusk is when the sun is ten degrees under horizon. However, Al–Biruni found that the dusk happens when the sun goes 18 degrees under the horizon. Al-Birunis al-Lam'at explains his observations on this issue.The Indians had their own system whereas the Muslims used the knowledge of the Arabians and the annual calendar (taqwim) that predicted and explained the meteorological, agricultural and medical events. The Muslims were perhaps responsible for the establishment of the system of forecast meteorology. Al–Biruni studied all of the information through old observation methods, general knowledge as well as popular ideas that were related to this matter during that era. However, he had discovered that the idea (Anwa') was not universal. (Abd. LatifSamian, 1992) He stated scientifically that the idea of Anwa' related to the movement of sun in zodiac. Astrology has received a great deal of attention by Al –Biruni's interest. Many astrologers had referred to Al–Biruni's works and treatises up to date. Al–Biruni's Book of Instruction in the Elements of the Art of Astrology, an English version of his al–Tafhim–li–AwailSina'at al–Tanjim, a book that contains vast amount of knowledge in the field of astrology has received a great deal of attention from people around the globe. The picture of Islamic astrology that emerges is very similar to the Greek model as exemplified in Ptolemy's Tetrabiblos though with differing attributions and correspondences to reflect a different cultural environmental–Biruni makes frequent comparisons with Indian practices – along with the occasional dry note of disapproval where they offend his sense of propriety. His extensive list of the 'Arabian parts' was taken from Abu–Ma'shar though the concept was much older.It was a popular technique amongst Muslim astrologers and so, it became closely associated with them.Al–Biruni lists over 150 parts or 'lots' and still criticized that it is impossible to enumerate the lots which, haven been invented for the solution of horary questions as they increase in number every day. The lunar mansions or stations of the Moon is one purely Arabic concept, though Al–Biruni limited himself to the astronomical description only.It is the astronomical dimension to Al–Biruni's astrology that distinguishes it from the classical texts, reflecting the advances and refinements of Islamic science. His discussion of the subtleties of interpretation arising from different phases of the planetary orbits puts our present understanding of accidental dignity to shame.

Al–Biruni's Book of Instruction in the Elements of the Art of Astrology, an English version of his al–Tafhim–li–AwailSina'at al–Tanjimby R. Ramsay Wright, was written for Lady Rayhanah, one of the members of the Khwarizm court carried off to Ghaznah by Mahmood in 1017. Virtually nothing is known about her, though R. Ramsey Wright rather patronizingly says, 'she is marked out among oriental women by her craving for scientific knowledge and by the rare distinction of having a book dedicated to her [9].

Al–Biruni's instructions to Rayhanah were comprehensive – According to Wright, the Book of Elements may be regarded as a primer of 11th century science. The assertion made by the School of Mathematics ofUniversity of St. Andrews that is untrue:"It appears clear that, despite his many works on astrology, al–Biruni did not believe in the 'science' but used it as a means to support his serious scientific work." (J. J. O' Conner & E. F. Robertson, 1999)

Al–Biruni took the time to actually compose the Book of Instructions, which is a basic astrology text. In the beginning of the Book of Instructions, he states:"The comprehension of the structure of the Universe, and of the nature of the form of the Heavens and the Earth and all that is between them, attained by rehearsing the information received is extremely advantageous in the Art of Astrology ... I have begun with Geometry and proceeded to Arithmetic and the Science of Numbers, then to the structure of the Universe and finally to Judicial Astrology, for no one who is worthy of the style and title of Astrologer who is not thoroughly conversant with these for sciences." (Al-BiruniMainpage, 2005)

The Book of Instructions begins with sections on geometry and arithmetic leading to a thorough exposition of Ptolemaic astronomy that includes a detailed description of the use of the astrolabe. This is followed by sections on geography and chronology. Al–Biruni insisted that no one is entitled to call himself an astrologer without a good knowledge of these ancillary sciences. All these clearly indicate that he had used science extensively in his works.He recognized five divisions of judicial astrology. The first, natural astrology is concerned with meteorology, earthquakes, floods, and all other 'vicissitudes and disasters of nature'. The second is mundaneastrology, which deals with the rise and fall of kingdoms, battles, revolutions and etc. Individual natalastrology constitutes the third division where, like Ptolemy, Al–Biruni was fully aware that considerations of heredity and environment should modify any astrological indications.

The fourth division has to do with all human activities and occupations that are found on beginnings or origins. This would include horary and evectional astrology, though this area shades into the fifth divisionwhere astrology reaches a point which threatens to transgress its proper limits. The astrologer is on one sideand the sorcerer on the other one enters a field of omens and divinations which has nothing to do withastrology although the stars may be referred to in connection with them.

IV. AL-BATTANI'S CONTRIBUTIONS TO ASTRONOMY

Abu Abdallah Mohammad ibn Jabir Al–Battani is one of the most important role–model in the development of science. The reason for this can be clearly seen from the influence of his work on scientists such as Tycho Brahe, Keppler, Galileo and Copernicus. A great debate has been going on how Al–Battani managed to produce more accurate measurements of the motion of the sun to that of Copernicus. Some sources indicate that Al–Battani obtained more accurate results simply because of the location of his observations, which were made from more southerly latitude.This is explained by the effect of refraction which were relatively little on his meridian observations during the winter solstice at the southerly site of Raqqah whereby the sun was higher in the sky. From his observations at Aracte and Damascus, where he died, he was able to correct some of Ptolemy's results, previously taken on trust. One of the Al-Battani's well known discoveries is the remarkably accurate determination of the solar year as being 365 days, 5 hours, 46 minutes and 24 seconds; which is very close to the latest estimates. Following that discovery, Dr Muhammad Saud asserted that: "He noticed an increase of 16° 47' in the longitude of the sun's apogee since Ptolemy's time. This led to the discovery of the motion of the solar apsides and of slow variation in the equation of time." (Muhammad Saud, 1986)Al–Battani compiled new tables of the Sun and Moon, long accepted as authoritative, discovered the movement of the Sun's apogee and assigned to annual precession the improved value of 55". This implied the important discovery of the motion of the solar apsides and of a slow variation in the equation of time. He did not believe in the trepidation of the equinoxes, although Copernicus held it. Al–Battani determined with remarkable accuracy the obliquity of the ecliptic, the length of the seasons and the true and mean orbit of the sun. (N. Swerdlow, 1972) [10].

Al–Battani proved, in sharp contrast to Ptolemy, the variation of the apparent angular diameter of the sun and the possibility of annular eclipses. However, according to Swerdlow, the influence of Ptolemy was remarkably strong on all medieval authors, and even a brilliant scientist like Al–Battani probably did not dare to claim a different value of the distance from the Earth to the Sun from that given by Ptolemy. (N. Swerdlow, 1972) this was despite the fact that al–Battani could deduce a value for the distance from his own observations that differed greatly from Ptolemy's. (J. J. O' Conner & E. F. Robertson, 1999) According to Phillip Hitti, a well–versed scholar in Islamic history from the Princeton University: "He (Battani) made several emendations to Ptolemy and rectified the calculations for the orbits of the moon and certain planets. He proved the possibility of annular eclipses of the sun and determined with greater accuracy the obliquity of the seasons and the true and mean orbit of the ecliptic, the length of the tropical year and the seasons and the true and mean orbit of the sun" (Abu Abdullah Al-Battani)

He rectified several orbits of the moon and the planets and propounded a new and very ingenious theory to determine the conditions of visibility of the new moon. His excellent observations of lunar and solar eclipses were used by Dunthorne in 1749 to determine the secular acceleration of motion of the moon. Dunthorne, then determined many astronomical coefficients with great accuracy: Precession of Equinoxes 54.5" a year and inclination of the Ecliptic 23º35'. It is also from a perusal of Al–Battani's work on apparent motion of fixed stars that Hevilius discovered the circular variation of the moon. Al-Battani wrote many books on astronomy and trigonometry. His most famous book, *Kitab al–Zij*, an astronomical treatise with tables, was translated into Latin in the twelfth century with the title *De ScientaStellarum – De NumerisStellarumetmotibus.* His *Zij*was, in fact, more accurate than all others written by that time. His treatise on astronomy was extremely influential in Europe till the Renaissance, with translations available in several languages. His original discoveries both in astronomy and trigonometry were greatly discussed in his *Zij*. The overall work contained 57 chapters. Besides his observations, it contains a description of the division of the celestial sphere into the signs of the zodiac. The necessary background and the mathematical tools needed, such as the arithmetical operations on sexagesimal fractions and the trigonometric functions were also introduced. The third chapter of his *Kitabal–Zij*is devoted to Trigonometry.

He was the first to replace the use of Greek chords by sine's, with a clear understanding of their superiority. As an astronomer as well as a mathematician at the same time, he found more accurate values for the length of the year, the annual precession of the equinoxes and the inclination of the ecliptic. He also improved the calculation for the sinusoidal functions and had developed the concept of cotangent, furnishing their table in degrees. Al–Battani also provided very ingenuous solutions for some problems of spherical trigonometry using the methods of orthographic projection. (Encyclopedia of Islam, Leiden)Al–Battani's *Kitab al–Zij*is by had also discussed a large number of different astronomical problems following to some extent

material from the Almagest – the subject of planetary motions in particular. Towards the end of his text, he had discussed the construction of a number of astronomical instruments. (Encyclopedia of Islam, Leiden)

V. FINDINGS

These thesis depicts that it isreevaluate Muslim input to astronomy. We have glorious past in all sections of study. A major disadvantage of this study that we didn't know about their sacrifice for us, that's the main drawbacks The Pathfinder study has shown that the collection of relevant information which required for linkingwith past history, can be cumbersome and time consuming. All relevant information should ideally be put intoone paper format from the start, but there is also a need for a proper and unbiased biography of those scientist of those data before they can be used in a linking exercise.

VI. RECOMMENDATIONS

Recommendation # 1: Cyber authority should review there biography with great honors and keep their life style, there study sector in different website.

Recommendation #2: The authority in cyber law department should find all the website or journal or related source & check whether their resources are correct.

Recommendation # 3: The government of all Muslim countries should keep their resources to central library, that's the good idea to spread their knowledge among youngster.

Recommendation # 4: There are many resources are not discovered to known world we can make committee to find those things.

VII. CONCLUSION

Al-Biruni& Al-Battani's are one of the most important Muslim authorities on the history of religion. They were pioneer in the study of comparative religion. They studied Zoroastrianism, Judaism, Hinduism, Christianity, Buddhism, Islam, and other religions. They treated religions objectively, striving to understand them on their own terms rather than trying to prove them wrong. There underlying concept was that all cultures are at least distant relatives of all other cultures because they are all human constructs. They were disgusted by scholars who failed to engage primary sources in their treatment of Hindu religion. They found existing sources on Hinduism to be both insufficient and dishonest. Guided by a sense of ethics and a desire to learn, they sought to explain the religious behavior of different groups.

REFERENCES

[1] Abd. LatifSamian, 1992. (ed.), Al–Biruni: Zaman, KehidupandanPeranannya, (Kuala Lumpur: DewanBahasadanPustaka)
[2] Abu Abdullah Al-Battani."http://www.islamvoice.com/islam/sience/Scentists/battani.html
[3] Abu RaihanBiruni: Philosopher, Physicist Mathematician and Astronomer", Iranian Personalities, in www.iranchamber.com.
[4] Al-BiruniMainpage, 2005. Retrieved 9 Jan http://www.renaissance astrology.com/albiruni.htmlAl–Quran, Surah Al–Baqara, verse 189 Al–Quran, Surah al–Dukhan, verse 38
[5] Arvind Sharma, 1983. Studies in Alberuni's India, (Wiesbaden: Otto Harrassowitz)
[6] David, A. King, 1986. Islamic Mathematical Astronomy, (London: Variorum Reprints)
[7] David Plant, 2005. "Al Biruni and Arabic Astrology.", Skyscript Astrology Pages, Skyscript, Retrieved 4 Apr. http://www.skyscript.co.uk/albiruni.html
[8] Dick Teresi, 2003. Lost Discoveries: The Ancient Roots of Modern Science-from the Babylonians to the Maya. (USA: Simon & Schuster) Encyclopedia Britannica
[9] Martin Nick, "Who was Al–Biruni?, Al-Shindagah, <www.alshindagah.com.
[10] Mohaini Mohamed, 2000. Great Muslim Mathematicians, (Johor: U. T. M)Muhammad Saud, 1986. Islam and Evolution of Science, (Islamabad: Islamic Research Institute and International Islamic University)Swerdlow, N., 1972. "Al-Battani's Determination of the Solar Distance," (Centaurus 17(2): 97-105.

American Journal of Engineering Research (AJER)
e-ISSN: 2320-0847 p-ISSN : 2320-0936
Volume-4, Issue-8, pp-104-107
www.ajer.org
Research Paper Open Access

Electrical Conductivity of Water in Some Selected Areas of Delta State, Nigeria

K. Emumejaye* and R.A Daniel – Umeri
Department of Science Laboratory Technology, Delta State Polytechnic, Ozoro
*Corresponding author. Email: ekugbere@gmail.com

Abstract: *The electrical conductivity of water estimates the total amount of solids in it. Hence determines the water quality. The water samples were collected during the raining season from four selected locations of Abraka, Oleh, Ozoro and Warri. The samples were analyzed for electrical conductivity (µs/m), pH, TDS (mg/l), TSS, Turbidity (NTU), Iron content (mg/l), salinity (Cl^-) mg/l, and Nitrate Nitrogen (NO_3N) mg/l. The concentrations of investigated parameters in the water samples were within the permissible limits of the world health organization. However, the pH values of river water samples from Oleh call for concern as all water analyzed were acidic, and indicated corresponding high values in electrical conductivity and iron content, thus there is need to periodically examined water for their pH, total iron content, electrical conductivity to avoid health hazards associated with these parameters.*
Keywords: *electrical conductivity, water quality, turbidity, salinity, water pollution*

I. Introduction

The electrical conductivity of water estimates the total amount of solids in water. Hence, could be used to determine the water quality. Assessment of water quality is very salient for knowing its suitability for different uses (Choubey *et al*., 2008). Urbanization, rapidly growing human population and industrialization results in increase of waste water discharge into fresh water ecosystems and the release of pollutants into the atmosphere, thus impairing water quality, sometimes to an unacceptable level, thereby, limiting its beneficial use (Tanimu *et al.*, 2011).

Water is one of the most important constituents for healthy living of human society. In Delta State, some people in the areas investigated depend on ground water, surface water and rain water for both drinking and domestic purposes.

Water pollution has been reported for several urban centres around the world (cross, 1980; Rivett et al., 1990; Shahin, 1988; Sharma, 1988; Gosk et al., 1990). A wide range of pollutants has been identified: heavy metals, phenols, cyanides, pesticides, chlorinated hydrocarbons. Continuous and high frequency monitoring of streams to improve the understanding of the river water quality can be expensive; there is, therefore, a need to develop an economic and effective method for continuous estimation of nutrients in streams and other sources of water (Gali et al.,2012). Electrical conductivity is a measure of a solution's ability to conduct a current and has been used widely to measure soil salinity, clay, and water content (Kachanoski et al., 1988;

Williams and Hoey, 1987), soil nutrient levels (Rhoades et al., 1989), total dissolved solids in solution (Hem, 1985), as an indicator of concentration of soluble ions in glacial melt studies (Collins, 1979) and in hydrograph separation studies (Heppell and Chapman, 2006; Pellerin et al., 2008). The use of Electrical Conductivity data as a surrogate to estimate nutrient concentrations in streams would be ideal as it is an inexpensive approach. The goal of this study is to investigate electrical conductivity as a tool for measurement of water quality.

II. Material and methods

Study area: The study area comprises of four major towns in different local government areas (Ozoro in Isoko North, Oleh in Isoko South, Abraka in Ethiope East and Warri, Warri South) of Delta State. One thing common to these towns is that directly or indirectly petroleum exploration activities take place in and around these areas which may have contributions to the quality of water samples analysed. The area experience wet and dry season which are typical seasons in Nigeria (Eteng Inya , 1997; Etu – Efeotor,1998). The geology consist of sand, sandstones, gravel and clay (Tchokossa et al.,2013).

Sample collection

A total of 4 samples were collected from each location in clean acid free plastic bottles from four different towns of Delta state, Nigeria. All the water samples were collected consecutively within two days in July, 2014. Rain water samples were collected directly (not from roofs) in plastic bottles with funnel and were placed on an object 1 metre above the ground level. This was done to ensure that the rain water is free from possible contamination from the ground. The taps were allowed to run for about 30 seconds before samples of borehole water were collected into bottles. Well water samples were collected using clean fetching bucket at different sites. Stream/ river water samples were also collected from these four locations. All samples were properly covered, carefully labeled and were taken the laboratory for analysis.

Physio-chemical Analysis

The collected samples were analyzed for major physical and chemical water quality parameters like pH**,** Electrical conductivity (EC), Total Dissolved solids (TDS), Turbidity (NTU), Fe^{2+}**,** nitrate nitrogen as per the method Assessment of Ground Water Quality described in "Standard methods for the examination of water and wastewater American Public Health Association (APHA,1995).The parameters present in the water sample can be calculated by using various methods (Manivasakam,1996) . The pH of all the water samples was determined using a pH meter. Electrical conductivity was measured using a conductivity meter.

Results

Table1 shows the result of the physiochemical analysis of various samples

Location	Sample code	pH	Electrical conductivity(µs/m)	Temp (^{0}c)	TDS (mg/l)	TSS	Turbidity	Fe^{2+} (mg/l)	Total iron content
Warri	RW1	6.8	15.0	28	792	7	1.5	0.25	0.50
	BW1	7.2	14.8	28	752	1	1.0	0.19	0.20
	WW1	8.5	14.4	28	794	4	1.5	0.31*	0.50
	RV1	8.2	31.2	28	1661*	8	2.5	0.33*	0.90
Abraka	RW2	5.4	15.5	28	780	6	1.0	0.18	0.46
	BW2	7.8	15.2	28	766	1	1.0	0.2	0.30
	WW2	6.2	15.0	28	755	6	1.5	0.22	0.30
	RV2	7.7	28.9	28	1452*	7	1.5	0.36*	1.20
Ozoro	RW3	6.1	13.1	28	656	7	1.0	0.22	0.33
	BW3	6.9	12.9	28	650	1	1.0	0.02	0.12
	WW3	7.3	11.9	28	601	4	1.3	0.26	0.35
	RV3	6.2	27.6	28	1392*	7	2.0	0.36*	1.40
Oleh	RW4	8.2	16.2	28	842	6	2.0	0.29	0.40
	BW4	7.1	14.9	28	760	2	1.0	0.25	0.28
	WW4	6.5	21.0	28	1049*	3	1.7	0.29	0.40
	RV4	8.6*	28.1	28	1411*	6	2.5	0.39*	0.80
	Mean	7.2	18.5		945	5	1.5	0.26	0.53

* above WHO limits

III. Discussion

Electrical Conductivity

From the result of analysis the mean electrical conductivity is 18.5 µS/m in the range between 11.9 to 31.2 µS/m with RV1 indicating the highest value as shown in fig.1. the least value of electrical conductivity was in WW3.

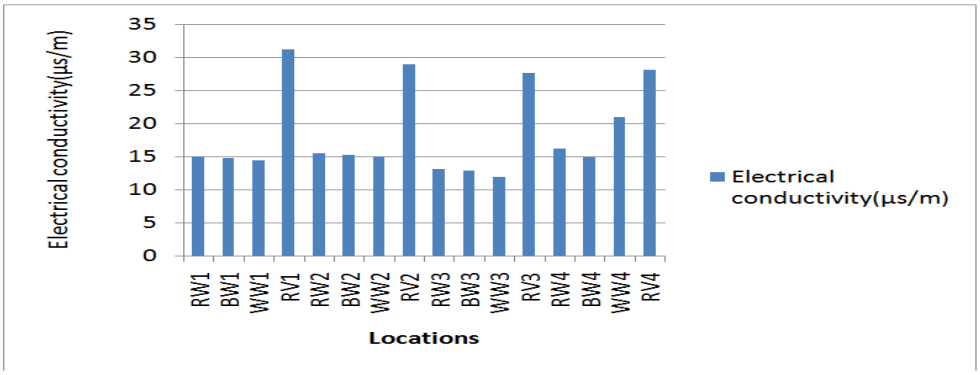

Fig. 1 Plot of Electrical conductivity of samples by Location

Total Dissolved Solids (TDS)

The TDS of samples analyzed indicated a trend in that high values of electrical conductivity showed corresponding high values in TDS of same samples. The mean value of TDS was 945µS/m with the highest value in RV1 and least in WW3 in fig.2.

Water from these rivers is of low quality since the Electrical conductivity and TDS are high. This might be as a result of indiscrimate waste disposal in these rivers. Also well water ww4 indicated high values of Electrical conductivity and TDS.

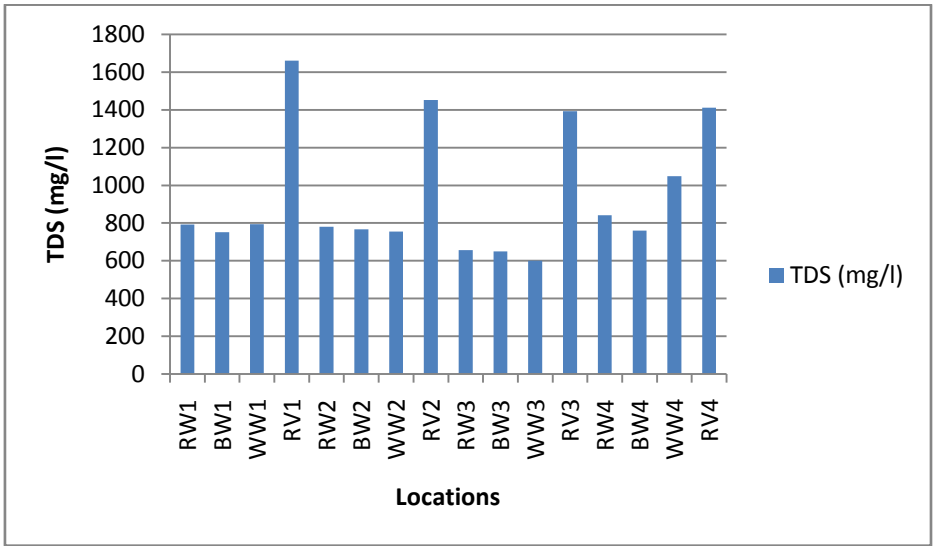

Fig. 2 A Plot of TDS of samples by Location

Iron content

WHO (1996; 2007) set the maximum permissible limits of iron (0.3mg/l) in water. All the water samples analyzed in this work were not fully within these limits; however it will pose no danger to consumers as these values are concerned.

IV. Conclusion

The TDS in mg/l of the four rivers sampled were above WHO permissible limits for water and have the high corresponding electrical conductivity values. The mean electrical conductivity is 8.5 µS/m with highest value in samples from Abraka river (RV3). This study reveals that electrical conductivity is a sufficient parameter to determine the quality of water in terms of physiochemical properties, and is cost effective and time saving. Through extensive monitoring over long period, data in this study area, better relationships can be developed resulting in a possible method for estimating more accurate determination of water quality.

References

[1] Choubey, V. K., Sharma, M. K., & Dwivedi, . (2008). Water Quality Characteristics of the Upper Bhopal Lake, M.P., India. *Proceedings of the 12th World Lake Conference, Taal 2007, published by the International Lake Environment Committee*, 366-372.

[2] Tanimu, Y., Bako, S. P., & Adakole, J. A. (2011). Effects of domestic waste water on water quality of three reservoirs supplying drinking water. *Waste water-evaluation and management*, Intech open access publisher, Rijeka, Croatia.

[3] Manivasakam N.(1996) Physical Chemical examination of water, sewage and industrial effluents 3rd Ed, Pragati Prakashan, Meeret, India.

[4] APHA(1995), Standard methods for analysis of water and wastewater.19th Ed. *American Public Health Association, Inc*., Washington D C. 19.

[5] Eteng- Inya A., (1997). The Nigerian State, Oil Exploration and Community Interest: Issues and Perspectives. University of Port Harcourt, Nigeria conf paper

[6] Etu – Efeotor J.O (1998). Hydrochemical analysis of surface andground waters of Gwagwalada area of central Nigeria. Globa J Pure Appl. Sci – 4 (2): 153 – 163.

[7] World Health Organization WHO (1996) Guideline for drinking water quality, health criteria and other supporting information Geneva.

[8] World Health Organization, WHO (2007). International Drinking Water Standards. 3rd edition.

[9] Tchokossa, P, Olomo, J.B, Balogun, F.A & Adesanmi, C.A (2013) Assessment of radioactivity contents of food in the oil and gas producing areas in Delta State, *Nigeria.international Journal of science and technology* 3(4): 245-250

[10] Gali,R.K, Soupir,M.L & Helmers, M.J (2012) Electrical Conductivity as a tool to estimate chemical properties of drainage water quality in the Des Moines Lobe, Iowafor presentation at the 2012 ASABE Annual International Meeting Sponsored by ASABE Hilton Anatole Dallas Dallas, TX July 29 – August 1, 2012

[11] Cross,H.J (1980) Ground water contamination by road salt, Nova Scotia, Canada.

[12] Gosk, E, Bishop, P.K, Lerner, D.N & Burston, M (1990) Field investigation of solvent pollution in the ground-waters of Coventry, UK.
[13] Rivett, M.O.,Lerner, D.N, Lloyd,J.W & Clark, L. (1990) Organic contamination of the Birmingham acquifer. Journal of Hydrol. 113: 307-323.
[14] Shahin, M.M.A.(1988) Impacts of urbanization of the greater Cairo area on the ground water in the underlying acquifer. Proc. Symp. Hydrological processes and water management in urban areas, Duisburg, FRG, April 24 – 28. Pp. 517-524
[15] Sharma, V.P. (1988) Ground water and surface water quality in and around Bhopal city in India. Proc. Symp. Hydrological processes and water management in urban areas, Duisburg, FRG, April 24 – 28. Pp. 525-532
[16] Collins, D.N. 1979. Hydrochemistry of meltwaters draining from an alpine glacier. *Arctic and Alpine Research.* 13(3): 307-324.
[17] Kachanoski, R.G., Gregorich, E.G. & Van- Wesenbeeck, I.J (1988) Estimating spatial variations of soil water content using noncontacting electromagnetic inductive methods. *Can. J. Soil. Sci.* 68: 715-722.
[18] Williams, B.G, & Hoey, D (1987) The use of electromagnetic induction to detect the spatial variability of the salt and clay content of soils. *Aust. J. Soil. Res.* 25: 21-27.
[19] Rhoades, J.D., Manteghi, N.A., Shouse, P.J. & Alves, W.J. (1989) Soil electrical conductivity and soil salinity: New formulations and calibrations. *Soil Sci. Soc. Am. J.* 53: 433-439.
[20] Hem, J. (1985) Study and interpretation of the chemical characteristics of natural water. *U.S. Geological Survey Water-Supply. Paper No. 2254.* United States Printing Office. Washington, D.C.
[21] Pellerin, B.A., Wollheim, W.M. , Feng, X. & Vorosmarty, C.J.(2008) The application of electrical conductivity as a tracer of hydrograph separation in urban catchments. *Hydro. Proc.* 22:1810-1818.
[22] Heppell, C.M., & Chapman, A.S. (2006) Analysis of a two-component hydrograph separation model to predict herbicide runoff in drained soils. *Agricultural Water Management.* 79(2):177-207.

American Journal of Engineering Research (AJER)
e-ISSN : 2320-0847 p-ISSN : 2320-0936
Volume-04, Issue-08, pp-108-119
www.ajer.org
Research Paper Open Access

Development of high efficiency gas-cleaning equipment for industrial production using high-intensity ultrasonic vibrations

V.N. Khmelev, A.V. Shalunov, R.S. Dorovskikh, R.N. Golykh, V.A. Nesterov
Biysk Technological Institute (branch) of Altay State Technical University named after I.I. Polzunov, Russia

ABSTRACT: *The article presents the results of research aimed at increase of the efficiency of gas cleaning equipment based on the Venturi tube using high-intensity ultrasound. Carried out theoretical analysis of dust-extraction unit operation let determine the possibility of efficiency increase and dust reduction of gas at the output of the plant at the application of ultrasonic action, especially at collecting of high-disperse particles (for the particles with the size of 2 μm the efficiency of the plant rose from 74.8 % to 99.1 %). It was determined, that sound pressure level no less than 150 dB and frequency of ultrasonic influence 22 kHz provide maximum efficiency of the Venturi tube. It was stated, that the application of 2 ultrasonic radiators of 370 mm in diameter provides dust concentration at the output of the dust-extraction plant of no more than 0.255 g/Nm^3; four radiators – no more than 0.225 g/Nm^3; six radiators – no more than 0.2 g/Nm^3 at burning of coal from Kharanor coal deposit (dust concentration at the output without ultrasonic influence is more than 0.8 g/Nm^3). Evaluated modes and conditions of ultrasonic action allowed developing special ultrasonic transducer. The developed design of ultrasonic transducer with a heat exchanger provides continuous operation at high temperatures (170°C). The received theoretical and experimental results allow providing maximum efficiency of dust-extraction plant.*

Keywords - *Dust extraction plant, Venturi tube, ultrasonic impact, coagulation, dispersed particles*

I. INTRODUCTION

At present for collection of dispersed phase particles (1-10 μm) from industrial emissions different apparatuses, which differ from each other in construction and method of precipitation of suspended particles in gas, are developed and used.In industry wet dust-collecting apparatuses are widely used as a part of gas-cleaning unit, among which Venturi turbulent apparatuses (scrubbers) are the most efficient [1, 2]. They provide efficiency of collecting of dispersed ash particles up to 94-96%. However such efficiency of dust collecting is insufficient due to the modern environmental requirements. At that further efficiency increase of such types of the dust-collectors due to changes of the construction and modes of movement of gas-dispersed and liquid phases does not bring desired results. The reason is that it is impossible to increase probability of collision of dispersed particles with the particles of sprayed water. To increase the probability of collision of collecting dispersed particles with sprayed water drops is possible due to providing of vibrating motion to dispersed particle relative to heavier water particles. It can be realized the most effectively by acoustic action on gas-dispersed flow – ultrasonic coagulation of dispersed particles [3].

For estimation of efficiency of dispersed particle coagulation in Venturi tube and their collection degree in all dust extraction plant at the use of additional action of high-intensity ultrasonic vibrations it is necessary to solve the following tasks:

– to study coagulation mechanism of dispersed particles in Venturi tube;

– to determine optimum modes and conditions, at which ultrasonic action can provide maximum efficiency increase of dust extraction in the dust-extraction plant;

– to develop and study the operation of the ultrasonic radiators, which are able to act on gas-dispersed flow in the conditions of high temperatures;

– to determine number and location of the ultrasonic radiators in Venturi tube providing optimum conditions of ultrasonic action and protection of the radiators from abrasive wear by solid particles of flue gases.

II. Methods and Approaches Used at the Design of Dust-extraction Plant Model

Carried out analysis of the multiphase flow model showed, that Lagrange model considers fully the main factors influencing on the process efficiency of dispersed particles collecting in the dust-extraction plant (both at the presence and absence of ultrasonic action).

According to this model in polydisperse flow containing particles of various sizes coagulation effect occurs due to particle speed differential (orthokinetic coagulation), which influences mostly on intensity of particles collision.

At the absence of ultrasonic action under the action of inertial forces large particles move slower than little ones, and thereby probability of collision increases. At the presence of ultrasonic action large water drops are not involved into vibrational motion retaining initial trajectory, and small particles of ash (no more than 10 μm) vibrate on a large scale (i.e. with doubled amplitude) up to 100 μm increasing the space of effective interaction with water drops [4].

As existing procedures of calculation of gas-cleaning equipment do not take into consideration the possibility of ultrasonic action for the decrease of residual dust content of flue gases, we use universal methods of mathematical modeling of current and interaction of multiphase flows realized by numerical calculations on the computer with the application of special programs based on finite-element method. They let take into account a large number of determining factors, minimize assumptions and perform numerical calculations with high accuracy and at rather short period of time.

III. Determination of Optimum Modes of Ultrasonic Action Providing Maximum Efficiency of Dust-extraction Plant Operation

For carrying out calculations on operation efficiency of the dust-extraction plant we designed 3d geometric model consisting of Venturi tube and cyclone-drop catcher (Fig. 1). Geometry and standard size of the model correspond to existing constructions of the dust-extraction plant applied in industry [2].

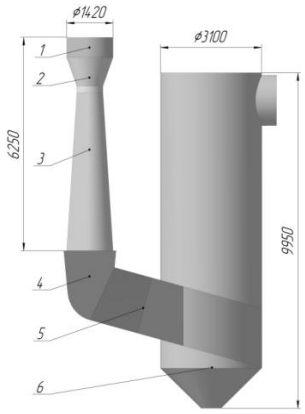

1 – input nozzle; 2 – confuser; 3 – diffuser; 4 – curved part of the air pipe (pipe bend);
5 – connecting pipe; 6 – cyclone-drop catcher

Fig. 1. 3D model of the dust-extraction plant on the base of Venturi tube

At the design of calculated model of Venturi scrubber it is assumed that:

– there is a laminar flow, i.e. gas moves in layers without mixing and pulsations(irregular and quick changes of speed and pressure);

– friction and adhesion of the particles on walls of Venturi pipe are not taken into consideration, at that inelastic reflection of the particles (ash and water drops) from the wall of Venturi tube is assumed;

– settling of ash and drop particles on the wall of the drop catcher;

– absence of heat transfer between the phases and as a consequence absence of water drop evaporation;

– one-way interaction of continuous and dispersed phases (influence of dispersed particles on gas flow does not take into account).

To calculate efficiency of the plant we take following initial data corresponding to the operating parameters of the most dust-extraction plants exploited at present:

1. The temperature of flue gases before the installation is 170° C, that corresponds to the density of gas flow of 0.78 kg/m^3;

2. Mean size of the drops of sprayed water is 150…250 μm;

3. The volume of output flue gases is 100000 m³/h that corresponds to speed of gas flow at the input of Venturi tube equal to 17.4 m/s.

4. Dust content before the plant is 17.0 g/Nm³ that corresponds to mass output of ash of 0.35 kg/s;
5. Speed of flue gases in the confuser of Venturi tube is 50-70 m/s;
6. Water discharge on the spraying of Venturi tube is 10 t/h;
7. Size of ash particles formed at the combustion of coal is defined according to scientific-technical data [5, 6] and it can be of 2…90 μm.

The results of modeling of gas flow motion in the dust-extraction plant are shown in Fig. 2.

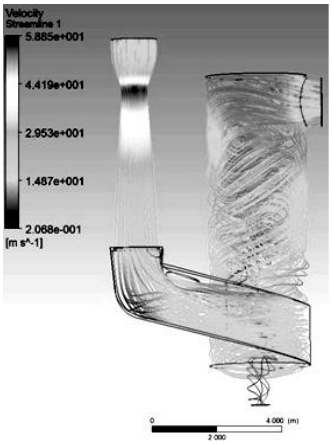

Fig. 2. Pattern of gas flow motion in the dust-extraction plant

As it follows from obtained results, speed of gas flow in the opening of Venturi tube achieves 58.8 m/s. At that in the papers [1, 2] the range of values is 50–70 m/s that proves adequacy of used model of gas flow motion.

The presence of ultrasonic vibrations in Venturi tube is taken into consideration as additional force acting on individual particle located in the ultrasonic field. This force consists of two components:

– orthokinetic (different degree of involvement of dispersed particles into vibrational motion, which is in inverse proportion to their diameter and mass);

– hydrodynamic (occurrence of forces of attraction between the particles caused by asymmetry of flow field of dispersed particles in the ultrasonic field).

Moreover at the calculation of addition to force deviation of the form of ash particle from the spheric one was considered. Thus total addition to the force acting on ash particle from the side of gas flow caused by the presence of ultrasonic vibrations is defined by the equation (1):

$$\Delta F = 3\pi d\mu(k_B \cos^2\theta + k_N \sin^2\theta)\times(U_1 + U_2)\sin(2\pi ft), \quad (1)$$

where d is the largest diameter of the ellipsoid particle, m; μ is the viscosity of gas flow, Pa·s; θ is the angle between smaller semi-axis of the particle and the direction of ultrasonic field, rad; k_B is the streamlining coefficient of the particle at flow motion along smaller semi-axis; k_N is the streamlining coefficient of the particle at flow motion along larger semi-axis; f is the frequency of vibrations (22 kHz); U_1 is the amplitude of disturbance of gas flow speed from the side of initial ultrasonic field, m/s; U_2 is the amplitude of disturbance of gas flow speed from the side of water particles, m/s; t is the time, s.

The force addition from the side of gas flow at the calculations is taken into account only at the presence of the particles in the volume of Venturi tube.

According to the results of carried out calculations the dependences of efficiency and residual dust content of gas flow of Venturi tube on the size of ash particles were obtained (Fig. 3).

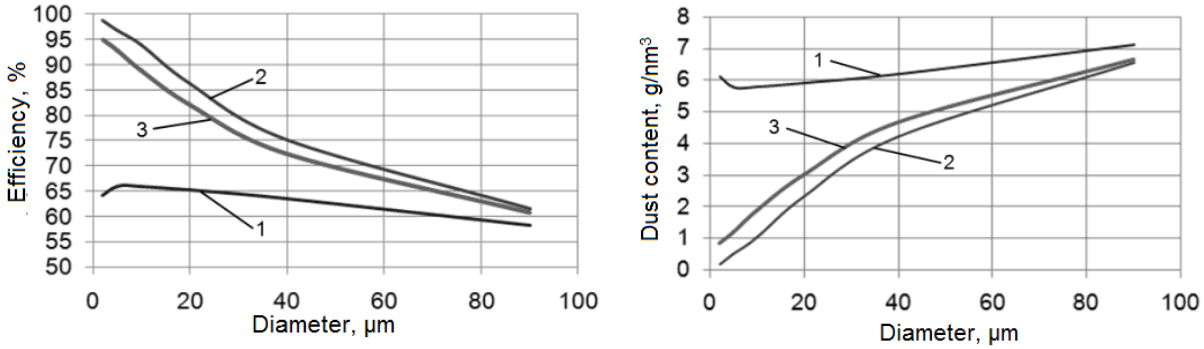

a) b)

1 – without ultrasound; 2 – with ultrasound 150 dB; 3 – with ultrasound 145 dB

Fig. 3. Dependence of efficiency (a) and residual dust content (b) of Venturi tube on the size of ash particles at different levels of acoustic pressure

From presented results (Fig. 3) it follows, that the application of ultrasonic vibrations with the level of acoustic pressure of 150 dB provides no less than twofold dust reduction at the output of Venturi tube for the particles with the size of up to 20 μm and in 1.5 times for the particles with the size of more than 20 μm.

It proves high efficiency of the application of ultrasonic vibrations for coagulation of suspended particles and mainly thin-dispersed ones (2–5 μm), for which sixfold dust content reduction is provided.

Further the calculations of determination of optimum zone of ultrasonic action at different levels of acoustic pressure were carried out (Fig. 4).

From obtained results it can be concluded, that to provide maximum efficiency of the coagulation process it is necessary to achieve uniform ultrasonic field in all volume of Venturi tube (simultaneous ultrasonic action on the confuser and the diffuser).

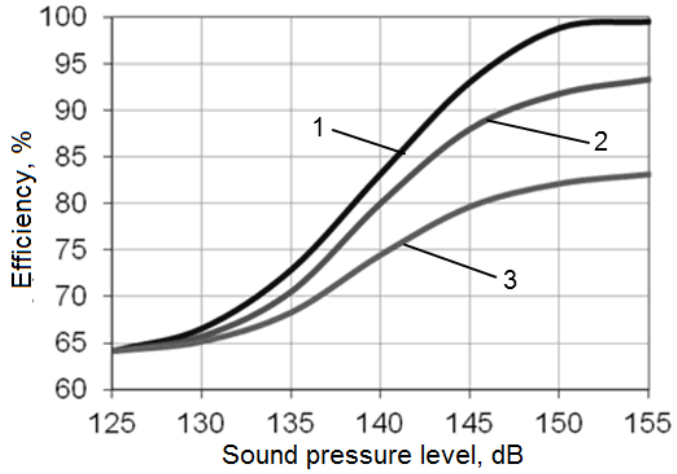

1 – Confuser+diffuser; 2 – Diffuser; 3 – Confuser

Fig. 4. Dependence of Venturi tube efficiency on the level of acoustic pressure at different zones of ultrasonic action

Fig. 5 shows the dependences of efficiency and residual dust content of the gas flow of all dust-extraction plant on the size of the ash particles.

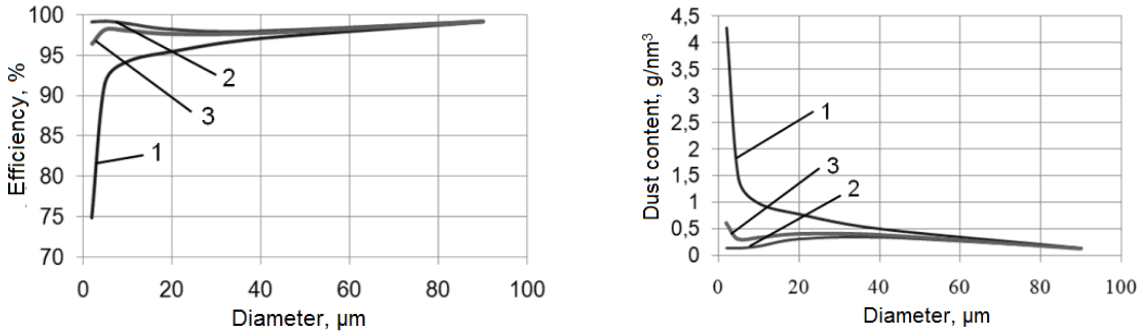

a) b)

1 – without ultrasound; 2 – with ultrasound 150 dB; 3 – with ultrasound 145 dB

Fig. 5. Dependences of efficiency (a) and residual dust content (b) of the gas flow of all dust-extraction plant on the size of the ash particles at different levels of acoustic pressure

From the presented dependences, it follows, that the application of ultrasonic action provides essential efficiency increase of the operation of the dust-extraction plant especially in the zone of high-dispersed particles. So for the particles of 2 μm efficiency of the plant rises from 74.8 % to 99.1 %.

Thus the use of ultrasonic action with frequency of 22 kHz is the most efficient for the particles of less than 20 μm. Larger particles are influenced by ultrasonic vibrations to a lesser degree, however for the particles of 20 μm to 40 μm the efficiency of the dust-extraction plant increases from 95.4 % to 98.2 %.

Efficiency decrease after the application of ultrasound for large particles is leveled by high starting efficiency (without ultrasonic action) of collecting of such particles.

That is why, it can be concluded that the application of ultrasonic action for the efficiency increase of the dust-extraction plant on the base of Venturi tube is expedient to reduce the content of high-dispersed ash fraction in flue gases.

At the final stage of the analysis theoretically achieved gas dust content at the output of the dust-extraction plant at known powder of ash at the input was determined. Residual dust content of the gas was calculated on the base of obtained data on fractional efficiency of the dust-extraction plant (Fig. 5) by the following expression (2):

$$\eta_p = \frac{\sum_{i=1}^{N} \eta(d_i) W_i}{\sum_{i=1}^{N} W_i}, \qquad (2)$$

where η_p is the collecting efficiency of polydisperse ash, %; $\eta(d_i)$ is the dependence of collecting efficiency of monodisperse ash on the diameter d_i, %; i is the amount of the groups of ash particles sizes; d_i is the size of the particles of i-group, m; W_i is the mass fraction of ash particles of i-group.

For objective efficiency estimation of the application of ultrasound the data on powder of flue ash obtained from reliable free sources [6] were used.

Fig. 6 shows the results of calculation for ash obtained after burning of brown coal of Kharanor deposit ground by the mill MV 50–160 in the boiler BKZ 210–240 of Vladivostok heat station-2.

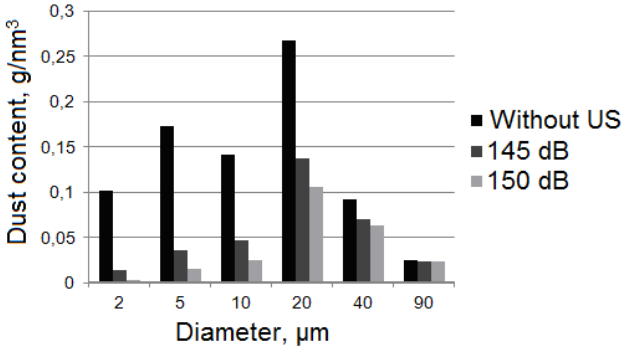

Fig. 6. Ash powder at the output of the dust-extraction plant

From obtained data it follows, that at the output of the dust-extraction plant with the application of ultrasonic action with the level of acoustic pressure of 150 dB fractions with the size of particles of 2-5 μm are not observed (less than 0.05 g/Nm^3). Total dust content at the output of the dust-extraction plant is: without ultrasonic action – 0.802 g/Nm^3 (the efficiency is 95.2535 %); at the level of acoustic pressure of 145 dB – 0.329 g/Nm^3 (the efficiency is 98.065 %); at the level of acoustic pressure of 150 dB – 0.237 g/Nm^3 (the efficiency is 98.611 %).

Thus obtained results prove efficiency and prospects of the application of ultrasonic vibrations for efficiency increase of the dust-extraction plants on the base of Venturi tubes.

In order to achieve maximum efficiency of dust-extraction plant operation it is necessary to provide ultrasonic action at the frequency of 21…24 kHz and level of acoustic pressure of 145…150 dB.

IV. Development and Study of Ultrasonic Radiator Operation for the Action on Gas-dispersed Flow Providing Defined Action Modes

For ultrasonic influence on gas-dispersed flow acoustic radiator in the form of stepped-variable disk with the diameter of 370 mm was developed [7]. The form of the radiator and distribution of its vibration amplitudes are shown in Fig.7.

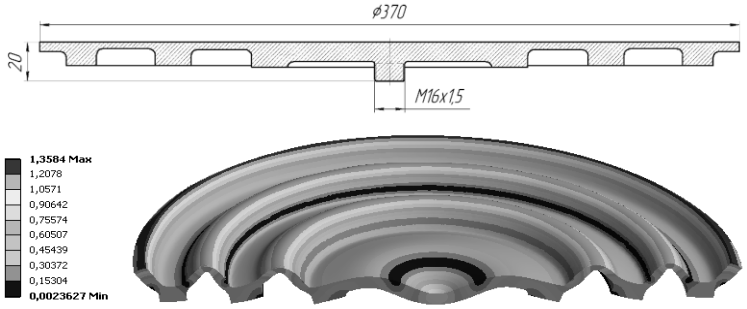

Fig. 7. Form of ultrasonic disk radiator with the diameter of 370 mm and distribution of vibration amplitudes (in relative units)

For excitation of vibrations of the disk at specified frequency the ultrasonic vibrating system shown in Fig. 8 was designed.

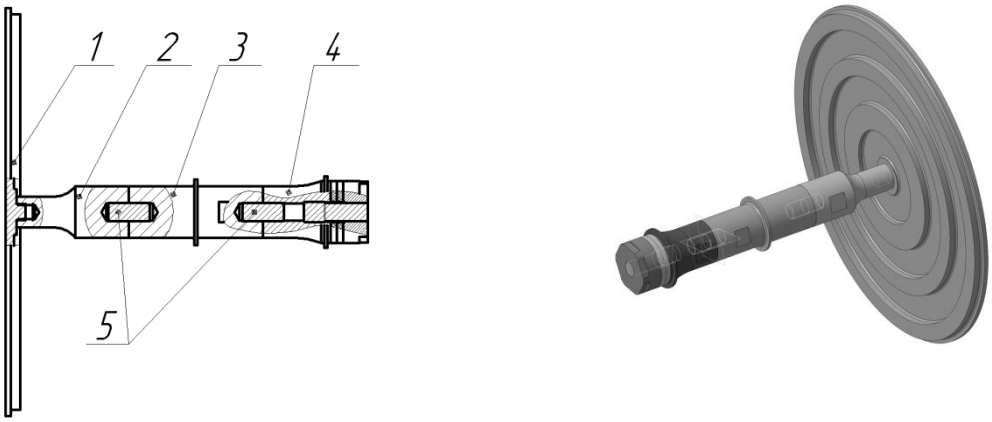

1 – source of ultrasonic pressure in the form of the disk; 2 – concentrator
3 – waveguide; 4 – piezoelectric transducer; 5 – studs
Fig. 8. Ultrasonic vibrating system with the disk radiator

The development of the piezoelectric transducer was carried out on the base of known procedures described in the papers [8, 9].

Taking into account the fact that temperature of gas in Venturi tube is about 170^{o}C, during action of the ultrasonic radiator on gas-disperse flow at high temperatures the efficiency of the transducer decreases, vibration amplitude of the disk radiator drops and the level of acoustic pressure falls due to low efficiency of the piezoelectric conversion in the materials of the transducer [10].

To provide optimum temperature mode of the operation of the piezoelectric transducer in the construction of the vibrating system there is an additional (intermediate) section of the waveguide for the installation of thermal cutoff unit providing fluid cooling of the transducer during the operation (Fig. 9).

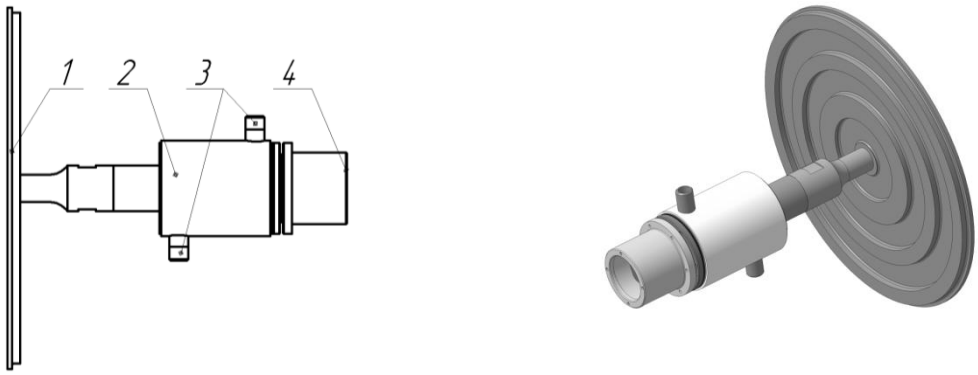

1 – Ultrasonic vibrating system with the disk radiator; 2 – heat exchanger; 3 – branch pipes for input and output of cooling liquid; 4 – case of the piezoelectric transducer

Fig. 9. Draft of designed ultrasonic vibrating system with the heat exchanger

In order to verify the operation efficiency of the thermal cutoff unit the calculations of thermal modes of the ultrasonic vibrating system operation were carried out. The initial temperature condition of the disk radiator and the concentrator was established equal to the temperature of the operating medium 200^{o}C. As it follows from the results of calculation liquid cooling maintains temperature of the reflecting cover-plate at the level of 40-45 ^{o}C. The application of liquid cooling of the reflecting cover-plate of the piezoelectric transducer and the waveguide provides establishing stationary temperature mode in 1000 sec. At such mode the piezoceramic rings are heated to the temperature of no more than 80 ^{o}C.

Thus carried out calculations allow determine, that cooling of the ultrasonic vibrating system with the disk radiator for providing of required temperature mode should be assured by water (with the temperature of no more than 60 degrees Centigrade) with the consumption of no less than 12–15 l/h.

Further researches were aimed at the determination of the disk radiator parameters. At the first stage vibration amplitude on the surface of the disk radiator was measured for the comparison with the results of the theoretical calculations.

For the study of distribution of vibration amplitude two diametral straight lines were drawn on the disk surface, on which studied points and vibration zeros were marked. Figure 10 shows the distribution of vibration amplitudes on the disk surface in studied points.

The measurements were carried out with the help of developed test bench (Figure 6) at the temperature of the radiator of 20 ^{0}C. As a result of the measurement it was determined, that the ratio of experimental values of vibration amplitudes in different zones of the disk to vibration amplitude in its center varies with theoretical ones in no more than 10%. It proves the adequacy of used model of vibrating solid.

Maximum level of acoustic pressure was observed at the distance of 25 cm and it was 158 dB.

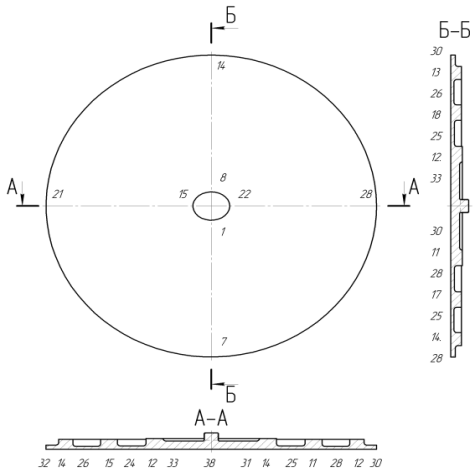

Fig.10. Distribution of vibration amplitudes in studied points (in μm)

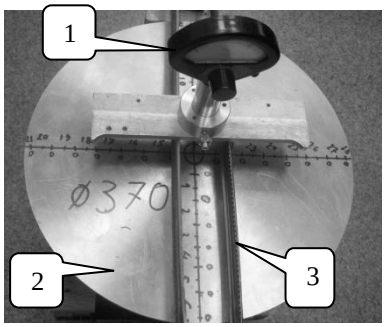

1 – travel indicator of watch-type (the scale interval is 1 μm); 2 – ultrasonic disk radiator; 3 – skids
Fig. 11. Test bench for measurements of vibration amplitudes

The estimation of influence of operating medium temperature on the parameters of the ultrasonic radiator (resonance frequency, level of acoustic pressure, consumed power and distribution of vibration amplitude) during its operation was carried out on developed test bench, shown in Figure 12.

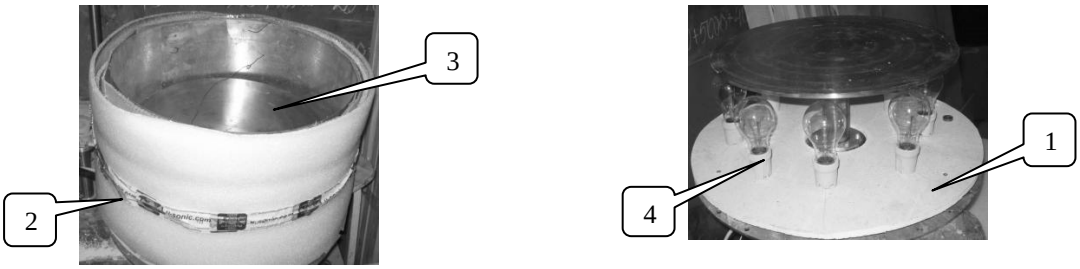

1 – collar with cooling volume; 2 – cylinder sidewall; 3 – ultrasonic vibrating system with the disk radiator; 4 – heating elements
Fig. 12. Photo of the test bench for heating and measuring of vibration amplitude of the disk radiator surface

The test bench consisted of cylinder operating chamber with the diameter of 450 mm and height of 400 mm made of noncombustible material, in which the ultrasonic vibrating system with the heat exchanger was placed. The internal volume of the chamber was heated by incandescent lamps. To reduce heat losses the chamber was covered by thermal insulation material outside. Water was used as a cooling fluid for the ultrasonic vibrating system.

The results of measurements of the resonance frequency depending on the temperature of the disk radiator are shown in Fig. 13.

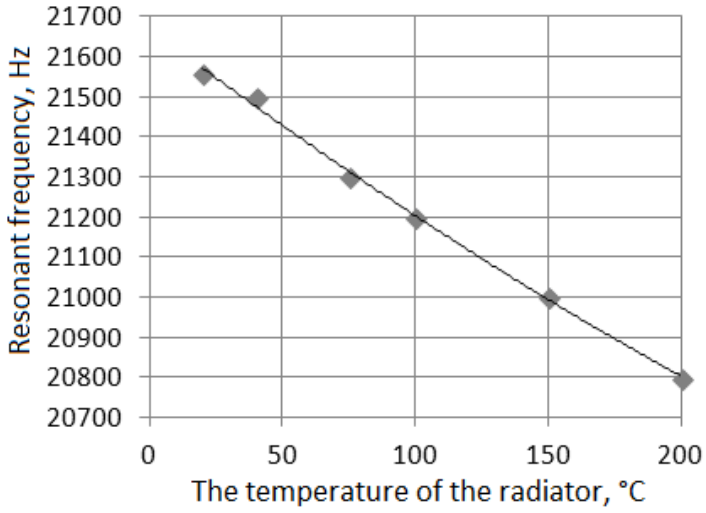

Fig. 13. Dependence of resonance frequency of the ultrasonic vibrating system on the temperature of the disk radiator

As it is evident from the graph, that the resonance frequency decreases linearly with the temperature increase in the range under study.

To determine dependences of the level of acoustic pressure on the temperature the measurements were carried out at the distance of 0.25 m and 1 m from the surface of the disk radiator. Obtained dependences are shown in Fig. 14.

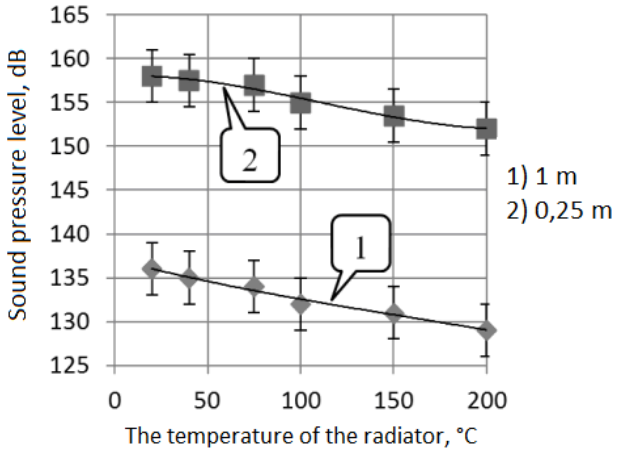

Fig. 14. Dependence of the level of acoustic pressure on the temperature of the ultrasonic disk radiator

The analysis of the obtained dependences allows determine, that the level of acoustic pressure decreases with the temperature increase that is caused by the reduction of density of heated gas. At the same time temperature increase of the radiator causes insufficient rise of vibration amplitude of the disk surface.

V. Determination of Number and Places of the Ultrasonic Radiators Providing Maximum Efficiency of Dust Collecting in the Dust-extraction Plant

Taking into account obtained distribution of vibration amplitude on the surface of the disk radiator of 370 mm in diameter we calculated the distribution of level of acoustic pressure in the volume of Venturi tube with the application of boundary element method. The method is based on the fact, that calculation of distribution of acoustic pressure is carried on the surface of measurement environment, and then acoustic pressure is defined in the volume by the surface values.

The distribution of acoustic pressure in Venturi tube was calculated by Helmholtz equation (3) describing propagation of acoustic vibrations in the medium:

$$\Delta p + k_*^2 p = 0, \tag{3}$$

where k_* is the efficient wave number of gas medium taking into account absorption of ultrasonic vibrations in the medium, m^{-1}; p is the complex amplitude of acoustic pressure in gas medium with boundary conditions (4)

$$4\pi^2 f^2 \rho A_n = (\nabla p, \mathbf{n}), \tag{4}$$

where **n** is the vector of outer normal line to the radiator surface; f is the frequency of ultrasonic vibrations equal 22 kHz; ρ is the density of gas medium, kg/m^3; A_n is the function of distribution of normal vibration amplitude on the radiator surface.

To calculate level of acoustic pressure it is necessary to determine installation position of the disk radiators. Installation position should exclude possibility of abrasive wear of the disk surface by ash dispersed particles.

One of possible variants excluding abrasive wear of the ultrasonic radiators is their location on the cap of Venturi tube in the place of joining to the confuser (Fig. 15) at an angle to the axis providing the most even distribution of acoustic field in Venturi tube.

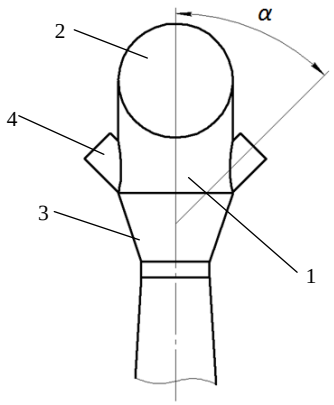

1 – cap; 2 – input pipe; 3 – confuser; 4 – pipe for installation of the ultrasonic radiator; α – angle between the axis of Venturi tube and the ultrasonic radiator

Fig.15. Scheme of installation of the ultrasonic radiators into the cap of Venturi tube

The installation of 2 radiators is minimal for providing of uniformity of acoustic action in the volume of Venturi tube.

The calculations of distribution of acoustic pressure at different installation angles of the ultrasonic radiators in Venturi tube and specified level of acoustic pressure of 145 dB (near the center of the radiating surface at the operation of the radiator in unlimited space) were carried out. Further taking into consideration obtained data mean value of the level of acoustic pressure in all volume of Venturi tube was calculated by the following formula:

$$L_{avg} = \frac{\int_V L(\mathbf{r})\partial V}{V}, \tag{5}$$

where L(**r**) is the level of acoustic pressure in point *r*; *V* is the volume.

Obtained results are shown in Fig. 16.

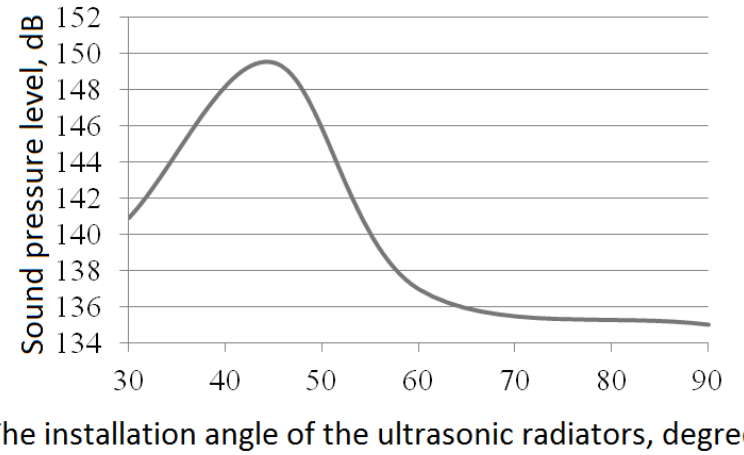

Fig. 16. Dependence of mean value of the level of acoustic pressure on the installation angle of the ultrasonic radiators

From presented dependences it follows, that optimum installation angle of the ultrasonic radiators is 45º, at which mean value of the level of acoustic pressure in Venturi tube is maximum. Moreover at the optimum angle maximum level of acoustic pressure is achieved in the confuser and the diffuser of Venturi tube.

For carrying out experiments on distribution of level of acoustic pressure in the volume of Venturi tube with the application of developed ultrasonic radiator we designed laboratory setup (model) of Venturi tube at a scale of 1:1, shown in Fig. 17.

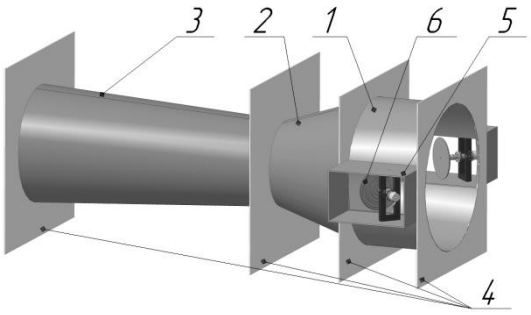

1 – cap of Venturi tube; 2 – confuser; 3 – diffuser; 4 – framework; 5 – rotating unit; 6 – ultrasonic disk radiator

Fig. 17. 3D model of the laboratory setup

On the cap of Venturi tube two opposite-directed rotating units, in which there were two disk radiators, were placed. The rotating unit is intended for the installation of the disk radiator at different angles in order to provide maximum level of acoustic pressure and even distribution of ultrasonic vibrations in the volume of Venturi tube.

The measurements of the level of acoustic pressure in the laboratory setup were carried along 5 cross-sections, in 17 points of each cross-section by the noise and vibration analyzer "Assistant".

Obtained results proved the presence of optimum angle (45º), at which maximum level of acoustic pressure in the mouth of Venturi tube achieved 145 dB.

As results of measurements showed, the difference between theoretical and experimental data was 5 dB. It was caused by the following factors, as inelastic reflection of ultrasonic waves from the walls (at the theoretical calculations absolute elasticity was assumed).

Further theoretical calculations of the determination of dependence of Venturi tube and the dust-extraction plant efficiency on the size of ash particles for different number of developed ultrasonic radiators of 370 mm in diameter were carried out. Obtained results are shown in Fig. 18, 19.

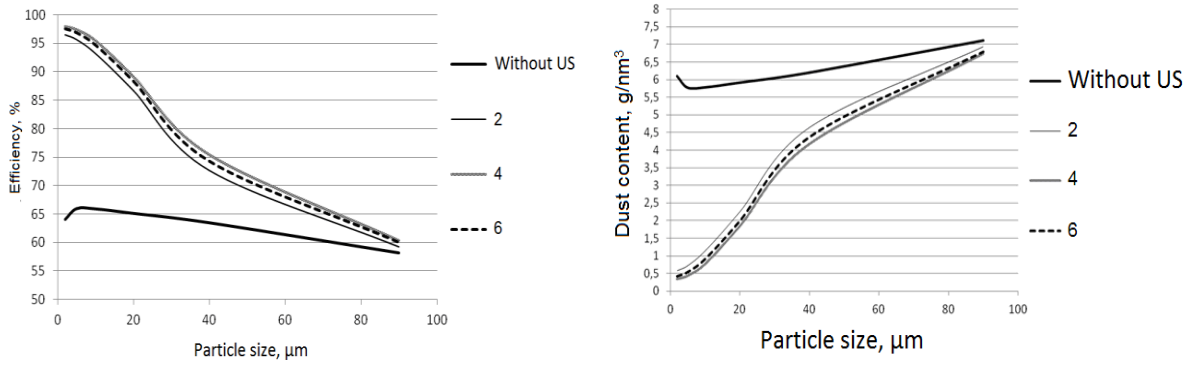

a) b)

Fig. 18. Dependence of Venturi tube efficiency (a) and dust concentration at its output (b) on size of ash particles at different number of the ultrasonic radiators

It was stated, that the application of 2 ultrasonic radiators of 370 mm in diameter provides dust concentration at the output of the dust-extraction plant of no more than 0.255 g/Nm^3; four radiators – no more than 0.225 g/Nm^3; six radiators – no more than 0.2 g/Nm^3 at burning of coal from Kharanor coal deposit.

Further efficiency increase of dust extraction is concerned with the increase of number of applied ultrasonic radiators. However the installation of more than 4 radiators is economically unpractical and is caused by constructional limits of Venturi tube.

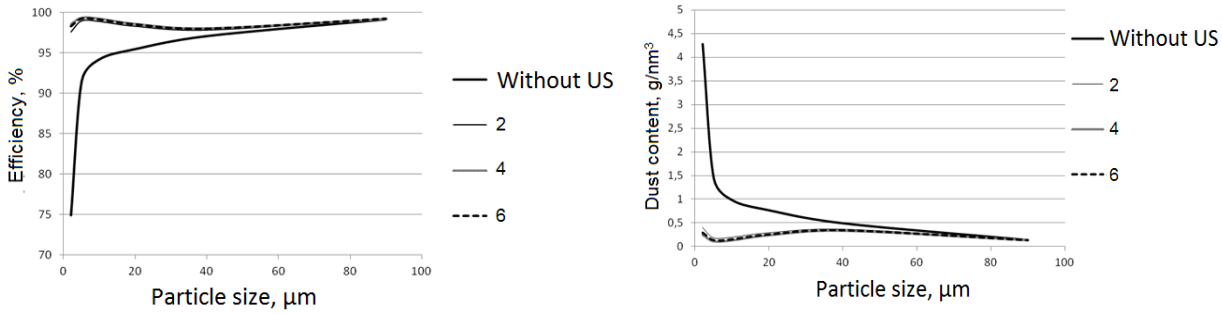

а) б)

Fig. 19. Dependence of efficiency of the dust-extraction plant (a) and dust concentration at its output (b) on the size of ash particles at different number of the ultrasonic radiators

To increase output acoustic power and as a sequence efficiency of dust-extraction plant operation it is necessary to enlarge area of radiation surface, i.e. the diameter of the ultrasonic radiators.

Thus, obtained results allow determining optimum number and installation position of the ultrasonic radiators providing fulfillment of necessary requirements on efficiency and residual dust concentration at the output of the dust-extraction plant.

VI. Conclusion

After carrying out studies following results are obtained:

1. it is determined, that the process of ultrasonic coagulation occurs due to orthokinetic (different degree of involvement of dispersed particles into vibrational motion, which is in inverse proportion to their diameter and mass) and hydrodynamic (occurrence of forces of attraction between the particles caused by asymmetry of flow field of dispersed particles in the ultrasonic field) mechanisms;
2. theoretical calculations show, that the use of ultrasonic action provides essential efficiency increase of the dust-extraction plant operation especially for high-dispersed particles (for the particles of 2 µm the efficiency of the dust-extraction plant increases from 74.8 % to 99.1 %);
3. the construction of the ultrasonic radiator excluding overheating of the piezoelectric transducer at the operation in the conditions of high temperatures is developed;
4. the number and position of the ultrasonic radiators in Venturi tube providing optimum conditions of ultrasonic action and protection of the ultrasonic radiators from abrasive wear by solid particles of flue gases are determined.

VII. Acknowledgements

The study was supported by grant of the President of Russian Federation No. MK-957.2014.8.

References

[1] V.N. Uzhov, A.U. Waldberg, B.I. Myagkov, I.K. Reshidov, *Cleaning of industrial gases from dust* (M.: Chemistry, 1981). In Russian.
[2] L.I. Kropp, A.I. Akbrut, *Dust-collectors with Venturi tubes at thermal power stations* (M.: Energy, 1977). In Russian.
[3] V.N. Khmelev, A.V. Shalunov, K.V. Shalunova, S.N. Tsyganok, R.V. Barsukov, A.N. Slivin, *Ultrasonic coagulation of aerosols* (Altay State Technical University, Biysk: Publishing of Altay State Technical University). In Russian.
[4] V.N. Khmelev, A.V. Shalunov, R.V. Barsukov, S.N. Tsyganok, D.S. Abramenko, Acoustic coagulation of aerosols, *Polzunov bulletin, 1(2)*, 2008, 66-74. In Russian.
[5] N.N. Chernov, *Acoustic methods and means of precipitation of suspended particles of industrial flue gases*, doctoral diss. ,Taganrog, 2004. In Russian.
[6] L.Y. Skryabina, *Industrial and sanitary purification of gases. Atlas of industrial dusts. Part I. Flue ash of the thermal power stations* (Central institute of scientific-technical information and technical-economical studies of chemical and oil mechanical engineering, M., 1980). In Russian.
[7] V.N. Khmelev, A.V. Shalunov, V.A. Nesterov, R.N. Golykh, R.S. Dorovskikh, Increase of separation efficiency in the inertial gas-purifying equipment by high-intensity ultrasonic vibrations, *International Conference and Seminar on Micro / Nanotechnologies and Electron Devices*, Novosibirsk, RU, 2014, 233-239.
[8] V.N. Khmelev, S.S. Khmelev, A.V. Shalunov, S.N. Tsyganok, A.N. Lebedev, A.N. Galakhov, Development of the piezoelectric ultrasonic vibrating systems for intensification of processes in gas media, *Bulletin of Tula State University, Issue 1*, 2010, 148-153. In Russian.
[9] V.N. Khmelev and others, Design and modeling of the ultrasonic vibrating systems, *Measurements, automation and modeling in industrial and scientific studies*, Biysk, RU, 2003, 211-216. In Russian.
[10] V.N. Khmelev, R.V. Barsukov, E.V. Ilchenko, Studies of temperature influence on the parameters of the ultrasonic vibrating systems, *South-Siberian scientific bulletin, 2(4)*, 2013, 46-49. In Russian.

American Journal of Engineering Research (AJER) 2015
American Journal of Engineering Research (AJER)
e-ISSN: 2320-0847 p-ISSN : 2320-0936
Volume-4, Issue-8, pp-120-124
www.ajer.org
Research Paper Open Access

Seasonal variation in the physico-chemical Parameters of Tirana river

[1]Enkelejda KUCAJ, [2]Uran ABAZI
[1] *Department of Agro Environment & Ecology, Agricultural University of Tirana, Albania.*
[2]*Department of AgroEnvironment & Ecology, Agricultural University of Tirana, Kodër-Kamëz 1029, Tirana, Albania*

ABSTRACT: *Water quality has become a major concern due to ever increasing human developmental activities that over exploit and pollute the water resources. As the Economic and financial centre of Albania, Tirana has an extensive experienced urban expansion after 1990 with a very high cost in environmental degradation The aim of the present study is to examine the water quality of Tirana River Nile through several physico-chemical analyses. Results obtained from two seasons (June-September, during 2011-2013) . Water samples were taken at different locations and indicators were analyzed: temperature, pH, DO, TDS, NBO5, $NO3^-$, NO_2^-, NH_4^+, P_{total} and PO_4^{3-}. Based on the results of the analysis and the rates set by Albanian state standards catalogue (KSSH, 2012) has shown that the river was highly polluted due to urban and industrial effluent in the urban and the water of these river classified as class IV and V. High concentrations of NH3, total dissolved solids (TDS), biological oxygen demand (BOD), total alkalinity, turbidity and recognizable depletion in dissolved oxygen (DO) were recorded. Increasing pollution and negative impact of discharges in these river ecosystems is a disturbing problem and requires constant monitoring and a final solution by treatment of these waters before pouring them into the sea.*

Keywords: *Physico-chemical analyses, Pollution, Surface water quality, Tirana river.*

I. INTRODUCTION

Tirana is the city with the largest inflows demographic fact that has led to an increased number of productive activities in industry and agriculture. These processes have contributed significantly to increasing levels of pollution in surface waters. Tirana river passes through the capital city, and in this area are many urban discharges. During the last years of water pollution has reached very high levels by affecting the water quality and on the other hand affecting directly to the ecosystems of the area (Abazi et al., 2008). Tirana River is one of the branches of the Ishmi river, which flows into the Adriatic Sea near the Rodoni Bay. It has a length of 35 km and is the shortest river of this region compared with Erzeni and Terkuza.

This river stems in the Hurmëza village being supplied with water selita and several streams that flow into his bed. Passes through the Shali area, Zall Dajtit, Brar, Tufinë, Ferraj and traverses the field of Tirana, pervades Domje village and join with Terkuza river to forming Ishmi river, which continues the path to shed in the Adriatic Sea. In the upper of the river have Cretaceous carbonate sediments of Paleocene (Zone Dajtit Zall), thus disrupting the terrigenous carbonate deposits in the area Brarit. The average flow capacity per year is 3.1 m^3/sec (with a minimum value 0.94 m^3/sec at the maximum 5 m^3/sec). Surface of Tirana River watershed basin is about 71 km^2 (Kabo et al., 1991). Largest flow of water from precipitation: 80% -82% during the wet season and 18% -29% during the dry season. Tirana river from the Brari bridge to Kamza bridge, serves as a collector for the discharge of untreated wastewater portion of sewerage network to Tirana and many commercial activities and industrial. Numerous studies conducted since 1998 have demonstrated the highest pollution in Tirana River (Çullhaj A., Hasko A., Miho A., Scanz F., Brandl H., Bachoren R., 2005), (Bode A. 2012) not only for the physical-chemical parameters but also heavy metals in water and sendimente. Population growth permanently, the importance of Tirana river for the area ecosystem, its use of the many residents who live edge of the river are necessary indicators for ongoing evaluation of water quality of the Tirana river. Based on these important indicators for the life of residents in the area, the objective of the study was the assessment of water quality in Tirana river.

II. MATERIALS AND METHODS

Sampling for assessment of water quality of these river is done in such a way to present its changes in time and space. Determining of the number of sampling sites in rivers was relying on some size and, specifically in the surface of the them, their length and slope. Sampling points that are selected, considering the characteristic places in which have waited pollution from anthropogenic activities (industrial activities, traffic, sewage, agricultural land, etc.). During this study (2011-2013) were measured physico-chemical parameters in water which are important determinants in aquatic systems (A. Sargaonkar and V. Deshpande, 2003;, (Pavendan P.,; Anbuselvan S. and Rajasekaran C. Sebastian, 2011; Kamble Pramod N.,; Gaikwad Viswas B. and Kuchekar Shashikant R, 2011). The sampling was done at four (4) stations, T1 (Brari Bridge), T2 (Babrru Bridge), T3 (Kthesa Kamzës Bridge) and T4 (Laknas Bridge), were established on the river during June- September according to the methodology defined by the USEPA in 2011.

Water samples were collected in the morning with polythene bottles, (500 ml) and were transported to the laboratory by refrigeration at 4 grade before sending to the laboratory. At each station was measured water temperature, pH, dissolved oxygen, TDS, COD, BOD_5, is also made assessment of nitrates, nitrites, ammonium and phosphates. Some of this parameters are measured insitu used portable sensor multiparameter. The found results were compared with Norms set by Albanian State Standards Catalogue (KSSH, 2012) and assessment of water quality.

III. FIGURES AND TABLES

To assess the water quality was done based on Norms of the State Standards Catalogue (KSSH, 2012) and Water Framework Directive of the EU (Directive 76/160 / EEC, Table 1).

Table 1. Limit values of chemical parameters in rivers under the EU Framework Directive (Directive 76/160/EEC).

Parameters	Unit meas.	Limit values of chemical parameters				
		High Condition	Good condition	Moderate Condition	Poor condition	Poor state
DO		>7	>6	>5	>4	<3
BOD_5	mg/l	<2	<3.5	<7	<18	>18
pH (acid)			>6.5	>6		
pH (alkalin)			<8.5	<9		
NH_4	mg/l	<0.05	<0.3	<0.6	<1.5	>1.5
NO_2	mg/l	<0.01	<0.06	<0.12	<0.3	>0.3
NO_3	mg/l	<0.8	<2	<4	<10	>10
PO_4	mg/l	<0.05	<0.10	<0.2	0.5	>0.5
P-total	mg/l	<0.1	<0.20	<0.4	<1	>1

Table 2. Site and results of the physico-chemical parameters of Tirana River (During June-September 2011-2013)

Year	Parameters	Unit meas	T1			T2			T3			T4		
			June	Sept.	Mean	June	Sept.	Mean	June	Sept.	Mes.	June	Sept.	Mean
2011	Temp.	^{0}C	20.3	11.02	15.66	19.8	14.2	17	20.8	15.7	18.25	22.5	17.4	19.95
	pH	pH	7.80	8.26	8.03	7.65	7.96	7.805	7.75	7.90	7.825	8.15	8.67	8.41
	DO	mg/l	7.05	9.26	8.155	5.96	5.63	5.795	7.03	5.54	6.285	7.32	8.28	7.8
	TDS	mg/l	30.8	32.0	31.4	31.0	38.6	34.8	37.4	72.0	54.7	27.6	80.9	54.25
	NKO	mg/l	6	9	7.5	51	46	48.5	42	37	39.5	8	7	7.5

	NBO5	mg/l	4	3	3.5	30	20	25	25	15	20	40	28	34
	N-NO2	mg/l	0.007	0.001	0.004	0.02	0.04	0.032	0.016	0.003	0.0095	0.04	0.038	0.043
	N-NO3	mg/l	0.42	0.33	0.375	0.86	0.48	0.67	0.70	0.42	0.56	0.78	0.198	0.48
	N-NH4	mg/l	0.083	0.183	0.133	11.2	16.9	14.05	13.40	15.40	14.4	6.36	8.64	7.5
	P total	mg/l	0.012	0.11	0.061	0.63	2.07	1.35	0.66	1.35	1.005	1.28	1.35	1.315
	P-PO4	mg/l	0.009	0.007	0.008	0.59	2.03	1.31	0.61	1.33	0.97	1.27	1.32	1.295
2012	Temp.	^{0}C	12.3	15.4	13.85	15	15.7	15.35	17.2	16.6	16.9	17.8	17.2	17.5
	pH	pH	7.43	7.68	7.555	7.16	7.64	7.4	7.03	7.78	7.405	7.08	7.79	7.435
	DO	mg/l	8.49	8.48	8.485	7.68	7.87	7.775	7.06	7.94	7.5	7.61	8.32	7.965
	TDS	mg/l	12.5	9.3	10.9	27.4	28.5	27.95	34.1	15.3	24.7	35.3	17.6	26.45
	NKO	mg/l	9	4	6.5	27	62	44.5	23	80	51.5	27	84	55.5
	NBO5	mg/l	4	2	3	10	30	20	8	38	23	9	40	24.5
	N-NO2	mg/l	0.05	0.04	0.045	0.08	0.03	0.061	0.091	0.027	0.059	0.13	0.014	0.072
	N-NO3	mg/l	0.57	0.19	0.38	0.92	0.07	0.495	0.87	0.05	0.46	0.79	0.041	0.415
	N-NH4	mg/l	0.54	0.019	0.279	8.80	8.42	8.61	6.35	10.82	8.585	7.42	11.13	9.279
	P total	mg/l	0.015	0.023	0.019	0.34	0.66	0.5	0.36	0.89	0.625	0.34	1.08	0.71
	P-PO4	mg/l	0.014	0.017	0.015	0.35	0.64	0.499	0.34	0.86	0.6	0.28	1.06	0.67
2013	Temp.	^{0}C	18.4	15	16.7	21	16.5	18.75	21.7	17.2	19.45	27.5	18	20.55
	pH	pH	7.48	7.60	7.54	7.56	7.38	7.47	7.78	7.90	7.84	8.32	7.43	7.875
	DO	mg/l	6.81	6.20	6.505	6.03	5.97	6	5.68	5.87	5.775	5.60	5.82	5.71
	TDS	mg/l	16.4	33.6	25	142	16.7	79.35	178.4	69.0	123.7	221	109.2	165.4
	NKO	mg/l	43	6	24.5	52	18	35	58	27	42.5	63	54	58.5
	NBO5	mg/l	6	2	4	20	10	15	25	17	21	31	25	28
	N-NO2	mg/l	0.012	0.09	0.051	0.12	0.01	0.072	0.139	0.025	0.082	0.15	0.017	0.087
	N-NO3	mg/l	0.267	0.074	0.170	0.75	0.13	0.4455	0.943	0.156	0.5495	0.96	0.105	0.534
	N-NH4	mg/l	0.097	0.048	0.072	4.66	6.73	5.6995	5.98	13.08	9.53	6.17	15.09	10.63
	P total	mg/l	0.028	0.034	0.031	0.54	0.57	0.5555	0.638	0.672	0.655	0.73	0.758	0.747
	P-PO4	mg/l	0.026	0032	0.002	0.53	0.56	0.549	0.647	0.784	0.7155	0.73	0.843	0.790

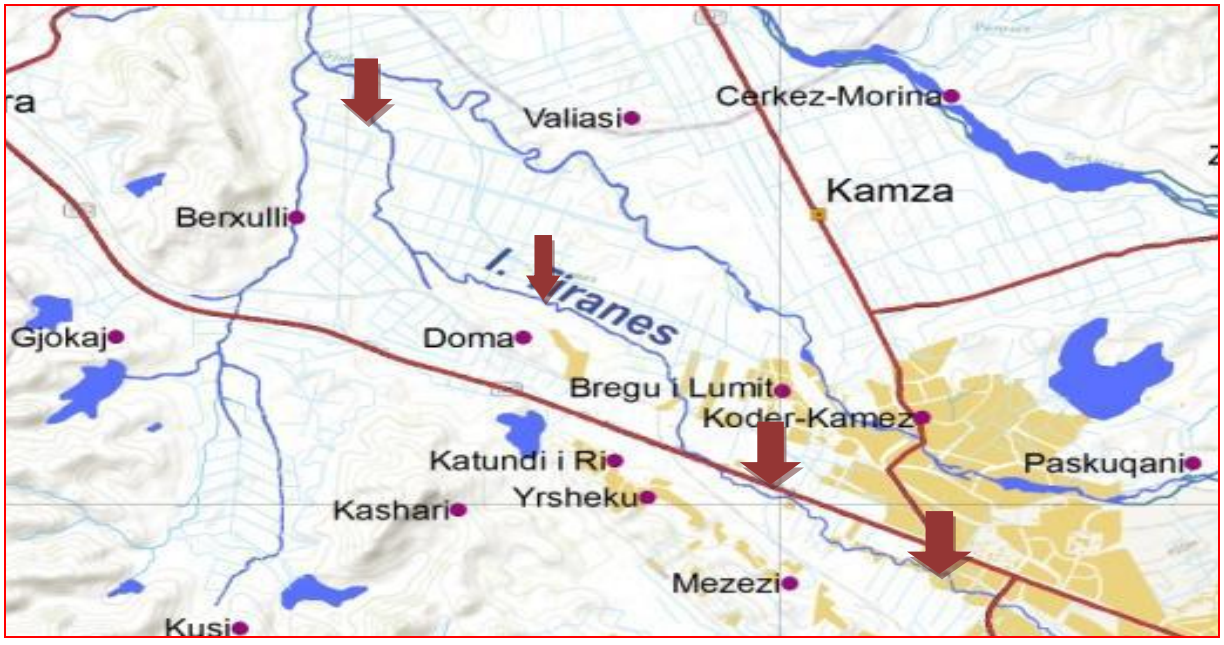

Figure 1. Sampling site in Tirana river

IV. RESULTS AND DISCUSSION

Results have demonstrated the value of water temperatures with different tendencies during three years of study. During the year 2011 is observed that temperatures have increased from the beginning to the end of monionitorimit. The reverse has happened in 2012 and 2013, as a result of climate change.

The pH ranging with different values for all samples in three year from 7.7 to 8.24. The pH values of 6.5 to 8.5 is normally acceptable under the guidelines suggested. Minimum value (7.12) is registered at the station T2 in 2012 and maximum values 8.67 is registred at theT4 in 2011, ranking in class IV. Different value comes as a result of accumulated urban discharge materials at all stages of the river.

Mean values of the Total Dissolved Solids in the analyzed samples contain about 15 times more than the ranging in class V, a fact that makes the necessary treatment of these waters. Minimume value measured in the water river si 9.3 mg/l at the station T1 in 2012 and maximume value is 221.6 mg/l at the T4 in 2012.

Throughout the study period 2011-2013, there has been a shortage of dissolved oxygen in the sample. The value of DO ranging from 5.54 mg/l minimume at st T3 in 2011and maximume 9.26 mg/l at st T1 in 2011. Low oxygen content in the water is usually associated with organic pollution. The value of thisparameters classify these waters in class III-IV.

Generally COD values resulted very high during the monitoring period.The influence of climatic factors, the increase of dilution has led to an increase of 15% of the COD values. Results have demonstrated a very high value of COD.The minimum value of COD is 4 mg/l at st T1 in 2012, while the maximum value result is 84.4 mg/l at st T4 observed in the same year. The COD values are very high compared with the legal norms belonging to class IV.

High variability has also resulted NBO_5 in the same year and between the years water monitoring. The minimum values of BOD_5 ranging from 2 mg/l at st T1 in 2012 and max. 40 mg/l at st T4 to the same year. Compared with the permissible values for BOD_5 wastewater spilling into the environment (20mg / l) and based on the values that have resulted over limits during all years of monitoring that go up to 30% of the samples analyzed, we believe it must treatment these waters. Compared with the norms value, the levels of nitrate exceeding the recommended amount.

Minimume value measured in the water river si 0.041 mg/l at the station T4 in 2012 and maximume value is 0.964 in 2013. High content of NO_3 in Tirana river is an indicator of pollution by urban and agricultural origin ending in groundwater from run off and erosion.

Minimume value measured in the water river si 0.001 mg/l at the station T1 in 2011 and maximume value is 0.158 in 2013. The content of NO_2 in water is an indicator of pollution by sewage discharges.

The values of the nitrogen content resulting from 0.019 in 2012-15.4 mg/l in 2011. Maximum values have resulted higher than allowable values of KSSH demonstrating a very high pollution due to the discharge of waste, wastewater and Slaughterhouses waste (rubbish). Generally increasing tendency of NH_{4+} from the first station at the last shows the negative effect of such discharges to surface waters.

The maximum value of P - PO4 resulted 1,32 mg/l at st. T4 in 2011 while other values found in the analyzed samples have been lower in 2012 and 2013. Tendency of P-PO4 ions from the first station monitoring in fourth station has resulted in an increase during the year 2011 and the same tendency observed for 2013. While in 2012 the values have been variability and is not observed the same tendency. The same trend has also led to the total phosphorus content, the content which has resulted higher in the first year of study in urbanized area that crosses the river length at T4.

The maximum value of the P total content is observed as the puntual value at the second station in the first year (2.07 mg / l). This high value found only in one case appears to be random due to discharges with high water content, waste and other effluents that contain high levels of phosphates.

V. CONCLUSION

Based on the finding conclude that the water quality of the river Tirana, comes down from the first station at the fourth as a result of the increased pollution. Results found classify waters of the river Tirana in class IV-V. The main cause of this contamination is the water used, the discharge of waste into surface waters, agricultural discharges, agricultural and industrial. Another cause is the erosion process, especially when favored by atmospheric factors. Use of these waters for irrigation of crops and for other uses washing, livestock and recreational purposes can have consequences for the human health. Regular monitoring and continual water quality of Tirana River is necessity as a result of continued pollution and protection of aquatic ecosystems and is a priority obligation of Albania at the regional level.

REFERENCES

[1] A. SARGAONKAR AND V. DESHPANDE, "DEVELOPMENT OF AN OVERALL INDEX OF POLLUTION FOR SURFACE WATER BASED ON A GENERAL CLASSIFICATION SCHEME IN INDIAN CONTEXT," *ENVIRONMENTAL MONITORING AND ASSESSMENT, VOL. 89, NO. 1, 2003, PP. 43-67.*

[2] Çullhaj A., Hasko A., Miho A., Scanz F., Brandl H., Bachoren R., 2005: The quality of Albanian natural waters and human impact. *Environment Internacional 31. f. 133-146.*

[3] Kamble Pramod N., Gaikwad Viswas B. and Kuchekar Shashikant R.; Monitoring of Physico Chemical Parameters and Quality Assessment of Water from Bhandaradara Reservoir; *Der Chemica Sinica, 2011, 2 (4):229-234.*

[4] Mendez G., A. Flores R., S. Palacios M., 1997. Disponibilidad de Cd, Fe, Mn y Pb en suelos agricolas de Tecamachalco, Edo. De Puebla. Pp. 60. In: Memorias del XXVIII, Congreso Nacional de la Ciencia del Suelo, Villahermosa, Tabasco.

[5] Pavendan P., Anbuselvan S. and Rajasekaran C. Sebastian, Physico Chemical and microbial assessment of drinking water from different water sources of Tiruchirappalli District, South India; Pelagia Research Library *Eur. J. Exp.Bio.,2011,1(1):183-189.*

[6] Bratli L.J.2000: *Classification of the Environmental Quality of Freshwater in Norway. Hidrological and limnological aspects of lake monitoring.* Heinonen et al. (ed). John Willey & Sons Ltd.f.331-343

[7] Kabo M. (ed.), 1991: *Physical Geography of Albania*. Vol. I & II, Academy of Sciences, Geographic Centre, Tirana. R.E. Moore, *Interval analysis* (Englewood Cliffs, NJ: Prentice-Hall, 1966).

[8] Katalogu i Standarteve Shtetërore Shqiptare, 2012. Botim i Drejtorisë së Përgjithshme të Standarteve, (D.P.S.).

[9] USEPA, 2011. Methods for Chemical Analysis of Water and Wastes, 2nd ed. Washington, D.C.:U.S. Environmental Protection Agency, 2011

[10] Bode A. 2012: *Impakti ambiental i faktorëve antropogjenë në pellgun ujëmbajtës të Tiranës*. Phd thesis.

[11] Tamariz F,. 1996. *Contaminación de los suelos agricolas por metales pesados en el municipio de Atlixo, Puebla*. Tesis de Mestria en Edafologia. Faculdad de Ciencias, Universidad Nacional Autonoma de México, México.

[12] D.S. Chan, *Theory and implementation of multidimensional discrete systems for signal processing*, doctoral diss., Massachusetts Institute of Technology, Cambridge, MA, 1978.

[13] Abazi, U. and Balliu, A. 2008. Environmental impact of heavy metals presence in the Fan and Shkumbin Rivers. 43rd Croatian and 3rd International Symposium on Agriculture, Opatija, Croatia, *Proceedings, pp. 111-114.*

[14] Hilsenhoff, W.L., "Use of arthropods to evaluate water quality of streams", Department of Natural Resources, Madison W.I. *Tech. Bull, No. 100, pp. 15, 1977.*

American Journal of Engineering Research (AJER)
e-ISSN: 2320-0847 p-ISSN : 2320-0936
Volume-4, Issue-8, pp-125-139
www.ajer.org
Research Paper Open Access

Performance evaluation of existing ASP & SBR (30 MLD capacity) STP's at PCMC, Pune (MH) – A case study.

Er. Mahesh Kawale[1], Er. Devendra Dohare[2], Er. Pravin Tupe[3]
[1]*PG Student, M.Tech. (Environmental Engg.), CE-AMD, SGSITS, Indore, M.P, INDIA*
[2]*Assistant Professor, CE-AMD, SGSITS, Indore, M.P, INDIA*
[3]*Joint City Engineer(E/M), Pimpri Chinchwad Municipal Corporation, Pune Maharashtra, INDIA*

ABSTRACT : *The present study was undertaken to evaluate performance of sewage treatment plants working on Activated Sludge process (ASP) and Sequencing Batch Reactor Process (SBR) of 30 MLD capacities each at Chinchwad, Pimpri Chinchwad Municipal Corporation, Pune, Maharashtra, INDIA. To evaluate performance of ASP & SBR, both plants were monitored for normal operation, samples were collected and analyzed for the major water quality parameters, such as pH, Colour, Temperature, Conductivity, Total solids, TSS, TDS, DO, BOD, COD, Chlorides, Alkalinity, Total Hardness, Nitrogen(Nitrates), Phosphates and Total Organic Carbon. The % Variations, % parameter removal efficiency, Effluent water quality indexes in terms of CCMEWQI, statistical co-relations between parameters of inlet, outlet, and % parameter removal efficiency were evaluated and based on these information performance of ASP & SBR had been compared. It was found out that ASP was working with average % removal efficiency for BOD & suspended solids as 83.59% & 75.55% respectively which were lower than design values whereas SBR was working with average % removal efficiency for BOD & suspended solids as 94.94% & 92.12% respectively which were higher than design values.*

Keywords- *% incremental efficiency, % removal efficiency, Activated Sludge Process (ASP), CCMEWQI, Sequencing Batch Reactor (SBR), Statistical co-relations*

I. INTRODUCTION

Pimpri Chinchwad Municipal Corporation (PCMC), Pune & Maharashtra Industrial Development Corporation (MIDC) lifts @435 MLD & supply @330 MLD raw water from Pavana River. As per Indian River Standards Pavana River was of Class C up to the raw water lifting point at Ravet but onwards it was Class D type and Non-Perennial River in the PCMC area. The industrial effluent was discharged through secondary and primary natural channels in to Pavana River. As well as treated water i.e. effluents from all STP's were also discharged in to Pavana River. As the effluents from all STP's were discharged into Pavana River it may be one of the reasons for Pavana River pollution. So it became necessary to check quality of effluents discharged into Pavana River as well as to evaluate the performance of the all STP's. For this purpose two STP's 1) 30 MLD STP at Bhatnagar, Pimpri-Chinchwad Link Road (ASP Process) and 2) 30 MLD STP at Laxminagar, Chinchwad (SBR Process) were taken for study of Performance evaluation of ASP & SBR for domestic sewage treatment as a case study. After treatment effluents were tested only for pH, BOD, COD, DO & TSS and maintained as per these parameters only. As per the Indian Effluent Standards laid by CPCB, effluent should be tested by using methodology specified in various parts in Indian Standards IS 3025 and compared with limits prescribed in the Indian Effluent Standards for parameters like pH, BOD, COD, DO, TSS, TDS, Nitrogen as Nitrates, Phosphates, Total Organic Carbon, Colour, Hardness and Chlorides. As effluents from all STP are wasted in river, the requirements of Indian River Standards laid for Class D River should be fulfilled by effluents. Parameters such as pH, Colour, Temperature, Conductivity, Total solids, TSS, TDS, DO, BOD, COD, Chlorides, Alkalinity, Total Hardness, Nitrogen (Nitrates), Phosphates and Total Organic Carbon were selected for present study. Samples were collected, analyzed and compared with limits prescribed in the Indian Effluent Standards & Indian River Standards. Based on this information % parameter removal efficiency, Effluent water quality indexes in terms of CCMEWQI, statistical co-relations between parameters of inlet, outlet, % removal efficiency & parameters were evaluated. Performance of ASP & SBR had been compared with design % removal efficiency and performance data prescribed in 'CPHEEO Manual', published by the Govt. of India.

II. DESCRIPTION OF WORK AREA

30 MLD STP at Bhatnagar, Pimpri-Chinchwad Link Road (ASP Process)

The sewage treatment plant was designed on Activated Sludge Process Technology popularly known ASP of capacity 30 MLD for purification of domestic sewage obtaining from the municipal corporation residential areas and constructed at Bhatnagar link road Chinchwad. The plant was designed in accordance with the characteristics of influent and effluent as provided and according to the guidelines set up by the 'CPHEEO Manual', published by the Govt. of India. The plant was designed for raw water characteristics as BOD_5 at 20°C – 350 mg/ltr, Suspended solids – 400 mg/ltr and effluent characteristics as BOD_5 at 20°C – 20 mg/ltr, Suspended solids – 30 mg/ltr with % removal efficiency for BOD & suspended solids as 94.29% & 92.50% respectively.

Location Coordinates: 18°37'39"N 73°47'44"E

30 MLD STP at Laxminagar, Chinchwad (SBR Process)

The sewage treatment plant was designed on Sequencing Batch Reactor Technology popularly known as SBR of capacity 30 MLD for purification of domestic sewage obtaining from the municipal corporation residential areas and constructed at Laxminagar, Chinchwad. The plant was designed in accordance with the characteristics of influent and effluent as provided and according to the guidelines set up by the 'CPHEEO Manual', published by the Govt. of India. The plant was designed for raw water characteristics as BOD_5 at 20°C – 250 mg/ltr, Suspended solids – 300 mg/ltr and effluent characteristics as BOD_5 at 20°C – 20 mg/ltr, Suspended solids – 30 mg/ltr with % removal efficiency for BOD & suspended solids as 92% & 90% respectively.

Location Coordinates: 18°37'51"N 73°47'32"E

III. METHODOLOGIES

1 Sample collection

Samples were collected at Parshall flume as inlet (influent) and after chlorination as outlet (effluent).

2 Experimental Methodologies

Samples were collected and analyzed for the major water quality parameters, such as pH, Colour, Temperature, Conductivity, Total solids, TSS, TDS, DO, BOD, COD, Chlorides, Alkalinity, Total Hardness, Nitrogen(Nitrates), Phosphates and Total Organic Carbon as per test procedure prescribed in Indian Standards IS:3025.

3 Computation Methodologies

Removal efficiencies were calculated by using formula % removal efficiency = (IC-EC) x100/IC which contains IC – Influent concentration, EC – Effluent concentration. Negative Removal efficiency shows that parameter had increased in effluent instead of decreasing so negative removal efficiency considered as incremental efficiency. Statistical co-relations were established by computing correlation coefficient (r) & coefficient of determination (r^2) by using eleven test data points. Computation of water quality indexes (WQI) done by using method prescribed by Canadian Council of Ministers of Environment (CCMEWQI) as per limits prescribed in Indian River Standards for Class D.

4 Result Comparison Methodologies

Test parameters were compared with limits prescribed for effluent characteristics in Indian Effluent Standards IS 2490:1982, limits prescribed for inland surface water class A to E in Indian River Standards IS 2296:1982 and design % removal efficiency along with average performance data of % removal efficiency of ASP & SBR prescribed in 'CPHEEO Manual', published by the Govt. of India.

IV. RESULTS & DISCUSSION

Samples were collected and analyzed for the major water quality parameters, such as pH, Colour, Temperature, Conductivity, Total solids, TSS, TDS, DO, BOD, COD, Chlorides, Alkalinity, Total Hardness, Nitrogen (Nitrates), Phosphates and Total Organic Carbon as per test procedure prescribed in Indian Standards IS:3025. The test results observed and noted in table no 1 along with calculated average & % variations & % parameter removal efficiency for each parameter.

Table no 1 Test Results

Sr.No.	Parameter	ASP			SBR		
		Inlet	Outlet	% Variations	Inlet	Outlet	% Variations
1	**pH**						
1	Min	6.84	6.93	1.11	6.70	7.10	4.41
2	Max	7.40	7.53	4.28	7.05	7.60	11.94
3	Average	7.22	7.40	2.40	6.89	7.46	8.25
2	**Temperature (°C max)**						
1	Min	24	22	0.00	26	26	0.00
2	Max	25	25	8.33	30	30	7.14
3	Average	24.36	23.36	4.15	27.91	27.45	1.62
3	**Dissolve oxygen (DO) recovery (mg/ltr min)**						
1	Min	0	2.7		0.0	5.5	
2	Max	0	4.7		0.0	5.9	
3	Average	0	3.91		0.00	5.79	
Sr.No.	**Parameter**	**ASP**			**SBR**		
		Inlet	**Outlet**	**% Removal Efficiency**	**Inlet**	**Outlet**	**% Removal Efficiency**
4	**Colour (Hazen units max)**						
1	Min	757	385	47.16	759	43	86.35
2	Max	1208	571	65.06	1172	160	94.33
3	Average	1051	463.55	55.67	1021.09	108.00	89.79
5	**Conductivity (µs max)**						
1	Min	236	261	-9.22	369	341	5.25
2	Max	465	577	-24.09	591	551	9.70
3	Average	412.27	469.91	-13.69	472.36	438.82	7.12
6	**Total solids (mg/ltr max)**						
1	Min	332	253	15.71	288	178	31.30
2	Max	471	322	35.03	488	285	43.55
3	Average	413.64	298	27.55	399.64	246.09	38.12
7	**TSS (mg/ltr max)**						
1	Min	138	25	71.18	102	6	88.78
2	Max	255	68	85.12	205	23	94.12
3	Average	193.9	48.09	75.55	147.55	11.82	92.12
8	**TDS (mg/ltr max)**						
1	Min	194	223	-9.25	186	172	4.78
2	Max	232	287	-23.71	295	276	9.89
3	Average	219.73	249.82	-13.64	252.09	234.27	7.08
9	**BOD (mg/ltr max)**						
1	Min	140	18	78.67	110	6	93.33
2	Max	190	32	88.00	160	8	96.25
3	Average	161.82	26.45	83.59	141.82	7	94.94

Sr.No.	Parameter	ASP			SBR		
		Inlet	Outlet	% Removal Efficiency	Inlet	Outlet	% Removal Efficiency
10	**COD (mg/ltr max)**						
1	Min	240	60	66.67	230	20	88.00
2	Max	320	100	76.00	340	30	94.12
3	Average	269.09	78.18	70.85	298.18	23.64	91.98
11	**Chloride (mg/ltr max)**						
1	Min	30	36	-9.68	56	42	10.00
2	Max	62	68	-23.81	78	66	15.38
3	Average	42.73	48.91	-14.83	61.45	53.09	13.52
12	**Alkalinity (mg/ltr max)**						
1	Min	241.20	247.60	-1.31	227.00	260.20	-13.62
2	Max	269.00	275.40	-4.78	267.40	317.20	-21.81
3	Average	252.22	258.43	-2.48	247.19	291.85	-17.99
13	**Total Hardness (mg/ltr max)**						
1	Min	84	96	-5.56	128	112	4.55
2	Max	160	192	-26.32	192	176	15.79
3	Average	138.55	155.64	-12.35	159.27	144.73	9.24
14	**Nitrogen(Nitrates) (mg/ltr max)**						
1	Min	24.60	18.30	25.61	24.00	5.70	76.25
2	Max	78.80	43.80	53.68	68.90	12.30	84.29
3	Average	60.25	34.66	41.10	47.35	8.70	81.15
15	**Phosphates (mg/ltr max)**						
1	Min	5.32	4.52	7.80	3.87	1.20	63.31
2	Max	5.87	5.20	18.41	6.38	2.20	79.66
3	Average	5.52	4.87	11.74	5.48	1.56	71.33
16	**Total Organic Carbon (mg/ltr max)**						
1	Min	46.00	38.80	11.56	55.56	31.37	39.43
2	Max	68.80	55.85	27.83	68.80	38.60	50.68
3	Average	58.17	48.93	15.74	61.42	34.18	44.26

Note: - Negative Values of % parameter removal efficiencies shows an increase in parameter in effluent than influent, hence considered as % parameter incremental efficiencies.

Parameters of Influents & Effluents

1) pH

pH of effluents from both plants were found within the limits prescribed in Indian Effluent Standards as 5.5 to 9. After treatment of sewage pH of effluents had increased in both process plants but increase in pH of effluent was higher in case of SBR plant than ASP plant. Fig no 1 shows graphs of % pH variations of both plants.

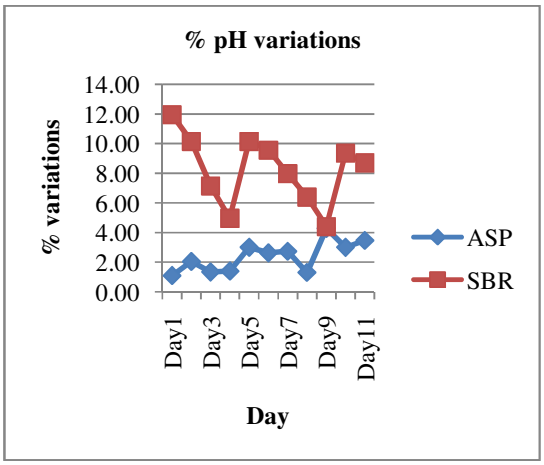

Fig no 1 % pH variations

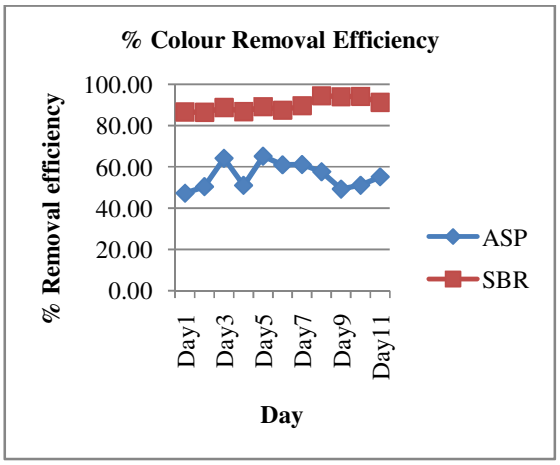

Fig no 2 % Colour removal efficiency

2) Colour

After treatment of sewage, Colour of treated water had decreased in both processes. It was observed that decrease in colour of effluent was higher in case of SBR than that of ASP. Limits for Colour of effluent were not prescribed in Indian Effluent Standards as well as Indian River Standards. Fig no 2 shows variations of % colour removal efficiency of both plants. SBR plant was working in range 86.35 to 94.33% colour removal efficiency with an average of 89.79%, whereas ASP plant was working in range 47.16 to 65.06% colour removal efficiency with an average of 55.67%. It was revealed that SBR plant was working at higher % colour removal efficiency than ASP plant.

3) Temperature

After treatment of sewage, Temperature of treated water was decreased most of the times in ASP but in case of SBR it was same and was found within the limits prescribed in Indian Effluent Standards as 40°C max. Fig no 3 shows % Temperature variations graphs of both plants. An average % Temperature variation of ASP plant was 4.15% which was higher than an average % Temperature variation of SBR plant as 1.62%.

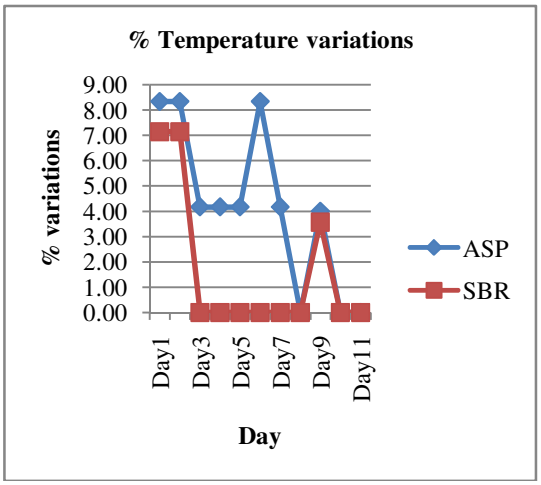

Fig no 3 % Temperature variations

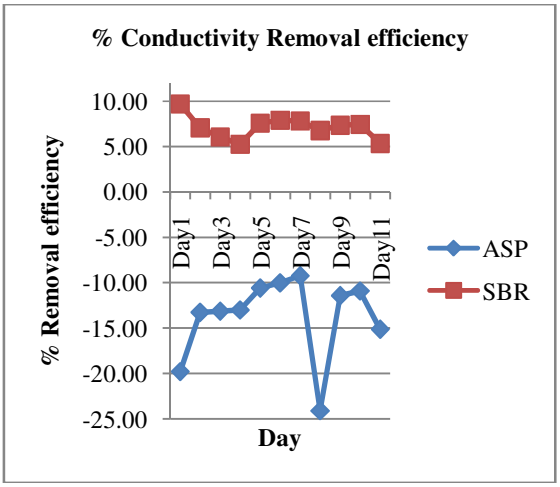

Fig no 4 % Conductivity removal efficiency

4) Conductivity

After treatment of sewage, Conductivity of effluent was augmented in ASP but in case of SBR it was lowered down. Limits for Conductivity of effluent were not prescribed in Indian Effluent Standards whereas Conductivity of effluent from ASP & SBR was found within the limits prescribed in Indian River Standards as 1000µs max. % Conductivity removal efficiency of both plants was plotted on graph as showed in fig no 4. SBR plant was working in range 5.25 to 9.70% conductivity removal efficiency whereas ASP plant was working in range -9.22 to -24.09% conductivity removal efficiency. ASP & SBR plants were working at -13.69% & 7.12%

average % conductivity removal efficiency respectively. Negative sign indicates an increase in conductivity of effluent than influent in case of ASP. SBR plant was working at higher % Conductivity removal efficiency than ASP plant.

5) Total Solids (TS)

Total solids in effluent were decreased in both plants after treatment of sewage. Limits for Total solids were not prescribed in Indian Effluent Standards as well as Indian River standards. Fig 5 describes variations in % Total solids removal efficiency of both plants. ASP plant was working in range 15.71 to 35.03% TS removal efficiency whereas SBR plant was working in range 31.30 to 43.55% TS removal efficiency. ASP & SBR plants were working at 27.55% & 38.12% average % TS removal efficiency respectively. ASP plant was running at lesser % Total solids removal efficiency than SBR plant.

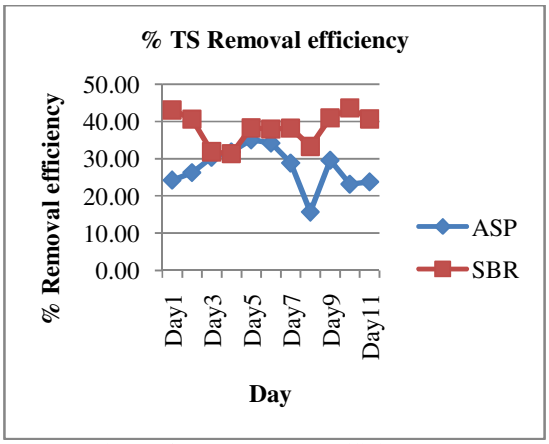

Fig no 5 % TS removal efficiency

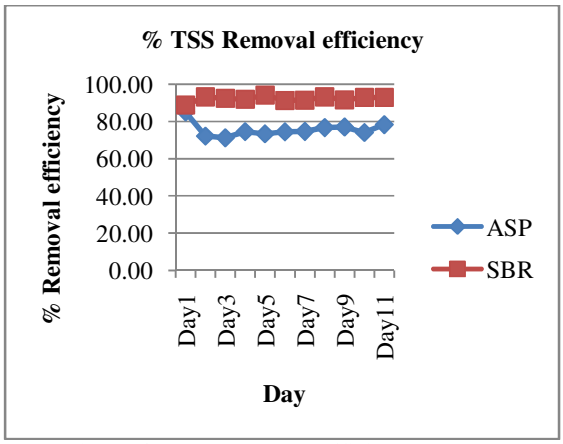

Fig no 6 % TSS removal efficiency

6) Total Suspended Solids (TSS)

After treatment of sewage, Total suspended solids in effluents from ASP & SBR were decreased & found within the limits prescribed in Indian Effluent Standards as 100 mg/litre max. ASP plant was operating in range 71.18 to 85.12% TSS removal efficiency whereas SBR plant was operating in range 88.78 to 94.12% TSS removal efficiency as plotted in Fig no 6. Both plants were working at 75.55% & 92.12% average % TSS removal efficiency respectively for ASP & SBR. It was observed that SBR was working at higher % Total suspended solids removal efficiency than ASP. Also it was discovered that ASP was designed for % TSS removal efficiency 92.50%, and it was working with average % TSS removal efficiency 75.55% which was lower than design value. SBR was designed for % TSS removal efficiency 90%, and it was working with average % TSS removal efficiency 92.12% which was higher than design values.

As per 'CPHEEO Manual', published by the Govt. of India performance of ASP & SBR as % TSS removal efficiency was 85 to 90% & 85 to 97% respectively. It was found that ASP plant was working with lesser efficiency than % TSS removal efficiency prescribed in CPHEEO manual on Day2 to Day11 and the design % TSS removal efficiency on all days. Whereas SBR plant was working within the range of % TSS removal efficiency prescribed in 'CPHEEO Manual', published by the Govt. of India on all days and the design % TSS removal efficiency on all days excluding day1.

ASP plants needs to provide efficient excess sludge removal system at secondary settling tank to enhance its % TSS removal efficiency and to reduce rising of sludge in secondary settling tank as it will also help to reduce total dissolved solids & conductivity in effluent.

7) Total Dissolved Solids (TDS)

TDS in effluent was increased in ASP but in case of SBR it was lowered down. Total Dissolved solids in effluent from ASP & SBR were found within the limits prescribed in Indian Effluent Standards as 2100 mg/litre max. ASP plant was working in range -9.25 to -23.71% TDS removal efficiency whereas SBR plant was working in range 4.78 to 9.89% TDS removal efficiency as drawn in fig no 7. ASP & SBR plants were working at -13.64% & 7.08% average % TDS removal efficiency respectively. Negative sign indicates increase in Total Dissolved Solids in case of ASP. ASP plants needs to provide efficient aeration & sludge removal system at secondary settling tank to enhance its % TDS removal efficiency and to reduce rising of sludge in secondary settling tank, it will also help to reduce total suspended solids & conductivity in effluent. % TDS removal efficiency was higher in case of SBR plant than ASP plant.

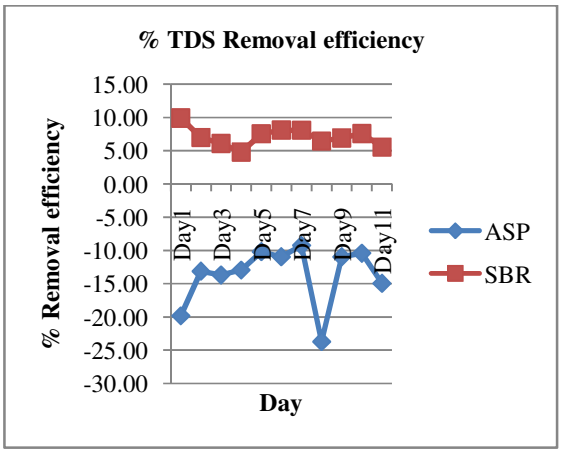

Fig no 7 % TDS removal efficiency

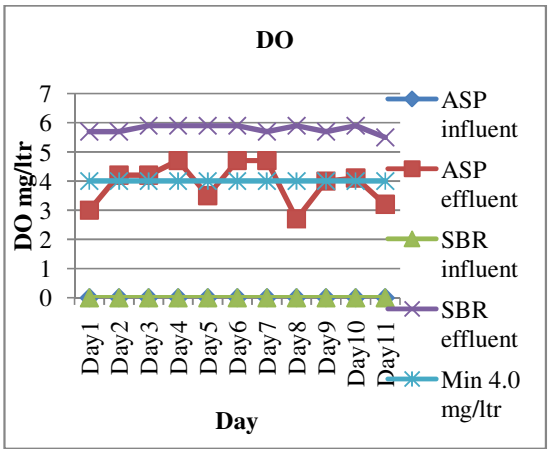

Fig no 8 DO in influents & effluents

8) Dissolved Oxygen (DO)

Limits for Dissolved Oxygen in effluents were not prescribed in Indian Effluent Standards whereas Dissolved oxygen in effluent from ASP was found less than the minimum limits prescribed in Indian River Standards for Class D as 4mg/litre min on Day1, Day5, Day8 & Day11 as 3, 3.5, 2.7 & 3.2 respectively. Dissolved oxygen in effluent from SBR was found within the limits prescribed in Indian River Standards for Class D as 4mg/litre min. DO in effluents was recovered in ASP & SBR plants with an average of 3.91 & 5.79 mg/litre respectively. DO in influents & effluents were showed in fig no 8. Higher and uniform DO recovery was observed in case of SBR plant than ASP plant because SBR plant was provided with Auto control of diffused aeration with the help of SCADA as compared to surface aerators used for aeration at ASP plant without SCADA.

9) Biochemical Oxygen Demand (BOD)

In ASP & SBR plants overall BOD of effluent was reduced after treatment of sewage. BOD of effluent from ASP was found higher than the limits prescribed in Indian Effluent Standards as 30 mg/litre max excluding Day2. Whereas BOD of effluent from SBR was within the limits prescribed in Indian Effluent Standards as 30 mg/litre max. ASP plant was running in range 78.67 to 88% BOD removal efficiency whereas SBR plant was running in range 93.33 to 96.25% BOD removal efficiency with an average of 83.59% & 94.94% BOD removal efficiency respectively. Fig no 9 shows the graphs of % BOD removal efficiency of both plants. It was found that ASP plant was working with lesser % BOD removal efficiency than SBR plant. In 'CPHEEO Manual', published by the Govt. of India performance of ASP & SBR for % BOD removal efficiency was prescribed as 85 to 95% & 89 to 98% respectively. ASP plant was working on lesser % BOD removal efficiency than % BOD removal efficiency prescribed in manual on Day1 to Day8 and the design % BOD removal efficiency on all days. ASP plants needs to provide efficient aeration system to enhance its % BOD removal efficiency. Whereas SBR plant was working within the range of % BOD removal efficiency prescribed in manual on all days and also it was working at higher % BOD removal efficiency than the design value on all days.

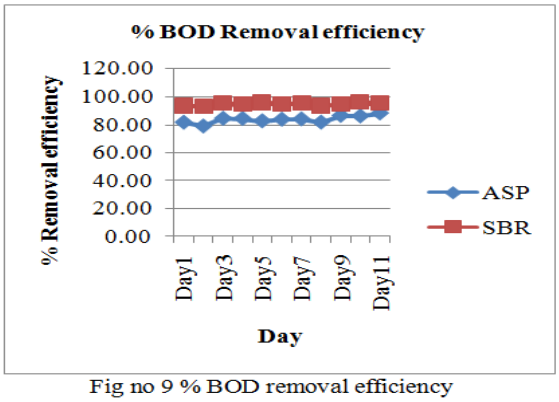

Fig no 9 % BOD removal efficiency

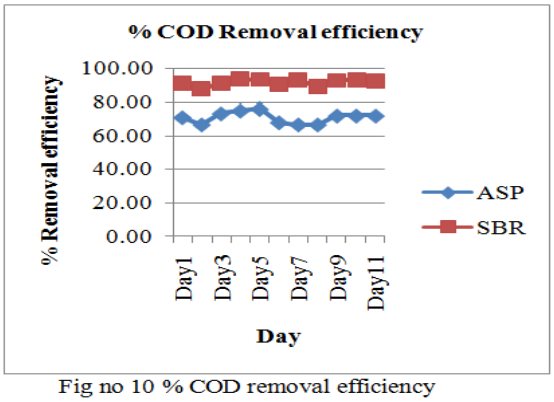

Fig no 10 % COD removal efficiency

10) Chemical Oxygen Demand (COD)

After treatment of sewage, COD of effluent was lowered down in both plants. COD of effluents from ASP & SBR were found within the limits prescribed in Indian Effluent Standards as 250 mg/litre max & % COD removal efficiency Graphs drawn as showed in Fig no 10. It was found that SBR had higher COD removal efficiency than ASP. ASP plant was operating in range 66.67 to 76% COD removal efficiency whereas SBR plant was operating in range 88 to 94.12% COD removal efficiency. ASP & SBR plant was working with an average of 70.85% & 91.98% COD removal efficiency respectively.

11) Chlorides

It was revealed that after treatment Chlorides in effluent were increased in ASP but decreased in effluent from SBR plant. Chlorides in effluent from ASP & SBR were found within the limits prescribed in Indian Effluent Standards as 1000 mg/litre max. SBR plant had higher and more uniform % Chlorides removal efficiency than ASP plant as showed in fig no 11. ASP plant was working in range -9.68 to -23.81% Chlorides removal efficiency whereas SBR plant was working in range 10 to 15.38% Chlorides removal efficiency. ASP & SBR plant was working with an average of -14.83% & 13.52% Chlorides removal efficiency respectively. Negative sign indicates increase in Chlorides in case of ASP plant which resulted in increase in Total hardness and Conductivity of effluent in case of ASP plant. ASP plants needs to provide efficient aeration system to enhance its % chlorides removal efficiency; it will also help to reduce total suspended solids, total hardness & conductivity in effluent.

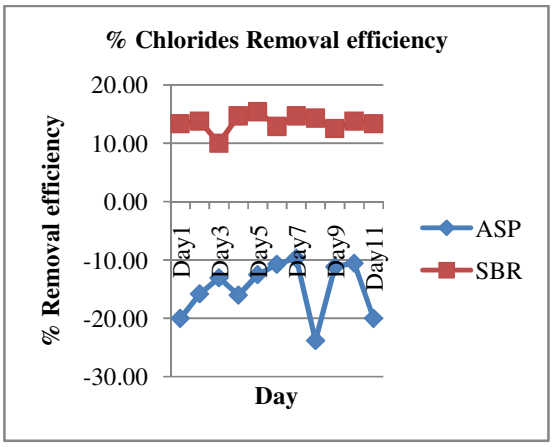

Fig no 11 % Chlorides removal efficiency

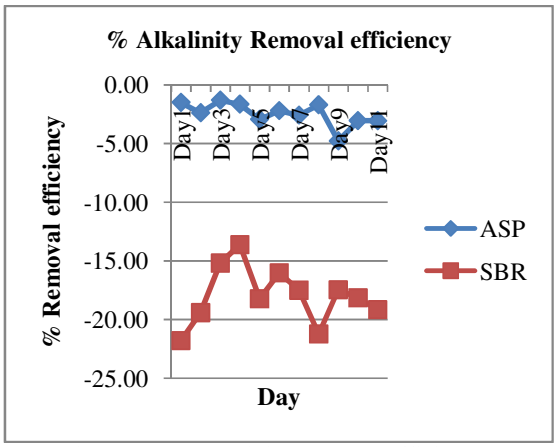

Fig no 12 % Alkalinity removal efficiency

12) Alkalinity

Alkalinity of effluent was increased after treatment in ASP & SBR plants. Limits for Alkalinity were not prescribed in Indian Effluents Standards & Indian River Standards. ASP plant was working in range -1.31 to -4.78% whereas SBR plant was working in range -13.62 to -21.81% Alkalinity removal efficiency as drawn in fig no 12. ASP & SBR plant was working with an average of -2.48% & -17.99% Alkalinity removal efficiency respectively. Negative sign indicates increase in Alkalinity in effluents from both plants. So % Alkalinity removal efficiency was considered as % incremental efficiency. SBR plant had higher % Alkalinity incremental efficiency than ASP plant.

13) Total Hardness

Total Hardness in effluent had increased in ASP but in case of SBR it was found decreased. Limits for Total Hardness were not prescribed in Indian Effluents Standards as well as in Indian River Standards for Class D. Fig no 13 shows graphs of % Total Hardness removal efficiency of both plants and it was observed that SBR plant was operating with higher % Total Hardness removal efficiency than ASP plant. ASP plant was operating in range -5.56 to -26.32% whereas SBR plant was operating in range 4.55 to 15.79% Total Hardness removal efficiency. ASP & SBR plant was working with an average of -12.35% & 9.24% Total Hardness removal efficiency respectively. Negative sign indicates an increase in Total Hardness in case of ASP plant resulted in an increase in Conductivity of effluent. ASP plants needs to provide efficient aeration system to enhance its % Total Hardness removal efficiency; it will also help to reduce total suspended solids, chlorides & conductivity in effluent.

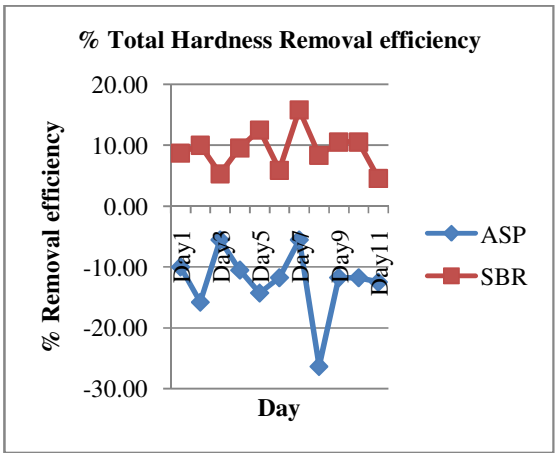

Fig no 13 % Total Hardness removal efficiency

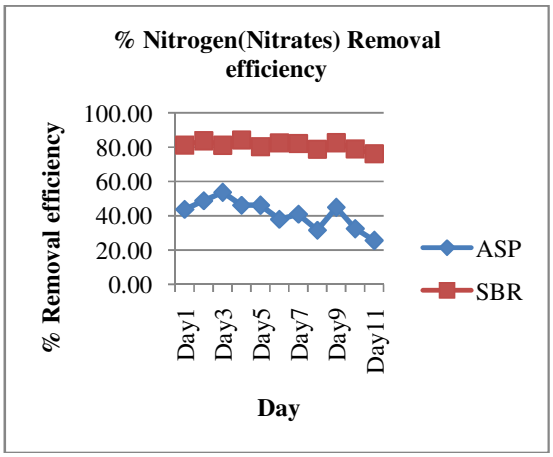

Fig no 14 % Nitrogen (Nitrates) removal efficiency

14) Nitrogen (Nitrates)

Nitrogen (Nitrates) in effluent was reduced after treatment in ASP & SBR plants. Limits for Nitrogen (Nitrates) in effluent were not prescribed in Indian Effluent Standards as well as Indian River Standards for Class D. In fig no 14 graphs of % Nitrogen (Nitrates) removal efficiency of both plants were plotted. SBR plant was working at very high % Nitrogen (Nitrates) removal efficiency than ASP plant. ASP & SBR plant was working with an average of 41.10% & 81.15% Nitrogen (Nitrates) removal efficiency respectively. Performance of SBR as % removal efficiency for Total nitrogen removal was >75% and no treatment in case of ASP plant was described in 'CPHEEO Manual', published by the Govt. of India . It was noticed that SBR plant & ASP plant was running at 76.25 to 84.29% & 25.61 to 53.68% Nitrogen (Nitrates) removal efficiency respectively.

15) Phosphates

It was observed that Phosphates in effluent reduced in both ASP & SBR plants. Phosphates in effluent from ASP were found higher on Day3 & Day8, whereas in case of SBR Phosphates in effluent were less than the limits prescribed in Indian Effluent Standards as 5 mg/litre max. In fig no 15 graphs of % Phosphates removal efficiency of both plants were plotted. From this graphs it was revealed that SBR plant was working with very high % Phosphates removal efficiency than ASP plant. No treatment & 57 to 69% efficiency range was described for Biological Phosphorus removal efficiency of ASP & SBR plants respectively in manual whereas it was discovered that ASP was working with 7.80 to 18.41% & SBR was working with 63.31 to 79.66% range of % Phosphates removal efficiency. ASP & SBR plant was working at 11.74% & 71.33% average % Phosphates removal efficiency respectively.

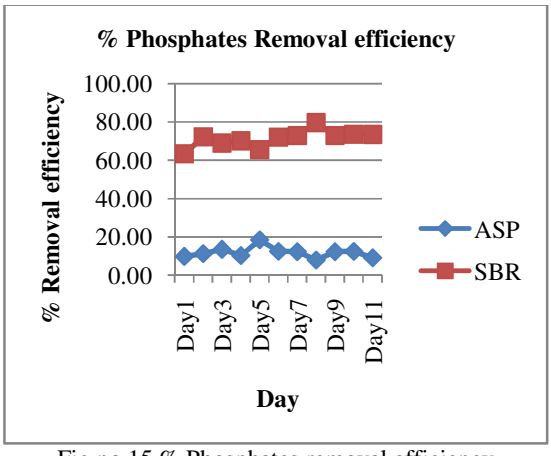

Fig no 15 % Phosphates removal efficiency

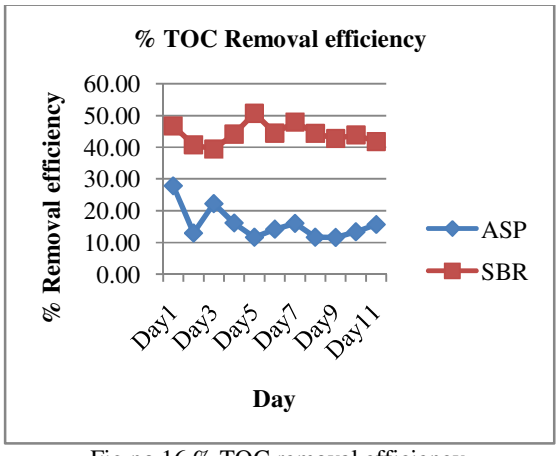

Fig no 16 % TOC removal efficiency

16) Total Organic Carbon (TOC)

After treatment of sewage, Total organic carbon in effluent had decreased in ASP & SBR plants. In Indian Effluent Standards & Indian River Standards for Class D no limits were prescribed for TOC. % TOC removal efficiency graphs were plotted as shown in fig no 16. It was found that SBR had higher % Total organic carbon removal efficiency than ASP plant. ASP plant was working in range 11.56 to 27.83% TOC removal efficiency whereas SBR plant was working in range 39.43 to 50.68% TOC removal efficiency. ASP & SBR plant was working at 15.74% & 44.26% average % TOC removal efficiency respectively.

Statistical co relations

Statistical co-relations between parameters of influents and effluents, % removal efficiency and parameters were evaluated by using eleven test data points and noted as in table no 2 of ASP and table no 3 for SBR. Statistical co-relations of very high degree between parameters such as TSS & Total solids, Total Hardness & Conductivity, TDS & Conductivity, Chlorides & Conductivity, Chlorides & TDS, Alkalinity & pH and Phosphates & Conductivity were detected in case of ASP. Statistical co-relations of very high degree between parameters such as TSS & Total solids, TDS & Conductivity, TDS & Total solids, Total Hardness & Conductivity, Total Hardness & TDS, Total solids & Conductivity, Total Hardness & Total solids, Phosphates & Total solids, Phosphates & TDS, COD & Alkalinity were detected in case of SBR.

Table no. 2 Statistical co-relations summary of ASP

Sr. No	Y			X			Co-relation Coefficient (r)	Coefficient of determination (r^2)	Slope (m)	Inter-cept (c)
	Inlet	Outlet	%RE/variations	Inlet	Outlet	%RE/variations				
ASP										
1	TSS			Total solids			0.97	0.94	0.93	-192.58
2	Total Hardness			Conductivity			0.98	0.97	0.31	9.15
3		Total Hardness			Conductivity		0.97	0.95	0.29	18.91
4			TDS			Conductivity	1.00	0.99	0.98	-0.22
5			Chlorides			Conductivity	0.93	0.87	0.97	-1.57
6			Chlorides			TDS	0.92	0.85	0.98	-1.53
7			Alkalinity			pH	0.95	0.90	0.91	-0.28
8	TSS					Total Solids	0.89	0.78	6.56	13.10
9		Temperature				Temperature	-0.97	0.93	-0.36	24.86
10		BOD				BOD	-0.83	0.70	-1.27	132.94
11		Phosphates				Conductivity	-0.87	0.76	-25.76	772.22

Note: - Statistical co-relations were evaluated on the basis of test data for eleven data points. More accurate Statistical co-relations can be evaluated by using more data points.

Table no. 3 Statistical co-relations summary of SBR

Sr. No	Y			X			Co-relation Coefficient (r)	Coefficient of determination (r^2)	Slope (m)	Intercept (c)
	Inlet	Outlet	%RE/variations	Inlet	Outlet	%RE/variations				
SBR										
1	TSS			Total solids			0.91	0.82	0.56	-75.88

Sr. No	Y			X			Co-relation Coefficient (r)	Coefficient of determination (r^2)	Slope (m)	Intercept (c)
	Inlet	Outlet	%RE/variations	Inlet	Outlet	%RE/variations				
2	TDS			Conductivity			0.92	0.85	0.39	67.25
3	TDS			Total solids			0.86	0.74	0.44	75.88
4	Total Hardness			Conductivity			0.98	0.97	0.27	30.24
5	Total Hardness			TDS			0.93	0.86	0.61	6.75
6		Total solids			Conductivity		0.91	0.83	0.42	62.10
7		TDS			Conductivity		0.92	0.85	0.39	61.42
8		TDS			Total solids		0.99	0.98	0.92	7.42
9		Total Hardness			Conductivity		0.98	0.97	0.30	14.50
10		Total Hardness			Total solids		0.90	0.82	0.59	-1.30
11		Total Hardness			TDS		0.91	0.82	0.64	-5.32
12		Phosphates			Total solids		-0.90	0.82	-0.01	3.43
13		Phosphates			TDS		-0.90	0.80	-0.01	3.46
14			TDS			Conductivity	0.99	0.97	1.08	-0.63
15	Colour					Colour	-0.91	0.82	-41.68	4763.07
16	BOD					BOD	0.91	0.82	18.63	-1627.36
17	COD					Alkalinity	0.84	0.70	12.14	516.59
18		Colour				Colour	-0.99	0.98	-14.07	1371.24

Note: - Statistical co-relations were evaluated on the basis of test data for eleven data points. More accurate Statistical co-relations can be evaluated by using more data points.

Water quality indexes

Water quality indexes in terms of CCMEWQI of influent and effluents were evaluated as per the method described by Canadian Council of Ministers of Environment (CCMEWQI) which was based on a formula developed by the British Columbia Ministry of Environment, Lands and Parks and modified by Alberta Environment. Daily water quality indexes were evaluated for influent and effluents as per Indian River Standards of Class D and showed on graph in fig no. 17.

CCMEWQI and its ranges of ASP influents & effluents were found 1) on daily basis between 14.36 to 14.44% & 14.48 to 21.05% respectively, 2) over total test period as 14.38 & 18.72% respectively and 3) average over total test period as 14.38 & 18.67% respectively, which was categorized as poor.

CCMEWQI and its ranges of SBR influents & effluents were found 1) on daily basis between 14.36 to 14.41% & 21.22 to 21.42% respectively, 2) over total test period as 14.38 & 21.31% respectively and 3) average over total test period as 14.38 & 21.32% respectively, which was categorized as poor.

It was revealed that the requirements of Indian Standards laid for Class D River IS 2296:1982 were not fulfilled by characteristics of effluent. Water quality of influent was improved after treatment in both process but in case of SBR quality of effluent was better & uniform than ASP.

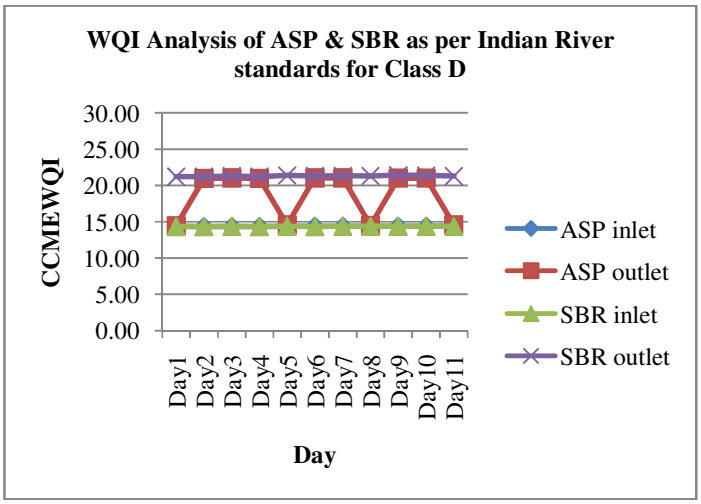

Fig no 17 CCMEWQI of ASP & SBR plants

Differentiation of ASP & SBR plants

Differentiation of ASP & SBR plants based on % parameter removal efficiency, Effluent water quality indexes in terms of CCMEWQI & statistical co-relations between parameters & % removal efficiency had been done and noted in table no 4.

Table no 4 Performance of ASP & SBR

Sr. No.	Parameters	Activated Sludge process STP			Sequencing Batch Reactor STP		
		Design	Range	Average	Design	Range	Average
1	Variations						
	pH		1.11% to 4.28%	2.40%		4.41% to 11.94%	8.25%
	Temperature		0 % to 8.33%	4.15%		0 % to 7.14%	1.62%
2	DO recovery		2.7 to 4.7 mg/liter	3.91 mg/liter		5.5 to 5.9 mg/liter	5.79 mg/liter
3	Removal efficiencies						
	Colour		47.16% to 65.06%	55.67%		86.35% to 94.33%	89.79%
	Conductivity		-24.09% to -9.22%	-13.69%		5.25% to 9.70%	7.12%
	Total solids		15.71% to 35.03%	27.55%		31.30% to 43.55%	38.12%
	TSS	92.50%	71.18% to 85.12%	75.55%	90%	88.78% to 94.12%	92.12%
	TDS		-23.71% to -9.25%	-13.64%		4.78% to 9.89%	7.08%
	BOD	94.29%	78.67% to 88%	83.59%	92%	93.33% to 96.25%	94.94%
	COD		66.67% to 76%	70.85%		88% to 94.12%	91.98%
	Chlorides		-9.68 % to -23.81%	-14.83%		10% to 15.38%	13.52%
	Alkalinity		-1.31% to -4.78%	-2.48%		-13.62% to -21.81%	-17.99%
	Total Hardness		-5.56% to -26.32%	-12.35%		4.55% to 15.79%	9.24%
	Nitrogen (Nitrates)		25.61% to 53.68%	41.10%		76.25% to 84.29%	81.15%
	Phosphates		7.80% to 18.41%	11.74%		63.31% to 79.66%	71.33%

Sr. No.	Parameters	Activated Sludge process STP			Sequencing Batch Reactor STP		
		Design	Range	Average	Design	Range	Average
	Total Organic Carbon		11.56% to 27.83%	15.74%		31.37% to 38.60%	44.26%
4	Performance (Design)	ASP plant was working with average % removal efficiency for BOD & suspended solids lower than design values.			SBR plant was working with average % removal efficiency for BOD & suspended solids higher than design values.		
5	Performance (CPHEEO manual range)	ASP plant was working with lesser % removal efficiency for BOD & suspended solids than the range prescribed in CPHEEO manual.			SBR plant was working within the range of % removal efficiency for BOD & suspended solids prescribed in CPHEEO manual.		
6	Statistical co-relations	Statistical co-relations between parameters such as TSS & Total solids, Total Hardness & Conductivity, TDS & Conductivity, Chlorides & Conductivity, Chlorides & TDS, Alkalinity & pH and Phosphates & Conductivity were detected in case of ASP.			Statistical co-relations between parameters such as TSS & Total solids, TDS & Conductivity, TDS & Total solids, Total Hardness & Conductivity, Total Hardness & TDS, Total solids & Conductivity, Total Hardness & Total solids, Phosphates & Total solids, Phosphates & TDS, COD & Alkalinity were detected.		
7	WQI(CCMEWQI) as per Indian River standards for Class D						
	Daily	14.48 to 21.05% Categorization- poor.			21.22 to 21.42% Categorization- poor.		
	Total test period	18.72% Categorization- poor.			21.31% Categorization- poor.		
	Average over Total test period	18.67% Categorization- poor.			21.32% Categorization- poor.		
	Quality	Less improved quality than SBR.			Better & uniform improved quality than ASP.		

Note: - 1. Negative (-) values of % parameter removal efficiencies shows an increase in parameter in effluent than influent, hence considered as % parameter incremental efficiencies.
2. Statistical co-relations were evaluated on the basis of eleven test data points. More accurate Statistical co-relations can be evaluated by using more data points.

V. CONCLUSIONS

- It was revealed that ASP plant was working at lesser efficiency of TSS & BOD removal than range prescribed in CPHEEO manual. For ASP plant No treatment was prescribed in manual for Nitrogen (Nitrates) and Phosphates but it was found that ASP was working in range of 25.61% to 53.68% & 7.80% to 18.41% removal efficiency respectively. In case of SBR plant, it was working within the ranges prescribed in CPHEEO manual for removal of TSS, BOD, Nitrogen (Nitrates) and Phosphates.
- It was found that ASP was working with average % removal efficiency for BOD & suspended solids as 83.59% & 75.55% respectively which were lower than design values.
- It was observed that SBR was working with average % removal efficiency for BOD & suspended solids as 94.94% & 92.12% respectively which were higher than design values.
- Average % Variations in pH and Temperature were noticed as 2.40% & 4.15% in case of ASP whereas 8.25% & 1.62% noticed in SBR.
- An average of 3.91 mg/liter & 5.79 mg/liter DO was recovered in treated effluents from ASP & SBR respectively.
- ASP was found working with average % removal efficiency for Colour, Conductivity, Total solids , TDS , COD, Chlorides, Alkalinity, Total Hardness , Nitrogen (Nitrates), Phosphates & Total Organic Carbon as 55.67%, -13.69%, 27.55%, -13.64 %, 70.85%, -14.83%, -2.48%, -12.35% , 41.10 %, 11.74 % & 15.74% respectively. Note:- Negative (-) sign shows an increase in parameter in effluent than in influent, hence considered as % parameter incremental efficiencies.
- SBR was observed working with average % removal efficiency for Colour, Conductivity, Total solids, TDS, COD ,Chlorides, Alkalinity, Total Hardness , Nitrogen (Nitrates), Phosphates & Total Organic Carbon as 89.79%, 7.12%, 38.12%, 7.08 %, 91.98 %, 13.52%, -17.99%, 9.24%, 81.15 %, 71.33% & 44.26% respectively. Note:- Negative (-) sign shows an increase in parameter in effluent than in influent, hence considered as % parameter incremental efficiencies.

- pH, Temperature, TSS, TDS, COD, Chlorides & Nitrogen (Nitrates) in effluents from ASP & SBR plants were found within limits prescribed in Indian Effluent Standards.
- DO in effluent from SBR found within limits but DO in effluent from ASP within limits excluding 4 days as per Indian River Standards for Class D as > 4 mg/litre.
- BOD found within limits excluding one day and Phosphates found within limits excluding two days in effluent from ASP as per Indian Effluent Standards. BOD & Phosphates in effluent from SBR were observed within the limits given in Indian Effluent Standards.
- Limits for Colour, Total solids, and Total organic carbon were not prescribed in Indian Effluent Standards but were found decreased in ASP & SBR. Colour of effluents found in range 385 to 571 hazen units & 43 to 160 hazen units in ASP & SBR respectively. Total solids in effluents detected in range 253 to 322 mg/liter & 178 to 285 mg/liter in ASP & SBR respectively. Total organic carbon in effluents observed in range 38.80 to 55.85 mg/liter & 31.37 to 38.60 mg/liter in ASP & SBR respectively.
- Limits for Conductivity & Total Hardness were not prescribed in Indian Effluent Standards but were found decreased in SBR and increased in ASP. Conductivity in effluents found in range 261 to 577 µs & 341 to 551 µs in ASP & SBR respectively. Total Hardness in effluents revealed in range 96 to 192 mg/liter & 112 to 176 mg/liter in ASP & SBR respectively.
- Limits for Alkalinity were not prescribed in Indian Effluent Standards but were found increased in both plants. Alkalinity in effluents found in range 247.60 to 275.40 mg/liter & 260.20 to 317.20 mg/liter in ASP & SBR respectively.
- It was revealed that the requirements of Indian River Standards for Class D IS 2296:1982 were not fulfilled by characteristics of treated effluents from ASP & SBR plants. Water quality of influent was improved after treatment in both plants but in case of SBR quality of effluent was better & uniform than ASP.
- Statistical co-relations between parameters such as TSS & Total solids, Total Hardness & Conductivity, TDS & Conductivity, Chlorides & Conductivity, Chlorides & TDS, Alkalinity & pH and Phosphates & Conductivity were detected in case of ASP. Statistical co-relations between parameters such as TSS & Total solids, TDS & Conductivity, TDS & Total solids, Total Hardness & Conductivity, Total Hardness & TDS, Total solids & Conductivity, Total Hardness & Total solids, Phosphates & Total solids, Phosphates & TDS, COD & Alkalinity were detected. Note: - Statistical co-relations were evaluated on the basis of eleven test data points. More accurate Statistical co-relations can be evaluated by using more test data points.
- It is recommended that the existing ASP plant can be modified by using SBR as a biological treatment of sewage which will help to upgrade quality of treated effluent.

VI. ACKNOWLEDGEMENTS

It is my pleasure to acknowledge my guides, Er. Devendra Dohare, Assistant Professor, CE-AMD, SGSITS, Indore, M.P, INDIA and Er. Pravin Tupe, Joint City Engineer (E/M), Pimpri Chinchwad Municipal Corporation, Pune Maharashtra, INDIA for their guidance and support at every step.

REFERENCES

[1] Ali Akbar Azimi Sayyad Hossein Hashemi, Gholamreza Nabi Bidhendi and Rohallah Mahmooddkhani (2005) "Aeration Ratio effect on efficiency of Organic Materials Removal in Sequencing Batch Reactors." *Pakistan Journal of Biological Sciences 8 (1): 20-24, 2005*

[2] B. Manoj Kumar and S. Chaudhari (2003) "Evaluation of sequencing batch reactor (SBR) and sequencing batch biofilm reactor (SBBR) for biological nutrient removal from simulated wastewater containing glucose as carbon source." *Water Science and Technology Vol. 48 No 3 pp 73–79, 2003*

[3] B. S. Akın, A. Ugurlu (2005) "Monitoring and control of biological nutrient removal in a Sequencing Batch Reactor", *Process Biochemistry, Vol. 40, No. 8, pp. 2873 - 2878, 2005*

[4] D. Obaja, S. Mac e, J. Mata-Alvarez (2005) "Biological nutrient removal by a sequencing batch reactor (SBR) using an internal organic carbon source in digested piggery wastewater." *Bio resource Technology 96 (2005), 7–14, 2005*

[5] Dahu Ding Chuanping Feng a, Yunxiao Jin a, Chunbo Hao a, Yingxin Zhao a, Takashi Suemura (2011) "Domestic sewage treatment in a sequencing batch biofilm reactor (SBBR) with an intelligent controlling system." *ELSEVIER Desalination 276 (2011) 260–265*

[6] Debaskar Anupam, Somnath Mukherjee And Siddhartha Datta (2007) "Sequencing Batch Reactor (SBR) Treatment for Simultaneous Organic Carbon and Nitrogen Removal – A Laboratory Study", *Journal of Environmental Science and Engineering, Vol. 48, No.3, pp. 169-174, 2007*

[7] E. C. Ukpong (2013) "Performance Evaluation of Activated Sludge Wastewater Treatment Plant (ASWTP) At QIT, Ibeno Local Government Area of AkwaIbom State, Nigeria." *The International Journal Of Engineering And Science (IJES), Volume 2, Issue 7, Pages 01-13, 2013*

[8] Er. Devendra Dohare, Shri. Vishnu k. Pathak, Miss Nupur Kesharwani (2014) "Biological process modification using sequential batch reactor in the sewage treatment plant of Bhilai steel plant: A case study" *International Journal of Emerging Trends in*

Engineering and Development, Issue 4, Vol.5 ,2014

[9] Fu E. Tang, and Vun J. Ngu (2011) " A study of performance of wastewater treatment systems for small sites", *World Academy of Science, Engineering and Technology, 2011, Vol. 5, pp. 12 – 29*

[10] H.L.S. Tam, D.T.W. Tang, W.Y. Leung, K.M. Ho and P.F. Greenfield (2004) "Performance evaluation of hybrid and conventional sequencing batch reactor and continuous processes." *Water Science and Technology Vol. 50 No 10 pp 59–65, 2004*

[11] Ilgi Karapinar Kapdan, Rukiye Ozturk (2005) "Effect of operating parameters on colour and COD removal performance of SBR: Sludge age and initial dyestuff concentration." *ELSEVIER, Journal of Hazardous Materials B123 (2005) 217–222*

[12] Isolina Cabral Goncalves, Susana Penha, Manuela Matos, Amelia Rute Santos, Francisco, Franco1 & Helena Maria Pinheiro (2005) "Evaluation of an integrated anaerobic/aerobic SBR system for the treatment of wool dyeing effluents(Purification of wool dyeing effluent in a SBR)." *Biodegradation (2005) 16: 81–89, Springer 2005*

[13] K. Sundara Kumar (2011) Computer aided design of waste water treatment plant with activated sludge process. *International Journal of Engineering Science and Technology (IJEST), Vol. 3 No. 4 April 2011*

[14] K. Sundara Kumar P. Sundara Kumar, Dr. M. J. Ratnakanth Babu (2010) "Performance evaluation of waste water treatment plant." *International Journal of Engineering Science and Technology, Vol. 2(12), 2010, 7785-7796*

[15] Kayranli Birol and Aysenur Ugurlu (2011) "Effects of Temperature and biomass concentration on the performance of Anaerobic Sequencing Batch Reactor treating low strength wastewater", *Desalination, Vol. 278, No. 1-3, pp. 77-83, 2011*

[16] Mahvi A. H. (2008) "Sequencing Batch Reactor: A Promising Technology in Wastewater Treatment", *Iran Journal of Environmental Health Science Engineering, 2008, Vol. 5, No. 2, pp. 79-90*

[17] Mauro P. Moreira, Celso S. Yamakawa and Ranulfo M. Alegre (2002) "Performance of the sequencing batch reactor to promote poultry wastewater nitrogen and COD reduction". *Revista Ci˜enciasExatas e Naturais, Vol. 4, no 2, Jul/Dez 2002*

[18] Prachi N. Wakode and Sameer U. Sayyad (2014) "Performance Evaluation of 25MLD Sewage Treatment Plant (STP) at Kalyan." *American Journal of Engineering Research (AJER), Volume-03, Issue-03, pp-310-316, 2014*

[19] Pradyut Kundu, Anupam Debaskar and Somnath Mukherjee (2014) "Performance Studies on Biological Treatment of Slaughterhouse Wastewater Using Mixed Culture in sequencing Batch Reactor." *Asian Journal of Water, Environment and Pollution, vol. 11, No. 2, pp 67-79, 2014*

[20] R. Lognathan, K. Rasappan, M. Issac Solomon Jebamani and M. Johnson Naveen Kumar (2012) "Biological Treatment of Domestic Wastewater Using Sequential Batch Reactor (SBR)." *Indian Journal of Environmental Protection, vol. 32, No. 7, July 2012*

[21] S. Murat, E. Ates¸ Genceli, R. Tas¸ lı, N. Artan and D. Orhon (2002) "Sequencing batch reactor treatment of tannery wastewater for carbon and nitrogen removal." *Water Science and Technology Vol. 46 No 9 pp 219–227, 2002*

[22] Shuokr Qarani Aziz1, Hamidi A. Aziz, Amin Mojiri, Mohammed J.K. Bashir, Salem S. Abu Amr (2013) " Landfill Leachate Treatment Using Sequencing Batch Reactor (SBR) Process: Limitation of Operational Parameters and Performance", *International Journal of Scientific Research in Knowledge (IJSRK), 1(3), pp. 34-43, 2013*

[23] Sílvia C. Oliveira Sílvia C. Oliveira and Marcos von Sperling (2011) "Performance evaluation of different wastewater treatment technologies operating in a developing country." *Journal of Water, Sanitation and Hygene for Development, 01.1, 2011*

[24] Stricker Anne- Emmanuelle and Michel Béland (2006) "Sequencing Batch Reactor versus Continuous Flow Process for pilot plant research on activated sludge", *Water Environment Foundation, Vol. 20, No. 3, pp. 414-426, 2006*

[25] Soledad Gutierrez Adrian Ferrari, Alejandra Benıtez, Dayana Travers, Javier Menes, Claudia Etchebehere and Rafael Canetti (2007) "Long-term evaluation of a sequential batch reactor (SBR) treating dairy wastewater for carbon removal." *Water Science & Technology Vol. 55 No 10 pp 193–199, IWA Publishing 2007*

[26] Vaishali Sahu and V. Geetha Varma (2013) "Comparative Performance Evaluation of Sewage Treatment Plants in Gurgaon." *Asian Journal of Water, Environment and Pollution, vol. 10, No. 4, pp 89-97, 2013*

[27] Wisaam S. Al-Rekabis, He Qiang and Wei Wu Qiang (2007) " Review on Sequencing Batch Reactors.", *Pakistan Journal of Nutrition, Vol. 6, No. 1, pp. 11-19, 2007*

[28] CPHEEO (2012) *"Manual on Sewerage and Sewage Treatment."* Second Edition, The Central Public Health and Environmental Engineering Organization Ministry of Urban Development, New Delhi., May 2012

[29] Metcalf and Eddy (2003) *'Waste Water Engineering Treatment and Reuse'*, 4th edition 2003, Tata McGraw Hill Publishers, 2003

[30] Ankur Shahji (2011) *Performance evaluation of Kabitkhedi sewage treatment plant (78MLD), Indore And Computer Aided Design of an up flow anaerobic sludge blanket reactor (UASB) based sewage treatment plant,* SGSITS Indore, RGPV, Bhopal, INDIA, 2011

[31] Pranay Kumar (2013) *Computer Aided Hydraulic Process Design of conventional municipal sewage treatment plant without and with up gradation,* SGSITS Indore, RGPV, Bhopal, INDIA, 2013

[32] Amr m. Abd-el-Kader (2009) "Comparison study between sequencing batch reactor And conventional activated sludge by using Simulation mathematical model" *Thirteenth International Water Technology Conference*, IWTC 13, Hurghada, Egypt, 2009

American Journal of Engineering Research (AJER)
e-ISSN: 2320-0847 p-ISSN : 2320-0936
Volume-4, Issue-8, pp-140-144
www.ajer.org
Research Paper Open Access

Flocculator Design for a Water Treatment Plant in a Rural Community with a River or Stream Water Source around Maiduguri Area, Borno State, Nigeria

Hussaini A Abdulkareem, Nuhu Abdullahi, Bitrus I Dangyara, Gideon I Orkuma
Department of Mechanical Engineering , School of Industrial Engineering , College of Engineering, Kaduna Polytechnic, Nigeria

ABSTRACT: *Flocculator, a major component of water treatment plant is required for attaining the International Standard for a potable drinking water is hereby design for rural domestic water supply. This is for an estimated population of 260,000 people with an average consumption rate of 0.057 mgd (million gallons daily). The dimension of the flocculator is 2m x 2m x 2.5m i.e. 10m^{3}in volume with a power input of 0.0036kw and detention time of 54.36min.Provision is also made for future expansion in the event of an increase in the communities' population. The sinuous channels principle used aided in minimal power requirement for the system.*
Key words: flocculator, sinuous channel, head loss, velocity gradient

I. INTRODUCTION

The use of gentle stirring in water, which floc has formed to induce the particles to coalesce and grow is known as flocculation. The bigger and denser the floc particles, the quicker are the rate of settlement.
The source of power for flocculating devices are mechanical and pneumatically. Generally speaking, seldom used in large plants, even though they possess quite useful features [2].When the dosed water carrying floc finally passes into the flocculator through the inlet port, a certain rolling motion is inevitable, which can be accentuated by baffles in Horizontal flow basin or in an upward flow basin by the sludge blanket. [1]
However in many basins there is ample evidence that better results can be obtained if mixing and flocculation can be intensified. In recent years much research has been done on both and sound theoretical rules have been laid down.

There are methods of theoretical approach, the mixing and flocculation can be carried out either by mechanical means in specially built chambers or in suitable baffled channel or interconnected chambers. The latter methods requires no mechanical equipment but lacks flexibility, because the system can be designed for maximum efficiency only at one rate of flow and at one temperature, where-as the speed of mechanical paddles can be adjusted to suit the variations of flow, temperature and silt conditions. However, the cost added to the complexity of mechanical equipment introduces additional complications to be avoided in a developing country, and in practice a sinuous inlet channel preceded by violent mixing generally provides a reasonable effective solution [1].

If the pipe or channel through WHICH the incoming water enters the basin is so dimensioned as to ensure a velocity > 1m/s, and if the channel or directed at an end wall so that the flow is forced to reverse abruptly through 180^o, any coagulant introduced into the water before that sudden reversal will be adequately mixed and floc will form almost instantaneously.
Unlike the absolute necessity for thorough mixing, the need for flocculation as a separate process may or may not be essential much depends on the nature of the suspended solids, for rivers carrying coarse and heavy sediment the main problem is to prevent the silt settling and blocking the inlet channels before it reaches the basin [1]. Shallow depth settling may present operational difficulties in developing countries, so separate flocculators are mostly found before conventional horizontal flow basins where colloids are a problem and the complication of additional machinery may be avoided by having the flocculating action imparted to the water by the gently rolling motion resulting from passing water along a sinuous channel. In practice a channel providing a velocity of flow of about 0.3m/s with cross-walls ensuring 12-20 changes of direction though 180^o (with well rounded corners), has often proved to be very effective, The emphasis must be placed on the comparative smoothness of flow required. Under no circumstances should velocity or turbulence be such as to break up the floc.

II. THEORETICAL APPROACH:

The stirring of water creates difference of velocity and therefore velocity gradients. The average temporal mean velocity gradient in a shearing fluid is denoted by G. For baffled basins or sinuous channels: -

$G = (\frac{\rho g h}{\mu T})^{1/2}$ ..... (1)

Also $T = \frac{\rho g h}{\mu G}$ ..... (2)

Where,

G is the velocity gradient, s^{-1}

ρg is the weight of water per unit volume

h is the head loss due to friction, m

μ Is the dynamic viscosity

T is the detention time, s.

For mechanical agitation, the velocity gradient relation G is given by;

$G = (\frac{P}{\mu V})^{1/2}$ ..... (3)

Where,

P is the power consumption, W

V is the volume of fluid, m^3

The total number of particle oscillation is proportional to GT, and is greater when there is a degree of turbulence as opposed to general rotation. It has been observed that in many of the more successful mixing and flocculating basins which are mechanically stirred the GT values are as shown in tables (1 & 2) below. Increase in contact time above 120 seconds achieves little, and excessive G values can be harmful [1].

Table: 1 Recommended GT Values for Flash Mixers [1]

Contact time T,s	Velocity Gradient G,s^{-1}	GT
20	1000	20,000
30	900	27,000
40	75	30,000
41-120	700	30,000

Table 2: Recommended GT Values for Flocculation [1]

Type	Velocity Gradient G,s^{-1}	GT
Turbidity or colour removal (without solids recirculation	20-100	20,000-150,000
Turbidity or colour removal (with solids recirculation)	75-75	25,000-200,000
Softeners (solid contact reactors)	30-200	200,000-250,000
Softener (ultra-high solid)	250-300	300,000-400,000

III. SINOUS CHANNELS

The permissible loading on a sinuous channel at any given value of GT is (from eqn. 2.0)

$\frac{Q}{V} = (\frac{Q\rho g h}{\mu V})^{1/2} / GT = (\frac{(Qgh}{\upsilon V})^{1/2} / GT$..... (5)

Where,

Q is the rate of flow, m^3/s

V is the channel volume, m^3

g is the acceleration due to gravity (9.81 m/s^2)

υ is the kinematic viscosity of the water, m^2/s

The useful power input is

$P = Q\rho gh$..... (6)

where P is the power watts for each meter of head lost, the useful power input is 9.8 x 10^3 watts per m^3/s, in practice, head losses are commonly 0.15-0.6m, velocities 0.15-0.5m/s and detention times 10.60min.

For channel with baffles (over and under or round the bend), the extra loss of head in the channel (in addition to normal channel friction) is,

$h = \frac{nV_1^2 + (n-1)V_2^2}{2g}$ ..... (4)

Where,

h is the addition head loss, m

n is the number of baffles
v_1 is the velocity between the baffles, m/s
v_2 is the velocity at the baffles slots, m/s
To approximate the total channel friction can be obtained by calculation using a Hazen Williams discharge coefficient c= 50 [5].

IV. FLOCCULATOR DESIGN

Since, the design is for a rural settlement, which should avoid excessive use of power and at lower cost, the flocculator should be a sinuous flow baffled channel type.
The number of baffles (n) is chosen to be 7, (over and under) [3] with an entry velocity V_1 = 0.36m/s (Velocity of water from mixer) [3] and a velocity between baffles V_2 = 0.5m/s.
The detention time in the channel is given by equation 2

$$T=\frac{\rho g h}{\mu G^2}$$

For turbidity or colour removal without recirculation G is taken to be $23s^{-1}$ (table 2). The head loss due to friction (hf) is given by Haizen Williams eqn with c = 50

$$hf = \left(\frac{1.594}{C}\right)^{1.85} \times \frac{L}{d^4 87} \times Q^{1.85}$$

Where L is the length of pipe which is 2m
d is the pipe diameter which is 0.1m
$Q = 0.003m^3/s$

$$hf = \left(\frac{1.594}{50}\right)^{1.85} \times \frac{L}{0.1^4 87} \times 0.003^{1.85}$$

hf = 0.0054m
ρg and μ at 35°C are $9.747x10^3 N/m^2$ and $0.7255x10^3 Ns/m^2$respectively(Appendix II)
Addition head loss in the channel is given by equation 4,

$$h = \frac{nV1^2 + (n-1)V2^2}{2g}$$

$$h = \frac{7 \times 0.36^2 + (7-1)0.5^2}{2 \times 9.81}$$

h = 0.123m
∴Total head loss = head loss due to friction + additional head loss.
Total head loss = 0.123 + 0.0054 = 0.1284m
Thus substituting values of head loss, ρg and μ in equation (2),

$$\text{The detention time } T = \frac{9.747 \times 10^3 \times 0.1284}{0.7255 \times 10^{-3} \times 23^2} = 361sec = 54.35min$$

$$\text{Thus from flow rate } Q = \frac{\text{volume discharged}}{\text{time}}$$

$$Q = \frac{V}{T}$$

$V = 0.003 \times 3261 = 9.8m^3 \cong 10m^3$
The dimension of the flocculator is 2m x 2m x 2.5m; hence the useful power inputs given by equation (6)
$P = \rho gQh$
$P = 9.747 \times 10^3 \times 0.003 \times 0.1230$
P = 3.6watts = 0.0036Kw
The permissible loading Q/V is given by equation (1)

$$Q/V = \frac{0.003}{10} = 0.03s^{-1}$$

and the GT value is thus, GT = 23 X 3261 = 75003.
This is within the recommended range as given in table 2.
The floor of the flocculator slopes from entry by 10% of the height. Thus 10% of 2m = 0.2, hence the height at entry = 2-0.2which is equals to 1.8m.

Thickness of the baffles are chosen to be 50mm, there are 3 upper baffles spaced 587.5mm apart and each 1.2m deep. The upper and lower baffles should lap by 0.4m (400mm) as shown in the diagram appendix I.
The flocculator basin is to be built with bricks and the surface is plastered to a smooth finish, the floor of the basin is of concrete. Since the flocculator is accompanied by a settlement basin, almost all floc formed will settle at the settlement basin and the remaining that settled at the flocculator is to be hand cleaned monthly.
The top of the flocculator is to be left open so as to assist further disinfection by ultraviolet radiation. The outlet diameter of the flocculator is to be the same with the inlet, i.e. 0.1m

V. CONCLUTION

For future expansion of the treatment plant due to increased water demand or population increase as pre-determined based on data of the 1963 census report, this expansion will be based on the population figure projected to that year. The provision for expansion has already been provided in the design and the addition of more chambers such as in the flocculator and settlement basins may be found necessary. The filter has been designed to last the life span of the project.

REFERENCES

[1] Smsrthurst G.: Basic Water Treatment 1979; Thomas Telford Ltd, London.
[2] M. Fair, Gordon C. Geyer, John A. Okun, Daniel. Water and Waste water Engineering Vol.1, 1968, John Willey and Sons Inc.
[3] H. A. Abdulkareem, S. B. Abdurrahman and Isyaku Umar, (Nov., 2014), "Design of a water treatment Mechanical Mixer for a pre-chlorination tank as an effective algae control, aeration and coagulation processing" International Journal of Engineering Science Invention ISSN (Online): 2319 – 6734, ISSN (Print): 2319 – 6726 www.ijesi.org Volume 3 Issue 11 November 2014, PP.25-36
[4] M. Fair, Gordon/C. Geyer, John/A. Okun, Daniel; Water and Waste water Engineering Vol. 2, 1968, John Willey and Sons Inc.
[5] Dunn, P.D.: Appropriate Technology Macmillan Press Ltd 1978

APPENDIXI

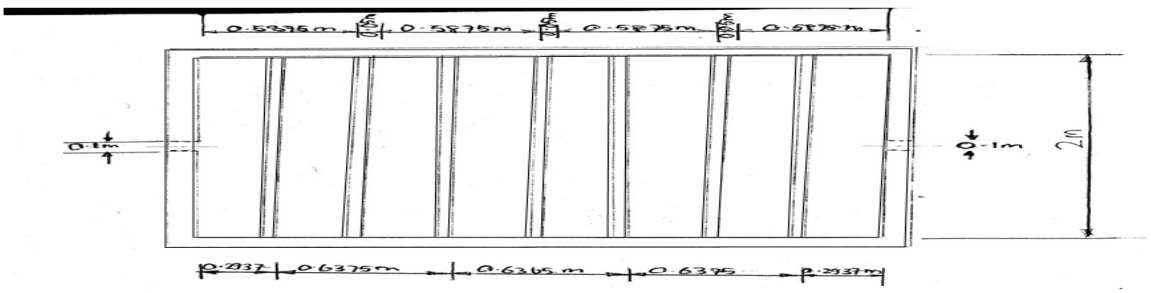

FLOCULLATOR PLAN VIEW

2.5m

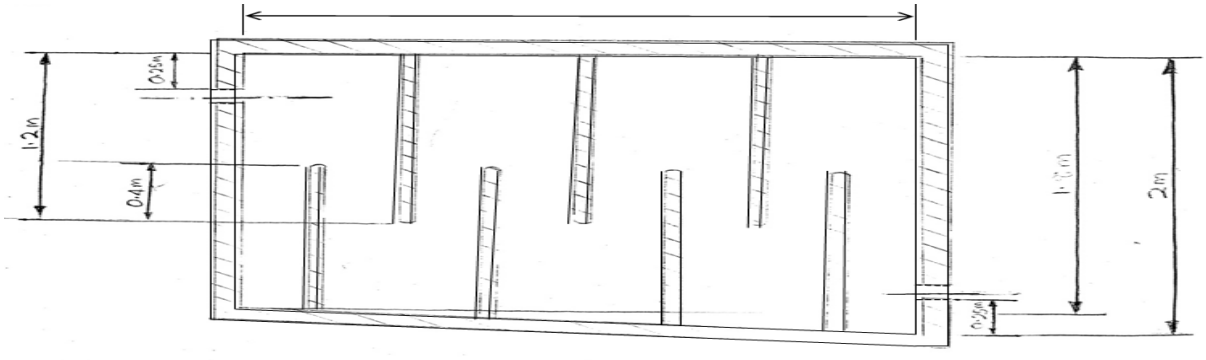

FLOCCULATOR SECTIONAL FRONT VIEW

APPENDIX II

Table A-2a Physical properties of water in English units

Temperature, °F	Specific weight lb. ft^3	Density ρ Slugs ft./	Viscosity μx10^3, sec ft^2 lb.	Kine-matic viscosity υ x 10^3 ft^2/sec	Heat of vapor-ization, Btu.lb	Vapor pressure p Pascal	Vapor pressure head *p* h ft.	Bulk modulus of elasticity E_tx 10^3 Pascal
32	’ 62.42	1.940	3.746	1.931	1075.5	0.09	0.20	293
40	62.43	1.940	3.229	1.664	1071.0	0.12	0.28	294
50	62.41	1.940	2.735	1.4 10	1065.3	0.18	0.41	305
60	62.37	1.938	2.359	1.217	1059.7	0.20	0.59	311
70	62.30	1.936	2.050	1.059	1054.0	0.36	0.84	320
80	62.22	1.934	1.799	0.930	104 8.4	0.51	1.17	322
90	62.1 1	1.931	1.595	0 826	1042.7	0.70	I .61	323
100	62. 00	1.927	1.424	0.739	1037.1	0.95	2.19	327
110	61.86	1.923	1.284	0.667	1031.4	1.27	2.95	331
120	61.71	1.918	1.163	0.609	1025.6	1.69	3.91	333
130	61.55	1.913	1.069	0.558	1019.8	2.22	5.13	334
140	61 38	1.908	0.981	0.514	1014.()	2.89	6.62	330
150	61 20	1.902	0 905	0.476	1008.1	3.72	8.58	328
160	61.00	1.896	0.838	0.412	1002.2	4.74	10.95	326
170	60.80	1.890	0.780	0.413	996.2	5.99	13.83	322
180	60. 58	1.883	0.726	0 385	990.2	7.51	17.33	318
190	60. 36	1.876	0.678	0.362	984.1	9.34	21.55	313
200	60.12	1 868	0.637	0 341	977.9	11.52	26.59	308
212	59.83	1.860	0.593	0.319	970.3	14.70	33.90	300

Table A - 2 A Physical properties of water in SI units

Temperature, °C	Specific weight **kN m^3**	Density ρ **kg m^3**	Viscosity μx10^3 **N sec m^2**	Kine-matic viscosity υ x 10^3 **m^2 sec**	Heat of vapor-ization **J gm.**	Vapor pressure p **kN m\ abs**	Vapor pressure head *p* m	Bulk modulus of elasticity E_t x 10-6 kN m:
0	9.805	999.8	1.781	1.785	2500.3	0.61	0.06	2.02
5	9.807	1000.0	1 518	1.519	2488. 6	0.87	0.09	2.**06**
10	9.804	999.7	1.307	1.306	2476.9	1.23	0.12	2.10
15	9.798	999.1	1.139	1.139	2465.1	1.70	0.17	2.15
20	9.789	998.2	1.002	1.1003	2453.0	2.34	0.25	2.18
25	9.777	997.0		0.893	244 1.3	3.17	0.33	2.22
30	9.764	995.7	0.798	0.800	24 29.6	4 24	0.44	2.25
40	9.730	992.2	0.653	0.658	2405.7	7.38	0.76	2.28
50	9.689	988.0	0.547	0.553	2381.8	12.33	1.26	2.29
60	9.642	983.2	0.466	0474 ,	2357.6	19.92	• 2.03	2.28
70	9.589	977.8	0.404	0.413	2333.3	31.16	3.20	2.25
80	9.530	971.8	0.354	0.364	2308.2	47.34	4.96	2.20
90	9.466	965.3	0 315	.0.326	2282.6	70.10	7.18	2.14
10	9.399	958.4	0.282	0.294	2256.7	101.33	10.33	2.07

American Journal of Engineering Research (AJER) 2015
American Journal of Engineering Research (AJER)
e-ISSN: 2320-0847 p-ISSN : 2320-0936
Volume-4, Issue-8, pp-145-156
www.ajer.org
Research Paper Open Access

Performance Analysis of Intermediate Band Solar Cell (IBSC)

Md. Kamal Hossain[1], Md Dulal Haque[2], Sumonto Sarker[3], Md. Arshad Ali[4], Md. Mizanur Rahman[5], Md. Mahbub Hossain[6]
(Department of Telecommunication & Electronic Engineering, Hajee Mohammad Danesh Science & Technology University, Dinajpur-5200, Bangladesh)

ABSTRACT: *To increase the efficiency of a single-junction solar cell the intermediate band solar cell is proposed. Renewable energy sources have become increasingly important; because of global environmental concerns. The intermediate band solar cell (IBSC) with potential to enhance the efficiency of the conventional single-junction cell. IBSCs have constraining efficiencies of 63.3%. In this solar cell an intermediate band placed in the band gap between the conduction and valence band. This implies that absorption of photons with energy below the band gap of the semiconductor is possible, and the photocurrent is thus increased. At the point when the carrier concentration in each of the three bands are portrayed by their own semi Fermi level the intermediate band does not influence the voltage if carriers are extricated from the conduction band and the valence band. An increment of proficiency is hence possible.*

KEYWORDS–*IBSC, Quasi-Fermi level,Solar Irradiance, Efficiency, Photon Energy.*

I. INTRODUCTION

According to the U.S. Energy Information Administration (EIA), the world's total energy consumption in 2007 was 495.2 quadrillion British Thermal Units (BTU) with 86% derived from fossil fuels[2] [**11**]. In the event that all nonrenewable sources[29] are considered, there is an extra 6% from atomic, bringing the world's total energy production from this category to 94%. The present asymmetries in the appropriation of nonrenewable wellsprings of vitality is unsustainable, meaning we can assume with complete assurance that with the status quo of energy production, exploitation of nonrenewable resources will consist in the progressive exhaustion of an initially fixed supply in which there will be no significant additions. At the point when will non-renewable be depleted? This is an exceptional inquiry encompassed by various territories of open deliberation. In 1956, M. King Hubbert explored this concept by realizing that there will be a point in time when the maximum rate of fossil fuel extraction will be reached and subsequently the rate of extraction enters a terminal decrease until the limited asset is totally depleted. The point in time when this most extreme rate is come to simply before the terminal decrease is called \peak". He was the first to offer ascent to the term crest and create extrapolating models anticipating top, utilizing his models to precisely focus top for U.S. oil creation would happen between years of 1965 and 1970 [12]. Further bothering the misuse of nonrenewable assets is the way that vitality interest is expanding. By 2035, the world's vitality utilization is anticipated to be 738.7 quadrillion BTU [11] or an increment of 49% from 2007. The essential thought of a sunlight based cell is to change over light vitality into electrical vitality. The vitality of light is transmitted by photons, little parcels or quantum of light. Electrical vitality is put away in electromagnetic fields, which thusly can make a current of electrons stream. In this manner a sun oriented cell changes over light, a stream of photons, to electric current, a stream of electrons. At the point when photons are consumed by matter in the sun based cell, their vitality energizes electrons higher vitality states where the electrons can move all the more openly. The measure of sun powered irradiance that hits the earth every year is pretty nearly 763,000 quadrillion Btu3 or more than 1000 times more vitality than what human vitality utilization is anticipated to be 2035. In the event that a modest part of vitality that earth gets could be changed over to helpful vitality, all our energy supply problems would be solved. So what is keeping us from tapping into this seemingly endless amount of energy that falls on the earth every day to solve the scarcity, environmental, and economic problems associated with non-renewable? The two main market penetration barriers of solar conversion devices include the current condition of innovation and financial aspects, both entwined.

1.1 World energy market

Most wellsprings of vitality on Earth begin from the Sun, the most dominant in today's world energy market being the burning of fossil fuels. At the present rate of utilization it is evaluated world supplies of oil will just last give or take an additional 30 years and coal supplies enduring an additional 250 years [13]. The urgency to find an efficient alternative energy source is compounded by the impact of a dangerous atmospheric devation anticipated to result in calamitous outcomes including rising ocean levels and expanded recurrence of amazing climate occasions.

1.2The standard solar cell

The solar cell converts sunlight into electric power, and thus understanding the radiation from the sun is therefore important for simulating the efficiency of a solar cell. A standard solar cell is shown schematically in figure 1.1. At the front surface there is a metallic grid (gray). Between the grid lines there is an anti-reflective layer (dark blue) covering a p-n junction (green/blue) made of a single semiconductor. The back surface of the cell is covered by a back contact (dark gray). Also shown is the external circuit where the electrons do work. The operation principle is described in the text. Sunlight is incident on the surface covered by a metallic grid acting as an electrical contact. Between the grid lines photons are absorbed in a semiconductor which is covered by an anti-reflective coating to reduce reflection. Photons with energies larger than the band gap E_G of the semiconductor excite electrons from the valence band to the conduction band, resulting in free charge carriers; electrons and holes. The charge carriers are separated by either a gradient in the charge carrier density or an electric field.

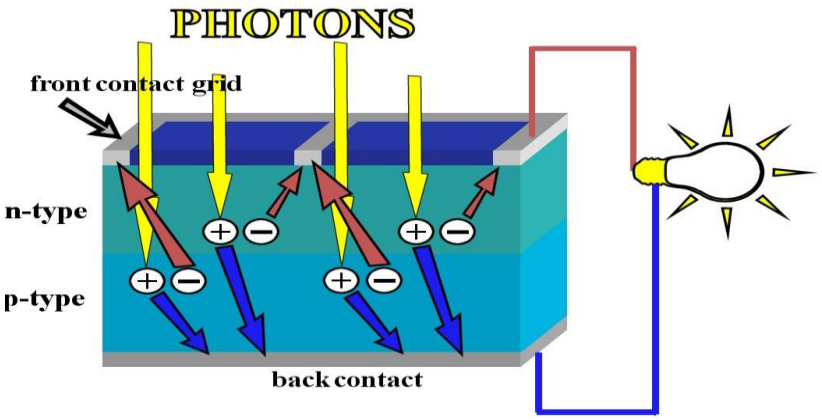

Figure 1.1: Structure of a standard solar cell shown schematically [**2**].

II. Intermediate band solar cells

Luque et al initially displayed the idea of expanding the productivity of sun based cells by photon incited moves at middle of the road levels in 1997 [1]. The intermediate band solar cell (IBSC) has the capability of accomplishing 63.1% productivity under most extreme concentrated daylight. This efficiency was calculated as occurring when the energy gap between the valence band and the conduction band was roughly 1.93 eV and when either the energy gap between the valence band and intermediate band or the conduction band and intermediate band was more or less 0.70 eV.The optimum efficiency of the IBSC relies on a material with three bands: a valence band (VB), an intermediate band (IB) and a conduction band. In addition, in order to achieve high efficiency, the Fermi level of the material must be located within the intermediate band (see figure 2.1).

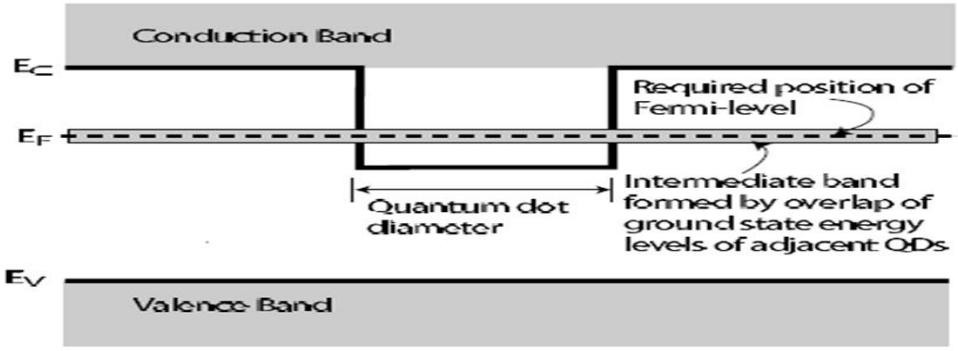

Figure 2.1: Band diagram of a quantum dot intermediate band solar cell.

Under these conditions there will exist both a supply of electrons fit for photon impelled move to the conduction band and in addition an expansive population of gaps that permit electrons to move from the valence band to the intermediate band. In respect to a material with two groups whose gap is equal in value to the widest band gap of the intermediate band solar, E_C-E_V in figure 2.1, the intermediate band solar cell will show an increase in photocurrent. Photon absorbtion is changed over into photocurrent that is extracted at a voltage restricted by the amplest band gap of the material, E_C-E_V in figure 2.1.

2.1 Generation and recombination

This area is taking into account [5]. The formation of free charge carrier in a semiconductor requires energy and is called generation. Recombination is the opposite occasion and discharges energy. In solar cells the most imperative generation procedure is absorbtion of photons. Diverse recombination procedures are demonstrated in figure 2.2. The procedures indicated are radiative recombination, non radiative recombination by means of trap states and non-radiative Twist drill recombination. All in all, every generation procedure is given its own particular generation rate G per unit time and unit volume. The recombination procedures have distinctive recombination rates, signified U. The rates will as a rule take distinctive qualities for electrons and holes. In warm harmony the recombination and generation rates are parallel.

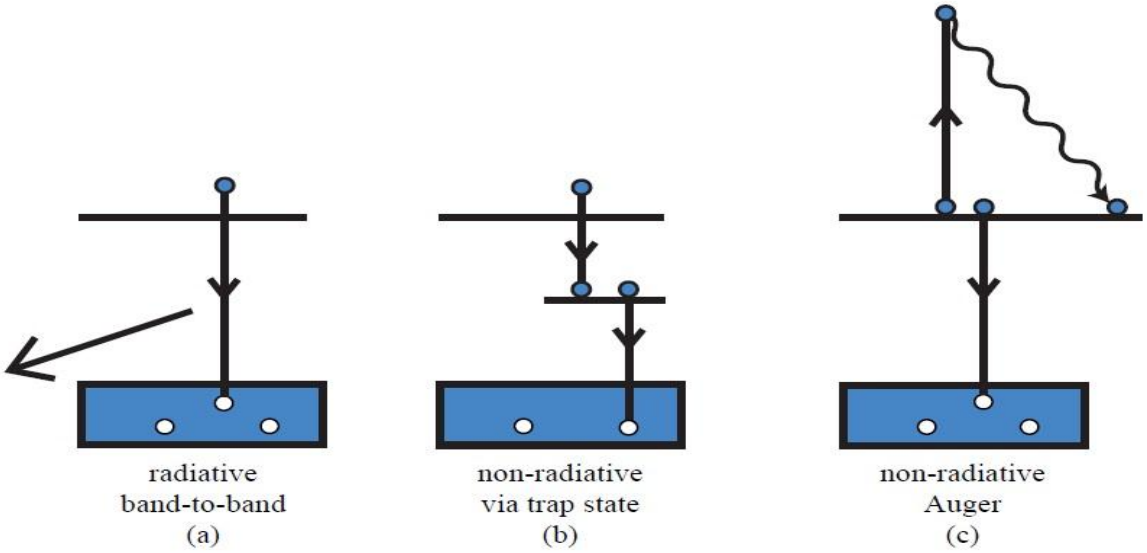

Figure 2.2: Recombination processes: (a) radiative, (b) non-radiative via trap states and (c) non-radiative Auger recombination.

Since it is the disturbance from thermal equilibrium which is important, the excess (over the thermal) generation and recombination rates are used.The only generation process considered in this thesis is absorption of photons from sunlight. When the photon energy is larger than the band gap of the semiconductor, an electron-hole pair may be generated. The recombination processes can be divided into unavoidable and avoidable processes. Unavoidable processes cannot be avoided through the use of perfect materials. They are identified with physical procedures in the material. Both radiative recombination and Auger recombination fall into this class. The third process emerges on the grounds that materials are not immaculate and dependably contain a few defects. Recombination may happen by means of imperfection states in the taboo crevice, starting now and into the foreseeable future alluded to as trap states taking after the terminology in [5], and the procedure is known as non- radiative. The era of charge bearers because of photon reusing is excluded in the model. Photon reusing is the procedure where photons produced by radiative recombination are reabsorbed in the material to create charge bearers. This procedure is discarded in the model of the reference cell and is additionally excluded here. In the constraining case the main recombination procedure included is radiative recombination.By having an intermediate band three radiative recombination processes are possible:

1) Recombination between the conduction band and the valence band
2) Recombination between the conduction band and the intermediate band
3) Recombination between the intermediate band and the valence band

2.2Current and voltage equation for a solar cell

The general current-voltage characteristic for a solar cell under illumination is given as

$$J = J_{light} - J_0\left(e^{\frac{qV}{k_BT}} - 1\right) - J_{dep,0}J_0\left(e^{\frac{qV}{2k_BT}} - 1\right) \quad \ldots\ldots(2.1)$$

From this equation the solar cell can be modeled as a circuit consisting of an ideal current source with current density J_{light} and two diodes in parallel with ideality factors equal to 1 and 2 as can been seen in figure 2.3.

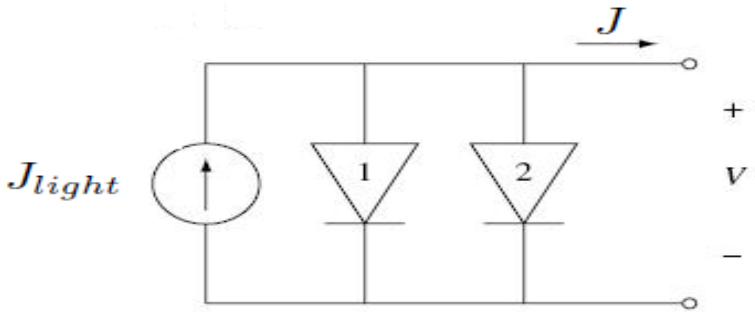

Figure 2.3: Modeling the solar cell as an circuit consisting of an ideal current source and twodiodes in parallel with ideality factor 1 and 2 [**3**].

Equation (2.1) can be rewritten by introducing the diode ideality factor A_0

$$J = J_{light} - J_{dark}\left(e^{\frac{qV}{A_0k_BT}} - 1\right) \quad \ldots\ldots(2.2)$$

A_0 has a value between 1 and 2 and varies with voltage and material quality. When non-radiative recombination in the depletion region dominates A_0 has a value approximately equal to 2, while when the recombination in the depletion region is not as important as the recombination in the p- and n-layers, A_0 has a value of 1.Often only the diode in figure 2.3 with ideality factor equal to 1 is considered; meaning that recombination in the depletion region is not included. This gives the current-voltage behavior shown in figure 2.4. There three important points are identified, that is the short-circuit current density J_{sc}, the open circuit voltage V_{oc} and the current density J_m and voltage V_m that gives the maximum power density Pm = J_mV_m. The short-circuit current density can be found by setting V equal to 0 in equation (2.2) and is equal to the photocurrent density J_{light}. The open circuit voltage can be found by setting J equal to 0 in equation (2.2) and is equal

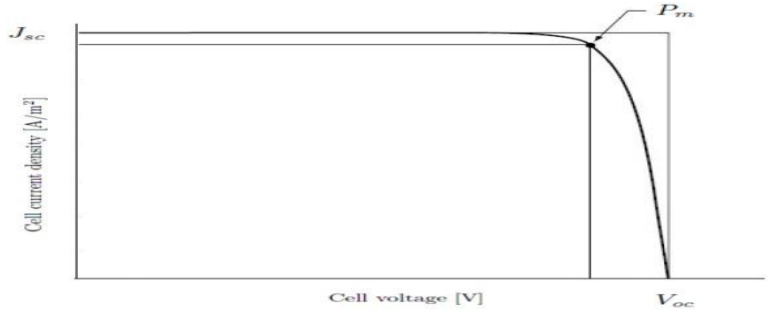

Figure 2.4: Current-voltage behavior for a solar cell showing the short-circuit current density J_{sc}, the open circuit voltage V_{oc} and the current density J_m and voltage V_m that gives the maximumpower density Pm = J_mV_m.

$$V_{oc} = \frac{A_0k_BT}{q}\ln\left(\frac{J_{light}}{J_{dark}} + 1\right) \quad \ldots\ldots(2.3)$$

The open circuit voltage differs subject to the recombination in the solar cell which are again reliant on the band gap of the semiconductor. The open circuit voltage is relied upon to change directly with the band hole of the semiconductor [4].

To obtain efficient solar cells, the main subject is to maximize the power. The ratio of maximum power density to the product of J_{sc} and V_{oc} is given the name fill factor, FF

$$FF = \frac{P_m}{V_{oc}J_{sc}} \quad \ldots\ldots(2.4)$$

The fill factor is always less than one and describes the squareness of the JV-curve. The most important term describing solar cells is the conversion efficiency, η, given as

$$\eta = \frac{P_m}{P_{in}} \quad \ldots\ldots (2.5)$$

where P_{in} is the incident power density, a quantity determined by the incident light.

III. Working principle for the intermediate band solar cell

The intermediate band solar cell uses a greater amount of the approaching photons from the sun through the utilization of the intermediate band. Notwithstanding the conduction band (CB) and the valence band (VB) the intermediate band solar cell contains a intermediate band (IB) put in the band gap between the conduction and valence band. As seen in figure 3.1 the band gap of the semiconductor E_G is isolated into two sub-band gap E_L and E_H. $E_H \equiv E_I - E_V$ is the difference between the balance Fermi energy of the intermediate band and the highest point of the valence band. $E_L \equiv E_C - E_I$ is the energy difference between the base of the conduction band and the balance Fermi energy of the intermediate band, and we have that $E_G = E_H + E_L$.The width of the intermediate band is assumed to be negligible. The conduction band, valence band and intermediate band are shown along with the equilibrium Fermi energy of the intermediate band. By absorbing photons three transitions are possible.

(1) an electron is transferred from the conduction band to the intermediate band.
(2) an electron is transferred from the intermediate band to the conduction band.
(3) an electron is transferred from the valence band to the conduction band. The symbols are explained in the text.

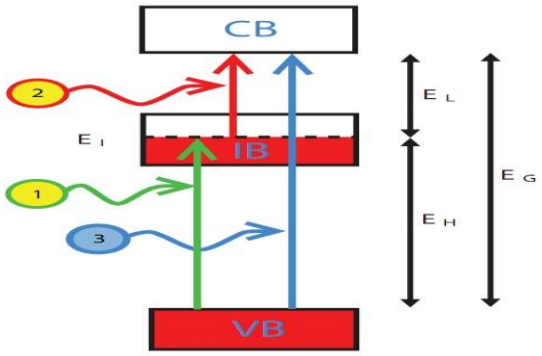

Figure 3.1: Band diagram of a material containing an intermediate band

The division of the aggregate band gap into two sub-band gaps makes retention of photons with energies not exactly the aggregate band gap conceivable, prompting an expanded photocurrent. To create an electron-hole pair by absorption of photons with energies less than E_G, two transitions are necessary. In one of the transitions an electron is transferred from the valence band to the intermediate band leaving a hole behind in the valence band, visualized as transition (1) in figure 3.1. In the second transition the electron is transferred from the intermediate band to the conduction band, visualized as transition (2) in figure 3.1. In addition we have the ”normal” creation of an electron-hole pair by absorption of a photon and the direct transfer of an electron from the valence band to the conduction band, visualized as transition (3) in figure 3.1.The intermediate band has to be partially filled with electrons to make both transition (1) and (2) possible. A partially filled band contains both void states to oblige electrons being exchanged from the valence band to the transitional band and filled states to discharge electrons being pumped into the conduction band. The Fermi energy of the intermediate band has to be placed within the intermediate band to fulfill this condition.

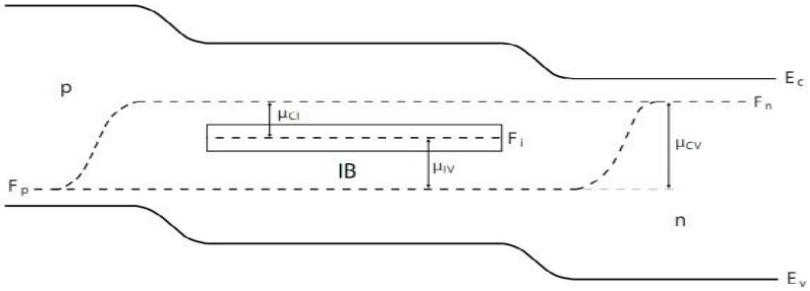

Figure 3.2: Quasi-Fermi levels and quasi-Fermi level splits in an intermediate band material placed between a p- and a n-layer. The symbols are explained in the text.

To get a high efficiency solar cell the photocurrent, as well as the voltage of the cell must be upgraded. A crucial condition in the hypothesis of intermediate band solar cells is that transporter focus in each of the groups can be depicted by its own particular semi Fermi level; F_p for holes in the valence band, F_i for electrons in the intermediate band and F_c for electrons in the conduction band, as shown in figure 3.2. This condition is fulfilled when the carrier relaxation time within each band is much shorter than the carrier recombination time between bands [**6**]. The quasi-Fermi level in the intermediate band is assumed to be fixed to its equilibrium position. No charge bearers are transported through the intermediate band, which is detached from the outside contacts by a p- and a n-layer put on every side of the moderate band material. The p-layer fixes the semi Fermi level for openings in the valence band in the middle of the road band material, while the n-layer fixes the semi Fermi level for electrons in the conduction band in the intermediate band material The voltage V of the cell is given by [**7**]

$qV = F_n - F_p$ ……..……..(3.1)

which has the same form as in a standard p-n solar cell. The voltage of the cell is thus unaffected by the intermediate band. The increase of the photocurrent in the intermediate band solar cell gives a higher efficiency.

3.1 Intermediate band solar cell design

The p- and n-layers in the intermediate band solar cell studied over in this proposition are in figure 3.3 indicated together with the area in the middle of where the intermediate band layer is put. The upper p-layer is trailed by an intrinsic layer of width wip,min. wip,min is the base width of the consumption locale between the p-layer and the intrinsic layer by setting Vp equivalent to a voltage Vmax,p equivalent to the open-circuit voltage over the p-i intersection. This intrinsic layer is incorporated since we need the majority of the intermediate band layer to be contained in a flat band region. For all voltages the width wip,min close to the p-layer is depleted, and it is then not necessary to have an intermediate band layer here.

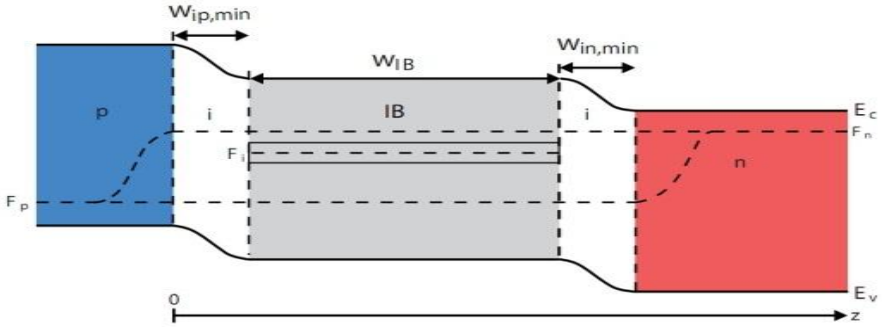

Figure 3.3: The structure of the forward biased intermediate band solar cell used in the modeling. Also shown are the quasi-Fermi level Fc of the electrons in the conduction band, the quasi-Fermi level Fi of the electrons in the intermediate band and the quasi-Fermi level Fp of the holes in the valence band.

After the intrinsic layer of width wip,min takes after a intermediate band material of width wIB, and we then have a second intrinsic layer of width win,min. win,min is the base width of the consumption locale between the n-layer and the i-layer by setting Vn equivalent to a voltage Vmax,n equivalent to the open-circuit voltage over the i-n intersection. At last the n-layer is set beneath the intrinsic material. The widths of the exhausted districts of the p-i and i-n intersection, wip and win, are subject to voltage. At the point when the thicknesses of the i-layers are equivalent to wip,min and win,min the i-layers on the p- and n-side are exhausted at all voltages. The piece of the intermediate band material contained in the drained districts close to the p-layer and the n-layer is in the models accepted to act like an intrinsic material with no quantum dots subsequent to the quantum dots in these areas are totally full or unfilled of electrons. Just the piece of the intermediate band material that is in the flat band district is taken to take after the conduct of a middle of the intermediate band material.

IV. Mathematical model of intermediate band solar cell

Intermediate band solar cell to analyses the current voltage characteristic the general equation under the illumination is given below:

$$I = J_{light} - J_{dark}\left(e^{\frac{qV}{A_0 k_B T}} - 1\right) \quad \text{……(4.1)}$$

Where A_0 is the ideality factor has a value between 1 and 2 and varies with voltage and material quality. k_B is the Boltzman constant J/K. T is the temperature used in article for solar cells in K. q is the charge of an electron in C. J_{light} is the light current density and J_{dark} is the dark current density. This equation used to analyses the current voltage relationship.

4.1 Relation between band density and concentration factor

Solar cells oblige some type of implicit asymmetry that will permit helpful energy to be separated before electrons and openings recombine. The dominant part of solar cells comprise of a p-n or p-i-n intersection to permit high carrier mobility and current to only flow in one direction. It shought to be noticed the partition of semi Fermi levels stays consistent all through the gadget expecting unending portability; truly this is a sensible rough guess for good quality solar cells. At the point when there is a sudden move from p-sort doping to n-sort doping the electrons and openings will diffuse to frame an area of lower electron and opening fixation known as the consumption district.The density state of conduction band is given by

$$N_c = 2\left(\frac{2\pi m_e k_B T}{h^2}\right)^{\frac{3}{2}} \dots\dots (4.2)$$

$$m_e = (0.0632 + 0.0856x + 0.023x^2)m_0 \dots\dots (4.3)$$

and

$$m_h = (0.50 + 0.2x)m_0 \dots\dots (4.4)$$

where k_B is Boltzmann's constant, T is the temperature of the cell, e is the charge of an electron, N_c is the density of states in the conduction, m_0 is the mass of electron, m_e and m_h are the are the effective electron and hole masses respectively and x is the concentration factor.

4.2 Relation betweenvoltage and concentration factor

The solar cell absorbs sunlight only from a small angular range, and this can be increased by using concentrators based on lenses or mirrors. Light is thus collected over a large area and focused to a solar cell of a smaller area. By using a ratio X between the collector and cell area the incident flux density is increased by a concentration factor equal to X. The photocurrent is directly proportional to the photon flux F. The photocurrent is thus increased by a factor X, and the open-circuit voltage increases logarithmically to

$$V_{oc}(X) = \frac{A_0 k_B T}{q} \ln\left(\frac{X J_{light}}{J_{dark}} + 1\right) \dots\dots (4.5)$$

By assuming a constant fill factor the efficiency η(X) is increased by a factor equal to

$$\frac{\eta(X)}{\eta(1)} = 1 + \frac{A_0 k_B T}{q V_{oc}(1)} \ln X \dots\dots (4.6)$$

where η(1) and $V_{oc}(1)$ are the efficiency and open-circuit voltage using no concentration, respectively. Concentration also increases the series resistance of the cell giving an increased voltage loss, and the temperature is raised leading to an increased dark-current. Both these effects lowers the open-circuit voltage and degrade the performance of the cell. Concentration may also give high injection conditions. This means that the photo generated carrier densities are comparable to the doping densities in the doped layers. The radiative and Auger recombination rates then become non-linear with the carrier densities n and p, meaning that the total current cannot be divided into an independent dark-current and a photocurrent. The concentration thus has an optimum value obtaining the highest efficiency for a solar cell.

4.3 Solar spectrum

The solar spectrum resembles as mentioned the spectrum of a black body with temperature 5760 K, and this spectrum is shown in figure 6.1. The emitted light is distributed over wavelengths from the ultraviolet to the visible and infrared part of the spectrum. Light is absorbed and scattered as it passes through the atmosphere. The attenuation of the light is quantized using the Air Mass. The Air Mass is the ratio between the optical length from the earth to the sun when the sun is placed at an angle γ_s and when the sun is placed directly overhead [5]

$$AM = \frac{1}{\cos\gamma_s} \dots\dots (4.7)$$

The power density from the Sun just outside the Earth's atmosphere is given by the solar constant 1353 ±21Wm^{-2}[**3**], dropping to approximately 1000Wm^{-2}on average at the Earth's surface attenuated by absorption in the atmosphere. Figure 6.1 compares the extraterrestrial solar spectrum, Air Mass 0 (AM0) to the standard terrestrial AM1.5 spectrum. The standard for solar cell efficiency measurements is the AM1.5 spectrum with an energy density of 1000W/m^2. The extraterrestrial solar spectrum can be closely modeled as a 6000K blackbody spectrum with the generalized Planck equation

$$n(E,T,\mu) = \epsilon(E)\frac{2\pi}{c^2h^3}\frac{E^2}{e^{\frac{E-\mu}{k_BT}}-1} \dots\dots (4.8)$$

where n is the photon flux as a function of energy E, ϵ is the emissivity, μ is the photon chemical potential and T is the temperature. For a blackbody, $\epsilon = 1$ for all energies and $\mu = 0$. The total density from the sun can be

obtained by multiplying the photon flux by the photon energy, E, and integrating over all energies to obtain the Stefan-Boltzmann law.

$$\int_0^\infty En(E,T)\,dE = \sigma T^4 \quad \text{……} \quad (4.9)$$

Where T = T_{sun} = 6000K equation 4.8 describes the photon flux at the surface of the sun and equation 4.9 describes the energy density at the surface of the sun. On Earth we receive sunlight from the solar disc subtending only a fraction of the hemisphere visible to the solar cell thus a dilution factor of $f_\omega = 2.16\times10^{-5}$ must be included to calculate the photon flux and energy density on Earth

4.4 Intermediate band solar cell with only radiative recombination in the flat band region

The electron and hole concentrations in the conduction band and valence band are influenced by the presence of an intermediate band. The electron concentration in the conduction band in an intermediate band material equals $n = \Delta n + n_{0,IB}$, where $n_{0,IB}$is the equilibrium electron concentration in the conduction band and Δn is the optically generated electron concentration. n can be expressed as

$$n = N_C e^{-\left[\frac{(E_C - F_i)}{k_B T}\right]} e^{\frac{(F_n - F_i)}{k_B T}}$$
$$= n_{0,IB} e^{\mu CI/k_B T} \quad \text{……} \quad (4.10)$$

where the last equality only holds if the quasi-Fermi level F_i of the intermediate band is pinned to its equilibrium position E_I [**8**]. N_C is the effective density of states in the conduction band and

$$n_{0,IB} = N_C e^{-\frac{E_L}{k_B T}} \quad \text{……} \quad (4.11)$$

In the same way the hole concentration in the valence band in an intermediate band material equals $p = \Delta p + p_{0,IB}$, where $p_{0,IB}$ is the equilibrium hole concentration in the valence band and Δp is the optically generated hole concentration. p can be expressed as

$$p = N_V e^{-\left[\frac{(F_i - E_V)}{k_B T}\right]} e^{\frac{(F_i - F_p)}{k_B T}}$$
$$= p_{0,IB} e^{-\frac{E_H}{k_B T}}, \quad \text{……} \quad (4.12)$$

where N_V is the effective density of states in the valence band and

$$p_{0,IB} = N_V e^{-\frac{E_H}{k_B T}}, \quad \text{……} \quad (4.13)$$

4.5 Intermediate band solar cell including both radiative and non-radiative recombination in the flat band region

In the limiting case only radiative recombination is included in the intermediate band material. Non-radiative recombination is present unless in the limit of perfect materials [**5**], and it has to be included in a more realistic model. Data for quantum dot solar cell prototypes grown by molecular beam epitaxy indicates that recombination is dominated by non-radiative processes possibly caused by defects at the interfaces between the dot and barrier material [**9**]. In this section non-radiative recombination is included in the model of the intermediate band solar cell.

The non-radiative recombination processes present in an intermediate band material are:

1) Non-radiative recombination between the conduction band and the valence band
2) Non-radiative recombination between the conduction band and the intermediate band
3) Non-radiative recombination between the intermediate band and the valence band

4.6 Material and sample parameters

As is clear from the preceding chapters several material parameters are involved in the expressions determining the current-voltage characteristic of a solar cell. To obtain the current voltage characteristic for specific solar cell numerical values for all these parameters must be known. The numerical values can either be measured for the solar cell in question or data has to be taken from literature. In this thesis data from literature is used, and material parameters are given. The solar cells considered in this thesis are made of InAs, GaAs and AlxGa1−xAs. The thicknesses and doping concentrations for the intermediate band solar cell made of InAs quantum dots in $Al_{0.35}Ga_{0.65}As$ are given in table 4.2. The mobility and lifetimes in $Al_{0.35}Ga_{0.65}As$ for these doping concentrations are given in table 4.2.

Doping (cm^{-3})	μ_p (cm^2/Vs)	μ_n(cm^2/Vs)	Γ_p(ns)	Γ_n(ns)
2×10^{19} (p^+)	-	1325	-	0.6
2×10^{18} (p)	-	1245	-	2.99
1×10^{14} (i)	378	8005	$\sqrt{7}\sqrt{7}$	
2×10^{17} (n)	245	-	33	-
2×10^{18} (n^+)	255	-	7.5	-

Table 4.1: Values of mobility and lifetimes in GaAs.

Doping (cm^{-3})	μ_p (cm^2/Vs)	μ_n(cm^2/Vs)	Γ_p(ns)	Γ_n(ns)
2×10^{19}(p+)	-	822	-	0.41
2×10^{18}(p)	-	1000	-	2.32
2×10^{17}(n)	102	-	3.2	-
2×10^{18} (n+)	64	-	0.8	-

Table 4.2 Values of mobility and lifetimes in Al0.35Ga0.65As

V. Efficiency of intermediate band solar cell

The third generation solar cells use different procedures to build the efficiency past the itemized equalization farthest point of 30.5 % for a single band gap material. The approaches to acquire efficiencies past this utmost are clarified in segment 5.1. The primary accentuation of this section is the intermediate band solar cell. General hypothesis concerning intermediate band solar cells is given in segment 5.2. Solar cell productivity is the proportion of the electrical yield of a solar cell to the episode vitality as daylight. The vitality change productivity (η) of a solar cell is the rate of the sun oriented vitality to which the cell is uncovered that is changed over into electrical vitality. This is computed by isolating a cell's energy yield (in watts) at its greatest force point (Pm) by the data light (E, in W/m2) and the surface territory of the solar cell (Ac in m2). The most imperative results from the hypothetical studies is that the partial filling of the intermediate band can be accomplished through photograph filling. For high light introduction the productivity is comparative for a photograph filled and prefilled (e.g. because of doping) IB sun oriented cell. The hypothetical examinations have likewise included advancement of a float dispersion model for photograph filled IB sunlight based cells, investigations of how thermalization of the populace in the IB influences the cell execution for a limited IB width lastly, how the IB sun powered cell can perform better if frightfully particular channels are being used.

5.1 Strategies to increase the efficiency

This segment is taking into account [3]. As said the restricting efficiency of a single band gap solar cell is 30.5 % by utilizing the guideline of itemized parity. The two most critical explanations behind this preferably low efficiency are that photons with vitality lower than the band hole of the semiconductor are not retained and that transporters created with E > EG lose active vitality by warm dissemination. Solar cell materials with more than one bandgap offer the likelihood to build the productivity of the solar cell past that of a single bandgap cell. The intermediate band solar cell (IBSC) is one such probability, where a intermediate band(IB) is set in the generally illegal bandgap of the solar cell material. Research on this gadget is spurred by high hypothetical efficiencies. The most extreme proficiency of an IBSC, having the perfect bandgaps of EL=0.71 eV, EH=1.24 eV and EG=1.97 eV, is as high as 63.2 %.The single bandgap cell has a productivity farthest point of 40.7%.
Theoretical efficiency limits for the intermediate band solar cell have been calculated under the assumption that the absorptivity of the solar cell is 1 for all photon energies larger than the smallest subband gap. In the present work, efficiency limits have been calculated under the assumption that the cell is covered by spectrally selective reflectors. The efficiency limit for the 1 sun 6000 K black body spectrum is found to increase from 46.8% to 48.5% and the limit for the AM1.5G spectrum (as defined by ASTM G173–03) is found to increase from 49.4% to 52.0%.
The conditions for cell estimation are institutionalized for examination purposes yet may not reflect genuine working conditions. Standard cell test conditions are 1000 Wm-2, 33°C. Concentrator cells are measured utilizing the immediate pillar AM1.5 range while other physical cells utilize the worldwide AM1.5 range that additionally incorporates diffuse light. All the cells are tried on a temperature controlled piece and warming impacts are overlooked. In genuine establishments the cell temperature rises prompting a proficiency reduction.The transitional band sun powered cell has the capability of accomplishing 63.1% productivity under greatest concentrated daylight. This proficiency depends upon a material with three groups: a valence band, and intermediate metallic band and a conduction band. With a specific end goal to accomplish high efficiencies, the Fermi level of the intermediate band must be well inside of the moderate band. The restricting efficiency

utilizing no focus is 46.0% for the band holes EL = 0.93 eV and EH = 1.40 eV [8]. Utilizing most extreme focus the constraining efficiency is 63.2% for the band crevices EL = 0.71 eV and EH = 1.24 eV

VI. Simulation and result

In this chapter results from the intermediate band solar cell is given. In my modeling the normalized Air Mass 1.5 spectrum is used giving an incident power density of 1000 W/m2. Tabulated measured data for the Air Mass 1.5 are taken from [**10**].

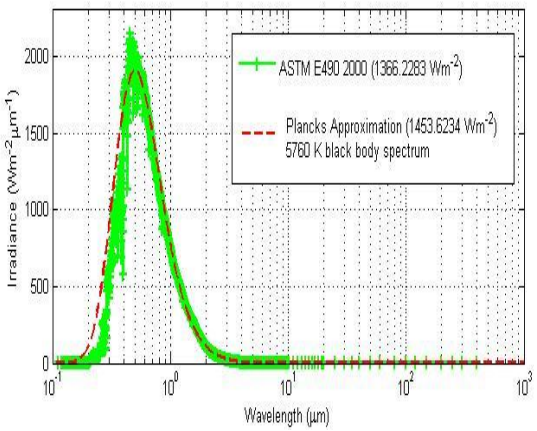

Figure 6.1: AM1.5 Solar Irradiance Vs Wavelength 0-1000 \μm

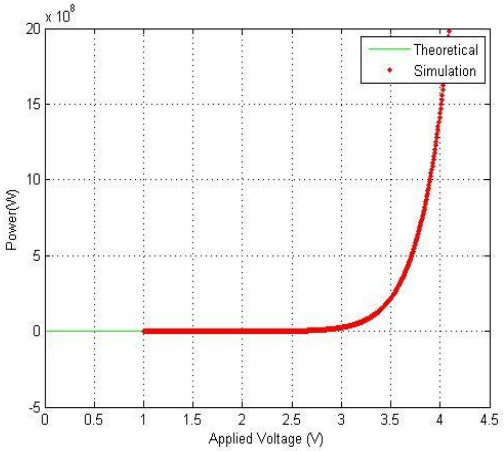

Figure 6.2: Power Curve at T=303K

The intermediate band solar cell two models are used, a simple model with only few layers included and a complete model with anti-reflective coating, window and front back surface field layers included. Power is increasing when photon energy is higher which is level in figure 6.2 and current is increasing in the same way which shown in figure 6.3.

When a load is connected to the solar cell, the current decreases and a voltage develops as charge builds up at the terminals. The resulting current can be viewed as a superposition of the short circuit current, caused by the absorption of photons, and a dark current, which is caused by the potential built up over the load and flows in the opposite direction. As a solar cell contains a PN junction (LINK), just as a diode, it may be treated as a diode. By increasing the lifetimes, the change in the current voltage curve is not seen, while decreasing the lifetime by factor 10^3 the change in the current voltage curve is clearly visible. The reason for this is the same as mentioned for the quantum efficiencies, when the diffusion lengths are much longer than the widths of the p- and n- layer they do not affect the dark-current much.

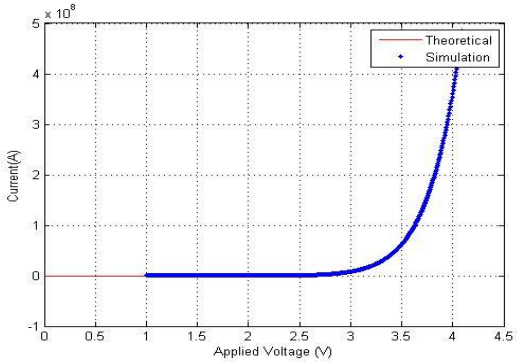

Figure 6.3: Light I-V Curve at T=303K

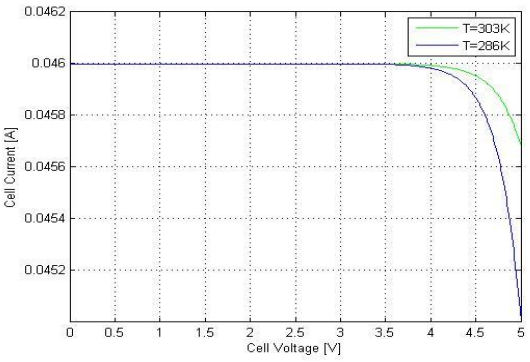

Figure 6.4: Current Voltage characteristic curve at T=303K and T=286K

The productivity and the photocurrent and voltage are extricated from the sunlight based cell. Effectiveness is the measure of what number of photons are changed over into recoverable electrons by the consolidated impact of the cell voltage and the photocurrent and the resistances and so on measured into the fill element. The productivity measure shought not change that much with irradiance aside from on account of warming the cell excessively. Then again, the photocurrent will change as much as less or more photons strike the cell and the voltage will change if the cell is warmed. At low light levels the dim current or the current from the parallel shunt resistance overwhelms the fill element. The level area in the effectiveness versus fixation is the place the fill element is diminishing with expanding light on the grounds that it is constrained by arrangement resistance and the voltage is as yet expanding logarithmically with light.

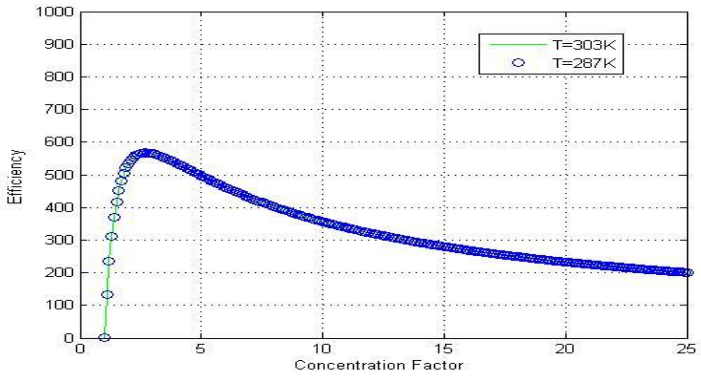

Figure 6.5: Efficiency Vs Concentration Factor at T=303K and T=287K

The conduction band measures the scope of vitality needed to free an electron from its bond to a particle. Once liberated from this security, the electron turns into a 'delocalized electron', moving openly inside of the nuclear grid of the material to which the particle has a place. Different materials may be grouped by their band gap: this is characterized as the contrast between the valence and conduction bands. In protectors, the conduction band is much higher in vitality than the valence band and it takes substantial energies to delocalize their valence electrons. Protecting materials have wide band holes. In semiconductors, the band gap is little. This clarifies why it takes a little vitality (as warmth or light) to make semiconductors' electrons delocalize and conduct power, subsequently the name, semiconductor. In metals, the Fermi level is inside no less than one band. These Fermi-level-intersection bands may be called conduction band, valence band, or something else relying upon condition.

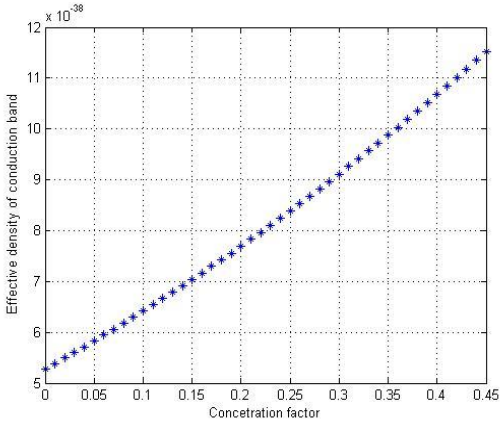

Figure 6.6: Conduction band density Vs Concentration factor at T=303K

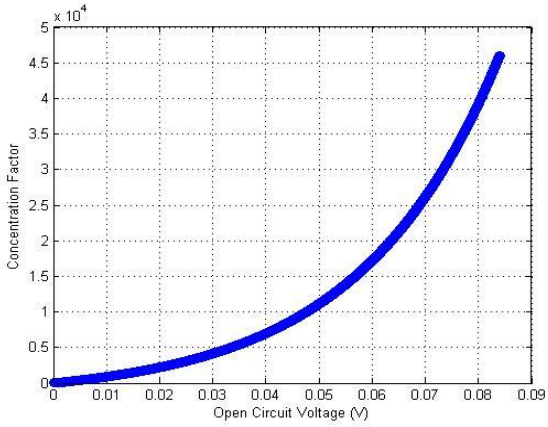

Figure 6.7: Concentration factor Vs Open circuit voltage

VII. Further work

This proposition is in light of a systematic methodology. One errand is to utilize numerical strategies to model a reference cell and a intermediate band solar cell taking into account the comparisons introduced in this theory. By utilizing numerical strategies radiative recombination can be incorporated in the i-layer in the p-i-n solar cell. The current-voltage characteristic under high-infusion may be inferred utilizing numerical techniques. Another assignment is to keep on utilizing the expository approach and develop the models given in this theory. The model of the reference cell can be further stretched out to incorporate band hole narrowing in the intensely doped layers. AlxGa1−xAs solar cells with other aluminum focuses than x=0.35 can be demonstrated to find the greatest efficiency for different estimations of the band gap EG. To get a solar cell with the most elevated efficiency, the thickness and doping centralization of the considerable number of layers in the reference cell may be fluctuated. An estimation of the arrangement and shunt resistances in the solar cells may be done and included in the model. The complete model of the intermediate band solar cell may be stretched out to model the intermediate band material put in the drained districts another way then regarding it as a characteristic material. A more practical instance of covering assimilation coefficients might likewise be incorporated in the model. How the estimations of the assimilation coefficients affect the present voltage trademark may.

VII. Conclusion

In this expert proposition intermediate band solar cells and suitable reference cells have been demonstrated for two unique estimations of fixation, X=1 and X=1000. The displaying of the reference cells demonstrates the significance of utilizing a window layer and intensely doped p+- and n+-layers to get a low successful surface recombination speed together with an against intelligent covering minimizing the reflection misfortunes. By utilizing these layers a high quantum productivity is gotten. Because of the non-presence of a model of a p-i-n solar cell with parts of the intrinsic material put in a level band region, a model of such a solar cell was produced. A comparative model with a intermediate band material put in the level band district was likewise created. A straightforward model of a intermediate band solar cell where just the intermediate band material is considered was taken from writing. Both radiative and non-radiative recombinations were incorporated in the flat band region of the intermediate band material in the models of the intermediate band solar cell. The force change proficiency of a intermediate band solar cell was anticipated to increment as the temperature of the cell was diminished because of a lessening in radiative and non-radiative recombination. A basic matlab model for ascertaining I-V bends and proficiency hypothetically anticipated how the effectiveness changed with temperature. By contrasting the outcomes from the demonstrating and trial information it is found that the model of the reference cell gives too high estimations of present and open-circuit voltage. The purpose behind this is relied upon to be the close estimation of disregarding band gap narrowing in the vigorously doped and layers and utilizing a reflectivity equivalent to zero when a hostile to reflective covering is available. Reenacting results uncovered that the effectiveness of our specimen GaAs intermediate band solar cell expanded reliably with diminishing temperature however errors in the middle of hypothesis and investigation were apparent.

Reference

[1] LUQUE, A. and MARTI, A., "Increasing the efficiency of ideal solar cell by photon-induced transitions at intermediate levels," Physical Review Letters, vol. 78, no. 26, pp. 5014-5017, 1997.

[2] Photovoltaic cells (solar cells), how they work. SPECMAT (Retrieved online on 2008-12 12). http://www.specmat.com/Overview$\%$20of$\%$20Solar$\%$20Cells.htm.

[3] J. L. Gray. The Physics of the Solar Cell. (John Wiley and Sons, Ltd, 2003).

[4] J. Nelson. Quantum-Well Structures for Photovoltaic Energy Conversion. (Thin Films, 21, 1995).

[5] J. Nelson. The Physics of Solar Cells. (Imperial College Press, 2007).

[6] A. Martí, C. R. Stanley, and A. Luque. Intermediate Band Solar Cells (IBSC) Using Nanotechnology, chapter 17 in Nanostructured Materials for Solar Energy Conversion. (Elsevier B. V., 2006).

[7] A. Martí, E. Antolín, E. Cánovas, N. López, P.G. Linares, A. Luque, C.R. Stanley, and C.D. Farmer. Elements of the design and analysis of quantum-dot intermediate band solar cells. Thin Solid Films 516, (2008) 6716.

[8] A. Luque and A. Martí. A Metallic Intermediate Band High Efficiency Solar Cell. Prog. Photovolt: Res. Appl. 9, (2001) 73.

[9] A. Luque, A. Martí, N. López, E. Antolín, E. Cánovas, C. Stanley, C. Farmer, and P. Díaz. Operation of the intermediate band solar cell under nonideal space charge region conditions and half filling of the intermediate band. J. Appl. Phys. 99, (2006) 094503-1.

[10] Reference solar spectral irradiance: Air mass 1.5. Renewabel Resource Data Center, National Renewable Energy Laboratory (Retrieved online on 2008-12-12). http://rredc.nrel.gov/solar/spectra/am1.5/.

[11] O_ce of Integrated Analysis and Forecasting. International energy outlook 2010. Technicalreport, U.S. Energy Information Administration, 2010.

[12] M. K. Hubbert. Nuclear energy and the fossil fuels. Drilling and Production Practice, 1956.

[13] Energy Information Administration. International Energy Annual. 2004.

Author's Biography

Md. Kamal Hossain received his B.Sc. degree in Telecommunication & Electronic Engineering from Hajee Mohammad Danesh Science & Technology University, Dinajpur, Bangladesh in 2015. His main working interest is based on software engineering, database optimization, discrete mathematics, Teletraffic Enginering, Digital Signal Processing and Networking. He likes cultural activities beside all other daily activities.

Md. Dulal Haque completed both B.Sc and M.Sc degree in Applied Physics and Electronic Engineering from Rajshahi University, Bangladesh. At present, He is serving as an assistant professor in the department of Telecommunication and Electronic Engineering at HajeeMohamadDanesh Science and Technology University, Bangladesh. His research interest is on electronic device fabrication and wireless communication.

Md. Arshad Ali Completed B.Sc in Computer Science and Engineering from Hajee Mohammad Danesh Science and Technology University, Bangladesh. He is serving as an assistant professor in the department of Computer Engineering at Hajee Mohammad Danesh Science and Technology University, Bangladesh. His research interest is Software development and Microwave.

American Journal of Engineering Research (AJER) 2015
American Journal of Engineering Research (AJER)
e-ISSN: 2320-0847 p-ISSN : 2320-0936
Volume-4, Issue-8, pp-157-162
www.ajer.org
Research Paper Open Access

Design & Simulation of Micro strip Patch Antenna at Nano Scale

Wahid palash, S. M. Ziyad Ahmed, Md. Hasibul Islam, Asaduzzaman Imon
[1](IICT, Bangladesh University of Engineering technology, Bangladesh)
[2](EEE, Bangladesh University of Engineering technology, Bangladesh)
[3, 4](EEE, American International University- Bangladesh, Bangladesh)

ABSTRACT: *Micro strip is a type of electrical transmission line which can be fabricated using printed circuit board technology, and is used to convey microwave-frequency signals. It consists of a conducting strip separated from a ground plane by a dielectric layer known as the substrate. Micro strip patch antennas are becoming increasingly useful because they can be printed directly onto a circuit board. Micro strip antennas are becoming very widespread within the mobile phone market. Patch antennas are low cost, have a low profile and are easily fabricated. Our objective is to design a micro strip patch antenna at Nano scale. Dielectric FR4 substrate was used in this design. The antenna has a band of operation from 1.5881 GHz to 1.7759 GHZ (187 MHz bandwidth) as a receive antenna, from 2.039GHz to 2.349 GHz (310 MHz bandwidth) as a transmit antenna, and a VSWR of 2:1 or lower.*

Keywords *–Micro strip, dielectric, lithographic, Bends, Feeding.*

I. INTRODUCTION

A microstrip patch antenna is a narrowband, wide-beam antenna fabricated by etching the antenna element pattern in metal trace bonded to an insulating dielectric substrate, such as a printed circuit board, with a continuous metal layer bonded to the opposite side of the substrate which forms a ground plane. Common microstrip antenna shapes are square, rectangular, circular and elliptical, but any continuous shape is possible. Some patch antennas do not use a dielectric substrate and instead are made of a metal patch mounted above a ground plane using dielectric spacers; the resulting structure is less rugged but has a wider bandwidth. Because such antennas have a very low profile, are mechanically rugged and can be shaped to conform to the curving skin of a vehicle, they are often mounted on the exterior of aircraft and spacecraft, or are incorporated into mobile radio communications devices [1]. A patchantenna (also known as a rectangular microstrip antenna) is a type of radio antenna with a low profile, which can be mounted on a flat surface. It consists of a flat rectangular sheet or "patch" of metal, mounted over a larger sheet of metal called a ground plane. The assembly is usually contained inside a plastic redone, which protects the antenna structure from damage. Patch antennas are simple to fabricate and easy to modify and customize. They are the original type of microstrip antenna described by Howell in 1972;the two metal sheets together form a resonant piece of microstrip transmission line with a length of approximately one-half wavelength of the radio waves. The radiation mechanism arises from discontinuities at each truncated edge of the microstrip transmission line. The radiation at the edges causes the antenna to act slightly larger electrically than its physical dimensions, so in order for the antenna to be resonant, a length of microstrip transmission line slightly shorter than one-half a wavelength at the frequency is used. A patch antenna is usually constructed on a dielectric substrate, using the same materials and lithography processes used to make printed circuit boards. Microstrip antennas are relatively inexpensive to manufacture and design because of the simple 2-dimensional physical geometry. They are usually employed at UHF and higher frequencies because the size of the antenna is directly tied to the wavelength at the resonant frequency. A single patch antenna provides a maximum directive gain of around 6-9 db. It is relatively easy to print an array of patches on a single (large) substrate using lithographic techniques. Patch arrays can provide much higher gains than a single patch at little additional cost; matching and phase adjustment can be performed with printed microstrip feed structures [2], again in the same operations that form the radiating patches. The ability to create high gain arrays in a low-profile antenna is one reason that patch arrays are common on airplanes and in other military applications. An advantage inherent to patch antennas is the ability to have polarization diversity.

Patch antennas can easily be designed to have vertical, horizontal, right hand circular or left hand circular polarizations, using multiple feed points, or a single feed point with asymmetric patch structures. This unique property allows patch antennas to be used in many types of communications links that may have varied requirements.

II. BENDS

In order to build a complete circuit in micro strip, it is often necessary for the path of a strip to turn through a large angle. An abrupt 90° bend in a micro strip will cause a significant portion of the signal on the strip to be reflected back towards its source, with only part of the signal transmitted on around the bend. One means of effecting a low-reflection bend, is to curve the path of the strip in an arc of radius at least 3 times the strip-width. However, a far more common technique, and one which consumes a smaller area of substrate, is to use a metered bend.

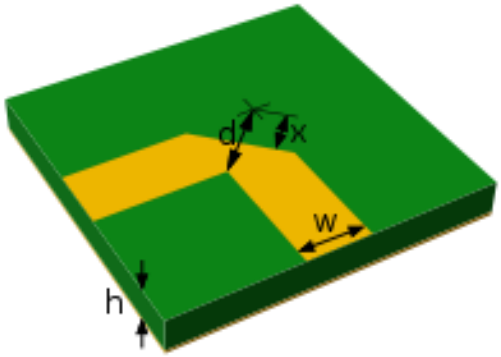

Figure 1: Micro strip 90° mitered bend.

To a first approximation, an abrupt un-miter bend behaves as a shunt capacitance placed between the ground plane and the bend in the strip. Mitering the bend reduces the area of metallization, and so removes the excess capacitance. The percentage miter is the cut-away fraction of the diagonal between the inner and outer corners of the un-miter bend. The optimum meter for a wide range of microstrip geometries has been determined experimentally by Douville and James. They find that a good fit for the optimum percentage miter is given by

$$M = 100\frac{x}{d}\% = (52 + 65e^{-\frac{27}{20}\frac{w}{h}})\%$$

Subject to $w/h \geq 0.25$ and with the substrate dielectric constant $\varepsilon_r \leq 25$. This formula is entirely independent of ε_r. The actual range of parameters for which Douville and James present evidence is $0.25 \leq w/h \leq 2.75$ and $2.5 \leq \varepsilon_r \leq 25$. Given by the formula at the minimum w/h of 0.25, the percentage miter is 98.4%, so that the strip is verynearly cut through.

III. FEEDING TECHNIQUE

Inset Feed

Previously, the patch antenna was fed at the end as shown here. Since this typically yields a high input impedance, we would like to modify the feed. Since the current is low at the ends of a half-wave patch and increases in magnitude toward the center, the input impedance (Z=V/I) could be reduced if the patch was fed closer to the center. Since the current has a sinusoidal distribution, moving in a distance R from the end will increase the current by cos(pi*R/L) - this is just noting that the wavelength is 2*L, and so the phase difference is 2*pi*R/(2*L) = pi*R/L. The voltage also decreases in magnitude by the same amount that the current increases. Hence, using Z=V/I, the input impedance scales as:

$$Z_{in}(R) = \cos^2\left(\frac{\pi R}{L}\right) Z_{in}(0)$$

In the above equation, Zin(0) is the input impedance if the patch was fed at the end. Hence, by feeding the patch antenna as shown, the input impedance can be decreased. As an example, if R=L/4, then cos(pi*R/L) = cos(pi/4), so that [cos(pi/4)]^2 = 1/2. Hence, a (1/8)-wavelength inset would decrease the input impedance by 50%. This method can be used to tune the input impedance to the desired value.

Fed with a Quarter-Wavelength Transmission Line

The microstrip antenna can also be matched to a transmission line of characteristic impedance Z0 by using a quarter-wavelength transmission line of characteristic impedance Z1.The goal is to match the input impedance (Zin) to the transmission line (Z0)[3]. If the impedance of the antenna is ZA, then the input impedance viewed from the beginning of the quarter-wavelength line becomes

$$Z_{in} = Z_0 = \frac{Z_1^2}{Z_A}$$

This input impedance Zin can be altered by selection of the Z1, so that Zin=Z0 and the antenna is impedance matched. The parameter Z1 can be altered by changing the width of the quarter-wavelength strip. The wider the strip is, the lower the characteristic impedance (Z0) is for that section of line.

Coaxial Cable or Probe Feed

Micro strip antennas can also be fed from underneath via a probe. The outer conductor of the coaxial cable is connected to the ground plane, and the center conductor is extended up to the patch antenna. The position of the feed can be altered as before control the input impedance. The coaxial feed introduces an inductance into the feed that may need to be taken into account if the height *h* gets large. In addition, the probe will also radiate, which can lead to radiation in undesirable directions [4].

Coupled (Indirect) Feeds

The feeds above can be altered such that they do not directly touch the antenna. For instance, the probe feed can be trimmed such that it does not extend all the way up to the antenna. The advantage of the coupled feed is that it adds an extra degree of freedom to the design [5]. The gap introduces a capacitance into the feed that can cancel out the inductance added by the probe feed.

Aperture Feeds

Another method of feeding micro strip antennas is the aperture feed. In this technique, the feed circuitry is shielded from the antenna by a conducting plane with a hole to transmit energy to the antenna**.** The upper substrate can be made with a lower permittivity to produce loosely bound fringing fields, yielding better radiation [6]. The lower substrate can be independently made with a high value of permittivity for tightly coupled fields that don't produce spurious radiation. The disadvantage of this method is increased difficulty in fabrication.

IV. DESIGN & EQUATIONS

The Micro strip patch antenna is often used in planar microwave radio active applications that require an Omni-directional pattern. The model of the dipole is shown in Fig.2. The dipole arm's width (W) and length (L)will be optimized for3. 0GHz operation, while the feed gap (g) and the substrate height (h)will be fixed. The model and simulation setup are outlined. The methods used to setup the simulation are outlined. In particular, the following topics are covered:

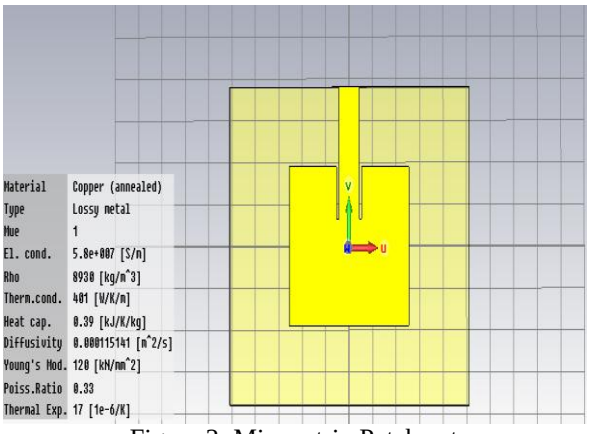

Figure 2: Micro strip Patch antenna

Infigure2, it shows the basic model of patch antenna. FR-4substrateusedinpatch antenna. FR-4isa grade designations signed to glass reinforce depoxy laminate sheets and printed board. Dielectric depend son height of patch antenna. Both Dipole arms are same length and same width. Gap between norms depends nits length. Ground plane of Antenna is 38.4 mm and Width is 46.8 mm, L & W of the patch is 28.8 mm & 37.2 mm.The patch width, effective dielectric constant, the length extension and also patch length are given by

$$w = \frac{C}{2f\sqrt{\varepsilon r}}$$

where *c* is the velocity of light, e is the dielectric content of substrate, *f* is the antenna working frequency, W isthe patch non resonant width, and the effective dielectric constant is egiven as,

$$\varepsilon_{eff} = \frac{(\varepsilon_r + 1)}{2} + \frac{(\varepsilon_r - 1)}{2}\left[1 + 10\frac{H}{W}\right]^{-\frac{1}{2}}$$

The extension length Δ is calculates as,

$$\frac{\Delta L}{H} = 0.412\frac{(\varepsilon_{eff} + 0.300)\left(\frac{W}{H} + 0.262\right)}{(\varepsilon_{eff} - 0.258)\left(\frac{W}{H} + 0.813\right)}$$

By using above equation we can find the value of actual length of the patch as,

$$L = \frac{c}{2f\sqrt{\varepsilon_{eff}}} - 2\Delta L$$

V. SIMULATION & RESULTS

The antenna radiation pattern is a measure of its power or radiation distribution with respect to a particular type of coordinates. We generally consider spherical coordinates as the ideal antenna is suppose dtoradiate in a spherically symmetrical pattern. However antennae in practice are not Omni directional but have a radiation maximum along one particular direction. For e.g. Dipole antenna is a broad side antenna where in the maximum radiation occurs along the axis of the antenna. The radiation pattern of a typical dipole antenna is shown in figure2.

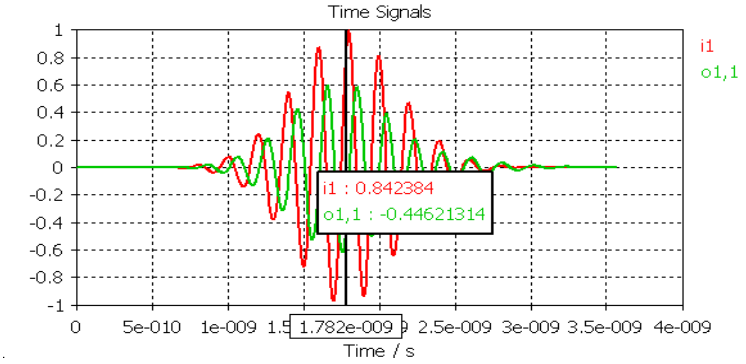

Figure 3: Time Signal.

In Figure 3 presents the graph of the time. It is clearly shown that lowest return loss is found at 1.60 GHz.And highest return loss found at 1 GHz frequency. Overall average return loss is not very effective per time.

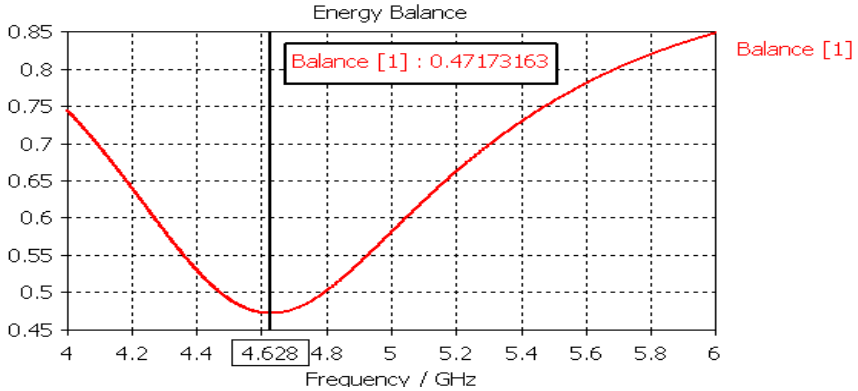

Figure 4: Frequency Vs Imaginary Impedance Graph.

In figure 4 describe the Impedance graph. There are two lines. One of them the upper one represents Imaginary Impedance graph and other one presents Real Impedance graph. We got Imaginary values are the highest in every frequency rather than real impedance graph. When frequency is 1.70 GHz found the highest impedance values for both graph.

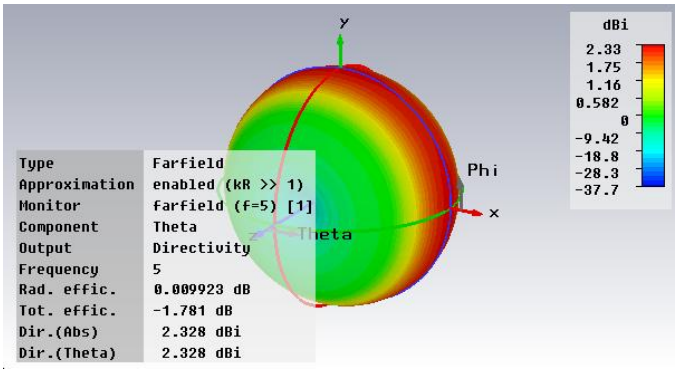

Figure 5: Radiation pattern of patch antenna.

In figure 5 describe the radiation graph. There are two lines. One of them the upper one light color graph represents patch antenna and other one presents dark red graph represents with microstrip lines. We got without far field values are the highest in every angel rather than other graph.

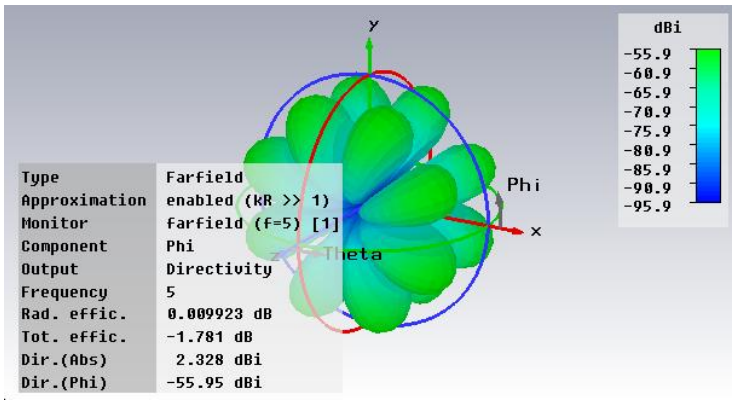

Figure 6: 3D pattern of microstrip patch antenna.

	Theta [deg]	rETotal [V] Setup : LastAdaptive Freq='0.9GHz' Phi='0deg'
1	-180.000000	447.377879
2	-175.000000	440.121530
3	-170.000000	431.593863
4	-165.000000	421.963485
5	-160.000000	411.437042
6	-155.000000	400.249550
7	-150.000000	388.653887
8	-145.000000	376.910252
9	-140.000000	365.276345
10	-135.000000	353.998841
11	-130.000000	343.306583
12	-125.000000	333.405660
13	-120.000000	324.476369
14	-115.000000	316.671854

We found at least 73 values from our simulation here we submit 14 values as a sample.it is clearly shown that it follow per 90 degree cycle that means per 90 degree its values at the nadir point and after that complete 90 degree it is in crest point.

VI. CONCLUSION

This thesis detailed the various aspects associated with the modeling of micro strip patch antenna. One of thegoals was the introduction of HFSS as an effectivetoolforelectromagneticanalysis.Aneffortwasmadeto imparting understanding of the design process in HFSS, which would aid the reader in building any simulation in HFSS.A comprehensive and graphic description of each step taken in creating the simulation of the patch antenna was presented. Achieved Gain is 4 db. Obviously there are some drawbacks of dipole antenna like:

- Lowbandwidth
- HighImpedance
- Movingspaceproblem
- Size

VII. Acknowledgements

We are earnestly grateful to one our group member, S. M Ziyad Ahmed, Graduated, Department of EEE, Bangladesh University of Engineering Technology. For providing us with his special advice and guidance for this project. Finally, we express our heartiest gratefulness to the Almighty and our parents who have courageous throughout our work of the project.

REFERENCES

[1] X. F. Shi, Z. H. Wang, H. Su and Y. Zhao, "A H-Type CPW Slot patch Antenna in Ku-band Using LTCC Technology with Multiple Layer Substrates," *Second International Conference on Mechanic Automation and ControlEngineering* (*MACE*), Hohhot, 15-17 July 2011, pp.7104-7106.

[2] U. Chakraborty, S. Chatterjee, S. K. Chowdhury and P. Sarkar, "A Compact shape Patch Antenna for Wireless Communication, *"Progress in Electromagnetics ResearchC*, Vol.18, 2011, pp.211-220.

[3] H. Sabri and Z. Atlasbaf, "Two Novel Compact Triple Band CPW Annular-Ring Slot Antenna for PCS-1900 and WLAN Applications," *Progress in Electromagnetics Research Letters*, Vol. 5, 2008, pp. 87-98.

[4] K. Kumar and N. Gunasekaran, "A Novel Wideband Slotted mm Wave Micro strip Patch Antenna," *International Conference on Signal Processing, Communication, Computing and Networking Technologies* (*ICSCCN*), Thackeray, 21-22 July 2011, pp. 10-14.

[5] D. Xi, L. H. Wen, Y. Z. Yin, Z. Zhang and Y. N. Mo, "A Compact Dual Inverted C Shaped Slots Antenna for WLAN Application," *Progress in Electromagnetics ResearchLetters*,Vol.17,2010,pp.115-123.

[6] G. M. Zhang, J. S. Hong and B. Z. Wang, "Two Novel Band-Notched UWB Slot Antennas Fed by Z shapeLine," *Progress in Electromagnetics Research*, Vol. 78, 2008, pp. 209-218.

American Journal of Engineering Research (AJER) 2015
American Journal of Engineering Research (AJER)
e-ISSN: 2320-0847 p-ISSN : 2320-0936
Volume-4, Issue-8, pp-163-169
www.ajer.org
Research Paper Open Access

Numerical Comparison of Variational Iterative Method and a new modified Iterative Decomposition Method of solvingIntegro-differential Equations

S. Emmanuel[1], M. O. Ogunniran[2], N. S. Yakusak[3]
[1](Department of Mathematics, Federal University Lokoja, Lokoja Nigeria)
[2](Department of Mathematics, Nigerian Turkish International Colleges, Abuja Nigeria)

ABSTRACT : *In this paper, a modified iterative decomposition method is proposed to solve the nth order linear and nonlinear integro differential equations. The solution was obtained by decomposition of the solution of the integro differential equations and the initial approximation was obtained by the evaluation of the source term. Subsequent approximations were obtained by applying the nonlinear operator on the sum of previous solutions obtained. The results obtained confirmed the accuracy and efficiency of the method when compared with the other methods found in literature. Some examples were given to illustrate the variational iterative method and the modified iterative decomposition method.*

Keywords: *Integro-differential Equations (IDEs), Iterative Decomposition Method (IDM), Variational Iterative Method (VIM),*

I. INTRODUCTION

Integral and integro-differential equations arise in many scientific and engineering applications. A type of the equations can be obtained from converting initial value problems with prescribed initial values. However another type can be derived from boundary value problems with the given boundary conditions. It is important to point out that converting initial value problems to an integral equation and converting an integral equation to initial value problems are commonly used in the literature. However converting boundary value problem to an integral equation and integral equation to equivalent boundary value problems are rarely used. In recent time researchers have worked on integral equations and lots of discoveries have been recorded. Adomian G. (1994)[1] presented the decomposition method, Aslam, Noor (2008)[2] had the Solution of Integro Differential Equations by Variational Iterative Method, Daftardar-Gejji V. and Jafari H.(2006)[4] produced an iterative method for solving nonlinear functional equations, He J. H. (1999)[7] produced the Homotopy perturbation technique of solution, Hemeda A. A. (2012)[8] presentented a new Iterative Method of aplication to nth-Order Integro-Differential Equations.

II. TECHNIQUES AND METHODOLOGY

A. Standard Variational Integration Techniques

Consider the differential equation

$$Lu + Nu = g(x) \tag{1}$$

Where L and N are linear and non-linear operators respectively and g(x) is the source term and equation (1) is formed non-homogeneous.

According to Variational Iteration Method by Aslam Noor (2008)[2] we constructed a correct functional as follows

$$u_{n+1}(x) = u_n(x) + \lambda\int_0^x (Lu_n(t) + Nu_n(t) - g(t))dt \quad (2)$$

Where λ is a general Lagrange multiplier which is identified optimally via variational theory, noting that in this method λ may be a constant or a function and $U_n(x)$ is a restricted value. The subscript n denotes the nth approximation. Hence, $\delta u_n = 0$ where δ is a variational derivative. For a complete use of the VIM, we followed two steps

1. The determination of the Lagrange multiplier λ that is identified optimally and
2. With λ determined, we substituted the result in (2) where the restriction is omitted.

Taking the variation with respect to independent variable u_n, we have.

$$\frac{\delta u_{n+1}}{\delta u_n} = 1 + \frac{\delta}{\delta u_n}(\int_0^x \lambda(t)(Lu_n(t) + Nu_n(t) - g(t))dt) \quad (3)$$

or equivalently

$$\delta U_{n+1} = \delta u_n + \delta(\int_0^x \lambda(t)(Lu_n(t)dt) \quad (4)$$

Integration by parts is usually used for the determination of $\lambda(t)$. In other word, we used

$$\int_0^x \lambda(t)u_n'(t)dt = \lambda(t)u_n(t) - \int_0^x \lambda'(t)u_n(t)dt \quad (5)$$

$$\int_0^x \lambda(t)u_n''(t)dt = \lambda(t)u_n'(t) - \lambda'(t)u_n(t) + \int_0^x \lambda''(t)u_n(t)dt \quad (6)$$

$$\int_0^x \lambda(t)u_n''(t)dt = \lambda(t)u_n''(t) - \lambda'(t)u_n'(t) + \lambda''(t)u_n(t) - \int_0^x \lambda'''(t)u_n(t)dt \quad (7)$$

and so on. These identities are obtained by integration by parts. E.g If $Lu_n(t) = u_n'(t)$ in (3) then (4) becomes

$$\delta u_{n+1} = \delta u_n + \delta\left\{\int_0^x \lambda(t)(Lu_n(t)dt)\right\} \quad (8)$$

or

$$\delta u_{n+1} = \delta u_n(t)(1+\lambda)|_{t-x} - \int_0^x \lambda'(t)\delta u_n(t)dt \quad (9)$$

but the extremum condition requires that δu_{n+1} on the LHS of (8) is zero and as a result, the RHS should be zero as well and this yields the stationary condition. This gives:

$$\lambda = -1 \quad (10)$$

Also if $Lu_n(t) = u_n''(t)$ in (8), then it becomes

$$\delta u_{n+1} = \delta u_n + \delta(\int_0^x \lambda(t)(Lu_n(t)dt)) \quad (11)$$

Integrating the integral of (11) by parts, we have:

$$\delta u_{n+1} = \delta u_n + \delta\lambda(u_n)'|_0^x - (\lambda'\delta u_n)|_o^x + \int_0^x \lambda''\delta u_n dt \quad (12)$$

or

$$\delta u_{n+1} = \delta u_n(t)(1-\lambda'|_{t=x} + \delta\lambda(u_n)'_{t=x} + \int_0^x \lambda''\delta u_n dt \quad (13)$$

where $\delta u_{n+1} = 0$, and these yield stationary condition

$$1-\lambda'|_{t=x} = 0, \lambda(t)|_{t=x}, \lambda''|_{t=x} = 0 \quad (14)$$

$$\lambda = t - x \tag{15}$$

The Langrange multiplier is determined from the the general formula

$$\lambda(t) = \frac{(-1)^i (t-x)^{i-1}}{(i-1)!} \tag{16}$$

Where i is the order of the differential equation. Having determined the Langrange multiplier $\lambda(t)$, the successive approximation $u_{n+1}(x), n \geq 0$ of the solution $u(x)$ is readily obtained using selective function $u_0(x)$, However for fast convergence the function $u_0(x)$ should be selected by using the initial conditions as follows.

$$\left.\begin{aligned} u_0(x) &= u(0), \text{for the first order,} \\ u_0(x) &= u(0) + xu'(0), \text{ for the second order.} \\ u_0(x) &= u(0) + xu'(0) + \frac{x^2}{2}u''(0), \text{for the third order} \\ &\vdots \\ u_0(x) &= u(0) + xu'(0) + \frac{x^2}{2}u''(0) + \ldots + \frac{x^{n-1}}{n-1}u^{n-1}(0), \text{for the nth order} \end{aligned}\right\} \tag{17}$$

Consequently the solution

$$u(x) = \lim_{n\to\infty} u_n(x) \tag{18}$$

In other words, the correct functional (2) will give several approximate solution which will tend toward the exact solution. The correct functional for the IDE is

$$u_{n+1}(x) = u_n(x) + \int_0^x \lambda(u_n^{(n)}(t) - f(t) - \int_0^t K(x,r)u_n(r)dr)dt \tag{19}$$

If $n = 0,1,2,\cdots k-1$ then equation (19) becomes

$$\left.\begin{aligned} u_1(x) &= u_0(x) + \int_0^x \lambda\left(u_0^{(n)}(t) - f(t) - \int_0^t K(t,r)u_0(r)dr\right)dt \\ u_2(x) &= u_1(x) + \int_0^x \lambda\left(u_1^{(n)}(t) - f(t) - \int_0^t K(t,r)u_1(r)dr\right)dt \\ &\vdots \\ u_k(x) &= u_{k-1}(x) + \int_0^x \lambda\left(u_{k-1}^{(n)}(t) - f(t) - \int_0^t K(x,r)u_{k-1}(r)dr\right)dt \end{aligned}\right\} \tag{20}$$

B. Derivation of the Modified IDM on General Problem

The general nth-order integro-differential equation is

$$y^{(n)} + f(x)y(x) + \int_{h(x)}^{g(x)} k(x,t)y^q y^{(m)}dt = g(x) \tag{21}$$

with

$$y(a) = \alpha_0, y'(a) = \alpha_1, y''(a) = \alpha_2, ..., y^{(n-1)}(a) = \alpha_{(n-1)} \quad (22)$$

where $\alpha_i, i = 0,1,...i-1$ are real constants. m, n and q are integers with $q \le m < n$ in (21). The function f(x), g(x) and k(x,t) are given and the unknown function $y(x)$ to be determined, we assumed that equation (21) has a unique solution.

Let us consider the following general non-linear equation

$$y = f + N(y) \quad (23)$$

where N is a non linear operator from a Banach space $B \to B$ and f is a known function, we assumed an approximate solution y of equation (23) of the form

$$y = \sum_{n=0}^{\infty} y_n \quad (24)$$

The non-linear operator N is defined as

$$N(\sum_{n=0}^{\infty} y_n) = N(y_0) + \sum_{n=1}^{\infty} \left\{ N(\sum_{k=0}^{\infty} y_k) - N(\sum_{k=0}^{n-1} y_k) \right\} \quad (25)$$

Thus, from equations (24) and (25), equation (23) is equivalent to

$$\sum_{n=0}^{\infty} y_n = f + N(y_0) + \sum_{n=1}^{\infty} \left\{ N(\sum_{k=0}^{\infty} y_k) - N(\sum_{k=0}^{n-1} y_k) \right\} \quad (26)$$

We defined the recurrence relation as

$$\left.\begin{aligned} y_0 &= f \\ y_1 &= N(y_0) \\ y_2 &= N(y_0 + y_1) - N(y_0) \\ y_3 &= N(y_0 + y_1 + y_2) - N(y_0 + y_1) \\ &\vdots \\ y_{n+1} &= N(y_0 + y_1 + y_2 + ... + y_n) - N(y_0 + y_1 + ... + y_{n-1}) \end{aligned}\right\} \quad (27)$$

The nth-term approximate solution for equation (27) is given as:

$$y = y_0 + y_1 + y_2 + ... + y_{n-1} \quad (28)$$

III. NUMERICAL EXAMPLES

In this section, we demonstrated the standard VIM and the Modified IDM on some numerical examples. We considered the comparison of the methods in four examples in which two are linear and the other two are non-linear integro-differential equations and the degree of approximation; n = 6. The errors were also considered.

Example 1

Consider

$$u'(x) = 1 - \frac{x}{3} + \int_0^1 xtu(t)dt, \quad u(0) = 0$$

The Exact solution is given as: $u(x) = x$

Table 1: Numerical Results of VIM and Modified IDM for Example 1 and the Errors obtained

x	Exact	VIM Result	IDM Result	Error for VIM	Error for IDM
0.0	0.0	0.0000000000	0.0000000000	0.0000000000	0.0000000000
0.1	0.1	0.0999999936	0.09999999921	6.36 E-09	7.90 E-10
0.2	0.2	0.1999999746	0.1999999968	2.45 E-08	3.20 E-09
0.3	0.3	0.2999999428	0.2999999928	5.72 E-08	7.20 E-09
0.4	0.4	0.3999998983	0.3999999873	1.02 E-07	1.27 E-08
0.5	0.5	0.4999998411	0.4999999801	1.59 E-07	1.99 E-08
0.6	0.6	0.5999997711	0.5999999714	2.29 E-07	2.86 E-08
0.7	0.7	0.6999996885	0.6999999611	3.12 E-07	3.89 E-08
0.8	0.8	0.7999995931	0.7999999491	4.07 E-07	5.09 E-08
0.9	0.9	0.8999994850	0.8999999356	5.15 E-07	6.44 E-08
1.0	1.0	0.9999993420	0.9999999205	6.58 E-07	7.95 E-08

Example 2

Consider the second order integro differential equation

$$y''(x) = 2 - \frac{x}{2} + \int_0^1 xy(t)y'(t)dt$$

with initial conditions $y(0) = y'(0) = 0$; the Exact solution is given as $y(x) = x^2$

Table 2: Numerical Results of VIM and Modified IDM for Example 2 and the Errors obtained

x	Exact	VIM Result	IDM Result	Error for VIM	Error for IDM
.0.0	0.0000000000	0.0000000000	0.0000000000	0.0000000000	0.0000000000
0.1	0.0100000000	0.0099938228	0.0099999980	6.18 E-06	1.70 E-09
0.2	0.0400000000	0.0399505826	0.0399999860	4.94 E-05	1.36 E-08
0.3	0.0900000000	0.0898332164	0.0899999540	1.67 E-04	4.58 E-08
0.4	0.1600000000	0.1596046611	0.1599998910	3.95 E-04	1.09 E-07
0.5	0.2500000000	0.2492278537	0.2499997880	7.72 E-04	2.12 E-07
0.6	0.3600000000	0.3586657312	0.3599996330	1.33 E-03	3.67 E-07
0.7	0.4900000000	0.4878812305	0.4899994180	2.12 E-03	5.82 E-07
0.8	0.6400000000	0.6368372887	0.6399991310	3.16 E-03	8.69 E-07
0.9	0.8100000000	0.8054968427	0.8099987620	4.50 E-03	1.24 E-06
1.0	1.0000000000	0.9938228295	0.9999983020	6.18 E-03	1.70 E-06

Example 3

Consider the third order volterra fredhom integro differential equation, giving as

$$u'''(x) = 2sinx - x - 3\int_0^x (x-t)u(t)dt + \int_0^1 u(t)dt$$

with initial conditions

$$u(0) = u'(0) = 1, u''(0) = -1$$

the exact solution is giving as

$$u(x) = sinx + cosx$$

Table 3: Numerical Results of VIM and Modified IDM for Example 3 and the Errors obtained

x	Exact	VIM Result	IDM Result	Error for VIM	Error for IDM
0.0	1.0000000000	1.0000000000	1.000000000	0.000000000	0.000000000
0.1	1.0948375820	1.0951049000	1.095105400	2.67318 E-04	2.67318 E-04
0.2	1.1787359090	1.1808661320	1.180870200	2.13022 E-03	2.13022 E-03
0.3	1.2508566960	1.2579985000	1.258012100	7.14180 E-03	7.14180 E-03
0.4	1.3104793360	1.3272464300	1.327278500	1.67671 E-02	1.67671 E-02
0.5	1.3570081000	1.3893426000	1.389405200	3.23345 E-02	3.23345 E-02
0.6	1.3899780880	1.4449622900	1.445069300	5.49842 E-02	5.49842 E-02
0.7	1.4090598740	1.4946734600	1.494841000	8.56136 E-02	8.56136 E-02
0.8	1.4140628000	1.5388851500	1.539128000	1.24822 E-01	1.24822 E-01
0.9	1.4049368780	1.5777897200	1.578119300	1.72853 E-01	1.72853 E-01
1.0	1.3817732910	1.6113047500	1.611722800	2.29531 E-01	2.29531 E-01

Example 4

$$u^{iv}(x) = 1 + \int_0^x e^{-x} u^2(t)dt$$

$$u(0) = u'(0) = 1, u(1) = e, u''(1) = e \quad Exact: u(x) = e^x$$

Table 4: Numerical Results of VIM and Modified IDM for Example 4 and the Errors obtained

x	Exact	VIM Result	IDM Result	Error for VIM	Error for IDM
0.0	1.0000000000	1.0000000000	1.0000000000	0.0000000000	0.0000000000
0.1	1.1051581800	1.1161649000	1.1051707990	1.1000 E-02	1.1908 E-07
0.2	1.2214022700	1.2323962000	1.2214026690	1.0994 E-02	8.9160 E-08
0.3	1.3498588000	1.3608493000	1.3498580830	1.0991 E-02	7.4246 E-07
0.4	1.4918246900	1.5028023000	1.4918184720	1.0977 E-02	6.2256 E-06
0.5	1.6487212700	1.6596591000	1.6486976610	1.0938 E-02	2.3610 E-05
0.6	1.8221188000	1.8329540000	1.8220479640	1.0835 E-02	7.0836 E-05
0.7	2.0137527000	2.0243571000	2.0135713730	1.0604 E-02	1.8133 E-04
0.8	2.2255409200	2.2356765000	2.2251306430	1.0135 E-02	4.1029 E-04
0.9	2.4596031100	2.4688607000	2.4587584240	9.2576 E-03	8.4469 E-04
1.0	2.7182818200	2.7259981000	2.7166666020	7.7163 E-03	1.6158 E-03

IV. GRAPHS OF COMPARISON

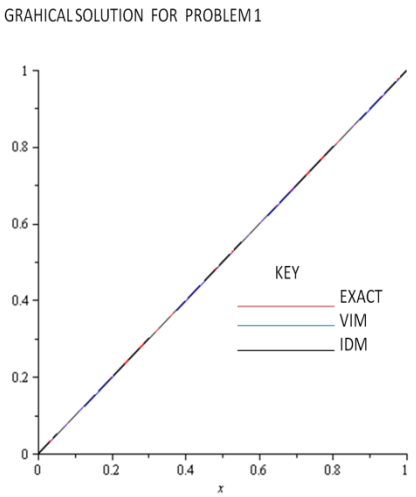

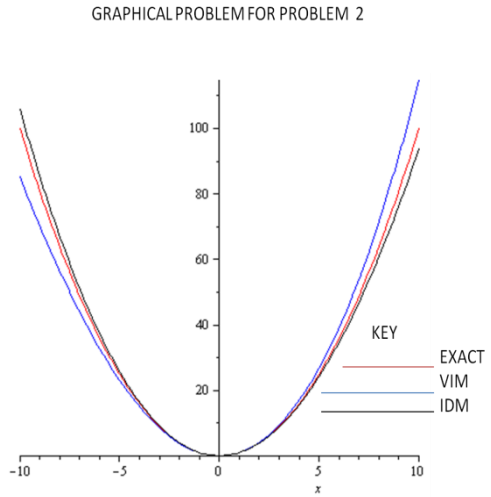

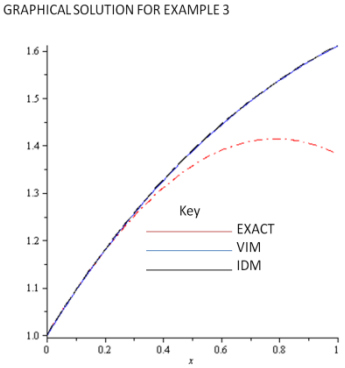

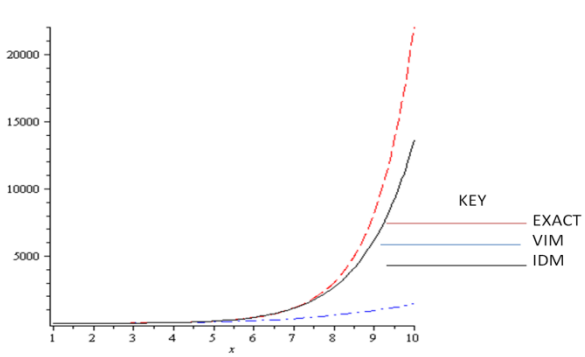

V. DISCUSSION OF RESULTS AND CONCLUSION

It is very clear and easy to observe that the newly proposed method performed creditably well when it was applied to solve integro-differential equation. It compete favourably with the existing variational iteration method in the examples considered, we discovered that the results obtained using the modified iterative

decomposition method are in close agreement with the exact solution and performed better than the other existing methods. in the case of Fredholm integro differential equations, when the newly proposed scheme was applied, we saw a great convergence to the exact solutions, infact there is a better performance in terms of errors obtained and closeness to the exact solutions than the variational iteration method. The modified iterative decomposition method performed creditably well when applied to solve integro-differential equations, infact it had an edge over the VIM. Moreover the new modified iterative decomposition method gives better results than those obtained by the variational iteration method, evident are shown in the table of results

Acknowledgements

We would like to acknowledge the effort and contributions of Ass. Prof. O. A. Taiwo of Department of Mathematics, University of Ilorin, Ilorin Kwara State Nigeria for the success of this work.

REFERENCES

[1] Adomian G. (1994): Solving Frontier problems of physics: The decomposition method, Kluwer,Scientific Research Academic Publisher 2, No 8.
[2] Aslam, Noor (2008): The Solution of Integro Differential Equations by Variational Iterative Method, Appl Anal 87, 1023-1038.
[3] Bhalekar S. and Daftardar-Gejji V. (1991): Solving Riccati differential equations of fractional order using the new iterative method.
[4] Daftardar-Gejji V. and Jafari H.(2006): An iterative method for solving nonlinear functional equations, J. Math. Anal. Appl., 316 , 753-763.
[5] Esmail Hesammeddoni and Azam Rahini (2013): The computational methods for differential equations presented a new numerical scheme for solving systems of integro-differential equations, Australian Jorn. of Basic and Applied Sciences, 1(2),108-119.
[6] He J. H. (1998): Approximate analytical solution for seepage flow with fractional derivatives in porous media, Comput. Meth. Appl. Mech. Engn., 167, 57-68.
[7] He J. H. (1999): Homotopy perturbation technique, Comput. Meth. Appl. Mech. Eng., 178 , 257-262.
[8] Hemeda A. A. (2012): New Iterative Method: Application to nth-Order Integro-Differential Equations, International Mathematical Forum, 7, (47), 2317-2332.
[9] Kamel-Al-Khaled (2005): The decomposition method for solving nonlinear IDEs, Appl. Math and Comp. 165(2), 473-487
[10] Kahani (2008): A simple numerical method for solving nonlinear Volterra IDEs.,Appl. Mathematical Sci. 2(51), 2531-41.
[11] Manafianheris (2012): The solution of IDE using the modified laplace Adomian decomposition method, Journal of Mathematical Extension 6(1) 41-55.
[12] Sweilam N. H., Hemeda A. A. (2007): Fourth order integro-differential equations using variational iteration method, Comput. Math. Appl., 54, 1086-1091.
[13] Taiwo O. A. (2009): Approximate solution of variational problems by an iterative decomposition method, Maejo Int. Jornal pf Sci. and Technology,3(03), 426-433
[14] Taiwo O. A. and Odetunde O. S. (2012): Numerical Approximation of Fractional Integro-differential Equations by an Iterative Decomposition Method, Pioneer Journal of Advances in Applied Mathematics, (6), 1-10.
[15] Taiwo O. A., Jimoh A. K. and Bello A. K. (2014): Comparison Of Some Numerical Methods For The Solution Of First And Second Orders Linear Integro Differential Equations, American Journal of Engineering Research (AJER) 03(01), pp 245-250.
[16] Wang S.Q. and He J.H. (2007), Variational iteration method for solving integro-differential equations, Phys. Lett. A, 367, 188-191.
[17] Wazwaz A. M. (2011) Methods and Applications of linear and nonlinear integral equations.

American Journal of Engineering Research (AJER) 2015
American Journal of Engineering Research (AJER)
e-ISSN: 2320-0847 p-ISSN : 2320-0936
Volume-4, Issue-8, pp-170-178
www.ajer.org
Research Paper Open Access

Numerical simulation of the bulk forming processes for 1345 aluminum alloy billets

Fakhreddine. KHEROUF [1], Smail. BOUTABBA [2], Kamel. BEY [3]
[1]*LMI, Department of Mechanical Engineering, Badji Mokhtar University, BP 12, Annaba 23000, Algeria.*
[2]*Applied Mechanics Laboratory of New Materials, 8 May University, BP: 401. Guelma 2400, Algeria*

ABSTRACT : *This paper presents an improved numerical simulation of bulk metal forming processes. It takes into the account the advanced formalism of large displacements and large deformations. Also, the interface workpiece formalism in considered. Metallographic studies are conducted to determine the evolution of the micro hardness as a function of annealing time and that to characterize accurately the plastic range of aluminum alloy for a range of plasticity 120%. The obtained results of metallographic studies are used to simulate a hot upsetting under the friction law of the plastic wave. Several simulations of forging operations of an axisymmetric billet by a rigid axisymmetric conical tool are performed with ABAQUS/standard computer code and that for preheated billets from 20 °C to 500 °C. The numerical study of the evolution of the normal stress at the interface has shown that the latter is independent of the tool roughness for a temperature close to 500 °C. The numerical study also allowed us to define the three areas of forging whatever cold; warm and hot forging. The effects of friction coefficient on the metal flow and contact pressure are numerically explored.*
Keywords -*Bulk forming, Finite elements, Roughness, Metallography, Plasticity*

I. INTRODUCTION

Forging is a bulk metal forming process which gives either a single geometric shape billet or a complex predetermined one and that by using a specific tools [1]. This process is widely used because the obtained parts have higher strength than ones obtained by machining or casting for equivalent masses.

These parts are resistive to strain and to impact resistance and that is due to metallurgical properties obtained during the bulk forming. Today, the automotive and aerospace industries are the predominant application because they use more than four-fifths of the produced parts by forging. Economic and technological interests of shaping metals are undeniable: high production rates, good geometric and mechanical quality, and low falls rate.

In the bulk forming processes, the friction plays an important role which is sometimes difficult to control. In the literature, several experimental tests are carried out to characterize the friction in plastic forming were reported [2].In the field of plastic forming, ring compression test is often used [3-6]. Also, a conventional test of a cylinder could be used to characterize the friction of the bulk forming operations [7-8]. The most sophisticated manufacturing processes have never produced perfect smooth surfaces. The characterization of the state roughness measurement plays major role in the study of friction.

In this context, modeling and numerical simulation can be used to predict material's flow, the analysis of deformations, the stress and the temperature distribution [9-11]. Also, in industrial applications, the finite element method is widely used [12-14]. In the numerical simulation development of thermo-mechanical's materials processing, surface behavior of existing laws fall within the modeling of contact by considering or no the friction are constantly being improved to better approximate the actual conditions. Therefore, a new friction law, known as the plastic wave has been studied for several years [15] for contacts between a rigid punch and an elastic-plastic. In order to characterize the friction law of the plastic wave, three parameters must be identified [16]. The first one is the flow of the materiel law in the vicinity of the contact interface between the tool and the workpiece.

In the present work this parameter (plastic flow) will be identified by a torsion test for which the plastic deformation zone is higher than in a tensile test. Thus, the torsion test was carried out on specimens of 1345 aluminum alloy to identify the law of the materiel flow. The identified parameter will be used into the simulation program. The studies on the state of specimens subjected to test upsetting showed a micrographic structure mainly characterized by large grains [17]. The annealing was performed on specimens before torsion tests in order to approximate this micro-structural state.

The simulation of the forging process is carried out by the FEM via the ABAQUS software using very fine mesh at the interface contact. The ABAQUS code offers the possibility to implement the plastic wave friction model using the user subroutine ".for". The main objective of this simulation is the comparison on the microscopic level of the sensitivity of the stress according to the temperature.

The paper is structured as follows: in section two, the theory of plastic wave friction is presented. The experimental procedure (hardness test, micrographic study, torsion test) is detailed in section three, the numerical simulation of the bulk forming processes is given in section four. The paper ends with concluding remarks and conclusion.

II. SUMMARY OF THE THEORY

The classical friction tests for bulk forming processes are usually based on simple compression by a rigid punch. This test induces a heterogeneous strain hardening in the billets [18].

A lot of microscopic models are developed in order to obtain a law of macroscopic friction [19-20]. The plastic wave model, formulated with slip line theory [21] and the upper bound, consider a plane strain field in a perfectly rigid plastic triangular asperity is based on a 2D geometry and actual roughness, of circular shape, is replaced by a triangular geometry of the same average height R and the same wavelength AR [22]. This model will allows to obtain a friction law at the interface according to normal contact stress, the roughness of the tool, the workpiece material yield stress and local constant friction coefficient. In this model, the friction force opposes the sliding of the rough surface and the resulting growth in the plastic wave material of the workpiece.

Table 1. Geometry of punch.

Cone Angle	R (µm)	AR (µm)
7°	20.985	359.060

III. EXPERIMENTAL DETAILS

3.1. Hardness test

In this section the experimental tests are presented, cylindrical samples of 7 mm thickness and 20 mm diameter were cut from the heat-treated rods of the furnace at 320°C. A minimum of four readings were taken on each sample in order to obtain reasonable statistics for the measured hardness values.

3.1.1. Hardness before heat treatment

All hardness tests were carried out on the external faces [23] of the samples previously polished, under a consistent load of 300 kgf applied for about 15 seconds as shown in Table.2.

Table 2. Hardness before heat treatment.

	Test1	Test2	Test3	Test4	Average
Vickers Hardness	40.1	40	42.6	41.1	40.95

3.1.2. Hardness after heat treatment

The annealing treatments of re-crystallization, which give new crystals, increase considerably the plasticity however, the elastic limit, the load rupture and the hardness are decreased.

To change the micro-structural properties, a thermal annealing is carried out on samples at 320 °C for a time period of 1 hour to 8 hours. After cooling, the hardness measurement tests are performed and the results are presented in Table 3.

Table 3. Hardness after heat treatment.

Annealing time	Test1	Test1	Test1	Test1	Average
1h	34	32.6	33	32.1	32.92
1h30	27.3	25.8	27.9	26	26.75
2h	25.4	23.6	26.1	25	25
3h	21.6	22.9	22.3	20.3	21.77
4h	22.8	22.3	20.9	21	21.75
5h	23.8	19.3	21.2	20	21.07
8h	21.5	21.7	20	21.2	21.02

According to the obtained results, the hardness of the specimen drops significantly during the first three hours of annealing and then stabilizes at 21 HV (figure 1). One can deduce that it is necessary to have the same hardness as that obtained after upsetting test, to subject samples to annealing for a minimum time of at least 4 hours.

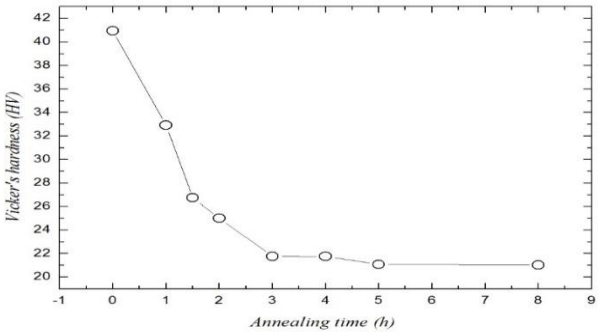

Fig. 1. Hardness evolution according annealing time.

3.2. Micrographic study

To study the microstructure, the specimens were prepared to be in accordance with the standard metallographic procedure. Before performing the micrographic control specimens, polishing was performed using abrasive paper of finer silicon carbide, a finishing with Alumina is performed by a diamond paste to get fine surface. To bring out the grain boundaries and in order to obtain a contrast between different grains, a chemical attack using appropriate Keller's reactive (distilled water, hydrofluoric acid, nitric acid, hydrochloric acid) was performed for 30 and 40 seconds. Metallographic microscope which is equipped with a camera connected to a PC to get shots of each samples.

3.3. Evaluation of microstructure

In figure 2, analysis of shots is carried out and the following remarks can be made: For specimen without heat treatment, there are a few grains that are not clear. Annealing for 1 hour, no grain boundary is visible even by increasing the zoom. An annealing of 1h30 gives a lightly difference suppose an enlargement grains.

On this specimen, the grain boundary is visible. In the annealing of 2 hours and there is no exploitable visible change. Whereas, in the annealing of 3 hours, a significant difference compared to the other specimens is visible; grain boundaries begin to appear and we can easily identify the various grains on the figure e. Less grains are observed after 4 hours of annealing compared to one of 3 hours. After 5 hours of annealing, it is found that the microstructure of the specimen has completely changed. From figure h which corresponds to 8 hours of annealing, a significant increase is observed in grain size of specimen material. The latter is directly related to the annealing time. A great similarity is observed between the microcrystalline state micrograph of the specimen heated for 8 hours and the state of the specimen subjected to upsetting test.

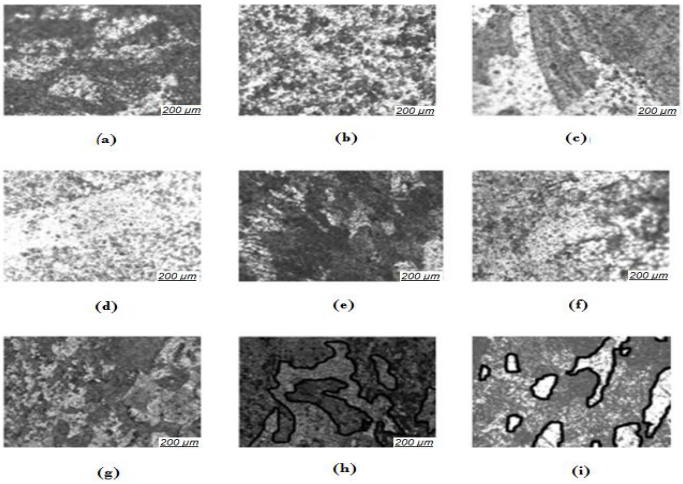

Fig. 2. (a) Without heat treatment ×100, (b) After 1 hour of heat treatment, (c) 1 h30, (d) 2 h, (e) 3 h, (f) 4 h, (g) 5 h, (h) 8 h, (i) Metallographic aspect of the specimens having undergone a upsetting test [17].

3.4. Mechanical characteristics and material

Numerical modeling of bulk forming processes (forging, stamping, punching ...) requires the prior determination of the mechanical characteristics of materials in the elastic range as well as those in large plastic deformations (100% to 300%). Accurate knowledge of those mechanical properties is usually required in various engineering applications such as aeronautical [24-25], automotive [26-27], naval [28-29] and in the mechanical manufacturing areas [30].

To determine the mechanical characteristics of the material, tensile test are used, from where the Young modulus and the Poisson's ratio of the material are measured. In [16], the tensile test is used and extrapolated the results to a larger plastic strain.

In this work, we performed a torsion test to determine the mechanical properties of the material for which we have a larger plastic strain. The specimens of 1345 Aluminum alloy with an initial diameter of 8 mm and an initial length of 160 mm, were subjected to a preliminary annealing at 320 °C for 8 hours . Then, the test torsion is performed. The stress-strain curve has been raised to 120% as given by figure 3.

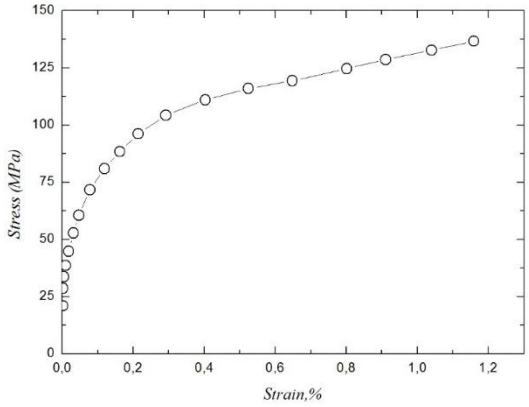

Fig. 3. Stress-strain curve of the billet material.

For the numerical modeling of the upsetting process, the punch material is supposed to be rigid with the combination of the following mechanical and thermal properties. See table 4. The billet is perfectly plastic material, the mechanical and thermal properties are shown in table 5.

Table 4. Thermal and mechanical properties of the punch.

Properties	Values
Young modulus E	210000 MPa
Poisson ratio ν	0.28
Mass density ρ	7700 Kg/m^3
Thermal expansion coefficient α	1.3e-005 /K°
Thermal conductivity K	50 W/m/°K
Specific heat C_p	460 J/kg/°K

Table 5. Thermal and mechanical properties of the billet.

Properties	Values
Young modulus E	69000 MPa
Poisson ratio ν	0.33
Yield stress σ_0	125 MPa
Mass density ρ	2700 Kg/m^3
Thermal expansion coefficient α	2.4e-005 /K°
Thermal conductivity K	230 W/m/°K
Specific heat C_p	1000 J/kg/°K

IV. NUMERICAL SIMULATION

4.1. 4.2. Mesh and boundary conditions

The problem similarity allows considering calculation only for one half of the higher punch and a quarter of the billet. The geometries of the dies and billet are meshed with, 4-node axisymmetric thermally coupled quadrilateral elements with bilinear displacement and temperature shape functions, reduced integration, hourglass control. A mesh refinement is applied to the interface tool/workpiece (20 elements in front of each tool asperity). This simulation leads to 13875 elements for the mesh from the billet and 453 for the tool.

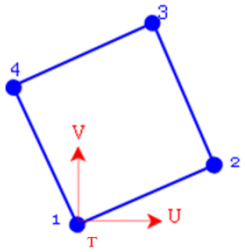

Fig. 4. Quadrilateral element.

The billets are cylindrical with an initial diameter of 6 mm and an initial height of 8 mm, the top base is conical with angle inclination set to 7°. The interface is modeled with the assumption that the friction is not considered (perfect sliding) and the mesh is made very fine in the vicinity in the contact area. The punch goes down at a constant speed with a stroke of 1.2 mm subdivided in different positions. As for the boundary conditions, the transverse displacement is blocked on the level of the base as well as radial displacement on the symmetry axis. See figure 5.

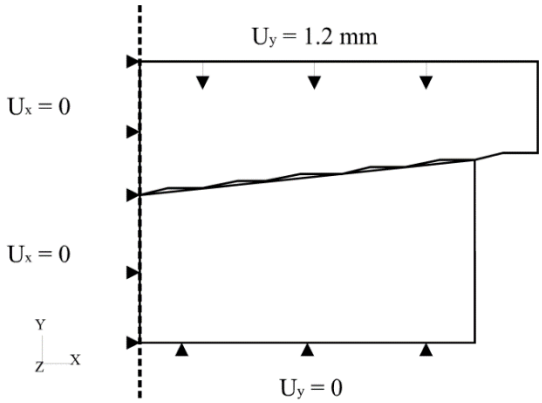

Fig. 5. Boundary conditions.

V. RESULTS AND DISCUSSIONS

5.1. Contact pressure distribution

5.1.1 Effect of friction coefficient on contact pressure

The important parameters which influence friction include normal stress along the tool–material interface, the lubrication condition, the relative velocity, temperature, surface roughness, and mechanical properties of the material and / or tool. ABAQUS is one of the most powerful finite element calculation software. In the processes of bulk forming metals, many studies have considered the contact pressure as a parameter. Figure 6 shows the effects of friction on the amplitude of the maximum contact pressure. It is observed a decrease of pressure in the vicinity of the contact surface depending on the variation of the friction coefficient. It is also noted that the value of contact pressure is higher (753.9 MPa) for a zero friction coefficient and its value (525 MPa) for the case of dry friction with a coefficient equal to 0.45. The shape of the curve shows a significant effect of the friction on the contact pressure.

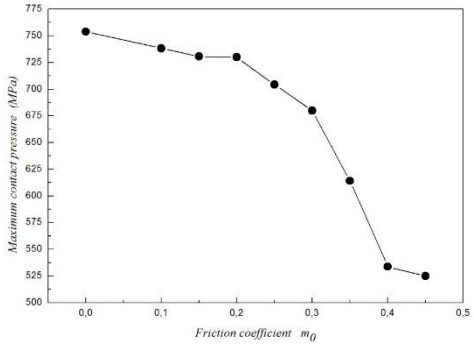

Fig. 6. Effect of friction on the maximum contact pressure.

5.2. Plastic flow in the workpiece

The pressure distribution in the vicinity of the contact surface results in a plastic flow of the billet material. During the bulk forming process, the contact pressure in the upper region of the billet is much larger than that of the lower region, as shown in Fig. 7. By observing the directions shown on the figure it is observed that the diameter of the upper region is larger than that of the lower region of a deformed workpiece.

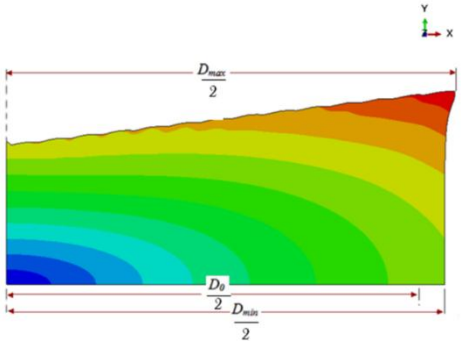

Fig. 7. Deformed workpiece for m_0.=0.1

Accordance to the literature, we can evaluate quantitatively the plastic flow of a deformed slug with the following relationship:

$$\phi_D = \frac{D_{\max} - D_{\min}}{D_0} \times 100\% \qquad (1)$$

D is the diameter of the workpiece,Dmax and Dmin are the maximum and minimum diameters of the deformed surface of a workpiece, respectively.

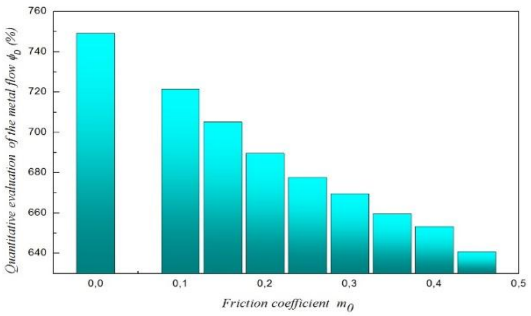

Fig. 8. Effect of friction on the plastic flow.

Figure 8 shows the effect of friction coefficient on the plastic flow of axisymmetric billets. It is noted that decreases substantially linearly when the friction coefficient increases. At the end of the upsetting for a punch stroke of 1.2 mm, we notice that the value of is 749.234 for zero friction, taking the values 721.42, 705.131, 689.533, 677.701, 669.609, 659.637, 653.248, 640.850 for, respectively, the friction coefficients of 0.1, 0.15, 0.2, 0.25, 0.3, 0.35, 0.4 and 0.45.

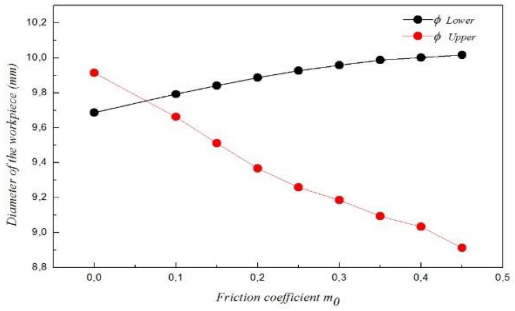

Fig. 9. Workpiece diameter evolution.

Figure 9 shows the influence of friction on a diameter of the deformed workpiece, we find that the diameter increases with lower friction. In contrast to the larger diameter it decreases when the friction increases. In fact, the friction tool / workpiece interfaces not only affect the surface quality of the product but also changes in the geometry and physical properties. Experimental tests enable to validate the numeric simulation taking into account the friction at the interface.

5.3. Upsetting analyzes

Some bulk forming processes are carried out at hot conditions to decrease the efforts, because the temperature determines the flow stress value of the material to be deformed. Figure 10 shows the predicted Von Mises stress distribution in workpiece surface during the simulation results history for various workpiece temperatures included between 20°C and 500°C. These results show that on the interface, more the temperature is high, less is important the stress σ and its fluctuations: so, the material becomes easy to forge.

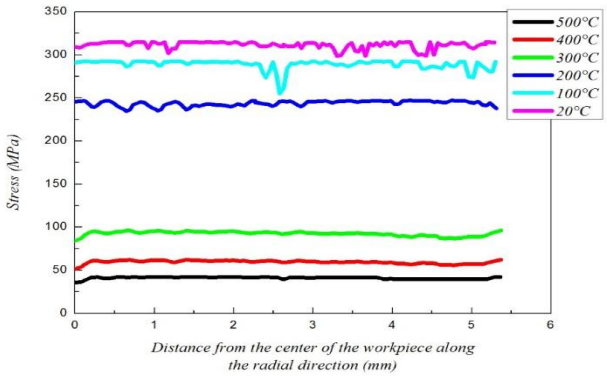

Fig. 10. Von Mises stress distribution in workpiece surface along the radial direction.

Several of the billet preheat temperatures were studied in order to distinguish the various areas from the stress evolution during the upsetting process.

The numerical simulations were made for temperatures varying between 20°C and 500°C and that to locate the variation points, it can be found from figure 11 the yield stress evolution according to the billet pre heating temperature. On this Figure we notice three different zones:

Zone I: for temperatures going from 20°C to 100°C, the stress is practically constant, between 2.92E+02 MPa and 2.89E+02 MPa.

Zone II: change of the behavior is noted with a stress varying of 2.89E+02 MPa, for a pre-heating of 100°C, and with 9.28E+01 MPa for a temperature of 300°C.

Zone III: the stress is stabilized, for a zone of temperature of 200°C, between 9.28E+01 MPa and 4.12E+01 MPa.

These areas correspond with the three zones of forging indicated in the literature, the first zone corresponds perfectly to the cold forging zone during which the evolution of the material's structure is caused only by the work hardening, where the flow stress increases and the ductility decreases. The second is included in the warm forging zone for which notable reduction in work hardening is observed. The flow stress is a decreasing function of the temperature. For the hot or with warm processes the conclusions are similar. The third zone starts at the higher temperatures of the zone of warm forging and extends until the zone of the hot forging.

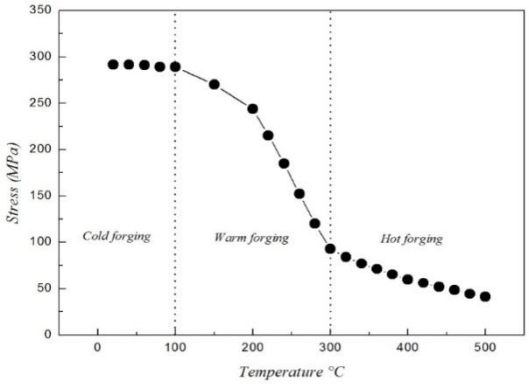

Fig. 11. Yield stress evolution for aluminum alloy according to the temperature.

VI. CONCLUSION

We have presented in this paper, an improved numerical simulation of bulk metal forming processes. Our contribution concerns the precise characterization of materials in the deformation area. Torsion tests of specimens on Aluminum alloy were carried out to characterize material in the plastic range and micrographic tests were conducted on specimens subjected to annealing in order to obtain a metallographic state similar to that of specimens undergone a upsetting test. The obtained data were introduced into ABAQUS to simulate the behavior near the interface tool-workpiece in a bulk forming operation. In this simulation, the friction coefficient is modeled by so-called "plastic wave" friction law. The influence of the temperature on the metals bulk forming process was studied as well as the determination of the cold, warm and hot forging zones. It has been observed that roughness does not have any influence on the operations of hot bulk forming

REFERENCES

[1] Felder, E. Procédés de mise en forme, Introduction, Techniques de l'Ingénieur, 2000.
[2] Zhang, Q.; Arentoft, M.; Bruschi, S.; Dubar, L.; Felder, E. Measurement of friction in a cold extrusion operation: Study by numerical simulation of four friction tests. *Int J Mater Form*, 1,2008, 1267-1270.
[3] Petersen, S.B.; Martins, P.A.F.; Bay, N. Friction in bulk metal forming: a general friction model vs. the law of constant friction. *Journal of Materials Processing Technology*, 66,1997, 186-194.
[4] Joun, M.S.; Moon, H.G.; Choi, I.S.; Lee, M.C.; Jun, B.Y. Effects of the friction law on metal forming processes. *Tribology International*, 42,2009, 311-319.
[5] Hasan, S.; Jahan, R. On the measurement of friction coefficient utilizing the ring compression test. *Tribology International*, 32,1999, 327-335.
[6] Stembalski, M.; Pres´, P.; Skoczyn´ski, W. Determination of the friction coefficient as a function of sliding speed and normal pressure for steel C45 and steel 40HM. *archives of civil and mechanical engineering*,13 , 2013, 444 –448.
[7] Ebrahimi, R.;Najafizadeh, A. A new method for evaluation of friction in bulk metal forming. *Journal of Materials Processing Technology*, 152, 2004, 136-143.
[8] Tan, X. Comparisons of friction models in bulk metal forming. *Tribology International*, 35, 2002, 385-393.
[9] Tisza, M. Numerical modelling and simulation in sheet metal forging. Journal of Materials Processing Technology, 151,2004, 58-62.
[10] Weronski, W.; Gontarz, A.; Pater, Z. b.The reasons for structural defects arising in forgings of aluminiumolloysanalysed using the finite element method. *Journal of Materials Processing Technology*, 92-93,1999, 50-53.
[11] Xinghui, H.; Lin, H. 3D FE modeling of contact pressure response in cold rotary forging. *Tribology International*, 57,2013, 115-123.
[12] Yaakoubi, M.; Kchaou, M.; Dammak, F. Simulation of thermomechanical and metallurgical behavior of steels by using ABAQUS software. *Computational Materials Science*, 68, 2013, 297-306.
[13] Rojek, J.; Onate, E.; Postek, E. Application of explicit FE codes to simulation of sheet and bulk metal forming processes. *Journal of Materials Processing Technology*, 80-81, 1998, 620-627.
[14] Cui, X. Y.; Li, G. Y. Metal forming analysis using the edge-based smoothed finite element method. *Finite Elements in Analysis and Design*, 63, 2013, 33-41.
[15] Baillet, L. Modélisation du frottement pour les opérations de matriçage, INSA-Lyon,1994.
[16] Vidal-Sallé, E. ;Boutabba, S. ; Cui, Y. ; Boyer, J. C. An improved « plastic wave » friction model for rough contact in axisymmetric modelling of bulk forming processes. *Int. J. Mater. Form*, 1, 2008, 1263-1266.
[17] Morival, S.; Boyer, J. C. Endommagement ductile des surfaces de produits forgés, rapport de PFE, INSA-Lyon, 2010.
[18] Vidal-Sallé, E.; Maisonnette-Masson, S.; Boyer, J. C.About the validity of the plastic wave model for an actual roughness of axisymmetric tooling in bulk forming. *Int J Mater Form*, 2, 2009, 217-220.
[19] Hélénon, F.; Vidal Sallé, E.; Boyer, J. C.Lubricant flow between rough surfaces during closed-die forging. *Journal of Materials Processing Technology*, 154, 2004, 707-713.
[20] Challen, J. M.; Oxley, P. L. B. Anexpiation of the different regimes of friction and wear using asperity deformation models. *Wear*, 53, 1979, 229 – 243.

[21] Vidal-Salle, E.; Dubois, A.; Dubar, M.; Dubar, L.; Boyer, J. C. Experimental identification and validation of the plastic wave approach in hot forging of steels. *Wear*, 286-287, 2012, 35-44.
[22] Kherouf F, Boutabba S, Bey K, Chettah A and. Boyer J.-C., Mesoscopic comparison of interface tool/workpiece for simulation by FEM of EN AW 1350 bulk forming alloy. Mechanics & Industry; 3 (16), 2015, 309.
[23] Shittu, M. D., Ibitoye, S. A., Olawale, J. O.Mechanical properties of cast hypoeutectic Al-Si alloy in hexachloroethane-coated mould. *Journal of Engineering Science and Technology*, 7, 2012, 529-539.
[24] Karagiozova, D.; Mines, R. Impact of aircraft rubber tyre fragments on aluminium alloy plates: II-numerical simulation using LS-DYNA. *International Journal of Impact Engineering*, 34, 2007, 647-667.
[25] Varas, D.; Zaera, R.; López-Puente, J.Numerical modelling of the hydrodynamic ram phenomenon. *International Journal of Impact Engineering*, 36, 2009, 363-374.
[26] Rusinek, A.; Zaera, R.;Forquin, P.; Klepaczko, J.R. Effect of plastic deformation and boundary conditions combined with elastic wave propagation on the collapse site of a crash box. *Thin-Walled Structures*, 46, 2008, 1143-1163.
[27] Kazanci, Z.; Bathe, K. Crushing and crashing of tubes with implicit time integration. *International Journal of Impact Engineering*, 42, 2012, 80-88.
[28] Zong, Z.; Zhao, Y.; Li, H. A numerical study of whole ship structural damage resulting from close-in underwater explosion shock. *Marine Structures*, 31, 2013,24-43.
[29] Ehlers, S. The influence of the material relation on the accuracy of collision simulations. *Marine Structures*, 23, 2010, 462-474.
[30] Hui, W.; Ying-bing, L.; Friedman, P.; Ming-he, C.; Lin, G. Warm forming behavior of high strength aluminum alloy AA7075. *Trans. Nonferrous Met. Soc. China*, 22, 2012, 1-7.

American Journal of Engineering Research (AJER) 2015
American Journal of Engineering Research (AJER)
e-ISSN: 2320-0847 p-ISSN : 2320-0936
Volume-4, Issue-8, pp-179-185
www.ajer.org
Research Paper Open Access

Innovative Concepts of Fuzzy logic which Improve the Human and Organizational Capabilities

Mehzabul Hoque Nahid[1]
[1](Faculty coordinator, Computer science and engineering Department, Royal University of Dhaka, Bangladesh)

ABSTRACT: *This thesis has been realized following a design science approach, it therefore aims at first creating innovative concepts which improve the actual human and organizational capabilities, secondly, at evaluating these concepts by providing concrete instantiations. According to this research paradigm, the objectives of this thesis are the following: The first objective of this thesis is to extend the querying ability of the fuzzy classification approach proposed by Schindler. By adding new clauses to the fuzzy Classification Query Language, the user should be given more powerful means for selecting elements within a fuzzy classification. The second objective of this thesis is convert classical value to fuzzy value which base on fuzzy membership function such as S shape membership function, Pi shape membership function and Z shape membership junction. The third objective is, considering the application domain specificities, to extend the original fuzzy queries approach by new concepts which provide additional capabilities to the system and proved that the proposed intelligent fuzzy query is faster than the conventional query and it provides the user the flexibility to query the database using natural language. The fourth and last objective is to also make a comparison between traditional database and fuzzy database by computing the time cost of classical query over classical database, fuzzy query over classical database and fuzzy query over fuzzy database.*

Keywords – *Fuzzy Database, Query, Boolean, Set, Function.*

I. CONCEPT OF FUZZY SETS

The fuzzy logic theory is based on fuzzy sets which are a natural extension of the classical set theory. A sharp set (also called crisp set) is defined by a bivalent truth function which only accepts the values 0 and 1 meaning that an element fully belongs to a set or does not at all, whereas a fuzzy set is determined by a membership function which accepts all the intermediate values between 0 and 1[1]. The values of a membership function, called membership degrees or grades of membership, precisely specify to what extent an element belongs to a fuzzy set, i.e. to the concept it represents. A fuzzy set is built from a reference set called universe of discourse. The reference set is never fuzzy. Assume that $U = fx1; x2; : : : ; xng$ is the universe of discourse, then a fuzzy set A in U (A ½ U) is defined as a set of ordered pairs

$$f\,(xi;\ ^1A(xi))g$$

Where $xi\ 2\ U$, $^1A: U!$ [0; 1] is the membership function of A and $^1A(x)\ 2$ [0; 1] is the degree of membership of x in A.

Consider the universe of discourse $U = f1; 2; 3; 4; 5; 6g$. Then a fuzzy set A holding the concept 'large number' can be represented as

$$A = f\,(1; 0); (2; 0); (3; 0:2); (4; 0:5); (5; 0:8); (6; 1)\ g$$

With the considered universe, the numbers 1 and 2 are not 'large numbers', i.e. the membership degrees equal 0. Numbers 3 to 5 partially belong to the concept 'large number' with a membership degree of 0.2, 0.5 and 0.8. Finally number 6 is a large number with a full membership degree [2]. It is important to note that the definition of the membership degrees is subjective and context dependent, meaning that each person has his own perception of the concept 'large number' and that the interpretation is dependent on the universe of discourse and the context in which the fuzzy set is used. In Example 2.2 for instance, the membership degrees of the elements would be quite different if the universe of discourse contained numbers up to 100 or even 1000. In a similar

manner, the concept 'large profit' would have a distinct signification for a small and a large enterprise. Fuzzy sets are commonly represented by a membership function. Depending on the reference set, the membership functions are either discrete or continuous. Figure 2.3 shows the truth function of a sharp set in comparison to the membership functions of a discrete and a continuous fuzzy set.

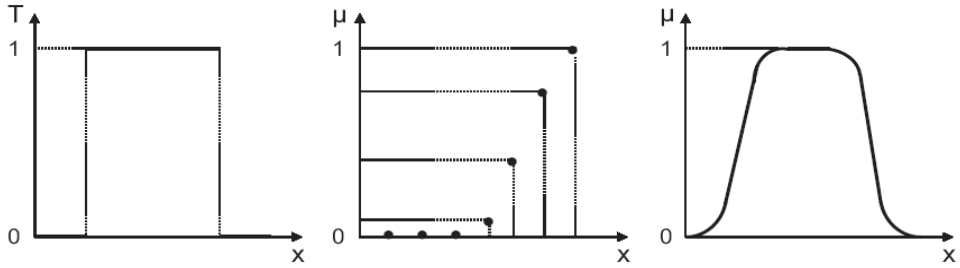

Figure 1: Truth function of a sharp set and membership functions of a discrete and a continuous fuzzy set

Usually, several fuzzy sets are defined on the same reference set forming a fuzzy partition of the universe. A linguistic expression from the natural language can label the fuzzy sets in order to express their semantics. In the case the reference set can hold the concepts 'young', 'middle-aged' and 'old' at the same time allowing a continuous transition between them (see Figure 2). This construct is essential in the fuzzy logic theory and is called a linguistic variable [3]. A linguistic variable is a variable whose values are words or sentences instead of numerical values. These values are called terms (also linguistic or verbal terms) and are represented by fuzzy sets.

A linguistic variable is characterized by a quintuple

$$(X; T; U; G; M)$$

where X is the name of the variable, T is the set of terms of X, U is the universe of discourse, G is a syntactic rule for generating the name of the terms and M is a semantic rule for associating each term with its meaning, i.e. a fuzzy set defined on U.

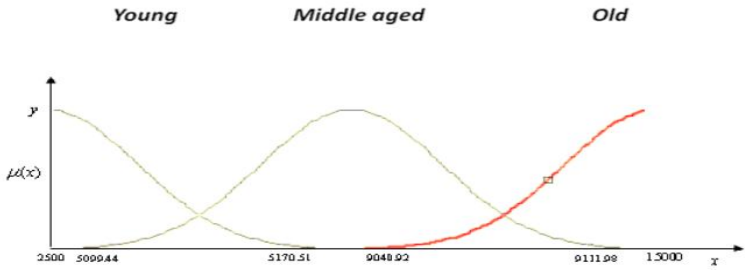

Figure 2: Fuzzy partition of the reference set with labeled fuzzy sets

The ability of giving a partial belonging to the elements allows a continuous transition between the fuzzy sets instead of having sharply fixed boundaries. This way, it is possible to better reflect the reality where everything is not black or white but often differentiated by grey values. The definition of a fuzzy set can therefore adequately express the subjectivity and the imprecision of the human thinking. Furthermore, the concept of linguistic variable is the basis for representing the human knowledge with within human oriented rules or queries which can be processed by computers.

II. FUZZY VS BOOLEAN

Fuzzy logic is extension of normal Boolean logic, which is extended to identifier partially truth. What means, something between absolute truth and absolute false. Advantage of fuzzy logic is mathematical ability catch up information described by words. This gives us possibility to work with ambiguous term like “small”, “near”, “far”, “about”, “very” and with number of other words used in human language. Basic problem is, how to handle words, which meaning is hard to define. Is close 50m, 100m or 1 kilometer. If 50m is close, so 51m is not? Is it far? Exactly number of ambiguous in common language represents problem, which cannot be solved by Boolean logic. To learn computer systems human speech, it is necessary to solve this problem. Fuzzy sets are probably one of solution. Boolean logic model become basement form of classic querying languages among which belong SQL (Structured Query Language)[4]. Boolean algebra brings logic operators and (conjunction), or (disjunction), and not (negation). By using these operators when searching with imprecise or not complete

information, it is not ensured that we get requested data. By using AND, some inaccuracy resides in problem of results, because information which do not match one of conditions or more than one conditions are the same. There is no differences between information, which meet different number of conditions in query.
Disadvantage of strict evaluations AND operator express in this situation: User is looking for information and he is sure that information exist in database. Conditions, which exactly identify searching data are composed into query using and operator. If user enters only one wrong condition, than result will not include requested information. User has to do corrections in his query. If there are no information meeting query conditions, than user will be pleased if he gets information which meet conditions with some degree. That is hardly handled by classic approach. In case of operator OR, there is no chance to differentiate information matching different number of conditions. Result consists of data, which meet one condition or two and more conditions. This can leads to huge number of tuples among which is wanted tuple.
Empirical research shows, that strict form of evaluation Boolean operators do not match human thinking, appreciation and decision. Human tolerance, displayed by do not eliminating solutions, which do not meet all his conditions is in contrast to strict evaluation and operator [5].
Basic difference between fuzzy approach and Boolean one is ability to get rated result, which can be ordered by real number from <0, 1> interval. User has chance to deal only by the most valuable information, what is not possible to handle by Boolean logic. Next difference is direct in query, where fuzzy statement can be used. It is allowed to use words like average, big, far, near.

III. PROPERTIES OF FUZZY SET

As the fuzzy set theory is an extension of the classical set theory, crisp sets are specific cases of the fuzzy sets. For this reason, the existing properties of the classical sets have to be extended and some new properties are introduced [6]. Among the extended properties of the classical sets are the definitions of emptiness, equality, inclusion and cardinality. In order to take the wider scope of the fuzzy sets into account, the definitions of convexity, support, ®-cut, kernel, width, height and normalization have been introduced.

A fuzzy set is considered to be empty if the membership degrees of all the elements of the universe are equal to zero.
A fuzzy set A, defined over a reference set U, is empty if

$$A = ?\ ,\ {}^{1}A(x) = 0;\ 8x\ 2\ U$$

Two fuzzy sets are equal if their membership degrees are equal for all the elements of the reference set, i.e. if the two fuzzy sets have the same membership function. The support of a fuzzy set A defined over a reference set U is a crisp subset of U that complies with

$$Supp(A) = fx\ 2\ U;\ {}^{1}A(x) > 0g$$

The ®-cut, resp. the strong ®-cut, of a fuzzy set is the crisp subset of the universe where the membership degrees are greater or equal, resp. greater, than the specified ® value.

IV. FUZZY MEMBERSHIP FUNCTION

The membership function values need not always be described by discrete values. Quite often these turn out to be as described by a continuous function. We know different types of fuzzy membership function such as S shape, Z shape, Pi shape, Trapezoidal, Triangle, Singleton membership function. But in this paper we use three membership function S shape, Z shape, and Pi shape membership function.

zmf - Z-shaped built-in membership function**,** this paper we classify this membership function in three linguistic terms such as S1= *very low*, S2= ***low*** and S3= *not so low*.

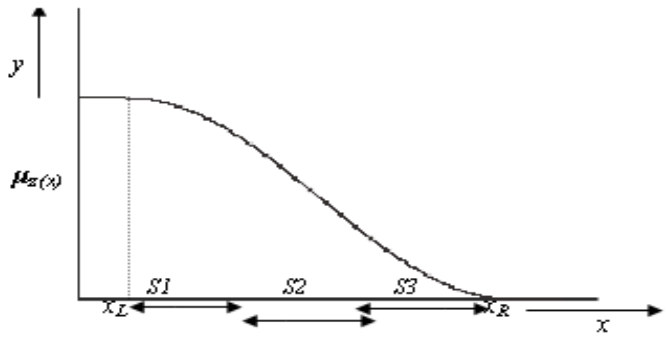

Figure 3: Z-shaped membership function

$$y_z = \begin{cases} \frac{1}{2} + \frac{1}{2}\cos\left(\frac{x_R - x}{x_R - x_L}\right)\pi, & \text{if } x_L \le x \le x_R \\ 0 & \text{if } x > x_R \\ 1 & \text{if } x < x_L \end{cases}$$

smf - S-shaped built-in membership function, this paper we classify S membership function in three linguistic terms such as S1= not so high, S2= high and S3= very high.

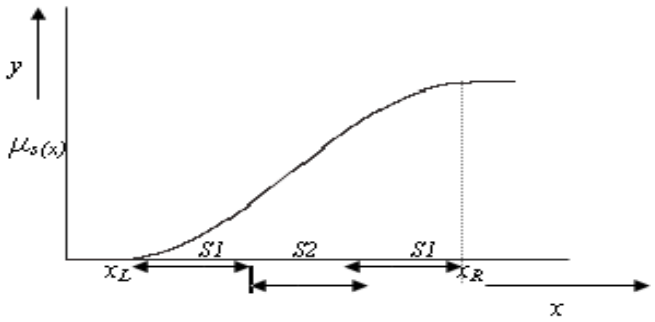

Figure 4: *S*-shaped membership function

$$y_s = \begin{cases} \frac{1}{2} + \frac{1}{2}\cos\left(\frac{x - x_L}{x_R - x_L}\right)\pi, & \text{if } x_L \le x \le x_R \\ 0 & \text{if } x < x_R \\ 1 & \text{if } x > x_R \end{cases}$$

pimf - Π-shaped built-in membership function, In this paper we classify this membership function in three linguistic terms such as XL,XR= not so medium, S1= medium and S3= very medium

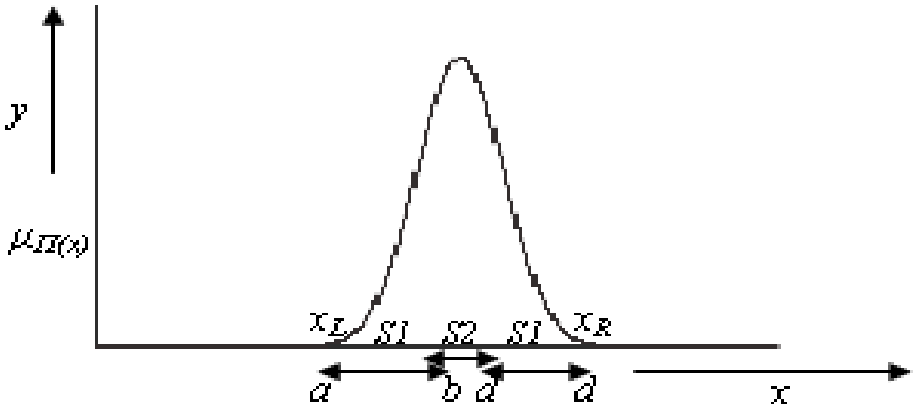

Figure 5: Pi-shaped membership function

y_{π} = $(x, [a,b,c,d])$

$$y_s = \begin{cases} 0 & \text{if } x = a \text{ or } x = d \\ 2\left(\frac{x-a}{b-a}\right)^2 & \text{if } a < x \le \frac{a+b}{2} \\ 1-2\left(\frac{x-b}{b-a}\right)^2 & \text{if } \frac{a+b}{2} < x < b \\ 1-2\left(\frac{x-c}{d-c}\right)^2 & \text{if } c < x \le \frac{c+d}{2} \\ 2\left(\frac{x-d}{d-c}\right)^2 & \text{if } \frac{c+d}{2} < x < d \\ 1 & \text{if } b \le x \le c \end{cases}$$

V. OPERATION OF FUZZY LOGIC

The operations of complement, intersection and union of the classical set theory can also be generalized for the fuzzy sets. For these operations, several definitions with different implications exist. This section only presents the most common operators from the Zadeh's original proposition [7]

The complement of a fuzzy set is 1 minus the membership degrees of the elements of the universe. This definition respects the notion of strong negation.

The complement of a fuzzy set a defined over a reference set U is defined as

$$\sim A = {}^1\sim A(x) = 1 \text{ ¡ } {}^1A(x);\ x\ 2\ U$$

For the intersection (resp. the union), Zadeh proposes to use the minimum operator (resp. the maximum operator). These operators have the advantages of being easily understandable and very fast to compute. The intersection (resp. the union) of two fuzzy sets is the minimum (resp. the maximum) value of the membership degrees of the two fuzzy sets for all the elements of the reference set.

The intersection of two fuzzy sets A and B defined over a reference set U is defined as

$$A \setminus B = {}^1A\setminus B(x) = {}^1A(x) \wedge {}^1B(x) = min\ ({}^1A(x);\ {}^1B(x));\ x\ 2\ U$$

The union of two fuzzy sets A and B defined over a reference set U is defined as

$$A\ [B = {}^1A\ [B(x) = {}^1A(x)\ \_\ {}^1B(x) = max\ ({}^1A(x);\ {}^1B(x));\ x\ 2\ U$$

Based on the intersection definition of two fuzzy sets, it is possible to introduce the notion of possibility (also called consistency or consensus) which is the fundament of the possibility theory which is briefly treated in Subsection 2.5.1. The possibility of two fuzzy sets, which determines the agreement degree between the concepts represented by the fuzzy sets, measures to what extent the fuzzy sets superpose each other and is defined as the highest membership degree of the intersection of these two fuzzy sets. In the case of Zadeh's definition of the intersection this operation is called the max-min operation since it considers the maximum of the minimum values of the fuzzy sets.

VI. APPLICATIOS FIELD

The fuzzy set theory has been successfully applied in various domains. The most important application areas are the fuzzy control, the fuzzy diagnosis, the fuzzy data analysis and the fuzzy classification. This section aims to explicit the implication of the fuzzy set theory in some of these domains [8]. First, Subsection introduces the possibility theory as a basis for the approximate reasoning which allows the integration of the natural language into the reasoning process. Based on the approximate reasoning, Subsection presents the fuzzy control theory in comparison to the modern control theory. Examples of fuzzy diagnosis and fuzzy data analysis areas are fuzzy expert systems depicted in Subsection and the fuzzy classification approach presented [9] Last but not least, Subsection presents different approaches which enable the representation and the storage of the imprecision, i.e. fuzzy databases systems.

Nowadays a large number of real-world applications take advantages of the approximate reasoning. Many other applications fields could have been discussed like the neural networks, the genetic algorithms, the evolutionary programming, the chaos theory, etc., but their presentation is beyond the scope of this thesis.

VII. Query Cost of Classical Query Over Classical Database

The necessary steps require to retrieve a record from classical database by suing fuzzy queries, this are given below,

Procedure find (value V)
Set C=root node
While C is not a leaf node begin

Let Ki=smallest search key value, in any greater than V

If there is no such value then begin

Let m= the number of pointers in the node

Set C= node pointed to by Pm

End

Else set C=the node pointed to by Pi

End

If there is a key value Ki in C such that Ki=V

Then pointer Pi directs us to the desired record

Else no record with key value k exists

End procedure.

For example, the fuzzy query

Q "fined the all account numbers whose balance is very high"

The output of this query statement is shown in Table 1

Table 1: Output of query statement Q.1

A_no	A_name	B_name	Balance	F_Balance	L_Balance
2008	Karim	Chittagong	25000	1	Very high

In our example, k=2, n=4, m=1.

$$\text{The query cost} = \left(\log\left\lceil\frac{4}{2}\right\rceil 2+1\right)\times(4+0.1)$$

$$= (1+1)\times(4+0.1)$$

$$= 2\times 4.1$$

$$= 8.2\text{ms}$$

As a result we can say that, classical query over classical database and fuzzy query over classical database require the same time for search a key. But our propose implication fuzzy query over fuzzy database reduce time for search a key.

VIII. Conclusion

Recently there exists a huge application of fuzzy sets and their properties and one of those is databases. Fuzzy sets represent basement of fuzzy database systems, which lead to further step of joining computer systems and human. They bring opportunity to query data by language close to human speech. This paper focuses on fuzzy query. We explained fuzzy sets, fuzzy logic form of storage fuzzy data, parallelism of query operators and fuzzy SQL. Current fuzzy database systems are extension to actual database systems, which allows applying fuzzy terms into the systems using Boolean logic. This paper designs classical query in classical database, fuzzy query in classical database and fuzzy query in fuzzy database and calculates the query cost. In classical database system, it has only one index file to save the information. If search a record in classical database, it search the approximately n records. As a result it requires more time than other query. Fuzzy query in classical database requires the same time as the classical query in classical database. This research proposes implication of fuzzy query in fuzzy database and creation of nine index files to save the records.. So if any record is required that is represented by the linguistic term not so moderate then it directly goes to not so moderate index file. So extra time to compute fuzzy value is not killed during search any record from the database. So, we can say that, searching time of one record from the fuzzy database using fuzzy query is also reduced. This time is more effective when the database is so large and the node size is also large.

IX. Acknowledgements

We are earnestly grateful to one our group member, Md. Galib Anwar, Graduated, Department of EEE, American International University-Bangladesh. For providing us with his special advice and guidance for this project. Finally, we express our heartiest gratefulness to the Almighty and our parents who have courageous throughout our work of the project.

REFERENCES

[1] Ndress Meier, Nicolas Werro, Martain Albrecht, Fuzzy Classification Query Language for Customer Relationship Management.
[2] Liberios Vokorokos, Anton Balaz, Norber Adam, Parallelism in fuzzy Database, Teach media, 5th Edition, 5th Edition, 2006.
[3] A. H. M. Sejedul Haque , Data Mining using Fuzzy Associative Rules.
[4] Rabindra Nath Shil & Subash Chandra Debnath, An Introduction to the Theory of Statistics.
[5] N. Werro, A. Meier, C. Mezger, and G. Schindler. Concept and Implementation of a Fuzzy Classification Query Language. In Proceedings of the International Conference on Data Mining, DMIN 2005, World Congress in Applied Computing, pages 208_214, Las Vegas, USA, June2005.
[6] N. Werro, H. Stormer, and A. Meier. Personalized Discount _ A Fuzzy Logic Approach. In Proceedings of the 5th International Federation for Information Processing Conference on eBusiness, eCommerce and eGovernment, I3E 2005, pages 375_387, Poznan, Poland, October 2005.
[7] Y. Takahashi. A Fuzzy Query Language for Relational Databases. In P. Bosc and J. Kacprzyk, editors, Fuzziness in Database Management Systems, volume 5 of Studies in Fuzziness, pages 365_384. Physica Publisher, Heidelberg, 1995.
[8] A. Meier, C. Savary, G. Schindler, and Y. Veryha. Database Schema with Fuzzy Classification and Classification Query Language. In Proceedings of the International Congress on Computational Intelligence _ Methods and Applications, CIMA 2001, pages 1-7, Bangor, UK, June 2001.
[9] A. Meier, G. Schindler, and N. Werro. Fuzzy Classification on Relational Databases. In J. Galindo, editor, Handbook of Research on Fuzzy Information Processing

American Journal of Engineering Research (AJER) 2015
American Journal of Engineering Research (AJER)
e-ISSN: 2320-0847 p-ISSN : 2320-0936
Volume-4, Issue-8, pp-186-190
www.ajer.org
Research Paper Open Access

Secured UAV based on multi-agent systems and embedded Intrusion Detection and Prevention Systems

K.Boukhdir[1], F.Marzouk[1], H.Medromi[1], S.Tallal[1], S.Benhadou[1]
[1](Systems Architecture's Team, ENSEM)

ABSTRACT : *Unmanned aerial vehicles, or drones, are a relatively recent area of research and in full effervescence with more and more amateur and academic projects. Initially associated to the military, these vehicles are way to be used in many other areas. In effect, demand is growing for various applications within of this type of technology. Inspection of buildings, search and rescue of missing or in distress people are some examples. This research paper highlights a lightweight intrusion detection system with the objective to secure UAVs. Our IDP(Intrusion and Prevention System) uses real-time architecture, based on the multi-agent systems so it can be autonomous and distributed between the ground control station(GCS) and the UAV is more suited to be embedded in low computation resources devices in general and especially UAVs.*

Keywords *-UAV security, Intrusion and Prevention systems, multi-agent systems.*

I. INTRODUCTION

The main goal of the project is to create a secure UAV (Unmanned Aerial Vehicle), stable and efficient, operating in several modes: full autonomy (Autopilot), partial autonomy (planning instant flight) or instant driving.The UAV includes a set of features and equipment, enabling it to undertake different kind of tasks like flying in tactical or strategic objective, recognition, monitoring objectives or inspection. Furthermore, our drone must be secured against all types of attacks that may arise. However, some security techniques do not translate well to embedded systems, where constraints such as low-power, low-memory, and real-time operations may impact the computational capability of the system. The need to secure systems that express complex logic is well understood and presents many challenges –strict timing requirement, computational and storage limitation, adaptability and ubiquitous presence. Our security model is characterized by its board and lightweight nature insofar as it helps to ensure a level of security - confidentiality, integrity and availability- without soliciting too many computational resources.Existing intrusion detection and prevention systems undergo the following problems: intrusion detection system cannot detect and block all the malicious traffic; signature database are not updated on a regular basis; different intrusion detection and prevention systems are not interoperable; and most of all they are not suitable to protect embedded systems because due to structural problems, in other aspects of the architectures can not meet the strict timing and restriction in resources. In this paper, we present a modular and extensible approach to building a system helps solve the complex problems in an embedded intrusion and detection system. It divides the problem into the aspects of information gathering, pre-processing and classification, analysing and configuration. Lightweight agents have been developed to retrieve information from the ground control station, classify and analyse the data and prevents threats, and stores the logs into a database. We also demonstrate how dynamic agents provides a convenient mechanism for extending existing objects and allows us to quickly add new features to the system.

II. BACKGROUND

The extensive use of information and communication technologies (ICT) to solve complex, significant-applied problems has profoundly affected critical infrastructures and systems conception. Such evolutions implicate the exposition to new kinds of security threats. Moreover, the dependence to those technologies has become critical due to the evolution and development of networks in terms of users and provided services. However the need to secure systems that express complex logic is well understood and presents many challenges [1] –strict timing requirement, computational and storage limitation, adaptability and ubiquitous presence for data analysis and monitoring- that have nothing new for security experts. Afterwards, the traditional intrusion detection paradigm based on a hypervisor to create a safe environment from which a analyze entity can operate is impractical to secure critical infrastructures

However, some security techniques do not translate well to embedded systems, where constraints such as low-power, low-memory, and real-time operation may impact the computational capability of the system [5].

A. State Of The Art.

While many work have been done to secure various kinds of wireless based communication like sensor networks (WSN) [6]-[7]-[15] and mobile ad-hoc networks [8], these models cannot be useful to secure usual UAVs. Modeling of UAVs communication is harder and distinctive from other networks for its wider complexities and vast discrepancy in various properties. The use of different channels of different type, the various range of communications (short/long), different power requirements for different components, different types of traffic flows involving commands, video, audio, image and more, the disponibility and integrity and confidentiality requirements, are roughly the features which make security requirements of a UAV dissimilar from other state of the art systems.

Very little research to date has been done to secure UAVs and their communication with the GCS (Ground Control Station) and this resulted in many attacks to those systems. In the next chapter we have reported some of the knows attacks against UAVS

B. Known attacks

Till 1997 there were reports about cyber-attacks targeting UAV systems throughout the world. This is due to the relatively recent of use of those systems in the developed nations. Israeli experts [10] recently determined that the Hezbollah leader Hassan Nasrallah and claims taken over - by an IDF (Israel Defense Forces) drone in the scene of Squadron 13 Banzriih night between 4 and 5 September 1997 are authentic. Nasrallah explained that his organization had intercepted the filming at the time, and that it allowed its fighters to ambush the soldiers [11]. In 2009, the arrest of a terrorist group leads to the detection of the recording of UAV video. The unencrypted video footage was assembled by the terrorists using software called SkyGrabber, which is used to capture satellite data using a satellite antenna [9].

In December 2011 members of Iran's elite Revolutionary Guards put on show a US unmanned aerial vehicle they claimed to have brought down electronically. US officials later confirmed the aircraft was captured in Iran but insisted it malfunctioned and was not hijacked. [12].

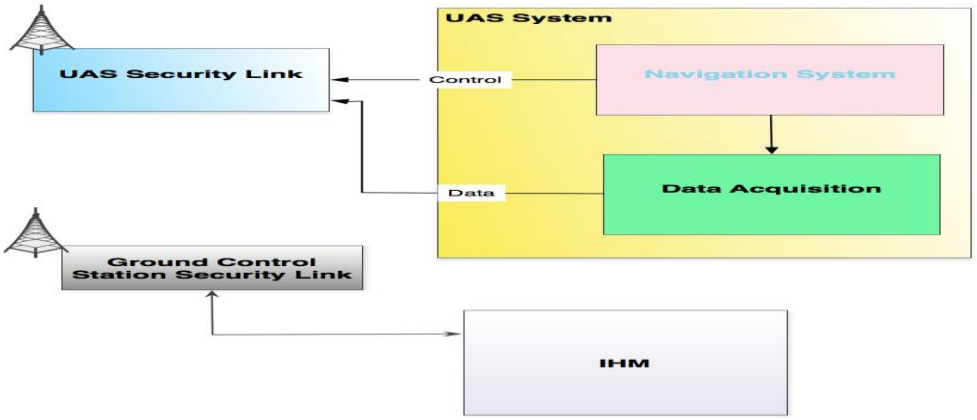

Figure 1 UAV Architecture with security links

III. SYSTEM DESIGN

The system is designed to deliver highmanoeuvrability – vertical Take Off and Landing (can land on very small areas) and able to perform stationary/slow flight (useful to perform long time tasks in the same position) and can easily fly in small and cluttered environment by performing hovering and slow motion.

The hexacopter can be flown in different modes using manual/autonomous control. In the standard mode, hexacopter attitude (roll and pitch), yaw rate and thrust is manipulated with a standard flight radio RC Transmitter, whilist in the autonomous mode, the attitude and thrust are being calculated using the autopilot module wich use a set of data fusion using sequences of PID and some extended filters (figure 2).

To ensure that our security solution won't affect the control system, which needs finely grained timing like controlling the throttle, we plugged it as an expansion board that runs real time Linux. We separated the low-level control loops (PIDs) and all the sensing and filtering that are considered time critical stuff to the autopilot hardware and then run highlevelintrusion detection on the embedded linuxon the Raspberry Pi Card.

III.2. Agents and multi-agent sytems

Agents can push further the level of abstraction and the flexibility of component coupling, notably through self-organization abilities.

An agent is anything that can be viewed as perceiving its environment through sensors and acting upon that environment through its effectors to maximize progress towards its goals [2][3].

Multi-agent Systems have emerged as one of the most promising solution to cater for the complex, robust[16], and reliable security processes. (Ferber, 1999; Stone &Veloso, 2000; Sycara, 1998; Weiss, 1999) have suggested that MASs are well suited for applications that are distributed, complex, modular, scalable and flexible, where problems in the security fields exhibit these characteristics [3].

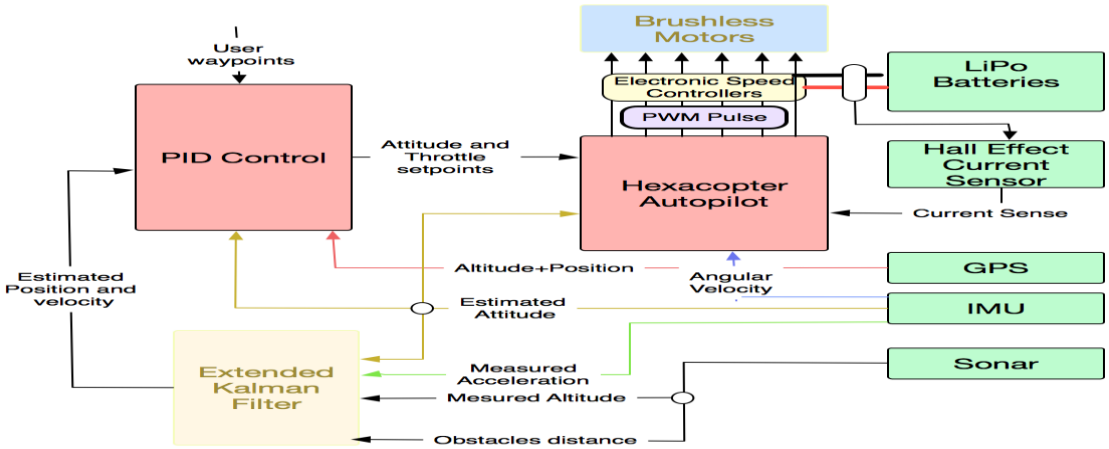

Figure 2 Autopilot design

III.2. UAV IDPS Engine agents Architecture

To overcome the deficits of traditional IDPS systems, the software design use an effective lightweight detection technology witch is the pre-filtering combined with full analysis. The overall structure of the agents composing the IDPS Engine is shown in Figure 3.

Listener Agent is purely a reactive agent with the charge of capturing traffic data. The continuous traffic flows between the GCS and the drone is captured in order to be sent to the preprocessor Agent for processing.

Preprocessor Agent: after receiving traffic data from the listener, it's pre-processed in order to be analyzed. Once the data has been pre-processed, it's sent to the analyzer agent. The task of a preprocessor is to segment the traffic, remove excessive information, defragmentation, checksum validation, connection tracking, and stream re-assembly. And convert into a form that can be feasibly processed by the Analyzer Agent.

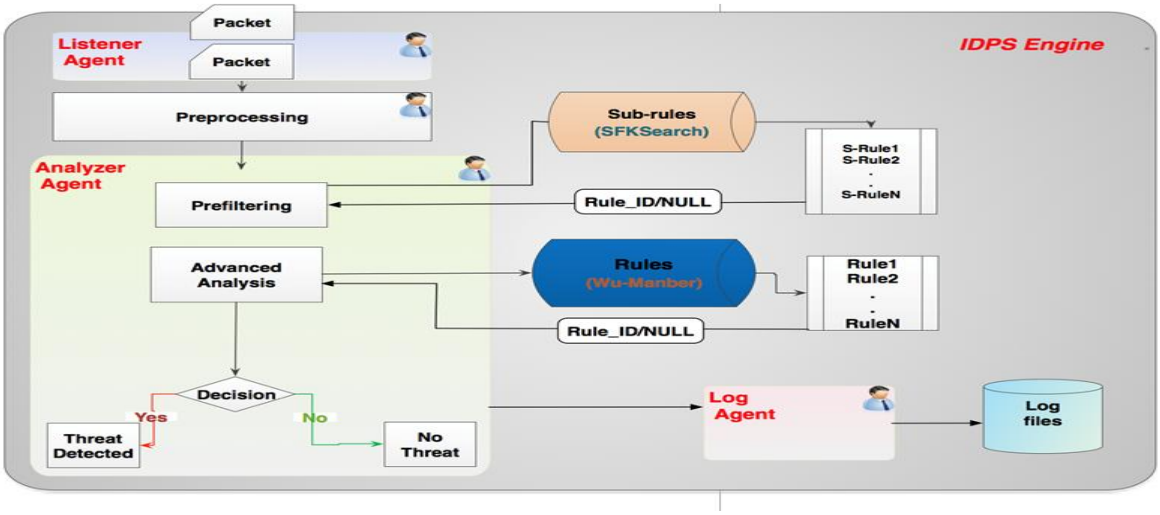

Figure 3 IDPS Engine Architecture

AnalyzerAgent: This intelligent agent is embedded in the analyze stage in order to investigate the pre-processed traffic data. Preprocessed incoming data arrive to the pre-filtering sub-module, which reveals the probably activated rule in a set of sub-rules using the algorithm SFKSearch[13][14]. This algorithm builds a tree and each level in the tree is a sequential list of sibling nodes that contain a pointer to matching rules, a character that must be matched to traverse to their child node, and a pointer to the (next) sibling node. The algorithm uses a bad character shift table to advance through search text until it encounters a possible start of a match string, at which point it traverses the tree looking for matches. If there is a match between the character in the current node and the current character in the packet, the algorithm follows the child pointer and increments the character packet pointer. Otherwise, it follows the sibling pointer until it reaches the end of the list, at which point it recognizes that no further matches are possible. In the case that matching fails, the algorithm backtracks to the point at which the match started, and now considers matches starting from the next character in the packet.

In the worst case, the SFKSearch algorithm can make L · P memory references where L is the length of the longest pattern string and P is the length of the packet examined.

If in the pre-filtering stage a rule has already been activated, the information's about the rule are reported to the advanced analysis sub-module. This sub-module is responsible for content matching and deep analyzing by using the Wu-Manber[13][14]algorithm. This algorithm starts by pre-computing two tables, a bad character shift table, and a hash table. When the bad character shift fails, the first two characters of the string are indexed into a hash table to find a list of pointers to possible matching patterns. These patterns are compared in order to find any matches and then the input is shifted ahead by one character and the process repeats.

An interface between the pre-filtering and the advanced analysis sub-module should be used to feed the advanced analysis sub-module with the identification (ID) of the matched sub-rules and their exact position in the rule database.

Log Agent: This agent is responsible for storing and maintaining the log data in order to be used to generate detailed reports about the communication and the threats detected. This log is also needed to check the performance of the IDPS Engine by studying it.

The IDPS Engine assures near real-time analyses by analyzing information sources gathered by the listener agent on a real-time basis. Thus, it is important to provide responses before an attacker significantly damages the systems.

III.3. Summary

The proposed architecture ensures that the IDPS is using the minimal resource in the systems when monitoring. In fact, the minimal resource could avoid the shortage of the systems resource and prevent the system from possible crash caused by overloading. In order to respect real time constraint and to use the minimal possible resources in the system, the pre-filtering agent witch uses a set of sub-rules extracted from full rules and a very efficient matching algorithm (SFKSearch). The most complicated task of the pre-filtering is to figure out an effective way to generate a tiny rule (sub-rule) of the each original intrusion detection rule-set and that the sub-rule must be representative of the full rule so that the amount of activated rules in the Pre-filtering phase would be as significant as possible.

IV. EXPERIMENTAL RESULTS

To test our architecture, we used a Raspberry Pi computer (ARM1176JZF-S CPU and 512 MB SDRAM) embedded in our UAV. The performance of the Raspberry Pi computer is far too low compared to a usual computer with high computational power, but the fact that it weights less than 45 g (1.6 oz) and its battery very low battery consumption makes it more suitable to be embedded in a UAV in order to host our lightweight IDPS.

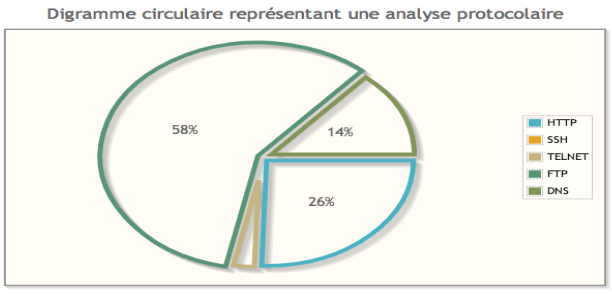

Figure 4 : Report Chart

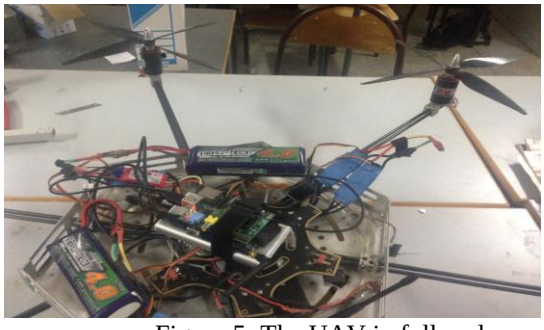

Figure 5: The UAV in full scale

We tested our IDPS against several threats techniques. Most of the threats tested are samples that help demonstrate the capabilities and the efficacy of the detection and prevention approach. Those threats code were written with the only purpose to test the platform and the test was conducted mainly while embedding the system in the UAV (Fig.4). Fig.5 shows screenshots of the result after testing the IDPS with a set covering a large scope of attacks (badTraffic, evasionTechniques, shellCodes, DOS/DDOS) and a ruleSet which are basic rules testing. These attacks are supposed to be detected by the rules sets shipped with the IDPS.

V. CONCLUSION

Intrusion detection and prevention systems are a good solution to mitigate threats but the state of the art IDPSs are not suitable to protect embedded systems because due to structural problems, like strict timing and restriction in resources.In this paper, we presented a modular and extensible approach to building a system helps solve the complex problems in an embedded intrusion and detection system that divides the problem into the aspects of information gathering, pre-processing and classification, analysing and configuration. The use of lightweight agents helped modularizing the platform in order to make it more suitable for embedded devices.

However an overall security threat analysis of the UAVs system must be conducted to mitigate other threats like GPS spoofing and signal jamming and also expand the platform to help secure the ground control station (GCS).

REFERENCES

[1] J. Reeves, AshwinRamaswamy, Michael Locasto, Sergey Bratus, Sean Smith "Intrusion detection for resource-constrained embedded control systems in the power grid Original Research Article" International Journal of Critical Infrastructure Protection, Volume 5, Issue 2, July 2012, Pages 74-83

[2] Book Chapter in the book "Multi-AgentSystems - Modeling, Control, Programming, Simulations and Applications", ISBN 978-953-307-174-9, InTech, April4, 2011

[3] CHAIB-DRAA : « Systèmesmultiagents : Versuneapprocheformellebaséesurl'action et l'interaction » Décembre 2009.

[4] A. Sayouti and H. Medromi. "Autonomous and Intelligent Mobile Systems based on Multi-Agent Systems".

[5] P. Kocher, et al., Security as a new dimension in embedded system design, in: 41st Design Automation Conference, 2004.

[6] Bo Sun; Osborne, L.; Yang Xiao; Guizani, S., "Intrusion detection techniques in mobile ad hoc and wireless sensor networks," Wireless Communications, IEEE , vol.14, no.5, pp.56,63, October 2007

[7] Esfandi, A., "Efficient anomaly intrusion detection system in adhoc networks by mobile agents," Computer Science and Information Technology (ICCSIT), 2010 3rd IEEE International Conference on , vol.7, no., pp.73,77, 9-11 July 2010.

[8] Patrick Traynor, Kevin Butler, William Enck, Patrick McDaniel, Kevin Borders, "malnets: large-scale malicious networks via compromised wireless access points", Journal of Security and Communication Networks, Special Issue on Security in Mobile Wireless Networks, Vol. 3, Issue 2-3, June 2010.

[9] AvielMagnezi, "The Naval Disaster Report", ynet 01/07/14 http://www.ynet.co.il/articles/0,7340,L-3980739,00.html.

[10] YAAKOV KATZ 06/12/2012 "IDF encrypting more drones amid hacking concerns" http://www.jpost.com/Defense/IDF-encrypting-more-drones-amid-hacking-concerns.

[11] SIOBHAN GORMAN, YOCHI J. DREAZEN and AUGUST COLE Dec. 17, 2009 "Insurgents Hack U.S. Drones" http://online.wsj.com/news/articles/SB126102247889095011

[12] CNN Wire Staff, "Obama says U.S. has asked Iran to return drone aircraft", http://www.cnn.com/2011/12/12/world/meast/iran-us-drone

[13] BenfanoSoewito et al. / International Journal of Engineering Science and Technology (IJEST)

[14] Nathan Tuck et al. "Deterministic Memory-Efficient String Matching Algorithms for Intrusion Detection",

[15] O. Kachirski, R.K. Guha, Effective intrusion detection using multiple sensors in wireless ad hoc networks, in: Proceedings of HICSS, 2003, 57 pp.

[16] M. Fisk, G. Varghese, Fast content-based packet handling for intrusion detection, Tech. Rep. CS2001-0670, Department of Computer Science, University of California, San Diego, May 2001.

American Journal of Engineering Research (AJER) 2015
American Journal of Engineering Research (AJER)
e-ISSN: 2320-0847 p-ISSN : 2320-0936
Volume-4, Issue-8, pp-191-195
www.ajer.org
Research Paper Open Access

Queuing Model for Banking System: A Comparative Study of Selected Banks in Owo Local Government Area of Ondo State, Nigeria

[1]Raimi Oluwole Abiodun & [2]Nenuwa Isaac Omosule
[1]*M.Tech Student, Mechanical Engineering Department, Federal University of Technology, Akure, Nigeria*
[2]*Assistant Lecturer, Mechanical Engineering Department, Rufus Giwa Polytechnic, Owo, Nigeria*

ABSTRACT: *Comparative study of two selected banks (Wema & Skye Bank) in Owo Local Government Area of Ondo state was investigated. The research study employed a queuing model for both banking system to measure the behavioural queuing characteristics of customers in terms of their arrival and service rate respectively. The data for the arrival and service rate of the two banks were collected simultaneously at the space of three days. The data collected was also analysed separately with respect to the queuing theory parameters ($L_s, L_q, W_s, and\ W_q$). Findings showed that Wema bank has a high waiting service time value (0.019%) which may have a negative significant effect on customers on waiting lines. When compared with Skye bank, we realized that Skye bank has an advantageous effect of service time value (0.000022%) which will have a positive significant effect on customers in experiencing little or no queue at all. This clearly indicates that for optimum efficiency in the banks, there is need to increase the number of servers. Also, the result of the respective banks shows that waiting lines reduces when the number of servers increases. The analysis in this study is very effective and practical, and is hereby recommended for the management of the banks to review for better efficiency and performance.*

KEYWORDS: *Queuing model, Banking system, Waiting lines, Customers, Owo*

Notations

P_n = Probability of exactly n customers in the system
L_s = Expected number of customers in the system
L_q = Expected number of customers in the queue
W_s = Average time a customer spends in the system
W_q = Expected waiting time of customers in the queue
X = Number of servers
λ = The mean arrival rate(Expected number of arrival per unit time)
μ = The mean service rate for overall systems

I. INTRODUCTION

Challenges encountered by most commercial or business organisation are the problem of waiting lines. It is so serious that most customers complained of lack of special treatment and care by the management of the commercial organisation. There is need to give customers a special care during service delivery because when a particular customer is satisfied to a certain level, all available customers are attracted to the organisation, this brings about the expected high profit.

Kasum *et al.*, (2006) evaluated queue efficiency in Nigeria banks through comparative analysis of old and new generation banks. Their study employ a primary data collected from selected bank through a well structured questionnaire along the inverted funnel method. The questionnaires were administered by the customers of the banks. Their findings showed that time spent on queue for services in old generation bank is in aggregate longer than in the new generation bank. Also, their findings showed that new generation banks are more efficient in timely service delivery than the old generation banks.

Pei-Chun *et al.,* (2006) examined the service efficiency of 26 banking institutions in Taiwan (including the postal banking services) through the application of queuing theory by evaluating service efficiency of ATMs functions composed of cash withdrawal, fund transferring, password alternations and balance inquiry. They fitted a queuing model for evaluating the service efficiency of ATMs. They collected a field data from July to August 2004. Their findings suggested that some bank should add more ATMs to reduce customer waiting time.

Tian *et al.,* (2011) examined the queuing system of bank based on business process reengineering. They evaluated the bottleneck problems of bank queuing as well as the concept, classification and methodologies of business process reengineering. They used simulation method to analyse the number of open servers of the bank system. Their findings showed that if the bank use simulating method to determine the number of open servers by referring to dynamic statistics; it will improve much in flexibility and make full use of the current resources.

Toshiba *et al.,* (2013) established an optimization model of queuing theory for the improvement of bank service. In their study, they converted the M/M/Z∞FCFS model into M/M/1/∞FCFS to know which one is more efficient, a line or more lines. Their findings showed that the efficiency of commercial banks is improved by the queuing number, the service stations number, and the optimal service rate; therefore making the results effective and practical, and increasing customer satisfaction.

II. METHODOLOGY

Optimization Method

The study made use of two selected banks in Owo Local Government Area of Ondo State, Nigeria. The banks are Wema Bank and Skye Bank respectively. The queuing system in the selected banks is the bank service system. The following assumptions were made for the queuing system at the selected banks, in accordance with the queuing theory:

- Poisson arrival rate of λ customers per unit of time.
- Exponential service times of μ customer per unit of time.
- Queue discipline is first come first served basis by any of the server.
- The waiting line has two or more identical servers.
- There is no limit to the number of the queue (infinite).
- The average arrival rate is greater than average service rate.

Model Formulation

All the model adoption in this work is the (M/M/X): (∞/FCFS) Multi Server Queuing Model. This is the extensional form of single server model where customer in a waiting line can be served by more than one server simultaneously. There are n numbers of customers in the queuing system at any point in time. If n<X, (number of customers in the system is less than the number of servers), then there will be no queue. However, X–n number of servers will not be busy. The combined service rate will then be $\mu n = n\mu$; n<X. And, if n≥X (number of customers in the system is more than or equal to the number of servers) then all servers will be busy and the maximum number of customers in the queue will be n – X. The combined service rate will be $\mu n = X\mu$; n ≥X.
Following are the properties of the Multi-Server Queuing Model:
Utilization factors i.e. the fraction of time servers are busy:

$$\rho_X = \frac{\lambda}{X\mu} \qquad (1)$$

The probability of having n customers in the system is given by:

$$P_0 = \left[\sum_{n=0}^{X-1} \frac{1}{n!}\left(\frac{\lambda}{\mu}\right)^n + \frac{1}{X!}\left(\frac{\lambda}{\mu}\right)^Z \frac{X\mu}{X\mu-\lambda}\right]^{-1} \qquad (2)$$

$$P_n = \begin{cases} (\rho^n/n!)P_0 & n \le X \\ \rho^n/(X!X^{n-X})P_0 & n > X \end{cases} \qquad (3)$$

When n≥Z, it is that the number of customers in the system is not smaller than the number of servers, the next customers must wait, that is,

$$C(X,\rho) = \sum_{n=X}^{\infty} P_n = \frac{\rho^X}{X!(1-\rho_X)} P_0 \qquad (4)$$

Expected number of customers waiting on the queue:

$$L_q = \left[\frac{1}{(X-1)!}\left(\frac{\lambda}{\mu}\right)^X \frac{\mu\lambda}{(X\mu-\lambda)^2}\right] P_0 \qquad (5)$$

Expected number of customers in the system:

$$L_s = L_q + \frac{\lambda}{\mu} \qquad (6)$$

Expecting waiting time of customers in the queue:

$$W_q = \frac{L_q}{\lambda} \quad (7)$$

Expecting waiting time of customers in the system:

$$W_s = \frac{L_s}{\lambda} \quad (8)$$

Data Analysis

The collected data for the two banks use in this research study were collected simultaneously at the same time range. The data is collected for three days and it comprises the arrival and service rate of customers. The data values for the arrival and service rate for the two banks is shown below:

Table 1: Wema Bank

Arrival Rate	Service Rate
77	69
43	36
49	43

Source: Authors Computation

Overall arrival rate of the Wema bank system is:

$\lambda_T = \lambda = \lambda_1 + \lambda_2 + \lambda_3$

$\lambda = 77 + 41 + 49 = 169$

Overall service rate of the Wema bank system is:

$\mu_T = \mu = \mu_1 + \mu_2 + \mu_3$

$\mu = 69 + 36 + 43 = 148$

Table 2: Skye Bank

Arrival Rate	Service Rate
125	89
94	77
123	85

Source: Authors Computation

Overall arrival rate of the Skye bank system is:

$\lambda_T = \lambda = \lambda_1 + \lambda_2 + \lambda_3$

$\lambda = 125 + 94 + 123 = 342$

Overall service rate of the Skye bank system is:

$\mu_T = \mu = \mu_1 + \mu_2 + \mu_3$

$\mu = 89 + 77 + 85 = 251$

The numbers of server (X) for the two banks are not the same. For Wema bank, the number of servers is 7, while for Skye bank, the number of server is 11.

Estimating Queuing Parameters for Wema Bank

Let's assume 7 waiting lines for the customer in the bank.

When there is a line, $X = 7, \lambda = 169, \mu = 148, \rho = \frac{169}{148}, n = 0, 1, 2, \ldots, 6.$

$$P_0 = \left[\sum_{n=0}^{X-1} \frac{1}{n!}\left(\frac{\lambda}{\mu}\right)^n + \frac{1}{X!}\left(\frac{\lambda}{\mu}\right)^X \frac{X\mu}{X\mu - \lambda}\right]^{-1}$$

Where:

$$\sum_{n=0}^{X-1} \frac{1}{n!}\left(\frac{\lambda}{\mu}\right)^n = 3.1322$$

$$P_0 = \left[3.1322 + \frac{1}{7!}\left(\frac{169}{148}\right)^7 \frac{7\times148}{(7\times148)-169}\right]^{-1} = 0.3192$$

$$L_q = \left[\frac{1}{(7-1)!}\left(\frac{169}{148}\right)^7 \frac{148\times169}{[(7\times148)-169)^2}\right] \times 0.3192 = 0.000038$$

$$L_s = L_q + \frac{\lambda}{\mu} = 0.000038 + \frac{169}{148} = 1.1419$$

$$W_s = \frac{L_s}{\lambda} = 0.0068$$

$$W_q = \frac{L_s}{\lambda} = \frac{0.000038}{169} = 0.0000002$$

When there are two lines, $\frac{\lambda}{2} = 84.5, \mu = 148, \rho = 0.5709$

$L_s = \frac{\rho}{1-\rho}$ =1.3305

$L_q = \frac{\rho^2}{1-\rho}$ =0.7596

$W_s = \frac{1}{\mu-\lambda}$ =0.0157

$W_q = \frac{\rho}{\mu-\lambda}$ =0.0090

Similarly, the analysis is same for, when the lines are 3, 4, 5, 6, & 7 respectively.

The Table 3 gives the summary of the queuing parameters of the assumed number of lines to the bank if the number of servers remains unaltered.

Probability that an arriving customer or customers will have to wait for service at the bank is given by the formula:

$P_w = \left(\frac{\lambda}{\mu}\right)^X \frac{P_0}{X!\left(1-\frac{\lambda}{X\mu}\right)}$

Where: $X = 7;\ \lambda = 169;\ \mu = 148;\ P_0 = 0.3192;$ *by substituting into the formula,*

$P_w = 0.00019$ *or* 0.019%.

Estimating Queuing Parameters for Skye Bank

Let's assume 11 waiting lines for the customer in the bank.

When there is a line, $X = 11, \lambda = 342, \mu = 251, \rho = \frac{342}{251}, n = 0, 1, 2, \ldots, 10.$

$P_0 = \left[\sum_{n=0}^{X-1} \frac{1}{n!}\left(\frac{\lambda}{\mu}\right)^n + \frac{1}{X!}\left(\frac{\lambda}{\mu}\right)^X \frac{X\mu}{X\mu-\lambda}\right]^{-1}$

Where:

$\sum_{n=0}^{X-1} \frac{1}{n!}\left(\frac{\lambda}{\mu}\right)^n = 3.9061$

$P_0 = \left[3.9061 + \frac{1}{11!}\left(\frac{342}{251}\right)^{11} \frac{11\times342}{(11\times251)-342}\right]^{-1} = 0.2560$

$L_q = \left[\frac{1}{(11-1)!}\left(\frac{342}{251}\right)^{11} \frac{251\times342}{[(11\times251)-342)^2}\right] \times 0.2560 = 0.000000031$

$L_s = L_q + \frac{\lambda}{\mu} = 0.000000031 + \frac{342}{251} = 1.3625$

$W_s = \frac{L_s}{\lambda} = 0.0040$

$W_q = \frac{L_s}{\lambda} = \frac{0.000000031}{342} = 0.000000000091$

When there are two lines, $\frac{\lambda}{2} = 171, \mu = 251, \rho = 0.6813$

$L_s = \frac{\rho}{1-\rho}$ =2.1377

$L_q = \frac{\rho^2}{1-\rho}$ =1.4564

$W_s = \frac{1}{\mu-\lambda}$ =0.0125

$W_q = \frac{\rho}{\mu-\lambda}$ =0.0085

Similarly, the analysis is same for, when the lines are 3, 4, 5, 6, 7, 8, 9, 10, & 11 respectively.

The Table 4 gives the summary of the queuing parameters of the assumed number of lines to the bank if the number of servers remains unaltered.

Probability that an arriving customer or customers will have to wait for service at the bank is given by the formula:

$P_w = \left(\frac{\lambda}{\mu}\right)^X \frac{P_0}{X!\left(1-\frac{\lambda}{X\mu}\right)}$

Where: $X = 11;\ \lambda = 342;\ \mu = 251;\ P_0 = 0.2560;$ *by substituting into the formula,*

$P_w = 0.00000022$ *or* 0.000022%.

Table 3: The queuing system characteristics of Wema bank

Number	λ	μ	L_s	L_q	W_s	W_q
1	169	148	1.1419	0.000039	0.0068	0.0000002
2	84	148	1.3305	0.7596	0.0157	0.0090
3	56	148	0.6145	0.2339	0.01091	0.0042
4	42	148	0.4072	0.1144	0.0095	0.0027
5	33	148	0.2960	0.0676	0.0088	0.0020
6	28	148	0.2350	0.0447	0.0083	0.0015
7	24	148	0.1949	0.0318	0.0081	0.0013

Source: Authors Computation

Table 4: The queuing system characteristics of Skye bank

Number	λ	μ	L_s	L_q	W_s	W_q
1	324	251	1.3625	0.000000031	0.0040	0.000000000091
2	171	251	2.1377	1.4564	0.0125	0.0085
3	114	251	0.8322	0.3780	0.0073	0.0033
4	85	251	0.5165	0.1759	0.0060	0.0021
5	68	251	0.3746	0.1021	0.0055	0.0015
6	57	251	0.2937	0.0667	0.0052	0.0012
7	48	251	0.2416	0.0470	0.0049	0.00096
8	42	251	0.2053	0.0350	0.0048	0.0008
9	38	251	0.1784	0.0270	0.0047	0.0045
10	34	251	0.1578	0.0215	0.0046	0.00060
11	31	251	0.1414	0.0175	0.0045	0.00056

Source: Authors Computation

III. DISCUSSION OF FINDINGS

The comparative analysis of the two banks under review differs significantly with respect to the queuing theory. The result of the respective banks shows that waiting lines is highly reduced if the number of servers is drastically increased so as to satisfy customers at an optimum advantage. Based on the number of servers of the two banks, when an arriving customer will have to wait until he or she is attended to, Wema bank has the highest waiting probability service value (0.019%) when compared with Skye bank value (0.000022%). This value indicates that for optimum efficiency in the bank, there is need to increase the service station. This gave Skye bank a practical advantage over Wema bank that no queue exists in their banking system. That is, the probability that a customer will have to wait is very infinitesimal when compared with Wema bank. This can also be seen in the parameters of the queuing theory under consideration that the expected number or waiting time of customers on the queue or in the banking system reduces irrespective of the waiting lines. The higher the number of servers, the lesser the waiting lines, the lower the number of servers, the more the waiting lines. This is the practical cause of the two banks in this research study.

IV. CONCLUSION

The queuing number, the number of servers, and the optimal probability service as investigated by means of queuing theory are the three measures that improve the efficiency of commercial banks. The analysis in this study as carried out by the two banks is effective and practical. It was also investigated that the optimal queuing model is feasible.

REFERENCES

[1] Kasum, A. S., Abdulraheem, A., & Olaniyi, T.A., (2006):" Queue Efficiency in Nigeria Banks: A Comparative Analysis of Old and New Generation Banks". *Ilorin Journal of Sociology*, Vol.2, No.1, pp 162-172. ISSN II7-9448I, June.

[2] Pei-Chun, L., & Ann, S.Y., (2006): "Service efficiency evaluation of automatic teller machines- a study of Taiwan financial institutions with the application of queuing theory". *Journal of Statistics and Management Systems*, Vol.9, No.3, pp 555-570.

[3] Tian, H., & Tong, Y., (2011):" Study on Queuing System Optimization of Bank Based on BPR". 3rd *International Conference on Environmental Science and Information application Technology (ESIAT)*, Pp 640-649, Available online at: www.sciencedirect.com

[4] Toshiba, S., Sanjay, S., & Anil, K.K., (2013):" Application of Queuing Theory for the Improvement of Bank Service". *International Journal of Advanced Computational Engineering and Networking*, Vol. 1, issue 4, pp 15-18. ISSN 2320-2106, June

American Journal of Engineering Research (AJER) 2015
American Journal of Engineering Research (AJER)
e-ISSN: 2320-0847 p-ISSN : 2320-0936
Volume-4, Issue-8, pp-196-204
www.ajer.org
Research Paper Open Access

Some Fixed Point and Common Fixed Point Theorems in 2-Metric Spaces

Rajesh Shrivastava[1], Neha Jain[2] , K. Qureshi[3]
[1]*Deptt. of Mathematics, Govt. Science and comm. College Benazir Bhopal (M.P) India*
[2]***Research Scholar, Govt. Science and comm. College Benazir Bhopal (M.P) India***
[3]*Additional Director, Higher Education Dept. Govt. of M.P., Bhopal (M.P) India*

Abstract : *In the present paper we prove some fixed point and common fixed point theorems in 2-Metric spaces for new rational expression . Which generalize the well known results.*

Keywords : *Fixed point , 2-Metric Space , Common fixed point , Metric space , Completeness .*

I. Introduction

The concept of 2-metric space is a natural generalization of the metric space . Initially , it has been investigated by S. Gahler [1,2] . The study was further enhanced by B.E. Rhoades [6] , Iseki [3] , Miczko and Palezewski [4] and Saha and Day [7] , Khan[5] . Moreover B.E. Rhoades and other introduced several properties of 2- metric spaces and proved some fixed point and common fixed point theorems for contractive and expansion mappings and also have found some interesting results in 2-metric space , where in each cases the idea of convergence of sum of a finite or infinite series of real constants plays a crucial role in the proof of fixed point theorems . In this same way, we prove a fixed point theorem and common fixed point theorems for the mapping satisfying different types of contractive conditions in 2-metric space.

II. Definitions and Preliminaries

Definition 2.1 :- Let X be a non empty set . A real valued function d on $X \times X \times X$ is said to be a 2-metric in X if

(i) To each pair of distinct points x, y in X . There exists a point $z \in X$ such that $d(x, y, z) \neq 0$

(ii) $d(x, y, z) = 0$, When at least of x, y, z are equal.

(iii) $d(x, y, z) = d(y, z, x) = d(x, z, y)$

(iv) $d(x, y, z) \leq d(x, y, w) + d(x, w, z) + d(w, y, z)$ for all $x, y, z, w \in X$

When d is a 2-metric on X , then the ordered pair (X, d) is called 2- metric space.

2.2 A sequence $\{x_n\}$ in 2-metric space (X, d) is said to be convergent to an element $x \in X$ if $\lim_{n\to\infty} d(x_n, x, a) = 0$ for all $a \in X$.

It follows that if the sequence $\{x_n\}$ converges to x then

$\lim_{n\to\infty} d(x_n, a, b) = d(x, a, b)$ for all $a, b \in X$

2.3 A sequence $\{x_n\}$ in 2-metric space X is a Cauchy sequence if $d(x_m, x_n, a) = 0$ **as** $m, n \to \infty$ for all $a \in X$.

2.4 If a sequence is convergent in a 2-metric space then it is a Cauchy Sequence .

2.5 A 2-metric space (X, d) is said to be complete if every Cauchy Sequence in X is convergent.

Proposition 2.6 :-

If a sequence $\{x_n\}$ in 2-metric space converges to x then every subsequence of $\{x_n\}$ also converges to the same limit x .

Proposition 2.7

Limit of a sequence in a 2-metric space , if exits , is unique .

3 Main Results :

Theorem 3.1

Let T be a mapping of a 2-metric spaces into itself. If T satisfies the following conditions: $T^2 = I$, where I is identity mapping ---------- (1.1)

$$d(Tx - Ty, a) \geq \alpha \frac{d(x - Tx, a)\, d(y - Ty, a)}{d(x - y, a)}$$
$$+\beta \frac{d(y - Ty, a)\, d(y - Tx, a)\, d(x - Ty, a) + [d(x - y, a)]^3}{[d(x - y, a)]^2}$$
$$+\gamma \left[\frac{d(x - Tx, a) + d(y - Ty, a)}{2}\right]$$
$$+\delta \left[\frac{d(x - Ty, a) + d(y - Tx, a)}{2}\right] + \eta d(x - y, a) \quad \text{……..(1.2)}$$

Where $x \neq y, a > 0$ is real with $8\alpha + 10\beta + 4\gamma + 2\delta + 3\eta > 4$.

Then T has unique fixed point.

Proof :- Suppose x is any point in 2-metric space X .

Taking $y = \frac{1}{2}(T + I)x$, $z = T(y)$

$$d(z - x, a) = d(Ty - T^2 x, a) = d(Ty - T(Tx), a)$$
$$\geq \alpha \frac{d(y - Ty, a)\, d(Tx - T(Tx), a)}{d(y - Tx, a)}$$
$$+\beta \frac{d(Tx - T(Tx), a)\, d(Tx - Ty, a)\, d(y - T(Tx), a) + [d(y - Tx, a)]^3}{[d(y - Tx, a)]^2}$$
$$+\gamma \left[\frac{d(y - Ty, a) + d(Tx - T(Tx), a)}{2}\right]$$
$$+\delta \left[\frac{d(y - T(Tx), a) + d(Tx - Ty, a)}{2}\right]$$
$$+\eta [d(y - Tx, a)]$$

$$\geq \alpha \frac{d(y-Ty,a)d(Tx-x,a)}{\frac{1}{2}d(x-Tx,a)}$$

$$+\beta \frac{d(Tx-x,a)\left[d(Tx-y,a)+d(y-Ty,a)\right]d(y-x,a)+\left[d(y-Tx,a)\right]^3}{\frac{1}{4}\left[d(x-Tx,a)\right]^2}$$

$$+\gamma\left[\frac{d(y-Ty,a)+d(Tx-x,a)}{2}\right]$$

$$+\delta\left[\frac{d(y-x,a)+d(Tx-y,a)+d(y-Ty,a)}{2}\right]$$

$$+\eta\left[d(y-Tx,a)\right]$$

$$\geq 2\alpha d(y-Ty,a)$$

$$+\beta \frac{d(Tx-x,a)\left[\frac{1}{2}d(x-Tx,a)+d(y-Ty,a)\right].\frac{1}{2}d(x-Tx,a)+\frac{1}{8}\left[d(x-Tx,a)\right]^3}{\frac{1}{4}\left[d(x-Tx,a)\right]^2}$$

$$+\gamma\left[\frac{d(y-Ty,a)+d(Tx-x,a)}{2}\right]$$

$$+\delta\left[\frac{\frac{1}{2}d(x-Tx,a)+\frac{1}{2}d(x-Tx,a)+d(y-Ty,a)}{2}\right]+\frac{\eta}{2}d(x-Tx,a)$$

$$\geq 2\alpha d(y-Ty,a)$$

$$+\frac{\beta}{2}\left\{4\left[\frac{1}{2}d(x-Tx,a)+d(y-Ty)\right]+\frac{\left[d(x-Tx,a)\right]^3}{\left[d(x-Tx,a)\right]^2}\right\}$$

$$+\gamma\left[\frac{d(y-Ty,a)+d(Tx-x,a)}{2}\right]$$

$$+\delta\left[\frac{d(x-Tx,a)+d(y-Ty,a)}{2}\right]$$

$$+\frac{\eta}{2}\left[d(x-Tx,a)\right]$$

$$\geq 2\alpha d(y-Ty,a)+\frac{\beta}{2}\left[2d(x-Tx,a)+4d(y-Ty,a)+d(x-Tx,a)\right]$$

$$+\frac{\gamma}{2}\left[d(y-Ty,a)+d(Tx-x,a)\right]+\frac{\delta}{2}\left[d(x-Tx,a)+d(y-Ty,a)\right]+\frac{\eta}{2}d(x-Tx,a)$$

$$\geq d(x-Tx,a)\left(\frac{3\beta}{2}+\frac{\gamma}{2}+\frac{\delta}{2}+\frac{\eta}{2}\right)+\left(2\alpha+2\beta+\frac{\gamma}{2}+\frac{\delta}{2}\right)d(y-Ty,a)$$

$$\geq \frac{1}{2}d(x-Tx,a)(3\beta+\gamma+\delta+\eta)+\frac{1}{2}d(y-Ty,a)(4\alpha+4\beta+\gamma+\delta)$$

Now for

$$d(u-x,a)=d(2y-z-x,a)=d(Tx-Ty,a)$$

$$\geq \alpha\frac{d(x-Tx,a)d(y-Ty,a)}{d(x-y,a)}+\beta\frac{d(y-Ty,a)d(y-Tx,a)d(x-Ty,a)+\left[d(x-y,a)\right]^3}{\left[d(x-y,a)\right]^2}$$

$$+\gamma\left[\frac{d(x-Tx,a)+d(y-Ty,a)}{2}\right]+\delta\left[\frac{d(x-Ty,a)+d(y-Tx,a)}{2}\right]+\eta d(x-y,a)$$

$$\geq \alpha\frac{d(x-Tx,a)d(y-Ty,a)}{\frac{1}{2}d(x-Tx,a)}$$

$$+\beta\frac{d(y-Ty,a)\frac{1}{2}d(x-Tx,a)\left[\frac{1}{2}d(x-Tx,a)\right]+\frac{1}{8}\left[d(x-Tx,a)\right]^3}{\frac{1}{4}\left[d(x-Tx,a)\right]^2}$$

$$+\gamma\left[\frac{d(x-Tx,a)+d(y-Ty,a)}{2}\right]+\delta\left[\frac{\frac{1}{2}d(x-Tx,a)+\frac{1}{2}d(x-Tx,a)}{2}\right]$$

$$+\frac{\eta}{2}d(x-Tx,a)$$

$$\geq 2\alpha d(y-Ty,a)+\beta d(y-Ty,a)+\frac{\beta}{2}d(x-Tx,a)$$

$$+\gamma\left[\frac{d(x-Tx,a)+d(y-Ty,a)}{2}\right]+\frac{\delta}{2}d(x-Tx,a)+\frac{\eta}{2}d(x-Tx,a)$$

$$\geq d(x-Tx,a)\left(\frac{\beta}{2}+\frac{\gamma}{2}+\frac{\delta}{2}+\frac{\eta}{2}\right)+d(y-Ty,a)\left(2\alpha+\beta+\frac{\gamma}{2}\right)$$

$$\geq \frac{1}{2}d(x-Tx,a)(\beta+\gamma+\delta+\eta)+\frac{1}{2}d(y-Ty,a)(4\alpha+2\beta+\gamma)$$

Now

$$d(z-u,a)=d(z-x,a)+d(x-u,a)$$

$$\geq \frac{1}{2}d(x-Tx,a)(3\beta+\gamma+\delta+\eta)+\frac{1}{2}d(y-Ty,a)(4\alpha+4\beta+\gamma+\delta)$$

$$+\frac{1}{2}d(x-Tx,a)(\beta+\gamma+\delta+\eta)+\frac{1}{2}d(y-Ty,a)(4\alpha+2\beta+\gamma)$$

$$\geq \frac{1}{2} d\left(x-Tx,a\right)\left(3\beta+\gamma+\delta+\eta+\beta+\gamma+\delta+\eta\right)$$

$$+\frac{1}{2} d\left(y-Ty,a\right)\left(4\alpha+4\beta+\gamma+\delta+4\alpha+2\beta+\gamma\right)$$

$$\geq \frac{1}{2} d\left(x-Tx,a\right)\left(4\beta+2\gamma+2\delta+2\eta\right)$$

$$+\frac{1}{2} d\left(y-Ty,a\right)\left(8\alpha+6\beta+2\gamma+\delta\right)----------(1.3)$$

$$d\left(z-u,a\right)=d\left(T\left(y\right)-T\left(2y-z\right),a\right)$$

$$=d(T(y)-2y+T(y),a)$$

$$=2d\left(Ty-y,a\right)----------(1.4)$$

So,

$$2d\left(Ty-y,a\right)\geq \frac{1}{2} d\left(x-Tx,a\right)\left(4\beta+2\gamma+2\delta+2\eta\right)+\frac{1}{2} d\left(y-Ty,a\right)\left(8\alpha+6\beta+2\gamma+\eta\right)$$

$$\Rightarrow\left[4-\left(8\alpha+6\beta+2\gamma+\eta\right)\right]d\left(y-Ty,a\right)\geq\left(4\beta+2\alpha+2\delta+2\eta\right)d\left(x-Tx,a\right)$$

$$\Rightarrow d\left(x-Tx,a\right)\leq\frac{4-\left(8\alpha+6\beta+2\gamma+\eta\right)}{4\beta+2\gamma+2\delta+2\eta}d\left(y-Ty,a\right)$$

$$\Rightarrow d\left(x-Tx,a\right)\leq kd\left(y-Ty,a\right)as\left(8\alpha+10\beta+4\gamma+2\delta+3\eta>4\right)$$

Where, $k=\frac{4-\left(8\alpha+6\beta+2\gamma+\eta\right)}{4\beta+2\gamma+2\delta+2\eta}<1$

Let $R=\frac{1}{2}\left(T+I\right)$, then

$$d\left(R^2\left(x\right)-R\left(x\right),a\right)=d\left(R\left(R\left(x\right)\right)-R\left(x\right),a\right)$$

$$=d\left(R\left(y\right)-y,a\right)=\frac{1}{2}d\left(y-Ty,a\right)$$

$$<\frac{k}{2}d\left(x-Tx,a\right)$$

By the definition of R we claim that $\left\{R^n\left(x\right)\right\}$ is a Cauchy sequence in X, $\left\{R^n\left(x\right)\right\}$ is converges to so element x_0 in X.

So $\lim_{n\to\infty}\left\{R^n\left(x\right)\right\}=x_0$. So $\left\{R\left(x_0\right)\right\}=x_0$

Hence $T\left(x_0\right)=x_0$

So x_0 is a fixed point of T.

Uniqueness

If possible let $y_0 \neq x_0$ is another fixed point of T. Then

$$d(x_0 - y_0, a) = d(Tx_0 - Ty_0, a)$$

$$\geq \alpha \frac{d(x_0 - Tx_0, a)\, d(y_0 - Ty_0, a)}{d(x_0 - y_0, a)}$$

$$+\beta \frac{d(y_0 - Ty_0, a)\, d(y_0 - Tx_0, a)\, d(x_0 - Ty_0, a) + \left[d(x_0 - y_0, a)\right]^3}{\left[d(x_0 - y_0, a)\right]^2}$$

$$+\gamma \left[\frac{d(x_0 - Tx_0, a)\, d(y_0 - Ty_0, a)}{2}\right]$$

$$+\delta \left[\frac{d(x_0 - Ty_0, a) + d(y_0 - Tx_0, a)}{2}\right]$$

$$+\eta d(x_0 - y_0, a)$$

$$\geq \beta d(x_0 - y_0, a) + \delta d(x_0 - y_0, a) + \eta d(x_0 - y_0, a)$$

$$\geq (\beta + \delta + \eta) d(x_0 - y_0, a)$$

Which is contradiction so $x_0 = y_0$

Hence fixed point is unique **Hence proved**

Theorem 3.2 :-

Let T and G be two non expansive mappings of a 2-metric space X into itself . T and G satisfy the conditions:

(2.1) T and G commute .

(2.2) $T^2 = I$ and $G^2 = I$, where I is identity mapping .

(2.3)

$$d(Tx - Ty, a) \geq \alpha \frac{d(Gx - Tx, \mathrm{a})\, d(Gy - Ty, a)}{d(Gx - Gy, a)}$$

$$+\beta \frac{d(Gy - Ty, a)\, d(Gy - Tx, a)\, d(Gx - Ty, a) + \left[d(Gx - Gy, a)\right]^3}{\left[d(Gx - Gy, a)\right]^2}$$

$$+\gamma \left[\frac{d(Gx - Tx, a) + d(Gy - Ty, a)}{2}\right] + \delta \left[\frac{d(Gx - Ty, a) + d(Gy - Tx, a)}{2}\right] + \eta \left[d(Gx - Gy, a)\right]$$

For every $x, y \in X$, $\alpha, \beta, \gamma, \delta, \eta \in [0,1]$ with $x \neq y$ and $d(Gx, Gy) \neq 0$ and $\beta + \delta + \eta > 1$

Then there exist a Unique Common Fixed Point of T and G such that $T(x_0) = x_0$ and $G(x_0) = x_0$.

Proof :-

Suppose x is point in 2-metric space X it is clear that $(TG)^2 = I$

$$d(TG.G(x) - TG.G(y), a) \geq \alpha \frac{d(G(G^2x) - T(G^2x), a)\, d(G(G^2y) - T(G^2y), a)}{d(G(G^2x) - T(G^2y), a)}$$

$$+\beta \frac{d(G(G^2y) - T(G^2y), a)\, d(G(G^2y) - T(G^2x), a)\, d(G(G^2x) - T(G^2y), a) + [d(G(G^2x) - G(G^2y), a)]^3}{[d(G(G^2x) - G(G^2y), a)]^2}$$

$$+\gamma \left[\frac{d(G(G^2x) - T(G^2x), a) + d(G(G^2y) - T(G^2y), a)}{2} \right]$$

$$+\delta \left[\frac{d(G(G^2x) - T(G^2y), a) + d(G(G^2y) - T(G^2x), a)}{2} \right]$$

$$+\eta [d(G(G^2x) - G(G^2y), a)]$$

$$\geq \alpha \frac{d(Gx - TG(Gx), a)\, d(Gy - TG(Gy), a)}{d(Gx - Gy, a)}$$

$$+\beta \frac{d(Gy - TG(Gy), a)\, d(Gy - TG(Gx), a)\, d(Gx - TG(Gy)) + [d(Gx - Gy, a)]^3}{[d(Gx - Gy, a)]^2}$$

$$+\gamma \left[\frac{d(Gx - TG(Gx), a) + d(Gy - TG(Gy), a)}{2} \right]$$

$$+\delta \left[\frac{d(Gx - TG(Gx), a) + d(G(y) - TG(Gx), a)}{2} \right]$$

$$+\eta d(Gx - Gy, a)$$

Taking $G(x) = p, G(y) = q$, where $p \neq q$

$$\geq \alpha \frac{d\left(p-TG(p),a\right)d\left(q-TG(q),a\right)}{d\left(p-q,a\right)}$$
$$+\beta \frac{d\left(q-TG(q),a\right)d\left(q-TG(p),a\right)d\left(p-TG(q),a\right)+\left[d\left(p-q,a\right)\right]^3}{\left[d\left(p-q,a\right)\right]^2}$$
$$+\gamma\left[\frac{d\left(p-TG(p),a\right)+d\left(q-TG(q),a\right)}{2}\right]$$
$$+\delta\left[\frac{d\left(p-TG(q),a\right)+d\left(q-TG(p),a\right)}{2}\right]$$
$$+\eta d\left(p-q,a\right)$$

Taking $TG=R$ we get

$$d\left(R(p)-R(q),a\right)\geq \alpha \frac{d\left(p-R(p),a\right)d\left(q-R(q),a\right)}{d\left(p-q,a\right)}$$
$$+\beta \frac{d\left(q-R(q),a\right)d\left(q-R(p),a\right)d\left(p-R(q),a\right)+\left[d\left(p-q,a\right)\right]^3}{\left[d\left(p-q,a\right)\right]^2}$$
$$+\gamma\left[\frac{d\left(p-R(p),a\right)+d\left(q-R(p),a\right)}{2}\right]$$
$$+\delta\left[\frac{d\left(p-R(q),a\right)+d\left(q-R(p),a\right)}{2}\right]$$
$$+\eta d\left(p-q,a\right)$$

It is clear by theorem (3.1) ; that $R=TG$ has at least one fixed point say x_0 in K that is

$$R\left(x_0\right)=TG\left(x_0\right)=x_0$$

and so $T.\left(TG\right)\left(x_0\right)=T\left(x_0\right)$

$$G\left(x_0\right)=T\left(x_0\right)$$

Now

$$d\left(Tx_0-x_0,a\right)=d\left(Tx_0-T^2(x_0),a\right)=d\left(Tx_0-T.T(x_0),a\right)$$
$$\geq \alpha \frac{d\left(G(\mathrm{x}_0)-\mathrm{T}(\mathrm{x}_0),\mathrm{a}\right)d\left(GT(\mathrm{x}_0)-\mathrm{T}(\mathrm{Tx}_0),\mathrm{a}\right)}{d\left(G(\mathrm{x}_0)-G(\mathrm{Tx}_0),\mathrm{a}\right)}$$
$$+\beta \frac{d\left(G(\mathrm{Tx}_0)-\mathrm{T}(\mathrm{Tx}_0),\mathrm{a}\right)d\left(G(\mathrm{Tx}_0)-\mathrm{T}(\mathrm{x}_0),\mathrm{a}\right)d\left(G(\mathrm{x}_0)-\mathrm{T}(\mathrm{Tx}_0),\mathrm{a}\right)+\left[d\left(G(\mathrm{x}_0)-G(\mathrm{Tx}_0),\mathrm{a}\right)\right]^3}{\left[d\left(G(\mathrm{x}_0)-G(\mathrm{Tx}_0),\mathrm{a}\right)\right]^2}$$
$$+\gamma\left[\frac{d\left(G(\mathrm{x}_0)-\mathrm{T}(\mathrm{x}_0),\mathrm{a}\right)+d\left(G(\mathrm{Tx}_0)-\mathrm{T}(\mathrm{Tx}_0),\mathrm{a}\right)}{2}\right]$$
$$+\delta\left[\frac{d\left(G(\mathrm{x}_0)-\mathrm{T}(\mathrm{Tx}_0),\mathrm{a}\right)+d\left(G(\mathrm{Tx}_0)-\mathrm{T}(\mathrm{x}_0),\mathrm{a}\right)}{2}\right]+\eta d\left(G(\mathrm{x}_0)-G(\mathrm{Tx}_0),\mathrm{a}\right)$$
$$=\left(\beta+\delta+\eta\right)d\left(\mathrm{Tx}_0-\mathrm{x}_0,\mathrm{a}\right)$$

So $T(x_0)=x_0 \quad (\beta+\gamma+\eta>1)$

That is x_0 is the fixed point of T.

But $T(x_0)=G(x_0)$ so $G(x_0)=x_0$.

Hence x_0 is the fixed point of T and G .

Uniqueness :-

If possible let $y_0 \neq x_0$ is another common fixed point of T and G.

Then

$$d(x_0-y_0,a)=d\left(T^2(x_0)-T^2(y_0),a\right)=d\left(T(T(x_0))-T(T(y_0)),a\right)$$

$$\geq \alpha \frac{d\left(G(Tx_0)-T(Tx_0),a\right)d\left(G(Ty_0)-T(Ty_0),a\right)}{d\left(G(Tx_0)-G(Ty_0),a\right)}$$

$$+\beta \frac{d\left(G(Ty_0)-T(Ty_0),a\right)d\left(G(Ty_0)-T(Tx_0),a\right)d\left(G(Tx_0)-T(Ty_0),a\right)+\left[d\left(G(Tx_0)-G(Ty_0),a\right)\right]^3}{\left[d\left(G(Tx_0)-G(Ty_0),a\right)\right]^2}$$

$$+\gamma\left[\frac{d\left(G(Tx_0)-T(Tx_0),a\right)+d\left(G(Ty_0)-T(Ty_0),a\right)}{2}\right]$$

$$+\delta\left[\frac{d\left(G(Tx_0)-T(Ty_0),a\right)+d\left(G(Ty_0)-T(Tx_0),a\right)}{2}\right]+\eta d\left(G(Tx_0)-G(Ty_0),a\right)$$

$$\geq \beta d(x_0-y_0,a)+\delta d(x_0-y_0,a)+\eta d(x_0-y_0,a)$$

$$\geq (\beta+\delta+\gamma)d(x_0-y_0,a)$$

But $\beta+\delta+\eta>1$

So $x_0=y_0$.

So Common Fixed point is Unique.

References

[1] S.Gahler , 2-metric Raume and iher topologische strucktur , Math. Nacher ., 26(1963) , 115-148 .

[2] S.Gahler , Uber die unifromisieberkeit 2-metrischer Raume , Math. Nachr. 28(1965) , 235-244.

[3] K. Iseki , Fixed point theorems in 2-metric space, Math. Seminar. Notes ,Kobe Univ.3(1975), 133-136 .

[4] A. Miczko and B. Palezewski , Common fixed points of contractive type mappings in 2-metric spaces, Math.Nachr., 124(1985) , 341-355.

[5] M.S., Khan, On fixed point theorems in 2-metrc spaces , Publ Inst. Math (Beograd) (N.S.), 27(41)(1980) , 107-112.

[6] B.E. Rhoades , Contractive type mappings on a 2-metric space , Math. Nachr., 91(1979) , 151-155.

[7] M. Saha and D. Day , On the theory of fixed points contractive type mappings in a 2-metric space, Int. Journal of Math . Analysis , 3(to be published in 2009), no.6, 283-293.

[8] M. Saha and A.P. Baisnab , Fixed point of mappings with contractive iterate, Proc. Nat, Acad, Sci. India, 63A, IV, (1993) 645-650.

[9] Saha and Day , Some results on fixed points of mappings in a 2-metric space, J .Contemp. Math. Sciences, Vol.4 No. 21 (2009) 1021-1028.

American Journal of Engineering Research (AJER) 2015
American Journal of Engineering Research (AJER)
e-ISSN: 2320-0847 p-ISSN : 2320-0936
Volume-4, Issue-8, pp-205-211
www.ajer.org
Research Paper Open Access

Compression Pressure Effect on Mechanical & Combustion Properties of Sawdust Briquette using Styrofoam adhesive as binder.

Abdulrasheed A.[1], Aroke U. O.[2], Ibrahim M.[3]
Department of Chemical Engineering
Abubakar Tafawa Balewa University, P.M.B. 0248, Bauchi state, Nigeria.

Abstract*: In this paper, briquettes were produced from sawdust at different compression pressure using Styrofoam (Polystyrene foam) adhesive as binding material. The effects of changing the compression pressure used in moulding of briquettes on its combustion and mechanical properties were investigated. In evaluating Combustion properties, 0.940kg of water was boiled using oven-dried sample of briquette in the combustion chamber with air flow velocity supplied to the combustion chamber at 10.2m/s. Combustion properties investigated were afterglow time, burning rate, specific fuel consumption, power output, percentage heat utilized, flame propagation rate and percentage ash content. The mechanical properties investigated included density, compressive strength, impact resistance, water resistance and abrasion resistance. The blends of sieved sawdust and binder were prepared in the ratio of 4:1 and compacted at pressures ranging from 40 – 90 kN/m^2 at 10 kN/m^2 interval in a hydraulic press machine with a dwell time of 5minutes. The pressures of moulding were varied to evaluate the range that gives the best quality in terms of combustion and mechanical properties of the briquette produced. The potential use of Polystyrene foam adhesive as a binder in production of briquettes was found promising.*

Keywords *- Adhesive, Briquette, compression pressure, sawdust, Styrofoam.*

I. INTRODUCTION

Sawdust can be regarded among the most abundant waste in the agricultural industries in Nigeria. The waste generated from processing of wooden products is estimated to be 15% of the total 1.72 million/m^3 wood processed [1]. Sawdust also referred to as wood dust is waste obtained from cutting, sanding, grinding, drilling and pulverizing of wood with the aid of a saw or other tools and machineries. It is a collection of small particles of wood in different sizes and mass. Sawdust is a flammable material when ignited which makes it useable as a source of fuel [2]. Based on the increase in utilization of wood resources, there is an expectation that fuel wood demand would rise to about 2.13 x 10^4 metric tonnes. As a result of this imbalance, a shift to a more sustainable and alternative energy resource is seriously needed especially in developing countries like Nigeria [3]. Thus, the use of wood or sawmill waste known as sawdust as an alternative energy source is imperative.Briquetting of biomass is defined as the compression of loose materials obtained as agricultural waste to produce a composite which is compact by pressure application [4]. Biomass are wastes or residues from agricultural products such as leaves, shells, sticks, cob, husks and straws or from industries that use bio-materials such as sawmills, plywood and furniture industries.According to Demirbas, [5] briquettes can be defined as cylinders made of compressed wood fibres that are of about 30 cm in length and have a gross calorific value of 4200kcal/kg. About 2.2 kg of briquette produces the same amount of energy during combustion as 1 litre of furnace oil. For effective utilization, the briquettes are dried properly, de-dusted and pressed into compacted form.The technology of briquetting has not been fully explored in many developing countries due to constraints in the technical ability of its production and difficulty in adopting existing technology to use local resources and conditions. As such, overcoming such challenges encountered with this technology and selecting the appropriate waste material for briquette production is very important in determining whether the production can be in commercial quantity [6]. Combustion properties of the produced briquettes analysed in this work with their respective formulae, units and sources were presented in Table 1. The same was carried out for mechanical properties as shown in Table 2.

Table 1: Test of combustion properties of Briquettes carried out.

S/N	COMBUSTION PROPERTIES	FORMULAE	UNITS	REFERENCES
1.	Afterglow Time	-	s	Kim *et al.*, 2001 [7].
2.	Percentage Heat Utilized	$\frac{m_w C_p (T_f - T_i) + m_w L}{m_b \times H_b} \times 100$	%	Ibrahim et al., 2015 [8].
3.	Power Output	$\frac{m_b \times H_b}{t}$	kJ/s	Kim *et al.*, 2001 [7].
4.	Specific Fuel Consumption	$\frac{m_b}{m_w}$	kg briquette/kg water	Ibrahim et al., 2015 [8].
5.	Burning Rate	$\frac{m_b}{t}$	kg/s	Kim *et al.*, 2001 [7].
6.	% Ash Content	$\frac{m_a}{m_b} \times 100$	%	Kim *et al.*, 2001 [7].
7.	Flame Propagation Rate	$\frac{D_b}{t}$	m/s	Ibrahim et al., 2015 [8].

KEY

- C_p = Specific heat capacity of water
- T_f = Final temperature of water
- T_i = Initial temperature of water
- L = Latent heat of vaporization of water.
- m_a= Mass of ash residue
- m_b = Mass of briquette used as fuel
- H_b = Calorific value of briquette
- m_w = Mass of water
- t = Time for flame propagation
- D_b = Graduated length of flame spread.

Table 2: Test of mechanical properties of Briquettes carried out.

	MECHANICAL PROPERTIES	FORMULAE	UNITS	REFERENCES
1.	Density	$\frac{\text{mass of briquette (kg)}}{\text{volume (m}^3\text{)}}$	kg/m^3	Obemberger and Thek, 2004 [9].
2.	Compressive Strength Test	$\frac{\text{Crushing load (kN)}}{\text{Area of sample (m}^2\text{)}}$	kN/m^2	Yadong and Henry, 2000 [10].
3.	Impact Resistance Test	$100 \times \frac{\text{Number of drops (N)}}{\text{Number of pieces (n)}}$	-	Richard, 1989 [11].
4.	Water Resistance Test	$100\% - \%\ water\ absorbed$	%	Obemberger and Thek, 2004 [9].
5.	Abrasion Resistance Test	$\frac{\text{Weight after tumbling}}{\text{Weight before tumbling}} \times 100$	%	Richard, 1989 [11].

II. MATERIALS AND METHODS

2.1 Sawdust Preparation

The sawdust material was sourced from sawmill in Muda Lawal market within Bauchi metropolitan area, Nigeria. The raw sawdust was sun-dried until stable moisture content range of 10 – 18% was obtained to give the briquette and was later subjected to size reduction through sieve analysis where a particle size of 1.18mm representing medium series was selected to produce uniform briquettes. Oversized materials were rejected and discarded.

2.2 Binder Preparation

Styrofoam was first collected from trash in bulk, pre-treated to be free of impurities and predetermined into smaller size particles by crushing. 400g of the crushed Styrofoam (about 20.43%) was then mixed with constituents such as gasoline, ethanol and dissolved gum Arabic of percent proportions; 42.90%, 8.07% and 28.09% respectively. The mixture was then stirred thoroughly forming polystyrene foam adhesive gradually. Consequently, about 0.51% proportion of silica gel was added to the content to enhance the emulsion characteristics of the adhesive, kept steady and undisturbed so as to further dehydrate the moisture in the adhesive [8].

2.3 Briquette Formation

The prepared binder constituting 30% by mass and sawdust were mixed in a vessel and thoroughly stirred to attain uniformity and enhance adhesion. The mixture was then fed into a mold (15cm height and 10cm diameter). The content in the mold was placed between round dies and positioned in the hydraulic powered press machine for compression into briquettes. The piston was actuated and a set pressure ranging between 40 - 90kN/m^2 was applied at a time to the material for 5minutes (dwell time). The briquette formed was then extruded and air-dried for 5 days and subsequently oven-dried for 24hrs at a constant temperature of 105^{0}C [8] [9] [10]. The detail procedure for the production process as stated by Ibrahim *et al.* is illustrated by Fig -1.

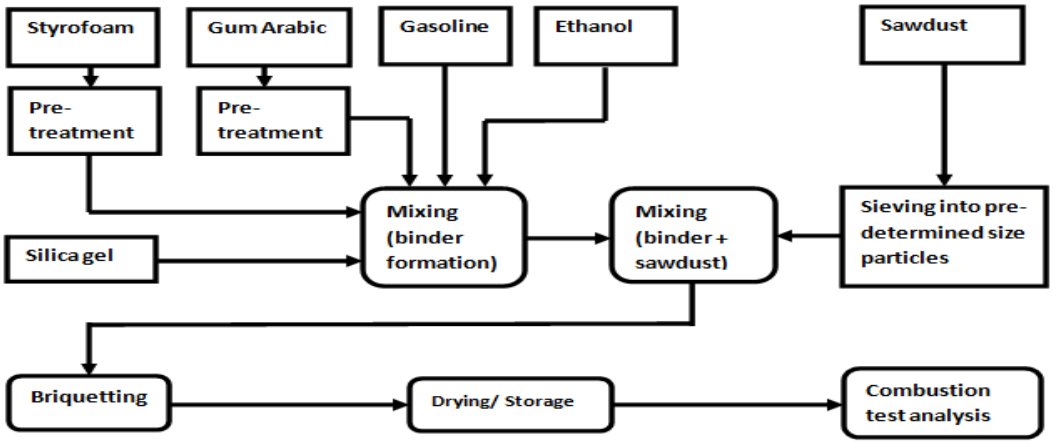

Fig -1: Block Diagram of processes involved in briquettes making from sawdust [8].

III. RESULTS AND DISCUSSION

3.1 Variations of combustion properties with molding pressure

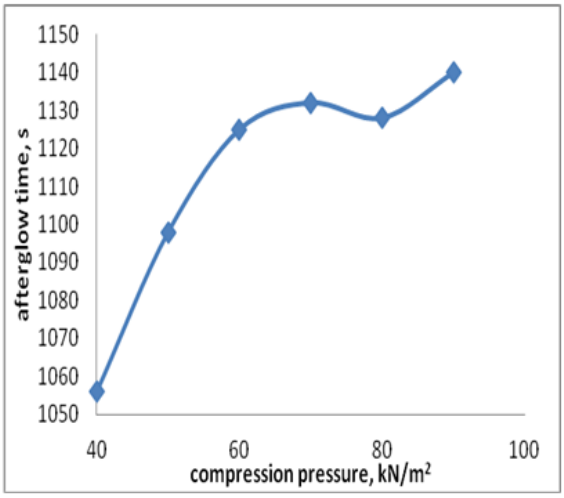

Fig -2: Sensitivity of afterglow time on compression pressure of briquette.

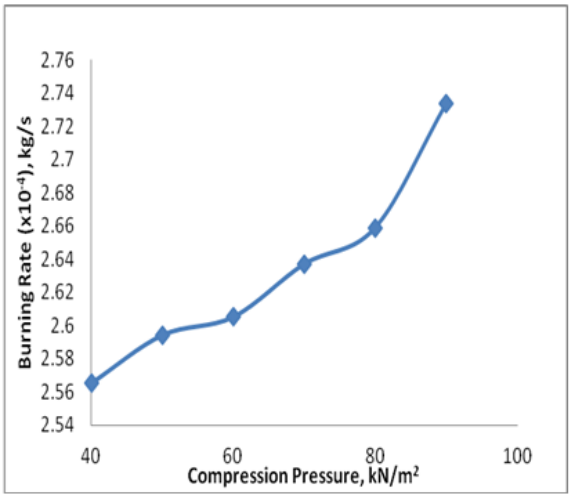

Fig -3: Sensitivity of burning rate on compression pressure of briquette.

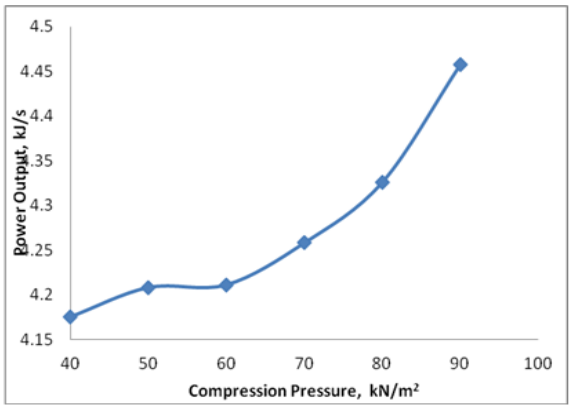

Fig -5: Sensitivity of power output on compression pressure of briquette.

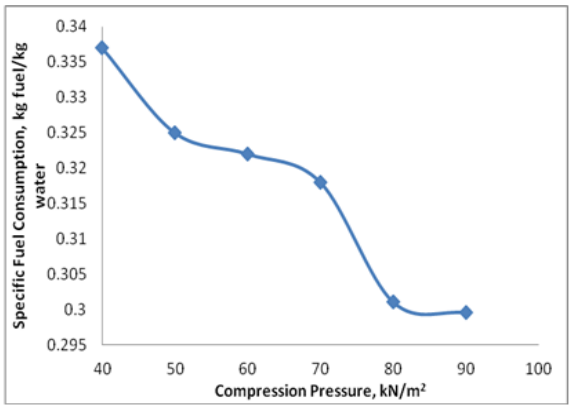

Fig -4: Sensitivity of specific fuel consumption on compression pressure of briquette.

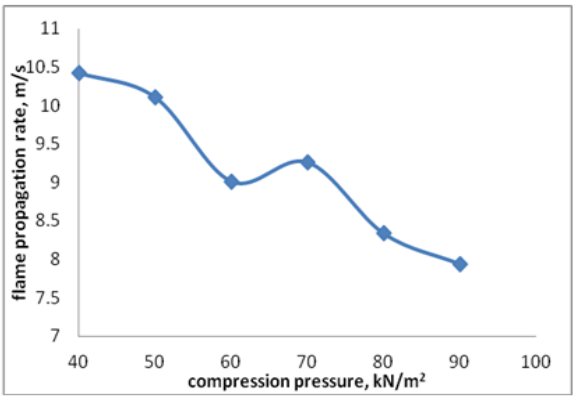

Fig -7: Sensitivity of flame propagation rate on compression pressure of briquette.

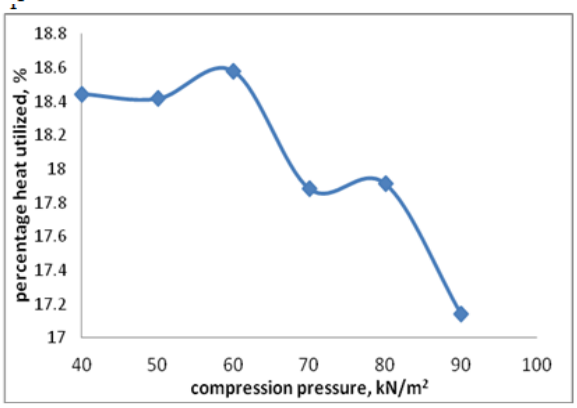

Fig -6: Sensitivity of percentage heat utilized on compression pressure of briquette.

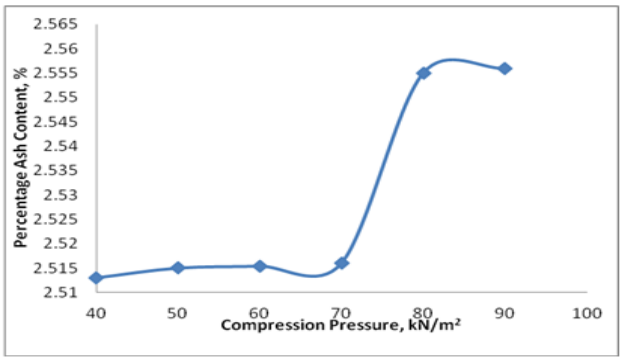

Fig -8: Sensitivity of percentage ash content on compression pressure of briquette.

The results obtained from water boiling tests showed that the afterglow time required for each set of briquettes to boil an equal volume of water increases with increase in the briquettes' compression pressure as shown in Fig -2 . The briquette with the lowest compaction pressure recorded lowest ignition time. The ignition time of the studied briquettes varied between 1,055 – 1,140s which showed a significant difference in variation at all level of compaction. This could be attributed to high porosity exhibited between particles which enable easy percolation of oxygen and out flow of combustion briquettes due to low compaction force. The observed values on ignition time showed that briquette bonded by Styrofoam adhesive took a longer time for it to burn out (1055 – 1140s) completely for each compaction as compared to the corresponding burn-out time (703 – 749s) of briquette bonded by cassava starch gel under 55 – 75 kN/m^2 compaction pressures as reported by (Onuegbu *et al.*, 2010) [8].

Fig -3 depicts the variation of burning rate with the compression pressure of the briquette. Briquettes with lower compaction burned faster than the ones with higher compaction. The study elucidated that increase in densification pressure increases the burning rate of the briquettes (ranging from 2.56 x 10^{-4} – 2.73 x 10^{-4}kg/s). In comparative of this result analyzed with those reported by (Onuegbu *et al.*, 2011) [11] ranging between (1.59 x 10^{-4} – 1.64 x 10^{-4}kg/s) showed a significant variation in the mass of briquette burnt per time.

The specific fuel consumption of briquette was found to decrease progressively with increase in compaction pressure which ranges from 0.3375 to 0.2988 kg fuel/kg water as depicted in Fig -4. This is from the fact that the mass of sawdust per volume would increase on increasing the compaction/compression pressure of moulding while the availability of air containing Oxygen for combustion is reduced and excessive consumption of fuel resulting to wastage of heat minimized. The efficiency of the analyzed data compete favourably with that of briquette bonded by starch as stated by Onuegbu et al. (2011) which experienced lower fuel consumption rate at higher compression pressure of 65 – 85 kN/m^2.

Fig -5 is a representation of the variation of power output with respect to changes in compression pressure. This is a measure of the energy released on burning the briquette. It increases progressively from sample of low compression pressure to high ranging from 4.176 to 4.461 kJ/s. These values were observed to be slightly greater than that of briquettes bonded by common starch.

Percentage heat utilized from briquette fuel was found to decrease with increase in pressure of compression. This is a measure of the thermal efficiency of the fuel. The result displayed in Fig -6 shows that briquettes produced from high compression pressure have low heat utilization which is due to longer time it requires to burn completely. In so doing, more heat is lost to the surroundings thereby reducing the amount of heat utilized in the heating process. Best utilization of heat were noticed at compression pressures of 40, 50, 60 kN/m^2 with corresponding values of 18.46, 18.42 and 18.58% respectively. These fuel efficiencies were less than that of briquettes bonded by starch obtained from Adeniji et al. (2007) [12] which is between the ranges of 28.17 – 29.05%.

From Fig-7, flame propagation rate which is the rate at which briquette burn over a graduated length decreases with increase in compression pressure. This trend is due to decrease in porosity and low oxygen percolation in the fuel biomass. There is a close range of values when compared with briquettes produced with cassava starch as adhesive and is in conformity with minimum requirement of DIN 51731[13] and that of Ajayi & Lawal (1995) [14].

Percentage ash content on burning sawdust briquette increases as the compression pressure increases as can be seen in Fig -8. The ash content was found to increase very slowly from compaction range of 40 - 70 kN/m^2 while it increases rapidly from 70 - 80 kN/m^2. It can be deduced from this trend that increment in compression of briquette results into increment in mass of sawdust per volume resulting to subsequent increment in ash formation. Briquettes produced at compression pressure of 40 &50 kN/m^2 produces the lower ash content which were 2.513& 2.515% respectively.

3.2 Variations of mechanical properties with molding pressure

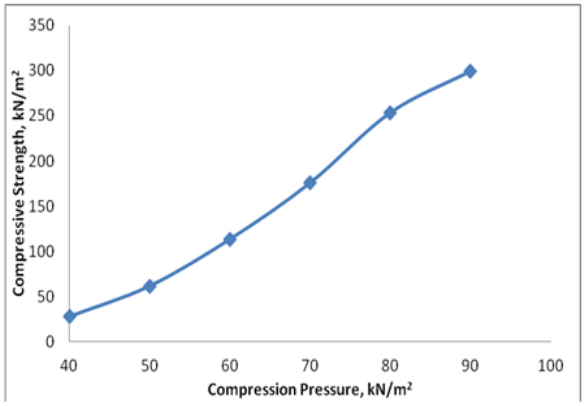

Fig -10: Sensitivity of compressive strength on compression pressure of briquette.

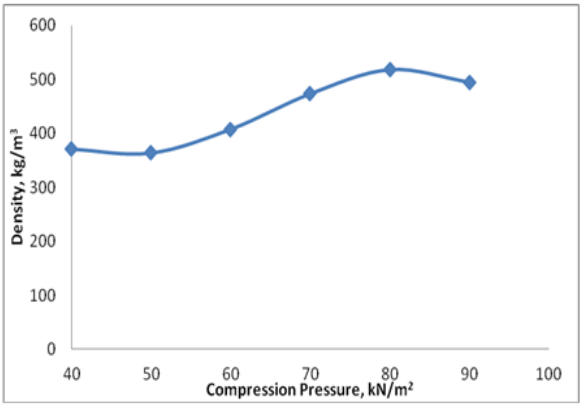

Fig -9: Sensitivity of density on compression pressure of briquette.

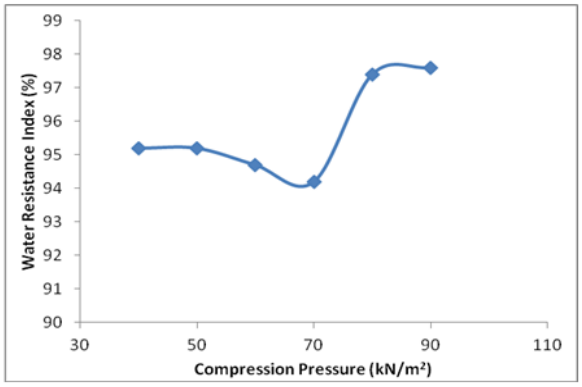

Fig -12: Sensitivity of water resistance on compression pressure of briquette.

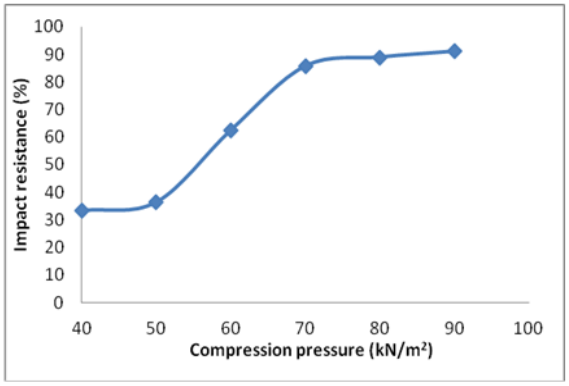

Fig -11: Sensitivity of impact resistance on compression pressure of briquette.

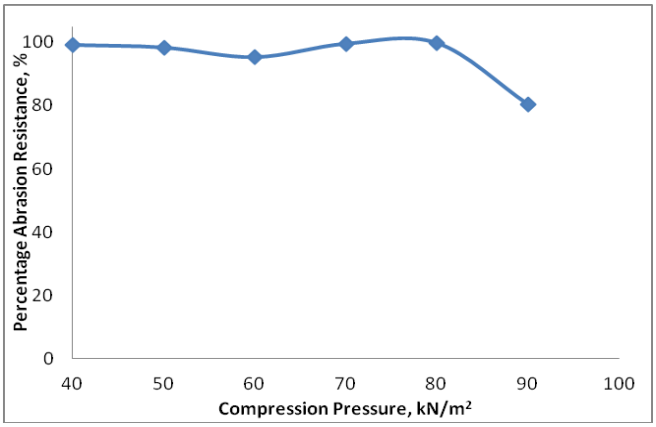

Fig -13: Sensitivity of Abrasion Resistance on compression pressure of briquette.

The density of briquettes was found to increase or the compaction was increased as depicted in F 9. As the compaction is increased, the particles that make the up material are forced closer to one another which minimize the void space between them. In so doing, the density of the briquettes is expected to increase on increased compaction for the fact that the briquettes particles which comprises of sawdust and Styrofoam are denser than the air pockets in void spaces. At slightly above 70 kN/m^2, the density of briquettes was no longer sensitive to compaction meaning further compaction results to no change in density.

Fig -10 shows the trend of compressive strength on increasing compaction of briquettes. It is an important parameter which indicates the ability of the briquettes to withstand loading capable reducing its sizes. It is critical in handling and transportation of the fuel. Increase in compaction result to increase in its compressive strength.

Fig -11 is a plot to show the effect of compaction on the ability of the briquettes to resist shock or high force applied to it in a short duration. It is a measure of the toughness of the briquettes. The impact resistance was found to increase as the compaction increases but more significantly at 50 – 70 kN/m^2. From 70 – 90 kN/m^2 compactions, the impact resistance was no longer sensitive to increase in compaction. The impact resistance of briquettes should be moderate because the biomass fuel is not frequently exposed to short time high force impact and also not to inhibit important combustion properties of the fuel.

From Fig -13, it was observed that the compression pressure has little effect on the abrasion resistance which is a measure of the briquette's ability to resist wearing of its surface when being in contact with the surface of another material. Compression pressure from 40 – 80 kN/m^2 produced briquettes at approximately 100% abrasion resistance. The only exception being at 90 kN/m^2 with percentage abrasion resistance of 80%. It can be deduced from this trend that the surface wear resistance of briquettes does not depend significantly on the compression pressure they are moulded.

Fig -12 shows the sensitivity of briquette fuel water resistance to variations of compression pressure in which higher resistance to water was obtained at higher compression pressure. The stability of briquette's resistance to water on changing the compression pressure was observed at 80 - 90 kN/m^2.

The strength of a briquette is a function of the pressure at which it was moulded as observed from Fig -9, 10 & 11 with the exception of the abrasion resistance which shows very low sensitivity as the compression pressure increases (Fig -13).

IV. CONCLUSIONS

The possibilities and potential use of Styrofoam as a binding material in sawdust briquetting was explored and found promising. The combustion and mechanical properties of the briquette was found to be dependent on the compression pressure with which it was moulded. Briquette quality is relative to its manner of application, transport and handling which determines the optimal compression pressure that best gives the required or desired properties of it. Optimization of the process should be carried out to ascertain the optimal conditions that give desired properties of the briquette. Cost analysis is relevant to evaluate the profitability of the process.

REFERENCES

[1] Badejo, S.O. 1990. "*Sawmill wood residue in Nigeria and their utilization*". Invited Paper. Proceedings of National on workshop on Forestry Management Strategies for self sufficiency in wood production, Ibadan 12th - 15th June, 1990.

[2]. Stout, B.A. and Best, G. 2001. "*Effective energy use and climate change: needs of rural areas in developing countries*". Agricultural Engineering International: the CIGR E-Journal of Scientific Research and Development. Vol. III, 19pp.

[3]. Yahaya, D. B. and Ibrahim, T. G. 2012. "*Development of Rice Husk Briquettes for use as fuel*". Research Journal in Engineering and Applied Sciences. *1(2) 130-133*.

[4]. Demirbas, A. and Sahin, A. 2001. "*Evaluation of Biomass Residue; Briquetting Waste Papers and Wheat Straw Mixtures*", *Journal on Fuel Processing Technology, (55) 175-183*.

[5]. Grover, P. D. and Mishra, S. K. 1996. "Biomass *Briquetting, Technology and Practices, Regional Wood Energy Development Programme in Asia*". Field document No. 46. FAO: Bangkok, Thailand.

[6]. Green, Harvey (2006) *Wood: Craft, Culture, History* Penguin Books, New York, page 403, ISBN 978-1-1012-0185-5.

[7]. Ibrahim M., Aroke U.O., Abdulrasheed A. (2015). "*Investigation of Mechanical & Combustible properties of Briquettes produced from Rice Husk using Polystyrene Foam Adhesive as a binder".* International Journal of Science, Engneering and Technology. *3(2) 449-454*.

[8]. Onuegbu, T. U., Okafor, I. Ilochi, N. O. Ogbu, I. M. Obumselu, O. F. and Ekpunobi, U. E. 2010. "*Enhancing the efficiency of coal briquette in rural Nigeria using Pennisetum purpurem".* Advances in Natural and Applied Sciences, *4: 299-304*.

[9] Emerhi, E. A. 2011. "*Physical and combustion properties of briquettes produced from sawdust of three hardwood species and different organic binders*" Advances in Applied Science Research, 2 (6):236-246.

[10] Ugwu, K. E. and Agbo, K. E. 2011. "*Briquetting of Palm Kernel Shell*" Journal of Applied Sciences and Environmental Management. *15 (3) 447 – 450*.

[11]. Onuegbu, T. U., Ekpunobi, U. E. Ogbu, I. M. Ekeoma, M. O. and Obumselu, F. O. 2011. "*Comparative studies of ignition time and water boiling test of coal and biomass briquettes blend*". International Journal of Research and Review in Applied Sciences, *7: 153-159*.

[12]. Adeniji, T. A., Sanni, L.O., Barimalaa, I.S., Hart, A.D. 2007. "*Nutritional and anti-nutritional composition of flour made from plantain and banana hybrid pulp and peel mixture*". Nigerian Food Journal, *25(2) 1-7*.

[13]. Standard DIN 51731. "Solid fuels testing, natural wood pressed pieces, demands and testing".

[14]. Ajayi, O. A. and Lawal G. T. 1995. "*Some Quality Indicators of Sawdust/Palm Oil Sludge Briquettes*": Journal of Agric Engineering and Technology, *3, 55-65*.

American Journal of Engineering Research (AJER) 2015
American Journal of Engineering Research (AJER)
e-ISSN: 2320-0847 p-ISSN : 2320-0936
Volume-4, Issue-8, pp-212-215
www.ajer.org
Research Paper Open Access

Conversion of Number Systems using Xilinx.

Chinmay V. Deshpande[1], Prof. Chankya K. Jha[2].
[1,2](Electronics & Tele-communication Department,
Sahyadri Valley College of Engineering & Technology, S. P. Pune University, India)

ABSTRACT: *There are different types of number systems. Binary number system, octal number system, decimal number system and hexadecimal number system. This paper demonstrates conversion of hexadecimal to binary number using Xilinx software.*

KEYWORDS – *Analyzer, IEEE, Verilog, VHDL, Xilinx*.

I. INTRODUCTION

Numbers are used to represent whole integers for example 1, 2, 3, 11 and so on. In our daily life we use decimal number system for carrying out functions like addition, subtraction, multiplication and division.
Other types of number systems used in computers and calculators are:

1] Binary number system: This system is having only two digits, binary logic 0 and logic 1. Thus, base of this number system is 2.

2] Octal number system: This system is having digits 0 through 7. E.g. 0, 1, 2, 3, 4, 5, 6, 7, 12, 23, 34, 45, 56, 67 are octal numbers. These numbers are constructed using only 0, 1, 2, 3, 4, 5, 6, 7 integers. Thus base of the system is 8. These numbers are represented as: $(1234)_8$, $(5672)_8$, $(4563)_8$.

3] Decimal number system: Decimal number system is having integers 0, 1, 2, 3, 4, 5, 6, 7, 8, 9. Thus base of this number system is 10. These numbers are represented as follows: $(123)_{10}$, $(904)_{10}$, $(456)_{10}$, $(786)_{10}$. We always consider base as 10 for writing numbers in system thus these numbers can also be written simply as: 123, 904, 456, 786 and so on.

4] Hexadecimal number system: Hexadecimal number system is having numbers from 0, 1, 2, 3, 4, 5, 6, 7, 8, 9, A, B, C, D, E, F. This number system is used for microprocessor and micro-controller as well as ASICs programming as assembly level language. Instruction's address is given in hexadecimal number system using this language. E.g. 10A0, 0010, 001E, 001F etc.

II. CONVERSION OF NUMBERS.

1. Octal to binary number conversion: Octal numbers are having base or radix 8. These numbers are represented as: $(345)_8$, $(756)_8$ etc. For conversion of octal numbers to binary number, binary equivalent of octal number is grouped into three binary bits.

E.g. $(3)_8 = (011)_2$, $(4)_8 = (100)_2$.

2. Decimal to binary conversion: For conversion of decimal numbers to binary numbers divide each decimal number by 2 and write remainder quotient and remainder outside.
For example, take $(10)_{10}$:

TABLE 1: CONVERSION OF DECIMAL NUMBER TO BINARY NUMBER.

Divider	Number/Quotient	Remainder
	10	
2	5	0
2	2	1
2	1	0
2	0	1

Arrange remainder from bottom to top for getting binary equivalent of decimal number.

3. Hexadecimal to binary conversion: Hexadecimal numbers are 0 to 9 and A, B, C, D, E, F. The base of this number system is 16. These numbers are represented as follows: $(1AFE)_{16}$, $(1ACE)_{16}$ etc.
For conversion of hexadecimal numbers to binary numbers, make group of 4 binary equivalent bits of hexadecimal number.
For example: $(0)_{16} = (0000)_2$, $(1)_{16} = (0001)_2$, $(2)_{16} = (0010)_2$, $(3)_{16} = (0011)_2$, $(A)_{16} = (1010)_2$, $(B)_{16} = (1011)_2$, $(C)_{16} = (1100)_2$, $(D)_{16} = (1101)_2$, $(E)_{16} = (1110)_2$, $(F)_{16} = (1111)_2$.
Decimal equivalent of hexadecimal alphabets A = 10, B = 11, C = 12, D = 13, E = 14 and F = 15.

4. Decimal to Octal number system: For conversion of decimal numbers to octal number divide decimal number by 8. Remainders will give octal equivalent of decimal numbers.
For example: $(389)_{10} = (?)_8$

TABLE 2: CONVERSION OF DECIMAL NUMBER TO OCTAL NUMBER.

Divider	Number/Quotient	Remainder
	389	
8	48	5 ↑
8	48	0 |
8	0	6 |

Arrange remainder from down to up for getting octal equivalent of number.
Thus, $(389)_{10} = (605)_8$.

5. Hexadecimal to decimal system: For conversion of Hexadecimal number to decimal number convert hexadecimal number into binary equivalent by grouping into four bits first then multiply the binary bits stream by equivalent of 2^n position of bits.

For example: $(BCD)_{16} = (?)_{10}$
$(BCD)_{16} = (1011\ 1100\ 1101)_2 = (1\times2^{11} + 0\times2^{10} + 1\times2^9 + 1\times2^8 + 1\times2^7 + 1\times2^6 + 0\times2^5 + 0\times2^4 + 1\times2^3 + 1\times2^2 + 0\times2^1 + 1\times2^0)_{10} = (3021)_{10}$.

6. Hexadecimal to Octal number system: For conversion of hexadecimal numbers to octal number, first convert hexadecimal number to binary number then group binary bits into group of three bits for getting equivalent conversion of hexadecimal number.
E.g. $(A23F)_{16} = (1010\ 0010\ 0011\ 1111)_2 = (1010001000111111)_2 = (001\ 010\ 001\ 000\ 111\ 111)_2 = (1\ 2\ 1\ 0\ 7\ 7)_8 = (121077)_8$.
If in grouping of three binary bits there are less bits then add zeros to left side for completing grouping of three bits.

7. Hexadecimal to binary number system: For conversion of hexadecimal to binary number system convert each hexadecimal number into binary group of four bits. Resulting number is binary equivalent of hexadecimal number.
For example: $(A123)_{16} = (1010\ 0001\ 0010\ 0011)_2$.

III. LITERATURE SURVEY.

History of Verilog Language: Verilog HDL was also consisting of Verilog Simulator. Verilog-XL, a new version of simulator with the enhanced language and simulator was introduced in 1985.
1989:
- Cadence bought Gateway.

1990:
- In early 90's Cadence split Verilog HDL and Verilog-XL simulator into separate products.
- Verilog was then released to public domain.
- OVI (Open Verilog International) was formed to control the language specification.
  - 1993:
- Of all design submitted to ASIC foundries in this year, 85% were designed and submitted using Verilog.
  - 1995:
- The Verilog language was reviewed and adopted by the IEEE as IEEE standard 1364.
  - Verilog can handle all levels of design abstraction.

- Verilog HDL allows different levels of abstraction to be mixed in the same model.

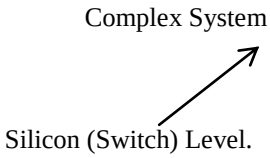

IV. FEATURES OF VERILOG

Universality:
Verilog is universal. It allows the entire design process to be performed within one design environment.

Industrial Support:
Verilog supports switch level modeling, hence has always been popular with ASIC designers, as it allows fast simulation & effective synthesis.

Extensibility:
The IEEE standard 1364 contains definition of PLI (Programming Language Interface) that allows for extension of Verilog capabilities.

Similarity with C:
Syntax is similar to the C programming language. Hence C programmers find it easy to learn Verilog.
"VERILOG is case – sensitive language."

Levels of Abstraction:
Verilog is both, behavioral and structural language. Designs in Verilog can be described at all the four levels of abstraction depending on the needs of design.

Behavioral Level:
It is used to model behavior of design without concern for the hardware implementation details. Designing at this level is very similar to C programming.

Dataflow Level [Register Transfer Level: RTL]:
Module is specified by specifying the data flow. The designer is aware of how the data flows between registers.

Gate Level:
Module is implemented in terms of logic gates & interconnections between these gates.
Design at this level is similar to describing design in terms of gate level logical diagram.

Switch Level:
Lowest level of abstraction is provided by Verilog. Module can be implemented in terms of switches, storage nodes & interconnection between them.

V. SOFTWARE REQUIRED.

Xilinx ISE 9.1

For conversion of hexadecimal number to binary number ⊕ = XOR operation is used.
The conversion of plaintext into binary code is done using Xilinx software and programming is done in Verilog.

Xilinx ISE tools:
Xilinx have different tools for viewing snapshots. Snapshots are the outputs of RTL schematic and technology schematic.
Other tools are: Constraints editor, core generator, schematic viewer, timing analyzer FPGA editor, FPGA editor, XPower Analyzer, iMPACT, SmartXplorer and so on.

VI. RESULTS OF EXPERIMENT.

For converting hexadecimal text i.e. plaintext into cipher text i.e. binary output stream of bits two processes are required which are implementation process and simulation process. Simulation process is required to simulate

i.e. to provide inputs to Behavioral Model. IEEE 1532 programming is supported by iMPACT when provided by an .ISE file.

Register Transfer Level (RTL) schematic:

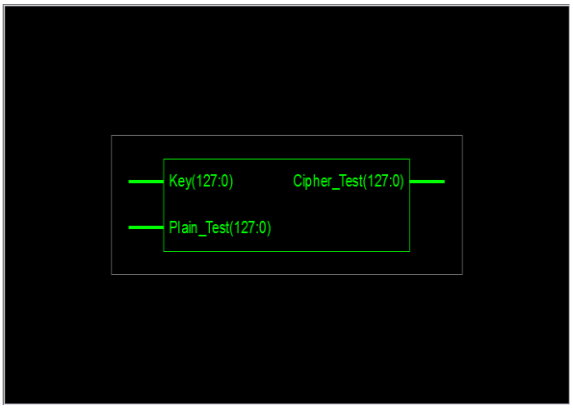

Figure 1: RTL Schematic.

Cipher output:

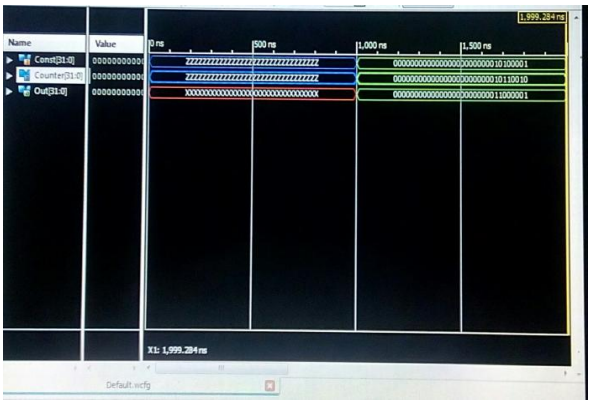

Figure 2: Binary output view.

VII. CONCLUSION.

In this project, for conversion of hexadecimal number given as input to cipher output i.e. a binary equivalent code of hexadecimal input Verilog programming is done using Xilinx ISE 9.1.
RTL schematic can be viewed by schematic viewer as shown in Figure 1. Binary output is given in Figure 2.

VIII. ACKNOWLEDGEMENTS

I place on record, my sincere thanks to all authors mention in references, my guide Prof. Chankya K. Jha and all my friends for their support.

REFERENCES

[1] J. Aumasson. On a bias of Rabbit, presented at the State of the Art of Stream Ciphers Workshop (SASC 2007).
[2] M. Boesgaard, M. Vesterager, T. Pedersen, J. Christensen, and O. Scavenius, "Rabbit: A new high-performance stream cipher," LectureNotes in Computer Science, vol. 2887, pp. 307–329, 2003.
[3] D. J. Bernstein, "Which eSTREAM ciphers have been broken?" Dept. Math., Statistics Comput. Sci. (M/C 249), Univ. Illinois, Chicago, IL, USA, 2008.
[4] S. Fischer, W. Meier, C. Berbain, J. Biasse, and M. J. B. Robshaw, "Non-randomness in eSTREAM candidates Salsa20 and TSC-4," FHNW 5210 Windisch, Switzerland, FTRD, 92794 Issy les Moulineaux, France, 2008.
[5] P. Crowley, "Truncated differential cryptanalysis of five rounds of Salsa20," presented at IACR Cryptology ePrint Archive, pp.375-375, Sep. 2005.
[6] Y. Tsunoo, T. Saito, H. Kubo, T. Suzaki, and H. Nakashima, "Differential cryptanalysis of Salsa20/8," in *Proc. Workshop Rec. SASC 2007: StateArt Stream Ciphers*, eSTREAM Rep. 2007/010, 2007.
[7] J. Hernandez-Castro, J. Tapiador, and J. Quisquater, "On the Salsa20/8 core function," *Lecture Notes in Computer Science*, vol. 5086, pp. 462–469, Feb. 2008.
[8] Mohsen A. M. El-Bendary*a*, AtefAbou El-Azm*b*, Nawal El-Fishawy*b*, FaridShawki*b*,Mostafa A. R. El-Tokhy*a*, Fathi E. Abd El-Samie*b*, and H. B. Kazemian*c*: SVD Audio Watermarking: A Tool to Enhance the Security of Image Transmission over ZigBee Networks.
[9] S. Sadoudi, C. Tanougast, and M. S. Azzaz: First experimental solution for channel noise sensibility in digital chaotic communications.
[10] Vimalathithan R. and M. L. Valarmathi : Cryptanalysis of Simplified-AES using Particle Swarm Optimization.
[11] Xiaoling Huang: A new digital image encryption algorithm based on 4d chaotic system.

Chinmay V. Deshpande is pursuing his M. E. in Electronics and Tele-communication Department (VLSI and Embedded Systems) from S. P. Pune University, India. He graduated in Electronics and Tele-communication Engineering from Sant Gadge Baba Amravati University, India. His areas of interest are wireless sensor networks, micro-processor and micro-controller and VLSI technology.

American Journal of Engineering Research (AJER) 2015
American Journal of Engineering Research (AJER)
e-ISSN: 2320-0847 p-ISSN : 2320-0936
Volume-4, Issue-8, pp-216-221
www.ajer.org
Research Paper Open Access

Fuzzy Logic Expert System-A Prescriptive Approach

Wahid palash[1], Md. Fuzlul Karim[2], Sumaiya Sultana Rika[3], Md. Faruque Islam[4]
[1] *(IICT, Bangladesh University of Engineering Technology, Bangladesh)*
[2] *(EEE, American International University- Bangladesh, Bangladesh)*
[3] *(CSE, Ahsanullah university of science and technology, Bangladesh)*
[4] *(EEE, American International University- Bangladesh, Bangladesh)*

ABSTRACT: *A membership value of a fuzzy set has been defined as the degree to which an element belongs to this fuzzy set. It is possible to give other interpretations to the membership degree like a certainty factor, a degree of truth, a degree of satisfaction and a degree of possibility. In 1978 Zadeh extended the fuzzy set theory to a possibility theory where the membership values are considered as degrees of possibility. Zadeh justies the possibility theory by the fact that the imprecision that is intrinsic in natural languages is, in the main, possibility rather than probabilistic in nature. In contrast to the statistical perspective of the information which is involved in the coding, the transmission and the reception of the data, the theory of possibility focuses on the meaning of the information. One of the reasons the scientific community took an interest in the fuzzy logic theory is the financial success of fuzzy control in home appliances in the Japanese industry. In 1990, the consumer products market using fuzzy controllers was estimated to 2 billion dollars. Interestingly enough L. A. Zadeh is a major contributor of the modern control theory. The control theory is a very precise and strict approach in order to model systems or phenomena.*

Keywords -*Linguistic variable, Fuzzy set, Control Theory, System, and operator.*

I. INTRODUCTION

One central concept in the possibility theory is the possibility distribution which is the counterpart of the probability distribution in the probability theory. A possibility distribution is a fuzzy set called fuzzy restriction, which acts as an elastic constraint, whose membership function determines the compatibility or the possibility with the concept of the fuzzy set. Given a possibility distribution it is possible to compute the possibility of another fuzzy set defined on the same universe [1]. Consider for instance the possibility distribution 'young' of a linguistic variable 'age' defined on the universe U and the fuzzy set 'around 35' also defined on U. By knowing that 'Mary is young' it is then possible to calculate the possibility that 'Mary is around 35'. Note that the possibility represents a degree of feasibility whereas the probability is related to a degree of likelihood implying that what is possible might not be probable and, conversely, what is improbable might not be impossible. The possibility theory opens the door to the fuzzy reasoning which can represent and manipulate the natural language. Almost all human related problems are so complex and so vague that only approximate linguistic expression can be used. The fuzzy approximate reasoning is based on different fuzzy inference patterns which deal with different implication interpretations and also determine the way the uncertainties are propagated. The fuzzy inference can then compute or deduct elastic constraints (fuzzy sets) determined by membership functions via the possibility concept.The idea of fuzzy logic was first advanced by Dr. Lotfi Zadeh of the University of California at Berkeley in the 1960s [2]. Dr. Zadeh was working on the problem of computer understanding of natural language. Natural language (like most other activities in life and indeed the universe) is not easily translated into the absolute terms of 0 and 1. (Whether everything is ultimately describable in binary terms is a philosophical question worth pursuing, but in practice much data we might want to feed a computer is in some state in between and so, frequently, are the results of computing.)Fuzzy logic includes 0 and 1 as extreme cases of truth (or "the state of matters" or "fact") but also includes the various states of truth in between so that, for example, the result of a comparison between two things could be not "tall" or "short" but ".38 of tallness."

II. FUZZY CONTROL THEORY

As all the aspects of the model have to be specified, modeling a complicated system is an extensive operation. For example, an application could be used to predict the path of a hurricane but if it has to be developed from scratch, the hurricane will be gone before the application is ready to use. In the control theory, the number of processes to be implemented grows exponentially relatively to the number of variables defining the system. For this reason some systems cannot be modeled even by high speed computers. A solution to this problematic is to roughly define systems with the help of the fuzzy logic theory. The fuzzy control is based on the approximate reasoning which offers a more realistic framework for human reasoning than the two-valued logic. The main advantages of fuzzy control over the classical control theory is its ability of implementing human expert knowledge, its methods for modeling non-linear systems and a shorter time to market development.

In the control theory systems are characterized by input and output variables as well as a set of rules. These rules define the behavior of the system [3]. The output variables are then calculated by inference based on the input variables and the given rules. An inference is the construct 'A implies B, B implies C then A implies C'. When a premise 'X implies Y' holds then Y is true if X is true and, conversely, X is false if Y is false. This is called a syllogism and a famous example is:

Implication: All men are mortal
Premise: Socrates is a man
Conclusion: Socrates is mortal

In the control theory the premises are defined by rules in the form 'If X is F Then Y is G' where X (resp. Y) is an input (resp. output) variable and F (resp. G) is a condition on X (resp. Y). Zadeh introduced in 1973 the compositional rule of inference which extends the inference mechanism in order to take the fuzziness into account. In 1993, Fullér and Zimmermann demonstrated the stability property of the conclusion using the compositional rule of inference which states that a conclusion depends continuously on the premise when the t-norm defining the composition and the membership function of the premise are continuous. This property guarantees that small changes in the membership function of the premise, eventually due to errors can imply only a small deviation in the conclusion.

The fuzzy rules can then be expressed in the natural language by the use of linguistic variables. Zadeh's fuzzy inference example where the conditions are expressed by the means of words is:

Implication: If a tomato is red then it is ripe
Premise: This tomato is very red
Conclusion: This tomato is very ripe

These words allow the fuzzy rules to integrate the semantics of the human knowledge and can be represented as fuzzy sets. The evaluation process of the fuzzy inference also differs from the classical control theory in the sense that all the rules involving a given output variable are computed simultaneously and their results are then merged in order to derive the value of the output variable. This is a major advantage over the classical control theory as it implies a compensation mechanism between the involved rules. As a result, a much smaller set of rules is required to model a system as the intermediate values of the input variables are dynamically interpolated from the existing rules. It also implies an inherent fault tolerance; consider that a rule has been erroneously implemented or that a hardware defect returns wrong results, the value of the output variable can be compensated by other rules defining this variable.

Many concrete applications using fuzzy control can be found. The most famous one is the opening in 1988 of a subway system in Sendai city (Japan) using the fuzzy control to accelerate and brake the trains more smoothly than a human driver. Compared to conventional control, this new approach achieved significant improvements in the fields of safety, riding comfort, accuracy of stop gap, running time and energy consumption. Other concrete applications can be found in domestic appliances like washing machines and vacuum cleaners, in visual systems like camera auto focus and photocopiers, in embedded car systems like anti-lock braking systems, transmission systems, cruise control and air conditioning, etc.

III. FUZZY EXPERT SYSTEM

Expert systems are a successful example from the broad field of artificial intelligence. Expert systems are knowledge-based systems which can derive decision or conclusion based on an extensive knowledge on a particular domain. More precisely, “an expert system is a program that can provide expertise for solving problems in a defined application area in the way the expert’s do”. This knowledge is represented in a set of 'If-Then' rules. By applying inferences on the specified rules, expert systems are able to derive optimal decisions.

A major problematic, however, is to convert the experts' knowledge into a set of 'If-Then' rules which are exact given that the human representation of the knowledge cannot be sharply determined. This drawback can be

overcome by introducing the fuzziness. This is done by allowing the definition of fuzzy rules, i.e. rules with words determined by a membership function, and by applying the previously defined fuzzy inference [4]. Just like in the fuzzy control, the fuzzy inference allows a dynamic compensation between the different fuzzy rules which results in the definition of a smaller set of rules. Fuzzy expert systems are usually involved when processes cannot be described by exact algorithms or when these processes are difficult to model with conventional mathematical models.Although the rules definition and the inference mechanism of fuzzy expert systems are similar to those in fuzzy controls, fuzzy expert systems do not come under the category of fuzzy control. Fuzzy control applications (often called fuzzy controllers) work in a closed loop schema where the output variables, which are derived from the input variables, directly act on the considered object. The rules are then executed in cycles in order to maintain a system. In the case of fuzzy expert systems and, more generally, for fuzzy diagnosis, fuzzy data analysis and fuzzy classification systems, the output information of a fuzzy system is dedicated to a human user or a monitoring device and hasn't any impact on the object itself.

Earl Cox has implemented different fuzzy expert systems which have been successfully applied to the following domains: transportation, managed health care, financial services, insurance risk assessment, database information mining, company stability analysis, multi-resource and multi-project management, fraud detection, acquisition suitability studies, new product marketing and sales analysis. By comparing fuzzy expert systems with conventional expert systems Cox stated that "generally, the final models were less complex, smaller, and easier to build, implement, maintain, and extend than similar systems built using conventional symbolic expert systems".

IV. FUZZY CLASSIFICATION WITH DEFINITION

The fuzzy classification is a natural extension of the traditional classification, the same way that the fuzzy sets extend the classical sets. In a sharp classification, each object is assigned to exactly one class, meaning that the membership degree of the object is 1 in this class and 0 in all the others. The belonging of the objects in the classes is therefore mutually exclusive. In contrast, a fuzzy classification allows the objects to belong to several classes at the same time; furthermore, each object has membership degrees which express to what extent this object belongs to the different classes [5].

Definition Let O be an object characterized by a t-dimensional feature vector xO of a universe of discourse U. Often U is the space Rt. Let C1; Cn be a set of classes which is given a priori or has to be discovered. A fuzzy classification calculates a membership vector M = fm1; : : : ;mng for the object O. The vector element mi 2 [0; 1] is the degree of membership of O in the class Ci.

In many real applications, a dichotomous assignment of an object in one class is often not possible as no unique conclusion can be derived from the object features and/or the object features cannot be exactly observed. This is particularly true for problems related to the human evaluation, intuition, perception and decision making where the problem structure is not dichotomous. The definition of the classes can be determined by using the knowledge of experts of the domain or can be automatically found by the use of data mining techniques like cluster analysis.

The fuzzy classification approach can be used for instance for diagnosis and for decision making support. In the case of a diagnosis system for ill persons, the classification procedure can derive the illness based on the symptoms of the patient or find a suitable therapy considering the illness of the patient. In a decision making process, the classification (also called segmentation depending on the context) is used to derive management decisions based on several characteristics of the objects. A major issue in this field is the complexity of the data, i.e. the abundance of information. This complexity is a source of uncertainty due to the limited capability of human beings to observe and handle large amounts of data simultaneously. As in the management field a large number of objects described by many features is usually considered, the classification approach, by grouping similar objects into classes, results in a complexity reduction which enables a better situation analysis. Furthermore, the fuzzy classification, in contrast to the classical one, by allowing objects to belong to several classes at the same time, reduces the complexity of the data and also provides much more precise information about the classified elements.

V. DATABASES & FUZZINESS

In practice, information systems are often based on very large data collections, mostly stored in relational databases. Due to an information overload, it is becoming increasingly difficult to analyze these collections and to generate business decisions. To address this issue, a toolkit for classification, analysis and decision support named FCQL (fuzzy Classification Query Language) has been developed. This toolkit is a combination of relational databases and fuzzy logic. Unlike statistical data mining techniques such as cluster or regression analysis, fuzzy logic enables the use of non-numerical values and introduces the notion of linguistic variables. Using linguistic variables and terms hides the complexity of the domain and enables a more intuitive and human-oriented querying process [6].

The proposed FCQL toolkit reduces the complexity of business data and extracts valuable hidden information through a fuzzy classification. The main advantage of a fuzzy classification compared to a classical one is that an element is not limited to a single class but can be assigned to several classes. Furthermore, each element has one or more membership degrees which illustrate to what extent this element belongs to the classes it has been assigned to. The notion of membership gives a much better description of the classified elements and also helps to reveal their potentials as well as their possible weaknesses.

The FCQL toolkit transforms FCQL queries into SQL (Structured Query Language) statements for sharp databases, thus allowing business managers to formulate and analyze uncap queries at a linguistic level. Being an additional layer above relational database systems the proposed fuzzy classification approach guaranties a full compatibility with legacy applications. The FCQL toolkit also provides a graphical user interface to define the fuzzy classifications, meaning that the fuzzy classes, the linguistic variables and terms as well as the membership functions can be defined using a user friendly wizard.

Another important issue, considering the size and the security concern of the data collections, is that neither modification of the underlying databases nor migration of the existing data have to be undertaken. The fuzzy classification is achieved by an extension of the relational database schema in such a way that it directly operates on the underlying databases and requires no migration of the raw data. Furthermore the SQL commands as well as the transaction and recovery mechanisms offered by the RDBMS (Relational Database Management System) are still available.

In everyday business life, many examples can be found where the fuzzy classification approach would be useful. In the customer relationship management for instance, a standard classification would sharply classify customers of a company into a certain segment depending on their buying power, age and other attributes. If the client's potential of development is taken into account, the clients often cannot be classified into only one segment anymore, i.e. customer equity. Other application domains discussed in the outlook of this thesis are the portfolio analysis, the credit worthiness, the marketing mix theory and some personalization issues.

VI. FUZZY SHAPE QUERIES

Querying and retrieving of data from a database is an important activity. Fuzzy querying allows users to formulate queries using linguistic words, hence it is more flexible than crisp querying. In addition, fuzzy queries produce naturally ranked results whereas conventional queries bring back only undifferentiated tuples. Fuzzy queries may also provide reasonable answers where crisp queries fail to find solutions. When querying the shape database, a user can formulate a query by searching the shape name and version. Frequent users may also query shapes using the shape ID, which is automatically generated by the computer. However, it is sometimes desirable to search shapes using natural-language-like shape descriptors, especially for occasional users. It is also desirable to allow users to express preferences and thus make the querying results more feasible. Using vague predicates represented by fuzzy sets to perform a query is one approach to achieve the above targets.

Query requirement analysis is based on the task the query will complete and the type of users. The aim of querying a shape database is to obtain the appropriate shape. People usually perceive a shape by commonly used regular shape names, by pictures or by shape description. For example, for a cubical shape, people will describe it as cube, cuboid, cubic, cubical, or square. Hence, the system should allow querying by shape descriptions. If the shape number of this cube in the shape database is 10 and the user knows this number, s/he may just ask “list out the 10th shape”. The query system should respect the diversity of querying, therefore multiple query options should be provided [7].

The users can be classified into primary users who use the system regularly and secondary users who use the system only casually. The query system should allow primary users to input their query as quickly as possible. This is achieved by querying the database using shape ID or name. For novice or casual users, the system should provide effective guidance. The Query-By-Example method and intelligent query assistant are usually employed to guide the query process. In the shape database, the underlying shape descriptors represent the geometric characteristics of shapes along different directions based on the shape representation approach. Although they are represented by words and can be understood by professional users, it is still hard for general users to understand and formulate shape queries using these descriptors. Hence, a Graphical User Interface is utilized to help users to formulate query. Commonly used shape descriptors are displayed in the GUI and they will be translated into underlying basic shape descriptors through a translator. In addition, the support messages, such as on-line help and error messages should be provided.

The shapes are classified into two classes: fuzzy shapes and crisp shapes. The main difference between these two kinds of shapes is the data associated with the shape parameters. For a crisp shape, each parameter has only one value whereas for a fuzzy shape, each parameter has a fuzzy set value. In the case of fuzzy query on crisp shapes, each tuple will be assigned a Degree of Fulfilment (DOF) to the fuzzy condition. In the case of fuzzy query on fuzzy shapes, the similar method as fuzzy query on crisp shapes can be employed but the calculation method for DOF is different and two DOFs are needed. In the latter case, we use the possibility and necessity degrees to measure the extent to which a datum satisfies a condition.

In a fuzzy database, the crisp data and the fuzzy data can be represented uniformly by fuzzy sets, and a crisp value is only a special case of a fuzzy value where the membership grade is one for a crisp element and zero for all others. Since the fuzzy shape database is mainly used for storing and retrieving initial fuzzy shapes that have fuzzy set values, hereafter we consider fuzzy queries on fuzzy data only. The possibility/necessity measures will be used to represent the upper and lower bounds of the satisfaction degree of a fuzzy datum with respect to a fuzzy condition.

The categories of fuzzy queries can be further classified into the following classes: simple query and combined query. A simple query refers to a query by a single condition. For example, the user inputs a single shape descriptor such as extremely round and a series of shapes will be retrieved from the database and will be displayed on the screen in multiple views. A combined query refers to a query composed of multiple descriptions. For example, a user inputs a combination of shape descriptions, such as extremely round and slightly bevel, and a series of shapes will be retrieved from the database and will be displayed on the screen.

Shape description combination can be classified into feasible combination and infeasible combination. Feasible combination means that two descriptors on the two sides of AND operator can be used to describe the same shape at the same time. For example, the descriptors extremely cylindrical and slightly bent can exist at the same time because they describe a shape that is a slightly bent cylinder. Infeasible combination means that two descriptors on the two sides of AND operator cannot be used to describe the same shape at the same time. For example, a cylindrical shape cannot be pyramidal. The feasible combination can be passed to the inference engine for deriving the result values. The infeasible combinations will be checked out by the system according.

VII. LIMITATION OF FUZZY LOGIC

Fuzzy logic is based on same principle as classical logic, the principle of truth-functionality. Logic is truth functional if the truth value of a compound sentence depends only on the truth values of the constituent atomic sentences, not on their meaning or structure. In the two-valued logic the mentioned principle is enough for all axioms. In case of all many-valued logics, including fuzzy logic, this principle is not sufficient and as a consequence these logics are not in the Boolean frame. More precisely, fuzzy logic is a precise many-valued logic where axioms of non-contradiction and excluded middle are not satisfied. It is obvious on following example: “WHERE attribute >5 and attribute <=5” (contradiction). In classical query it is obvious that criterion retrieves no record from database. In case of fuzzy query when the “WHERE attribute is Big and attribute is not big” criterion is used it could be expected that no record is retrieved because of non-contradiction axiom existence but min t-norm retrieves some records with QCI≤0.5. This is the consequence of not satisfied non-contradiction axiom. First way how to use the gradation in mathematics is to leave these axioms as non-adequate and accept the principle of truth functionality with all consequences. When the first way is chosen, it is possible to avoid this problem by selecting adequate t-norm or t-conform function for each query. A new t-norm T^ and a new t-conform C^, which depend on a parameter r in [-1, 1] or the correlation between the truth values of the operands are explained in.The second way is to go to the source of Boolean algebra and find the principle for gradation to be in the frame of the Boolean algebra. New approach to treating fuzziness or gradation in logic is based on the Interpolative Realizations of Boolean Algebra (IBA). The IBA ensures that the whole selection process will be in the frame of Boolean algebra and avoids theoretically possible situations when inappropriate functions are chosen.

VIII. PERFORMANCE MEASURE

The cost of query evaluation can be measured in terms of a number of different resources, including disk accesses, CPU time to execute a query and in a distributed or parallel database system, the cost of communication. In large database systems, however disk accesses which we measure as the number of transfers of blocks from disk are usually the most important cost, since disk accesses are slow compared to in memory operations. Moreover, CPU speeds have been improving much faster than have disk speeds. Thus, it is likely that the time spent in disk activity will continue to dominate the total time to execute a query. Finally estimating the CPU time is relatively hard, compared to estimating the disk access cost. Therefore, most people consider the disk access cost a reasonable measure of the cost of a query evaluation plan.

We use the number of block transfers from disk as a measure of the actual cost. To simplify our computation of disk-access cost, we assume that all transfers of blocks have the same cost. This assumption ignores the variance arising from rotational latency and seek time. To get more precise numbers, we need to distinguish between sequential input / output, where the blocks read are contiguous on disk, and random input/output, where the blocks are noncontiguous, and an extra seek cost must be paid for each disk input/output operation. We also need to distinguish between reads and writes of blocks, since it takes more time to write a block to disk than to read a block from disk. A more accurate measure would therefore estimate

1. The number of seek operations performed
2. The number of blocks read
3. The number of blocks written

And then add up these numbers after multiplying them by the average seek time, average transfer time for reading a block, and average transfer time for writing a block, respectively. Real-life query optimizers also take CPU costs into account when computing the cost of an operation. For simplicity we ignore these details, and leave it to you to work out more precise cost estimates for various operations.

The cost estimates we give ignore the cost of writing the final result of an operation back to disk. These are taken into account separately where required. The cost of all the algorithms that we consider depend on the size of the buffer in main memory. In the best case, all data can be read into the buffers and the disk does not need to be accessed again. In the worst case, we assume that the buffer can hold only a few blocks of data approximately one block per relation. When presenting cost estimates, we generally assume the worst case.

IX. CONCLUSION

The meaning and purpose of the previous query is understandable for the user who creates and uses it. In case of reuse of the same query in e.g. different time period or by different user the meaning and purpose of query is not obviously clear at the first glance. Fuzzy query contains logical conditions defined by linguistic expressions whereby the query becomes easy understandable and applicable. The meaning of a query remains the same, only the parameters and shapes of fuzzy sets are changeable to allow the query adaptation to new situations or requirements. A disseminated number without meaning (without explanatory metadata) does not tell very much to user. A number in a WHERE clause does not An Approach to Fuzzy Database Querying, Analysis and Realization explain the purpose of a query in many situations. As metadata are used to explain the meaning of the figures, the linguistic expressions are used to explain the meaning of a query. Fuzzy query enables also simplified and easy to use distance measurement of records around selected value. For this purposes normalized (fuzzy set is normalized if $ x,m A (x) = 1) and symmetric fuzzy sets shown in figure 4 are used. The criterion "WHERE attribute is approximately 5" can be described with "about" fuzzy set. The query retrieves all records that have attribute value equal to 5 and all records that have QCI>0 and QCI value is a distance value of each selected record.

ACKNOWLEDGEMENT

We are earnestly grateful to one our group member, Md. Fuzlul Karim, EEE, American International University-Bangladesh. For providing us with his special advice and guidance for this project. Finally, we express our heartiest gratefulness to the Almighty and our parents who have courageous throughout our work of the project.

REFERENCES

[1]. B. K. Bose, "*Expert systems, fuzzy logic, and network application control"*, Proceeding of the IEEE, vol.81, Aug. 1996.
[2]. L. H. Tsoukalas and R. E. Uhrig, "*Fuzzy and Neural Approaches in Engineering",* John Wiley, NY, 1997.
[3]. Math Works, Fuzzy Logic Toolbox User's Guide, Jan., 1998.
[4]. B. Jaychanda, simulation studies on "*Speed Sensor less Operation of Vector Controlled Induction Motor Drives Using NeuralNetworks"*, Ph.D. Thesis, IIT, Madras, Chennai.
[5]. T. Takagi and M. Sugeno, *"Fuzzy identification of a system andits application to modeling"*, IEEE Trans. Syst. Man and Cybern., vol.15, pp.116-132, Jan./Feb. 1985.
[6]. I. Milki, N. Nagai, S. Nishigama, and T. Yamada, *"fuzzy P-I controller"*, IEEE IAS Annu. Meet. Conf. Rec., pp. 342-346, 1991.
[7]. M. Nasir Uddin, Tawfik S. Radwan and M. Azizur Rahman, "Performances of Fuzzy-Logic-Based measurement", IEEE TRANSACTIONS ON INDUSTRY APPLICATIONS, VOL. 38, NO.5,SEPTEMBER/OCTOBER 2002, P1219.

American Journal of Engineering Research (AJER) 2015
American Journal of Engineering Research (AJER)
e-ISSN: 2320-0847 p-ISSN : 2320-0936
Volume-4, Issue-8, pp-222-228
www.ajer.org
Research Paper Open Access

Data Evaluation as a Guide in Water Treatment Process Selection

[1,4]H. A. Abdulkareem, [2]Bitrus Auta, [2]Habila Yusuf, [4]Bitrus I Dangyara
[1]*Department of mechanical Engineering, School of Industrial Engineering, College of Engineering, Kaduna, Polytechnic, Nigeria*
[2]*Applied Science Department, School of Science and Technical Education, College of Science and Technology Kaduna Polytechnic, Nigeria*

Abstract: *Data analysis and evaluation form the basis of all engineering design. In order to come up with a cost effective design of a water treatment plant in small communities around Maiduguri, Borno State, the population as well as the surface water within the selected localities were evaluated and analyzed leading to a process selection which is expected to provide potable drinking water that satisfies the requirement of WHO (world Health Organization) standard.*
Key words: *Data evaluation, water treatment, process selection*

I. Introduction

Absolutely pure water is rarely found in existence in nature, so there has always been a demand for pure portable water [3].

Most waters have to be purified before they can be used for portable purposes. Raw water is so infinitely variable in quality, that there is no fixed starting point to the treatment process, and within much narrower limits, there is no fixed starting point to the treatment process, and within much narrower limits, there is no rigidly fixed finishing point either.

There is virtually no water that is impossible to purify into potable standards. Accordingly it may be free from disease-producing organisms and poisonous or physiological undesirable substances[1].

The source of raw water determines its inherent quality, the quality of which is difficult to foresee, hence there is the need to collect samples of the raw water for a certain period of time and carry out some tests to ascertain the characteristic purities of the raw water and the relative quantity of each impurity.

Naturally occurring water can generally be classified as; groundwater, or surface water. Each has its own characteristic, but in general, ground water is the purest form of water available, and may not require much treatment compared to its counterpart (surface water).

Basic Needs

i. Due to health hazards experienced in different parts of the country, especially in rural communities; where the only supply of water is from a river source, free flowing stream or ponds which are not kept in good sanitary conditions, resulting in high epidemic rates such as cholera, typhoid guinea worm diseases etc.
ii. The needs to reduce the nation's high health bills due to epidemics, and other water borne diseases.
iii. The need to improve on the water supply system in rural communities.

II. History of Water Treatment

The History of water-quality improvement dates back to the history of man, when he realised that allowing water to stay for some hours or days improves its clarity. This is due to the gravitational forces acting on the suspended particles in water which causes them (naturally) to settle down at the bottom of the container to which they are kept. This simple art of allowing water to stay for some time in the bid to improve its clarity is called sedimentation. [5]

The use of sand as a form of filter dates back to the ninth century, where it was used as a form of deep-bed filter. Different layers of sands from the coarsest to the finest were arranged so that the raw water passes from the coarsest to the finest sand by means of gravity, thereby trapping the impurities, which are in the form of suspended solid particles along its way to the finest sand. [5]

The use of chemicals such as coagulants e.g. aluminum sulphate was used in conjunction with rapid sand filters in the late 19^{tn} century. The use of these chemical form a flocculent precipitate which traps suspended matter, and aids its removal by other chemicals like lime, iron sulphate were also used. [5]

Flocculation as a means of further improvement in the quality of water is a relatively new invention, which emergedin about the 19th century. This is the process whereby the water purification stage of coagulation is further enhanced by the rotating members to form large floc which become heavy and easy to settle in the bottom of the tank. [5]

The disinfection of water as the final process for assuring its safety for the consumer was not practiced until the first decade of the 20th century. The earliest form of chemicals used for this disinfection was bleaching powder, hypo-chlorides, and later chlorine gas, which were found to be successful in earlier water works. [5]

The first successful water treatment plant for domestic use was in New York (United States) in 1871, which was based on the slow sand filtration process, in addition to other purification techniques [4]. The first successfully use of chemical coagulants was that in 1884, also in the United States, which used metal salts, principal1y those of iron and aluminum [4].

Later developments of treatment plants both for domestic and industrial usage was enhanced by modern techniques, which dissolved new purification methods based on known scientific facts, and also the modification of previous techniques, by enhancing or combining separate processes together.

III. Quality of Water

The quality of water is defined in terms of its associated impurities. This gives a true picture of the type of impurities and their relative amounts, which vary with time, season of the year etc.
The quality of the raw water can be considered as the main design criteria, as it gives an idea of the treatment required for each impurity.

Thus, the design criteria or parameters used in the treatment of water based on its quality are [4].

i. Determine the class under which the impurity falls.
ii. Ascertain the TDS (Total dissolved salts) of the raw water.
iii. Decide on the degree of end-product purity.

From these criteria, it is possible to decide upon purification process/processes to be employed only rarely will a single method be adequate [4].

Usually the aim of this quality assessment is to compare the raw water quality with that of approved standards of potable usually these are standards set by public departments or those adopted from WHOs standard (World Health organization).

IV. Standards for Potable Water

There are no hard and fast rules as to the acceptable quality for potable supplies, but certain guidelines have been laid down. If these are not exceeded, no action is necessary, because the cost of providing and operating the treatment plant is appreciable and may represent an unwanted cost [1].

The World Health Organization has developed standards for developing nations which are as shown in appendix 1.0. This gives desirable concentrations, and also the maximum permissible concentration for each type of impurity [1].

V. Data Analysis and Process Selection

The essence of taking relevant data on the type, quality and quantity of the water in question is necessary, as it form the backbone of the design. Such information include, vertical head, distance from water source to outlet, purpose of water, altitude above sea level, pumping cycle, quality of water, legal right of water, power available and source of water. It is after a thorough analysis and consideration of the above key points or key factors that go along in determining the process or group of processes necessary for the economic treatment of raw water.

Data on Population Figures of Some Villages in Maiduguri Area (1963 Census)

Due to the unavailability of the 1991 CENSUS result for individual locality of Maiduguri area, that of 1963 CENSUS projected was used as a basis for the design. Though the figure as reported by the 1991 CENSUS of the nation's population is less than that of 1963, a sort of correction has to be made by the use of the dynamic nature of this water treatment plant capacity.

Table 1: Some statistical report of population figures of some villages in Maiduguri area projected from 1963 census.*

YEAR	MAFA	AUNO	DALRI	KONDUGA
1963	3,888	5,825	6,460	6,467
1991	7,762	11,629	12,897	9,840
1992	7,956	11,929	13,219	10,086
1993	8,155	12,218	13,555	10,338
1994	8,359	12,513	13,889	10,849
1995	8,568	13,157	14,236	11,391
1996	8,702	13,486	14,956	11,160
1997	8,801	13,823	15,350	12,559
1998	9,001	14,001	15,430	12,923
1999	9,254	14,169	15,714	13,186
2000	9,694	14,525	16,107	13,846

*National Population Commission Maiduguri Branch

VI. Data Analysis

From the data above, it is possible for one to have a rough idea of the number of people to be considered and hence the amount of water expected to be consumed by them, which is one of five key design features. Let the life span of the design be taken to be 15 years. This means that an estimate of the population in 15 years to come is needed starting from 1992. (i.e. to the year 2007). Thus we need to further project these figures to the year 2007. Since the design is not specified to a particular locality, but taken to a common locality, which happen to share some common characteristic, an average of the population is used in the form of arithmetic mean to serve as a representative of the group.

$$\text{Arithmetic mean (A.M)} = \frac{X1+X2+X3+\cdots Xn}{N}$$

$$= \sum_{i=1}^{N} X1/N$$

For 1963 census figure,

$$\text{A.M} = \text{Population of } \frac{(\text{Mafa}+\text{Auno}+\text{Konduga}+\text{Dalri}}{4}$$

$$= \frac{3,888+5,825+6,460+6,467}{4}$$

$$= \frac{2,2640}{4}$$

A.m. = 5,660

Hence the mean population in 1963 was 5,660.

Thus,

TABLE 2: Mean Population Projection

Year	Ave. No. of people
1963	5,660
1991	10,532
1992	10,798
1993	11,067
1994	11,403
1995	11,838
1996	12,076
1997	12,633
1998	12,839
1999	13,081
2000	13,543

To project to the year 2007, a graph of the years versus population figure needs to be drawn, and projected to that year, assuming a linear relationship between the two variables Fig. 1.

Fig 1: Graph of Population figure Vs Time

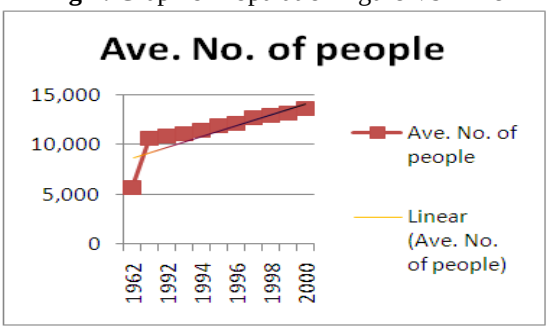

From this graph, the expected or approximate population at any instant of time may be determined by projecting to that year. Assuming all conditions remains unchanged. Thus since the design life span is to be 15 years, (i.e. up to the year 2007). Periodical adjustment need to be done say over 5 year intervals to cater for changes such as increased demand due to population increase. Thus for now, the population expected in the next 5 years is 12,400 (i.e. 1997), from the graph fig 1.

Thus, the population or number of heads to be considered in the first phase is 12,400. An approximated figured of 13,000 is to be used (i.e. an increase of 600) this is to serve some domestic animals who will also make use of the water.

The average rural water consumption is 20 liters/day. [7]. Thus, the water consumption per day is given by 13,000 people at 20 liters/head/day = 260,000 liters/day

Thus the daily water consumption is 260,000liters/day (56,968 Gals).

VII. Chemical Analysis of Water

The chemical analysis of the raw water was carried out and the results obtained are as indicated in tables 3 – 7

TABLE 3: Analysis for October 1991

PROPERTY	VALUE
Temperature at site	21.00°C
Temperature in lab	23.00°C
PH	7.80
Turbidity	23.00NTU
Specific conductance	133μmHos/cm
Colour	-
Dissolved oxygen	-
Bicarbonate ($CaCo_3$)	55.00 mg/1
Ammonia Nitrogen (N)	0.10 mg/1
Fluoride (F)	0.80 mg/1
Chloride (Cl_2)	11.00 mg/1
Sulphate (SO_4^2)	-
Hardness	42.00 mg/1
Phosphate (PO_4)	16.70 mg/1
Sodium (Na)	8.50 mg/1
Potassium (K)	6.60 mg/1
Boron (B)	
Carbon dioxide (CO_2)	
Magnesium (Mg)	
Calcium (Ca)	

TABLE 4: Analysis for November 1991

PROPERTY	VALUE
Temperature at site	31.00°C
Temperature in lab	33.00°C
PH	6.80
Turbidity	-
Specific conductance	130μmHos/cm
Colour	-
Dissolved oxygen	-
Bicarbonate ($CaCo_3$)	44.00 mg/1
Ammonia Nitrogen (N)	-
Fluoride (F)	-
Chloride (Cl_2)	13.00 mg/1
Sulphate (SO_4^2)	-
Hardness	20.00 mg/1
Phosphate (PO_4)	-
Sodium (Na)	6.00 mg/1
Potassium (K)	5.00 mg/1
Boron (B)	0.30 mg/1
Carbon dioxide (CO_2)	-
Magnesium (Mg)	14.00 mg/1
Calcium (Ca)	-

TABLE 5: Analysis for December 1991

PROPERTY	VALUE
Temperature at site	21.00°C
Temperature in lab	27.00°C
PH	7.55
Turbidity	-
Specific conductance	97.00μmHos/cm
Colour	-
Dissolved oxygen	-
Bicarbonate ($CaCo_3$)	44.00 mg/1
Ammonia Nitrogen (N)	-
Fluoride (F)	-
Chloride (Cl_2)	8.00 mg/1
Sulphate (SO_4^2)	3.00 mg/1
Hardness	26.30 mg/1
Phosphate (PO_4)	-
Sodium (Na)	-
Potassium (K)	-
Boron (B)	-
Carbon dioxide (CO_2)	38.00 mg/1
Magnesium (Mg)	8.00 mg/1
Calcium (Ca)	18.00 mg/1

TABLE 6: Analysis for January 1992

PROPERTY	VALUE
Temperature at site	22.30°C
Temperature in lab	25.00°C
PH	7.2
Turbidity	12.15 NTU
Specific conductance	125.00μmHos/cm
Colour	80.60 Mg/1
Dissolved oxygen	8.10
Bicarbonate ($CaCo_3$)	56.00 mg/1
Ammonia Nitrogen (N)	0.1
Fluoride (F)	0.5 mg/1
Chloride (Cl_2)	12.00 mg/1
Sulphate (SO_4^2)	3.50 mg/1
Hardness	40.00 mg/1
Phosphate (PO_4)	0.90 mg/1
Sodium (Na)	7.80 mg/1
Potassium (K)	6.80 mg/1
Boron (B)	0.30 mg/1
Carbon dioxide (CO_2)	-
Magnesium (Mg)	-
Calcium (Ca)	-

TABLE 7: Analysis for February 1992

PROPERTY	VALUE
Temperature at site	21.00°C
Temperature in lab	23.00°C
PH	7.80
Turbidity	23.00 NTU
Specific conductance	133.00μmHos/cm
Colour	135.00 Mg/1
Dissolved oxygen	-
Bicarbonate ($CaCo_3$)	-
Ammonia Nitrogen (N)	0.1 mg/1
Fluoride (F)	0.80 mg/1
Chloride (Cl_2)	11.00 mg/1
Sulphate (SO_4^2)	-
Hardness	42.00 mg/1
Phosphate (PO_4)	16.70 mg/1
Sodium (Na)	8.50 mg/1
Potassium (K)	6.60 mg/1
Boron (B)	-
Carbon dioxide (CO_2)	-
Magnesium (Mg)	-
Calcium (Ca)	-

Generally, there is no end to the type of treatment that can be carried out on water which depends mainly on the purpose to which the water is to be used (i.e. either for domestic or industrial). Thus a compromise between economy and necessities is made. Hence, from the data obtained on the Alau water which is the basis of design, the actual quality of the water is taken to be that obtained from the worst possible case as detected by the chemical analyst. This is due to the fact that the samples should have been taken over a 12 month period or more to get the true nature of the impurities been handled. Thus the respective values of the worst conditions of these impurities are as stated in table 8. These values are compared with those of WHO (World Health Organization). Appendix 1.0 since there is no set standard in Nigeria.

TABLE 8: Worst case values of water analysis

PROPERTY	VALUE
Temperature at site	31.00°C
Temperature in lab	33.00°C
PH	7.80
Turbidity	23.00 NTU
Specific conductance	133.00μmHos/cm
Colour	135.00 Mg/1
Dissolved oxygen	8.10 mg/1
Bicarbonate ($CaCo_3$)	56.00 mg/1
Ammonia Nitrogen (N)	0.10 mg/1
Fluoride (F)	0.80 mg/1
Chloride (Cl_2)	13.00 mg/1
Sulphate (SO_4^{2})	3.50 mg/1
Hardness	42.00 mg/1
Phosphate (PO_4)	16.70 mg/1
Sodium (Na)	8.50 mg/1
Potassium (K)	6.80 mg/1
Boron (B)	0.30 mg/1
Carbon dioxide (CO_2)	38.00 mg/1
Magnesium (Mg)	14.00 mg/1
Calcium (Ca)	18.0 g/1

Process Selection

The choice of the treatment process to be adopted depends on the impurities to be handled among others as previously discussed in VII. Thus, referring to Appendix 1.0, also on some design discretions a possible treatment process is given in the flow diagram below.

Fig 2: Process Selection Diagram

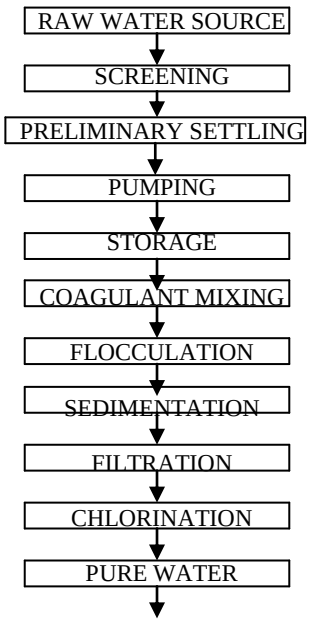

VIII. Conclusion

The need for proper data analysis most often depend on the data itself, there should be more appropriate and reliable means of water quality assessments in this country which has very poor data collection and management techniques. This may to a great extent alter many assumptions taken for a design; as such wide margins of error which were taken (to be on the safe side) for this design could have been avoided. The data on population census for individual localities should also be well documented for purposes such as these.

There should also be a standard for potable drinking water in this country which unfortunately there isn't. This data on potable water standards should be taken by well qualified personnel, so that a standard should be set for this country rather than depend on international standards, which may not really reflect the situation in this country.

References

[1]. Smsrthurst G.: Basic Water Treatment 1979; Thomas Telford Ltd, London.
[2]. M. Fair, Gordon/C. Geyer, John/A. Okun, Daniel. Water and Waste water Engineering Vol.1, 1968, John Willey and Sons Inc.
[3]. James G. V.: Water Treatment; 4th Edition, 1971, Technical Press.
[4]. Walter Lorch: Handbook of water purification, 1981, London; New York: McGraw-Hill (UK),
[5]. M. Fair, Gordon/C. Geyer, John/A. Okun, Daniel; Water and Waste water Engineer Vol. 2,1968, John Willey and Sons Inc.
[6]. Mogarr, F: Water and Waste water utilization in hot climate
[7]. Dunn, P.D.: Appropriate Technology;1978, McMillian Press Ltd
[8]. 8.Ernest F Branter, Horace W King, James E Lindell, C Y Wei 1996, Handbook of Hydraulics, McGraw-Hill, a Division of the McGraw-Hill Companies, Inc.

APPENDIX 1.0: RECOMMENDED TREATMENT

Treatment system	Bacteria, amoebas	Guinea-worm	Cercaria	Fe, Mn	Fluoride	Arsenic	Salts	Odour, taste	Organic matter	Turbidity
Straining through fine cloth Consists in pouring raw water through a piece of fine, clean, cotton cloth to remove some of the suspended solids.	–b	©©©	—	—	—	—	—	—	©	©
Aeration Oxidizes iron (Fe) and manganese (Mn). Good aeration of the water is also important for slow, sand filtration to be effective, especially if there is not enough oxygen in the surface water. Water can easily be aerated by shaking it in a vessel, or by allowing it to trickle through perforated trays containing small stones.				©©©				©©	©	
Storage/pre-settlement Storing water for only one day can eliminate some bacteria, but it should be stored for 48 hours to eliminate cercaria (snail larvae). The longer the water is stored, the more the suspended solids and pathogens will settle to the bottom of the container. The top water can then be used after sedimentation.	©		©©©	©				©	©	©©
Coagulation, flocculation and settlement In coagulation, a liquid coagulant, such as aluminium sulfate, is added to the water to attract suspended particles. The water is then gently stirred to allow the particles to come together and form larger particles (flocculation), which can then be removed by sedimentation, settlement or filtration. The amount of coagulant needed will depend on the nature of the contaminating chemical compounds and solids.	©		©	©	©©©	©©©		©	©	©©

Slow sand filtration Water passes slowly downwards through a bed of fine sand at a steady rate. The water should not be too turbid; otherwise the filter will get clogged. Pathogens are naturally removed in the top layer where a biological film builds up. A potential problem is that some households do not use this technology effectively and the water can remain contaminated.	©©©	©©©	©©©	©©		©©		©©	©	©©©
Rapid sand filtration The sand used is coarser than in slow sand filtration and the flow rate is higher. The method is used to remove suspended solids and is effective after the water has been cleared with coagulation/flocculation. There is no build-up of biological film, hence the water will still need to be disinfected. It is easier to remove trapped debris from up flow sand filters, compared to filters in which the water flows downwards.	©	©©	©	©©				©	©	©©
Charcoal filter Granular charcoal (or granulated activated carbon) can be used in filtration and is effective in improving the taste, odours and colour of the water. However, it should be replaced regularly, because bacteria can breed in it.		©©	©©	©				©©©		©
Ceramic filter The filter is a porous, unglazed ceramic cylinder and impurities are deposited on its surface. Filters with very small pores can remove most pathogens. Open, porous ceramic jars can also be used. The ceramic filter method can only be used with fairly clear water.	©©©	©©©	©©©					©©	©©	©©©
Solar disinfection Ultraviolet radiation from the sun will destroy most pathogens, and increasing the temperature of the water enhances the effectiveness of the radiation. In tropical areas, most pathogens can be killed by exposing the contaminated water to sun for five hours, centered around midday. An easy way to do this, is to expose (half-blackened) clear glass/ plastic bottles of water to the sun. Shaking the bottle before irradiation increases the effectiveness of the treatment. The water must be clear for this treatment to be effective.	©©©	©©	©©							

American Journal of Engineering Research (AJER) 2015
American Journal of Engineering Research (AJER)
e-ISSN: 2320-0847 p-ISSN : 2320-0936
Volume-4, Issue-8, pp-229-236
www.ajer.org
Research Paper Open Access

Architecture Design & Network Application of Cloud Computing

Mehzabul Hoque Nahid
(Faculty coordinator, Computer science and engineering Department, Royal University of Dhaka, Bangladesh)

ABSTRACT: *"Cloud" computing a comparatively term, stands on decades of research & analysis in virtualization, analytical distributed computing, utility computing, and more recently computer networking, web technology and software services. Cloud computing represents a shift away from computing as a product that is purchased, to computing as a service that is delivered to consumers over the internet from large-scale data centers – or "clouds". Whilst cloud computing is obtaining growing popularity in the IT industry, academic appeared to be lagging behind the developments in this field. It also implies a service oriented designed architecture, reduced information technology overhead for the end-user, good flexibility, reduced total cost of private ownership, on-demand services and many other things. This paper discusses the concept of "cloud" computing, some of the issues it tries to address, related research topics, and a "cloud" implementation available today.*

Keywords –*Network Cloud, CAPEX, OPEX, IBM, DEC.*

I. INTRODUCTION

Cloud computing is a model for enabling ubiquitous network access to a shared pool of configurable computing resources. Cloud computing and storage solutions provide users and enterprises with various capabilities to store and process their data in third-party data centers. It relies on sharing of resources to achieve coherence and economies of scale, similar to a utility over a network. At the foundation of cloud computing is the broader concept of converged infrastructure and shared services. Cloud computing, or in simpler shorthand just "the cloud", also focuses on maximizing the effectiveness of the shared resources. Cloud resources are usually not only shared by multiple users but are also dynamically reallocated per demand [1]. This can work for allocating resources to users. For example, a cloud computer facility that serves European users during European business hours with a specific application may reallocate the same resources to serve North American users during North America's business hours with a different application. This approach should maximize the use of computing power thus reducing environmental damage as well since less power, air conditioning, rack space, etc. are required for a variety of functions. With cloud computing, multiple users can access a single server to retrieve and update their data without purchasing licenses for different applications. The term "moving to cloud" also refers to an organization moving away from a traditional CAPEX model to the OPEX model.

Proponents claim that cloud computing allows companies to avoid upfront infrastructure costs, and focus on projects that differentiate their businesses instead of on infrastructure [2]. Proponents also claim that cloud computing allows enterprises to get their applications up and running faster, with improved manageability and less maintenance, and enables IT to more rapidly adjust resources to meet fluctuating and unpredictable business demand. Cloud providers typically use a "pay as you go" model.This can lead to unexpectedly high charges if administrators do not adapt to the cloud pricing model. The present availability of high-capacity networks, low-cost computers and storage devices as well as the widespread adoption of hardware virtualization, service-oriented architecture, and autonomic and utility computing have led to a growth in cloud computing. Companies can scale up as computing needs increase and then scale down again as demands decrease. Cloud vendors are experiencing growth rates of 50% per annum.

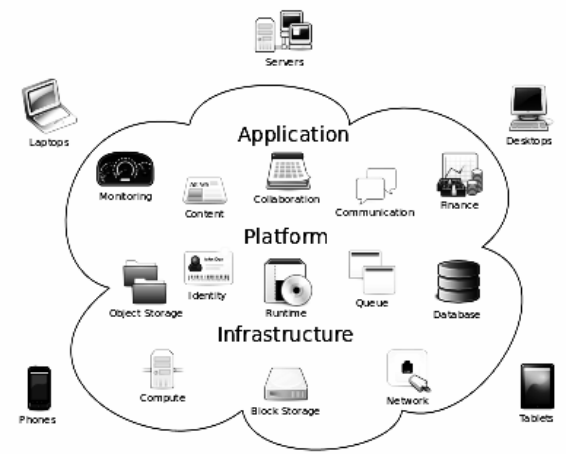

Figure 1: Cloud computing metaphor.

Figure 1 presents Cloud computing metaphor. For a user, the network elements representing the provider-rendered services are invisible, as if obscured by a cloud.

II. ORIGIN OF THE TERM "CLOUD COMPUTING"

The origin of the term cloud computing is unclear. The expression cloud is commonly used in science to describe a large agglomeration of objects that visually appear from a distance as a cloud and describes any set of things whose details are not inspected further in a given context. Another explanation is that the old programs to draw network schematics surrounded the icons for servers with a circle, and a cluster of servers in a network diagram had several overlapping circles, which resembled a cloud. In analogy to above usage the word cloud was used as a metaphor for the Internet and a standardized cloud-like shape was used to denote a network on telephony schematics and later to depict the Internet in [3]. With this simplification, the implication is that the specifics of how the end points of a network are connected are not relevant for the purposes of understanding the diagram. The cloud symbol was used to represent the Internet as early as 1994 in which servers were then shown connected to, but external to, the cloud.

The 1970s

During the mid-1970s, time-sharing was popularly known as RJE; this terminology was mostly associated with large vendors such as IBM and DEC. IBM developed the VM OperatingSystem to provide time-sharingservicesvia virtual machines.

The 1990s

In the 1990s, telecommunications companies, who previously offered primarily dedicated point-to-point data circuits, began offering virtual private network (VPN) services with comparable quality of service, but at a lower cost. By switching traffic as they saw fit to balance server use, they could use overall network bandwidth more effectively. They began to use the cloud symbol to denote the demarcation point between what the providers was responsible for and what users were responsible for. Cloud computing extends this boundary to cover all servers as well as the network infrastructure.

The New Millennium: 2000s

Since 2000 cloud computing has come into existence. In early 2008, NASA's Open Nebula, enhanced in the Reservoir European Commission-funded project, became the first open-source software for deploying private and hybrid clouds, and for the federation of clouds. In the same year, efforts were focused on providing quality of service guarantees to cloud-based infrastructures, in the framework of the IRMOS European Commission-funded project, resulting in a real-time cloud environment [4]. By mid-2008, Gartner saw an opportunity for cloud computing "to shape the relationship among consumers of IT services, those who use IT services and those who sell them" and observed that "organizations are switching from company-owned hardware and software assets to per-use service-based models" so that the "projected shift to computing .

III. TYPES OF COMPUTING

There are three different kinds of cloud computing, where different services are being provided for you. Note that there's a certain amount of vagueness about how these things are defined and some overlap between them.

- Infrastructure as a Service (IaaS) means you're buying access to raw computing hardware over the Net, such as servers or storage. Since you buy what you need and pay-as-you-go, this is often referred to as utility computing. Ordinary web hosting is a simple example of IaaS: you pay a monthly subscription or a per-megabyte/gigabyte fee to have a hosting company serve up files for your website from their servers.
- Software as a Service (SaaS) means you use a complete application running on someone else's system. Web-based email and Google Documents are perhaps the best-known examples. Zoho is another well-known SaaS provider offering a variety of office applications online [5].
- Platform as a Service (PaaS) means you develop applications using Web-based tools so they run on systems software and hardware provided by another company. So, for example, you might develop your own ecommerce website but have the whole thing, including the shopping cart, checkout, and payment mechanism running on a merchant's server. Force.com (from salesforce.com) and the Google App Engine are examples of PaaS.

IV. CHARACTERISTICS

Cloud computing exhibits the following key characteristics:

- **Agility** improves with users' ability to re-provision technological infrastructure resources.
- **Cost** reductions claimed by cloud providers. A public-cloud delivery model converts capital expenditure to operational expenditure. This purportedly lowers barriers to entry, as infrastructure is typically provided by a third party and does not need to be purchased for one-time or infrequent intensive computing tasks. Pricing on a utility computing basis is fine-grained, with usage-based options and fewer IT skills are required for implementation [6]. The e-FISCAL project's state-of-the-art repositorycontains several articles looking into cost aspects in more detail, most of them concluding that costs savings depend on the type of activities supported and the type of infrastructure available in-house.
- **Device and location independence**enable users to access systems using a web browser regardless of their location or what device they use. As infrastructure is off-site and accessed via the Internet, users can connect from anywhere.
- **Maintenance** of cloud computing applications is easier, because they do not need to be installed on each user's computer and can be accessed from different places.
- **Multitenancy** enables sharing of resources and costs across a large pool of users thus allowing for:
  - **Centralization** of infrastructure in locations with lower costs
  - **peak-load capacity** increases (users need not engineer for highest possible load-levels)
  - **Utilization and efficiency** improvements for systems that are often only 10–20% utilized.
- **Performance** is monitored, and consistent and loosely coupled architectures are constructed using web services as the system interface.
- **Productivity** may be increased when multiple users can work on the same data simultaneously, rather than waiting for it to be saved and emailed. Time may be saved as information does not need to be re-entered when fields are matched, nor do users need to install application software upgrades to their computer.
- **Reliability** improves with the use of multiple redundant sites, which makes well-designed cloud computing suitable for business continuity and disaster recovery.
- **Scalability and elasticity** via dynamic provisioning of resources on a fine-grained, self-service basis in near real-time, without users having to engineer for peak loads.
- **Security** can improve due to centralization of data, increased security-focused resources, etc., but concerns can persist about loss of control over certain sensitive data, and the lack of security for stored kernels. Security is often as good as or better than other traditional systems, in part because providers are able to devote resources to solving security issues that many customers cannot afford to tackle. However, the complexity of security is greatly increased when data is distributed over a wider area or over a greater number of devices, as well as in multi-tenant systems shared by unrelated users.

V. SERVICE MODELS

Infrastructure as a service (IaaS)

In the most basic cloud-service model & according to the IETF, providers of IaaS offer computers – physical or virtual machines and other resources IaaS clouds often offer additional resources such as a virtual-machine disk image library, raw block storage, and file or object storage, firewalls, load balancers, IP addresses, virtual local area networks (VLANs), and software bundles. IaaS-cloud providers supply these resources on-demand from their large pools installed in data centers. For wide-area connectivity, customers can use either the Internet or carrier clouds to deploy their applications, cloud users install operating-system images and their application software on the cloud infrastructure [7]. In this model, the cloud user patches and maintains the operating systems and the application software. Cloud providers typically bill IaaS services on a utility computing basis: cost reflects the amount of resources allocated and consumed.

Platform as a service (PaaS)

In the PaaS models, cloud providers deliver a computing platform, typically including operating system, programming language execution environment, database, and web server. Application developers can develop and run their software solutions on a cloud platform without the cost and complexity of buying and managing the underlying hardware and software layers. With some PaaS offers like Microsoft Azure and Google App Engine, the underlying computer and storage resources scale automatically to match application demand so that the cloud user does not have to allocate resources manually. The latter has also been proposed by an architecture aiming to facilitate real-time in cloud environments. Even more specific application types can be provided via PaaS, e.g., such as media encoding as provided by services as barcoding transcoding cloudor media.io.

Software as a service (SaaS)

In the business model using software as a service (SaaS), users are provided access to application software and databases. Cloud providers manage the infrastructure and platforms that run the applications. SaaS is sometimes referred to as "on-demand software" and is usually priced on a pay-per-use basis or using a subscription fee.In the SaaS model, cloud providers install and operate application software in the cloud and cloud users access the software from cloud clients. Cloud users do not manage the cloud infrastructure and platform where the application runs [8]. This eliminates the need to install and run the application on the cloud user's own computers, which simplifies maintenance and support. Cloud applications are different from other applications in their scalability—which can be achieved by cloning tasks onto multiple virtual machines at run-time to meet changing work demand. Load balancers distribute the work over the set of virtual machines. This process is transparent to the cloud user, who sees only a single access point. To accommodate a large number of cloud users, cloud applications can be multitenant, that is, any machine serves more than one cloud user organization.

The pricing model for SaaS applications is typically a monthly or yearly flat fee per user,so price is scalable and adjustable if users are added or removed at any point.

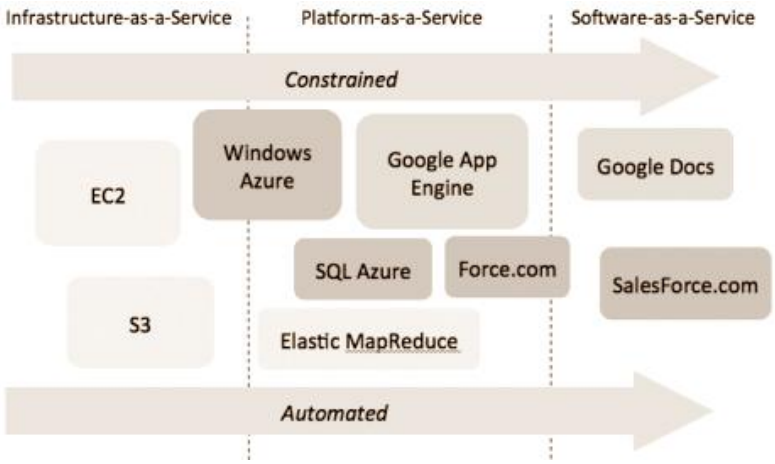

Figure 2: Service models of cloud computing

VI. DEPLOYMENT MODELS

Private cloud

Private cloud is cloud infrastructure operated solely for a single organization, whether managed internally or by a third-party, and hosted either internally or externally. Undertaking a private cloud project requires a significant level and degree of engagement to virtualize the business environment, and requires the organization to reevaluate decisions about existing resources. When done right, it can improve business, but every step in the project raises security issues that must be addressed to prevent serious vulnerabilities. Self-run data centers are generally capital intensive. They have a significant physical footprint, requiring allocations of space, hardware, and environmental controls. These assets have to be refreshed periodically, resulting in additional capital expenditures.

Public cloud

A cloud is called a "public cloud" when the services are rendered over a network that is open for public use. Public cloud services may be free. Technically there may be little or no difference between public and private cloud architecture, however, security consideration may be substantially different for services that are made available by a service provider for a public audience and when communication is effected over a non-trusted network. Generally, public cloud service providers like Amazon AWS, Microsoft and Google own and operate the infrastructure at their data center and access is generally via the Internet. AWS and Microsoft also offer direct connect services called "AWS Direct Connect" and "Azure Express Route" respectively, such connections require customers to purchase or lease a private connection to a peering point offered by the cloud provider.

Hybrid cloud

Hybrid cloud is a composition of two or more clouds (private, community or public) that remain distinct entities but are bound together, offering the benefits of multiple deployment models. Hybrid cloud can also mean the ability to connect collocation, managed and/or dedicated services with cloud resources.
Gartner, Inc. defines a hybrid cloud service as a cloud computing service that is composed of some combination of private, public and community cloud services, from different service providers. A hybrid cloud service crosses isolation and provider boundaries so that it can't be simply put in one category of private, public, or community cloud service. It allows one to extend either the capacity or the capability of a cloud service, by aggregation, integration or customization with another cloud service.

Varied use cases for hybrid cloud composition exist. For example, an organization may store sensitive client data in house on a private cloud application, but interconnect that application to a business intelligence application provided on a public cloud as a software service. This example of hybrid cloud extends the capabilities of the enterprise to deliver a specific business service through the addition of externally available public cloud services. Hybrid cloud adoption depends on a number of factors such as data security and compliance requirements, level of control needed over data, and the applications an organization uses [9].

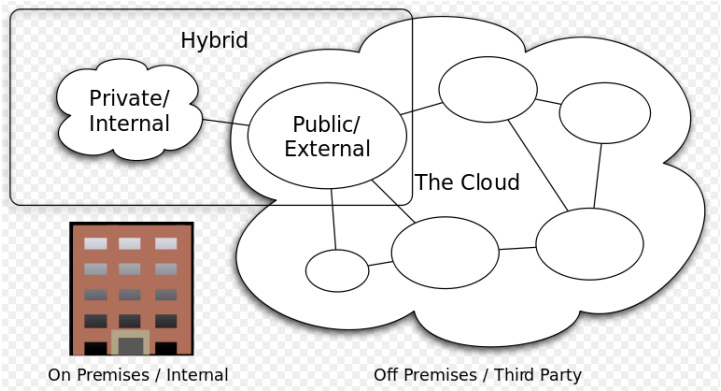

Figure 3: Deployment models

VII. ARCHITECTURE DESIGN

Enterprises and vendors follow some guidelines regarding where to use Layer 2 (switching) and Layer 3 (routing) in the network. Layer 2 is the simpler mode, where the Ethernet MAC address and VirtualLAN(VLAN) information are used for forwarding. The disadvantage of Layer 2 networks is scalability [10]. When we use Layer 2 addressing and connectivity in the manner specified previously for IaaS clouds, we end up with a flat topology, which is not ideal when there are a large number of nodes. The option is to use routing and subnets to provide segmentation for the appropriate functions at the cost of forwarding performance and network complexity.

VM migration introduces its own set of problems. The most common scenario is when a VM is migrated to a different host on the same Layer 2 topology. Consider the case where a VM with open Transmission Control Protocol (TCP) connections is migrated. If live migration is used, TCP connections will not see any downtime except for a short "hiccup." However, after the migration, IP and TCP packets destined for the VM will need to be resolved to a different MAC address or the same MAC address but now connected to a different physical switch in the network so that the connections can be continued without disruption. With VPLS and similar Layer 2 approaches, VM migration can proceed as before across the same Layer 2 network. Alternatively, it may be less complex to freeze the VM and move it across either a Layer 2 or Layer 3 network with the TCP connections having to be torn down by the counterpart communicating with the VM. This scenario is not a desired one from an application availability consideration, but it can lower complexity.

Another example of hybrid cloud is one where IT organizations use public cloud computing resources to meet temporary capacity needs that cannot be met by the private cloud.This capability enables hybrid clouds to employ cloud bursting for scaling across clouds. Cloud bursting is an application deployment model in which an application runs in a private cloud or data center and bursts to a public cloud when the demand for computing capacity increases. A primary advantage of cloud bursting and a hybrid cloud model is that an organization only pays for extra compute resources when they are needed. Cloud bursting enables data centers to create an in-house IT infrastructure that supports average workloads, and use cloud resources from public or private clouds, during spikes in processing demands.

The specialized model of hybrid cloud, which is built atop heterogeneous hardware, is called Cross-platform Hybrid Cloud. A cross-platform hybrid cloud is usually powered by different CPU architectures, for example, x86-64 and ARM, underneath. Users can transparently deploy applications without knowledge of the cloud's hardware diversity.This kind of cloud emerges from the raise of ARM-based system-on-chip for server-class computing.

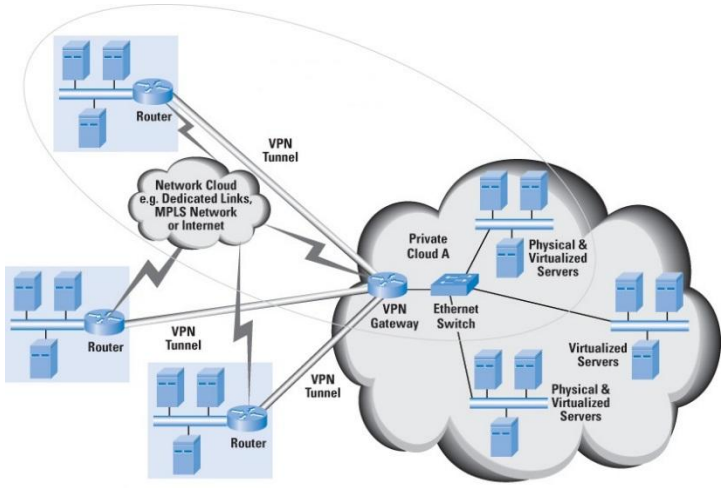

Figure 4: Architecture design of Computer cloud

VIII. SECURITY & PRIVACY

Cloud computing poses privacy concerns because the service provider can access the data that is on the cloud at any time. It could accidentally or deliberately alter or even delete information. Many cloud providers can share information with third parties if necessary for purposes of law and order even without a warrant. That is permitted in their privacy policies which users have to agree to before they start using cloud services [11]. Solutions to privacy include policy and legislation as well as end users' choices for how data is stored. Users can encrypt data that is processed or stored within the cloud to prevent unauthorized access.
According to the Cloud Security Alliance, the top three threats in the cloud are Insecure Interfaces and API's, Data Loss & Leakage, and Hardware Failure which accounted for 29%, 25% and 10% of all cloud security outages respectively together these form shared technology vulnerabilities. In a cloud provider platform being shared by different users there may be a possibility that information belonging to different customers resides on same data server. Therefore, Information leakage may arise by mistake when information for one customer is given to other. Additionally, Eugene Schultz, chief technology officer at Imagined Security, said that hackers are spending substantial time and effort looking for ways to penetrate the cloud. "There are some real Achilles' heels in the cloud infrastructure that are making big holes for the bad guys to get into". Because data from hundreds or thousands of companies can be stored on large cloud servers, hackers can theoretically gain control of huge stores of information through a single attack a process he called "hyper jacking".

Physical control of the computer equipment is more secure than having the equipment off site and under someone else's control. This delivers great incentive to public cloud computing service providers to prioritize building and maintaining strong management of secure services [12]. Some small businesses that don't have expertise in IT security could find that it's more secure for them to use a public cloud.

There is the risk that end users don't understand the issues involved when signing on to a cloud service. This is important now that cloud computing is becoming popular and required for some services to work, for example for an intelligent personal assistant Fundamentally private cloud is seen as more secure with higher levels of control for the owner, however public cloud is seen to be more flexible and requires less time and money investment from the user.

IX. FUTURE SCOPE

According to Gartner's Hype cycle, cloud computing has reached a maturity that leads it into a productive phase. This means that most of the main issues with cloud computing have been addressed to a degree that clouds have become interesting for full commercial exploitation. This however does not mean that all the problems listed above have actually been solved, only that the according risks can be tolerated to a certain degree. Cloud computing is therefore still as much a research topic, as it is a market offering. What is clear through the evolution of Cloud Computing services is that the CTO is a major driving force behind Cloud adoption. The major Cloud technology developers continue to invest billions a year in Cloud R&D; for example, in 2011 Microsoft committed 90% of its $9.6bn R&D budget to Cloud. Additionally, more industries are turning to cloud technology as an efficient way to improve quality services due to its capabilities to reduce overhead costs, downtime, and automate infrastructure deployment.

X. CONCLUSION

This article has served as a vendor-neutral primer to the area of cloud computing. We provided an introduction to the still-evolving area of cloud computing, including the technologies and some deployment concerns & also we provided a more detailed look at the networking factors in the cloud, security aspects, and cloud federation. We also highlighted some areas that are seeing increased attention with cloud-computing proponents and vendors. In theory, cloud computing is environmentally friendly because it uses fewer resources and less energy if 10 people share an efficiently run, centralized, cloud-based system than if each of them run their own inefficient local system. The area of cloud computing is very dynamic and offers scope for innovative technologies and business models. Ongoing work with respect to solutions is substantial, in the vendor research labs and product development organizations as well as in academia. It is clear that cloud computing will see significant advances and innovation in the next few years.

Acknowledgement

We are earnestly grateful to one our group member, MehzabulHoqueNahid, Masters in IT (2011), Swinburne University of Technology. For providing us with his special advice and guidance for this project. Finally, we express our heartiest gratefulness to the Almighty and our parents who have courageous throughout our work of the project.

References

[1] Sun Microsystems, Introduction to Cloud Computing Architecture, 2009

[2] FELLOWS, W.2008. Partly Cloudy, Blue-Sky Thinking about Cloud Computing. 451 Group.

[4] D. G EORGAKOPOULOS, M.HORNICK, AND A.S HETH, "An Overview of Workflow Management: From Process Modeling to Workflow Automation Infrastructure", Distributed and Parallel Databases, Vol. 3 (2), April 1995.

[5] RAYPORT, J. F. and HEYWARD, A.2009. *Envisioning the Cloud: The Next Computing Paradigm*. Market space.

[6] PASTAKI RAD, M., SAJEDI BADASHIAN, A.,MEYDANIPOUR, G., ASHURZAD DELCHEH, M., ALIPOUR, M. and AFZALI, H. 2009. A Survey of Cloud Platforms and Their Future.

[7] KHAJEH-HOSSEINI, A., SOMMERVILLE, I. and SRIRAM, I. "Research Challenges for Enterprise Cloud Computing,".(Submitted to 1st ACM Symposium on Cloud Computing, Indianapolis, Indiana, USA, June 2010, under paper id 54)

[8] IBM, *Staying aloft in tough times*, 2009

[9] PLUMMER, D.C., BITTMAN, T.J., AUSTIN, T., CEARLEY, D.W., and SMITH D.M., *Cloud Computing: Defining and Describing an Emerging Phenomenon*, 2008

[10] B. L UDSCHER, I.ALTINTAS, C.BERKLEY, D.HIG-GINS, E.JAEGER-FRANK, M.JONES, E.LEE, J.TAO, Y. Z HAO, "Scientific Workflow Management and the Keller System", Concurrency and Computation: Practice & Experience, Special Issue on Workflow in Grid Systems, Volume 18, Issue 10 (August 2006), pp. 1039–1065, 2006.

[11] MELL, P. and GRANCE, T. 2009. Draft NIST Working Definition of Cloud Computing.

[12] ERDOGMUS, H. 2009. Cloud Computing: Does Nirvana Hide behind the Nebula? *Software, IEEE* 26, 2, 4-6.

American Journal of Engineering Research (AJER) 2015
American Journal of Engineering Research (AJER)
e-ISSN: 2320-0847 p-ISSN : 2320-0936
Volume-4, Issue-8, pp-237-243
www.ajer.org
Research Paper Open Access

Analysis of Spectrum Sensing Techniques inCognitive Radio

Manjurul H. Khan[1], P.C. Barman[2]
[1] *ICT Department-System, Janata Bank Limited, Head Office, Dhaka, Bangladesh.*
[2] *Departments of Information & Communication Engineering, Islamic University, Kushtia, Bangladesh.*

ABSTRACT: *The growing demand of wireless applications has put a lot of constraints on the usage of available radio spectrum which is limited and precious resource. However, a fixed spectrum assignment has lead to under utilization of spectrum as a great portion of licensed spectrum is not effectively utilized. Cognitive radio is a promising technology which provides a novel way to improve utilizationefficiency of available electromagnetic spectrum. Spectrum sensing is a basic approach and requirement to implement cognitive radio technology.In this paper, analysis of Cooperative, Non-cooperative and Interference Based spectrum sensingtechniques are presented. We also highlight the strengths, weaknesses, parameters concerned and feasibilities of these techniques with comparison among them. Various challenges and the parameters which can affect performance of these techniques are also discussed.*

Keywords:*Cognitive, Cooperative spectrum sensing, Non-cooperative spectrum sensing, Interference Based Sensing.*

I.INTRODUCTION

Cognitive radio (CR) concept can be applied to many advanced and challenging communication as well as networking systems. The word cognitive means pertained to cognition or the action or process of knowing. It also means the mental process of getting knowledge through thought, experience and the senses. Thus, incommunication systems CR defines the radio with ability to sense reserved, idle communication spectra which can be utilized by secondary users for other applications during its idle period [1],[2].CR maximizes throughput of spectrum to increase spectrum efficiency and facilitate interoperability by providing access to secondary user group for other applications [3]. Cognitive radio concept may be applicable at 400-800 MHz (UHF TV bands) and 3-10GHz.Moreover, for long range communication applications these frequency bands have good propagation properties.Cognitive radio systems offer opportunity to use dynamic spectrum management techniques to immediately utilize available local spectrum. Interms of occupancy, sub bands of the radio spectrum may be categorized as follows:

i) Whitespaces: These are free of RF interferers, except for noise due to natural and/or artificial sources.
ii) Gray spaces: These are partially occupied by interferers as well as noise.
iii) Black spaces: The contents of which are completely full due to the combined presence of communication and (possibly) interfering signals plus noise [4].The Figure 1 shows the WhiteSpaces and Used Frequencies in Licensed Spectrum.

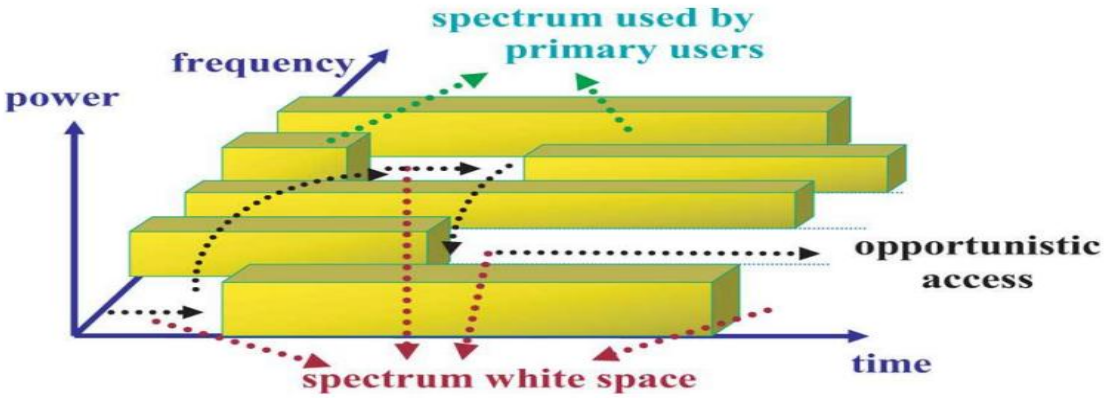

[Figure 1]: Illustration of White Spaces in Licensed Bands

When compared to all other techniques, Spectrum Sensing is the most crucial task for theestablishment of cognitive radio based communication mechanism.

This paper is organized as follows: Section II defines categorization of signal processing techniques for spectrum sensing. Section III presents most popular non-cooperative spectrum sensing techniques. In this section spectrum sensingtechniques are explained with their relative features and limitations. Cooperative sensing andits types are defined in section IV. In Section V Interference Based SensingTechniques are explained with their relative features and limitations and Section VI concludes this paper.

II. SPECTRUM SENSING TECHNIQUES

Classification of most popular spectrum sensing techniques for implementation of CR technology is shown in Figure 2. This figurealso categorizes non-cooperative and cooperative spectrum sensingTechniques.

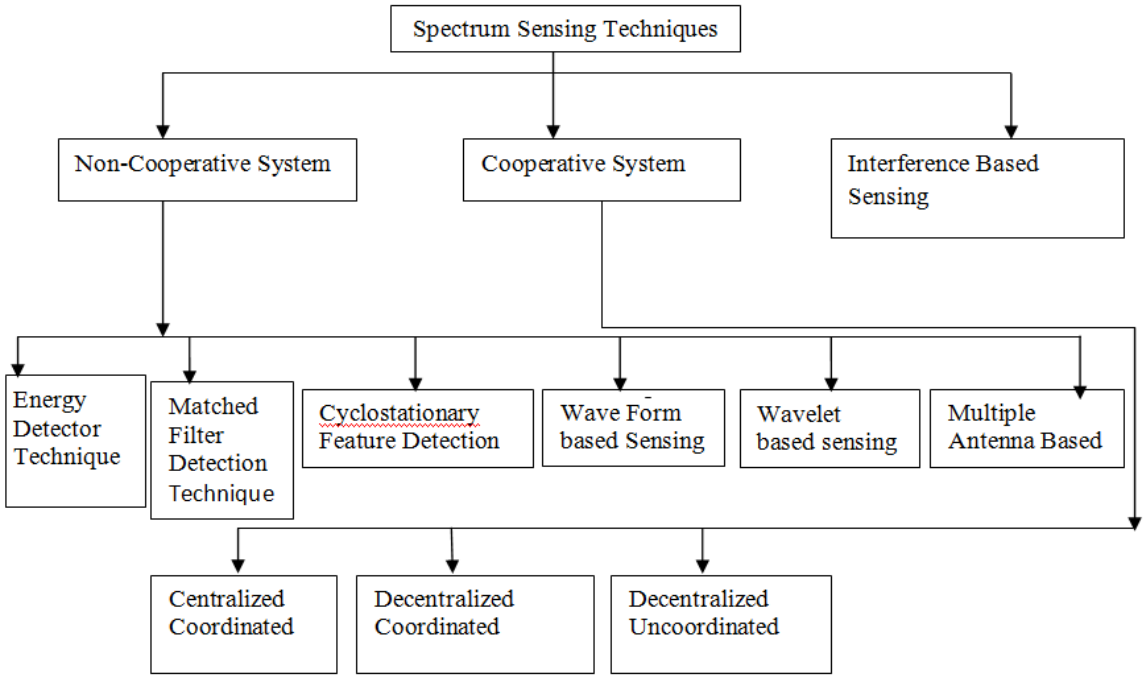

[Figure 2]: Classification of spectrum sensing techniques [5].

III. NON-COOPERATIVE SENSING

Non-cooperative sensing techniques need detection of primary user signal by some parameter measurement and filtering. The location of primary user is not known.It is based on following hypotheses

$$x(n) = \begin{cases} y(n) & Ho \\ s(n) + y(n) & H1 \end{cases}$$

In above equation H0 denotes absence of primary user and H1 shows its presence. y(n) and s(n) represents noise and primary user massage signal respectively. Popular non-cooperative Sensing techniques are:

3.1Energy Detector
3.2 Matched filter
3.3 Cyclostationary feature detection.
3.4Waveform Based Sensing
3.5 Wavelet Based Sensing
3.6Multiple Antenna Based Sensing

3.1 Energy Detector Technique

It is a straightforward detector that detects the whole energy content of the received signal over specific time length. it\'s the subsequent components:-

i)Band-Pass Filter (BPF):Limitsthe information measure of the received signal to the band of interest.
ii)Square Law Device: Squares every term of the received signal
iii) Summation Device:Add all the square values to calculate the energy.

A threshold worth is needed for comparison of the energy found by the detector. Energy bigger than the brink values indicates the presence of the first user.The principle of energy detection is shown in figure 3.1. The energy is calculated as

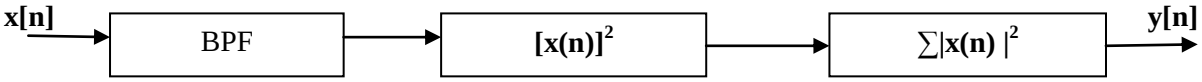

[Figure 3.1]: Principle of Energy Detection

Features:

(1) Energy detection method is popular due to its simplicity, ease of implementation and applicability. Noprevious information of the first user's signal needed. [6].

(2) It has low computational and implementation cost [6].

Limitations:

There are several limitations of energy detectors that might diminish their simplicity in implementation

(1) Threshold used for primary user detection is highly susceptible to changing noise levels. Presence of any undesired band possessing equal energy level might confuse the energy detector [6].

(2) Energy detector does not differentiate between primary user (PU) signals, noise and interference. So it cannot be beneficial to prevent interference [6].

(3) Energy detector is not useful for direct sequence, frequency hopping signals and spread spectrum signals [2].

(4) When there is heavy fluctuation in signal power so it becomes difficult to differentiate the desired signal [2].

(5) Compared to matched filter detection, energy detection technique requires longer time to achieve desired performancelevel [6].

(6)Problem associated with choosing a correct threshold for comparison functions.

3.2 Matched Filter Technique

The Matched Filter Technique is extremely vital incommunication because it is an optimum filtering technique that maximizes the signal to noise ratio (SNR).It is a linear filter and previous knowledge of the first user signal is extremely essential for its operation. Operation performed is adore a correlation. The received signal is convolved with the filter response that is the reflected and time shifted version of a reference signal. The figure 3.2 is outline of its function.

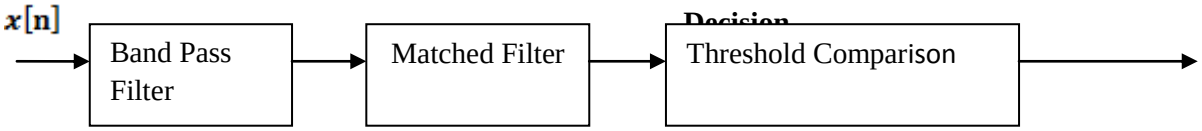

[Figure 3.2]: Principle of Matched Filter Technique.

Features:

(1) As Cognitive Radio user knows information of the licenseduser signal, matched filter detection requires less detectiontime due to high processing gain [7], [8], [9], [2], [3], [10].

(2) Matched filtering needs short time to achieve a certain probability of false alarm or probability of missed-detection [8], [3].

(3)Optimum detector it maximize the SNR ratio.

Limitations:

(1) It requires a prior knowledge of every primary signal [7].

(2) CR needs a dedicated receiver for every type of primary user [7].

(3) Cognitive radio needs receivers for all signal types; the implementation complexity of sensing unit is impractically large [8].

(4) Matched filtering consumes large power as various receiver algorithms need to be executed for detection [8].

3.3 Cyclostationary Feature Detection (CFD)Techniques

It exploits the periodicity in the received primary signal to identify the presence of primary users (PU). The periodicity is commonly embedded in sinusoidal carriers, pulse trains, spreading code, hopping sequences or cyclic prefixes of the primary signals. Due to the periodicity, thesecyclostationary signals exhibit the features of periodic statistics and spectral correlation, which isnot found in stationary noise and interference [11].The figure 3.3 shows block diagram of Cyclostationary feature detector.

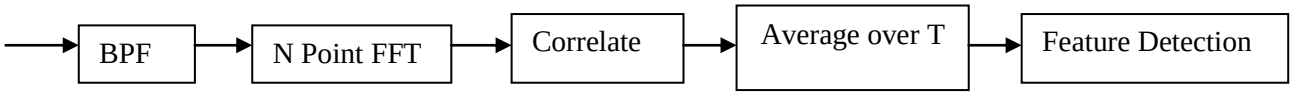

[Figure 3.3]: Block diagramof Cyclostationary feature detector [12]

Features:
(1) Cyclostationary feature detection performs better than Energy detection technique in low SNR regions [7], [9], [10].
(2) It is not affected by noise uncertainties. It is robust to noise [8], [9], [10].
(3) Frequency and phase synchronization of signal is not required.
Limitations:
(1) CFD requires long observation time, high sampling rate and higher computational complexity [8].
(2) CFD also requires the prior knowledge of primary user signal [8].
(3) There are possibilities of sampling time error.
(4) Since all the cycle frequencies are calculated that the machine complexness is above energy detector.

3.4 Waveform Based Sensing Technique

This type of sensing makes use of Preambles, pilot carrier and spreading sequences .These square measure other to the signal advisedly as data of such patterns facilitate in detection and synchronization functions. Preambles square measure set of patterns that square measure sent simply before the beginning of the data sequence whereas mid-ambles square measure transmitted within the middle of knowledge. The additional the lengths of these glorious patterns, additional are going to be the accuracy of the detection. The figure 3.4 highlights the most purposeful units of detector. The received signal is correlated with the celebrated patterns. The output of the correlator is compared with a threshold. In case the received signal is from the first users then it should have the celebrated patterns and so the correlation are going to be quite the edge or the case are going to be opposite just in case of noise.

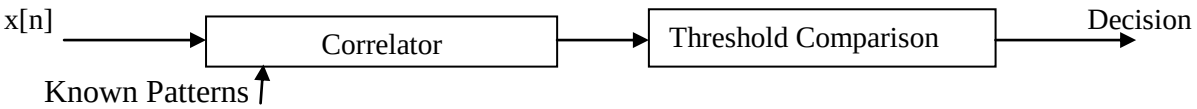

[Figure 3.4]: Waveform Based Sensing Method outline

Features:
(1)The Sensing time needed for the waveform based mostly detector is low as compared to energy detector.[13]
(2)It's additional reliable than energy detector.
Limitations:
(1) Higher accuracy needs a extended length of the proverbial sequences which ends up in lower potency of the spectrum.[13]

3.6 Wavelet Based Sensing Technique

A transition in frequency of an indication leads to edges within the frequency spectrum. This property may be terribly useful in detection algorithms. The waveband is sub-divided into variety of sub-bands every characterized by its own changes in frequency. The moving ridge rework is completed on these sub-bands to assemble the data regarding the irregularities or transitions. Moving ridge rework is applied and not standard Fourier rework as moving ridge rework offers the data regarding the precise location of the various frequency location and spectral densities. On the opposite hand Fourier rework is merely ready to show the various frequency parts however not the placement.The working principle [4] is illustrated in figure 3.5.the complete frequency vary is split into sub-bands. Rippling rework is applied to every of those sub-bands. The spectral densities of all the sub-bands are hunted for edges that represent transition from empty to occupied band. The presence of a grip indicates the presence of primary user within the band

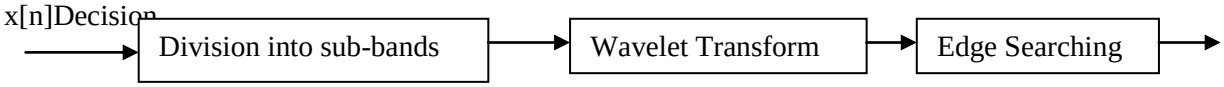

Figure 3.5: Principle of Wavelet Based Sensing

Features:
(1) Implementation price low as compared to multi-taper cost primarily based sensing technique.[13]
(2)It will simply adapt to dynamic Power Spectral density (PSD) structures.[13]
Limitations:
(1) So as to characterize the whole information measure higher sampling rates is also needed.[13]

3.6 Multiple Antenna Based SensingTechnique

Wireless transmissions via multiple transmit and receive antennas, or the thus referred to as multi input multi output (MIMO) systems have gained sizeable attention throughout recent times. MIMO systems typically use sensing schemes supported the Eigen values [14].In order to perform sensing for MIMO systems 2 basic steps are followed:-

Step-1:Planning of the check statistics that is obtained exploitation the chemist values of the co-variance matrix of the sample values. During this technique two algorithms are typically used, one being the utmost chemist worth detection and therefore the alternative being condition range detection.

Step-2:Account of the change density perform (PDF) of the check statistics or chemist values so sensing performance is quantified

Features:

(1) It does not need previous information of the received signal characteristics.[13]

(2) Since identical signal is received through multiple ways the noise power uncertainty is removed. [13]

Limitations:

(1)Use of multiple antennas will increase the value of the detector[13]

(2)The Quality of detector is additionally exaggerated. [13]

IV.COPERATIVE SENSING TECHNIQUES

High sensitivity requirements on the cognitive user can be alleviated if multiple CR users cooperate in sensing the channel. Various topologies are currently used and are broadly classifiable into three regimes according to their level of cooperation [15][16][17].Cooperative sensing techniques: a-Centralised Coordinated, b-Decentralised Coordinated, and c-Decentralised Uncoordinated.

4.1 Decentralized Uncoordinated Technique

Each CR user performs channel detection independently and does not support or share its information with other CR users [9].

4.2 Centralized Coordinated Technique

This technique designates a CR controller which is called fusion centre (FC). It is in strong connectivity with its nearby CR users inits range. FC selects desired frequency band and inform all CR in network to perform local sensing. CR user in network detects idle channel or primary user; inform to CR controller which shares thisinformation with all other CR users in network [9], [2], [18].

4.3 Decentralized Coordinated Technique

It does not require any CR controller or FC. Each CR user works as FC in network and provides coordination to other CR users [9]. It is also called distributed cooperative sensing technique.

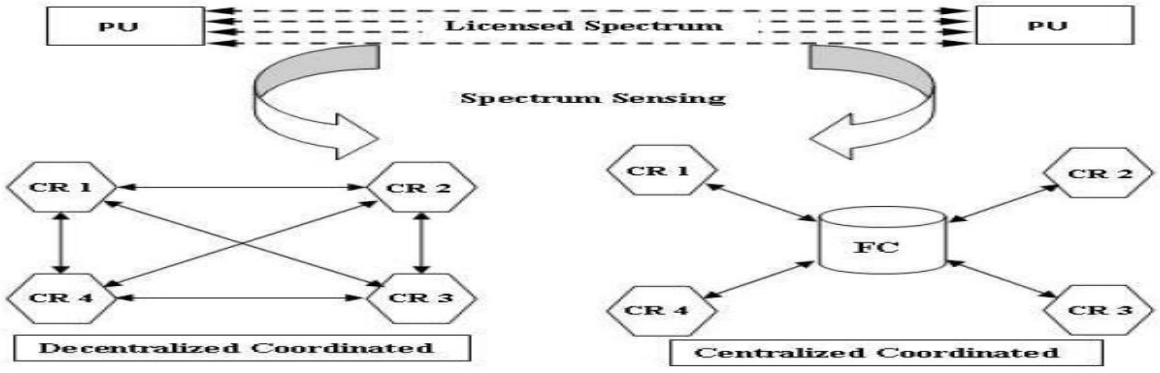

[Figure 4]: Cooperative Spectrum Sensing Techniques. [22]

The Figure 4 shows graphical representation of decentralized and centralized coordinated methods of cooperative spectrum sensing. In coordinated cooperative technique fusion centre (FC) is coordinating with 4 CR sensors while in uncoordinated technique all 4 CR sensors are connected with all the other CRs in network without existence of central fusion centre.

Features:

(1) Cooperative sensing decreases missed detection and false alarm probabilities [8].

(2) It solves hidden primary user problem and also decreases sensing problems [8].

(3) It provides higher spectrum capacity gains than local sensing [8].

(4) It requires less sensitive detectors, which result in flexibilities, reduced hardware cost and complexities [19].

Limitations:
(1) Combining sensing results of more than one CR users havingdifferent sensitivities, is a difficult task [2].
(2) This technique requires a control channel to convey informationamong all CR users [2].

V. INTERFERENCE BASED SENSING

Interference is typically regulated in a transmitter- centric way, which means interference can be controlled at the transmitter through the radiated power, the out-of-band emissions and location of individual transmitters. However, interference actually takes place at the receivers, as shown in Figure. 5.1 (a) &5.1 (b).[20]

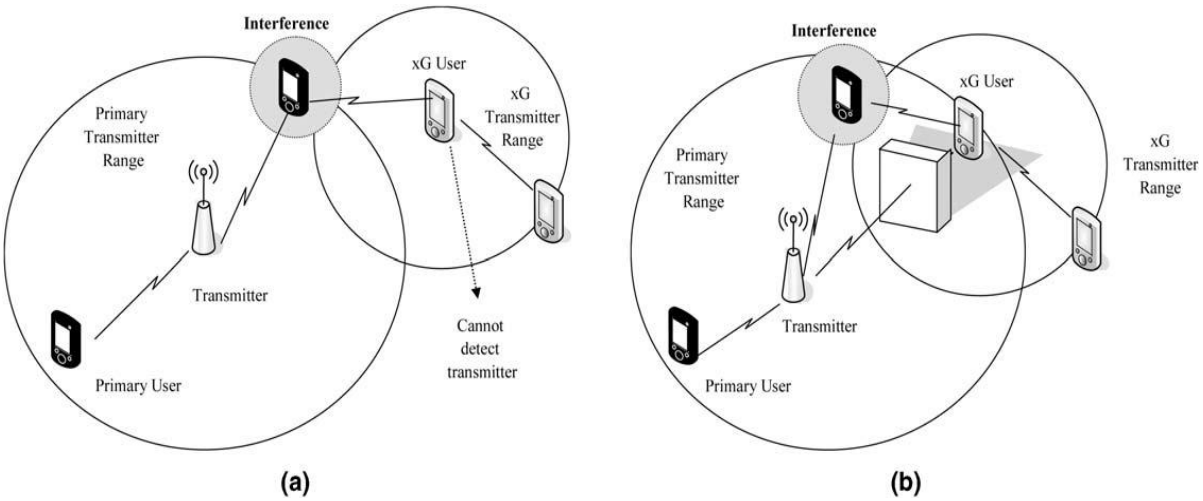

[Figure 5.1]: Transmitter detection problem :(a) Receiver uncertainty & (b)shadowing uncertainty.[20]

A new model for measuring interference, referred to as interference temperature shown in Figure 5.2 has been introduced by the FCC [21].

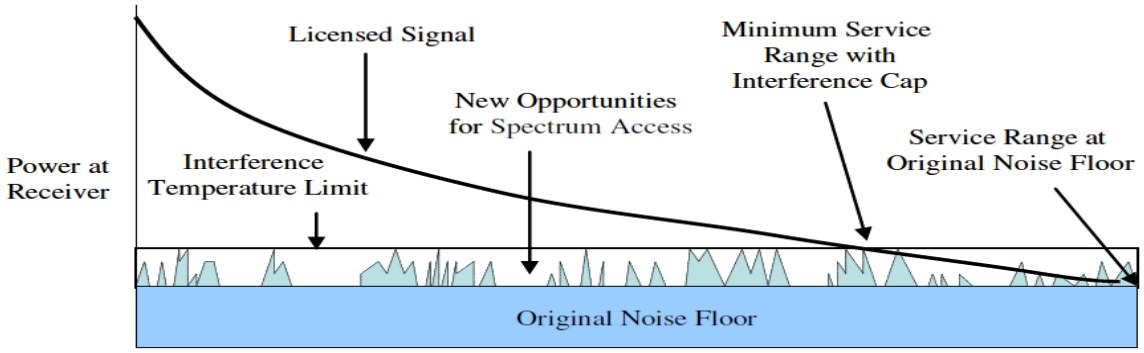

[Figure 5.2]: Interference temperature model [21].

The model shows the signal of a radio station designed to operate in a range at which the received power approaches the level of the noise floor.

Feature:
(1) As additional interfering signals appear, the noise floor increases at various points within the service area, as indicated by the peaks above the original noise floor.[20]
(2)The interference temperature model accounts for the cumulative RF energy from multiple transmissions and sets a maximum cap on their aggregate level. As long as xG users do not exceed this limit by their transmissions, they can use this spectrum band.[20]
Limitations:
(1) The interference is defined as the expected fraction of primary users with service disrupted by the xG operations.[20]
(2) This model describes the interference disrupted by a single xG user and does not consider the effect of multiple xG users.[20]
(3) If xG users are unaware of the location of the nearby primary users, the actual interference cannot be measured using this method.[20]

(4) CR users do not perform spectrum sensing for spectrum opportunities and can transmit rightWay with specified pre-set power mask.[10]
(5) The CR users can not transmit their data with higher power even if the licensed system is completely idle since they are not allowed to transmit with higher than the pre-set power to limit the interference at primary users.[10]
(6) The CR users in this method are required to know the location and corresponding upper level of allowedtransmit power levels. [10]

VI. CONCLUSIONS

In this paper, we discuss about three spectrum sensing techniques of cognitive radio such as cooperative, non-cooperative and interference based sensing.The main potential advantages introduced by cognitive radio are improving spectrum utilization and increasing communication quality. A novel approach to fulfil these requirements is to use CR concept.Cyclostationary feature detection shows the better detection performance as compared with the matched filter and energy detection techniques. We also said about important the importance of cooperation between Secondary users to avoid interference.Cooperative spectrum sensing raises the strength of cognitive radio network by combining efforts of multiple cognitive sensors. Most popular techniques for spectrum sensing are analysed in this paper.

REFERENCES

[1]. Mahmood A. Abdulsattar and Zahir A. Hussein, “Energy detection technique for Spectrum sensing in cognitive Radio,” International Journal of Computer Networks Communications (IJCNC) Vol.4, No.5, September 2012.
[2]. DanijelaCabric, ShridharMubaraqMishra, Robert W. Brodersen Berkeley Wireless Research Center, University of California, Berkeley IEEE Paper, “Implementation issues in spectrum sensing for cognitive radios,” in Proc. the 38th. Asilomar Conference on Signals, Systems and Computers, year 2004, pages 772-776.
[3]. TevfikYucek and HuseyinArslan, “A survey of spectrum sensing algorithms for cognitive radio applications,” IEEE communications surveys tutorials, Vol. 11, no. 1, first quarter2009.
[4]. S. Haykin, Cognitive Dynamic Systems, Proceedings of the IEEE, vol. 94, no. 11, Nov. 2006, pp. 1910-1911.
[5]. A. Rahim Biswas,Tuncer Can Aysal, SithamparanathanKandeepan, DzmitryKliazovich, RadoslawPiesiewicz, “Cooperative shared spectrum sensing for dynamic cognitive radio networks,” Broadband and Wireless Group, Create-Net International Research Centre, Trento, Italy, EUWB (FP7-ICT-215669).
[6]. Miguel Lpez-Bentez and Fernando Casadevall, “Improved energy detection spectrum sensing for cognitive radio,” This paper published in IET communication publication, IET Communications (2012), 6(8):785.
[7]. Sajjad Ahmad Ghauri, I M Qureshi, M. FarhanSohail, SherazAlam, M. Anas Ashraf, “Spectrum sensing for cognitive radio networks over fading channels,” International Journal ofComputer and Electronics Research Vol. 2, Issue 1, February 2013.
[8]. Anita Garhwal and ParthaPratim Bhattacharya, “A survey on spectrum sensing techniques in cognitive radio,” International Journal of Computer Science Communication Networks, Vol 1(2), 196-206.
[9]. V. Stoianovici, V. Popescu, M. Murroni, “A survey on spectrum sensing techniques for cognitive radio,” Bulletin of the Transylvania University of Brasov Vol. 15 (50) 2008.
[10]. Mansi Subhedar1 and GajananBirajdar, “Spectrum sensing techniques in cognitive radio networks: a survey,” International Journal of Next-Generation Networks (IJNGN) Vol.3, No.2, June 2011, DOI:10.5121/ijngn.2011.3203 37.
[11]. A. Tkachenko, D. Cabric, and R. W. Brodersen, (2007), “Cyclostationary feature detector experiments using reconfigurable BEE2,” in Proc. IEEE Int. Symposium on New Frontiers in Dynamic Spectrum Access Networks, Dublin, Ireland, Apr, pp: 216-219.
[12]. Shahzad A. et. al. (2010), “Comparative Analysis of Primary Transmitter Detection Based Spectrum Sensing Techniques in Cognitive Radio Systems,’’ Australian Journal of Basic and Applied Sciences, 4(9), pp: 4522-4531, INSInet Publication.
[13]. S. Joginder&R. MrsKestina “Spectrum Sensing in cognitive radio”, Chandigarh group of Colleges, Landran, Mohali, India, International Journal of Scientific and Research Publications, Volume 4, Issue 5, May 2014, ISSN 2250-3153.
[14]. Ying-Chang Liang, Guangming Pan, and YonghongZeng, "On the Performance of Spectrum Sensing Algorithms Using Multiple Antennas," GLOBECOM 2010, 2010 IEEE Global Telecommunications Conference, dec. 2010, pp. 1-5.
[15]. Ian F. Akyildiz, Brandon F. Lo, Ravikumar (2011), “Cooperative spectrum sensing in cognitive radio networks: A survey, Physical Communication”, pp: 40-62.
[16]. F.Zeng, Z. Tian, C. Li (2010), “Distributed compressive wideband spectrum sensing incooperative multi- hop cognitive networks”, in: Proc. Of IEEE ICC 2010, pp: 1-5.
[17]. A. Min, K. Shin, (2009), “An optimal sensing framework based on spatial RSS profile in cognitive radio networks”, in: Proc. of IEEE SECON, pp: 1-9.
[18]. NishantDevKhaira, PrateekBhadauria, “Cooperative spectrum sensing and detection efficiency in cognitive radio network,” International Journal of Electronics and ComputerScience Engineering ISSN-2277-1956.
[19]. Paul D. Sutton, Member IEEE, Keith E. Nolan, Member IEEE and Linda E. Doyle, Member IEEE, “Cyclostationary signaturesin practical cognitive radio applications,” IEEE journal on selected areas in communications, Vol. 26, no. 1, January 2008.
[20]. Ian F. Akyildiz, Won-Yeol Lee, Mehmet C. Vuran *, ShantidevMohanty” Next generation/dynamic spectrum access/cognitive radio wireless networks: A survey” Georgia Institute of Technology, Atlanta, GA 30332, United States, Computer Networks 50 (2006) 2127–2159.
[21]. FCC, ET Docket No 03-237 Notice of inquiry and notice of proposed Rulemaking, November 2003. ET Docket No. 03-237.
[22]. S. Md. Shahnawaz& G. Kamlesh “A Review of Spectrum Sensing Techniques for Cognitive Radio” AITR, Indore, International Journal of Computer Applications (0975 8887), Volume 94 - No. 8, May 2014.

American Journal of Engineering Research (AJER) 2015
American Journal of Engineering Research (AJER)
e-ISSN: 2320-0847 p-ISSN : 2320-0936
Volume-4, Issue-8, pp-244-249
www.ajer.org
Research Paper Open Access

Estimation of Modulus of Elasticity of Sand Using Plate Load Test

M. G. Kalyanshetti[1], Dr. S. A. Halkude[2], D. A. Magdum[3], K. S. Patil[4]
[1,2,3,4](Civil Engineering Department, Walchand Institute of Technology, Solapur, India)

Abstract: *Soil being a natural material, is very complex to understand mainly because of its heterogeneous nature. The other factors making the soil further complex are three phase system, non-linear stress-strain curve, loading and drainage conditions on field etc. Under all these circumstances evaluation of elastic constants of soil is a challenging task. The real challenge is to simulate the field condition precisely in the laboratory. Using tri-axial drained test, it is possible to simulate field condition for the evaluation of elastic constants such as modulus of elasticity (Es) and Poisson's ratio (μ). However, for sandy soil it is difficult to perform the tri-axial test because of its non-cohesive nature and limitation in the preparation of the test sample (cylindrical specimen). To overcome this limitation in the present study, an attempt is made to evaluate the modulus of elasticity using plate load test analogy. Loading frame is utilized for employing loads on the plates. Load settlement curves obtained from plate load tests are used for determination of the modulus of elasticity. The test is carried out using three plates of different sizes. The modulus of elasticity is calculated by assuming different values of Poisson's ratio. The study reveals that, modulus of elasticity is in the range of 22 to 25 MPa, which reasonably falls in the range given in different literature. The studied range of Poisson's ratio is not significantly influencing the Modulus of Elasticity of sand.*

Keywords: *Elastic theory, Loading frame, Load -settlement curve, Modulus of elasticity, Plate load test, Poisson's ratio.*

I. Introduction

Modulus of elasticity of soil is a measure of soil stiffness. The modulus of elasticity is often used for estimation of soil settlement and elastic deformation analysis. Generally, modulus of elasticity of soil is determined in the laboratory using tri-axial test. But, for sand it is difficult to carry out tri-axial test because of its non-cohesive nature leading to limitation in preparation of sample mould for testing. Therefore, in the present study an attempt is made to determine modulus of elasticity of sand using plate load test analogy. The loading on the plate may be applied by gravity loading or reaction loading. In gravity loading, a platform is constructed on a vertical column resting on plate. Loading on the plate is done by placing weighed sand bags on the platform. In reaction loading the load is applied through a proving ring and hydraulic jack by taking reaction against a fixed support. In the present study reaction loading is applied with the help of loading frame having capacity of 1000 kN. T. Warmate and H. O Nwankwoala [1] studied the use of plate load test in ascertaining elastic modulus, Es. The study is carried out in Calabar, Niger Delta, Nigeria. Four plate load tests were carried out within the area of investigation, with load settlement curve which indicates a firm to stiff partial cohesive soil. An average elastic modulus value was obtained in the elastic range (initial tangent modulus), which is indicative of firm clay. This value confirms reasonably with those obtained by method proposed using cone penetrometer test (CPT). Literature reveals that, there is wide range of modulus of elasticity of sand. As per J. E. Bowles [2], the modulus of elasticity for silty sand, loose sand and dense sand is in the range of 5-20 MPa, 10-20 MPa and 50-81 MPa respectively. From this wide range, it is difficult to pick up the appropriate value of modulus of elasticity for the sand under consideration. Hence, it is decided to carry out experiment for evaluation of modulus of elasticity of sand in the laboratory. Normally about 90 % of total settlement of sandy soil comprises of immediate settlement. The amount of immediate settlement (elastic) is a function of elastic modulus and Poisson's ratio. The modulus of elasticity, which is an indicator of the material stiffness and a fundamental material constant, gives an indication of the immediate settlement. Load settlement curve generated from the plate load test, helps in the extrapolation of reasonable elastic modulus where the soil does not exhibit significant variation. The elastic modulus, which characterizes the soil stiffness, can be graphically defined by the slope of the tangent in a stress-strain plot (tangent modulus) in the elastic range [1].

II. Experimental Study

Test Setup

The plate load set up is developed using a loading frame. For retaining the sand, a container of size 1.1 x 1.1 x 0.5 m is prepared. Two opposite sides of container are made up of steel plates and remaining two sides are made up of plywood of thickness 18 mm as shown in Fig. 1. The bottom of container is open so that influence zone of pressure under the plates is kept unconstrained.

Fig. 1 Sand container used for study

Fig.2 shows loading frame used for study.

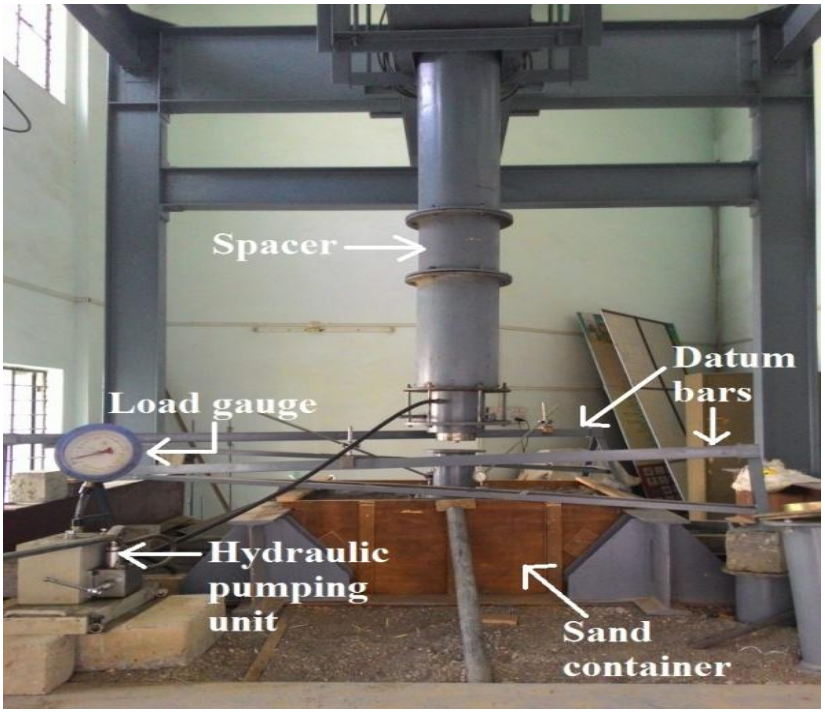

Fig. 2 Loading frame

Fig. 2 Loading frame

Proper care is taken to ensure lateral confinement of container. Stiffeners are provided on the ply woods to ensure lateral constraint & to avoid volume changes during application of load. Container is then filled with uniformly graded sand. This uniformly graded sand is having the size range 2.36 mm to 425 µ. Properties of sand used for test are shown in Table 1.

Table 1 Properties of sand

Sr. No.	Properties	Result
1	Specific Gravity	2.82
2	Water Absorption (%)	1.27
3	**Strength Parameters**	
	(a) Soil internal frictional angle (Ø) in degrees	51
	(b) Cohesion 'C' (kN/m^2)	0
4	Fineness Modulus	4.9
5	Unit Weight (kN/m^3)	18.01

Three rigid plates of different sizes are used for test which are shown in Fig. 3.

Fig. 3 Three rigid plates used in the study

Experiments are carried out to determine settlement beneath square plates resting on surface of sand. The settlement is measured with the help of sensitive dial gauges fixed on the surface of plate. The dial gauges are mounted on independently supported datum bars. As the plate settles, the ram of the dial gauge moves down and settlement is recorded. The load is indicated on the load–gauge of hydraulic jack. Fig. 4 shows plate load test setup.

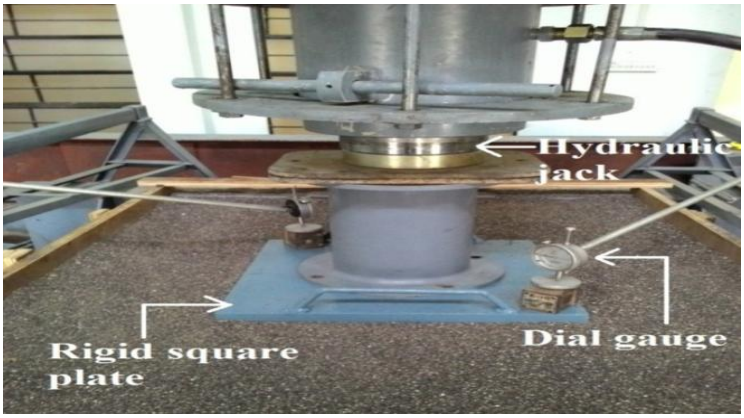

Fig. 4 Plate load test setup

Test Procedure

The plate is properly placed on sand at the center of container. The reaction load is applied with the help of a hydraulic jack. The maximum loads on plates are applied in such a way that their intensities of pressure under the plates are approximately equal to bearing capacity of sand under consideration. According to National Building Code of India, bearing capacity of cohesionless soil (medium, compact and dry) which reasonably confirms to the sand used for the study is in the range of 250 to 300 kN/m^2 [3]. The maximum loads on plates are applied equivalent to above pressure intensity. This loading is given in increment. The loads are applied in stages of 10 kN, 15 kN, 20 kN, 25 kN, 35 kN, 45 kN. For each load application settlement of plate is observed by dial gauges with sensitivity of 0.01 mm. Settlement is observed after an interval of 1, 2, 5, 15, 30 and 60 minutes and thereafter at hourly intervals until the rate of settlement becomes less than about 0.02 mm per hour [4]. After this, the next load increment is applied.

III. Results And Discussion

Load Settlement Curve

Settlements are recorded for three plates of different sizes. The values of loads and corresponding settlements of each plate are given in Table 2, Table 3 and Table 4.

Table 2 Load and corresponding settlement for plate no. 1

Load (N)	Pressure 'q' (N/mm^2)	Settlement 'S_i' (mm)
0	0	0
10000	0.111	2.280
15000	0.167	2.430
20000	0.222	3.480
25000	0.278	3.800
35000	0.389	4.620
45000	0.5	5.710

Table 3 Load and corresponding settlement for plate no. 2

Load (N)	Pressure 'q' (N/mm^2)	Settlement 'S_i' (mm)
0	0	0
10000	0.0711	1.665
15000	0.107	2.175
20000	0.142	2.600
25000	0.178	3.050
35000	0.249	3.540
45000	0.32	4.940

Table 4 Load and corresponding settlement for plate no. 3

Load (N)	Pressure 'q' (N/mm^2)	Settlement 'S_i' (mm)
0	0	0
10000	0.0494	1.370
15000	0.0741	1.500
20000	0.0988	1.585
25000	0.123	1.935
35000	0.173	2.710
45000	0.222	3.450

From these values, pressure v/s settlement curves are plotted as shown Fig. 5.

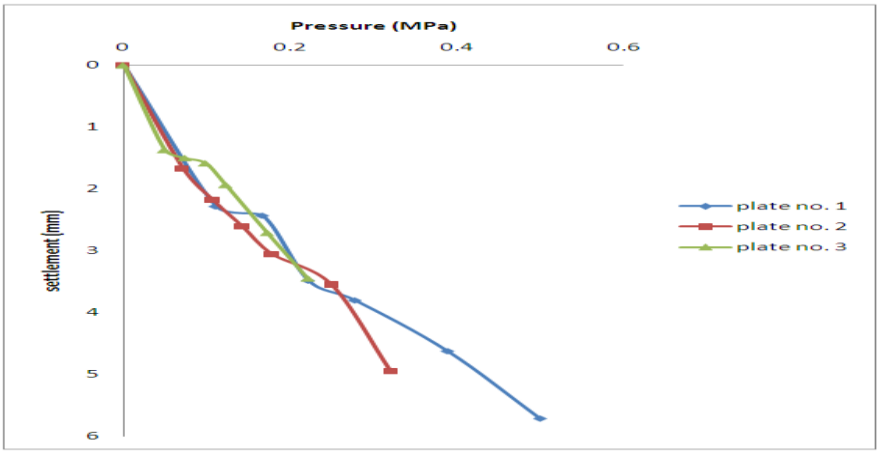

Fig. 5 Pressure v/s settlement curve for all plates

In Fig. 5, it is observed that in initial stages, rate of settlement is very less with increase in pressure. For plate no. 1 and 3 almost negligible settlements are observed in the initial stages. This is because of the resistance of sand particles to readjustment in the initial phase. After this phase sand undergoes the settlement almost in linear way.

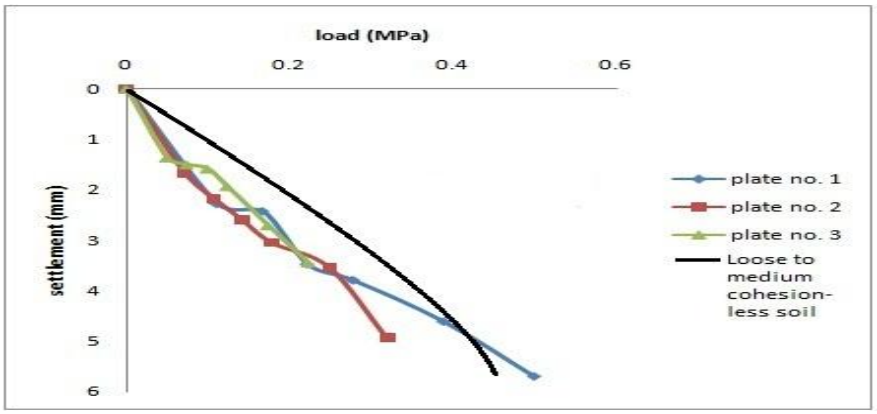

Fig. 6 Load settlement curve

Fig. 6 shows a typical load settlement curve for loose to medium cohesionless soil. Looking to the nature of load settlement curves of present study, it is observed that these curves are almost matching with the typical curve given for loose to medium cohesionless soil (Sandy soil), which almost matches with sand used for study. Hence, it may be inferred that the obtained load settlement curve of sand reasonably matches with the curves given in the literature.

Evaluation of Modulus of Elasticity (Es)

The theory of elasticity can be used to determine elastic settlement in soil caused by loads acting over footings of different geometrical shapes. The modulus of elasticity of sand can be computed from the following expression based on the theory of elasticity (Terzaghi).

$$S_i = qB\left[\frac{1-\mu^2}{E_s}\right] I_f \qquad (1)$$

Where, S_i is immediate elastic settlement of soil, q is intensity of contact pressure, B is least lateral dimension of footing, Es is modulus of elasticity of soil, μ is Poisson's ratio, I_f is influence factor.

It is difficult to determine Poisson's ratio for sand. However, the entire term $\left[\frac{1-\mu^2}{E_s}\right] I_f$ from eq. (1) is determined from plate load test by using three different size plates of the same shape. A plot between S_i and q.B gives a straight line, the slope of which is equal to $\left[\frac{1-\mu^2}{E_s}\right] I_f$. In the present study, loads applied on the plates are 10 kN, 15 kN, 20 kN, 25 kN, 35 kN and 45 kN. The values of S_i and q.B for all loads and plates are plotted and shown in Fig. 7.

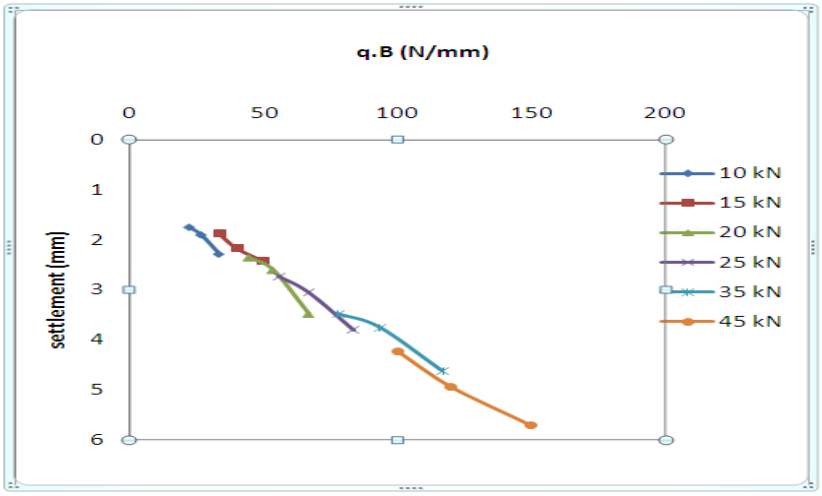

Fig. 7 Plot of S_i v/s q.B for all loads

It is observed from Fig. 7 that, variation of S_i with respect to q.B is almost straight line (linear). It is observed that slope of all the lines is almost same i.e. for various load values the modulus of elasticity remains the same. Thus, for experimentation any convenient load/pressure intensity can be used to obtain the modulus of elasticity.

Effect of Poisson's Ratio

From the literature it is revealed that, the Poisson's ratio of sand varies from 0.3 to 0.45 [5]. To understand the variation of modulus of elasticity with respect to Poisson's ratio, the Es value is calculated for Poisson's ration μ in the range of 0.3 to 0.46. Influence factor (I_f) is taken as 0.9 for the rigid square plate [6]. Table 5 gives the values of modulus of elasticity for different values of μ.

Table 5 Es value for different Poisson's ratios

Load (kN)	10	15	20	25	35	45
Slope= $\left[\frac{1-\mu^2}{E_s}\right]I_f$	0.3290	0.0333	0.0400	0.0333	0.0360	0.0360
Poisson's Ratio (μ)	Es (MPa)					
0.30	24.89	24.82	20.48	24.59	22.75	22.75
0.32	24.55	24.48	20.20	24.26	22.44	22.44
0.34	24.19	24.12	19.90	23.90	22.11	22.11
0.36	23.81	23.74	19.58	23.52	21.76	21.76
0.38	23.41	23.33	19.25	23.12	21.39	21.39
0.40	22.99	22.91	18.90	22.70	21.00	21.00
0.42	22.53	22.46	18.53	22.26	20.59	20.59
0.44	22.06	21.99	18.14	21.79	20.16	20.16
0.46	21.57	21.50	17.74	21.31	19.71	19.71

From Table 5, it is observed that for different values of μ, modulus of elasticity does not change very much. The modulus of elasticity of sand is in the range of 20 to 24 MPa. This variation is almost 16 %. The range of modulus of elasticity of sand as per literature is 10 to 25 MPa [2]. Therefore, it can be said that Es value which is experimentally determined confirms the range given in the literature for the soil under consideration.

IV. Conclusions

Plate load test on field requires reaction loading system on site which is time consuming and difficult task and also it is more cumbersome. Present study advocates the laboratory test is reasonably accurate and less cumbersome. From this study it is proved that, the loading frame can be used to develop the reaction loading system in the laboratory to perform the plate load test under much controlled conditions.

The elastic modulus obtained in the laboratory using plate load test is in the range 20 to 24 MPa. This value is reasonably confirming with the range of modulus of elasticity mentioned in the literature (Bowles).

Study reveals that, for different values of Poisson's ratio of sand (0.3 to 0.45), modulus of elasticity varies between 14 to 16 %. This variation is marginal. Hence, it can be inferred that Poisson's ratio is not significantly affecting the modulus of elasticity.

This method of evaluation of modulus of elasticity of sand in the laboratory using plate load test analogy is reasonably accurate than the cumbersome method of tri-axial where the major difficulty is the preparation of sample of sand.

References

[1]. T. Warmate, H.O. Nwankwoala, Determination of elastic modulus using plate load test in Calabar, South-Eastern Nigeria, *International Journal of Natural Sciences Research,* 2014, 2(11): 237-248.

[2]. Joseph E. Bowles, *Foundation Analysis and Design* (McGraw-Hill, 1997).

[3]. National Building Code of India, SP 7: 2005.

[4]. IS 1888: Method of load test on soil (second revision), Indian Standards Institution, New Delhi, 1982.

[5]. Narayan V. Nayak, *Foundation Design Manual*, (Dhanpat Rai Publications, 2006).

[6]. IS 8009 (Part I): Code of practice for calculation of settlements of foundations, Bureau of Indian Standards, New Delhi, 1976.